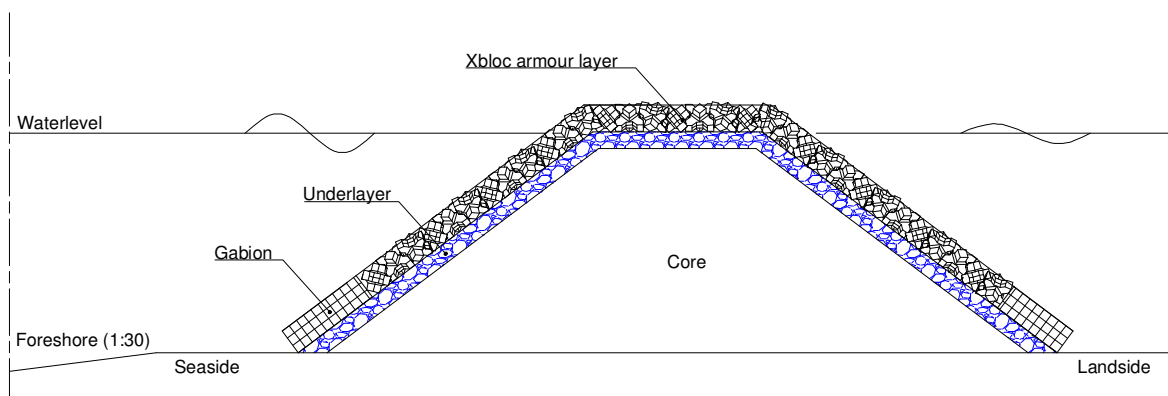


Stability of single layer armour units on low-crested structures

MASTER OF SCIENCE THESIS



Note: The Xblocs in the drawing are used as hatching for the armour layer, it gives no information on the actual number of rows.

List of trademarks used in this report:

- *Accropode* is a registered trademark of Sogreah Consultants, France;
- *Core-Loc* is a registered trademark of the US Army Corps of Engineers, USA;
- *X-Bloc* is a registered trademark of Delta Marine Consultants, The Netherlands.

The use of trademarks in any publication of Delft University of Technology does not imply any endorsement or disapproval of this product by the University.

GENERAL INFORMATION

Delft University of Technology
Faculty of Civil Engineering and
Geosciences
Section Hydraulic Engineering

Stevinweg 1
2628 CN Delft
The Netherlands
+31(0)152 787966
info@citg.tudelft.nl

Delta Marine Consultants
Department Coastal Engineering

H. J. Nederhorststraat 1
2801 SC Gouda
The Netherlands
+31(0)182 590431
dmc@dmc.nl

Master of Science thesis committee

Delft University of Technology

- Prof. drs. ir. J.K. Vrijling chairman
- Prof. dr. ir. W.S.J. Uijttewaal member
- Ir. H.J. Verhagen member

Delta Marine Consultants

- Ir. E. ten Oever member

Student

J.P. van der Linde

Peter_vd_linde@hotmail.com

Graduation topic

Stability of single layer armour units
on low-crested structures

Date of report

11 October 2009

ACKNOWLEDGEMENTS

This thesis is the final report of a research project undertaken to obtain the degree of Master of Science at Delft University of Technology. I would not have been able to complete this study by myself and therefore I want to thank all people who cooperated in my graduation project.

First of all I want to thank my parents for the unconditional support during my study.

I am grateful to Delta Marine Consultant for offering me a practical and both scientific internship for facilitating my graduation research. I thank all colleagues for their support and pleasant working atmosphere during this research.

I want to thank my graduation committee for their advice and supervision of my research process. From Delft University of Technology: Han Vrijling, Wim Uijttewaal and Henk Jan Verhagen. From Delta Marine Consultants I want to thank Erik ten Oever. Your enthusiasm for my research and your analytical point of view has been instructive and incentive for me. I also want to thank Markus Muttray. Your experience and input in the analysis of the test results were very valuable.

Peter van der Linde
October 2010

SUMMARY

A breakwater armour layer consists of rock or concrete elements. Concrete armour units are required for more severe design conditions. This study deals with the stability of single layer concrete interlocking Xbloc armour units on low-crested breakwaters. At this moment the Xbloc armour units are designed by $H_s/\Delta D_n = 2.8$. It is thus assumed that the armour units at the upper part of the slope and crest for low-crested breakwaters are as stable as elements near the waterline in the case of conventional breakwaters. The Newbiggin case indicates however that the stability decreases for low-crested breakwaters. One percent of the single layer interlocking Core-Loc armour units were broken after the structure's first winter. The stability number is probably taken too high for the armour layer design and breakage indicates that rocking is a sound failure mechanism.

This study is aimed at the execution of the first step in the process to a new stability formula for single layer armour units at low-crested breakwaters.

Two dimensional physical model tests are executed with Xbloc armour units on low crested structures to answer the objective. On the basis of findings in the literature study it can be expected that the stability of the Xbloc elements on low-crested breakwaters is a function of crest freeboard and crest width. The crest freeboard (R_c/D_n) varied from -0.8 to 0.8 in steps of 0.4 and the tested crest widths (W_c) are 3 and 9 armour units wide. Additionally all tests series are executed with a wave steepness of 2 and 4%. All test series are executed once except the reference test series ($R_c/D_n = 0$, $W_c = 3$) which are repeated four times to acquire insight into the reliability of the test results. The number of rocking and displaced armour units is registered for the total breakwater, seaside slope and crest (also termed breakwaters sections).

Settlements at both the sea- and leeward slope leads to openings in the armour layer at the transition from the seaside slope to the crest. As a consequence the interlocking properties of the upper part of the seaside slope and crest decreases and the area of the Xbloc crest elements normal to the wave induced flow increases. Moreover due to settlement the distance between two succeeding rows at the upper part of the slope increases whereas for the lower part of the slope it decreases. This together with the already decreased interlocking properties of the upper rows at the slopes and crest rocking results at both the upper part of the seaside slope and the outer seaward rows of the crest.

The armour layer stability (rocking and the displacement of armour units) in case of wave steepness 2% is significant smaller than for 4%. In case of rocking the stability of the total breakwater is minimal for submerged conditions in case of wave steepness 2% and maximal for a crest freeboard of 1.5 whereas the stability for wave steepness 4% shows an opposite trend. In case of displaced armour units both wave steepness's show a comparable trend over crest freeboard, the stability is maximal for submerged and emerged conditions and minimal for a crest freeboard of 1.5.

In case of rocking the stability at the seaside slope decreases from submerged to emerged conditions for wave steepness 2%. Whereas the stability in case of 4% wave steepness is maximal for submerged conditions and minimal for a crest freeboard of 1.5 after which the stability increases again. In case of displacement both wave steepness's show the same trend, the stability is maximal for submerged conditions and minimal for a crest freeboard of 1.5 after which the stability increases again slightly.

In case of rocking the stability at the crest is minimal for submerged conditions and becomes maximal for a crest freeboard of 1.5 after which the stability decreases slightly again. The minimum stability for submerged conditions is caused by the oscillating water flow over the crest. In case of displacement of the armour units the opposite trend is present, the stability is maximal for the most emerged and submerged conditions and minimal for a crest freeboard of 1.5. This applies for both a wave steepness of 2% and 4%.

The test results indicate that the design of the armour layer for a low-crested breakwater has to be based on the number of rocking elements instead of the number of displaced elements. Furthermore the wave steepness of 2 and 4% show comparable trends for the stability at the crest but not at the seaside slope and the total breakwater.

Independently of wave steepness the least stable crest freeboard is 1.5, this is caused due to the wave energy which is maximal around the still water line and the lower interlocking properties of the upper rows of the seaside slope.

CONTENTS

GENERAL INFORMATION	II
ACKNOWLEDGEMENTS	III
SUMMARY	IV
CONTENTS	VI
1. INTRODUCTION	1
1.1. ARMOUR LAYER STABILITY	1
1.1.1. <i>Armour layer stability</i>	1
1.1.2. <i>The Newbiggin Case</i>	2
1.1.3. <i>Hydraulic stability of concrete armour units</i>	4
1.1.4. <i>Lack of knowledge</i>	5
1.2. STUDY OBJECTIVE	5
1.3. STUDY METHODOLOGY	6
2. RUBBLE MOUND BREAKWATERS	7
2.1. FUNCTIONAL REQUIREMENTS	7
2.2. GENERAL BREAKWATER CROSS SECTION	8
2.2.1. <i>Hydraulic design considerations, wave structure interaction</i>	9
2.2.2. <i>Typical rubble mound breakwater cross sections</i>	10
2.3. STRUCTURAL FAILURE	12
2.3.1. <i>Loading of the armour layer</i>	13
2.3.2. <i>Failure modes armour layer</i>	15
3. LITERATURE STUDY ON ROCK ARMOUR STABILITY	17
3.1. DESCRIPTION OF LOADS AND RESISTANCE OF ROCK ARMOUR	17
3.1.1. <i>Load, wave induced flow forces on a stone</i>	18
3.1.2. <i>Strength, Stabilizing forces of a stone</i>	18
3.1.3. <i>Stability principle, load versus strength</i>	18
3.2. ARMOUR LAYER DESIGN FORMULAS	19
3.2.1. <i>Iribarren</i>	20
3.2.2. <i>Iribarrrens formula modified by Hudson (1959)</i>	21
3.2.3. <i>Hudson (1959)</i>	21
3.2.4. <i>Hudson</i>	21
3.2.5. <i>Van der Meer formula</i>	21
3.2.6. <i>Shields parameter</i>	24
3.2.7. <i>Conclusions on armour layer design formula</i>	24
3.3. PRIOR STUDIES LOW-CRESTED BREAKWATERS	24
3.3.1. <i>Mizutani et al. 1992, 1994</i>	25
3.3.2. <i>Van der Meer et al. 1994</i>	27
3.3.3. <i>Vidal et al. 1992</i>	29
3.3.4. <i>Burger 1995</i>	31
3.3.5. <i>Kramer et al. 2003</i>	31
3.3.6. <i>Vidal et al. (2007)</i>	35
3.3.7. <i>Numerical Modelling of velocity and turbulence fields around and within low-crested rubble mound breakwaters</i>	38
3.3.8. <i>Conclusions prior studies low-crested breakwaters with rock armour</i>	42
4. LITERATURE STUDY ON STABILITY SINGLE LAYER INTERLOCKING ARMOUR UNITS	44
4.1. CONCRETE ARMOUR UNITS	44
4.2. STABILITY	45
4.2.1. <i>Load</i>	45
4.2.2. <i>Resistance</i>	45
4.3. PRIOR STUDIES LOW-CRESTED BREAKWATERS	49
4.3.1. <i>Matsuda et al. 2003</i>	49

4.3.2. Dolos (double layer).....	50
4.3.3. Tetrapod (double layer).....	51
4.3.4. Accropode (single layer).....	51
4.3.5. Conclusions on design low-crested breakwaters with single layer armour units..	52
5. DESCRIPTIONS PHYSICAL MODEL TESTS	53
5.1. TEST FACILITY	53
5.2. SCALING.....	53
5.2.1. Scaling laws	54
5.2.2. Best suitable scaling law.....	55
5.2.3. Scale effects related to wave-structure interaction.....	56
5.3. MODEL.....	57
5.3.1. Cross section.....	57
5.3.2. Materials.....	60
5.4. TEST PROGRAMME	63
5.4.1. Waves.....	63
5.4.2. Programme	65
5.5. MEASUREMENTS.....	66
5.5.1. Waves.....	66
5.5.2. Xbloc movement and displacement.....	67
5.6. PERFORMED TESTS.....	68
5.6.1. Divergent tests from original test programme.....	68
5.6.2. Relative packing density.....	69
5.6.3. Placement crest elements.....	70
5.7. HYDRODYNAMICS.....	71
5.7.1. Waveheight.....	72
5.7.2. Wave steepness.....	72
5.7.3. Spectrum and waveheight distribution.....	73
5.7.4. Water level set up behind breakwater.....	75
6. GENERAL OBSERVATIONS.....	76
6.1. HYDRAULIC PROCESSES	76
6.1.1. Flow of Water over breakwater crest	76
6.1.2. Wave breaking.....	78
6.1.3. Transmitted waves.....	81
6.2. SETTLEMENTS ARMOUR LAYER.....	82
6.2.1. Initial settlements	82
6.2.2. Ongoing settlements.....	83
6.2.3. Course of the settlements	84
6.2.4. Consequences of settlements	85
6.3. PERFORMANCE XBLOC ELEMENTS ON THE CREST	87
6.3.1. Shift of crest armour	87
6.3.2. Rocking of Xbloc crest elements.....	88
6.3.3. Displacement of Xbloc crest elements.....	89
6.4. PERFORMANCE XBLOC ELEMENTS ON THE SLOPE	91
6.4.1. Rocking Xbloc slope elements	92
6.4.2. Displaced Xbloc slope elements	92
6.5. CONCLUSIONS	94
7. ANALYSIS ROCKING XBLOC ARMOUR UNITS	96
7.1. TEST RESULTS ROCKING ARMOUR UNITS	97
7.2. REFERENCE TESTS.....	98
7.2.1. Two percent wave steepness.....	99
7.2.2. Four percent wave steepness.....	102
7.2.3. Conclusions.....	104
7.3. ANALYSIS TEST RESULTS.....	105
7.3.1. Small crested breakwater, $s=2\%$	105
7.3.2. Wide crested breakwater, $s=2\%$	107
7.3.3. Small crested breakwater, $s=4\%$	108
7.3.4. Wide crested breakwater, $s=4\%$	110
7.4. ANALYSIS R_c/D_N	112
7.4.1. Influence crest freeboard.....	113
7.4.2. Influence crest width and relative placement density	126
7.4.3. Influence wave steepness	132

7.5. LOCATION OF ROCKING ARMOUR UNITS	136
8. DISPLACED ARMOUR UNITS	137
8.1. TEST RESULTS DISPLACED ARMOUR UNITS	137
8.2. REFERENCE TEST SERIES	140
8.2.1. Two percent wave steepness.....	140
8.2.2. Four percent wave steepness.....	143
8.2.3. Conclusions.....	145
8.3. ANALYSIS DISPLACED XBLOC ARMOUR UNITS	146
8.3.1. Small crested breakwaters, $s=2\%$	146
8.3.2. Wide crested breakwater, $s=2\%$	148
8.3.3. Small crested breakwaters, $s=4\%$	150
8.3.4. Wide crested breakwater, $s=4\%$	151
8.4. DISCUSSION TEST RESULTS	153
8.4.1. Influence crest freeboard.....	154
8.4.2. Influence crest width and relative placement density	160
8.4.3. Influence wave steepness	163
8.5. LOCATION OF DISPLACED ARMOUR UNITS	165
9. COMPARISSON TEST RESULTS.....	167
9.1. COMPARISSON ROCKING AND DISPLACED ELEMENTS	167
10. WAVE TRANSMISSION	174
11. FINAL CONCLUSION.....	177
12. REFERENCES.....	179
LIST OF FIGURES	182
LIST OF TABLES	188
APPENDIX A.....	189
APPENDIX B.....	190
APPENDIX C.....	193
APPENDIX D.....	195
APPENDIX E.....	223
APPENDIX F.....	232
APPENDIX G.....	249
APPENDIX H.....	255
APPENDIX I.....	256
APPENDIX I.....	257
APPENDIX I.....	258
APPENDIX J.....	259
APPENDIX K.....	273
APPENDIX L.....	281

1. INTRODUCTION

Breakwaters are widely used throughout the world, providing shelter from wave action and currents for vessels and port facilities. Besides giving shelter for port activities, breakwaters are also used to protect valuable habitats, prevent siltation of navigation channels and protect beaches which are exposed to erosion processes. There are different types of breakwaters such as the rubble mound, monolithic, composite, floating and pneumatic/hydraulic type of breakwaters. This study focuses on rubble mound breakwaters and more specific on the armour layer stability of low-crested structures.

1.1. ARMOUR LAYER STABILITY

A breakwater armour layer consists of rock or concrete elements. For moderate design wave conditions rock is most economical concrete armour units are required for more severe design conditions. A benefit of concrete over rock is that concrete armour units provide hydraulically stability by their own weight, interlocking and friction between adjoining units. In this way the individual weight of a concrete armour unit can be less than rock. This study deals with single layer interlocking concrete armour units.

1.1.1. ARMOUR LAYER STABILITY

There are different design guidelines for concrete en rock armour layers. A short description of these guidelines is given.

Rock armour layers

Non overtopped rubble mound breakwaters are usually designed according to the van der Meer or Hudson formula. Van der Meer gives the most advanced equation with parameters like permeability, damage level and wave steepness. On top of the just mentioned parameters, van der Meer makes a distinction between plunging and surging waves. Both formulas are based on model testing.

Concrete armour layers

Most concrete armour layers are designed according to the Hudson formula. The input parameters are the wave height at the toe of the structure, stability coefficient (K_d) and the slope angle. The stability coefficient is derived from model tests and depends on many factors. The coefficient is valid for one specific situation (one slope angle etc.), non common situations poses difficulties to the design of concrete armour layers. Stability coefficients for (overtopped) low-crested structures are not known by the author.

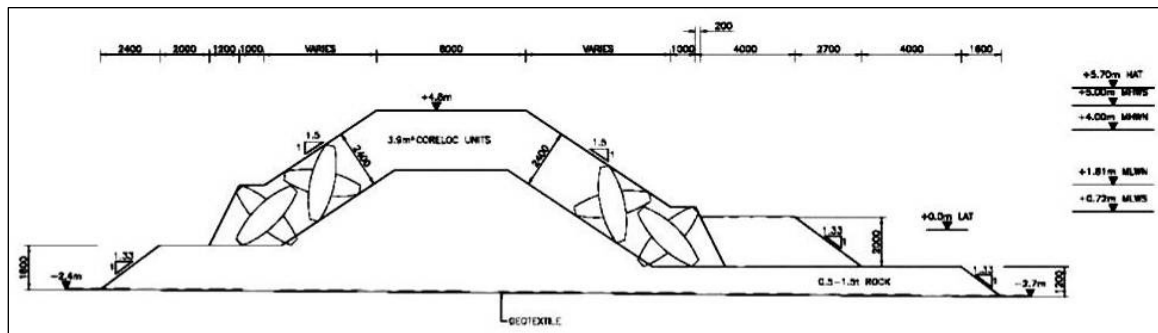
At this moment it is assumed that elements at the upper part of the slope and crest are as stable as element near the waterline in case of a conventional breakwater. Observations such as the Newbiggin case indicate that low-crested structures are less stable.

1.1.2. THE NEWBIGGIN CASE

To illustrate the lack of knowledge in the field of concrete armour units on Low-crested breakwaters, the example of New Biggin is given.

In Newbiggin a breakwater was constructed between April and November 2007 (see Figure 1.1). The breakwater armour layer consists of 3.9 m³ Core-Loc interlocking elements. The breakwater crest height is + 4.50 m and the highest astronomic tide + 5.70 m, the breakwater is thus a low-crested/submerged type.

Figure 1.1 Breakwater cross section Newbiggin



The breakwater is designed according to the Hudson formula and 2D and 3D model tests. Applying the Hudson formula with the design parameters given in Table 1-1 and the fact that there has been used a 3.9 m³ armour unit, it appears that the assumed K_d value is 16, this value is recommended as a design stability coefficient on breakwater trunk sections by the US Army Corps of Engineers

Table 1-1 Design parameters breakwater Newbiggin

Parameter	Value
design wave H_s	5.7 m
T_p	12 s
maximum water depth	8.6 m
length of structure	200 m
armour slope (V/H)	2/3

Several pictures (Figure 1.2 to Figure 1.5) were taken from the breakwater in 2008, giving the impression that the breakwater has suffered some damage. Figure 1.2 and Figure 1.5 indicates that some elements are moved from their original position. Figure 1.2 and Figure 1.3 shows that the breakwater has settled a considerably amount compared to the steel tube pile foundation of the monument. Figure 1.4 shows a bump at the front side of the breakwater, while the breakwater on the plan view (Figure 1.5) is completely straight, except for the breakwater heads.

Figure 1.2 Breakwater Newbiggin with monument



Figure 1.3 Original crest height breakwater relative to steel tube pile foundation of the monument

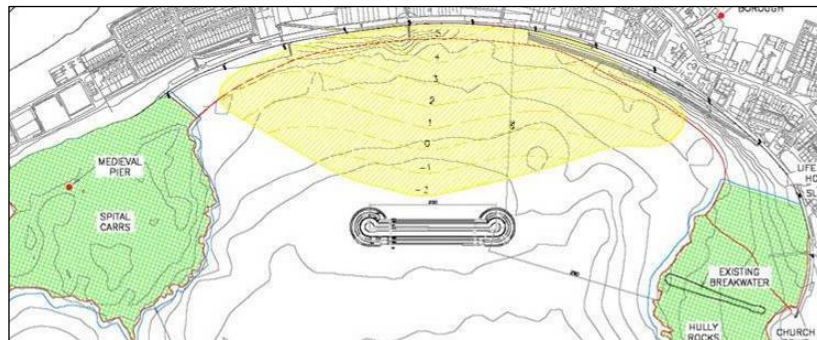


An inspection of the breakwater was carried out in June 2008 and confirmed the observed damage. Several Core-Loc units were found to have suffered damage during the structure's first winter. The number of breakages equates to approximately 1% of the total number [WAREING A.W. *et al.* 2009].

Figure 1.4 Breakwater Newbiggin with noticeable bump



Figure 1.5 Plan view breakwater Newbiggin



From the 1% breakage of the armour units in one year and the different photographs it can be concluded that the breakwater is not fully stable. The waves in front of the breakwater are depth limited, therefore the probability that the design wave height occurs is quite large. Therefore the breakwater will be exposed frequently to the design wave heights during its lifetime.

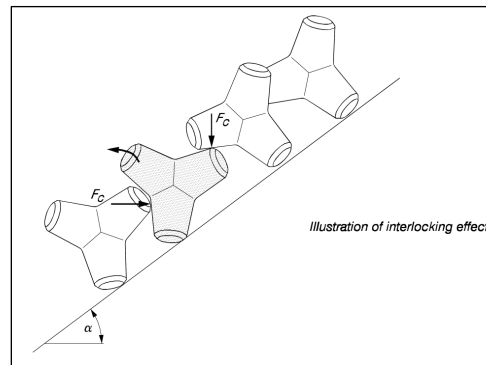
The performance of the breakwater armour layer has been validated in model tests. It is remarkable that the design has passed these tests, an explanation could be that rocking was not considered as failure mechanism or that it was hard to observe. The damage criteria would then be based on displacement of elements out of the armour layer.

The conclusions that can be drawn are that the stability coefficient is probably taken too high for the armour layer design and that breakage due to rocking is a sound failure mechanism.

1.1.3. HYDRAULIC STABILITY OF CONCRETE ARMOUR UNITS

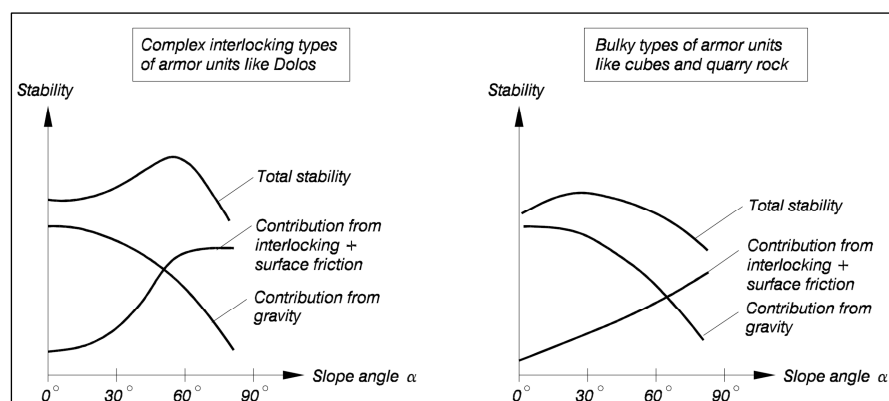
The stability of concrete armour units depends on their own weight, the amount of friction between the units and the amount of interlocking. Figure 1.6 illustrates the stabilizing interlocking effect caused by the contact forces. The contribution of the unit own weight to the stability can be determined in an analytical way, whereas the contribution of interblock friction and interlocking is determined experimentally nowadays.

Figure 1.6 Illustration of interlocking effect, one element is pulled out initiating contact forces (F_c)



The maximum interlocking effect in terms of pull-out resistance is obtained for fairly steep slopes, the size of which depends on the type and weight of the units. When interlocking armour units are placed on a horizontal breakwater section, the contribution from interlocking and surface friction becomes relatively small to the total stability (interlocking, friction, own weight i.e. gravity), see Figure 1.7. In this case the contribution from gravity to the total stability becomes dominant. The total stability (own weight, interlocking, inter-block friction) is maximal for fairly steep slopes compared to rock armour. In the case of bulky type of armour units the maximum is found for relatively gentle slopes. The difference between the maximum total stability and the total stability at a horizontal plane is smaller for a bulky type than for interlocking type of armour units. This shows the large influence interlocking and inter-block friction has on the stability.

Figure 1.7 Contribution of gravity, interlocking and surface to the total stability with varying slope angles [Price (1979)]



The number of rows above the still water line (where wave action and thus maximal loading of the armour units is present) is also of importance for the amount of interlocking of the armour units. The armour units at the toe experiences higher interlocking effects because the contact forces between the units for steep slopes are bigger at lower slope sections.

1.1.4. LACK OF KNOWLEDGE

In Newbiggen the stability is most likely influenced by the decreased interlocking properties for horizontal breakwaters sections and the absence of a number of rows above the still water line. It's not clear to what extent these features influence the stability of interlocking armour layers. This study is aimed at determining the stability of armour units on horizontal breakwater sections.

1.2. STUDY OBJECTIVE

At this moment there is not much known of the stability of single layer armour units at low-crested breakwaters. The design approach ($H_s/\Delta D_n$) of rock armour is also applied for single layer armour units. The calculated stability based on the present knowledge is not sufficient which is demonstrated by the damage in Newbiggin.

To enlarge the understanding of the stability of single layer armour units at low-crested breakwaters model tests have to be executed. A first step in the identification of the armour layer stability is the description of trends for different breakwater configurations and wave parameters. On basis of the identified trends the most important parameters and configurations can be studied further with as final objective a new stability formula for low-crested breakwaters.

This study is aimed at the execution of the first step in the process to a new stability formula for single layer armour units at low-crested breakwaters and the identification of trends for different breakwater cross sections and wave parameters with the aid of model tests. In this study Xbloc single layer armour units are used for the identification of the trends. The studied wave- and breakwater cross section parameters and are:

- wave height;
- wave steepness;
- crest freeboard;
- crest width.

These parameters are selected base on the literature study.

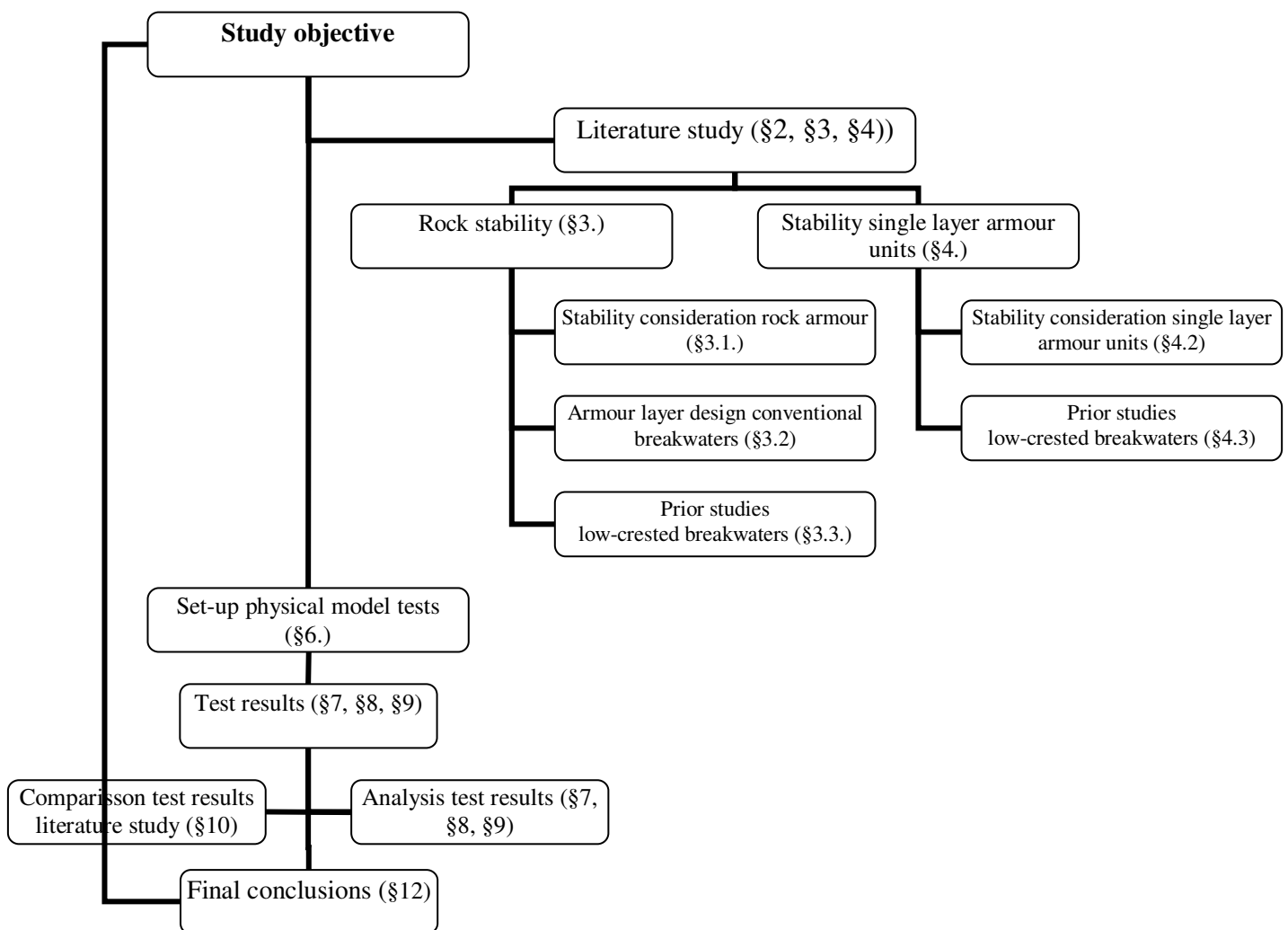
The influence of the above stated parameters is studied for the different breakwaters sections namely: seaside slope, crest and leeside slope. The identification of trends is based on the observed number of displaced and rocking elements in the model tests.

1.3. STUDY METHODOLOGY

To answer the study objective a number of steps have to be taken:

1. literature study, inventory of the present knowledge regarding the stability of single layer armour units at low-crested breakwaters;
2. set-up and execution of model tests;
3. analyses results from model tests;
4. comparison with current literature;
5. conclusions.

The study methodology is worked out in detail in the below mentioned flowchart.



An extensive study has been performed that touches various aspects of breakwater armour stability inclusive design research, model testing etc. This study is much wider than just a determination of armour stability on low-crested structures. This report is a complete documentation of all the work that has been done and contains thus plenty of information that is only marginally related to the study objective.

2. RUBBLE MOUND BREAKWATERS

The design of a breakwater is mainly based on the functional requirements (§2.1). A number of reasons can be thought of when a breakwater is not performing as intended for (§2.1), the following are worked out:

- breakwater cross section is not well designed (§2.2);
- structural failure occurs due to shortcomings in the design of breakwater elements (§2.3).

Not performing as intended for means that the breakwater is not or partially capable of fulfilling the functional requirements.

2.1. FUNCTIONAL REQUIREMENTS

Breakwaters can be used in a variety of situations, where each situation poses other functional requirements to the breakwater. The primary functions of a breakwater are:

- protection against waves;
 - vessels on berth;
 - sailing vessels;
 - port facilities;
 - shore protection;
- guiding of currents;
- protection against shoaling;
- provision of dock or quay facilities.

Protection against waves can be desirable in case of vessels on berth, sailing vessels, port facilities and shore protection. Vessels on berth put restrictions on the maximum wave height in the harbour basin because the moored vessel (to a rigid structure) can be damaged and (un)loading operations are not possible anymore when vessel movement becomes too large. Sailing vessels on the other hand are less vulnerable (depending on the type of certificate the vessel has), certainly when they can determine their own course and speed. But when a vessel is restricted in his course (navigation channel etc.), the situation changes unfavourable. Also the port facilities are bounded to maximum wave heights. Damage to jetties, quays and equipment can be the result of too high waves. Breakwaters are also used as shore protection, the incoming wave height is reduced such that the erosion of the shore is preserved.

A vessel that approaches the harbour will slow down, relatively far out of the coast, because it has a long stopping distance. When the vessel slows down the cross current makes it difficult to sail in a straight line. To avoid this difficulty a breakwater can be used to guide the currents away from the shore.

Longshore transport along sandy coasts will deposit sediment in the entrance channel to the harbour. A breakwater can be used to stop the deposition of sediment provided that the breakwater is long enough. At one side of the breakwater accretion takes place whereas on the other side erosion.

When breakwaters are used to protect a harbour basin the breakwater crest may be used for transport and access facilities. At the leeside there are mooring facilities for vessels. These activities demand a safe environment.

A number of reasons can be thought of when a breakwater is not performing as intended for (D'ANGREMOND *et al.*):

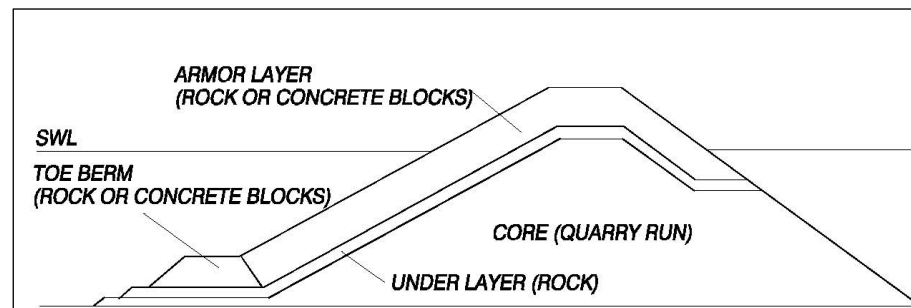
- the layout of the breakwater, lead to undesirable disturbance in the harbour basin, unsafe nautical conditions or undesirable accretion or erosion;
- the shape of the cross-section of the breakwater (see §2.2), lead to similar problems and also to unsafe conditions at the crest of the structure;
- the structural design of the breakwater (see §2.3), lead to stability problems etc.

The layout of the breakwater is not considered in this report, because it does not fit in the objective of this study, the shape of the cross section and the structural design are considered in the following sections.

2.2. GENERAL BREAKWATER CROSS SECTION

A breakwater is build out of different elements, each element with its own specific function. The functional requirements demand a certain level of hydraulic performance of a breakwater. To the hydraulic performance belongs wave run-up, wave transmission, wave overtopping and wave reflection see paragraph 2.2.1. Finally different typical rubble mound breakwaters and their hydraulic characteristics are described (§2.2.2).

Figure 2.1
Conventional multi
layer rubble mound
breakwater, [CEM
2006]



The main body of a breakwater comprises the core and consists usually out of wide graded dredged or quarry material. The armour layer is built of rock or concrete, depending on the local conditions. The armour layer prevents damage to the under-layer and core of the breakwater. The layer directly under the armour layer is called the first under-layer. The units forming this layer must not pass through the voids in the armour layer. In this way (if necessary) different under-layers can prevent erosion of the relatively fine core material. The toe berm is the lower support for the armour layer; it prevents sliding down of the armour layer.

2.2.1. HYDRAULIC DESIGN CONSIDERATIONS, WAVE STRUCTURE INTERACTION

The hydraulic performance of a breakwater can be assessed on the basis of:

- wave run-up and rundown;
- wave overtopping;
- wave transmission;
- wave reflection.

These points in combination with the functional demands can be used to determine a breakwater cross-section (see §2.2.2). For the loading of the armour layer only waves are considered as they are the most important for the objective of this study.

Wave run-up and rundown

Wave breaking on sloping structures causes run-up (R_u) and rundown (R_d). Run-up and rundown can be defined as the maximum and minimum water surface elevation measured (vertically) from the still water line. The wave run-up and rundown causes a water flow along the slope which influences the stability of the armour layer. This topic will be treated more extensively in (§1.1.)

Wave overtopping

Wave overtopping occurs when the run-up levels exceeds the crest freeboard. The allowable amount of overtopping depends on the functions which are utilised behind and on top of the breakwater crest. Examples are access roads and installations on the crest of breakwaters, behind the breakwater one can think of storage areas, buildings and berths for vessels. In the assessment of overtopping two levels can be considered, overtopping during normal service condition and overtopping during extreme design conditions where some damage to permanent installations might be allowed. Large quantities of overtopping water may be allowed when a breakwater has no other function than protecting harbour entrances (beaches, etc.). However significant overtopping can create waves which can damage moored vessels.

Wave transmission

Wave transmission can be expressed as the ratio between the incident- and the transmitted wave behind the breakwater. The transmitted wave is caused by wave overtopping and wave penetration in case of a permeable structure. When the wave period is relatively long and the breakwater permeable, wave energy can pass, creating waves behind the breakwater. The transmitted wave periods due to overtopping are generally shorter than the incident wave periods. The functional requirements determine the maximal allowable wave transmission.

Wave reflection

Incident waves are (partially) reflected by a breakwater, the extent of reflection depends on the type of breakwater. An impermeable vertical wall reflects almost all wave energy, whereas a porous sloping breakwater reflects far less. The combination of a considerably amount of reflected wave energy and incident waves creates a confused sea state. This sea state causes manoeuvre difficulties and it increases the sea bed erosion in front of the breakwater.

Wave energy dissipation takes place due to wave breaking, surface roughness and porous flow. The remaining wave energy is transmitted to the area behind the breakwater and partially reflected back into the sea.

2.2.2. TYPICAL RUBBLE MOUND BREAKWATER CROSS SECTIONS

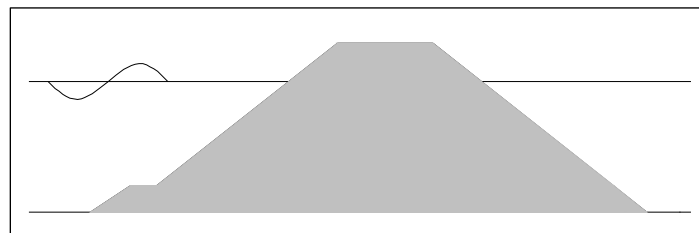
A number of typical rubble mound breakwater cross sections can be discerned:

- conventional breakwater;
- berm breakwater;
- low-crested breakwater;
- submerged breakwater.

For each breakwater cross section the importance for this study is discussed, subsequently the breakwater cross sections for the model tests are described.

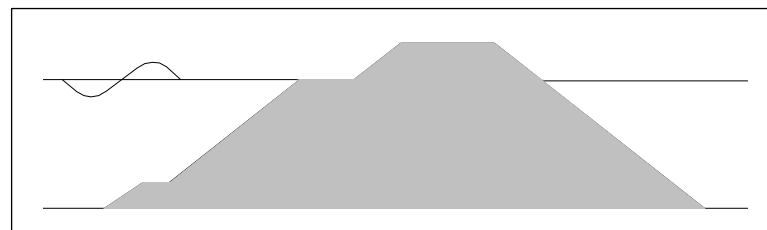
A conventional breakwater (Figure 2.2) has its crest well above the still water level such that wave overtopping is limited. The conventional breakwater is often the preferred solution when full wave protection is required (wave transmission small). In this study a conventional breakwater is not used as this type of breakwaters has been extensively studied in the past.

Figure 2.2
Conventional
breakwater



The berm breakwater (Figure 2.3) is a breakwater which has a berm in the seaward slope which reduces run-up and the amount of wave overtopping. A berm positioned at the still water line is the most effective. By applying a berm the breakwater height can be smaller compared to a conventional breakwater. In the case of single layer armour units a berm is usually not applied, when overtopping and run-up has to be reduced the breakwater crest is usually further elevated. Additional effects (wave-structure interaction due to the adjacent higher slope) play a role in the stability of single layer armour units on a berm. This study is aimed at gathering insight in the stability principle of single layer armour units on horizontal breakwater sections, because of the additional effect, the berm breakwater is not considered in this study.

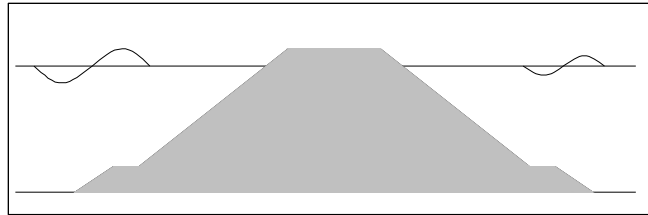
Figure 2.3 Berm
breakwater



Low-crested breakwaters are used when no full wave protection is required. Applications are protection of harbour entrances, creating artificial fishing grounds and shore protection measures. Low crested breakwaters have

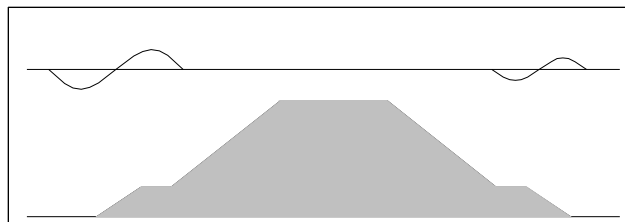
relatively high overtopping and transmission rates. An advantage of this type of breakwater is that it is less visible and that the amount of material needed is less.

Figure 2.4 Low crested breakwater



Submerged breakwaters have similar points as mentioned in low-crested breakwaters. The crest of these breakwaters is generally under water, which means that the breakwater itself is not visible. The amount of material needed for this type of breakwater is less than conventional breakwaters.

Figure 2.5 Submerged breakwater



Crest height

The crest level is generally dictated by the acceptable overtopping discharge or wave transmission based on the functional requirements that have been determined of the structure and its facilities in its lee [ROCK MANUAL 2007].

Rubble mound structures are mainly constructed out of permeable loose material. Wave transmission depends among other things on wave overtopping and the ratio of the permeability of the material to the wave period. Wave overtopping depends on the wave characteristics and wave run-up which again depends on a number of factors.

Crest width

The width of the crest depends mainly on the functional requirements like access roads and the construction method. If land based equipment is used for construction instead of water based equipment the crest has to be wide enough for dump trucks and a crane. In the user phase a crown wall or road can be present. If the crest width is not dependent on the construction method nor the functional requirements a minimum width of 3 to $4 \cdot D_{n50}$ is recommended. The crest width influences the amount of wave overtopping, a wider crest means less overtopping. Large overtopping rates affect the stability of the rear slope and crest. Wave transmission is also influenced by the crest width, mainly for structures with their crest around or under the still water level.

Structure subject to this study

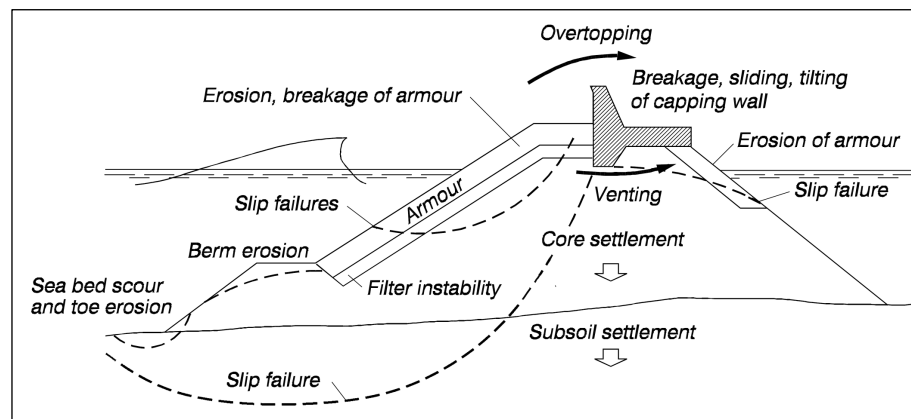
This study is aimed at describing the stability of single layer armour units on horizontal breakwater sections and the upper part of the slopes. Low-crested breakwaters are breakwaters with horizontal sections. The stability of single layer armour units at the upper part of the slope and the horizontal breakwater sections is affected by wave action. In the case of a berm breakwater, the berm

is mostly positioned at the still water level, because than it is most effective in reducing wave heights (and thus wave run-up, overtopping). Additional to the loading of a low-crested structure the stability of single layer armour units positioned on a berm (in the case of a berm-breakwater) is affected by wave-structure interaction due to the adjacent higher slope. To understand the principle of stability it is therefore preferable to test only the low-crested structures. A low-crested breakwater can be subdivided into an emergent and submerged breakwater

2.3. STRUCTURAL FAILURE

Different failure mechanisms related to geotechnical, hydraulic en structural stability have to be considered to obtain a balanced design of a breakwater (Figure 2.6).

Figure 2.6 Overview of breakwater failure modes, [CEM 2006]



Failure can be defined as total collapse of a structure but this definition is not very accurate. In the context of design reliability, it is preferable to define failure as stated below.

Failure: Damage that results in structure performance and functionality below the minimum anticipated by design.

For example, subsidence of a breakwater can be labelled as failure if the breakwater is no longer capable of serving its original purpose at or above the minimum expected level [CEM 2006].

Failure of breakwaters can be the cause of one or more of the following reasons:

- design failure, the structure as a whole cannot withstand the design loads or it perform not as anticipated for;
- load exceedance failure, the expected loads are larger than anticipated for;
- construction failure, failure occurs due to incorrect or bad construction or construction materials;
- deterioration failure, is the cause of deterioration and lack of maintenance.

In this study only failure of the armour layer is considered since it fits the objective best for this study. Design failure of the armour layer is the most important one because it's not clear how to assess the stability of concrete

armour units on horizontal breakwater sections. The other failure causes are therefore not taken into account in this study.

2.3.1. LOADING OF THE ARMOUR LAYER

In this section, the following loading mechanisms are clarified:

- type of wave breaking;
- wave run-up and rundown;
- turbulence.

Type of wave breaking

Wave breaking occurs as a result of instability which develops when the particle velocity (u) exceeds the wave celerity (c). Breaking arises because a wave is very steep or/and because the water is very shallow. Wave action on a slope can be described by the surf similarity parameter or breaker parameter ξ (-), also known as the Iribarren number, it gives the ratio between slope and wave steepness:

$$\xi = \frac{\tan \alpha}{\sqrt{s_0}} \quad (2.1)$$

Where:

α the slope angle of the structure ($^\circ$);

s_0 the influence of the wave period is often described using the fictitious wave-steepness s_0 :

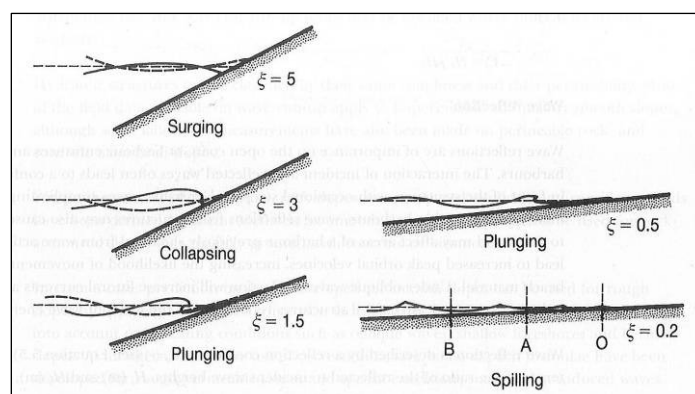
$$s_0 = H / L_0 = \frac{2\pi H}{g T^2} \quad (2.2)$$

Where:

L_0 the theoretical deep-water wavelength (m);

The surf similarity parameter describes the form of wave breaking on a beach or structure (Figure 2.7).

Figure 2.7 Breaker types as a function of the surf similarity parameter [CEM 2006]

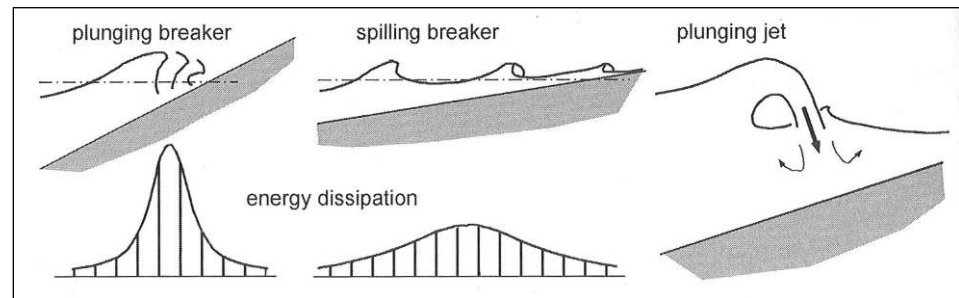


The transition between breaking and non breaking lies between $\xi = 2.5$ to 3, for higher values ($\xi = 3$ to 5) the water surges up and down the slope with minor air entrainment (surging breaker). Collapsing waves ($\xi = 3$) are between breaking and non breaking. The crest remains unbroken and relatively flat while the lower part of the front face steepens and then falls, forming irregular turbulent water surface that slides up the slope, without the development of a

bore like front. In a plunging ($\xi = 0.5 - 1.5$) type of breaker the crest curls over, enclosing an air pocket and impinges on the slope like a water jet (see Figure 2.8). Spilling waves ($\xi = 0.5$) occur when the wave crest becomes unstable at the top and the crest flows down the front face of the wave, producing an irregular foamy water surface that eventually takes the aspect of a bore.

The intensity of energy dissipation for a plunging breaker takes place at a small part of the slope, this implies great hydraulic loading for the armour layer.

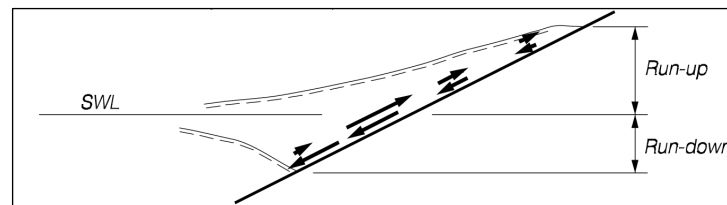
Figure 2.8 Energy disipation for two breaker types [SCHIERECK 2004]



Wave runup and rundown

Wave breaking on sloping structures causes run-up R_u and rundown R_d , see Figure 2.9. Run-up and rundown can be defined as the maximum and minimum water surface elevation measured (vertically) from the still water line [CEM 2006]. Wave run-up and rundown depends on the wave height, wave steepness, slope angle, surface roughness, permeability and porosity of the slope. Another factor of importance is the wave interaction with the previous (reflected) wave.

Figure 2.9 Up and downrush on impermeable slope [CEM 2006]



The wave run-up and rundown causes a turbulent water flow over and (in case of a permeable structure) through the armour layer elements. Due to the cyclic nature of the waves the load varies in time and direction. The wave run-up and rundown on permeable slopes increases with increasing surf similarity parameter [BRUUN AND GUNBANK 1976 as mentioned in HATTORI 1999].

The maximum flow velocities (perpendicular and parallel to the slope) are reached on impermeable smooth slopes. An illustration in vectors of the flow velocity over the course of a wave cycle is given in Figure 2.9 (impermeable slope) and Figure 2.10 (permeable slope). The main difference in velocities between the permeable and impermeable slope is that velocities are both parallel and perpendicular to the slope in the permeable case, whereas the velocities on an impermeable slope are only parallel.

Generally, the most critical flow field occurs in a zone around and just below the still water level (swl), where down-rush normally produces the largest destabilizing forces. Exceptions are slopes flatter than approximately 1:3.5 in which up rush is the most severe load. Permeability of the slope reduces the

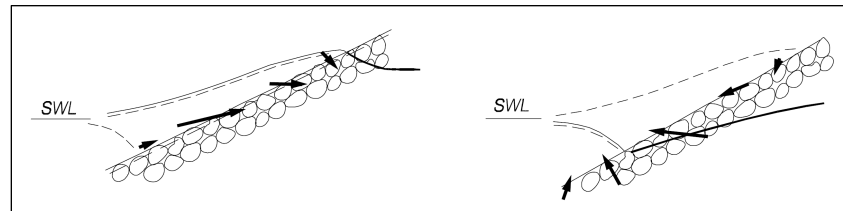
flow velocity along the slope surface because a larger proportion of the flow takes place inside the structure where the resistance is larger. The velocity is also affected by the surface roughness.

The maximum outflow velocity (from the underlayer) occurs near the point of maximum rundown [BRUUN EN JOHANNESSON 1976 as stated in HATTORI 1999]. It indicates that the minimum or incipient instability of armour units occurs in the vicinity of the lowest level of wave retreat where the velocity outside and inside the armour layer is maximum.

Plunging or collapsing breaking waves brings about high velocities in the breaking jet around the still water level. According to velocity measurements of MELBY *et al.* 1996 a large vertical upward velocity appears just below the steep wave front, which indicates that up-rush can cause armour layer instability.

Due to the fact that during up rush a bigger surface area is available for water penetration than during rundown internal setup can occur, especially for low permeable structures.

Figure 2.10 Up and down rush on permeable slope [CEM 2006]



Turbulence

A phenomenon which has a considerable impact on the stability is turbulence. Turbulence is an irregular motion of the water which affects the stability of an armour element. But at present it is still difficult to describe to which extent it influences the armour stability.

2.3.2. FAILURE MODES ARMOUR LAYER

Run-up and rundown causes a water flow over the armour which can initiate instability, different modes of instability exist (see Figure 2.11):

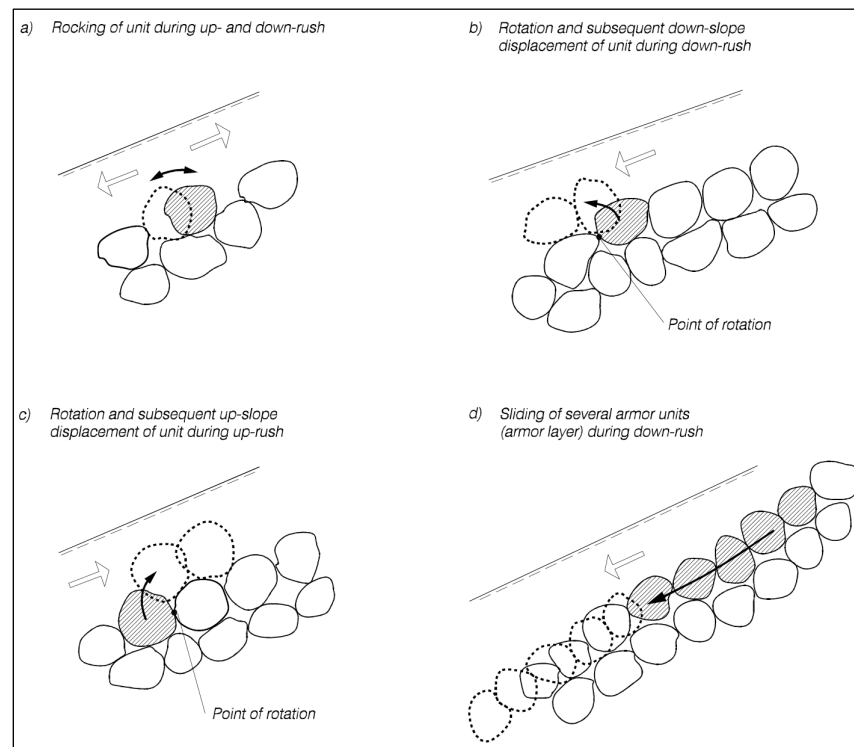
1. rocking of units during up- and downrush, which ultimately lead to breakage of units;
2. rotation and subsequent down-slope displacement of unit during down-rush;
3. rotation and subsequent up-slope displacement of unit during up-rush;
4. sliding of several armour units (armour layer) during down-rush;
5. Uplift.

Rocking of unit during up- and downrush

Armour units who are not completely clamped between each other have some space to move (an overturning motion) upslope or downslope. The upslope movement is caused by the up-rush motion of the water, the gravity and downrush tend to move the stone downslope. Due to the cyclic nature of waves the up- and downslope movement of the armour elements (rocking) can cause damage to the units. Rocking of concrete units is allowed to a limited degree because the units are made of unreinforced concrete which means that they will

break easily. Breakage of a concrete element will influence the stability of the surrounding elements, which can finally lead to failure of the armour layer.

Figure 2.11 Typical armour failure modes [BURCHARTH 1993]



Rotation and subsequent down-slope displacement of unit during down-rush
Gravity and downrush movement of the water can cause the armour units to be displaced (rolling) out of their original position. Rolling downslope of the armour units can damage other units. It is also possible that during uprush the unit is displaced in upslope direction and during downrush in downslope direction. This can occur a number of times before the unit ends up at the toe (under influence of gravity) of the breakwater. In this process different armour units can be damaged.

Rotation and subsequent up-slope displacement of unit during up-rush
The same as in 'Rotation and subsequent down-slope displacement of unit during down-rush' occurs, only in opposite direction.

Sliding of several armour units (armour layer) during down-rush
The downrush motion acting on an armour layer can cause the whole armour layer to slide downslope. The toe of the breakwater is not sufficiently strong to hold the armour layer on place.

Uplift

An armour element can be lifted out of the armour layer due to the lifting forces induced by the wave motion and the uplifting pressures from the core of the structure.

3. LITERATURE STUDY ON ROCK ARMOUR STABILITY

Breakwaters can be divided into statically and dynamically stable structures. Stability of individual stones is concerned in the case of static stability. For dynamic stability the transport capacity along the slope is important. Considering the scope of this study only static stability is of interest because the elements are not supposed to move.

The wave induced motion schematized by the flow velocity (v) is highly non stationary with respect to both velocity and direction. Thus all forces except the gravity force vary in size and direction with time. The magnitude of the flow velocity is dependent on several factors (see §2.3). The highest wave loads occurs at two times the design wave height (H_d) around the still water line. The forces at the contact points are static when no wave action and settlements are present, but will be quasi-static (pulsating) under wave action. Breaking waves can cause wave slamming which causes impact like contact forces. Solid body impart forces can occur when the units are moving [BURCHARTH 1993].

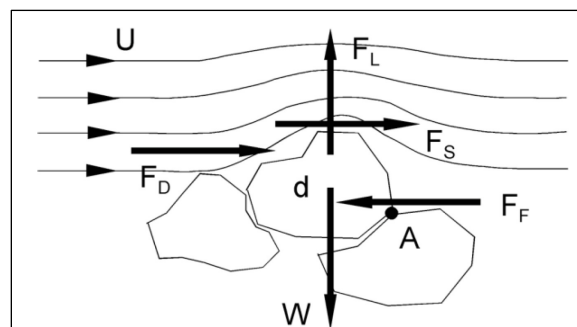
The stability analysis is based upon flow velocities induced by wave run-up and wave rundown due to wave motion. Impact forces from breaking waves and turbulence is not schematized in the present-day stability analysis. The analysis includes of the wave induced flow forces (load) and stabilizing forces (strength) such as own weight, friction and inertia. The proportionality between load and strength is called the stability number of the armour layer (§3.1.3). The stability number (a dimensionless parameter) makes it possible to compare the stability of different type of armour layers. In the stability analysis a current, for example a long shore current, is not taken into account.

Successively different armour layer design formulas and the comparison of these formulas are given in respectively paragraph 3.2 and 3.2.7.

3.1. DESCRIPTION OF LOADS AND RESISTANCE OF ROCK ARMOUR

The stability analysis is made for a stone in wave induced flow, globally the same analyses holds for a single layer armour unit, but additional forces play a role (§4.2).

Figure 3.1 Forces on a stone in flow
[SCHIERECK 2004]



3.1.1. LOAD, WAVE INDUCED FLOW FORCES ON A STONE

$$\text{Drag force (FD): } F_D = C_D \cdot \rho_w \cdot u^2 \cdot A_D \quad (3.1)$$

The drag force is exerted on the stone by the wave induced motion (flow). It can be seen as the resistance the stone experiences from the water. A pressure difference between the 'front' side (where the flow touches the stone first) and the rear side of the stone occurs. A lower pressure at the back of the stone is formed because the flow detaches from the stone.

$$\text{Lift force (FL): } F_L = C_L \cdot \rho_w \cdot u^2 \cdot A_L \quad (3.2)$$

The velocity of the water at the topside is higher than at the bottom side of the stone which results in a pressure difference, initiating an upward directed lift force.

$$\text{Shear force (FS): } F_S = C_S \cdot \rho_w \cdot u^2 \cdot A_S \quad (3.3)$$

The shear force is caused by the friction between the water and the stone.

In the above formula's C_i are empirical coefficients, A_i is the exposed surface areas of a stone to the wave induced motion.

3.1.2. STRENGTH, STABILIZING FORCES OF A STONE

$$\text{Weight of a stone (W): } W = (\rho_c - \rho_w) \cdot D_{n50}^3 \cdot g \quad (3.4)$$

The submerged weight of the stone is taken into account.

$$\text{Friction force (FF): } F_F = W \cdot \mu \quad (3.5)$$

The friction is influenced by its own weight and the friction coefficient.

$$\text{Inertia (FI): } F_I = \rho_c \cdot D_{n50}^3 \cdot \left(C_M \cdot \frac{du}{dt} \right) \quad (3.6)$$

The inertia term represents the amount of resistance to a variation in velocity, in this case of the armour units. The inertia coefficient is given by $C_M = C_m + 1$, where C_m represents the added mass.

3.1.3. STABILITY PRINCIPLE, LOAD VERSUS STRENGTH

The lift force is balanced directly by the (submerged) weight of the stone. Shear and drag, are balanced either by the moment around 'A' or by the friction force. If the flow field is assumed quasi stationary than the inertia forces may be neglected.

The different forces can be described by a proportionality:

$$\begin{aligned} F_L &= C_L \cdot \rho_w \cdot u^2 \cdot A_L \\ F_S &= C_S \cdot \rho_w \cdot u^2 \cdot A_S \quad \Rightarrow \quad F \propto \rho_w \cdot u^2 \cdot d^2 \\ F_D &= C_D \cdot \rho_w \cdot u^2 \cdot A_D \end{aligned} \quad (3.7)$$

All forces are proportional to the square of the velocity and since the surface is proportional to the square of the representative size d , the resultant load can be expressed in one term.

The proportionality between load and strength becomes:

$$\frac{\text{load}}{\text{strength}} \propto \left(\frac{\rho_w}{\rho_c - \rho_w} \right) \cdot \frac{u^2}{d_{n50} \cdot g} \quad (3.8)$$

The local characteristic flow velocity (v) induced by wave motion can be replaced by inserting the wave velocity ($v \approx \sqrt{g \cdot H}$), this gives the well known stability number:

$$N_s = \frac{H}{\Delta \cdot d_{n50}} \quad (3.9)$$

As earlier mentioned the stability number can be used to give the relationship between different structures. Structures such as caissons or structures with large armour units are characterized by small values of the stability number, however sand beaches and dunes represents large values of the stability number. In between there are gravel beaches, rock slopes, s-shaped- and berm breakwaters.

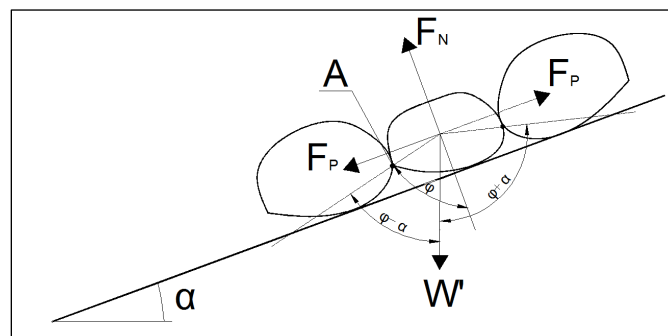
3.2. ARMOUR LAYER DESIGN FORMULAS

Most stability formulas have the stability number as common part. A derivation of the stability for a stone under wave action (could also be a single layer armour unit) is given which leads to a general equation. The assumed failure mechanism is 'Rotation and subsequent down- or upslope displacement of a unit during down- or up-rush' (see §2.3.1). From this general equation different formulas can be derived such as the well known Hudson formula. The derivation is presented to get an insight into stability mechanisms.

The analysis is based on VAN DER MEER 1988.

The wave forces are schematized by two forces, one parallel on the slope (F_P), and the other normal to the slope (F_N), see Figure 3.2.

Figure 3.2
Schematisation of
incipient motion



The momentum stability considered in point 'A' gives:

$$F_N \cdot \sin \varphi \cdot \frac{D}{2} + F_P \cdot \cos \varphi \cdot \frac{D}{2} = W \cdot \sin(\varphi - \alpha) \cdot \frac{D}{2} \quad (3.10)$$

The wave forces F_P and F_N are related to the wave height by the equation (HUDSON [1959]):

$$F = \rho_w \cdot g \cdot C \cdot D^2 \cdot H \quad (3.11)$$

Where:

- F wave force [N];
- C coefficient [-];
- D diameter of the stone [m].

Assuming C_1 for the normal wave force (F_N) and C_2 for the parallel wave force (F_P) and with equation (3.10) and assuming $D = K \cdot D_{n50}$ (k is a coefficient) the equation becomes:

$$\rho_w \cdot g \cdot C_1 \cdot D_{n50}^3 \cdot H \cdot \sin \varphi \cdot K + \rho_w \cdot g \cdot C_2 \cdot D_{n50}^3 \cdot H \cdot \cos \varphi \cdot K^3 / 2 = (\rho_c - \rho_w) \cdot D_{n50}^4 \cdot g \cdot \sin(\varphi - \alpha) \cdot K^4 / 2 \quad (3.12)$$

Or more elaborated:

$$\frac{H}{\Delta \cdot D_{n50}} = \frac{K \cdot \sin(\varphi - \alpha)}{(C_1 \cdot \sin \varphi + C_2 \cdot \cos \varphi)} \quad (3.13)$$

Implementing the friction coefficient (μ) in equation (3.13) defined according to Iribarren as $\mu = \tan \varphi$. The general equation finally becomes:

$$\frac{H}{\Delta \cdot D_{n50}} = \frac{K \cdot (\mu \cdot \cos(\alpha) - \sin(\alpha))}{(\mu \cdot C_1 + C_2)} \quad (3.14)$$

Artificial armour units can be described by the nominal diameter:

$$D_n = (W / \rho_c)^{1/3} \quad (3.15)$$

In that case the $H / (\Delta \cdot D_n)$ can be used instead of $H / (\Delta \cdot D_{n50})$.

The general equation (3.14) can be rewritten to a number of well known stability formulas.

3.2.1. IRIBARREN

Assuming that only a parallel wave force exists ($C_1 = 0$) equation (3.14) becomes Iribarren's formula as stated in VAN DER MEER 1988:

$$\frac{H}{\Delta \cdot D_{n50}} = K_1 \cdot (\mu \cdot \cos(\alpha) - \sin(\alpha)) \quad (3.16)$$

Where:

$$K_1 = K/C_2$$

Iribarrens derived his equation from an equilibrium consideration of forces acting on a block placed on a slope, no model tests were involved.

3.2.2. IRIBARRENS FORMULA MODIFIED BY HUDSON (1959)

Assuming only a normal force ($C_2 = 0$), equation (3.14) becomes Iribarrens formula modified by HUDSON 1959 as stated in VAN DER MEER 1988.

$$\frac{H}{\Delta \cdot D_{n50}} = \frac{K_2 \cdot (\mu \cdot \cos(\alpha) - \sin(\alpha))}{\mu} \quad (3.17)$$

Where:

$$K_2 = K/C_1$$

3.2.3. HUDSON (1959)

Hudson [as stated in VAN DER MEER 1988] assumed for rubble structures $\phi = 1$, which reduces equation (3.14) to:

$$\frac{H}{\Delta \cdot D_{n50}} = \frac{K \cdot (\cos(\alpha) - \sin(\alpha))}{C_1 + C_2} \quad (3.18)$$

3.2.4. HUDSON

Hudson [as stated in VAN DER MEER 1988] combined all different coefficients to one coefficient (K_D) and replaced the term $\cos \alpha - \sin \alpha$ by $(\cot \alpha)^{1/3}$. This reduces equation (3.18) to the well known Hudson formula, although written in a more simple form:

$$\frac{H}{\Delta \cdot D_{n50}} = (K_D \cdot \cot \alpha)^{1/3} \quad (3.19)$$

The Hudson formula can be rewritten to:

$$W_{50} = \frac{\rho_c \cdot g \cdot H^3}{K_D \cdot \Delta^3 \cdot \cot \alpha} \quad (3.20)$$

Hudson equation is based on model tests with regular waves on non-overtopped rock structures with a permeable core. It gives the relationship between the median weight of armour stone, W_{50} , and wave height

3.2.5. VAN DER MEER FORMULA

Research from THOMSON AND SHUTTLER 1975 and the work of van HIJUM AND PILARCZYK 1982 have been the basis for the research of van der Meer.

Deep water conditions

Van der Meer derived rock armour stability formulae for non-overtopped structures in deep water conditions. Deep water conditions are conditions where the water depth at the toe of the structure is larger than three times the significant wave height at the toe ($h > 3H_{s-toe}$). The formulas are valid for uniform slopes with their crest above the maximum run-up level. Van der Meer makes a distinction in the stability formula between plunging and surging waves:

for plunging waves ($\xi_m < \xi_{cr}$):

$$\frac{H_s}{\Delta \cdot D_{n50}} = c_{pl} \cdot P^{0.18} \cdot \left(\frac{S}{\sqrt{N}} \right)^{0.2} \cdot \frac{1}{\sqrt{\xi_m}} \quad (3.21)$$

for surging waves ($\xi_m \leq \xi_{cr}$):

$$\frac{H_s}{\Delta \cdot D_{n50}} = c_s \cdot P^{-0.13} \cdot \left(\frac{S}{\sqrt{N}} \right)^{0.2} \cdot \sqrt{\cot \alpha} \cdot \xi_m^P \quad (3.22)$$

Where:

N number of incident waves at the toe, which depends on the duration of the wave conditions [-];

ξ_m surf similarity parameter [-];

$$\xi_m = \frac{\tan \alpha}{\sqrt{\frac{2 \cdot \pi \cdot H_s}{g \cdot T_m^2}}} \quad (3.23)$$

Where:

T_m mean wave period [m];

P notional permeability of the structure $0.1 \leq P \leq 0.6$ [-];

c_{pl} coefficient (6.2);

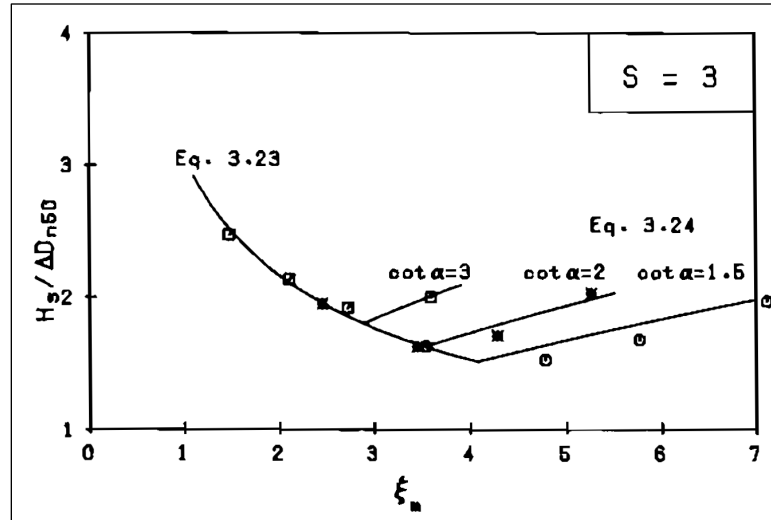
c_s coefficient (1.0).

The transition from plunging to surging waves is derived from the structure slope and can be calculated using a critical value of the surf similarity parameter:

$$\xi_{cr} = \left[\frac{c_{pl}}{c_s} \cdot P^{0.31} \cdot \sqrt{\tan \alpha} \right]^{\frac{1}{(P+0.5)}} \quad (3.24)$$

For slope angles more gentle than 1:4 only the equation for plunging waves should be used, independent of the surf similarity parameter.

Figure 3.3 Van der Meer formula



Shallow water conditions

In shallow water the wave height distribution deviates from a Rayleigh type distribution. Due to breaking of the waves the spectrum changes and the wave itself becomes more peaked and skewed. The influence of a non Rayleigh distribution can be taken into account by using the two percent wave height ($H_{2\%}$). The ratio $H_{2\%} / H_s$ is 1.4 for a Rayleigh distributed wave height, the van der Meer formula for deep water waves can be rewritten with this ratio, the H_s wave height is then replaced by the $H_{2\%}$ wave height. The ratio 1.4 for a Rayleigh distribution can be multiplied with the coefficients c_{pl} (6.2) and c_s (1.0), the new coefficients become c_{pl} (8.7) and c_s (1.4).

VAN GENT 2004 performed model tests to study rock stability in wave breaking conditions. By reformulation of the van der Meer formula the H_s wave height is replaced by the $H_{2\%}$ wave height and not by the ratio $H_{2\%} / H_s = 1.4$ as van der Meer. The spectral wave period ($T_{m-1,0}$) is used to calculate the surf similarity parameter. The coefficients (c_{pl} and c_s) are recalibrated and turn out to be $c_{pl} = 8.4$, $c_s = 1.3$.

For the stability of rock armour in shallow water conditions Van Gent formulated the following formulas:

For plunging conditions ($\xi_{s-1,0} < \xi_{cr}$)

$$\frac{H_s}{\Delta \cdot D_{n50}} = c_{pl} \cdot P^{0.18} \cdot \left(\frac{S_d}{\sqrt{N}} \right)^{0.2} \cdot \left(\frac{H_s}{H_{2\%}} \right) \cdot (\xi_{s-1,0})^{-0.5} \quad (3.25)$$

And for surging waves ($\xi_{s-1,0} \geq \xi_{cr}$)

$$\frac{H_s}{\Delta \cdot D_{n50}} = c_s \cdot P^{0.18} \cdot \left(\frac{S_d}{\sqrt{N}} \right)^{0.2} \cdot \left(\frac{H_s}{H_{2\%}} \right) \cdot (\xi_{s-1,0})^P \quad (3.26)$$

Where:

$H_{2\%}$ wave height exceeded by 2 per cent of the incident waves at the toe [m]

$\xi_{s-1,0}$ surf similarity parameter [-]

$T_{m-1,0}$ the spectral wave period [s]

3.2.6. SHIELDS PARAMETER

Assuming $H = u^2 / g$ in formula of the stability number (3.9) the agreement between the stability and the Shields parameter becomes clear. The Shields parameter is given by:

$$\psi = \frac{u^2}{g \cdot \Delta \cdot d_{n50}} \quad (3.27)$$

Different studies are executed to investigate the applicability of the Shields approach for the design of breakwater armour layers. The studies have been done for non-breaking waves, model test show good agreement with the predictions. Breaking waves creates impact like forces as a result of which the Shields approach is no longer valid.

3.2.7. CONCLUSIONS ON ARMOUR LAYER DESIGN FORMULA

In §3.2 the stability of a stone on a slope loaded by wave forces is considered. Following from this consideration Hudsons formula can be derived, Hudson himself based his formula on model tests. Van der Meer formula is also based on model tests but no theoretical derivation of the formulas is possible.

The main advantage of the Hudson formula is its simplicity and the wide range of armour units and configurations for which KD values haven been derived [ROCK MANUAL 2007]. This formula has however limitations:

- the use of regular waves only;
- no account of the wave period and storm duration;
- no description of armour damage level;
- the use of not-overtopped and permeable structures only.

The problems that may arise due to these shortcomings can be overcome by using various specific values of the stability coefficient. But it gives no physical insight in the stability principle.

The great advantage of the van der Meer formulae is that it includes the permeability, storm duration, wave period and a clearly defined damage level.

3.3. PRIOR STUDIES LOW-CRESTED BREAKWATERS

Different studies have been performed to understand and give stability relations for low-crested breakwaters:

- MIZUTANI *et al.* 1992, 1994;
- VAN DER MEER *et al.* 1994;
- VIDAL *et al.* 1992;
- BURGER 1995;
- MATSUDA *et al.* 2003;
- KRAMER *et al.* 2003;
- VIDAL *et al.* 2007;
- GARCIA *et al.* 2004.

3.3.1. MIZUTANI ET AL. 1992, 1994

The stability of armour units on a submerged breakwater is experimentally investigated (see Figure 3.4). The wave forces and the velocities in front of an armour unit were measured (see Figure 3.5), the wave forces are used to formulate a stability model. The theoretical stability is not described because among the input parameters the wave force is required, which is still difficult to determine for practical applications.

Figure 3.4 Model of tested submerged breakwater MIZUTANI *et al.* 1992

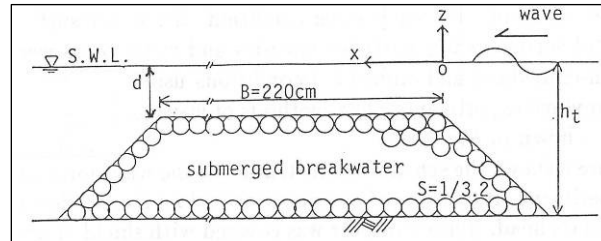
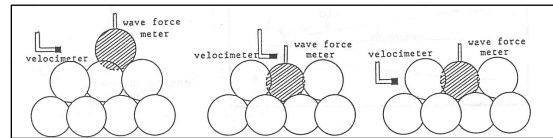


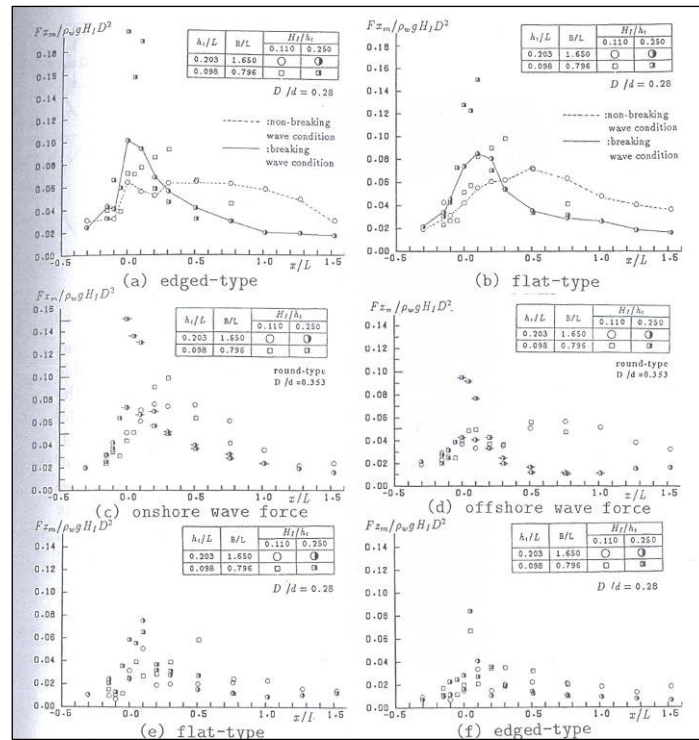
Figure 3.5 Methods of wave force and velocity measurements MIZUTANI *et al.* 1992



In MIZUTANI *et al.* 1992 only spherical armour units are considered, whereas in MIZUTANI *et al.* 1994 the shape of armour units is investigated. Both studies are described here, as it provides insight into the location of the most heavily attacked sections of a submerged breakwater, but also the influence of different parameters to describe armour unit stability become clear.

Figure 3.6 shows the variations of the dimensionless maximum wave forces $F_{x,m} / \rho \cdot g \cdot H_1 \cdot D^2$ (referred to as 'horizontal wave force') and $F_{z,m} / \rho \cdot g \cdot H_1 \cdot D^2$ (referred to as 'vertical wave force') with dimensionless distance from the leading crown-edge, x/L (referred to as 'distance'), as obtained from the wave force measurement experiments, where x (positive in onshore direction) is the horizontal distance measured from the leading crown edge and L is the wavelength at the structures toe (see Figure 3.4). The measured force is made dimensionless by the: density of the water (ρ), wave height (H_1), nominal diameter (D) and where subscript m denotes the maximal value of the force measured.

Figure 3.6 Variation of dimensionless maximum force MIZUTANI *et al.* 1994



Regardless of the variation of wave period, shape and size of armour units the horizontal wave force shows similar variation with the distance. As shown in Figure 3.6 the horizontal wave force increase with the distance and H_t/h_t on the slope ($x/L < 0$) and attains a maximum value near the crown edge, where h_t is the still water depth at the toe of the structure. On the crown ($x/L > 0$), the horizontal wave force decreases rapidly for wave breaking conditions, whereas it decreases gradually for non-breaking conditions. This may be attributed to the disturbance due to wave breaking and higher harmonic wave components generated on the crown. Similar tendency was observed for the vertical wave force, however the variation with the distance and H_t/h_t is not clear as compared with the horizontal wave force. Moreover, Figure 3.6 shows that the onshore wave forces are generally larger than the offshore wave force.

The relative crown depth, d/h_t also has a significant effect on wave force, d is the depth of the water from the crown and h_t the water depth at the toe of the structure. Experimental results show that a smaller d/h_t results in a larger wave forces, although the figures corresponding to larger d/h_t are not shown.

The shape effect of stones is not sensitive in the variations of the non-dimensional wave forces with the distance, it still shows the same trend with a peak at the crown edge. However the shape effect is very significant on the magnitude of the wave forces. The horizontal wave force on a round-type stone has almost the same magnitude as an equivalent sphere. For the edged-type shape stone flow separation takes place easier because of the edges of the stone leading to larger drag forces than for a round-type stone. On the other hand the horizontal wave force on flat-type stones is generally small compared to the other types of stones. The method of placement wherein the smallest cross-sectional area faces the horizontal flow gives the flat-type stones the smallest projected area which results to a smaller horizontal wave force. However the vertical wave force on flat-type stone is much larger than the other types of stone, because of the very large projected area. The stable weight is not much

affected by the stone shape since the shape effect on the stability is offset by the shape effect of the acting wave force.

The characteristics of wave forces are well correlated with the water particle velocities. On the slope the velocity becomes larger with increasing x/L , due to wave shoaling, then attains a maximum value at the crown edge. On the crown, the dimensionless maximum velocity decreases with x/L because of energy loss due to friction in the permeable structure and also due to wave breaking. The dimensionless maximum velocity increases as d/h_t decreases.

3.3.2. VAN DER MEER ET AL. 1994

VAN DER MEER *et al.* 1994 is a summary of the results concerning rock armour layer stability and wave transmission from: VAN DER MEER 1990A, VAN DER MEER AND PILARCZYK 1990, VAN DER MEER 1990B, DAEMEN 1991 and VAN DER MEER AND D' ANGREMOND 1991. Only rock armour layer stability is described considering the purpose of this study. The results are based on model tests. The applied armour on the front face, crest and rear is the same.

Low-crested breakwaters with crest above still water level

The stability of low-crested structures with their crest above still water level is related to the stability of non- or marginally overtopped structures. Stability formulas such as the Hudson formula or more advanced formulas (VAN DER MEER *et al.* 1988) can be used. The required rock armour diameter for an overtopped breakwater can then be determined by application of a reduction factor for the mass of the armour.

A long wave period gives higher run-up values on a slope than shorter periods. Therefore, more energy is lost by overtopping for a long wave period at the same crest level as for a short period. The increase in stability for low-crested structures is therefore a function of the wave period (or wave steepness).

The reduction in required nominal diameter D_{n50} is given as:

$$D_{n50} = \frac{1}{1.25 - 4.8 \cdot R_p^*} \quad \text{for } 0 < R_p^* < 0.052 \quad (3.28)$$

Where:

R_p^* dimensionless crest height [-];

$$R_p^* = \frac{R_c}{H_s} \cdot \sqrt{\frac{s_{op}}{2 \cdot \pi}} \quad (3.29)$$

Where:

R_c crest freeboard [m];

H_s significant wave height [m];

s_{op} fictitious wave steepness [-];

$$s_{op} = \frac{2 \cdot \pi \cdot H_{m0}}{g \cdot T_p^2} \quad (3.30)$$

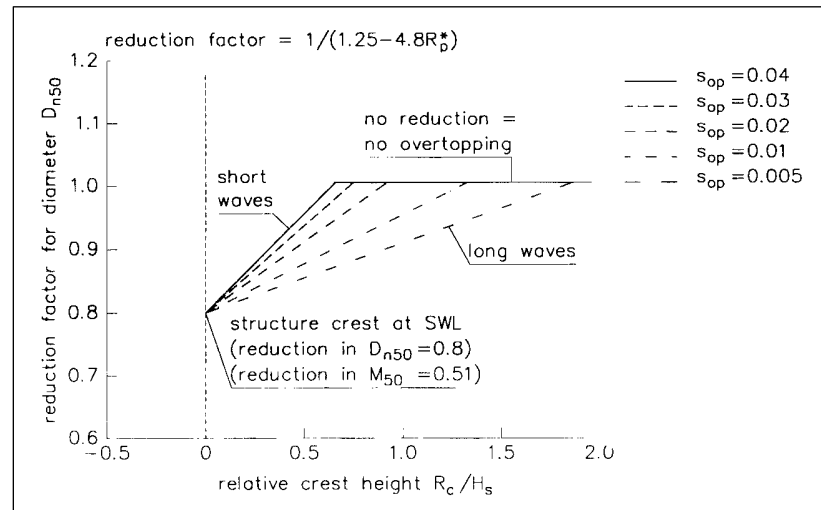
Where:

H_{m0} significant wave height $(4\sqrt{m_0})$ [m];

T_p peak wave period [s].

Equation (3.28) is presented in Figure 3.7 for various wave steepness's. The reductions factor of the nominal diameter can be read from this graph or can be calculated.

Figure 3.7 Design graph with reduction factor for rock diameter of low-crested structure, VAN DER MEER *et al.* 1994.



Low-crested breakwaters with crest below the still water level

The slope angle has large influence on non overtopped structures. In the case of submerged structures, the wave attack is concentrated on the crest and less on the seaward slope. Therefore excluding the slope angle of submerged structures may be legitimate. But because the derived formula is based on model tests with varying slope angles 1/1.5 – 1/2.5, the formula is only valid in the tested range of slope angles.

The stability of submerged breakwaters appeared only to be a function of the relative crest height h'_c/h , the damage level S and the spectral stability number N_s^* . The damage is characterized by S, S = 2 means start of damage, S = 5 represents moderate damage and S = 8 – 12 means severe damage.

The final design formula is given by:

$$\frac{h'_c}{h} = (2.1 + 0.1 \cdot S) \cdot e^{(-0.14 \cdot N_s^*)} \tag{3.31}$$

Where:

- h_c crest height before a test [m];
- S damage level [-];
- h water depth at toe of structure [m];
- N_s^{*} spectral (or modified) stability number [-];

$$N_s^* = \frac{N_s}{s_p^{1/3}} = \frac{H_s}{\Delta \cdot D_{n50}} \cdot \frac{1}{s_p^{1/3}} \tag{3.32}$$

Where:

- H_s significant wave height [m];
- Δ buoyant mass density [-];
- D_{n50} nominal diameter [m];
- s_p local wave steepness at structures toe [-];

$$s_p = H_s / L_p \tag{3.33}$$

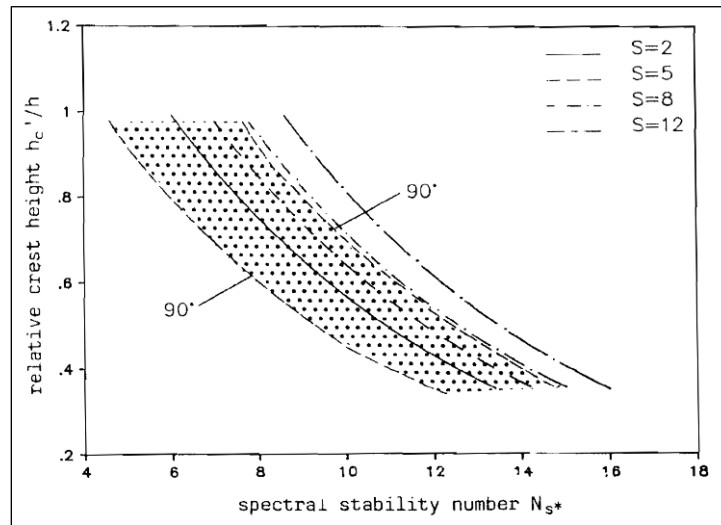
Where:

- H_s significant wave height at structures toe [m];
- L_p local wave length [m].

Where L_p is the Airy wave length calculated using the peak period of the wave energy density spectrum (T_p) and the water depth at the toe of the structure (h). In fact, a local wave steepness is calculated.

For fixed crest height, water level, damage level and wave height and period, the required ΔD_{n50} can be calculated with equation (3.31). Equation (3.31) is shown in Figure 3.8 for four damage levels.

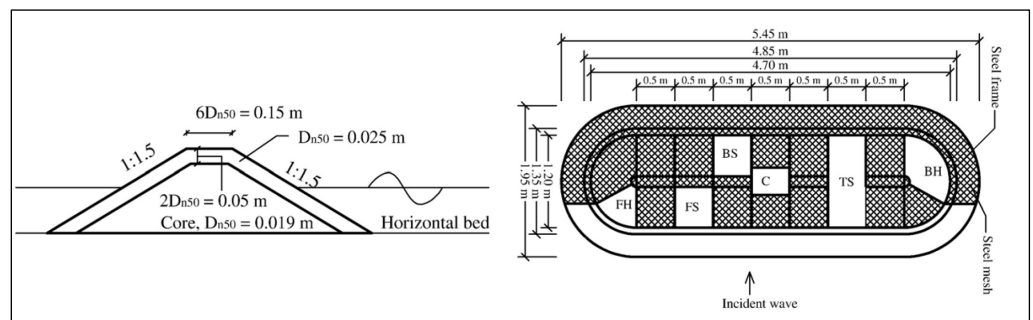
Figure 3.8 Design curves with 90% confidence bands for $S = 2$



3.3.3. VIDAL ET AL. 1992

VIDAL *et al.* 1992 performed model tests with low-crested structures including both trunk and roundheads. Only results for trunk stability are discussed.

Figure 3.9 Plan view and cross section of model by VIDAL *et al.* 1992



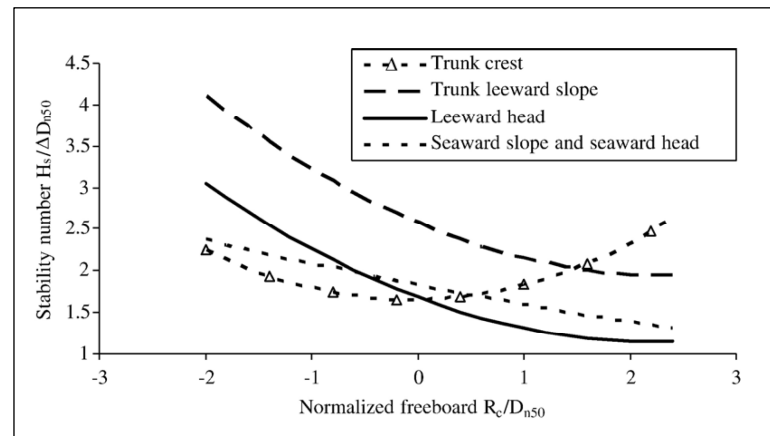
The water depth in the model tests varied between 0.38 and 0.65. The heights of the structure were 0.40 and 0.60 m and the tested R_c ranges between - 0.05 and + 0.06 m. Irregular waves perpendicular to the trunk with H_s between 0.05 and 0.19 m were used combined with two spectral peak periods, $T_p = 1.4$ and 1.8 s. During tests the wave period is kept constant and the significant wave height was increased.

The related number of waves in a test series was 3000 and 2600 respectively. The breakwater has a permeable core armoured with two layers of rock, a slope angle of 1/1.5 and a crest width of $6 * d_{n50}$. The tested model is shown in Figure 3.9.

The structure is divided into several sections (see Figure 3.9) in order to study the distribution of damage. It should be noted that the definition of crest in these tests contained the upper parts of the two slopes. A steel frame was covering the surface of the structure along the sections and a steel mesh was covering the parts where damage was not measured. Damage interactions among the sections were thereby not possible, the damage to the crest section could not influence damage to the seaward slope section and vice versa.

The results (Figure 3.10) shows that the trunk crest was the least stable part in case of submerged structures and that the trunk seaward slope was the least stable part for $R_c/D_{n50} < 0.5$.

Figure 3.10 Armour (rock) stability corresponding to initiation of damage, non depth limited waves perpendicular to the trunk, BURCHARTH *et al.* 2006



Seaward slope

The seaward slope shows a straight line suggesting a linear relation between the freeboard and the stability number. The minimum stability for the seaward slope corresponds to the non overtopped breakwater which is logical because no wave energy can pass the breakwater and the seaward slope has to dissipate all the wave energy.

Trunk crest section

The slope gradient of the curve 'seaward slope and seaward head' for positive freeboards is higher than for negative freeboard. The increase in stability is therefore greater for an increase of positive freeboards than for the decrease of negative freeboards. When the freeboard is positive, the armour units removed from the crest section by the waves are mainly carried with the forward movement of the waves to the 'Trunk leeward slope' section. By negative freeboards the armour units are mainly carried to the front slope with the backward movement of the waves. The number of units that moves to the trunk leeward and seaward slope also depends on the wave height. Progressive damage at the crest for positive freeboards decreases the crest freeboard and thereby the stability.

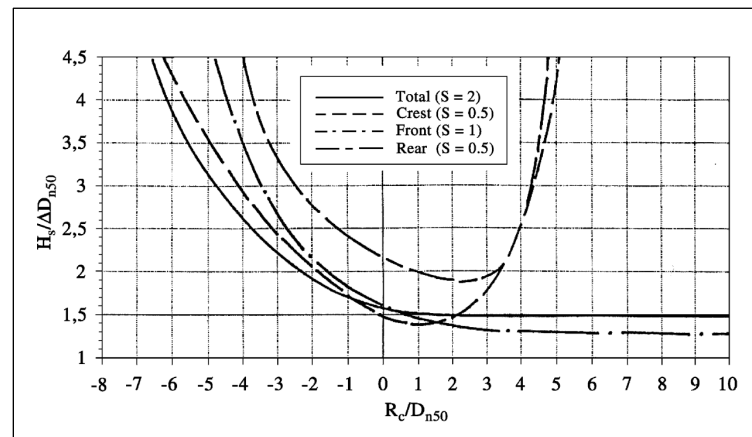
Trunk leeward slope

For negative freeboards, the waves go over the crest and break on the water that protects the back slope armour units. When the crest emerges, the water jet starts to impinge on the back slope armour units and the stability continues to decrease because the impinging flow of water works together with the gravity to dislocate the armour units.

3.3.4. BURGER 1995

BURGER 1995 re-analysed the existing tests reported by VAN DER MEER *et al* 1988 and VIDAL *et al.* 1992. The trunk was divided into seaward slope, crest and leeward slope. Stability, related to initiation of damage, was reported both for each sector and for total trunk sector see fig. 4.5. From the results it is evident that the crest is least stable part of the trunk under submerged and slightly emergent conditions. For an emerged the seaward slope is the least stable part.

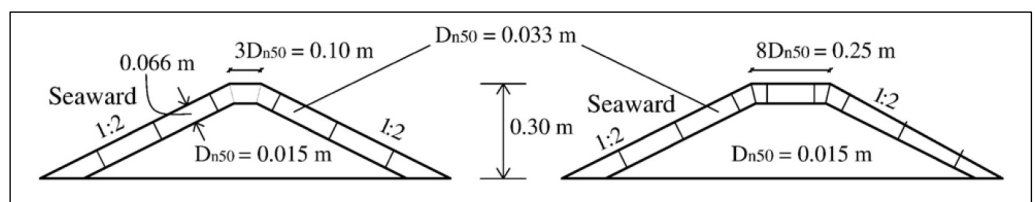
Figure 3.11 Trunk armour stability corresponding to initiation of damage BURGER 1995



3.3.5. KRAMER ET AL. 2003

KRAMER *et al.* 2003 performed 3D model tests on both trunk and roundhead stability. The test set-up and the results for trunk stability are discussed.

Figure 3.12 Trunk cross section KRAMER *et al.* 2003



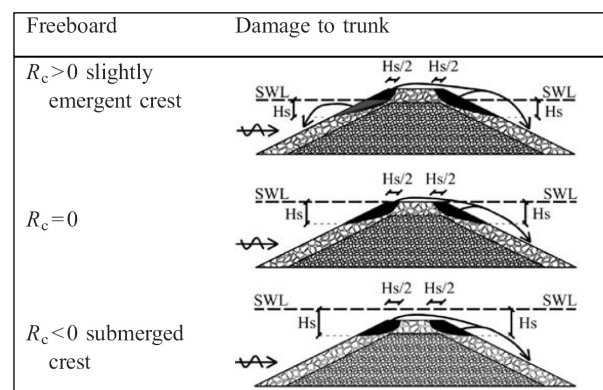
Both seaward and leeward slopes were 1/2 and crest widths of $3 \cdot D_{n50}$ and $8 \cdot D_{n50}$ were studied. Four crest freeboards ($R_c = -0.10, -0.05, 0.0$ and 0.05 m) were tested. A 1/25 foreshore and a 0.5 m horizontal plateau were arranged in front of the trunk. Two wave steepness's of 0.02 and 0.035 and an angle of wave incidence between -30° to $+20^\circ$ (0° corresponds to waves perpendicular to the trunk) were generated. The waves generated are irregular and the wave height is gradually increased in steps each containing 1000 waves.

Initiation of damage corresponds to the state when a few stones start to be displaced. A detailed description of the test set-up is given in KRAMER *et al.* 2003 and 2005. Figure 3.12 shows the two tested cross-sections.

The model tests performed are meant to increase the understanding of the influence on rubble stone stability of: obliquity of short crested waves, wave height and steepness, crest width and freeboard.

For the tested range the exposed areas of the trunk was found not to be depending on the crest width. Damage only takes place on edges of the trunk crest. In other words a few displaced stones cause the same damage to the trunk crest for the wide structure as to the more narrow structure. The exposed cross section covered an area from the edge of the crest and $H_s/2$ towards the centre (see Figure 3.13). Very narrow crest structures will be vulnerable to damage as the exposed area will cover the whole crest width. It is therefore recommended to choose a crest width at least equal to H_s when designing a low-crested breakwater. The damage occurs to one H_s under the still water level.

Figure 3.13 Sections prone to damage, filled black areas indicate exposed stones, KRAMER *et al.* 2003



shows the results of the armour stability tests for the trunk with varying freeboard, incident wave direction and steepness. The following conclusions can be drawn:

- Wave direction;
All parts of the trunk are slightly more stable under oblique wave attack than under normal incidence wave attack.
- Wave steepness;
From Figure 3.14 it can be seen that the data for $s_{0p} = 0.02$ and $s_{0p} = 0.035$ are fairly close. However, the series with $s_{0p} = 0.02$ (long waves) tend to give slightly more damage than the series with $s_{0p} = 0.35$ (short waves) meaning the structure is more stable for short waves.
- Crest width;
No significant difference in response can be identified for the tested crest widths indicating that for the tested range the influence of crest width is small.
- Freeboard;
The tests showed that stability is highly influenced by the freeboard.

Figure 3.14 Initiation of damage, KRAMER AND BURCHARTH 2003

Legend:
 SS seaward slope
 C crest
 LS leeward slope

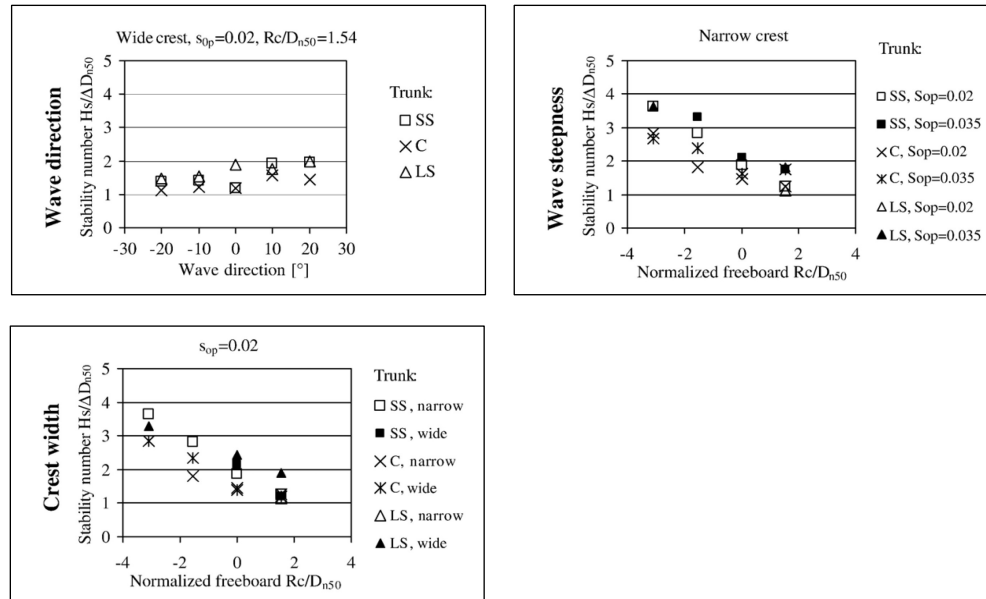
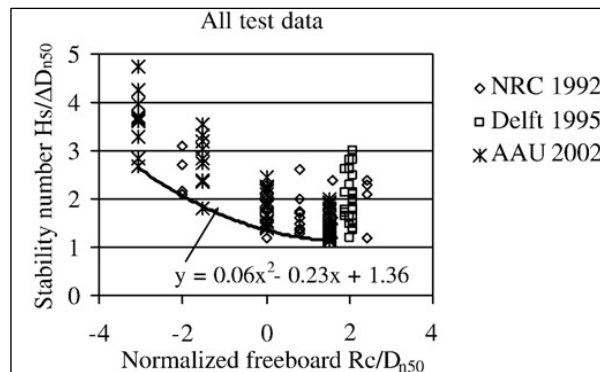


Figure 3.15 shows all the trunk and roundhead data available from the test performed by VIDAL *et al.* 1992 at NRC Canada, BURGER 1995 at Delft Hydraulics and KRAMER AND BURCHARTH 2003 at Aalborg University (AAU). The three sets of tests differ with respect to structure slope and waves (slope 1/1.5 and non-depth limited 2D waves in NRC and Delft Hydraulics test; slope 1/2 and depth-limited short-crested waves in AAU tests). All datasets are considered to be in reasonable agreement. The seawards slope is slightly more stable than in the AAU experiments especially under submerged conditions. The structure slope was gentler in the AAU experiments and a larger stability is therefore expected for the AAU structure.

Figure 3.15 Design graph for stability of low-crested breakwaters corresponding to initiation of damage KRAMER AND BURCHARTH 2003



The lower envelope curve represents initiation of damage in some parts of the structure. A design formula for the required stone size can be drawn up on the basis of this envelope curve for shallow water waves and depth limited waves.

Required stone size in shallow water waves

When designing a low-crested breakwater the highest significant wave heights must be calculated for different water depths caused by tide and storm surge. The corresponding necessary stone sizes for each of these water depths can then be found from figure Figure 3.15. In this way the worst condition will be the water depth giving the largest stone size. It is recommended to choose the stone size according to the lower line shown in Figure 3.15 given by:

$$\frac{H_s}{\Delta \cdot D_{n50}} = 0.06 \cdot \left(\frac{R_c}{D_{n50}} \right) - 0.23 \cdot \left(\frac{R_c}{D_{n50}} \right) + 1.36 \quad \text{for } -3 \leq \frac{R_c}{D_{n50}} < 2 \quad (3.34)$$

Where:

- H_s the significant wave height [m];
 R_c crest freeboard [m];
 D_{n50} the mean nominal diameter [m];
 Δ buoyant mass [-].

Required stone size in depth limited waves

If waves are depth limited and the breaking limit is represented as a limit ratio γ between significant wave height and the local water depth, among the incident wave height H_i , the water depth at structure toe h_s and structure freeboard R_c the following relation holds:

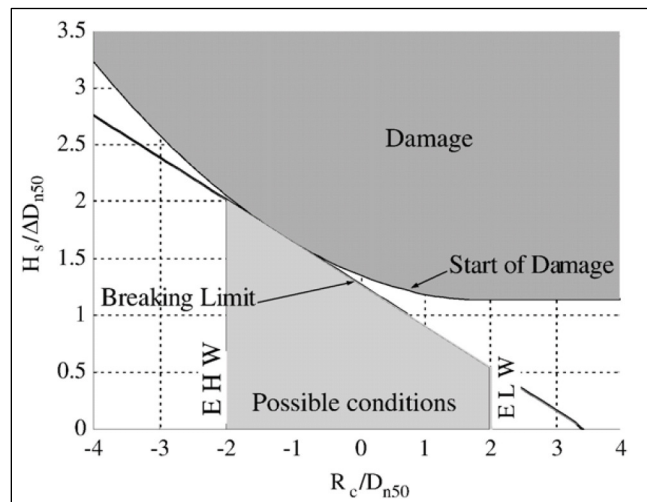
$$H_i = \gamma \cdot h_s = \gamma \cdot (h_c - R_c) \quad (3.35)$$

Where the breaker index γ depends on seabed slope, wave steepness and the characteristic wave height.

The shape of the two domains is such that stability is assured if breaking limit does not cross the start of damage curve (see Figure 3.16) or is tangent to it as a limit, i.e. if the discriminant of the combined equations (3.37) and (3.35) second order equation is zero, from which follows:

$$\frac{D_{n50}}{h_c} = \frac{\gamma/\Delta}{1.36 - (\gamma/\Delta - 0.23)^2 / (4 \cdot 0.06)} \quad (3.36)$$

Figure 3.16 Stability condition in depth limited waves, KRAMER *et al.* 2003



This leads to the hydraulic stability condition under variable water level and depth limited waves characterized by the significant wave height:

For a gentle foreshore slope the following rule of thumb can be found in case of depth limited waves ($\gamma = 0.6$, $\rho = 1.6$):

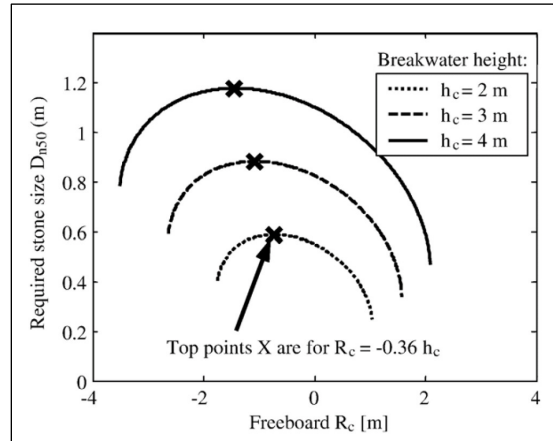
$$D_{n50} = 0.29 \cdot H_c \quad (3.37)$$

Where:

H_c structure height [m].

The rule of thumb is presented visually in Figure 3.17, in this specific design graph the largest required stone size at $R_c = -0.36 h_c$, which correspond to a slightly submerged conditions.

Figure 3.17 Design graph corresponding to damage initiation, equation (3.37) ($\gamma = 0.6$, $\rho_s = 2.65 \text{ t/m}^3$), KRAMER *et al.* 2003



3.3.6. VIDAL ET AL. (2007)

VIDAL *et al.* 2007 performed model tests on low-crested rubble mound structures with regular and irregular waves. Five wave periods and crest freeboards were tested. The experimental results are described by four types of damage, depending on the structure freeboard:

- Damage Type I occurs by low-crested breakwaters with high positive freeboards and low overtopping rates. The damage distribution is similar to the damage that occurs on non-overtopped rubble-mound breakwaters (see Figure 3.18A).
- Damage Type II occurred by low-crested breakwaters with positive freeboard near the still water level. As the wave overtopping increases, damage starts to occur also at the inner slope and at the outer edge of the crest. As wave period increases, Type I damage decreases while Type II increases (see Figure 3.18B).
- Damage Type III occurs by low-crested breakwaters near the still water level. The waves plunge on the crest, damaging the seaside edge of the crest and moving the units to the leeside slope. The run-down flow under the wave trough moves most of the stones from the crest to the seaside slope (see Figure 3.18C).
- Damage Type IV occurs by submerged structures. Overshooting created by the structure under the wave crest passage moves most of the stones to the leeside, where they are deposited (see Figure 3.18D).

Figure 3.18 Damage with regular waves

A. Damage Type I

$R_c=5\text{cm}$, $H=0.06\text{ m}$,
 $T=1.8\text{ s}$

B. Damage Type I/II

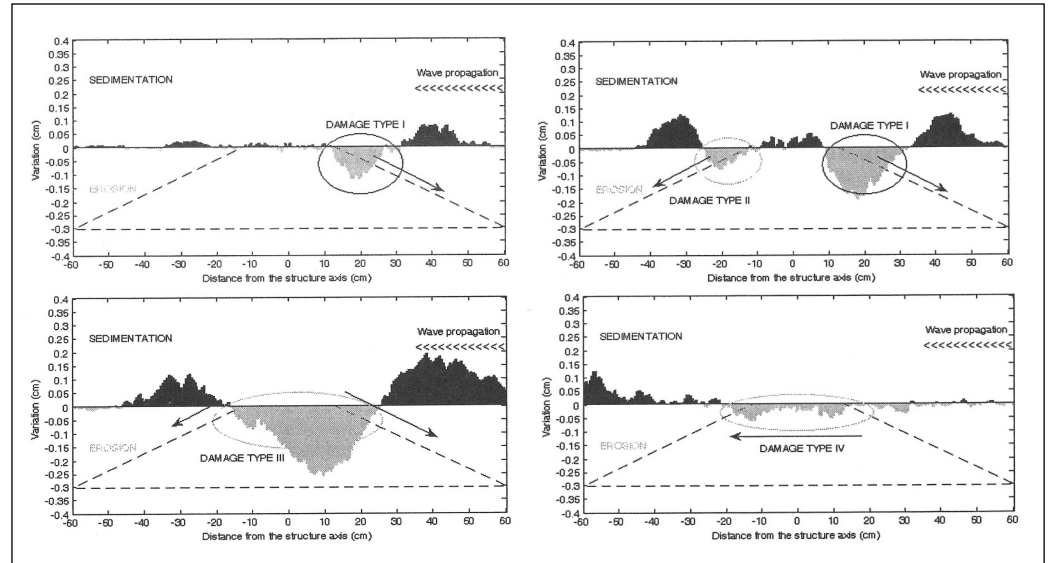
$R_c=-0.05\text{cm}$, $H=0.07\text{ m}$,
 $T=1.8\text{ s}$

C. Damage Type III

$R_c=-0.05\text{cm}$, $H=0.12\text{ m}$,
 $T=1.8\text{ s}$

D. Damage Type IV

$R_c=-0.25\text{cm}$, $H=0.18\text{ m}$,
 $T=3.4\text{ s}$



Different stability parameters are considered, namely the Mobility Parameter, Shields Parameter, Morison Drag Force Parameter and the Morison Lift Force Parameter (the formulas are described in Appendix B). Using the numerical model COBRAS, the evolution of some characteristic flow parameters around the structure are obtained. This evolution is then compared with the damaged geometry, being the Mobility Parameter that better describes the observed damage geometry on submerged breakwaters. This correlation is used to provide the following design formula for these structures.

Stability formula for rubble-mound submerged breakwaters

The mobility parameter is formulated with the maximum orbital velocity that occurs on the landward edge of the crest, U_{max} . The maximum velocity depends on the wave height, wave period, structure's freeboard and crest width. The most important ones are the wave height and the crest freeboard. With the aid of the numerical model the value of c can be determined in term of H_{50}/R_c .

The derivation and additional information about the stability is given in Appendix B. The design formula is given by:

$$S = 3.2 \cdot MP_{crit}^{1.45} - 0.30 \quad (3.38)$$

$$MP_{crit} = \frac{((c-1) \cdot U_{crit})^2}{(\Delta \cdot g \cdot D_{50})} \quad (3.39)$$

$$c = \frac{U_{max}}{U_{crit}} = 0.73 \cdot \ln\left(\frac{-H_{50}}{R_c}\right) + 2.3 \quad (3.40)$$

The formulas (3.38), (3.39) and (3.40) are applicable in the limits of the experimental range, given approximately by:

$$0.3 \leq \frac{-H_{50}}{R_c} \leq 0.9$$

Stability analysis for rubble mound low-crested breakwaters

For breakwaters with their crest around the still water line, other factors, different from the maximum values of flow parameters, should be taken into

account for the description of damage: turbulence generated by breaking waves over the units; the water jet created by plunging waves and forces originated by the down-rush at the seaward slope. That means a more empiric approach on the stability number is used to provide stability formulas in these cases.

For the empiric approach the following databases are used:

- DELOS Project UE EVK3-CT-2000-41, University Aalborg (2003);
- FEDER Project 1FD97-0404, University of Cantabria (2001);
- University of Cantabria, Vidal et al. (1998);
- Delft Hydraulics (1995);
- NRC-Canada, Vidal et al. (1992);
- Delft Hydraulics, Van der Meer (1988).

The data have been organized in groups with similar relative freeboard, $F_d = R_c / D_{n50}$. For each of the data groups, the following potential fit between the measured damage parameter and the measured stability number has been calculated for each of the low-crested structure sections:

$$S = a \cdot N_{s50}^b \quad (3.41)$$

Where:

$$N_{s50} = \frac{H_{50}}{\Delta \cdot D_{n50}} \quad (3.42)$$

To formulate a formula for the initiation of damage a damage criteria is needed. Re-analysis of the data from VIDAL *et al.* 1992 and KRAMER AND BURCHART [2003] to define the lower threshold values of S for initiation of damage for the different low-crested structure sections is given as:

seaward slope S value 1.0;
 crest S value 1.0;
 landward slope S value 0.5.

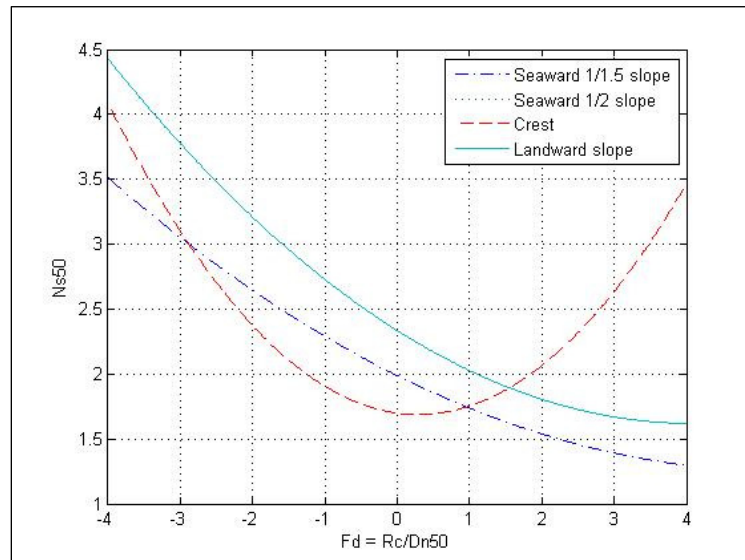
The formulas in Table 3-1 are formulated for the different breakwater sections.

Table 3-1 Design stability formulas of the different rubble mount breakwater sections

low-crested structure section	Expression (low 95% confidence band)	Validity range
seaward 1/1.5 slope	$N_{s50} = 0.0260 \cdot F_d^2 - 0.277 \cdot F_d + 1.989$	$-4 < F_d < 4$
seaward 1/2 slope	$N_{s50} = 0.043 \cdot F_d^2 - 0.351 \cdot F_d + 2.336$	$-4 < F_d < 4$
crest	$N_{s50} = 0.1298 \cdot F_d^2 - 0.0773 \cdot F_d + 1.700$	$-4 < F_d < 4$
landward slope	$N_{s50} = 0.043 \cdot F_d^2 - 0.351 \cdot F_d + 2.336$	$-4 < F_d < 4$

The formulas in Table 3-1 are presented in Figure 3.19, the stability formula for the 1/2 seaward and landward slope are same, therefore the landward slope is not visual in the graph.

Figure 3.19
Comparison stability
armour layer units on
different breakwater
sections according to
the formulas in Table
3-1



From Figure 3.19 the following conclusions can be drawn:

- the crest sector is the least stable in the range $-3 < F_d < 1$;
- for $F_d > 1$ the landward head sector is the low-crested structure's least stable;
- stability of the seaward sector of the trunk depends on the seaward slope angle, increasing the stability as the slope angle decreases;
- crest sector is the most stable for freeboards over +2;
- the trunk landward slope is less stable than the crest sector for $F_d > 2$ and its stability is similar to the seaward slope with $1/2$ slope angle.

3.3.7. NUMMERICAL MODELLING OF VELOCITY AND TURBULENCE FIELDS AROUND AND WITHIN LOW-CRESTED RUBBLE MOUND BREAKWATERS

The velocity and turbulence around and within low-crested rubble mound breakwaters is studied experimentally and numerically by GARCIA *et al.* 2004. With this information a number of elements of a low-crested structure are evaluated: functionality of the structure, structure stability, implications on the morphodynamics of nearby areas and the type of organisms that live in and around low-crested structures. Only elements which are of importance for this study are considered.

Influence structure freeboard

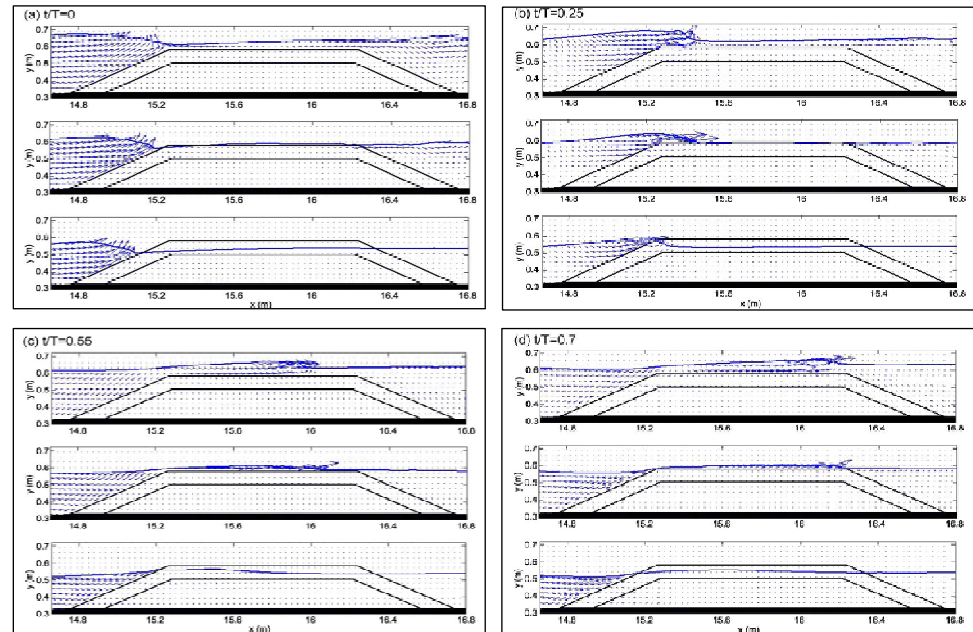
With zero structure freeboard the waves get steeper while passing on the initial gentle slope and then shoals on the seaside slope of the structure. The waves adopt an unstable profile earlier, as the relative depth is smaller, and the breaking point is slightly moved seaward.

By a positive freeboard the same phenomena of wave shoaling and breaking as in the previous cases can be observed with a slight transition seaward. Wave profiles reaches an unstable shape earlier, breaking occurs on the upper part of the slope.

Wave breaking conditions are obviously affected by the structure freeboard. Spilling breakers over the crest when the structure is submerged turn into plunging on the crest seaward edge in the case of zero freeboard, and

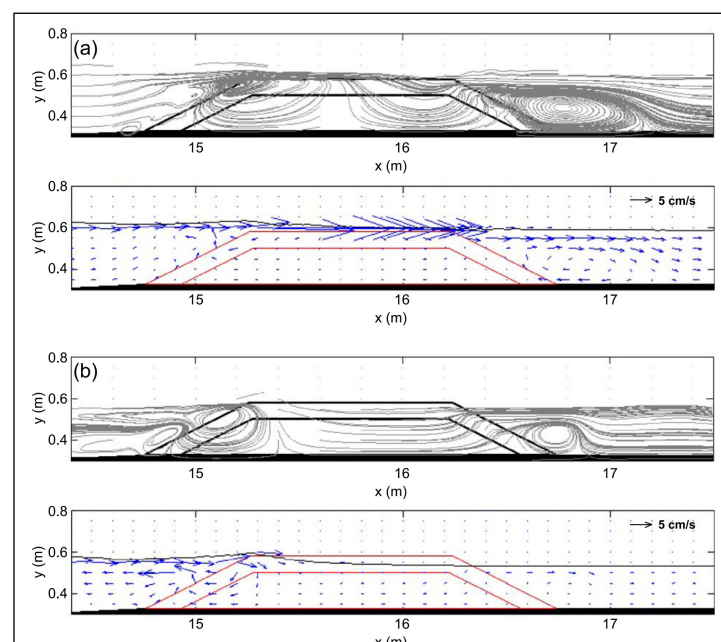
collapsing on the seaward slope when the structure emerges. Among the tested crest elevations, the breaking induced peak velocities are minimal when the structure is submerged and maximum when the freeboard is zero. The seaward edge of the crest seems then to be the most vulnerable zone of the structure. When the structure is submerged, the peak velocities associated with the propagation of the roller are distributed all along the crest zone and also affect the upper part of the leeward slope (Figure 3.20)

Figure 3.20
Snapshots of velocity field for different (positive, zero, negative) crest freeboards and t/T values



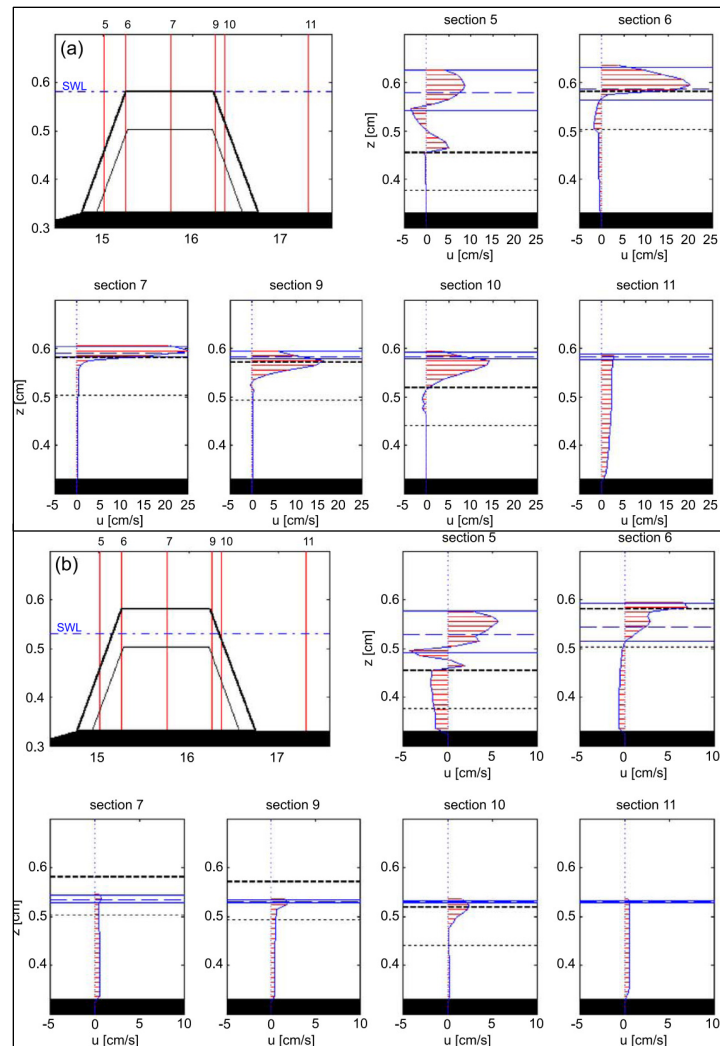
The perturbation of the mean flow pattern associated with wave breaking clearly appears in these Figure 3.21 and Figure 3.22. The high velocities over the crest in the case of a structure with zero freeboard, give rise to a strong mean current over the structure crest and a vortex cell at the lee, as for the submerged structure. A smaller vortex cell forms at the seaward edge of the crest and shows the vulnerability of this zone when the structure has zero crest freeboard. A vortex cell of reduced dimensions appears at the seaward toe of the structure.

Figure 3.21 Mean (ensemble averaged) flow, zero crest freeboard (a), and positive crest freeboard (b)



When the structure is emerged, the mean flow pattern is very different. A vortex is formed leeward but its dimensions are reduced with respect to the other tested depths. This cell is not associated with overtopping but with transmission through the structure. On the seaward slope the mean flow shows a rather complex structure, governed by the breaking conditions. Wave surging on the slope allows a greater penetration of the flow inside the porous media, and higher velocities are observed in the armour layer and the core of the seaward part of the structure. A mean current is formed in the offshore direction. In the transmission zone the onshore mean current is considerably reduced in comparison with the previous tested water depths.

Figure 3.22
Computed mean
(ensemble averaged)
velocity profiles,
structure freeboard (a)
zero crest freeboard,
(b) positive crest
freeboard



The spatial evolution of the mean flow pattern along the flume is more apparent in Figure 3.22, which shows the vertical distribution of the ensemble averaged velocities at different sections of the flume. In both $F=0$ and $F=5$ cm configurations, the vortices give rise to an inversion of the mean flow in the water column at Sections 5 and 6 corresponding to the seaward slope. At Section 5 the profile is rather complex, with a shoreward component above the trough level, a seaward component below and a shoreward component at the interface with the structure. As commented above, when the structure is emerged, higher velocities are reached inside the porous media and a significant mean current directed offshore can be observed in the armour layer at Section 5. This mean current is reduced at Section 6. The mean flow profile is more uniform at the other sections. The reduction of the mean current in the

transmission zone with the reduction of the structure freeboard can be clearly observed at Section 11.

Influence of structure crest width

The crest width affects the mode of energy dissipation at the structure and a combination of experimental and numerical results are used here to study the effect of a variation of the crest width on the wave breaking-induced near field flow pattern

Figure 3.23
Computed phase-averaged maximum velocity field and computed time averaged velocity field for different crest widths

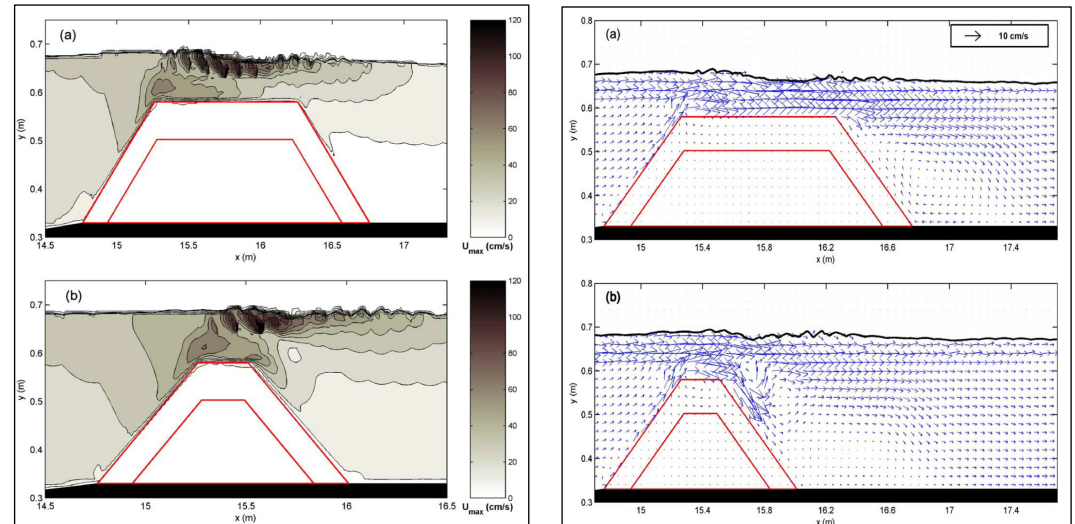


Figure 3.23 provides information on the potential vulnerability of the different zones of the structure, with armour stones of the leeside slope seen to be more likely to move downward in the case of the short-crested structure.

The velocity profiles in terms of magnitude and shape are, as expected very similar on the seaside of the breakwater for both widths of crests. As a consequence of the higher height of the transmitted wave in the case of the short-crested breakwater, the computed values of velocities are higher.

As a consequence of the lesser energy dissipation in the crest region in the case of the short-crested structure, the inner part of the crest and the upper part of leeside slope are affected by high values of maximum velocity intensity.

Figure 3.23 presents the variations in the mean flow pattern at the lee-side of both wide- and short-crested structures. A strong onshore current above the crest due to flow constriction and wave breaking and formation of vortex cells leeward of the structure. As can be seen in Figure 3.23 the maximum velocities at the leeside slope of the short-crested breakwater differ substantially from the wide crest geometry pattern. High values of mean velocities, directed downslope can be observed in the higher middle part of the slope.

3.3.8. CONCLUSIONS PRIOR STUDIES LOW-CRESTED BREAKWATERS WITH ROCK ARMOUR

Several studies have been done concerning the load and the stability of rock armour at low-crested breakwaters. In this section an overview of the results is given, a distinction is made between studies to the loading of the breakwater and studies to the stability of rock armour.

Loading breakwater

Both MIZUTANI *et al.* 1992/1994 and GARCIA *et al.* 2004 have investigated the load on a low-crested breakwater. MIZUTANI measured the wave forces at an armour unit and the velocities in front of an armour unit for different positions at the crest and the upper part of the seaside slope. GARCIA *et al.* 2004 studied experimentally and numerically the velocity and turbulence around low-crested breakwaters. From these studies the following can be concluded:

- Regardless of the variation of wave period, shape and size of the armour units the horizontal wave force shows similar variation with the distance from the seaside crest edge.
- The horizontal wave forces increases towards zero crest freeboards and becomes maximal at the crest edge. For wave breaking conditions the wave force decreases rapidly whereas it decreases gradually for non breaking conditions.
- Similar tendency is observed for the vertical wave force, however the variation with the distance and (non) breaking wave conditions is not clear.
- The onshore wave forces are in general larger than the offshore wave forces initiated by a water flow over the crest in seaside direction.
- The characteristics of the wave forces are well correlated with the measured water particle velocities.
- The velocity profile in terms of magnitude and shape are very similar on the seaside slope for both small and wide crest widths. For small crested breakwaters the inner part of the crest and the upper part of the leeside slope are affected by high maximum velocities whereas for wide crested breakwaters not.
- For emerged breakwaters higher velocities in the armour layer are present than in the case of zero and negative crest freeboard, a mean current is formed in the offshore direction.
- For positive crest freeboards the location of wave breaking shift more to the seaside slope compared to negative crest freeboards.

Stability rock armour

From studies of VAN DER MEER *et al.* 1994, VIDAL *et al.* 1992/2007 and KRAMER *et al.* 2003 the following conclusions can be drawn:

- Test series with 2% wave steepness tend to give slightly more damage than the series 3.5% wave steepness, VAN DER MEER states the opposite.
- No significant influence of crest width is observed.
- For positive crest freeboards the armour units removed from the crest section by the waves are mainly carried with the forward movement of the waves to the leeside slope. For negative freeboards the armour units are mainly carried to the front slope with the backward movement of the waves.

- For negative freeboards, the waves go over the crest and break on the water that protects the back slope armour units. When the crest emerges, the water jet starts to impinge on the back slope armour units and the stability continues to decrease because the impinging flow of water works together with the gravity to dislocate the armour units.
- The seaward slope shows a straight line suggesting a linear relation between the freeboard and the stability number. The minimum stability for the seaward slope corresponds to the non overtopped breakwater which is logical because no wave energy can pass the breakwater and the seaward slope has to dissipate all the wave energy.
- The crest sector is least stable for crest freeboards (R_c/D_{n50}) ranging from -3 to 1;
- For crest freeboards (R_c/D_{n50}) larger than 1 the leeside slope is the least stable section.
- The crest section is most stable for crest freeboards (R_c/D_{n50}) larger than 2.

In case of contradicting conclusions the conclusions of the most recent study are presented.

Four types of damage were observed in the study of VIDAL *et al.* 2007:

- Damage (Type I) at the upper part of the seaside slope occurs for low-crested breakwaters with high positive freeboards and low overtopping rates. The damage distribution is similar to the damage that occurs on non-overtopped rubble-mound breakwaters.
- Damage (Type II) at the upper part of the leeside slope occurred for low-crested breakwaters with positive freeboard near the still water level. As the wave overtopping increases, damage starts to occur also at the inner slope and at the outer edge of the crest. As wave period increases, Type I damage decreases while Type II increases.
- Damage (Type III) at upper part of the seaside slope and most dominantly at the seaside crest edge occurs for low-crested breakwaters near the still water level.
- Damage (Type IV) at the crest occurs for submerged structures.

4. LITERATURE STUDY ON STABILITY SINGLE LAYER INTERLOCKING ARMOUR UNITS

First an introduction is given to concrete armour units (§4.1). The stability of a concrete element under wave attack can be assessed in terms of load and strength. The wave attack can be schematized as a flow velocity and is called the load on a concrete element (§4.2.1). The resistance of a single layer armour unit is globally the same as for rock armour but additional stabilizing mechanisms such as interlocking has a positive influence on the stability (§4.2.2). Different studies have been done to the extent of interlocking and inter-block effect. Finally a number of stability formulas are given (§4.3).

4.1. CONCRETE ARMOUR UNITS

In Table 4-1 the chronological development of concrete armour units is represented.

Table 4-1
Development concrete
armour units

Cube 	Tetrapod 	Stabit 	Akmon 	Dolos 
-	1950	1961	1962	1963
Cob 	Antifer Cube 	Seabee 	Accropode I 	Shed 
1969	1973	1978	1980	1982
Haro 	Core-Loc I 	Diahitis 	A-Jack 	Xbloc 
1984	1995	1998	1998	2003
Accropode II 	Core-Loc II 			
2004	2006			

The armour units can be divided into categories related to their structural strength:

- massive or blocky type of units;
Cube, Antifer, Cube and Haro
- bulky type of units;
Stabit, Akmon, Accropode, Accropode II, Core-Loc II, Xbloc, Seabee, Diahitis and Xbloc
- slender type of units;
Tetrapod, Dolos, Core-Loc, A-Jack, Cob and Shed

The hydraulic efficiency can be evaluated by the hydraulic stability compared to the used concrete on a unit area of the slope. Hydraulic efficiency increases from the massive- to the slender units. Slender units are however more vulnerable to breakage. Massive units rely primarily on their own weight,

slender units on the other hand rely to a certain extent on their own weight but additional effects like interlocking plays an important role in the stability.

Some of the above mentioned elements can be used in a single layer, others demand a double layer. Mentioned single layer armour units in Table 4-1 are: Accropode, Core-Loc, Xbloc, Accropode II and Core-Loc II.

4.2. STABILITY

4.2.1. LOAD

The stability of armour units is affected by (as described in §2.3.1):

- wave run-up and wave rundown;
- type of wave breaking;
- turbulence.

The same consideration of rock armour units on a slope under wave induced flow can be made for single layer armour units. The difference in loading is caused by the different shear, drag and lift coefficients and the exposed areas normal to the flow. The shear, drag and lift coefficients for stone can be different than those for a single layer armour unit, just like the exposed area normal to the flow. Finally the coefficients multiplied with the exposed area normal to the flow can give other values than for rock.

With the roughness reduction factor the amount of wave overtopping can be calculated. Indirectly it gives an idea of the extent of wave run-up and wave rundown. A rough slope (low roughness factors) means relatively low levels of wave run-up, rundown and relatively small amounts of wave overtopping. Low roughness factors imply therefore high energy dissipating rates and large hydraulic loading of the armour layer.

4.2.2. RESISTANCE

Concrete armour layers rely for their stability on a number of mechanisms:

- their own weight;
- interlocking.

A simple consideration helps to understand the above mentioned principles. The armour unit experiences a force parallel and perpendicular to the slope due to its own weight. The steeper the slope the larger the parallel force component, whereas the perpendicular component becomes smaller. The frictional force between the elements depends upon the friction coefficient, contact surface area and the normal force between the elements. For steep slopes the frictional force increases due to the enlarged parallel force. As said before the perpendicular component decreases for steeper slope angles, so does the friction between the armour elements and the under-layer. In this respect the breakwater toe have to support (partially) the armour layer. This also implements that the top rows of the armour layer experiences almost no interlocking and interblock friction. The extent of interlocking increases due to the increasing parallel force component for steeper slope angles.

Interlocking and friction between rocks also contributes to the stability of rock armour layers. The contribution to the stability is however hard to quantify because of the large uncertainty and the wide scatter the values shows. The interlocking effect of concrete armour units clearly contributes to the stability, the influence of interlocking to the total stability of rock elements shows no clear influence. Therefore interlocking is not considered in the stability principle for rock in paragraph 3.1 **Fout! Verwijzingsbron niet gevonden.** and 3.2.

The influence of an armour units weight and inter-block friction on the stability can be considered the same as for rock. The interlocking capacities are however not comparable to rock elements, interlocking is the main feature through which a concrete element is more stable than a rock armour element.

Interlocking

When an armour unit is pulled out of the armour layer other surrounding units try to prevent this. Complementary to the weight of the unit that is pulled out the weight of the surrounding units is partially activated. The extent of interlocking depends upon a number of factors:

- slope angle;
- weight of the armour unit;
- smoothness (roughness) of the under-layer;
- block position.

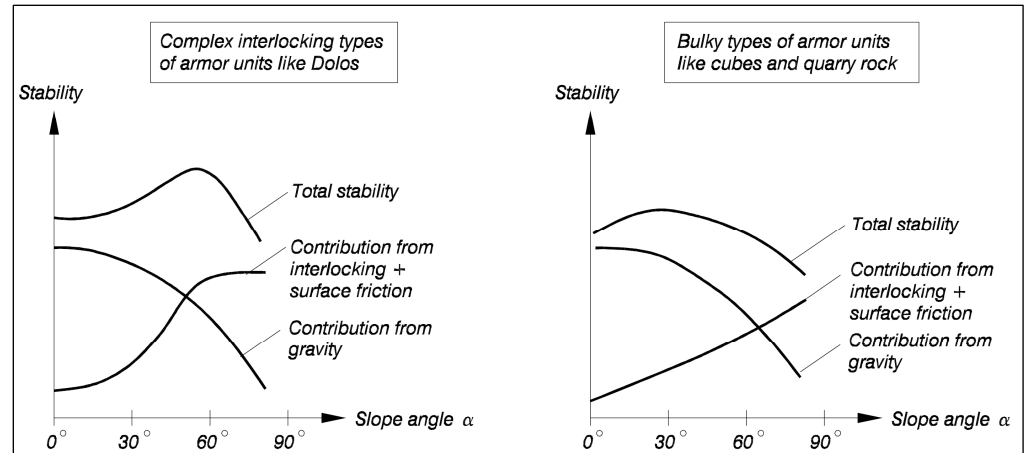
Different studies have been done to quantify the extent of interlocking for rock armour units and different type of concrete armour units.

BREBNER 1978 performed tests with Dolos and rock units on the bed in an open-channel under steady state turbulent flow. Brebner stated 'With the superior behaviour of the Dolos unit in an up-rush and downrush wave situation one might reasonably expect that, in a free non-oscillatory current, this interlocking property could play a significant role in making the Dolos unit more effective in resisting movement than an equal weight of quarry stone unit.' First, tests were conducted to determine the drag (C_D) and lift (C_L) coefficients for Dolos and rock units, it appeared that the drag and lift coefficients multiplied with the projected area normal to the flow for both units were essentially the same. This shows that the Dolos relies for a great part on the interlocking properties. Next tests were conducted in a flume on a bed of Doloses and rocks of identical mass. The water velocity in the flume was gradually increased until the point rock or Doloses were 'wiped out'. The velocity at which the units lost their stability was essentially the same. It can be concluded that interlocking becomes noticeable on sloping banks.

PRICE 1979 has done test to understand the interlocking capacities for rock and different double layer interlocking concrete blocks. The tests consisted of measuring the forces (normal to the slope) required to remove units from the armour layer. The tests were done on smooth slopes. Varying influencing effects on the interlocking capacities were taken into consideration, such as slope angle, effect of block position, block density and the effect of compaction. Compaction in reality takes place due to wave action. Results show that block position has no or minor influence, whereas the slope angle, block density and compaction has a substantial influence on the interlocking

effect. Compaction and a higher block density influence the interlocking positively. On average compaction increased the force necessary to remove a unit by 36%.

Figure 4.1
Contribution of gravity and surface friction to the total stability with varying slope angle [PRICE 1979]

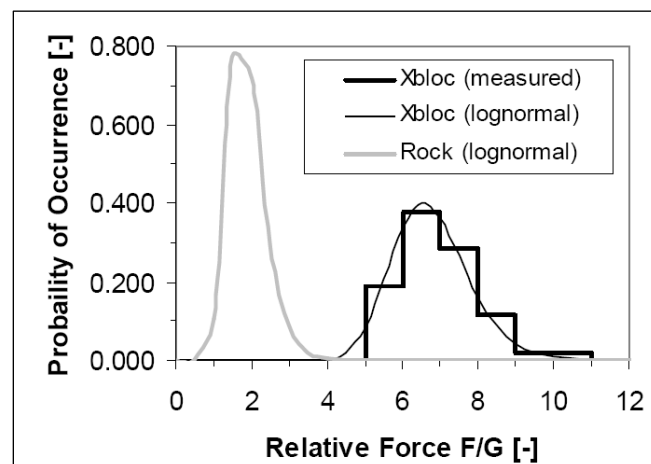


The contribution of interlocking and inter-block friction to the total stability attains a minimum on horizontal planes where the effect of the weight as stabilizing factor of a block maximizes. The increase of the interlocking effect is greatest between slope angles of 30° and 60°, for rock armour the rate of increase is almost constant. The maximal total stability occurs at a slope angle of approximately 55° for interlocking type of armour units. Maximal stability for rock armour stone occurs at a slope angle of approximately 25°.

HALD *et al.* 2000 performed pullout tests on rock armour layers to investigate the interlocking effect. Tests were performed on different slope angles (1:1.5, 1:2, 1:3) and on a 1:2 slope also the pull direction (60°, 90° normal to the slope, 120°, 150°) was varied. No influence of the slope angle has been observed, but as the direction of pull changes and becomes more upward directed (from 60° to 150°) the pullout resistance increases from approximately once the rocks own weight to 2.4 times the rocks own weight. The results on an 1:1.5 slope are plotted in Figure 4.2.

MUTTRAY *et al.* 2005 performed pullout tests normal to a slope of 1:1.5 for single layer Xbloc armour units, the results are shown in Figure 4.2.

Figure 4.2 Results pullout tests [MUTTRAY *et al.* 2005]



Delta Marine Consultant performed extensive pullout tests with the Xbloc single layer armour unit. The influence of different concrete densities (2102 kg/m³, 2465 kg/m³, 2915 kg/m³), slope angles (3:4, 1:2, 0:1), armour units position on the slope (row number 3 to 5, 9 to 11, 15 to 17) and under-layer roughness's are investigated (as an example see Figure 4.4). The Xbloc armour units are pulled out normal to the slope in all tests. The slope is vibrated to simulate the compaction of the armour units due to wave action.

The influence of the mass density of an armour units on the interlocking properties is not considered in this report because the density a constant. Interlocking increases with steeper slope angles (3:4, 1:2) in the case of a smooth under-layer whereas a rough under-layer shows no clear increase of interlocking for the steeper slope angles (3:4, 1:2). The extent of interlocking on a horizontal plane (0:1) is only tested with a rough under-layer. The pullout tests clearly shows lower interlocking values at horizontal slopes than for non horizontal slopes. The position on the slope also influences the extent of interlocking. A minimum of three rows above the pulled out unit is needed to generate the average interlocking of approximately four times its own weight (see §Figure 4.4). The extent of interlocking increases when the number of rows above the pulled out unit increases. For a smooth under-layer the increase is significantly in contrast to the rough under-layer. Vibrating the slope does not have the desired effect of giving the armour layer the characteristics of a prototype armour layer.

Figure 4.3 Results pullout tests Xbloc armour unit, slope 3:4, rough under-layer.

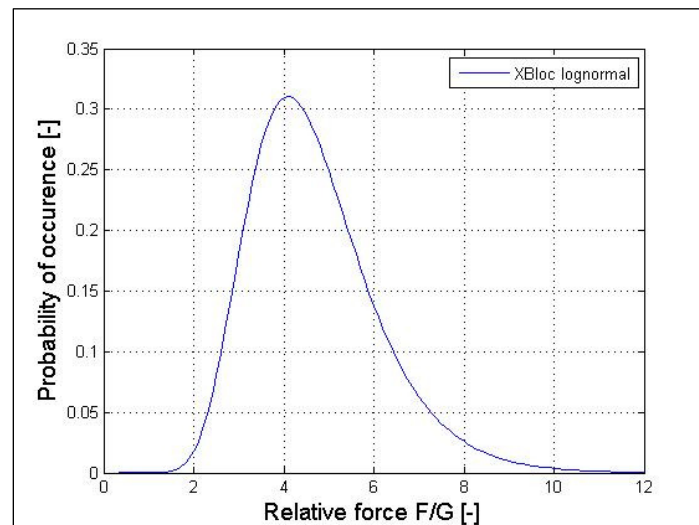
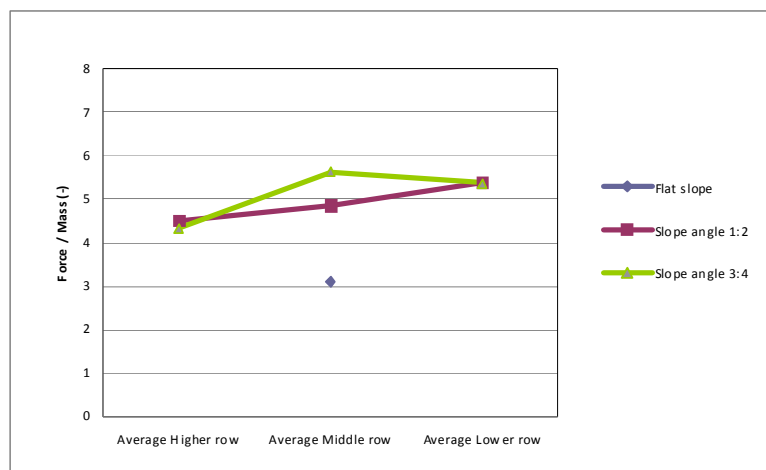


Figure 4.4 Results pullout tests Xbloc armour unit, various slope angles.



4.3. PRIOR STUDIES LOW-CRESTED BREAKWATERS

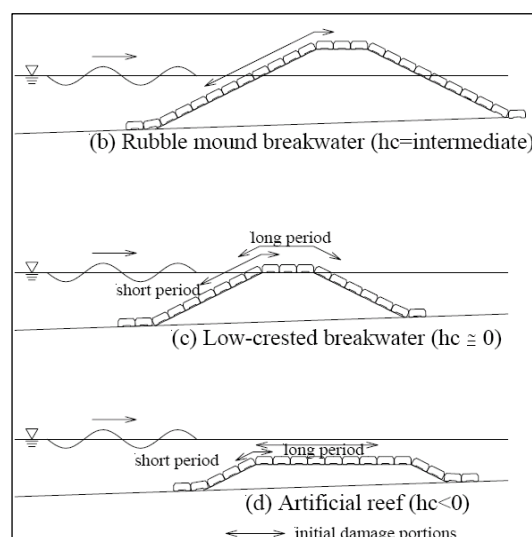
Holtzhausen performed model tests on Dolos armour units with a slope of 1:1.5 for non-overtopped structures. De Jong, Burcharth and Liu derived stability relations for Tetrapod armour units on overtopped and non overtopped structures. Van der Meer performed model tests on breakwaters armoured with Cubes, Tetrapods and Accropode. The stability of cubes and Tetrapods is tested on an 1:1.5 slope, whereas the Accropode on an 1:1.33 slope. The Accropode requires a steeper slope because it is applied in a single layer. The model tests were limited to one cross section (slope angle and permeability) for each armour unit. Therefore the slope angle and the surf similarity parameter are not present in the stability formula.

Given the perspective of the study only results for Dolosse, Tetrapod and Accropode are presented. These elements rely for their hydraulic stability heavily on their interlocking properties But also flat type of concrete armour units are discussed which have not interlocking properties (MATSUDA *et al.* 2003). At last the current design philosophy of single layer armour units is explained.

4.3.1. MATSUDA ET AL. 2003

MATSUDA *et al.* 2003 performed model tests with flat type concrete armour blocks, the blocks have no interlocking properties. Three slope gradients 1:2, 1:3, 1:5 were used. In the case of low-crested breakwaters shorter wave periods gave damage at the topside of the front slope. Long wave periods gave damage at the top side of the leeside slope and at the crest. In the case of a slope of 1:5, initial damage mainly occurred at the front slope because the waves did not hit the top side of the back slope and the crest. In the case of the artificial reef, the same tendency as in the low-crested breakwater was found (see Figure 4.5)

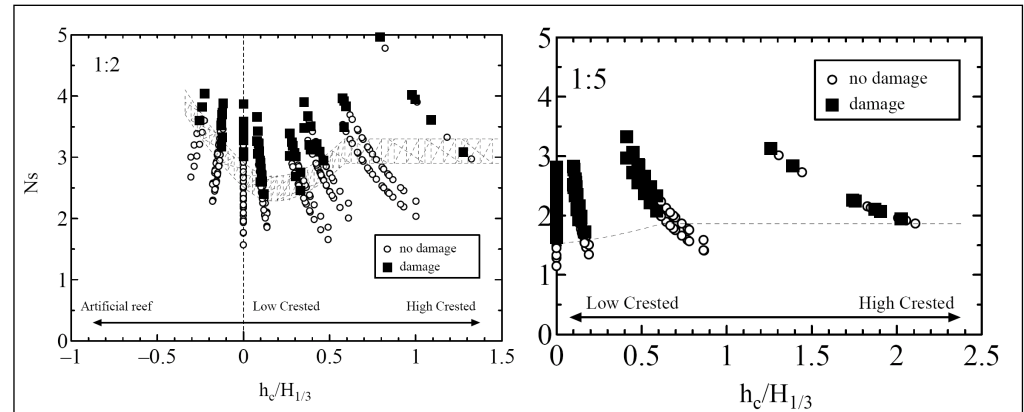
Figure 4.5 Sections with initial damage



When the slope was comparatively steep, surging breakers of wave groups running up and down the slope caused the armour blocks to rise and be pulled them out. On the other hand, when the slope was comparatively gentle plunging breakers directly attacked the blocks. Accordingly, the blocks received an impact force and were dislodged by only one wave.

When damage occurred at the top of the front slope, the armour blocks fell down the front slope, or they were turned up and moved to the back. When an armour block fell down the front slope, it was often observed that the part of the block had been landed the adjacent block at the crown before it fell down the slope. The cause of initial damage occurrence at the crest of the artificial reefs was mainly the result of wave breaking. When the slope was 1/2 initial damage often occurred around the top of the front slope even in the case of comparatively high crest. On the other hand, when the slope was 1/5 initial damage often occurred in the middle of the front slope even in the case of a low crest. The tendency for a slope 1/3 was placed between 1/2 and 1/5.

Figure 4.6 Relation between $h_c/H_{1/3}$ and N_s for an 1:2 and 1:5 slope



The following would be confirmed for the case of a slope of 1/2. N_s decreases with increasing $h_c/H_{1/3}$ in the range of $h_c/H_{1/3} < 0.2$. In the range of $0.2 < h_c/H_{1/3} < 0.6$, N_s increases with increasing $h_c/H_{1/3}$. N_s is almost constant in the range of $0.6 < h_c/H_{1/3}$. In the range of $0.6 < h_c/H_{1/3}$, the stability of the armour blocks would be rarely influenced by the crown height.

In the case of the 1/3 slope, N_s was minimal at nearly $h_c/H_{1/3} = 0$. And, it would be almost constant in the range of $N_s > 0.5$.

In the case of the 1/5 slope, N_s increases gently with increasing $h_c / H_{1/3}$ in the range of $0 < h_c/H_{1/3} < 0.7$. N_s is almost constant in the range of $0.7 < h_c/H_{1/3}$. The influence of the wave period on the stability number (N_s) is not clear.

4.3.2. DOLOS (DOUBLE LAYER)

BURCHARTH AND LIU 1993 developed the following formula for a 1:1.5 non-overtopped slope ($0.32 < r < 0.42$; $0.61 < \phi < 1$):

$$\frac{H_s}{\Delta \cdot D_n} = (17 - 26 \cdot r) \cdot \phi^{2/3} \cdot N_{od}^{1/3} \cdot N^{-0.1} \quad (4.1)$$

Where ϕ represents the packing density and r the waste ratio, which is the diameter of the central section over the unit height.

HOLTZHAUSEN (1996) presented the following equation for Dolos that is valid for packing density coefficients in the range $0.83 < \phi < 1.15$:

$$N_{od} = 6.95 \cdot 10^{-5} \left(\frac{H_s}{\Delta^{0.74} \cdot D_n} \right)^7 \cdot \phi^{1.51} \quad (4.2)$$

Equation (4.2) implies that as the packing density decreases the number of displaced units decreases. A physical explanation could be that higher packing densities do not allow optimum interlocking [CEM 2006].

4.3.3. TETRAPOD (DOUBLE LAYER)

A double layer of Tetrapods have a fair degree of interlocking, the stability is influenced by the wave period and storm duration. Longer wave periods increase the stability which is according to rock slopes [VAN DER MEER 1988]. The stability relationship turns out to be:

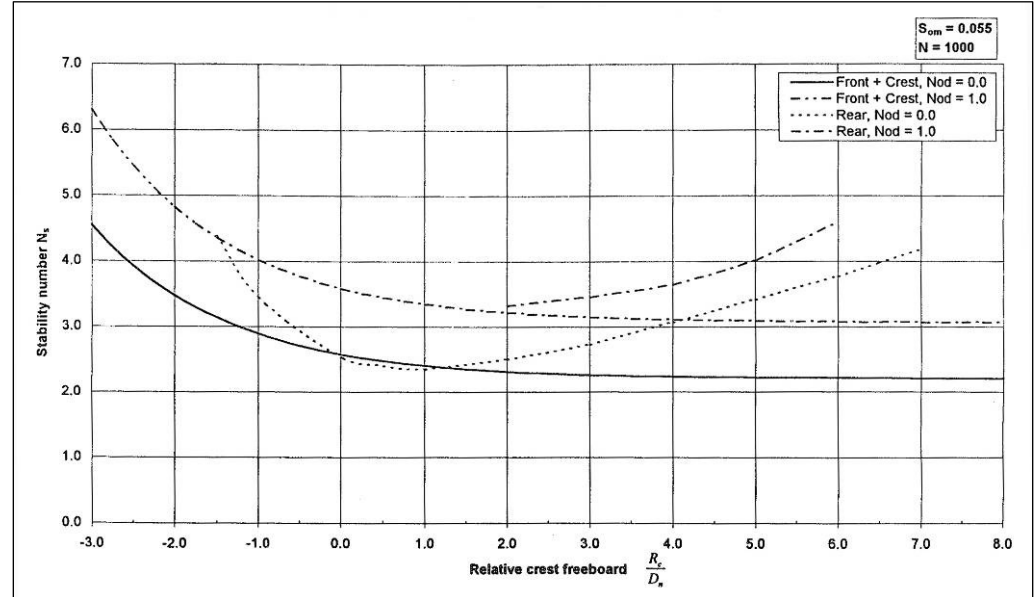
$$\frac{H_s}{\Delta \cdot D_n} = \left(3.75 \frac{N_{od}^{0.5}}{N^{0.25}} + 0.85 \right) \cdot S_{om}^{-0.2} \quad (4.3)$$

For plunging waves the following formula for the front slope plus crest is valid, also the influence of crest freeboard is taken into account [DE JONG 1996].

$$\frac{H_s}{\Delta \cdot D_n} = S_{om}^{0.2} \cdot \left(8.6 \cdot \left(\frac{N_{od}}{\sqrt{N}} \right)^{0.5} + 2.64 \cdot k_t + 1.25 \right) \cdot \left(1 + 0.17 \cdot \exp \left(-0.61 \cdot \frac{R_C}{D_n} \right) \right) \quad (4.4)$$

In which K_t is the layer thickness coefficient. The stability number is increased by a factor with respect to a lower crest height.

Figure 4.7
Comparison of
stability of front plus
crest with rear slope
[De Jong (1996)]



4.3.4. ACCROPODE (SINGLE LAYER)

The Accropode relies on a high degree of interlocking and it appears that the stability is not influenced by the storm duration and wave period. Two more important conclusions can be drawn. The stability for start of damage is very high compared to Tetrapods. This is caused by settlement of the steep slope (cot 4/3) during the bedding in tests with low waves. After settlement the armour layer acts as a 'blanket' where each unit contacts several neighbours. Start of damage and severe damage or failure, given by $N_0 > 0.5$ are very close,

however. This means that the initial stability of Accropode is very high, but that the structure fails in a progressive way. The stability can be described by two simple formulae [VAN DER MEER 1988]:

$$\text{Start of damage, } N_o = 0 \quad \frac{H_s}{\Delta \cdot D_{n50}} = 3.7 \quad (4.5)$$

$$\text{Failure, } N_o = 0.5 \quad \frac{H_s}{\Delta \cdot D_{n50}} = 4.1 \quad (4.6)$$

4.3.5. CONCLUSIONS ON DESIGN LOW-CRESTED BREAKWATERS WITH SINGLE LAYER ARMOUR UNITS

For double layer concrete armour units formula's exist to calculate the units required size and weight. For single layer concrete armour units however are designed according to the Hudson formula or the stability number. The stability coefficient (number) is derived from model tests and depends on many factors. The derived K_D value is valid for one standard situation (one slope angle etc.), non standard situations poses difficulties to the design of concrete armour layers. A design is usually based on a standardized K_D value and supplementary model test to make sure the breakwater performs as intended for.

5. DESCRIPTIONS PHYSICAL MODEL TESTS

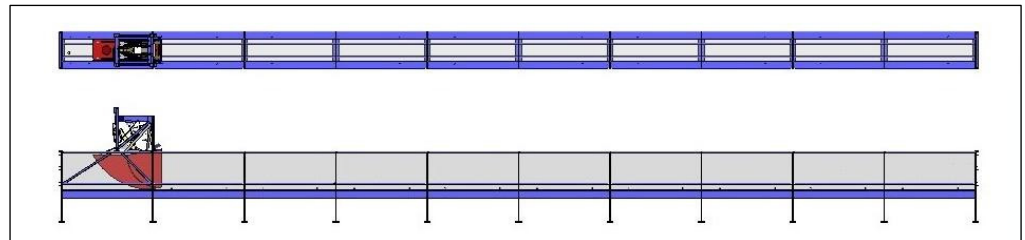
Physical model tests are performed to identify trends for the stability of low-crested structures (see §1.2, study objective). In this section the model set-up is discussed, the following subjects are threaded:

- test facility (§5.1);
- scaling (§5.2);
- model (§5.3);
- test programme (§5.4);
- measurements (§5.5).

5.1. TEST FACILITY

The wave flume consists of a long rectangular glass tank with a wave generator on one side, see Figure 5.1. The flume has a length of 25 m, a width of 0.6 m and a height of 1.0 m. The effective length of the flume is approximately 20 m. The maximal permissible water depth is 0.7 m with a maximal wave height of 0.3 m. The flume is equipped with an Edinburgh Designs piston wave generator, which can generate regular and irregular waves based on a spectrum. The Edinburgh Designs piston wave generator is able to measure the reflected wave and correct the paddle motion to absorb it.

Figure 5.1
Schematisation wave
flume Delta Marine
Consultants



The minimum water depth in which the wave maker is capable of generation waves is 40 cm, below this level the wave maker paddle does not have enough buoyancy to reach a stable centre position.

The maximum wave height which can be generated is a significant wave height of $H_{m0} = 20$ cm. The wave generator is bounded to a minimum and maximum frequency of 0.1563 Hz and 1.5 Hz which corresponds to a period of 0.67 s and 6.4 s.

5.2. SCALING

In paragraph 5.2.1 different scaling laws are discussed, in paragraph 5.2.2 scale effects related to waves structure interaction are discussed and finally the scaling laws used in this model are described. This section 'Scaling' is described on the basis of *Wave Action on Rubble Mound*

Breakwaters: the Problem of Scale Effects 2000. An extensive overview of scale effects is given such that the limitations of model test become clear.

In scale models, scale rules play an important role to guarantee similarity in behaviour in model and prototype. There are three types of similarity:

- geometric;
- kinematical;
- dynamic.

Geometrical similarity exists if all the linear dimensions of the prototype and model have the same scale ratio. This implies that the model has the same shape as the prototype.

$$N_L = \frac{x_m}{x_p} = \frac{y_m}{y_p} = \frac{z_m}{z_p} \quad (5.1)$$

Kinematical similarity implies similarity of motion in model and prototype. The vectorial components of motion have the same ratio for all particles at all time. Dynamic similarity exists for geometrical and kinematical similar systems if there is similarity in the force between prototype and model. The ratios of all the vectorial forces have to be equal. There is no fluid which can fulfil all force ratio requirements.

5.2.1. SCALING LAWS

In this section different scaling laws are considered to make clear which scale effects can arise. Four scaling laws are discussed:

- froude scaling;
- reynolds scaling;
- weber scaling;
- cauchy scaling.

Froude scaling

The Froude number gives the ratio between inertia and gravity forces and is defined by:

$$Fr = \frac{\text{Inertia force}}{\text{Gravity force}} = \frac{F_i}{F_g} \propto \frac{\rho \cdot U^2 \cdot L^2}{\rho \cdot g \cdot L^3} = \frac{U}{\sqrt{g \cdot L}} \quad (5.2)$$

In other words it represents the relative importance of inertia forces acting on a fluid particle to the weight of the particle. This results in terms of scale ratios:

$$\left(\frac{U}{\sqrt{g \cdot L}} \right)_p = \left(\frac{U}{\sqrt{g \cdot L}} \right)_m \Rightarrow \frac{N_U}{\sqrt{N_G \cdot N_L}} = 1 \quad (5.3)$$

Reynolds scaling

The Reynolds number indicates the ratio between inertia and viscosity.

$$\text{Re} = \frac{\text{Inertia forces}}{\text{Viscous forces}} = \frac{F_i}{F_v} \propto \frac{\rho \cdot U^2 \cdot l^2}{\mu \cdot U \cdot l} = \frac{\rho \cdot U \cdot l}{\mu} = \frac{U \cdot l}{\nu} \quad (5.4)$$

Where ν is the kinematic viscosity (μ/ρ). The Reynolds number will ensure that viscous forces are correctly scaled.

Weber scaling

The Weber number gives the ratio between surface tension forces and inertia. The Weber number is important in the case of air entrainment, but also for breaking waves, since the surface stress acts as a membrane. When the Weber number becomes too small, the shape of the breaking waves can be influenced. A first rule for models with short waves is that the wave height should not be smaller than about 5 cm in order to maintain similar breaking characteristics.

$$\text{Re} = \frac{\text{Inertia forces}}{\text{Surface tension forces}} = \frac{F_i}{F_s} \propto \frac{\rho \cdot U^2 \cdot l^2}{\sigma \cdot l} = \frac{\rho \cdot U^2 \cdot l}{\sigma} \quad (5.5)$$

Cauchy scaling

The Cauchy number gives the ratio between inertia and elastic forces.

$$\text{Ca} = \frac{\text{Inertia forces}}{\text{Elastic fluid forces}} = \frac{F_i}{F_e} \propto \frac{\rho \cdot U^2 \cdot l^2}{E \cdot l^2} = \frac{\rho \cdot U^2}{E} \quad (5.6)$$

The elasticity of air-water mixtures depends on air content, that may be significantly different in prototype and model and on ambient pressure, that does not scale down as a small pressure perturbation and therefore, the effect of elasticity scale is expressly represented. When the compressibility is the dominant factor, conversion to prototype should be made by using Cauchy law.

5.2.2. BEST SUITABLE SCALING LAW

None of the above scaling laws provides exact scaling of all the processes that occur in breakwater model tests. Main scale effects from prototype to model are due to intrinsic properties of the fluid that do not scale appropriately (viscosity, surface tension, air content etc.) and qualitative differences in processes in field and laboratory (obstruction of pores by algae and mussels in sea-water, reduced coalescence of air bubbles in sea-water).

For the scale reproduction of waves, the ratio between inertia and gravitational forces are dominant, therefore Froude scaling is applied. The other scaling laws provide scaling of less dominant parameters;

- The effect of viscous damping, in conventional reproduction of non-breaking laboratory waves, is negligible if water depths are greater than 2-3 cm and wave propagation is over a short distance.
- Surface tension can cause some scale effects on non-breaking laboratory wave propagation, but only if laboratory waves are very small and steep, heights and periods below 2 cm and 0.3 s.

- Short breaking waves causes scale effects on air entrainment. Compressibility of air-water mixture is much different in prototype or model conditions and therefore, causing a scale effect.

5.2.3. SCALE EFFECTS RELATED TO WAVE-STRUCTURE INTERACTION

Wave structure interaction describes the way in which a wave interacts with the breakwater. In model tests the wave structure interaction has to be similar to prototype. A number of wave structure interactions are considered which are essential in armour layer stability tests:

- wave impact on armour units;
- run-up and overtopping;
- structure deformation;
- porous flow.

Wave impact on armour units

Wave impacts on mound breakwaters are compounded of two parts: Impulsive load (sharp peak, high magnitude, short rise time); Pulsating (quasi-static) load associated to the mass of water ‘traveling’ through the structure. No major scale effects are evident when dealing with pulsating loads.

Impulsive loads induced by breaking waves involve compressibility of air during a very short time. The fluid interacting with the structure becomes a mixture of air and water and cannot be treated as an incompressible fluid. Froude and Cauchy law are not adequate for scaling model on impulsive events. Froude law overestimates the impulsive force because, the air content in sea water is significantly higher than in fresh water at model scale and the compression of air in the air water mixture is a non linear process controlled by the environmental pressure which does not scale down in the model. However, investigations of scale effects in armour stability tests have shown that if Reynolds number exceeds a certain critical value (Re_c) then the effects are very small. The characteristic velocity (U) is taken as $\sqrt{g \cdot H_s}$ in which H_s is the significant wave height. In this study the calculated Reynolds number amounts $3.45 \cdot 10^4$.

Run-up and overtopping

In a Froude model scale effects associated to viscous forces and surface tension are present. OPTICREST projects showed that run-up was underestimated in normal small scale models, and so is overtopping. Scale effect on overtopping are noticeable probably only for very small overtopping discharges but it is expected to be marginal for low crested structures where overtopping discharge is large. A recent set of experiments on wave overtopping at large and small scale suggests that bulk overtopping flows scale directly by Froude without need for any significant correction.

Structure deformation

An effect similar to compressibility of air is associated to structure compliance that can be due to element flexibility. In these model tests this is an important limitation, the concrete elements in the tests are much stronger than in reality. Rocking in reality can damage the elements severely, but in model test this is

impossible. One has to value the amount of rocking on bases of experience and feeling. Further considerations about the qualification of damage are given in paragraph §5.5.

Porous flow

Linear geometric scaling of core material diameter which follows from Froude scaling may lead to much too large viscous forces corresponding to too small Reynolds numbers especially in under-layers and core of small scale models. The related increase in flow resistance reduces the flow in and out of under-layers and core. This causes relatively larger up-rush and down-rush velocities. As a result run-up levels will be too high and armour stability too low BURCHARTH ET AL. 1999. A complete correction for this scale effect cannot be obtained just by further increasing the size (diameter) of the core material in the model with respect to the one given by the model length scale, because Reynolds number varies in time and space under the action of waves.

The method described in BURCHARTH *et al.* 1999 is used to determine the size of the core material. The method results in a diameter for the core material in the model that holds for a characteristic pore velocity. The pore velocity is chosen as the average velocity of a most critical area in the core with respect to the pore velocity. After calculating the d_{50} with BURCHARTH *et al.* 1999 it has to be checked whether geometric scaling leads to a bigger median sieve size. The largest median sieve size has to be used. Additional information on this method can be found in Appendix C.

5.3. MODEL

A breakwater can fail (structure performance and functionality below the minimum anticipated by design) for different reasons (see §2.1), one of these is structural failure of the armour layer (§2.3.2). The failure modes of the armour layer which are permitted during model test are:

- rocking of units during up and down-rush;
- rotation and subsequent down-slope displacement of unit during down-rush;
- rotation and subsequent up-slope displacement of unit during up-rush
- uplift of an armour unit.

Occurrence of other failure modes is prevented due to the model configuration.

Based on the permitted failure modes, the ‘Prior studies low-crested breakwaters (§3.3) and the ‘Hypotheses’ (chapter 5) a cross section of the model is drawn up (see §5.3.1). In paragraph 5.3.2 the used materials in the model and their dimensions are described.

5.3.1. CROSS SECTION

The cross section of the model can be subdivided into the breakwater cross section and the overall cross section (layout wave flume). First of all the breakwater cross section is treated, based here on the overall cross section is suited.

Breakwater cross section

Eight different configurations of the low-crested type of breakwater are tested, the crest freeboard and crest width are the two variables. The crest freeboard (R_c/H_s) varies between -0.8 to 0.8 in steps of 0.4, whereas the crest width is either three or nine armour elements wide.

The same Xbloc single layer armour units are used on all the different sections of the low-crested breakwater (seaward slope, crest and leeward slope). At the walls of the wave flume the Xbloc armour units can only partially interlock with the other Xblocs. Due the fact that one side of the unit cannot interlock with another unit the stability of these Xblocs will decrease and the chance of displacement will be higher. Therefore a steel chain is laid down on the Xblocs which are at the walls of the wave flume. The opted relative placement densities for the armour units in model tests are 100%. The Xbloc armour units are placed randomly which means that the orientation of the units is varied randomly. The number of armour unit rows at both slopes is a constant for the different breakwater configurations. Settlements of the armour layer are therefore comparable in all tests.

The under-layer is applied to make sure no core material can wash trough the armour layer. Furthermore possible settlements of the armour layer are modelled correctly; the extent of settlements is among other things influenced by the roughness of the under-layer. The under-layer thickness is $2 D_{n50}$, where the nominal diameter of the under-layer material is used.

The slope angle is chosen in accordance with the Xbloc specifications.

Table 5-1 Varying parameters (cross section)

Parameter	Value(s)	Unit
relative crest freeboard (R_c/H_s)	-0.8, -0.4, 0, 0.4, 0.8	-
crest width (w_c)	3, 9	nr. of armour units
sea- and landward slope ($\tan \alpha$)	3V/4H	-

Overall cross section

The overall cross section describes the layout of the wave flume (foreshore, water depth) and the position of the breakwater. Based on this layout numerical values can be assigned to the dimensions of the breakwater cross section.

A foreshore of 1:30 is applied to represent reality, as the low-crested type of breakwater is used often in coastal areas. The water depth and the bottom slope are responsible for the change of wave characteristics approaching the structure, that is whether waves are shallow or deep water, breaking or non breaking, linear or non linear.

Low-crested structures are by definition strongly overtopped structures, designed to allow the transmission of a certain amount of the incident wave energy. In most 2-D laboratory experiments on this type of structures, the overtopping gives rise to a piling-up of water in the leeside region of the structure and hence to an increase of the mean water level. This set-up in the transmission zone modifies the dynamics of the waves reformed in this region and the flow condition in the vicinity of the breakwater. It forces a strong return current flow over the structure which perturbs the wave breaking process on the structure seaward slope and crest, influencing the breaker type, position

and height. In real cases (of stretches of shore protected by low-crested structures) this phenomenon is not observed, as the potential piling-up behind the breakwater is relieved by 3-D circulation systems. Part of the flow is transmitted back to the seaward side through the permeable core, but a greater proportion returns to open sea by the sides of the breakwater, following pathways of lesser resistance.

2-D model tests have been done by LOSADA *et al.* 2000 within the DELOS project. A low-crested breakwater model with and without a flow-recirculation system (discharging the overtopping-induced excess of mass) has been tested. The absence of a flow recirculation system influences the flow pattern in the vicinity of the breakwater (crest, lee- and seaward slopes) in the flume. The flow recirculation system is fundamental in the adequate 2-D modelling of low-crested structure.

To prevent piling up of water behind the breakwater as much as possible, at the beginning of the foreshore a gap of 2 cm is present to allow flow recirculation (see Figure 5.2).

The test facility (see §5.1), foreshore and the breakwater cross sections leads to the following numerical values, see Table 5-2.

Table 5-2
Numerical
parameters, overall
cross section

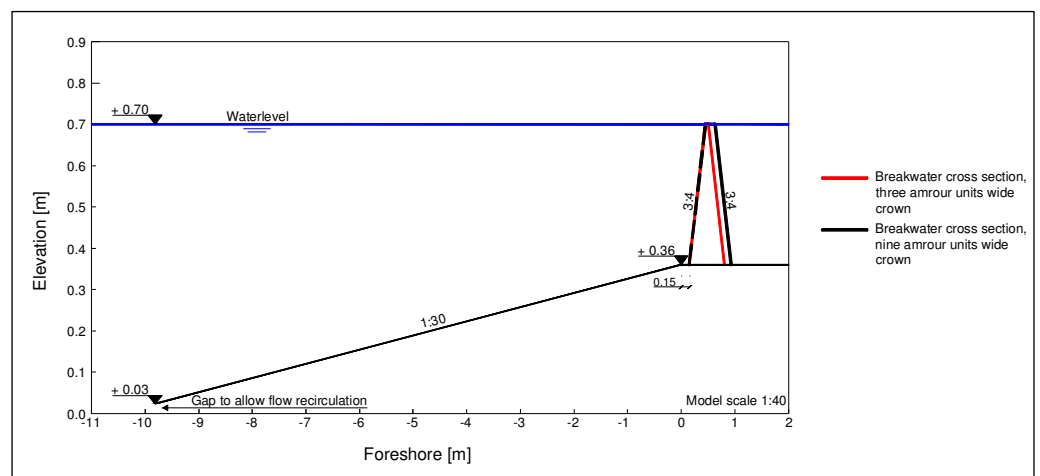
Parameter	Value(s)	Unit
<i>Water depths</i>		
wave paddle (h)	70	cm
toe breakwater (h_{toe})	33.9	m
<i>Foreshore</i>		
slope (β)	1:30	-
height	36.1	cm
length ($L_{foreshore}$)	9.93	m
gap height (h_{gap})	2	cm
<i>Xbloc</i>		
height (D)	4.3	cm
weight (W_{Xbloc})	62	g
nominal diameter (D_{n50})	2.98	cm
density material (ρ_{Xbloc})	2339	kg/m ³
Significant design wave height at the toe of the structure ($H_{s, toe}$)	11.06	cm
<i>Breakwater cross section</i>		
relative crest freeboard (Rc/H_s)	-0.8, -0.4, 0, 0.4, 0.8	-
crest height (h_c)	25.12, 29.52, 33.9, 38.3, 42.7	cm
crest width (w_c)	3 – 9	armour units
sea- landward slope ($\tan \alpha$)	3/4	-
number of Xbloc rows at the slope sections	14	-

The still waterline is kept constant in all tests; to realise the relative crest freeboard the structure height is varied. The advantage of testing in such manner is that the wave parameters are exactly similar for all tests. If in

contrary the water depth is adapted to obtain the different crest freeboards while the structure height remains the same, depth limited waves would occur in a number of tests (because of the limited maximum water depth of the wave flume). This would lead to different loading situations of the armour layer which makes a direct comparison impossible.

Due to the fact that the breakwater crest height is varied, the number of rows of armour units at the slopes varies in accordance. To keep the number of rows at the slopes constant, gabions are used as toe elements for the structures with a relative crest freeboard (R_c/H_s) larger than -0.8. The upslope length of the gabions compensates the increase in crest height such that the number of rows of armour elements at the slopes is constant. In the most submerged breakwater (relative crest freeboard (R_c/H_s) of -0.8) Xbases are used as toe elements. In total 14 rows of armour elements on each slope are used in each test.

Figure 5.2 Overall cross section



5.3.2. MATERIALS

The used materials in the different breakwater sections are described. The following breakwater sections are distinguished:

- core;
- underlayer;
- gabions;
- armour layer.

Core

The calculation of the rock size for the core is performed via the method proposed by BURCHARTH et al. 1999, see paragraph 5.2.3. The different cross sections and wave parameters (see §5.4) are of importance for the calculation of the core size material.

In general an higher wave steepness causes the size of the model core material to increase. This is due to the fact that the water in the core of the breakwater has less time to drain away before the next wave arrives compared to waves with a lower steepness (shorter wave period). Furthermore an increasing breakwater width leads also to an increasing size of the core material. The pore pressure gradient decreases with increasing distance from the bottom side of the under-layer. A decreasing gradient leads to lower flow velocities and increasing influence of resistance cause by the viscosity (decreasing turbulence). By increasing the core size material this can be prevented.

For the calculation a fictitious scale of 1:40 is assumed and a prototype core material with a D_{n50} of 0.21 m. The average D_{n50} for the different cross sections and wave parameters is calculated. For the model core a D_{n50} of 0,008 m is used with a grading of 1.62 (wide gradation).

Under-layer

Delta Marine Consultants recommends to use standard rock grading as specified in CUR/CIRIA and listed in the Xbloc design guidelines. If the use of this standard grading is not desired or cannot be applied, the following requirements are given:

$$\begin{aligned} W_{15} &\geq \frac{W_{Xbloc}}{15} \\ \frac{W_{Xbloc}}{11} &\leq W_{50} \leq \frac{W_{Xbloc}}{9} \\ W_{85} &\leq \frac{W_{Xbloc}}{7} \end{aligned} \quad (5.7)$$

The standard grading cannot be used in these model tests, therefore the above mentioned requirements are used:

$$\begin{aligned} W_{Xbloc} &= 62 \text{ g} \\ W_{15} &\geq 4,13 \text{ g} \\ 5,64 \text{ g} &\leq W_{50} \leq 6,89 \text{ g} \\ W_{85} &\leq 8,86 \text{ g} \end{aligned}$$

This results in a D_{n15} of 1.12 cm, $D_{n50} = 1.32$ cm and a D_{n85} of 1.5 cm.

Gabions

The gabions are filled with the same material as used in the underlayer, see Figure 5.3.

Figure 5.3 Gabions

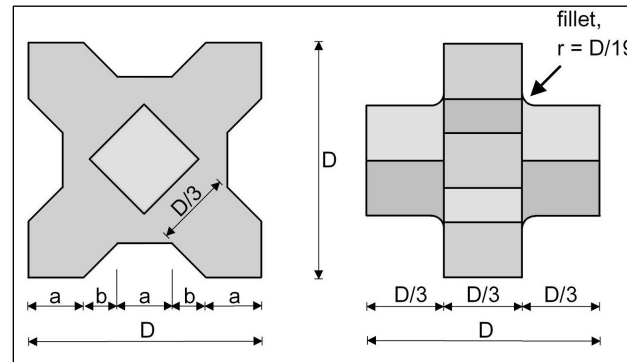


Armour layer

The Xbloc armour unit has an X shape base (four legs). On each side of the Xbase there are two noses. The specific shape gives the element interlocking capacities at all side of the unit. The shape and the dimensions are given in

Figure 5.4. The Xbase is a toe element which consists out of four legs (X shape base) and one nose.

Figure 5.4 Geometry Xbloc armour unit



Xbloc specifications

Xblocs with the specifications given in Table 5-3 are used in the tests.

Table 5-3 Parameters model and prototype Xbloc

Scale 1:40	Model breakwater	Prototype breakwater
D	4.3 cm	1.73 m
D_{n50}	2.98 cm	1.20 m
ρ_{Xbloc}	2339 kg/m ³	2400 kg/m ³

The Xbloc size in model cannot be scaled directly to prototype. The wave height is scaled with the scaling factor (1:40), due to the difference in specific weight of the model and prototype Xbloc, plus the difference in the specific weight of fresh and salt water, the size of the Xbloc is scaled with the aid of the stability number:

$$N_s = \frac{H_{s,m}}{\Delta_m \cdot D_{n,m}} = \frac{H_{s,p}}{\Delta_p \cdot D_{n,p}} \quad (5.8)$$

$$\Delta_m = \frac{\rho_{\text{Xbloc},m} - \rho_{\text{water},m}}{\rho_{\text{water},m}} \quad \Delta_p = \frac{\rho_{\text{Xbloc},p} - \rho_{\text{water},p}}{\rho_{\text{water},p}}$$

Placement density

For straight sections with a staggered placement pattern the packing density can be used to describe the quality of placement. Packing density provides an indication of the quality of the armour layer. If the placement pattern (staggered grid) and packing density are correct, the quality of the armour layer is likely to be in accordance with the specifications. The packing density is determined by measuring the distances between the centrelines of the units in x and y direction.

The relative placement density gives the ratio between the design packing density and the real (measured) packing density. The packing density should be between 98% and 105% of the design packing density [MUTTRAY *et al.* 2005]. This relative packing density is opted for all the breakwater sections (crest, seaward- and leeward slope)

The relative placement density can be calculated by equation (5.9).

$$RPD = \frac{(N_x - 1) \cdot (N_y - 1) \cdot dx \cdot dy \cdot D^2}{L_x \cdot L_y} \cdot 100\% \quad (5.9)$$

Where:

N_x	number of units in one row [-];
N_y	number of rows [-];
dx	1.3 [-];
dy	0.64 [-];
D	Xbloc unit height [cm];
L_x	length of row [cm];
L_y	length upslope [cm].

5.4. TEST PROGRAMME

A test programme for the described cross sections (§5.3.1) is formulated. The waves which will be used during the tests and the programme itself are worked out in respectively §5.4.1 and §5.4.2.

5.4.1. WAVES

First the wave height is calculated by which elements in a standard situation would be stable. A standard situation is referred to as a situation in which the slope is continues with an angle 3V:4H. Furthermore several (at least 3) rows of armour units have to be above the still waterline and none of the following situations are present:

- Foreshores steeper than 1:25;
- Concrete densities higher than 2500 kg/m³ and lower than 2350 kg/m³;
- Depth limited wave conditions (frequent occurrence of near design waves);
- Core with low permeability;
- Low-crested breakwaters ($R_c/H_s < 1$).

The model tests are performed with a Jonswap spectrum to generate the irregular waves. Every cross section is tested with two wave files each containing a different wave steepness.

Wave height

The wave height is calculated on the basis of the model Xbloc size with the stability number. The stability number is given as:

$$N_s = \frac{H_{s,m}}{\Delta_m \cdot D_{n,m}} \quad (5.10)$$

$$\Delta_m = \frac{\rho_{Xbloc} - \rho_{water}}{\rho_{water}}$$

With a stability number of 2.77 which is valid in standard situations for the Xbloc armour unit the significant wave height (or the design wave height) can be calculated.

$$2.77 = \frac{H_{s,m}}{2339 - 1000 \frac{H_{s,m}}{1000} \cdot 0.0298}$$

$$H_{s,m} = 0.1105 \text{ m}$$

The calculated wave height is the target wave height at the toe of the breakwater, but to generate the waves the wave height at the wave paddle is necessary. GODA 2000 developed a method which accounts for shoaling and breaking under the hypotheses of Rayleigh distributed irregular waves. Further GODA 2000 stated that, for the evaluation of the weight of armour stone at the shoreline, it may be safe to use the wave height at the depth of about $0.5 H_0$ for the areas shallower than that depth for the estimation of wave force and action on structures. In the case of these tests the water depth is larger than a half times the deepwater waveheight, thus the significant wave height at the toe of the structure can be used.

Fictitious wave steepness

Tests are performed with a fictitious wave steepness of 2% and 4%. In this manner the influence of varying wave steepness at low-crested structures can be compared to a standard situation, a long slope with a number of rows above the still waterline.

The fictitious wave steepness influences the type of wave breaking (see §2.3.1). The Iribarren number is used to give an idea of the type of wave breaking which can be expected, for waves with a steepness of 4% collapsing/surging breaker occur, waves with a steepness of 2% gives surging breakers. The classification used for wave breaking do not incorporate the influence of the overtopping waves.

The fictitious wave steepness is held constant during model tests, thus by increasing the wave height the wave period also increases (see equation (2.2)). The wave period remains constant during the wave propagation towards the breakwater; the wave period at the toe of the breakwater is the same as at the wave paddle.

The wave period is scaled according to Froude scaling, which results in:

$$T_p = T_m \cdot \sqrt{N_L} \quad (5.11)$$

Due to the fixed water level in the wave flume for all test series, only two wave files are needed, one for the 2% wave steepness and one for the 4% wave steepness. The advantage is that in all the test series the same wave file can be used and no large differences occur between the wave parameters.

Wave spectrum

To approach reality as best as possible irregular waves are used during the test series. There are various spectra available to model the irregular waves of a sea state, for instance the Jonswap spectrum for young sea states and the Pierson-Moskowitz spectrum for fully developed sea states. Because a fully developed sea state hardly ever occurs along the coast where breakwaters are located, because of the limited fetch and duration of a storm the Pierson-Moskowitz

spectrum is not a very realistic spectrum for coastal areas. Therefore tests are performed with the Jonswap spectrum to simulate a young sea state. The Jonswap energy density spectrum is given by:

$$E_{JONSWAP}(f) = \alpha \cdot g^2 \cdot (2\pi)^{-4} \cdot f^{-5} \cdot \exp\left[-\frac{5}{4} \cdot \left(\frac{f}{f_{peak}}\right)^{-4}\right] \cdot \gamma \cdot \exp\left[-\frac{1}{2} \cdot \left(\frac{f/f_{peak}-1}{\sigma}\right)^2\right] \quad (5.12)$$

In which:

E variance density [m²/Hz]

f frequency [Hz]

f_{peak} peak frequency [Hz]

g gravitational acceleration [m/s²]

α scaling parameter (Pierson-Moskowitz) [-]

γ scaling parameter (Jonswap peak-enhancement factor) [-]

σ scaling parameter (Jonswap peak-enhancement factor) [-]

σ = σ_a for f ≤ f_{peak}

σ = σ_b for f > f_{peak}

For the standard Jonswap spectrum the following holds:

σ_a = 0.07

σ_b = 0.09

γ = 3.3

The wave spectrum, generated in the experiments, is expected to be similar with the theoretical Jonswap wave spectrum. For narrow banded spectra in deep water H_{m0} is approximately equal to significant wave height (H_s) and is often referred to as the significant wave height. From the spectrum the significant wave height can be retrieved by:

$$H_{m0} = 4\sqrt{m_0} \quad (5.13)$$

In which:

$$m_0 = \int_0^{+\infty} E(f)df \quad (5.14)$$

5.4.2. PROGRAMME

A tests series consists of a number of tests in which the wave height is gradually increased until failure occurs. The wave height in a test is held constant, further each test lasts 1000 waves. The wave steepness is a constant, thus the peak period can be calculated, from which the test duration can be deduced from.

Based on Xbloc design table for standard breakwaters the wave height in the test series is increased in steps of 20% of the design wave height (H_d), starting from 60% of H_d up to a wave height which initiates failure. The tested structure is low-crested which means wave energy can overtop the breakwater; a 20% larger wave height does not automatically increase the load on the breakwater by 20%.

The different tests to execute are presented in Table 5-4.

Table 5-4 Programme test series
 S_0 fictitious wave steepness
 R_c/H_s relative crest freeboard

Crest width R_c/H_s	3 armour units $S_0 = 2\%$		9 armour units $S_0 = 2\%$	
	$S_0 = 2\%$	$S_0 = 4\%$	$S_0 = 2\%$	$S_0 = 4\%$
- 0.8	AI_2	AI_4	AII_2	AII_4
- 0.4	BI_2	BI_4	-	-
0	<i>CI_2 (4x)</i>	<i>CI_4 (4x)</i>	CII_2	CII_4
0.4	DI_2	DI_4	-	-
0.8	EI_2	EI_4	EII_2	EII_4

Explanation abbreviation: crest freeboard_crest width_wave steepness_serial number
 The italic printed tests are referred to as the reference test series.

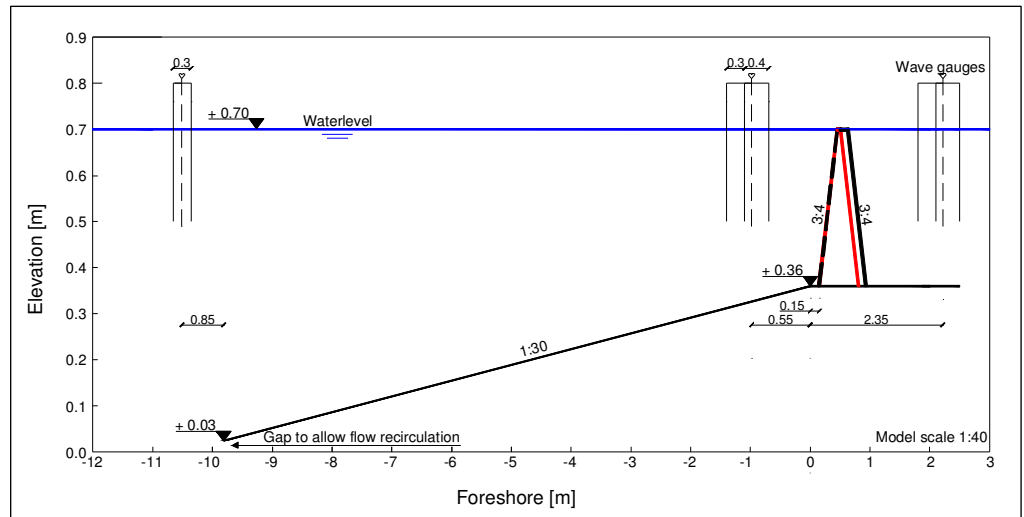
The breakwater cross section with crest freeboard of zero and three armour unit's wide crest is referred to as the reference cross section. Test series executed at the reference cross section are performed four times. In total eight reference tests because of the different wave steepness's. Other tests are performed once.

5.5. MEASUREMENTS

5.5.1. WAVES

In front and at the leeside of the breakwater two sets of three wave gauges are placed, this enables the measurement of waves. From the measurements of the waves the incident and reflected waves can be calculated, also the wave transmission can be calculated. In front of the foreshore also two wave gauges are present.

Figure 5.5 Location wave gauges



In many laboratory studies it is desirable to separate the measured wave train into its incident and reflected wave components so that model response can be related to parameters of the incident wave train. Therefore the surface elevation is measured with wave gauges.

The signal from the wave gauges is analysed with the program WAVELAB which is developed at the University of Aalborg. The program uses the method of MANSARD AND FUNKE 1980 for the reflection analysis of irregular waves.

The method requires a simultaneous measurement of the waves at three positions in the flume in reasonable proximity to each other and on a line parallel to the wave propagation. For the spacing between the gauges the following is recommended:

$$X_{1-2} = \frac{L_p}{10} \quad (5.15)$$

$$\frac{L_p}{6} < X_{1-3} < \frac{L_p}{3} \quad \text{and} \quad X_{1-3} \neq \frac{L_p}{5} \quad \text{and} \quad X_{1-3} \neq \frac{3 \cdot L_p}{10}$$

For the distance between the wave gauges there is according to equation (5.15) no single value recommended as the peak wave length for each run is different. A spacing of 0.3 m between the first and second gauge and 0.7 m between the first and third gauge is chosen (see Figure 5.5).

5.5.2. XBLOC MOVEMENT AND DISPLACEMENT

For single layer concrete armour units two types of failure can be distinguished; movement of one or more armour units and breakage of armour units. A broken unit may lose his function due to reduction of the gravitational force and possible interlocking effect. The broken parts can cause further breakage of other units, because they are thrown around by the waves. Movement according to BURCHARTH 1993 can be divided in:

- no movement;
- rocking;
 - incidental movement;
 - regular movement;
 - continuous movement.
- displacement of single armour unit from initial position, distance from original position between 0.5 D and 1.0 D;
- displacement > 1.0 D. Unit is said to be removed from the armour layer;
- sliding of multiple units; settlement entire or part of the armour layer.

In these tests the following definitions are used to characterize damage:

- Rocking, continuous and regular movement of armour units;
- start of damage, displacement of 1 armour unit from the armour layer (1 armour unit removed);
- failure, displacement of 10 armour units from the armour layer (10 armour unit removed);

The dislocation of one armour unit is characterised as start of damage. Around the displaced armour unit settlements occur and no further damage will occur at that location. However settlements lead to a fractured armour layer at the transition from the seaside slope to the crest in the case of low-crested structures.

General there are two ways to present the number of displaced armour units by more than one unit dimension, by the damage numbers N_d and N_{od} . N_d presents the number of displaced units as a percentage of the total number of units within a reference area. Van der Meer uses a different definition of damage, N_{od} . The damage is the number of displaced units out of the armour layer

within a strip with the width of the nominal diameter (D_n). For this research the method of Van der Meer is applied.

$$N_{od} = \frac{\text{number of displaced units}}{\text{width armour layer} / D_n} \quad (5.16)$$

The width of the wave flume is used as the width of the armour layer. The damage after each test is determined and photographed from a fixed position. In this way settlements and damage development is recorded. Two video cameras have been used to monitor the tests.

5.6. PERFORMED TESTS

In §5.6.1 the divergent tests from the original test programme are described. In §5.6.2 and §5.6.3 the relative placement density and the placement of the crest elements are described of the performed tests.

5.6.1. DIVERGENT TESTS FROM ORIGINAL TEST PROGRAMME

The actual performed tests are described below, the original test programme is given in Table 5-4 once more.

Table 5-5 Programme test series
 S_0 fictitious wave steepness
 R_c/H_s crest freeboard

Crest width R_c/H_s	3 armour units		9 armour units	
	$S_0 = 2\%$	$S_0 = 4\%$	$S_0 = 2\%$	$S_0 = 4\%$
- 0.8	AI_2	AI_4	AII_2	AII_4
- 0.4	BI_2	BI_4	-	-
0	CI_2	CI_4	CII_2	CII_4
0.4	DI_2	DI_4	-	-
0.8	EI_2	EI_4	EII_2	EII_4

Explanation abbreviation: crest freeboard crest width_wave steepness_serial number
 The italic printed tests are referred to as the reference test series.

As can be seen in Table 5-6 a number of tests are performed which are not in the original test programme. Tests in the first row of Table 5-6 have a clamped placement of the armour elements on the crest (see §5.6.3), because this is not a very realistic placement these tests are re-done.

Cross section DI was the least stable cross section of all tests with a small crest width, therefore test EII is replaced by DII.

Table 5-6 Performed tests

crest width	cross section A		cross section B		reference cross section C		cross section D		cross section E	
	AI_2	AI_4	BI_2	BI_4	CI_2	CI_4				
small	AI_2_1	AI_4_1	BI_2_1	BI_4_1	CI_2_1	CI_4_1	DI_2	DI_4	EI_2	EI_4
					CI_2_2	CI_4_2				EI_4_1
					CI_2_3	CI_4_3				
					CI_2_4	CI_4_4				
wide	AII_2	AII_4			CII_2	CII_4	DII_2	DII_4		
	AII_2_1									

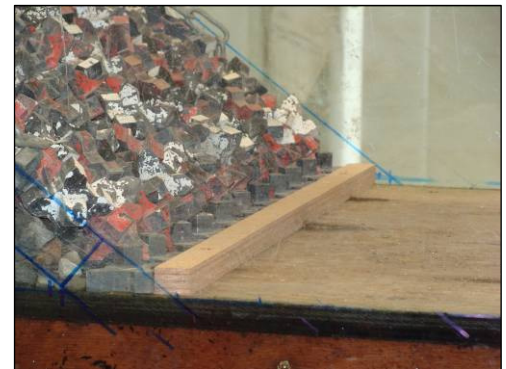
In test EI_4 the lowest positioned elements on the seaside slope lost their stability (see Figure 5.6), probably caused due to the missing interlocking between the gabion and the Xbloc. The damage continued to both sides of the slope and in upslope direction until complete failure occurred. The test is performed once more because this type of failure is not likely to occur, the wave forces are maximal around the still waterline and the resistance of the armour units minimal (see §4.2.2)

Figure 5.6 Damaged armour layer, lower positioned element, seaside slope.



In test AII_2 the Xbases displaced a significant distance resulting in excessive settlements in the armour layer of the leeward slope. The test is executed again (test AII_2_1) with fixed Xbases in lateral direction (see Figure 5.7).

Figure 5.7 Lateral displaced Xbases, test AII_2, fixed Xbase toe elements, test AII_2_1.



5.6.2. RELATIVE PACKING DENSITY

The quality of the placement is determined by the packing density and the interlocking. The packing density is measurable whereas interlocking can only be assessed by visual inspection, TEN OEVER *et al.* (2006).

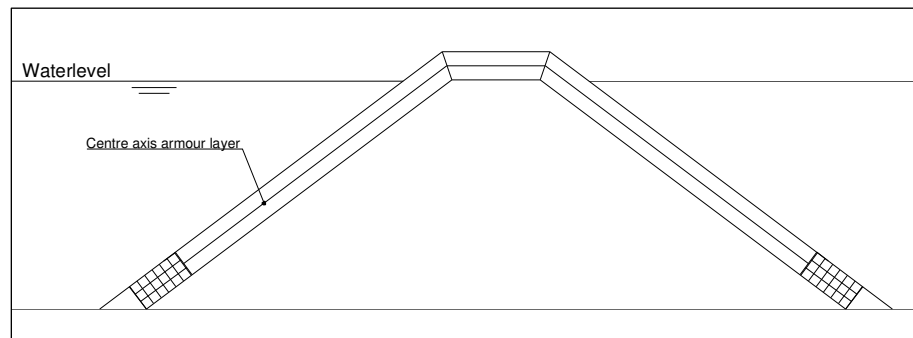
The relative placement density should be in between 98% and 105%. This is the opted relative placement density for all the breakwater cross sections. Theoretically it is possible to measure the relative placement density (see equation (5.9) in the model. However it appeared to be quite difficult because a small deviation in the measurement of the row- and upslope lengths gives an unrealistic relative placement density. The model scale is too small to obtain a reliable measurement of the relative placement density. Therefore the mean theoretical relative placement density is used. The total length of the centre

axis of the armour layer is calculated and with the number of rows known the mean theoretical relative placement density can be determined.

For the cross sections B to E the main point of the first Xbloc (above the gabions) on the slope is located $0.5 D$ above the gabions. Therefore in total $1 D$ has to be subtracted of the total length of the centre axis of the armour layer for the calculation of the total length of the centre axis.

In the case of cross section A this is not necessary, the first main point of the Xbloc on the slope is positioned where the under layer starts.

Figure 5.8 Calculation centre axis armour layer



The obtained mean theoretical relative placement densities are given in Table 5-7.

Table 5-7 Mean theoretical relative placement density

RPD [%]	cross section A		cross section B		Reference cross section C		cross section D		cross section E		
	var.	AI_2	AI_4	BI_2	BI_4	CI_2	CI_4				
103		AI_2_1	AI_4_1	BI_2_1	BI_4_1	CI_2_1	CI_4_1	DI_2	DI_4	EI_2	EI_4
						CI_2_2	CI_4_2				EI_4_1
						CI_2_3	CI_4_3				
100					CI_2_4	CI_4_4					
100		AII_2	AII_4			CII_2	CII_4	DII_2	DII_4		

Firstly the armour layer is applied on both the seaward- and leeward slope, next the crest armour units are placed. Because the crest elements are placed last the remaining space is filled with Xbloc armour units. This led in the case of tests BI_2, BI_4, CI_2 and CI_4 to an additional four element in the middle row of the three elements wide crest. In the case of test AI_4 an additional two elements were needed and for AI_2 two complete rows of additional armour units were needed. The additional armour units are required due to a slightly higher placement density on the slopes.

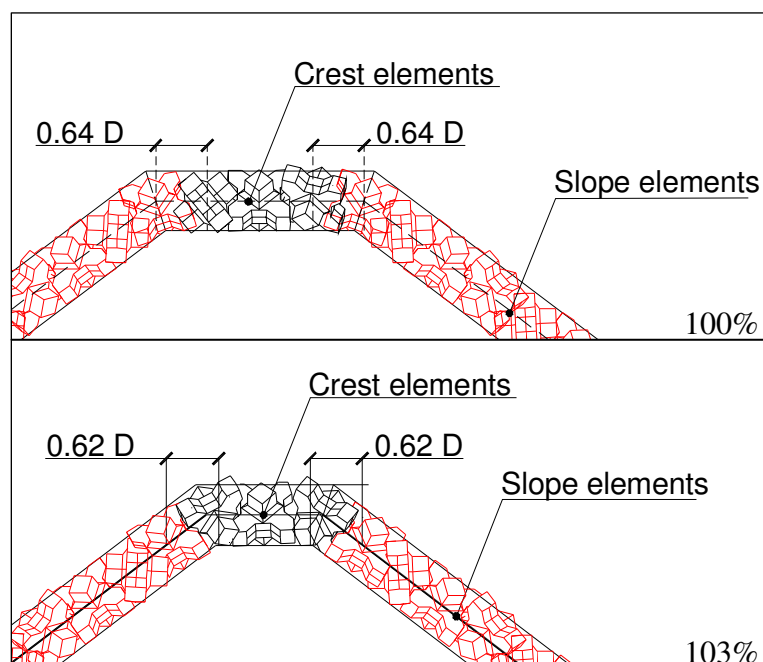
5.6.3. PLACEMENT CREST ELEMENTS

The placement of the Xbloc elements at the breakwater crest is carried out in the same way as at the breakwater slopes. The Xbloc elements are lifted by one of the legs and set down on one of the noses or one of the other legs. At the breakwater slopes the elements are placed on top of the previous (lower positioned) elements without forcing the element into a definite position into the armour layer. On horizontal sections the element is forced between the two preceding elements without dislocating them. But due to the lacking horizontal

force component the elements are not clamped between each other like on the slopes. The crest elements in the tests presented in the first row of Table 5-7 are placed clamped to each other. With clamped placement freedom of (little) movement is impossible, all elements are forced into position and are therefore clamped together, no movements is possible. But by placing the clamped elements the preceding elements are moved from their original position. This makes clamped placement not a very realistic or advisable one.

The crest elements in tests performed with small crest widths and relative placement densities of 103% have a different position than the elements placed in tests with a 100% relative placement density (Figure 5.9). When settlements on the breakwater slope occur, the outside crest elements in the case of a 103% relative placement density will follow these settlements in contrast to the tests with 100% relative placement density.

Figure 5.9 Placement crown elements for 100% and 103% relative placement density respectively.



5.7. HYDRODYNAMICS

The water depth in all test series is kept constant, therefore two wave files are sufficient to generate waves with a steepness of 2 and 4%. Within each wave file different significant wave heights (ranging from 60% H_d up to 180% H_d) can be selected for different tests. The wave files are converted into sea files such that the wave generator is able to reproduce the target waves. If the generator is not capable of generating the complete spectrum, the maximum wave height cuts off by a definite percentage. The two wave files used are cut off for tests with the higher waves in the test series, see Table 5-8.

Table 5-8 Clipped wave energy [%]

Opted waveheight	140% H_d (13.67 cm)	160% H_d (15.46 cm)	180% H_d (16.76 cm)
2% wave file	9	30	45
4% wave file	10	22	32

Table 5-8 shows significant clipped waves in the wave files for wave heights larger than 140% of the design wave height. The wave heights are smaller than the target wave heights. Rocking in the model tests occurred before 140% H_d .

5.7.1. WAVEHEIGHT

The target wave height and the measured mean significant (of all test series) incident wave height in front of the structure are (see §5.5 for the position of the wave gauges) given in Table 5-9, the measured wave heights for all individual test series are given in Appendix E.

Table 5-9 Measured mean (of all test series) incident waveheight and the target wave height

Wave file	H_s								
	2% + 4%	target	H_s (cm)	6.64	8.85	11.06	13.27	15.48	17.69
% H_d			60	80	100	120	140	160	180
4%	measured	H_{m0} (cm)	6.69	8.76	10.58	12.15	13.67	15.46	16.76
		% H_d	60	79	96	110	124	140	152
2%	measured	H_{m0} (cm)	6.44	8.37	8.96	10.70	12.37	14.46	16.90
		% H_d	58	76	81	97	112	131	153

Table 5-9 shows the measured and target wave heights, expressed in centimetres and as percentage of the design wave height for the applied Xbloc (11.06 cm). As can be seen in Table 5-9 the target wave heights are not reached. The wave height is not adapted during the tests because the damage criteria are reached, moreover if the wave height would have been adapted the more the wave energy would have been clipped, leading to an incorrect representation of the Jonswap spectrum.

5.7.2. WAVE STEEPNESS

Table 5-10 shows the calculated fictitious wave steepness and the measured mean (of all test series) wave height and period for the to wave files. Since the wave height is lower than anticipated for (increasing deviance for test with higher significant waves in the test series) and the wave period is approximately in accordance with the initial desired one, the wave steepness changes. This leads to decreasing wave steepness's for tests with higher waves in the test series.

Table 5-10 Measured mean wave period and target wave period

Wave file	H _s								
	4%	target	H _s (cm)	6.65	8.85	11.03	13.28	15.48	17.7
T _p [s]			1.03	1.19	1.33	1.46	1.58	1.68	1.79
measured		H _{m0} [cm]	6.69	8.76	10.58	12.15	13.67	15.46	16.76
		T _p [s]	1.02	1.22	1.33	1.46	1.6	1.73	1.8
		s ₀ [-]	0.041	0.038	0.038	0.037	0.034	0.033	0.033
2%	target	H _s [cm]	6.6	8.8	10.98	13.15	15.3	17.5	19.55
		T _p [s]	1.46	1.68	1.88	2.06	2.23	2.38	2.53
	measured	H _{m0} (cm)	6.44	8.37	8.96	10.7	12.37	14.46	16.9
		T _p [s]	1.46	1.73	1.94	2.13	2.21	2.42	2.58
		s ₀ [-]	0.019	0.018	0.015	0.015	0.016	0.016	0.016

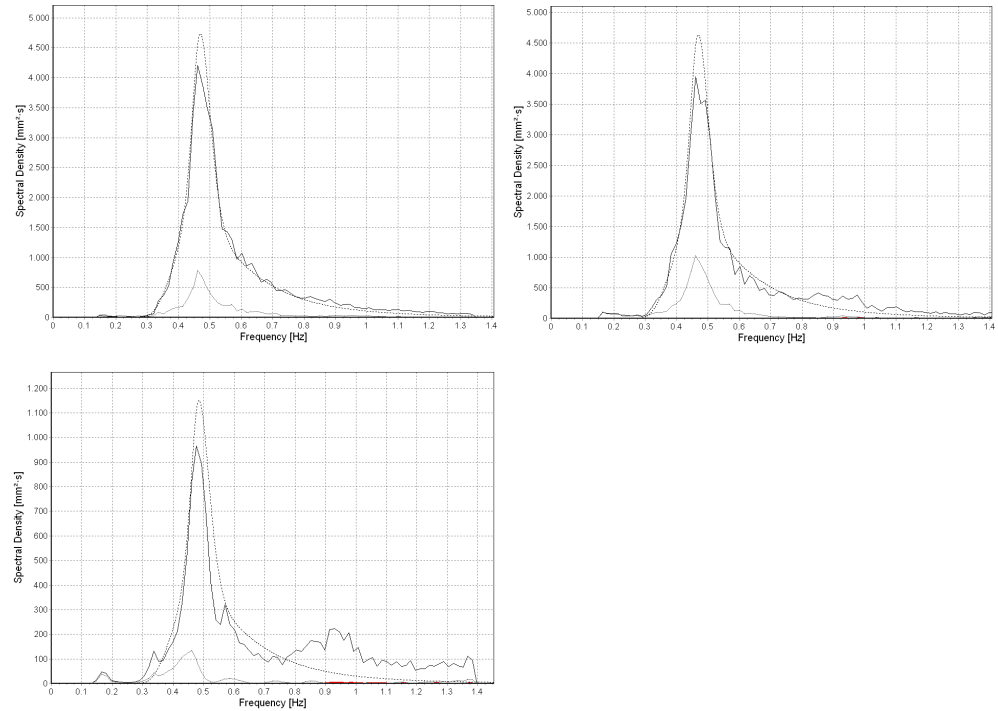
5.7.3. SPECTRUM AND WAVEHEIGHT DISTRIBUTION

Several spectra are presented to check the generated spectra with the theoretical Jonswap spectra. In addition, the transmitted spectra are of importance, the wave transmission coefficients only contain information about the wave heights behind the structure. The spectrum contains wave period information, which is often required for the calculation of morphological changes, wave run-up or overtopping at structures behind a low-crested structure. Wave height distributions give information on the probability of occurrence of the highest (measured) waves.

For each test with a different cross section and wave steepness, the wave height distributions and spectra are plotted for the design wave height of the Xbloc, see Figure 5.10 and Figure 5.11. This is done for three locations in the wave flume (where the wave gauges are located, see §5.5). In Appendix G the wave spectra of the reference situation for all tests in the test series CI_2_1 and CI_4_1 are plotted for the wave gauges located in front of the structure.

Energy density spectrum

The figures in which the incident spectra (solid line) are plotted also show the Jonswap spectra (dashed line) and the reflected spectra (dotted line). For the Jonswap spectra the measured significant wave height and period are used, the peak enhancement coefficient is 3.3. As an example in Figure 5.7 the spectra for cross section CI_2_1 at three different locations are shown.

Figure 5.10 Spectra
CI_2_1

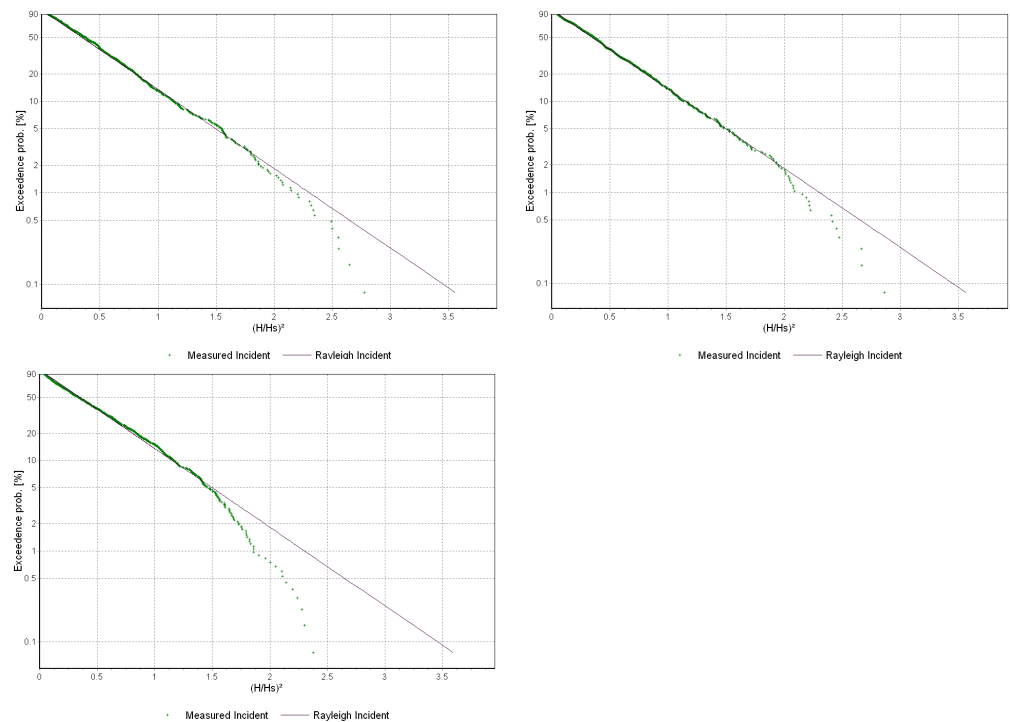
In Appendix G the clipped wave energy is clearly visible for the tests with waves higher than 120%. It is unlikely that the difference between the Jonswap spectrum and the measured incident spectrum is completely caused by wave breaking, because the ratio $H_s/h = 0.48$ in case the highest significant wave height in a test series is used. The new peak in the spectrum for the highest significant wave height indicates that some wave breaking is nevertheless present.

Waveheight distribution

The wave height distribution is plotted with the measured waves, the plus-signs represents the measured waves. The solid line depicts the Rayleigh distribution. The wave height distribution is measured at the locations of the wave gauges.

The Rayleigh distribution does not apply in shallow water where wave heights are limited due to forced wave breaking when the height exceeds approximately 0.8 times the water depth. Also the significant wave height is restricted by the water depth, on a flat sloping seabed the maximum wave height H_s will be approximately 0.6 times the water depth. Furthermore, the spectrum has to be very narrow ($\epsilon \rightarrow 0$) to approach the Rayleigh wave height distribution. If the spectrum is very wide ($\epsilon \rightarrow 1$) the wave height distribution approaches a Gaussian distribution.

Figure 5.11 Rayleigh waveheight distribution and measured wave height CI_2_1



In Figure 5.11 and in Appendix F the wave height distribution is plotted for the design wave height of the Xbloc. The last wave height distribution in Figure 5.11 represents the transmitted waves, therefore the deviation of the Rayleigh wave height distribution can be quite large. From these figure the highest measured wave can be retrieved.

The wave height distribution approaches the Raleigh distribution for tests with lower ($60\% H_d$) wave heights. Tests with increasing wave heights shows that the wave height distribution deviates increasingly of the Rayleigh type of distribution. This suggests that wave breaking does play a role.

5.7.4. WATER LEVEL SET UP BEHIND BREAKWATER

Set-up (of the water level) behind the breakwater can occur in the case of low-crested structures. Set-up (in 2-D model tests) is a mechanism which influences the stability of the armour layer by the return current over the crest, and is therefore of interest for this study. In real cases (for example stretches of shore protected by low-crested structures) this phenomenon is not observed, as the potential piling-up behind the breakwater is relieved by 3-D circulation systems (see 5.3.1). Set-up is tried to prevent by an opening at the rear end and a small gap at the beginning of the foreshore. The set-up for the tested cross sections was limited.

6. GENERAL OBSERVATIONS

The hydraulic processes which results from wave interaction with the breakwater are described in §6.1 these processes together with the incident waves form the loading of the armour layer. Subsequently the following observations are described:

- settlements armour layer (§6.2);
- Xbloc crest elements (§6.3);
- Xbloc slope elements (§6.4).

In paragraph 6.5 the conclusions regarding the observations are described.

6.1. HYDRAULIC PROCESSES

The performance of the Xbloc armour unit is closely correlated with the loading. The loading consists of the incident waves and the hydraulic processes as a result of wave interaction with the breakwater. The location and the extent of loading varies with crest freeboard, crown width and wave steepness. The influences of these parameters on the following hydraulic processes are described:

- water flow over breakwater crest (§6.1.1);
- wave breaking (§6.1.2);
- transmitted wave (§6.1.3).

6.1.1. FLOW OF WATER OVER BREAKWATER CREST

As a consequence of overtopping and propagating (breaking) waves two types of water flow over the crest are observed:

- water flow in landward direction;
- water flow in seaward direction.

The water flow has a large influence on the Xbloc units on the crest.

Water flow in landward direction

The flow in landward direction is caused by the propagating and overtopping waves. The incident waves cause wave run-up and run-down, if the slope is not long enough and the crest not wide enough the waves overtop the breakwater (see Figure 6.1) and a flow in landward direction originates. Also for submerged breakwaters this water flow is present

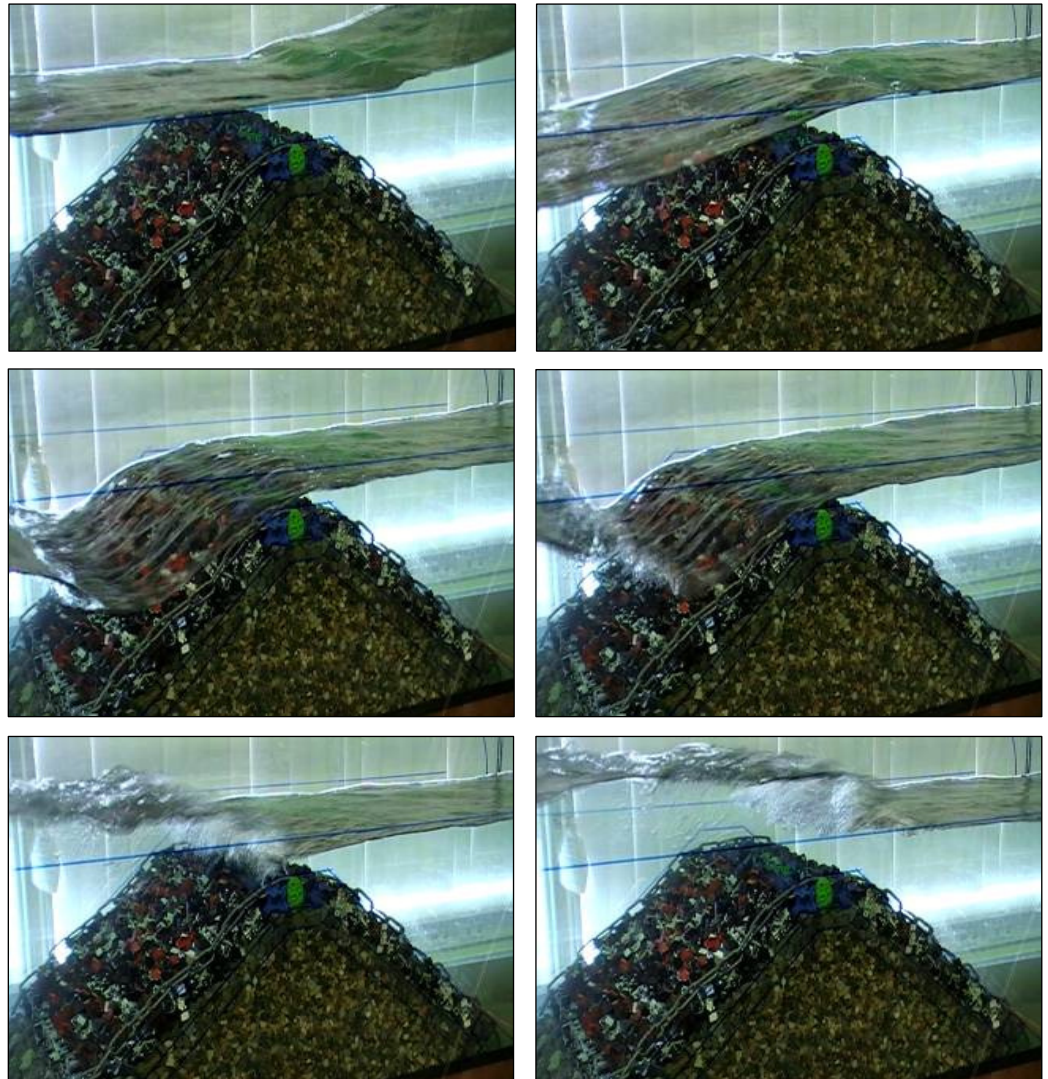
Figure 6.1
Overtopping wave for
cross section EI



Flow in seaward direction

A current in seaward direction over the crest of the breakwater develops as a result of a wave trough in front of the breakwater and a water level equal to the still water line at the leeside. Sometimes also a raised water level at the leeside is present due to a passing incident wave crest. Figure 6.2 shows the current development over the breakwater crest for different moments in time for a significant wave height of 14.4 cm and a wave steepness of 2%. The magnitude of the current becomes smaller for decreasing wave heights (constant wave steepness) and increasing wave steepness's. The influence of the inertia term of the water flow increases for higher wave steepness's, therefore the water flow develops less.

Figure 6.2 Current in
seaward direction
over breakwater crest
for test series BI_2



The observed water depth on the crest becomes smaller near the seawards crests edge. With the assumption that not much water above the crest flows into the breakwater, the flow velocity becomes critical (maximal) near the seawards crests edge.

Figure 6.3 Waterflow in seaside direction for a wide crested breakwater



For the wide crested breakwaters also a water flow in seaward direction occurs but it is less severe (see Figure 6.3). This can be explained by the fact that the column of water above the crest is larger than for small crested breakwaters. Therefore the influence of the inertia term increases. Additionally the gradient over a wide crested breakwater is smaller than is the case for a small crested breakwater. The difference in water level at the lee- and seaside of the breakwater is the same for both wide- and small crested breakwaters whereas the crest width differs.

6.1.2. WAVE BREAKING

The different crest freeboards of the breakwater are obtained by varying the breakwater crest height instead of the water level. In this manner waves at the breakwater toe are similar for all tests.

In the case of low-crested breakwaters the type of wave breaking cannot fully be described according to the surf similarity parameter, because the wave structure interaction is different for a low-crested type of breakwater than for a conventional one. Therefore the breaking waves are described based on observations, supplementary to the surf similarity parameter.

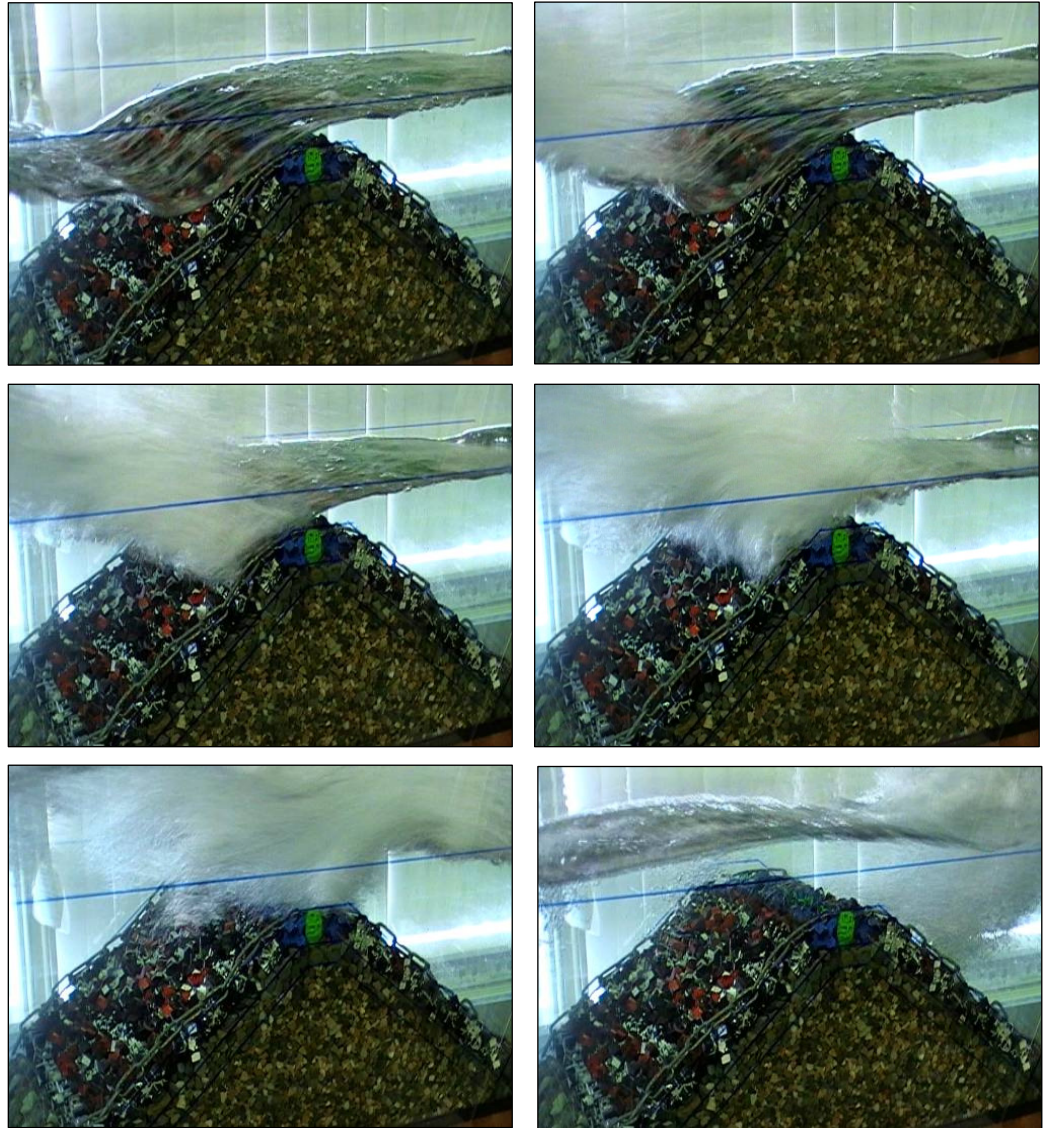
First of all wave breaking at the foreshore is described and subsequently at the breakwater.

Foreshore

For the 2% and 4% waves spilling breakers at the foreshore are observed in the case of wave heights of 160% and 180% H_d . For smaller wave heights no wave breaking is observed.

For emerged structures the spilling breakers hits the seaside slope. Whereas in the case of zero and negative crest freeboard the spilling breaker runs into the upper part of the seaside slope and/or the crest, depending on the preceding wave trough. In the case of a preceding wave trough which is not deep, the load is concentrated at the crest section. This load at the seaside slope and crest is decreased due to a water cushion (for submerged breakwater), formed by the water flow over the crest in seaward direction, see Figure 6.4.

Figure 6.4 Water cushion between spilling breaker (from the foreshore) and breakwater crest, seaside slope

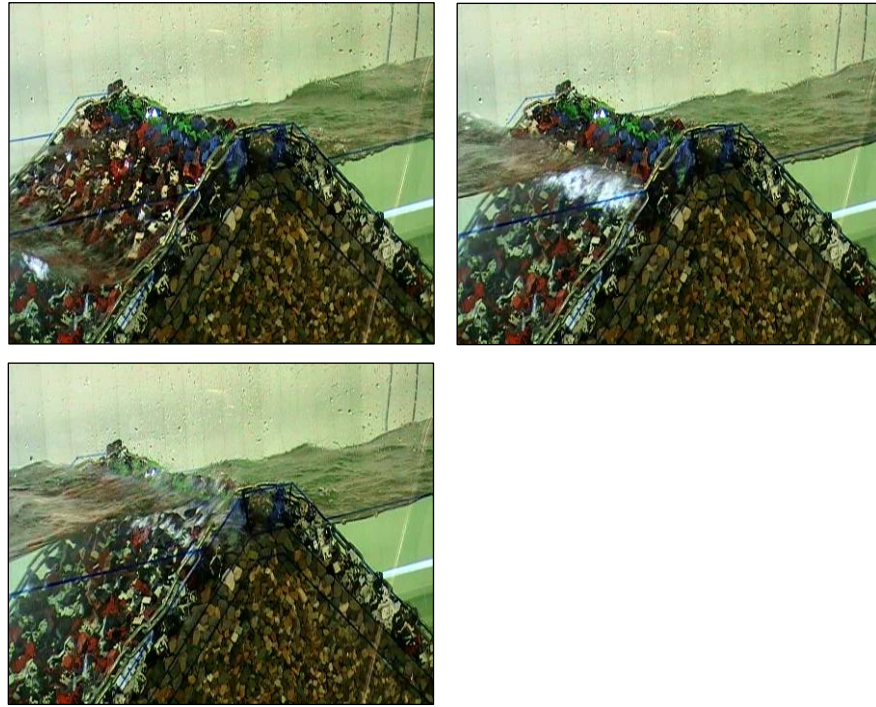


Breakwater

The type of wave breaking at the breakwater is determined by the geometry of the breakwater (crest freeboard, crest width) and the wave parameters (wave height, wave steepness). In the case of the tested cross sections the crest freeboard, crest width and wave steepness are the most important parameters.

Surging breakers are observed for the 2% wave file and collapsing/surging breakers for the 4% wave file (see Figure 6.5) in the case of positive crest freeboard. For negative crest freeboards waves with a steepness of 2% get steeper and sometimes a collapsing breaker is formed as a consequence of the current in seaward direction. The 4% waves break more frequently due to their higher steepness but the observed influence of the water flow in seaward directions on the wave breaking is less than is the case for the 2% waves. For tests with wide crests more wave breaking is observed for both the 2% and 4% wave file.

Figure 6.5 Collapsing breaker (test DI_4_100)



The point of wave breaking shift from the seaside slope for positive crest freeboards to the leeside slope for negative crest freeboards. Due to the submergence (water cushion) no direct loading of the leeside armour layer takes place, as is the case for the seaside slope of emerged structures. The overtopping waves for the tested emerged breakwaters never impinge on the leeside slope, it seems that the leeside slope is steeper than the path that the overtopping wave follows (see Figure 6.6).

Figure 6.6 Overtopping wave (the white lines show the path of the overtopping wave and the leeside slope)

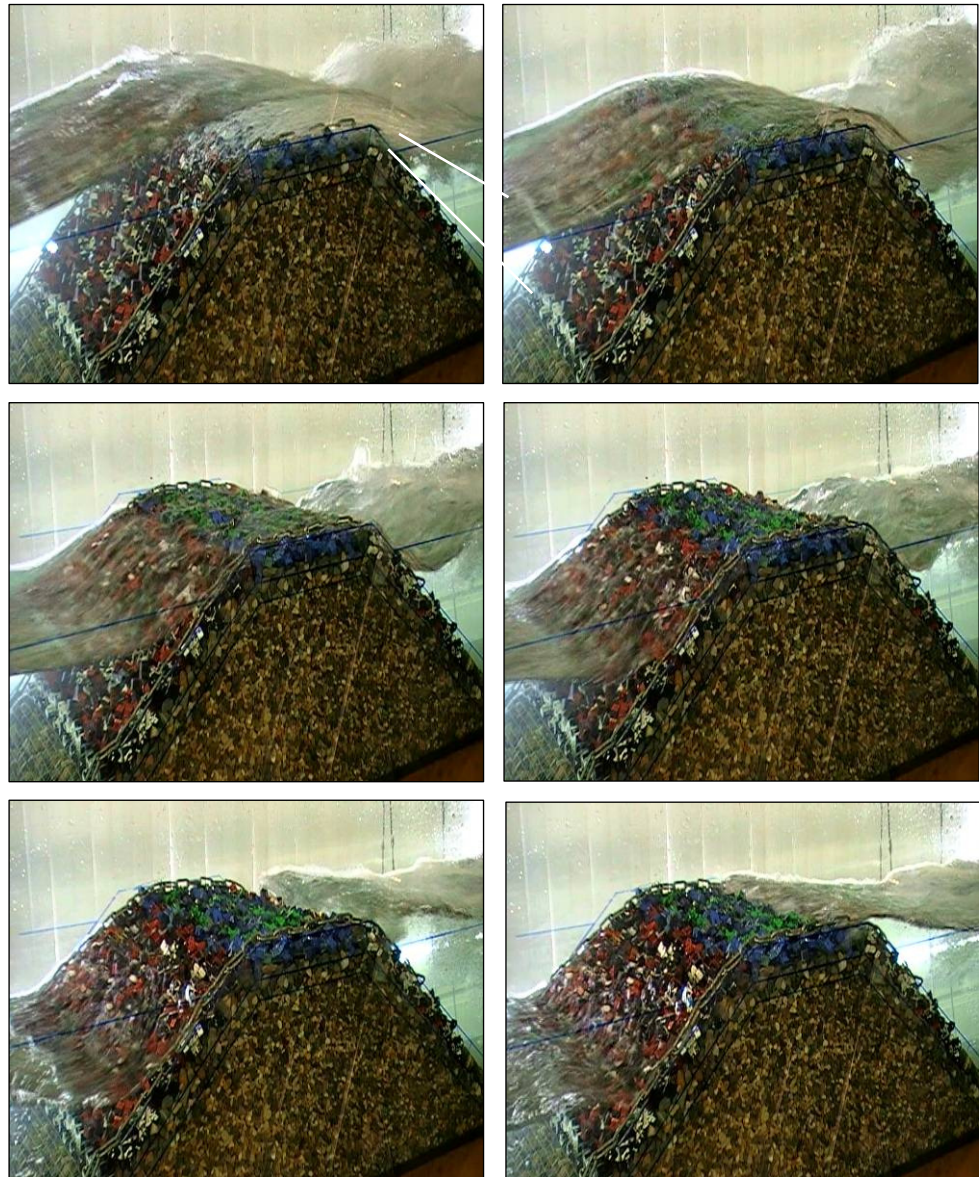


For positive crest freeboards the incident wave only interacts with the breakwater, whereas in addition to that, for negative crest freeboards, the interaction of the incident waves with the water flow in seaward direction becomes important. Due to shoaling the water particles gain a velocity in landward direction. As a result of the water flow in seaward direction the velocity and or the direction of the water particles changes. A situation originates in which the top side of the wave still has an initial velocity in landward direction whereas in the lower part of the wave the velocity and or the direction deviate from the initial situation leading to breaking waves.

6.1.3. TRANSMITTED WAVES

For positive and zero crest freeboard two transmitted waves are observed, one propagating into landward direction and the other in seaward direction. Due to the non perpendicular impact of the water jet like overtopping wave, two in opposite propagating waves originate. The wave which propagates into landward direction is the biggest one, see Figure 6.7. The overtopping wave does not directly load the leeside slope as already described in §6.1.2. The transmitted wave which propagates into seaside direction overtops the breakwater regularly for structures with zero crest freeboard and occasionally for emerged breakwaters in the case of wave heights in the order of 160% to 180% H_d .

Figure 6.7
Overtopping wave,
the forming of two in
opposite propagating
waves



6.2. SETTLEMENTS ARMOUR LAYER

In this section firstly the observed settlements in the armour layer are discussed and subsequently the consequences for the stability of the armour layer of low-crested structures (§0).

The settlements completely originate from the armour layer except for the most submerged tested cross section (cross section A). For this cross section Xbase toe elements are used, whereas for the other cross sections fixated gabions are applied.

To correctly represent settlements in model scale a number of parameters are of importance under which:

- the loading of the armour layer in model scale has to be identical to that of prototype scale.
- the roughness of the under layer which depends on the shape and size of the material;
- friction coefficient (μ) of the model Xbloccs which has to be identical to that of the concrete prototype armour units to correctly represent inter-block friction [DORRINGTON METTAN 1980];

The under layer is identical to that of in prototype scale, whereas the loading is and the friction coefficient are different. The loading of the armour layer can not fully be modelled according to prototype scale; therefore in general some simplifications are made which are insuperable. The friction coefficient of plastic model units is smaller than for concrete model units, however to what extent is not known. Therefore the extent of settlements (and the hydraulic stability) shows conservative values.

The total settlements in the armour layer are composed of two parts:

- Initial settlements, which are defined as the settlement of several rows of armour units at the same moment in time and occur for relatively small wave heights (60% to 80% H_d). The whole armour layer settles at once which makes initial settlements well perceptible by eye (§6.2.1).
- Ongoing settlements, occur after the initial settlements have taken place and are characterized by their gradual occurrence throughout the tests. These settlements proceed until equilibrium is found between the resistance to settlements and the load from wave action. Due to their gradual occurrence they are not perceptible by eye, trough photos which are taken from exact the same location before and after each test the settlements are perceptible (§6.2.2).

6.2.1. INITIAL SETTLEMENTS

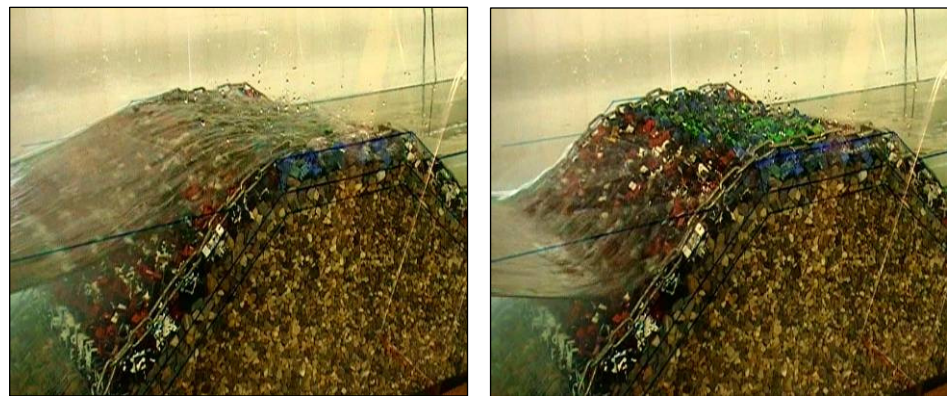
Initial settlements are observed mostly for emerged breakwater at the seaside slope whereas for the most submerged tested breakwaters initial settlements are not observed. This is caused due to the fact that the total acting wave energy at the seaside slope for submerged breakwaters is significantly smaller than for emerged breakwaters. For that same reason no initial settlements are observed

at the leeside slope. Further no difference between the tested small and wide crown breakwaters is observed.

Concerning the wave parameters initial settlements are observed more for tests with a wave steepness of 2% than 4%. Furthermore the observed extent of initial settlements is larger in case of 100% relative placement density than in the case of 103% relative placement density.

Initial settlements are caused by a high wave in the spectrum followed by a deep down rush motion (see Figure 6.8). The down rush motion loads the Xbloc elements by a drag force parallel to the seaside slope and gives rise to settlements in the armour layer. Since for emerged breakwaters not much wave overtopping takes place all wave is still present in during wave run-down and thereby initiating initial settlements.

Figure 6.8 Hydraulic conditions at which initial settlements occur



6.2.2. ONGOING SETTLEMENTS

Ongoing settlements are described based on comparison of photos which are taken from the start and end situation of each test. Ongoing settlements are observed for all types of tested breakwaters at both the sea- and leeside slope. Due to the cumulative character of the ongoing settlements the total amount of settlements increases until failure or the maximum generated wave height is reached (approximately 152%).

For submerged breakwaters ongoing settlements at the seaside slope are observed from wave heights of 60% H_d (no initial settlements are observed). Settlements at the leeside slope are observed for wave heights slightly above the design wave height. No clear influence of wave steepness is observed. For emerged breakwaters firstly initial settlements are observed before ongoing settlements take place at the seaside slope. Ongoing settlements at the leeside slope are observed for wave heights starting at 80% H_d , these settlements increases by increasing wave heights. For the 2% wave steepness settlements at the leeside slope occur earlier in the test series than is the case for a 4% wave steepness, no clear influence of wave steepness at the seaside slope is observed.

Settlements in the case of submerged structures are caused by the propagating and breaking waves for both the lee- and seaside slope. Moreover the settlements at the seaside slope are stimulated by the water flow in seaward direction.

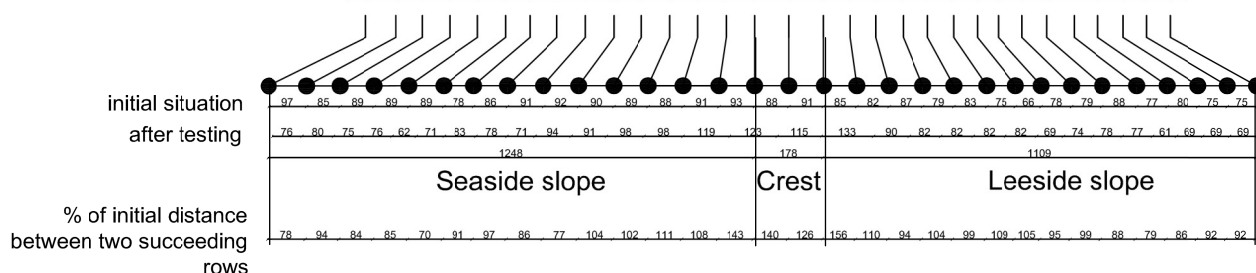
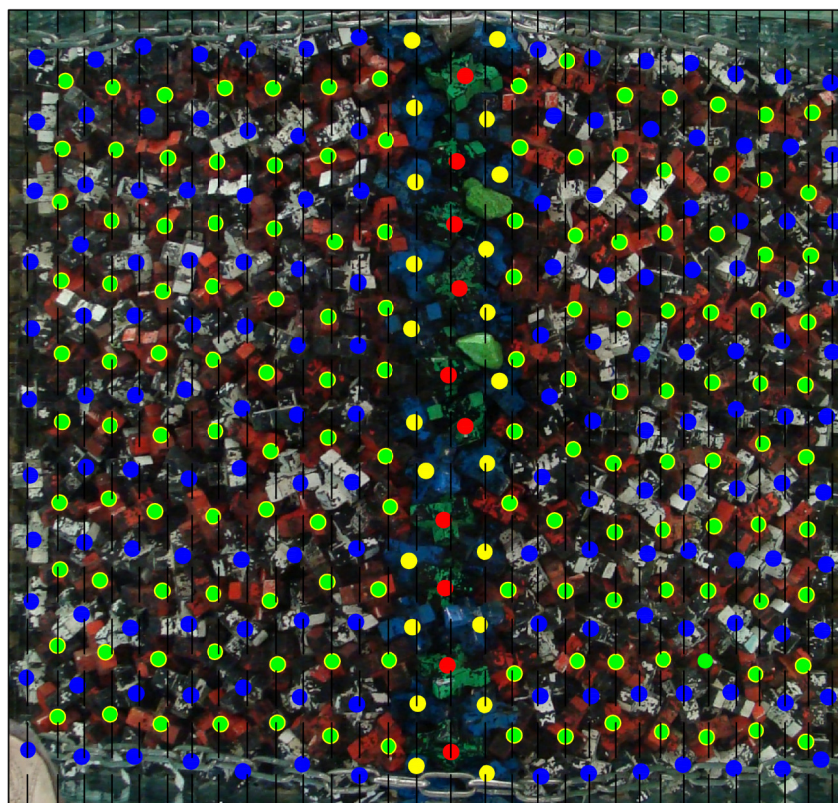
Settlements at the leeside slope for emerged breakwaters are caused to a large extent by the displacement of the crest section in landward direction (see

§6.3.1) and to a less extent by the overtopping waves. The displaced crest elements press the armour layer at the leeside slope down. Additionally the overtopping wave creates a current parallel to the leeside slope and thereby loading the armour layer and initiating settlements. Settlements at the seaside slope for emerged breakwater are caused by the breaking waves and by the up- and down-rush movement of the waves.

6.2.3. COURSE OF THE SETTLEMENTS

If for all tested breakwaters the upslope distance between two rows is considered for the upper part and the lower part of the armour layer the following can be concluded regarding the course of the settlements. The lower positioned elements in the armour layer experiences higher contact forces (parallel force to the seaside slope as a result of the armour units own weight) than the upper positioned elements. Therefore in the case of settlements the upslope distance for the lower positioned elements decreases more than for the higher positioned elements. Depending on the crest freeboard the upslope distance for the higher positioned elements actually increases, the number of rows where this applies from submerged to emerged conditions. This is caused by the lacking contact forces, the bottom friction the Xbloc elements experiences and the wave run-up. In wave run-up all incident wave energy is present, whereas for wave run down the total active energy is less due to the overtopping volume of water, therefore the upslope distance increases.

Figure 6.9 Top view reference breakwater with representation of settlements



In this consideration no distortions of the camera lens and the water level are taken into account.

The visual interpretations of the breakwater top views confirm the findings stated above. The following general conclusions can be drawn:

- Due to the settlements the distance between two succeeding rows is decreased for the lower positioned rows for both the sea- and leeside slope.
- Due to settlements and wave run-up the distance between two succeeding rows increases for the upper positioned rows for both the sea- and leeside slope.
- Settlements results in an increased distance of approximately 1.5 times the initial distance between the upper row of the slopes and the outer rows of the crest.
- The distance between the crest rows is increased considerable.

It should be noted that in the case of positive crest freeboard the crest elements are displaced to the leeside slope (see §6.3.1), as a result the armour layer at the leeside slope is more compacted than in the case of submerged or zero crest freeboard breakwaters. Therefore it is likely that the distance between the upper rows of the leeside slope decreases and that the distance between the upper row of the leeside slope and the outer landward row of the crest also decreases.

6.2.4. CONSEQUENCES OF SETTLEMENTS

A number of consequences result from settlements in the armour layer at the sea- and leeside slope.

Due to settlements the packing density increases in the lower positioned rows at the slopes and thereby the hydraulic stability of the armour layer. Whereas the hydraulic stability decreases for the upper rows due to the increased upslope distance. But for low-crested breakwaters that is the part of the armour layer at the seaside slope which is loaded most severe and does not benefit from the improved hydraulic stability due to settlements.

For all tested breakwaters settlements are present at both the sea- and leeside slope. Since the crest armour units cannot follow these settlements, a gap between two succeeded rows (crest and slope row) of armour units originates and a fractured armour layer result. The fractured armour layer has a number of consequences:

- Increased exposed surface area of the Xbloc crest armour units to the wave induced motion. The wave induced motion (§6.1.1) is formed by the overtopping, breaking propagating waves in landward direction and the water flow in seaward direction;
- The upper rows of armour units at the sea- and leeside slope have lost interlocking and inter-block friction with the crest elements.

Emerged breakwater

For emerged structures only overtopping waves are present, these overtopping waves displace the crest elements in landward direction. The displacement of crest elements is among other things the cause of settlements in the leeside slope (see §6.2.2), therefore no fractured armour layer develops at the landward side of the crest. At the seaside section of the crest the fractured armour layer

becomes for that reason twice as large, after all the settlements at the lee- and seaside slope form this crack.

Initial settlements of the seaside slope give rise to an increase of the exposed surface area of the crest elements to the overtopping waves. Therefore the crest elements are displaced more easily into landward direction and cause settlements in the leeside slope. Subsequently the exposed surface area to the overtopping waves is further increased and the possibility of displaced crest elements increases further.

Figure 6.10 Fractured armour layer for emerged breakwater at transition of the crest tot the seaside slope (test DI_4_160)

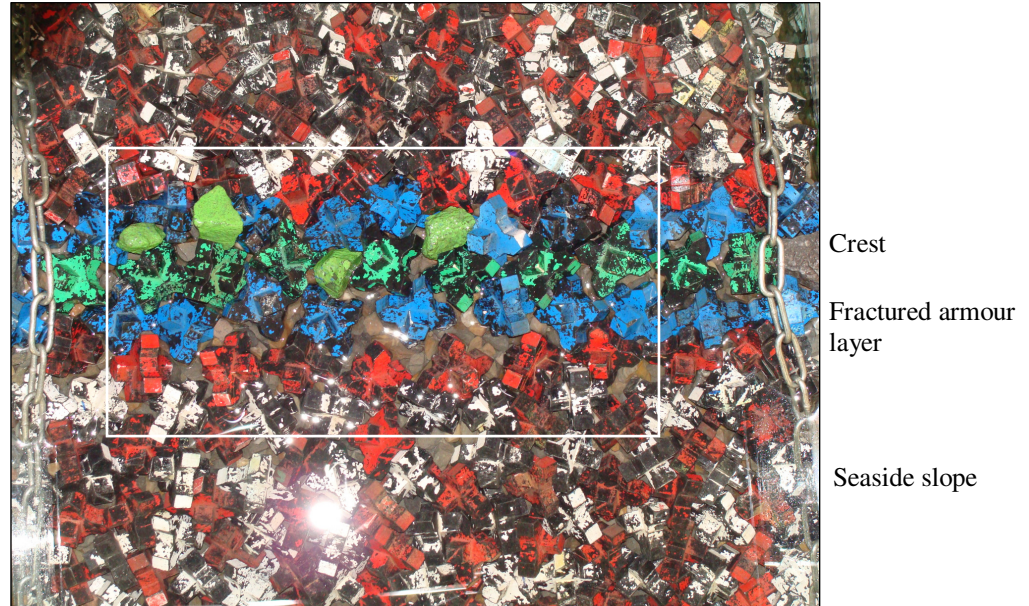


Figure 6.11 Enlarged white boxed area in Figure 6.10

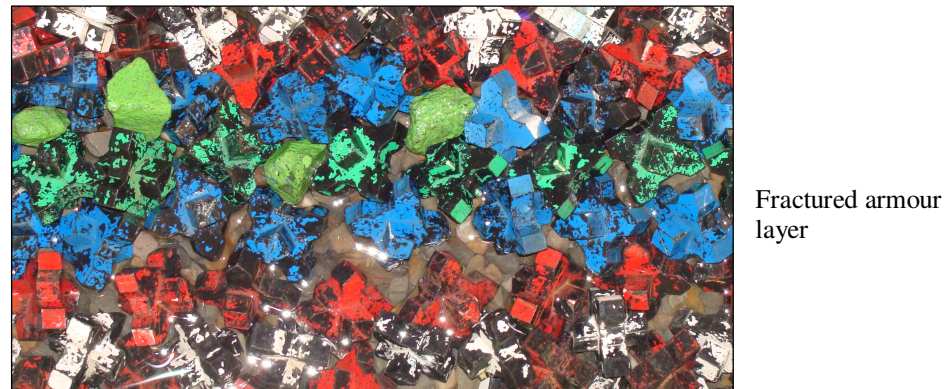


Figure 6.10 and Figure 6.11 shows the above described fractured armour layer after a test with $140\% H_d$ and wave steepness 4% . The cracked armour layer is visible at the seaside section of the crest, whereas it is not at the leeside section.

Submerged breakwater

For submerged breakwaters overtopping breaking waves and a water flow in seaward direction are present. The settlements at the lee- and seaside slope which originate from these hydraulic processes give rise to a armour layer which opens up at the transitions from the slopes to the crest. In contrast to emerged breakwaters two openings are formed, at the seaside crest section and at the landward crest section. Due to the oscillating water flow (formed by the breaking, propagating waves and the water flow in seaward direction) the crest elements are not displaced to one direction. As a result of the forming of two cracks, the crack width is smaller than is the case for emerged breakwaters.

6.3. PERFORMANCE XBLOC ELEMENTS ON THE CREST

The performance of the Xbloc crest elements is described in this section. The following subjects are treated:

- displaced crest (§6.3.1);
- rocking Xbloc crest elements (§6.3.2);
- displaced Xbloc crest elements (§6.3.3).

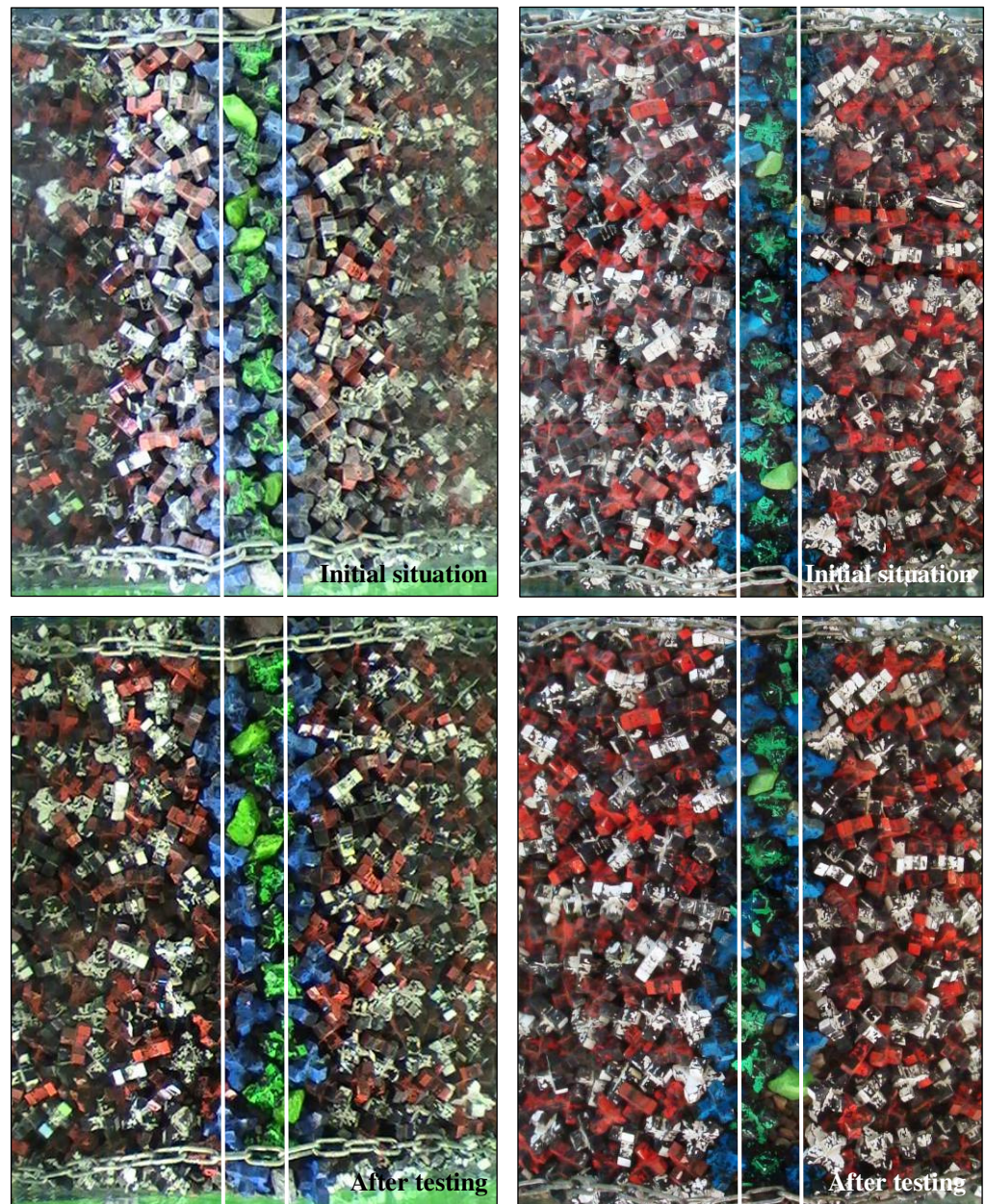
6.3.1. SHIFT OF CREST ARMOUR

Shift of crest armour stands for the shift of the whole crest armour into seaward or landward direction.

Due to the overtopping, propagating (breaking) waves and the water flow in seaward direction the crest section remains on average at the same position for submerged and zero crested freeboard breakwaters. Whereas for emerged breakwaters the crest section displaces into landward direction due to continuous overtopping waves, no oscillating water flow is present as is the case for submerged breakwaters. Settlements further stimulate the displacement of the crest armour units in landward direction, due to the increased surface area of the Xbloc elements (at the seaside section of the crest).

Figure 6.12 shows four photos of the crest section for two different tests and two moments in time, the initial situation and the situation after a series of tests up to 152% H_d . The photo of the emerged breakwater (left photo) clearly shows the displaced crest section, whereas for the submerged structure on average the crest section maintains at the same location. Some elements follow the settlements of the slopes and are therefore somewhat displaced, this is also caused due to the placement (see §5.6.3). The same phenomenon is observed after tests with smaller wave heights

Figure 6.12
 Displacement crest
 section, initial
 situation and situation
 after test with 153%
 Hd, the white lines
 are reference lines
 Left: test EI_4_1
 Right: test AI_4_1



For tests with a wide crest the same observations have been done as for a small crest.

6.3.2. ROCKING OF XBLOC CREST ELEMENTS

For emerged breakwaters only a current in landward direction is observed due to overtopping waves (see §6.1.1). The Xbloc elements are therefore loaded by a force which varies in magnitude but not in direction. Therefore some movement of crest elements is observed (but no rocking) until they have found a more stable position. Rocking of Xbloc crest elements was only observed if an element has freedom to move in the direction of the propagating wave. The moment the wave overtops the structure the element tilts over until its movement is restricted by surrounding elements, when the overtopping wave passes by the element returns to its initial static stable position. Most of the rocking armour units are observed at the outer seaside row and the second row (counted from the outer seaside row) of the crest, for both the wide and small crested breakwaters. Settlements in the seaside slope results in an increased surface area of the armour units normal to the water flow. The total

force exerted on the Xbloc armour units by the overtopping waves increases and therefore creating a larger overturning moment. Units which were initially statically and dynamically stable may be go rocking.

For submerged breakwaters an oscillating water flow is present (see §6.1.1). The elements cannot find a stable position, as is the case for submerged breakwaters, due to the oscillating load. As a consequence more rocking elements are observed at the moment of displacement of the Xbloc elements. Furthermore due to settlements in both sea- and leeside slope the distance between to succeeding crest armour rows increases. Whereas for emerged breakwaters the succeeding distance only increases at the transition from the seaside slope to the crest. Rocking is therefore observed more scattered over the crest for small crested breakwaters, for wide crested breakwaters the observed rocking is mostly concentrated at the seaside edge of the crest. This is caused by the water flow in seaward direction over the crest which is maximal at the seaside section of the crest.

Rocking is observed long before start of damage or failure occurs, this shows the relative importance of rocking. At the moment of failure or at the maximum generated wave height almost all crest armour units are rocking. No clear difference for rocking between the two and four percents wave steepness is observed.

6.3.3. DISPLACEMENT OF XBLOC CREST ELEMENTS

Displacement of crest Xbloc elements is observed from wave heights of 112% up to 153% H_d in the case of wave steepness 2%. Whereas for waves with a steepness of 4% only in test DII_4, wide crest and crest freeboard of 1.5 D_n , a significant number of crest elements was displaced. In the other tested cross sections none or only one or two Xbloc crest elements were displaced. The observed displacement is mainly at the seaside part of the crest and occasionally some scattered displacement at the leeside part. As a consequence of settlements, in the sea- and leeside slope, the stability of the crest Xbloc elements decreases, the cause is two sided, the load increases and the stabilizing properties of the Xbloc elements decreases.

- Due to settlements and sometime the displacement of the upper seaside row elements, the area normal to the load increases because of the development of a fractured armour layer at the transition of the seaside slope to the crest.
- Due to settlements the Xbloc elements get more space. Therefore the already decreased interlocking and inter-block friction properties of the Xbloc armour unit, due to the horizontal application, reduces further as a result of the decreasing packing density. At the moment of displaced Xbloc crest elements a lot of crest elements are continues rocking due to the oscillating flow, whereas for emerged breakwaters this is not observed.

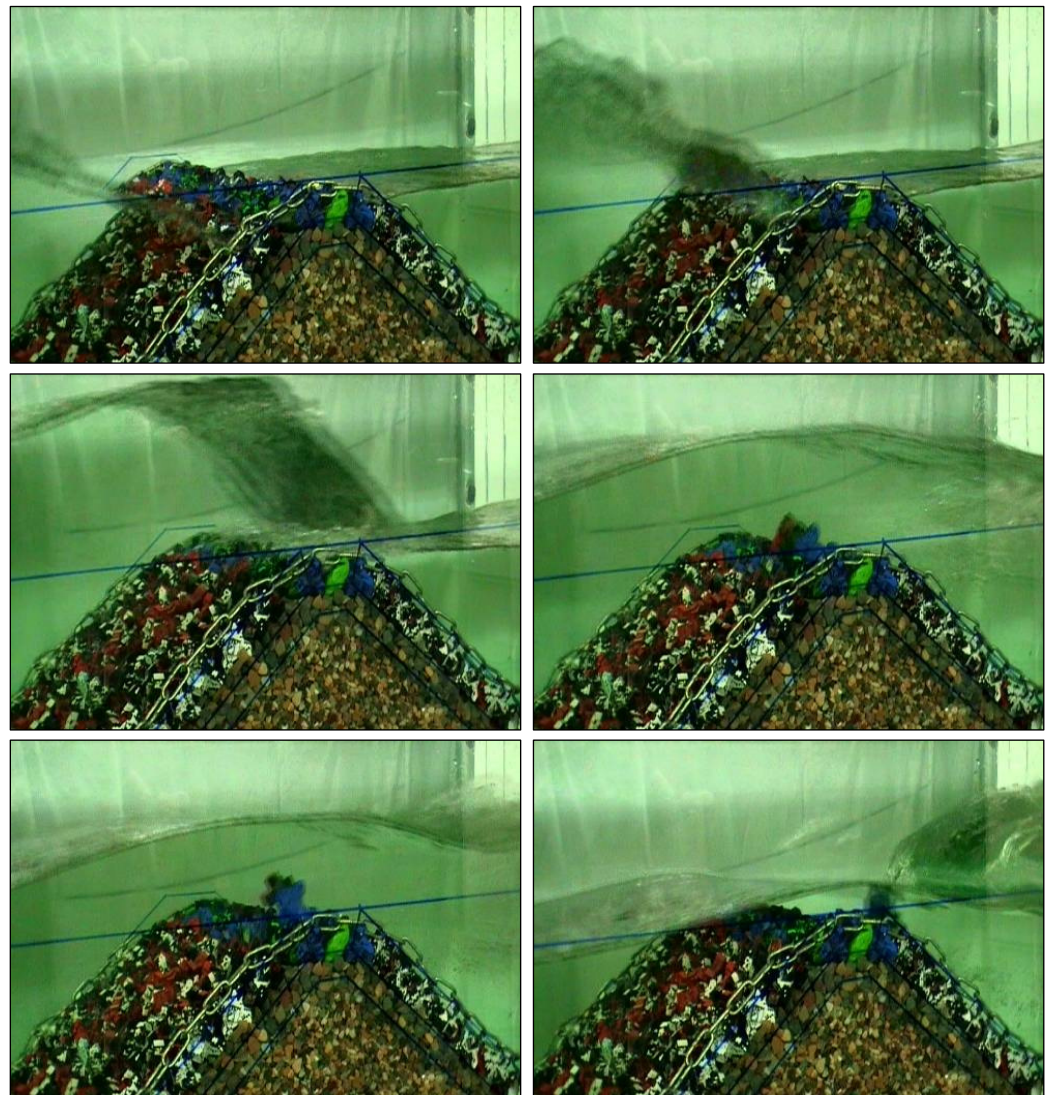
The increasing load and the decreasing stability of the Xbloc elements ultimately lead to the displacement of crest elements at the seaside part of the crest. The decrease in stability at the leeside part of the crest is the same as at the seaside, but the load (incident waves, water flow in seaward direction) is smaller and therefore almost no displaced armour units are observed.

For emerged breakwaters the entire crest section is displaced to the leeside part of the breakwaters (see §6.3.1). The displacement of the crest section is attempted to resist by the leeside slope elements. As a consequence sometimes an accumulation of Xbloc crest and leeside slope elements originate. Due to a number of succeeding high waves a large part of the crest and leeside slope is displaced in a small amount of time.

For the other tested breakwaters the crest element displacement is observed until failure of the complete breakwater occurs. Most of the elements are displaced within a test in a test series. At the moment of several dislocated armour units the damage progression develops fast and within some high waves a large part of the crest is dislocated (see Appendix J).

Figure 6.13 shows for different moments in time the displacement of a crest Xbloc element. In this case the element is displaced to the landward side of the breakwaters, whereas in other situations the element is displaced to seaside part of the breakwater. Sometimes an element is displaced out of its initial position by the incident waves and by the water flow in seaside direction the element rolls back to its initial position.

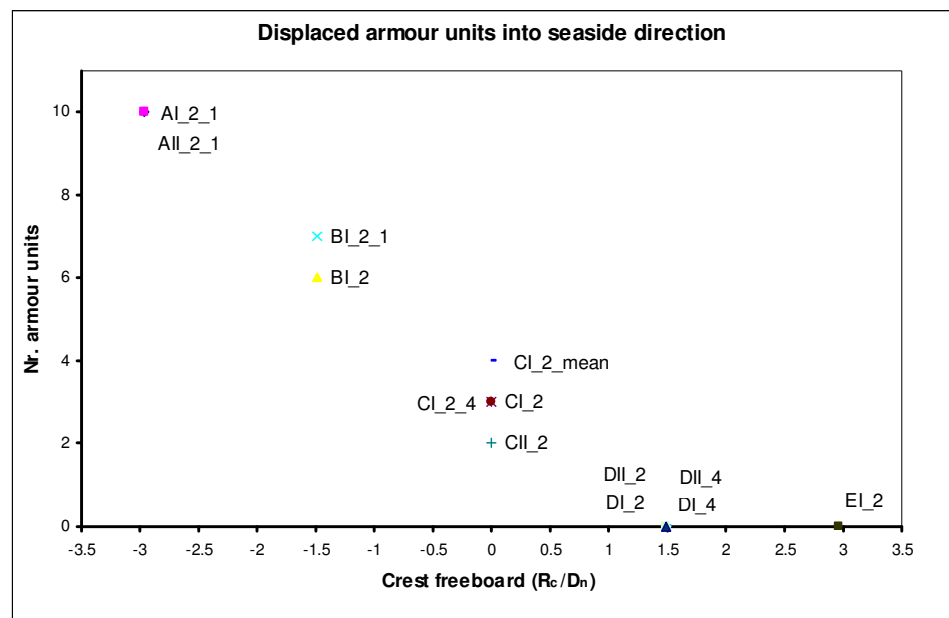
Figure 6.13
Displacement Xbloc
crest elements for
different moments in
time



The displacement of the crest elements is caused by the enlarged area normal and the decrease stability of the element due to settlements. In Figure 6.13 initially it seems that no Xbloc elements are at the point of displacement. Due to the water flow over the crest a lift and drag force acts at the armour unit. When the resulting force becomes large enough and lasts long enough such that it overcomes the inertia term of the Xbloc element it rolls over the neighbouring armour units. In some cases the elements at the crest have so much space that the element rolls firstly over the crest which simplifies the displacement because of the momentum it gained.

The same considerations as stated above holds for the water flow in seaside direction. Figure 6.14 shows how much elements of the total breakwater are displaced into seaside direction by the water flow in seaside direction for breakwaters which failed. It clearly shows that for the most submerged conditions the water flow in seaside direction is the displacement mechanism, whereas for increasing crest freeboard the influence of the water flow decreases.

Figure 6.14 Number of displaced armour units in seaside direction for breakwaters at which failure occurred (10 displaced armour units)



6.4. PERFORMANCE XBLOC ELEMENTS ON THE SLOPE

The performance of the Xbloc elements at the lee- and seaside slope is described on basis of:

- rocking Xbloc elements (§6.4.1);
- displaced Xbloc slope elements (§6.4.2).

An overview of the acting mechanisms which influences rocking and the displacement of the slope elements are given. Single layer armour units rely for their stability on interlocking and their own weight. After settlements in the sea- and leeside slope, the top row elements have no interlocking anymore with the crest elements. Additionally the top row elements of the slopes have no parallel force component from higher positioned rows, which influences the hydraulic stability negatively, see §1.1.3 and §4.2.2. In the case of emerged breakwaters only the element on the seaside slope loses contact with the crest

elements due to the displacement of the crest section. The course of settlements (see §6.2.3) results in an increased upslope distance for the top rows, thus an lower relative placement densities, lower interlocking and inter-block properties.

6.4.1. ROCKING XBLOC SLOPE ELEMENTS

Rocking at the leeside slope is only observed in one test series with zero crest freeboard (CI_2_1), whereas rocking at the seaside slope is observed for each test series from wave heights of 60% H_d up to the maximum generated wave height in a test series.

Most of the rocking armour units are observed in the top rows of the seaside slope (due to the mechanisms described in §6.4). The number of rows, in which rocking armour units mostly occur, increases from submerged to emerged breakwaters from approximately one to four row(s). Furthermore waves with a steepness of 4% show more rocking elements in lower positioned rows than is the case for wave steepness 2%. For increasing wave heights the number of rocking elements increases. At the moment of displacement of several armour units, the Xbloc elements in the top rows of the seaside slope are rocking continues and are partially lifted from the under layer in case of larger waves than the design wave height.

Due to the natural properties of single layer amour units and the course of the settlements and the settlements itself along with the fact that the maximal wave energy is concentrated around the still water line results in a large number of rocking Xbloc elements in the case of emerged breakwaters. More rocking Xbloc elements at the seaside slope are observed for emerged breakwaters than is the case for submerged breakwaters.

No clear influence of crest width was observed, this seems logical in case of emerged structures because the incident waves do not interact with the water flow in seaside direction as is the case for submerged breakwaters. The velocity of the water flow in seaside direction is smaller for wide crested breakwaters than is the case for small crested breakwaters (§6.1.1). Due to a different velocity of the water flow, the number of rocking armour units at the seaside slope could be different in case of submerged breakwaters, although this is not observed.

6.4.2. DISPLACED XBLOC SLOPE ELEMENTS

Only for test CI_2_4 and DII_2 some elements are displaced at he leeside slope, whereas for all other test series only displaced elements are observed at the seaside slope. The first displaced elements are observed for wave heights of approximately 110% H_d in the case of wave steepness 2%. Displacement of the first Xbloc element and failure for a wave steepness of 4% occurs for larger wave heights than is the case for wave steepness 2%. Furthermore the Xbloc elements are more easily displaced from the seaside slope of emerged breakwaters than from submerged breakwaters.

Most of the Xbloc elements are displaced from the higher positioned rows at the seaside slope. This is caused by reasons given in §6.4. After the first

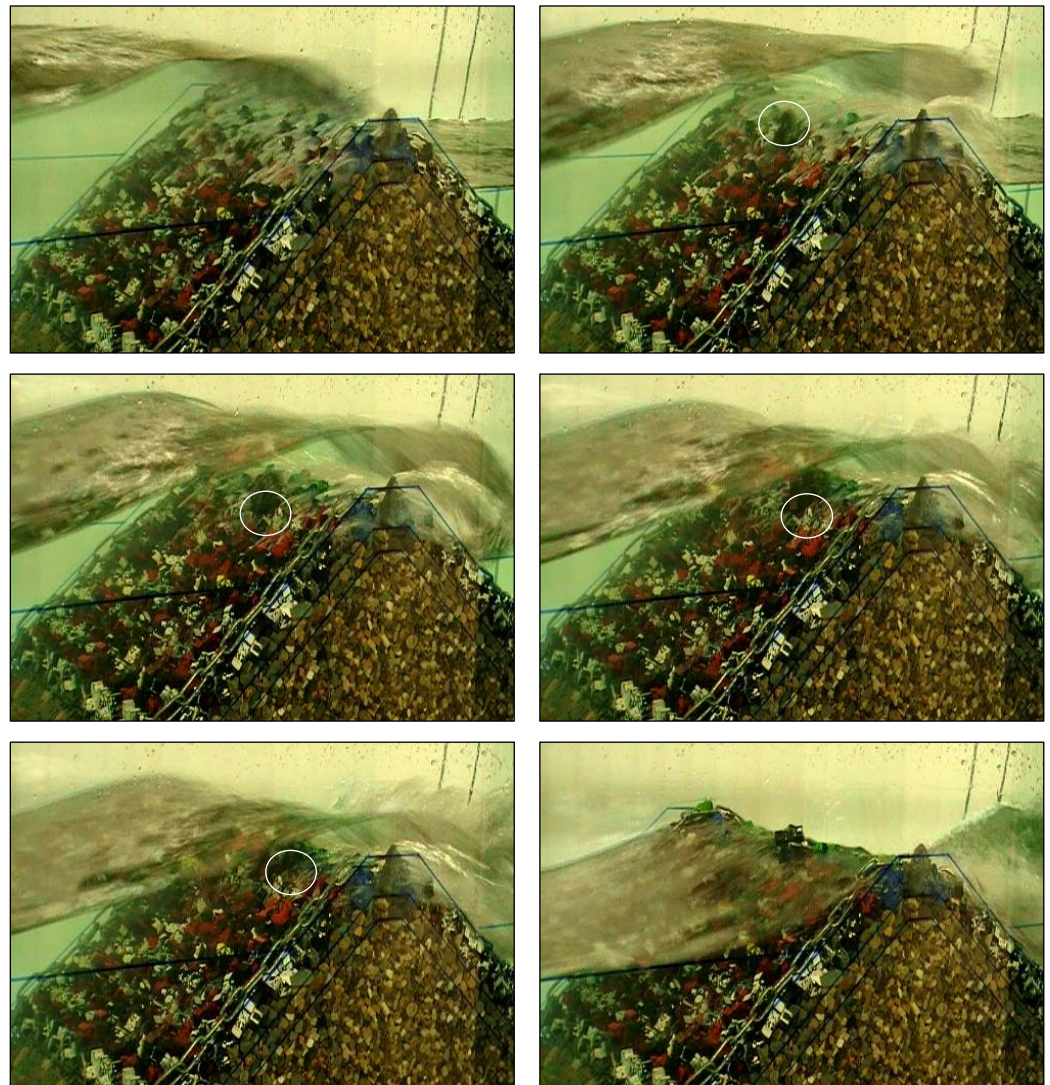
elements is displaced the surrounding elements starts to move more easily and get displaced to.

No clear influence of the crest width is observed for both the submerged and emerged breakwaters.

The displacement of the Xbloc seaside slope elements is correlated with the displaced Xbloc crest elements. If some Xbloc crest elements are displaced the elements in the upper rows of the seaside slope are also more easily displaced and the other way around.

Figure 6.12 shows for different moments in time the displacement of an Xbloc at the seaside slope. The elements at the seaside slope have a decreased hydraulic stability trough settlements and the course of settlements in combination with wave action. At the moment of displacement the elements move continuously, a high wave in combination with an unfavourable positioned element leads to the displacement of this element. Just as in the case of the displacement of crest elements the same consideration holds, with the lift and drag forces and inertia term, as for the displacement of the Xbloc slope elements. The element is displaced by rolling over the higher positioned Xbloc element, sometimes it is firstly displaced to the crest section and by the following wave to the leeside slope (as is the case in Figure 6.15).

Figure 6.15
Displacement Xbloc
element at the seaside
slope for different
moment in time



6.5. CONCLUSIONS

A number of conclusions can be drawn from the observations:

- A water flow over the breakwater crest acts in both seaside and landward direction. The water flow in seaside direction is caused by a wave trough in front of the breakwater and normal or raised water level at the leeside of the breakwater. The water flow in landward direction is caused by the overtopping waves.
- The velocity of the water flow in seaward direction is larger for 2% than 4% wave steepness. This is caused by the larger inertia of the water mass on top of the breakwater in case of 4% wave steepness.
- At the foreshore spilling breakers are observed whereas at the breakwater surging breaker for the 2% wave steepness and surging/collapsing breakers in case of the 4% wave steepness are observed. Not only the breakwater itself initiates wave breaking but also the water flow in seaward direction.
- Waves which overtop the breakwater do not impinge on the leeside slope. The seaward slope and crest are attacked by some wave breaking from the foreshore.
- Two types of settlements can be distinguished, initial settlements which occur for relative small wave heights and are perceptible by eye and ongoing settlements which take place after the initial settlements and are not perceptible by eye due to their gradual occurrence. Initial settlements are in the first place observed for emerged breakwaters at the seaward slope and ongoing settlements are observed for both the sea- and leeward slope and all crest freeboards.
- The largest displacement of the elements due to settlements is observed for the top rows at both slopes. The upslope distance between the higher positioned rows at both the seaward and leeward slope increases due to settlements and wave action.
- As consequence of settlements at both slopes the distance between two succeeding rows of crest armour units increases. Furthermore a fractured armour layer develops at the transitions from the slope to the crest. Due to the displacement of the crest armour units in landward direction for emerged breakwaters only at the transition from seaward slope to crest a fractured armour is present.
- For submerged breakwaters the crest armour units are loaded by an oscillating water flow whereas for emerged breakwaters only the overtopping waves are present therefore submerged breakwaters show more scattered rocking over the crest than emerged breakwaters. Although most of the rocking elements are located at the seaside part of the crest.
- Due to settlements at the slopes the exposed surface area normal to the flow increases for the outer rows of the crest. Therefore the crest elements located at the seaside part of the crest are the first displaced crest elements. For submerged conditions the elements are mainly displaced by the water flow in seaside direction whereas for emerged breakwaters the displacement is caused by the overtopping waves. Rocking of the crest armour units is observed long before start of damage and failure.
- Due to settlements and the increased distance for two succeeding rows the stability of the higher positioned Xbloc element at the slope decreases. This in combination with the already decreased stability of the higher positioned Xbloc elements leads to rocking and the displacement of the upper part of

the seaside slope. The already decreased stability of the Xbloc elements is caused by the decreased interlocking properties, inter-block friction and the absence of a force parallel to the seaward slope.

7. ANALYSIS ROCKING XBLOC ARMOUR UNITS

Rocking armour units finally lead to breakage of the elements and thereby to a significant decrease of the interlocking capacities. DE ROVER *et al.* performed tests with broken Xbloc armour units in an armour layer on standard breakwater slopes. Start of damage was observed for lower stability numbers and no significant differences for failure were observed in comparison to an armour layer with non broken armour units. The behaviour of broken armour units may well be different for low-crested structures, therefore rocking is a failure mechanism (§2.3.2) which in the current design philosophy is not allowed.

Rocking in these tests is defined as the continuous and regular movement of one or more armour units.

Rocking of the armour units is considered a form of instability because the units are dynamically not stable. The larger the numbers of rocking elements the less stable the armour layer is considered.

For the quantification of the amount of rocking elements the same principle is used as for the number of displaced elements (N_{od}). The amount of rocking elements is defined as:

$$N_{or} = \frac{\text{number of rocking units}}{\text{width armour layer} / D_n} \quad (9.1)$$

Each moving armour unit is registered by eye until the total number of moving armour units becomes approximately 10 to 15, although higher registered numbers are also present.

The damage is the number of rocking armour units in the armour layer within a strip with the width of the nominal diameter (D_n). This means that one rocking armour unit gives the same value of N_{or} for the total breakwater and for instance the seaside slope.

The analysis of the number of rocking Xbloc armour units is divided into the following parts:

- test results rocking armour units (§7.1);
- reference test series, which enables the determination of the 90% confidence band interval for the reference tests and the qualitative valuation of the other test series (§7.2);
- analysis test results (§7.3);
- discussion test results (§7.4).

7.1. TEST RESULTS ROCKING ARMOUR UNITS

Since the absence of clear damage numbers (expressed in N_{or}), as is the case for displaced armour units, the number of rocking armour units is plotted against the stability number, instead of presenting the results for fixed damage level curves over different crest freeboards. Tests with clamped placed crest elements (see §5.6.1 and §5.6.3) are not taken into account, the number of rocking elements was not yet registered for these tests.

In Appendix J the test results for the different breakwater sections of each individual test series is plotted into a figure. This enables the comparison of the ratios of damage for different breakwater sections. In the same figures also the number of displaced armour units is plotted to emphasize that rocking is a mechanism which acts (long) before start of damage or failure occurs.

The total number of rocking armour units is plotted for the total breakwater (Figure 7.1) and the different breakwater sections, seaside slope (Figure 7.2) and crest (Figure 7.3). Results for the leeside slope are not plotted because only test series CI_2_1 and DI_4 show some rocking elements. For a clear definition of the different breakwater sections see §5.6.3.

The total breakwater implies all breakwater sections, thus also the leeside slope. Figure 7.1, Figure 7.2 and Figure 7.3 shows in general a continuous increasing number of rocking armour units. For some lines a temporary negative gradient is present although the stability numbers increases. Furthermore two clusters of lines at a stability number of 1.5 are perceptible, most of the lines, which represents a relative placement density of 100%, start in the higher positioned cluster of lines.

Figure 7.1 Test results rocking armour units, Total breakwater

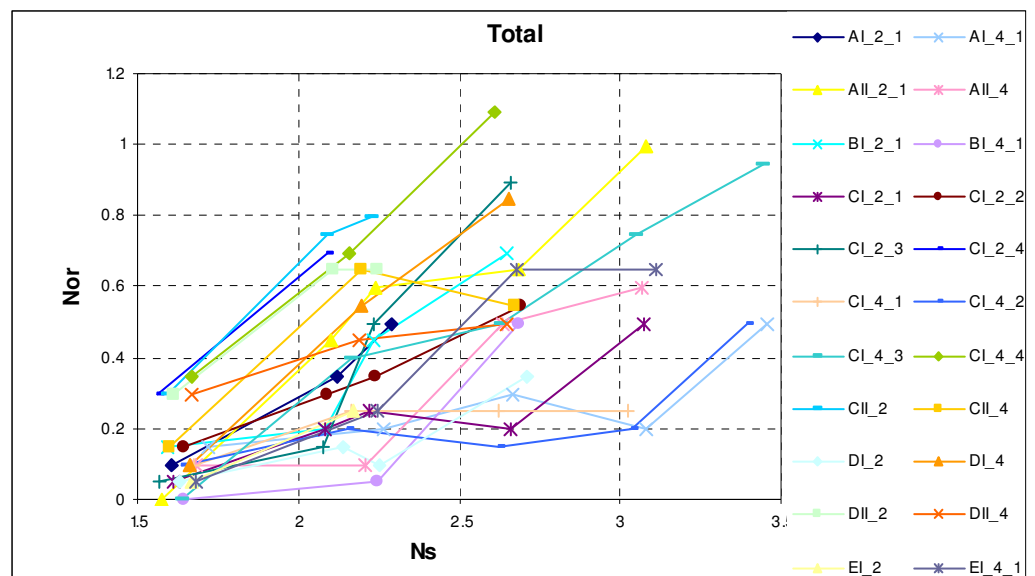


Figure 7.2 Test results rocking armour units, Seaside slope

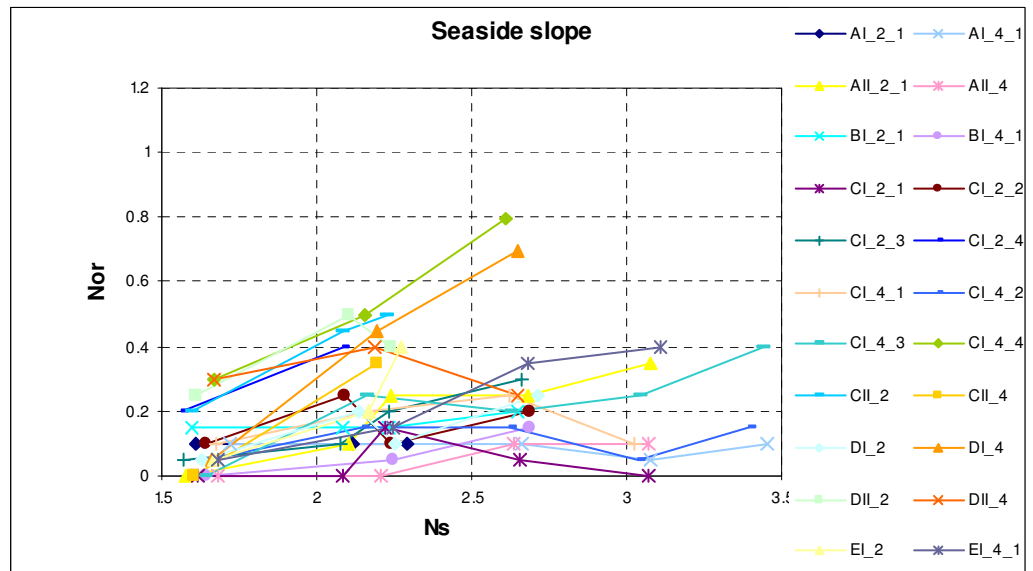
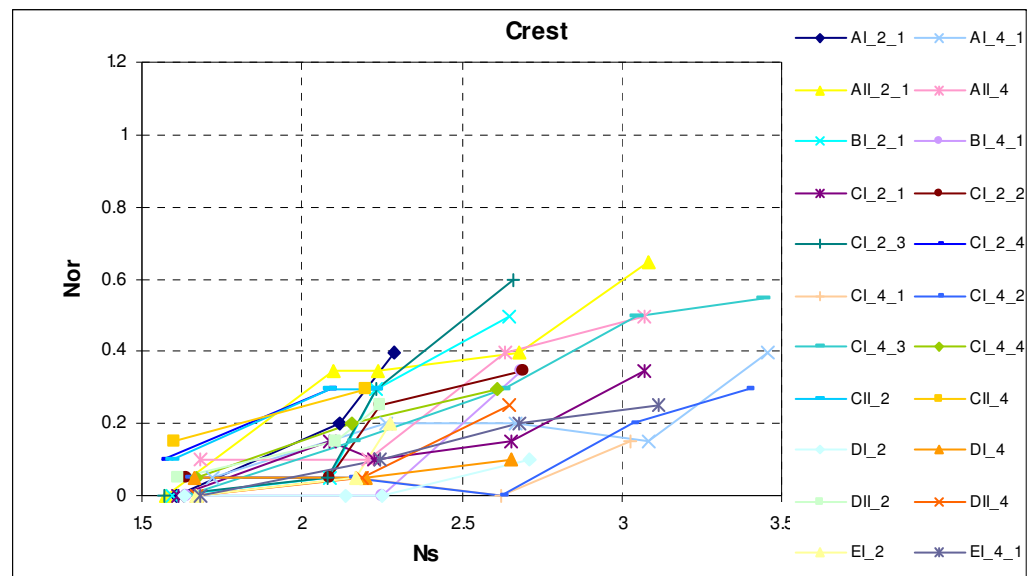


Figure 7.3 Test results rocking armour units, Crest



7.2. REFERENCE TESTS

Tests at the reference cross section, zero crest freeboard and small crest width, are performed three times to acquire insight into the reliability of the test results. But it enables also the valuation of the reliability of test results for the other cross sections.

In the case of wave steepness 2% tests CI_2_1, CI_2_2 and CI_2_3 are referred to as the reference test series whereas in case of the 4% wave steepness these test series are CI_4_1, CI_4_2, CI_4_3.

Results of the reference test series are visualised by plotting the number of rocking elements (N_{or}) against the stability number (N_s). In this way the progression of the number of rocking elements for increasing wave heights is obtained (see for example Figure 7.3). The mean number of rocking elements (CI_2 mean, CI_4 mean) for the reference test series per stability number is calculated and plotted together with its 90% confidence band interval. The lines which represent the upper and lower limit of the confidence band interval

are plotted black dashed, whereas the mean number of rocking elements is plotted in a black solid line. Trend lines are added for the mean number of rocking elements and the upper- and lower limits in respectively a red solid line and a red dashed line. Furthermore test series CI_4_4 and CI_2_4 are plotted in the same figures; these test series were executed with a relative placement density of 100% whereas for the reference test series it was 103%.

The above described figure is made for the total breakwater armour layer, seaside slope and crest (see §5.6.3 for a clear definition of the different breakwater sections). Also a distinction is made between the 2 and 4% wave steepness. First the figures of the 2% wave steepness are discussed (§7.2.1) and subsequently the 4% wave steepness (§7.2.2).

7.2.1. TWO PERCENT WAVE STEEPNESS

No observations have been done for a stability number of approximately 3.3 except for test series CI_2_1, therefore this observation is not taken into account in the calculation of the mean and the 90% upper and lower limit values for all breakwaters sections.

At a stability number of 1.6, start of the test series, almost no elements are rocking at the crest (see Figure 7.6) in contrast to the seaside slope (see Figure 7.5). Figure 7.4 shows the total number of rocking armour units for the total breakwater. The mean number of rocking elements at a stability number of 1.65, start of the test series, is almost zero for the crest section whereas for the seaside slope the number of rocking element is 0.05. For increasing stability numbers the gradient of the mean number of rocking elements for the crest section increases in contrast to the gradient of the seaside slope. The number of rocking elements for the crest section reaches a maximum of 0.2 in case of extrapolation of the trend line. Due to the number of rocking elements at the beginning of the test series is 0.07. The gradient of the mean trend line increases for increasing stability numbers. For a stability numbers smaller than 2.85, at the seaside slope most of the rocking elements are observed whereas for larger stability numbers most of the rocking elements are positioned at the crest.

The 90% confidence band interval increases until the design stability number and then becomes approximately constant in case of the crest section. Whereas for the seaside slope the 90 % confidence band interval is constant for stability numbers lower than the design stability number and increases for higher stability numbers. This leads an ever increasing confidence band interval for the number of rocking elements of the total breakwater.

Figure 7.8 shows that for a relative placement density of 100% (test series CI_4_4) more armour units at the seaside slope are rocking than is the case for a relative placement density of 103%. The number of rocking elements at the crest section is larger than the average number of rocking elements but still in the 90% confidence band interval of the reference tests. The number of rocking elements at the start of a test series in case of a relative placement density of 100% is significantly higher than in case of the reference test series, furthermore the gradient of the line CI_4_4 is larger than the mean line of the reference tests.

The number of rocking armour units for the total breakwater therefore shows also some rocking elements at the start of a test series. The gradient of the line 'CI_2 mean' for the seaside slope decreases slowly towards the design stability number and it seems that a maximum number of rocking armour units is reached of approximately 0.2. Whereas for the crest section the gradient increases for increasing stability numbers and thereby thus the number of rocking elements. Due to the course of the trend lines which represent the number of rocking elements for the seaside slope and the crest the number of rocking elements increases for the total breakwater. The seaside slope shows the largest number of rocking elements for stability numbers smaller than 2.1, for larger stability numbers rocking at the crest becomes dominant.

The 90% confidence band interval is initially small for the crest section but increases rapidly for increasing stability numbers, whereas for the seaside slope the interval increases slowly. The confidence band interval in case of the total breakwater is almost constant until a stability number of 2.08, from there on the interval increases rapidly until the design stability number. The confidence band interval is larger for the crest section than for the seaside slope.

Both at the seaside slope, crest and total breakwater significant more elements are rocking in the case of a relative placement density of 100%. This is not an arbitrariness observation due to the fact that the line which represents the number of rocking elements, for test series CI_2_4, is located well outside the 90% confidence band interval of the reference test series. The higher number of rocking elements in the case of 100% relative placement density is caused to a large extend by the higher number of rocking armour units at the start of the test series and due to the larger gradient of the line.

Figure 7.4 Number of rocking armour units, reference test series (s=2%), total breakwater

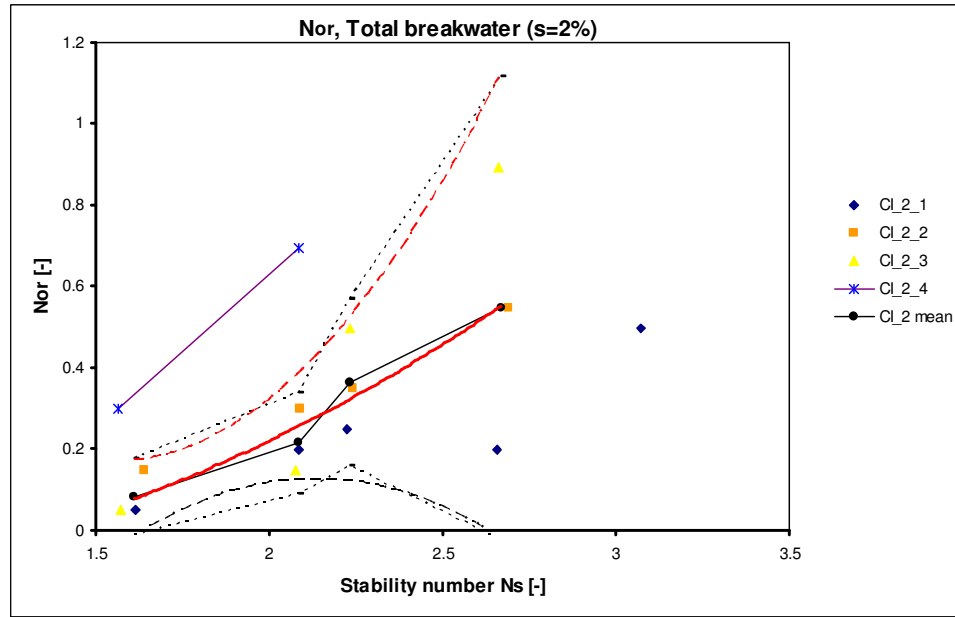


Figure 7.5 Number of rocking armour units, reference test series (s=2%), seaside slope

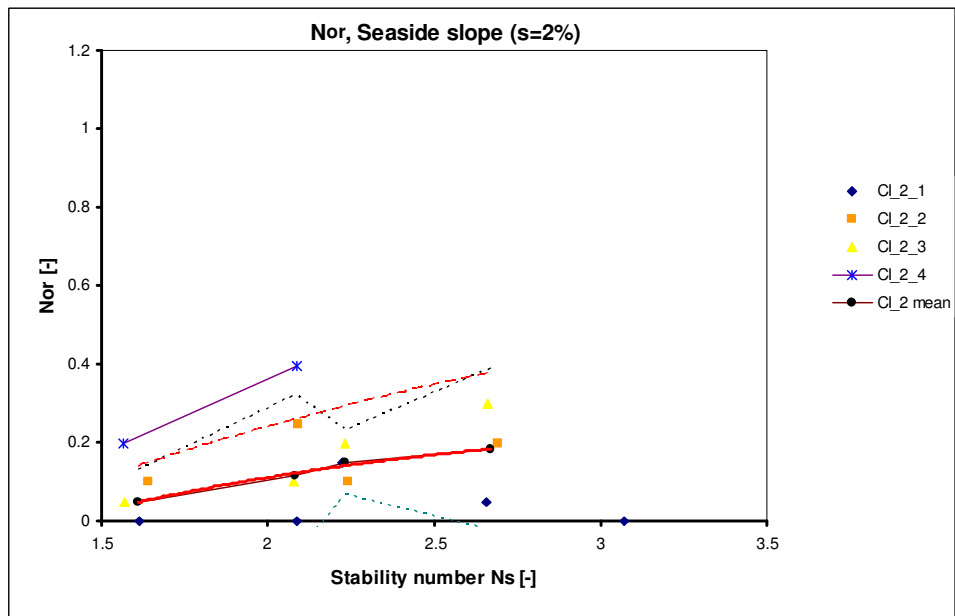
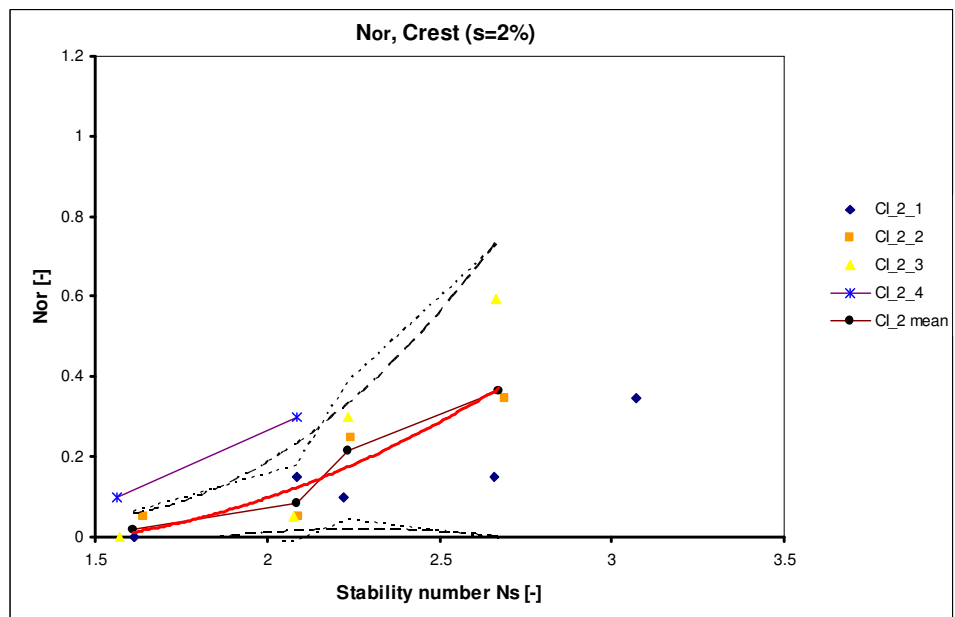


Figure 7.6 Number of rocking armour units, reference reference test series (s=2%), crest



7.2.2. FOUR PERCENT WAVE STEEPNESS

Figure 7.7 shows the total number of rocking elements whereas in Figure 7.8 and Figure 7.9 respectively the number of rocking armour units for the seaside slope and crest are plotted.

The mean number of rocking elements at a stability number of 1.65, start of the test series, is almost zero for the crest section whereas for the seaside slope the number of rocking armour units is 0.05. For increasing stability numbers the gradient of the mean number of rocking elements for the crest section increases in contrast to the gradient of the seaside slope. The number of rocking elements for the crest section reaches a maximum of 0.2 in case of extrapolation of the trend line. Due to the number of rocking elements at the crest and the seaside slope the total number of rocking elements at the beginning of the test series is 0.07. The gradient of the mean trend line increases for increasing stability numbers. For stability numbers smaller than 2.85, at the seaside slope most of the rocking element are observed whereas for larger stability numbers most of the rocking elements are positioned at the crest.

The 90% confidence band interval increases until the design stability number and then becomes approximately constant in case of the crest section. Whereas for the seaside slope the 90 % confidence band interval is constant for stability numbers lower than the design stability number and increases for higher stability numbers. This leads an ever increasing confidence band interval for the number of rocking elements of the total breakwater.

Figure 7.8 shows that for a relative placement density of 100% (test series CI_4_4) more armour units at the seaside slope are rocking than is the case for a relative placement density of 103%. The number of rocking elements at the crest section is larger than the average number of rocking elements but still in the 90% confidence band interval of the reference tests. The number of rocking elements at the start of a test series in case of a relative placement density of 100% is significantly higher than in case of the reference test series, furthermore the gradient of the line CI_4_4 is larger than the mean line of the reference tests.

Figure 7.7 Number of rocking armour units, reference reference test series (s=4%), total breakwater

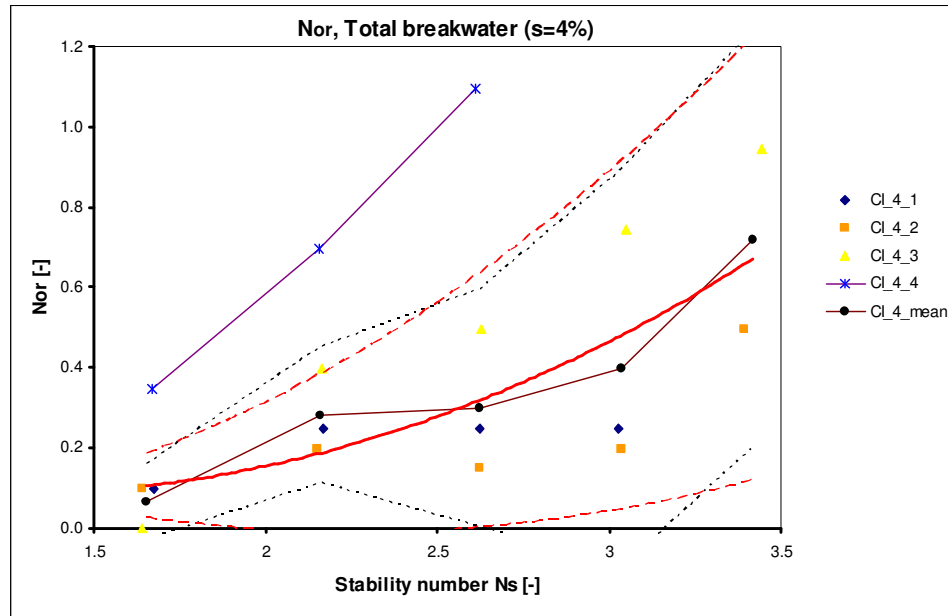


Figure 7.8 Number of rocking armour units, reference test series (s=4%), seaside slope

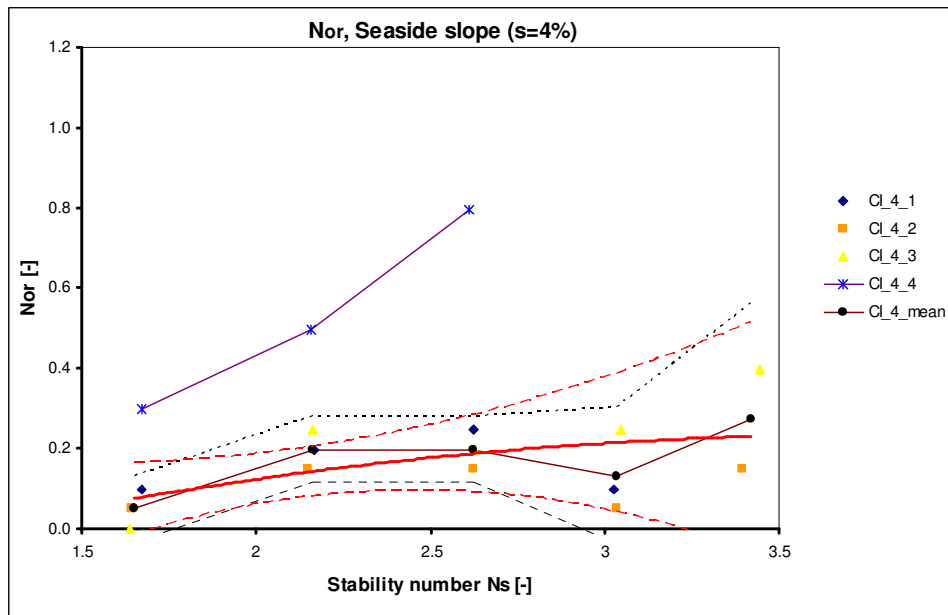
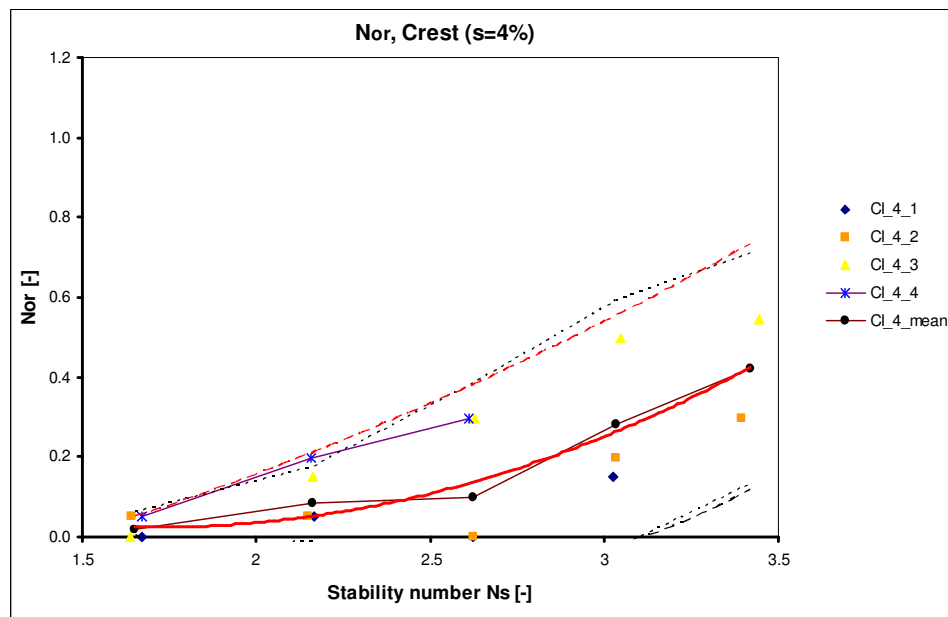


Figure 7.9 Number of rocking armour units, reference test series (s=4%), crest

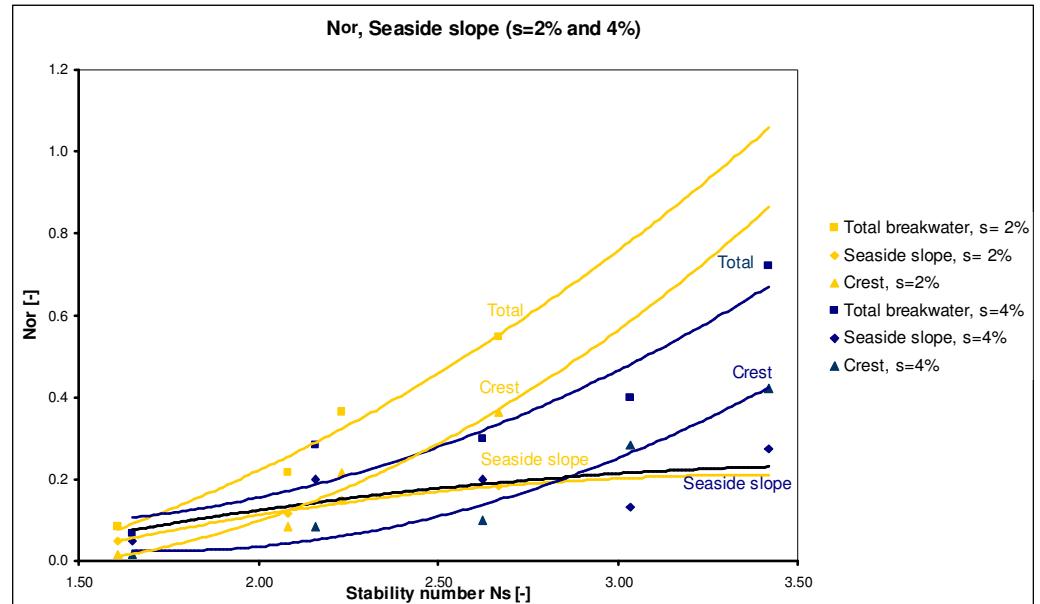


7.2.3. CONCLUSIONS

A number of conclusions can be drawn from the analysis of the reference test series for the 2 and 4% wave steepness.

To give an overview and enable the comparison of the results for the 2 and 4% wave steepness all results are plotted in Figure 7.10. It should be noted that the trend lines of the 2% wave steepness are obtained by extrapolation beyond a stability number of 2.7.

Figure 7.10 Number of rocking armour units, reference test series, all breakwater sections



The following conclusions can be drawn regarding the number of rocking elements in case of the reference test series:

- The total number of rocking elements is always larger for a 2% wave steepness than for a 4% wave steepness.
- Initially more rocking elements are observed at the seaside slope, but this alters to the crest earlier for the 2 than the 4% wave steepness.
- The number of rocking elements at the seaside slope is independent of wave steepness and reaches a maximum whereas the crest section does not reach a maximum.
- For both wave steepness's the seaside slope shows already some rocking elements at a stability number of 1.62, whereas the crest section shows almost no rocking.
- The 90% confidence band interval of the mean number of rocking elements at the total breakwater increases for increasing stability numbers. Around the design stability number the interval is largest for the 2% wave steepness.
- The 90% confidence band interval of the mean number of rocking element at the crest increases for wave steepness 4% until the design stability number, it then becomes constant whereas for the seaside slope it is the other way around. The confidence band interval for wave steepness 2% increases all the time for the crest section and for the seaside slope it is initially constant and increases after for stability numbers larger than 2.23.
- The number of rocking elements in case of a 100% relative placement density is significantly larger than in the case of a relative placement density of 103%. Only for crest section and wave steepness 4% the amount of rocking in case of a relative placement density 100% is larger than mean

number rocking elements of the reference test series but still within the 90% confidence band interval.

With these results of the reference tests regarding the mean number of rocking armour units and the confidence band intervals the other test series can be placed into perspective concerning the reliability.

7.3. ANALYSIS TEST RESULTS

In this section all test series are discussed, a distinction in the analysis is made between:

- small crested breakwater, $s=2\%$ (§7.3.1);
- wide crested breakwater, $s=2\%$ (§7.3.3);
- small crested breakwater, $s=4\%$ (§7.3.2);
- wide crested breakwater, $s=4\%$ (§7.3.4).

For all of the above stated tests, graphs with the number of rocking armour units are plotted against the stability number for the total breakwater, seaside slope and crest. Furthermore in every graph the mean number of rocking armour units for the reference test series is plotted together with the 90% confidence band interval (dashed lines). In §7.4 the influence of the varied parameters is discussed, in this section only the test results are compared to each other.

7.3.1. SMALL CRESTED BREAKWATER, $S=2\%$

In this section all test series with a small crest and wave steepness 2% are considered.

Figure 7.11 Number of rocking armour units small crested breakwaters, all 2% test series, all breakwater sections

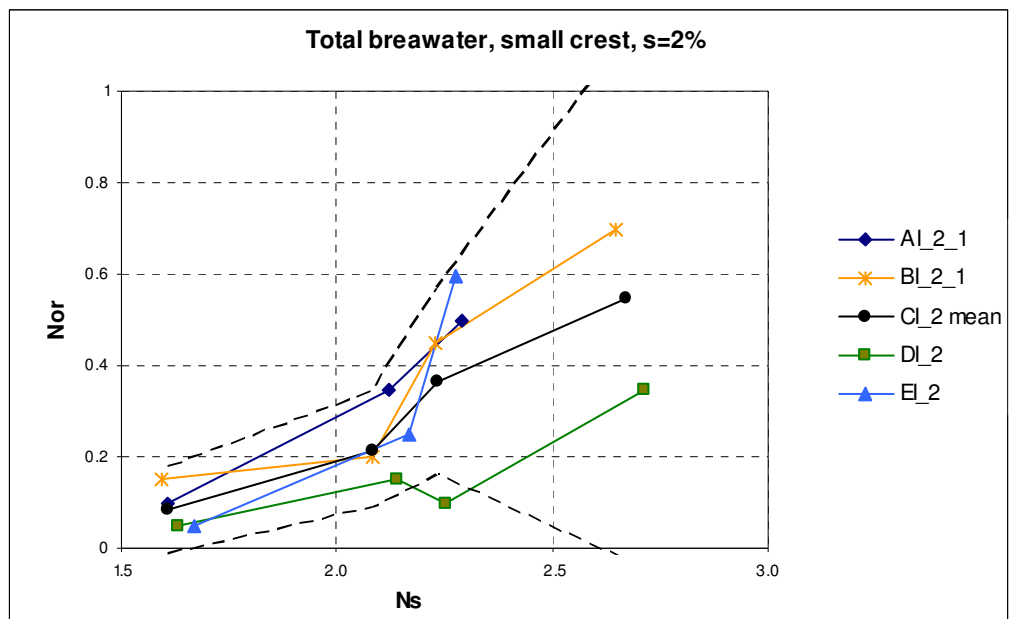


Figure 7.11 total number of rocking armour units for the total breakwater. Test series DI_2 shows the least number of rocking elements throughout the test series whereas initially test series AI_2_1 shows the largest number of rocking armour units. In general the number of rocking armour units increases for

negative crest freeboards. Only test series EI_2 shows a divergent pattern. Before a stability number of approximately 2.2 more rocking elements are present than is the case for DI_2, whereas after a stability number of 2.2 EI_2 shows the most rocking elements. All test series fall inside the 90% confidence band interval of the reference test series.

Figure 7.12 Number of rocking armour units small crested breakwaters, all 2% test series, seaside slope

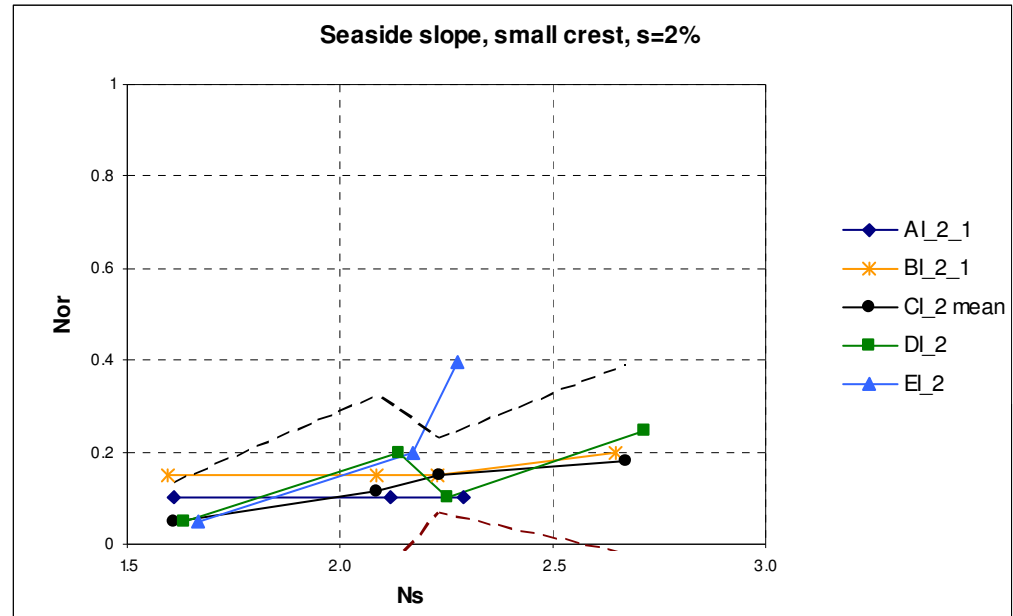


Figure 7.13 shows the number of rocking armour units at the seaside slope. For submerged conditions a substantial number of armour units is already rocking at the beginning of the test series but remains constant for increasing wave heights. Test series BI_2_1 shows that from a stability number of 2.24 the number of rocking elements increases slightly. For zero and positive crest freeboard the number of rocking armour units at the start of a test series is smaller than is the case for negative crest freeboard. Furthermore the number of rocking armour units increases for increasing stability numbers, and increasing crest freeboard. Until stability number 2.1 test series DI_2 and EI_2 shows almost the same amount of rocking armour units, for larger stability numbers rocking increases fast for test EI_2.

Figure 7.13 Number of rocking armour units small crested breakwaters, all 2% test series, crest

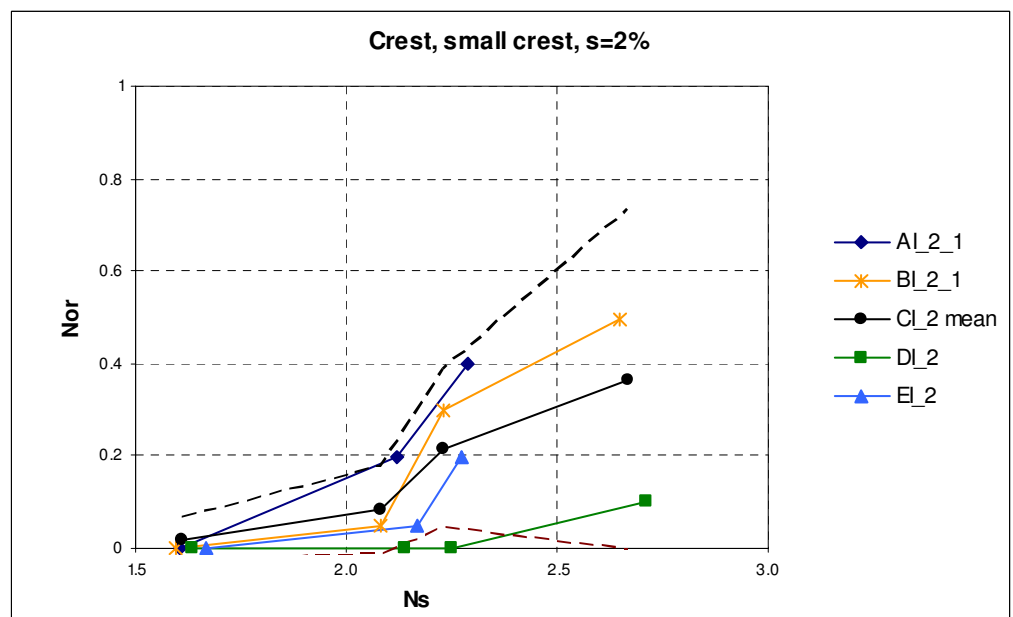


Figure 7.13 shows the number of rocking elements at the crest. The number of rocking elements in general increases from emerged to submerged breakwaters. Only test EI_2 and DI_2 diverges from this trend, the number of rocking elements of test EI_2 is larger than test DI_2. From a stability number of 2.1 to 2.3 the number of rocking armour units increases fast after which the gradient decreases again.

7.3.2. WIDE CRESTED BREAKWATER, S=2%

In this section all test series with a wide crest and wave steepness 2% are considered. These tests have been performed with a relative placement density of 100% whereas the small crested breakwaters with 103% (CI_2_mean).

Figure 7.14 Number of rocking armour units wide crested breakwaters, all 2% test series, all breakwater sections

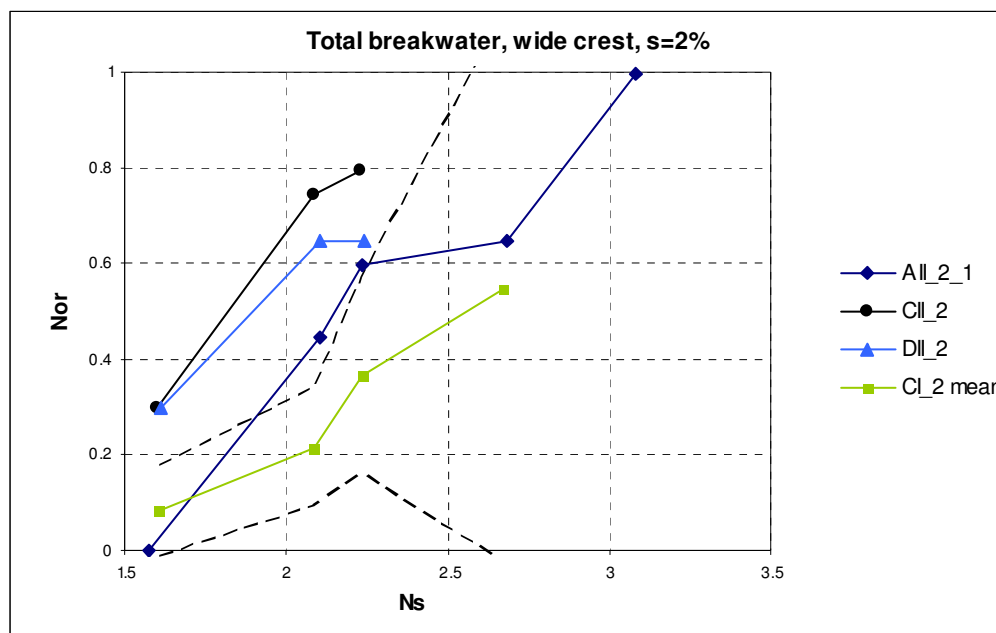


Figure 7.14 shows the number of rocking elements for the total breakwater. At the start of the test series test AII_2_1 no armour units are rocking in contrast to the other tests. For test AII_2_1 the least number of armour units are rocking and an increasing number of armour units from DII_2 to CII_2.

Figure 7.15 Number of rocking armour units wide crested breakwaters, all 2% test series, all breakwater sections

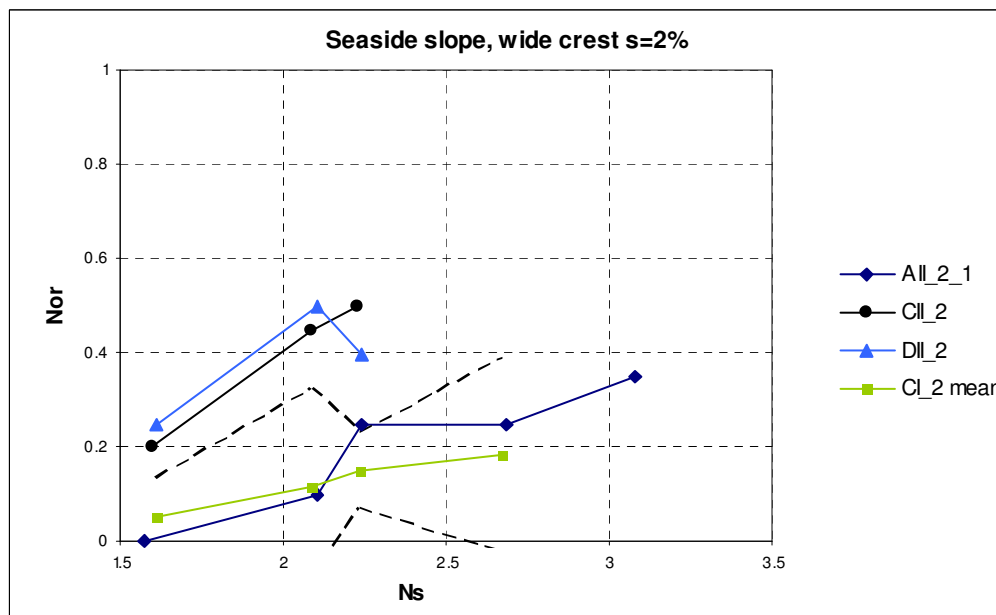


Figure 7.15 shows the number of rocking armour units at the seaside slope. Test AII_2_1, negative crest freeboard, shows no rocking elements at the start of a test series in contrast to zero- and positive crest freeboard. The number of rocking armour units increases from submerged to emerged breakwaters. Only test DII_2 shows a decreasing number of rocking elements for a stability number of 2.25.

Figure 7.16 Number of rocking armour units wide crested breakwaters, all 2% test series, all breakwater sections

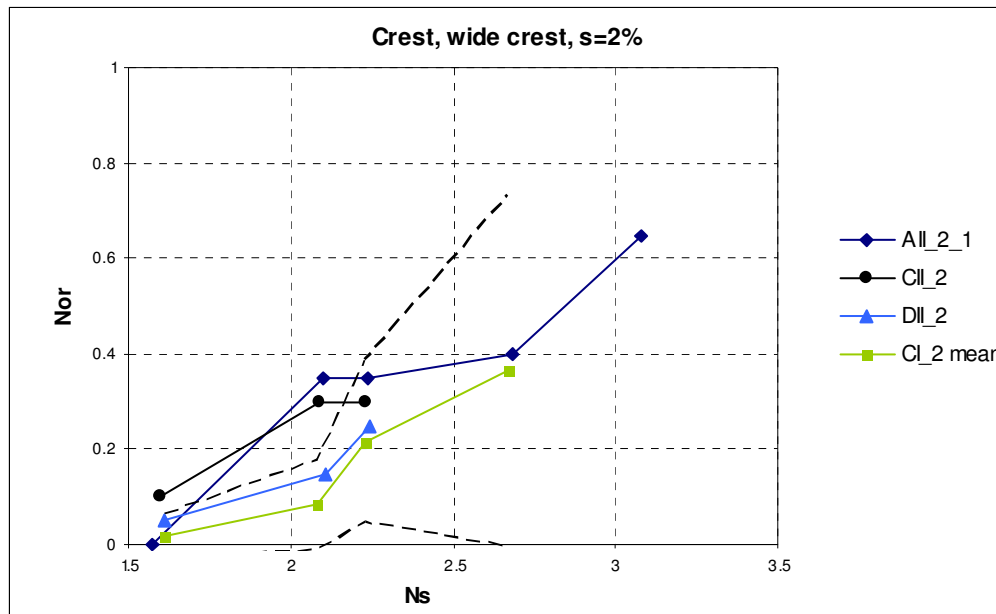


Figure 7.16 shows the number of rocking armour units at the crest. The number of rocking armour units increases from emerged to submerged breakwaters. The number of rocking armour units shows some scattered values at the start of a test series, no armour units are rocking for test series AII_2_1 in contrast to CII_2 and DII_2.

7.3.3. SMALL CRESTED BREAKWATER, S=4%

In this section all test series with a small crest and wave steepness 4% are considered.

Figure 7.17 Number of rocking armour units, all 2% test series, all breakwater sections

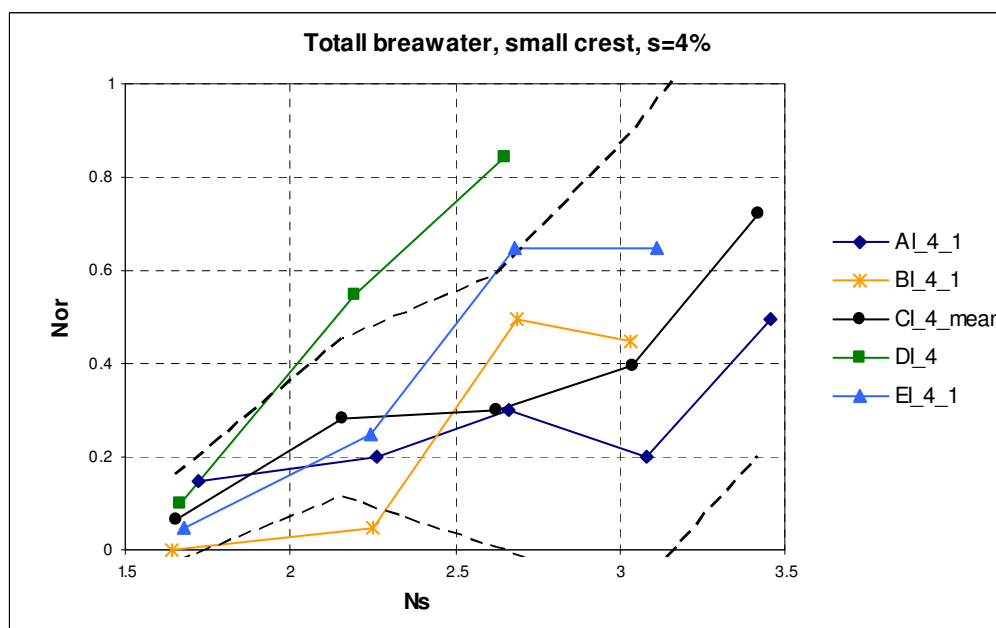


Figure 7.17 shows the number of rocking elements at the total breakwater. In general the number of rocking elements is larger for emerged breakwaters than is the case for submerged breakwaters, where test series DI_4 shows the most rocking armour units. Furthermore the following remarks can be made. At a stability number of 1.6 the largest number of rocking armour units is observed for test series AI_4_1 whereas for test series BI_4_1 no armour units are rocking. The number increases fastest for test series DI_4 and EI_4_1. For test series EI_4_1 no further increase in the number of rocking elements is observed for stability number larger then the design stability number. Structures with a negative crest freeboard show a temporal decreasing number of rocking elements after the design stability number whereas for the positive crest freeboard test series and CI_4_mean the number of rocking elements respectively increases and remains constant.

Figure 7.18 Number of rocking armour units, all 2% test series, all breakwater sections

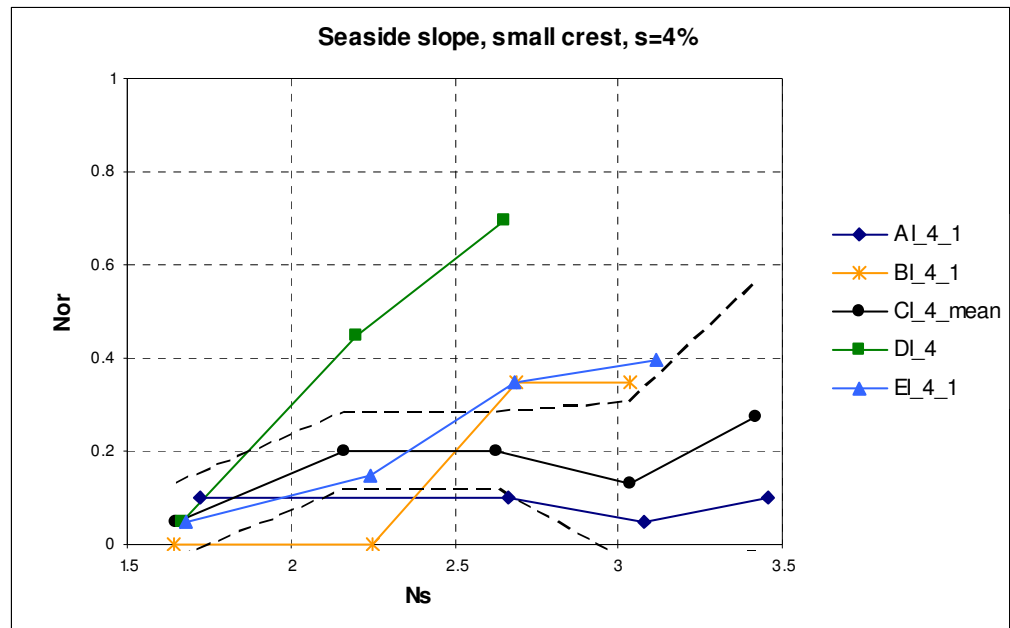


Figure 7.18 shows the number of rocking elements for the seaside slope. The number of rocking armour units is largest for test AI_4_1 at a stability number of 1.6, the other tests show approximately the same number of rocking armour units except for test BI_4_1 for which no armour units are rocking.

For increasing stability numbers the number of rocking armour units remains constant for test series AI_4_1 until a stability number of 2.7, it then decreases slightly and subsequently increases to a larger number of rocking elements. The reference test series shows a similar trend except from the increased rocking at the the lower stability numbers. For test test series BI_4_1 the number of rocking elements is constant until a stability number of 2.25, the number of rocking armour units then increases and becomes constant again. Test series DI_4 clearly show the most rocking elements.

Figure 7.19 Number of rocking armour units, all 2% test series, all breakwater sections

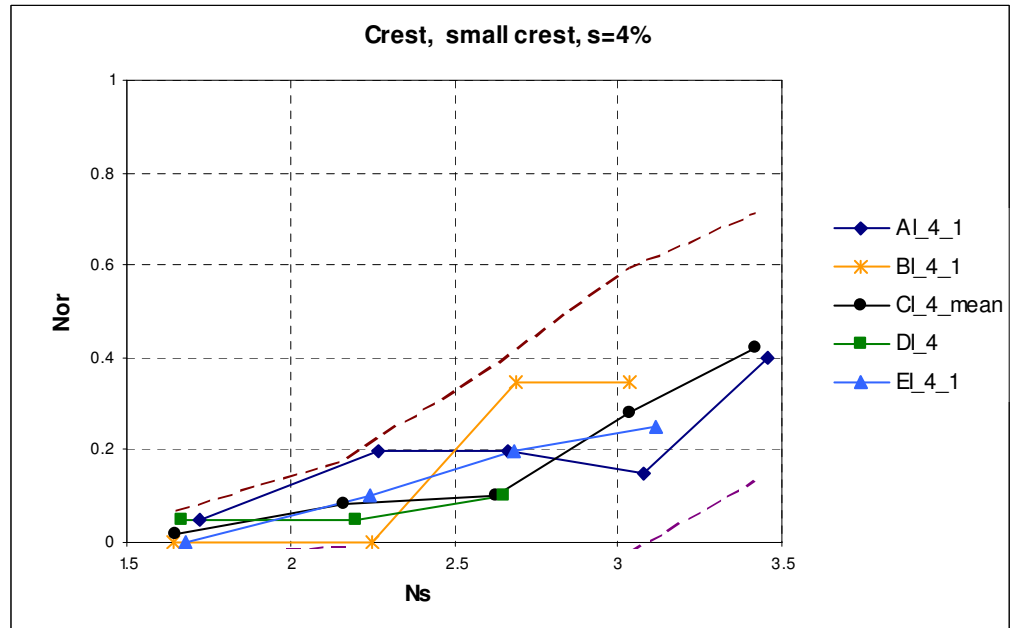


Figure 7.19 shows the number of rocking elements for the crest section. All test series show approximately the same number of rocking elements at a stability number of 1.6. Initially test series AI_4_1 shows the highest number of rocking armour units, whereas for stability numbers larger than the design stability number the relative amount of rocking in comparison to the other test series decreases. Test series BI_4_1 shows exactly the opposite trend as AI_4_1, initially no armour units are rocking and for increasing stability numbers the relative amount of rocking elements becomes maximal. For emerged breakwaters, the amount of rocking is initially constant for test series DI_4 and then gradually increases, whereas for EI_4_1 initially no armour units are rocking but for increasing stability numbers the number of rocking armour units also increases.

7.3.4. WIDE CRESTED BREAKWATER, S=4%

In this section all test series with a wide crest and wave steepness 4% are considered together with the reference situation of the 4% wave steepness.

Figure 7.20 Number of rocking armour units, all 2% test series, all breakwater sections

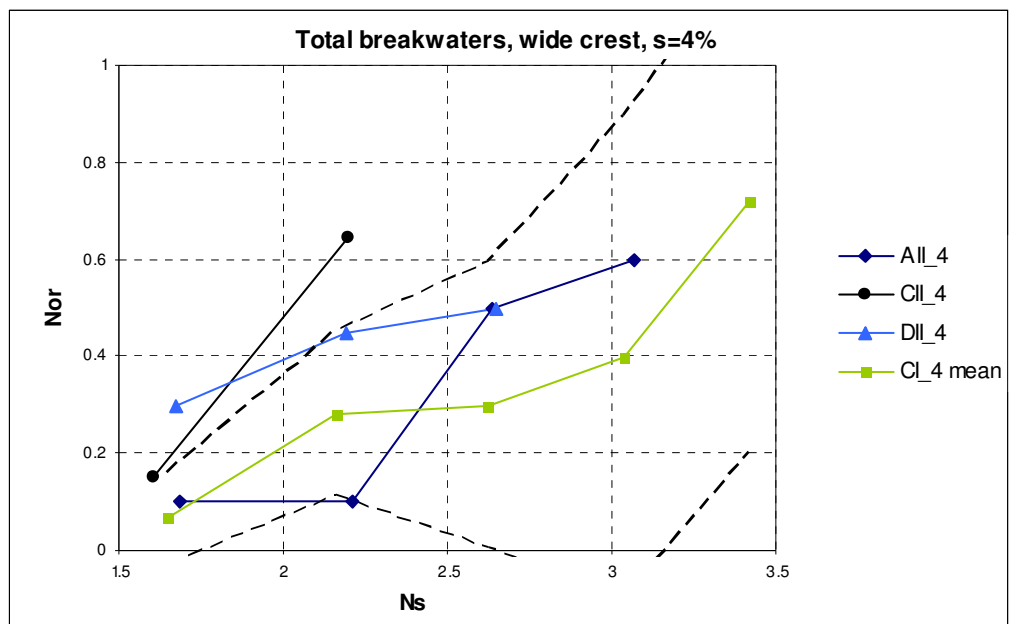


Figure 7.21 shows the number of rocking elements for the total breakwater.

Figure 7.21 Number of rocking armour units, all 2% test series, all breakwater sections

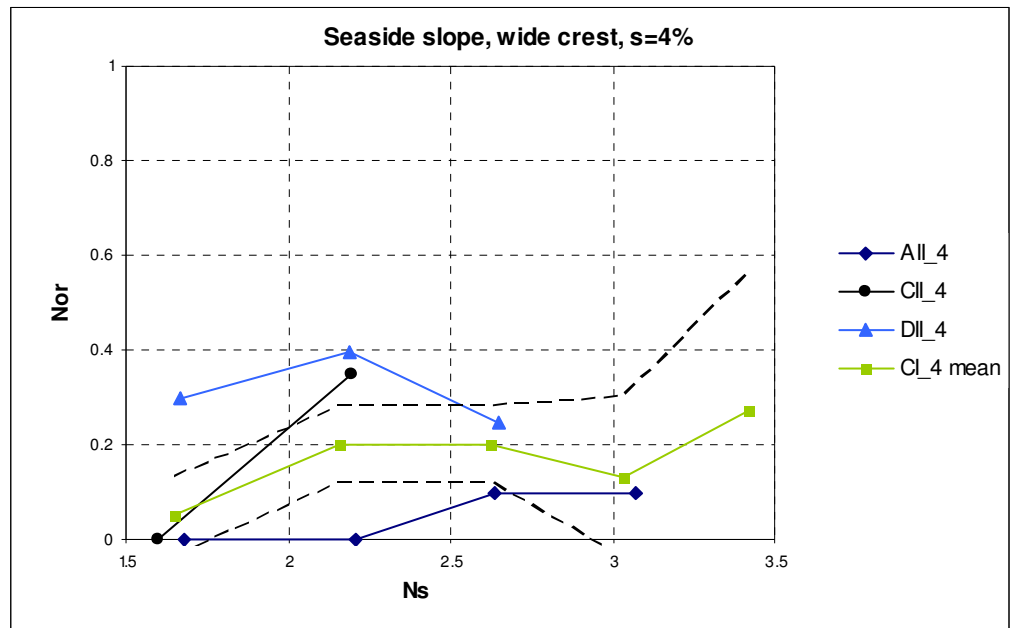


Figure 7.21 shows the number of rocking armour units at the seaside slope. Initially test series CII_4 and DII_4 show no rocking armour units in contrast to test series DII_4. Test series AII_4 show initially no rocking elements, the number increases towards the design stability number whereas it decreases for test series DII_4.

Figure 7.22 Number of rocking armour units, all 2% test series, all breakwater sections

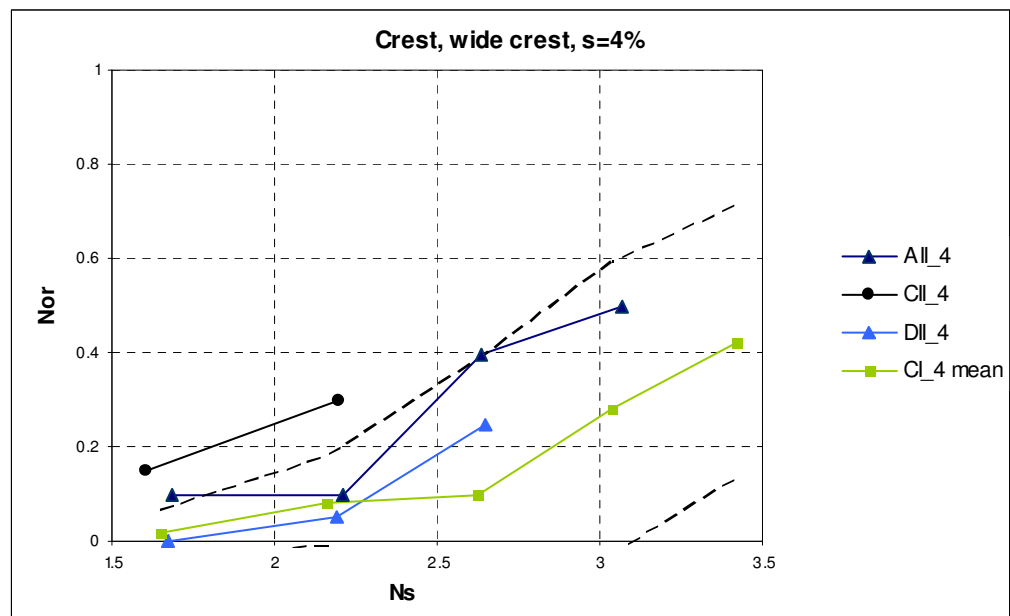


Figure 7.22 shows the number of rocking elements at the crest together with the reference test series. Initially no elements are rocking at the crest for test series DII_4 in contrast to the test series CII_4 and AII_4. Test series DII_4 shows the largest number of rocking elements at the crest whereas test series DII_4 show the least number of rocking elements. The least number of rocking armour units are observed at the crest.

7.4. ANALYSIS R_C/D_N

In the discussion of the test results of the number of rocking armour units for the total breakwater, seaside slope and crest the following subject are treated:

- influence crest freeboard (§7.4.1);
- influence crest width (§7.4.2);
- influence wave steepness (§7.4.3).

This study is aimed at the stability of the Xbloc single layer armour unit at low-crested breakwaters, therefore the influence of crest width and wave steepness is discussed in relation to the stability number and crest freeboard.

The number of rocking armour units is plotted against the stability number (at the y-axis) and crest freeboard (at the x-axis). Through fixed number of rocking elements a trend line is drawn. For the reference test series the mean values are used. Red points with the number of rocking elements between brackets indicate that these points are presumed to enable the drawing of the damage lines. Also the design stability number is plotted to place the number of rocking elements in more perspective. The trend lines are not correlated with the other breakwater sections, $N_{or}=0.1$ at the seaside slope and crest does not imply that the number of rocking elements (N_{or}) at the total breakwater is 0.2. The ratios of the number of rocking elements can not be retrieved from these results. If the same number of rocking elements is observed more than once in a test series, the damage number which occurs at the lowest stability number is used for the determination of the position of the trend line. In the case the required number of rocking armour units for drawing the trend line falls between two observations of the number of rocking armour units the stability number required is calculated by interpolation.

The above described figures show for fixed damage levels the stability number over the crest freeboard. The figures don't give any easily readable information over the damage ratios for the different breakwater sections in case of a fixed total damage number. Therefore plots are made with the crest freeboard on the x-axis and the damage number (N_{or}) on the y-axis. For the plotted fixed damage levels in the above described graph the ratio of damage is plotted for the different breakwater sections. The summated damage numbers for the seaside slope and crest are not always equal to the damage number for the total construction because in some cases elements are rocking at the leeside slope. These figures are of interest because for increasing wave heights (larger damage number) the wave structure interaction and the most severe loaded part of the breakwater can change. A higher number of rocking elements for the total breakwater in case of increased wave heights could for example be caused completely by the higher number or rocking elements at the crest or seaside slope.

7.4.1. INFLUENCE CREST FREEBOARD

The influence of crest freeboard is discussed for wave steepness 2 and 4% and for both wide and small crested breakwaters. The comparison of the results for both wave steepness's is done in §7.4.3.

Small crested breakwater, $s = 2\%$

Figure 7.23 shows the number of rocking armour units for the total breakwater armour layer and Figure 7.24, Figure 7.25 respectively the seaside slope and crest.

The stability of the total breakwater increases from a negative to a positive crest freeboard of 1.5 after which the stability slightly decreases again to a crest freeboard of 3. The declination of the trend line towards a crest freeboard of 3 is unexpected because the design stability number is valid for conventional breakwaters, crest freeboard $(R_c/D_n) \geq 3.75$, where no rocking is allowed. The trends are observed for both damage levels ($N_{or}=0.2$ and $N_{or}=0.3$).

The stability of the seaside slope is maximal for negative crest freeboards and decreases for increasing crest freeboards, the stability is minimum for test series EI_2 ($R_c/D_n = 3$).

The crest section is least stable for the most negative crest freeboards, from there on the stability increases to a maximum for test series DI_2 and remains approximately constant. Actually it should still show an increasing line because finally for emerged breakwaters no wave overtopping takes place and thus also no rocking. Furthermore the number of rocking armour units for test series DI_2 falls outside the expected course of the trend line, this is remarkable because this is not the case for the seaside slope. Due to the fact that the trend line is based on a total of seven test series (including the reference test series) it is reasonable to expect that it shows the right trend and on average the right number of rocking elements.

Figure 7.23 Rocking armour units, total breakwater, $s=2\%$

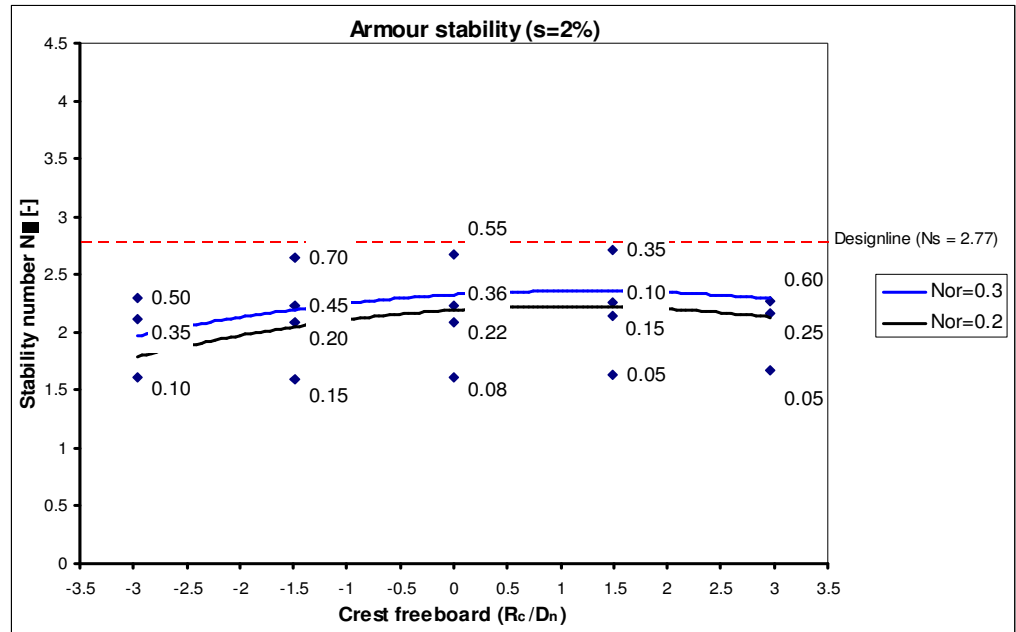


Figure 7.24 Rocking armour units, seaside slope, $s=2\%$

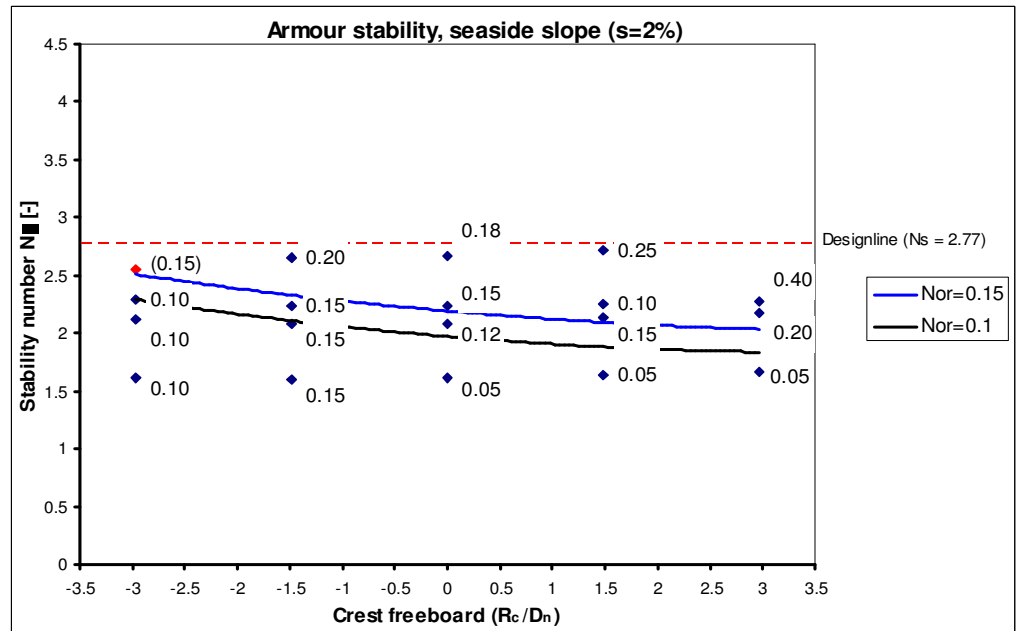


Figure 7.25 Rocking armour units, crest, $s=2\%$

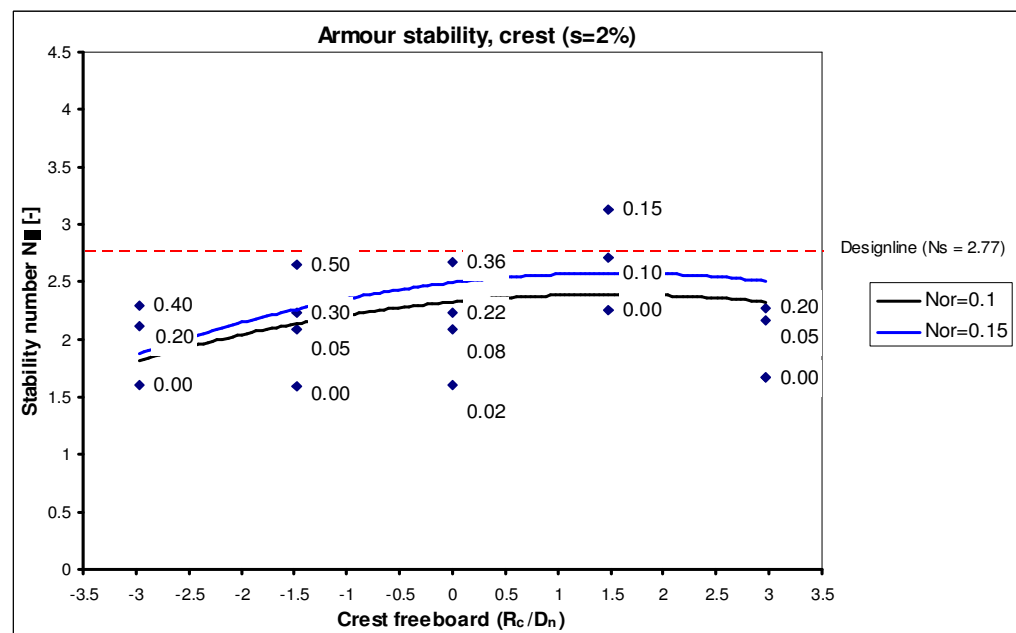


Figure 7.26 Damage ratios for the different breakwater sections, $s=2\%$

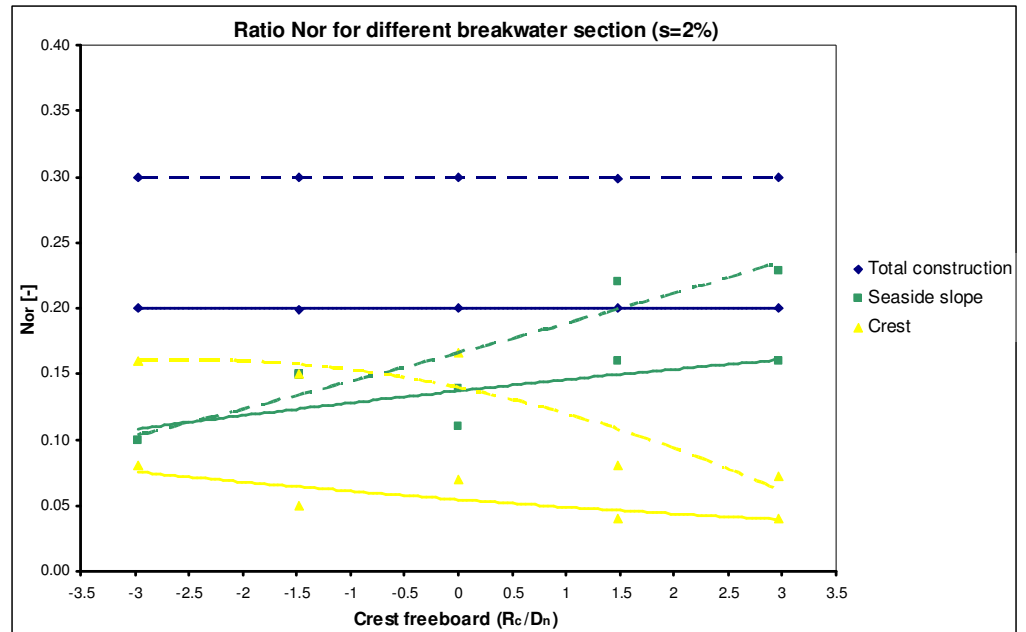


Figure 7.25 shows the ratios of damage for the different breakwaters sections. The dashed trend lines represent a number of rocking elements of 0.3 for the total breakwater, whereas the solid line represents a number of rocking elements of 0.2 for the total breakwater.

For a damage number of $N_{or}=0.3$ and submerged conditions most of the rocking elements are observed at the crest, whereas for $N_{or}=0.2$ most of the rocking element are located at the seaside slope. The number of rocking elements at the seaside slope is independent of the total damage number in case of a crest freeboard (R_c/D_n) of -3. This indicates that rocking at the seaside slope does not necessarily increase for larger wave heights in the case of crest freeboard $R_c/D_n = -3$. For increasing crest freeboard the increase in the total number of rocking elements is mostly caused by rocking elements at the seaside slope, the contribution of the crest to the total number of rocking elements becomes smaller.

For a damage number of $N_{or}=0.2$ the seaside slope shows relatively the most rocking elements for all crest freeboards, whereas for $N_{or}=0.3$ most of the rocking elements are for submerged conditions observed at the crest and for increasing crest freeboard at the seaside slope.

Wide crested breakwater, $s=2\%$

Figure 7.27 shows the number of rocking armour units for the total wide crested breakwater armour layer and Figure 8.28, Figure 8.29 respectively the seaside slope and crest.

The stability of the total breakwater is largest for the most negative crest freeboards and decreases to a minimum for a crest freeboard of 0 to 0.5 in case of $N_{or}=0.3$ and $N_{or}=0.5$ respectively. After the minimum the stability increases slightly again. Both damage levels show a comparable trend line over the crest freeboards.

The stability of the seaside slope (Figure 8.28) is maximal for submerged conditions and decreases for increasing stability numbers to a minimum at a crest freeboard (R_c/D_n) of 0.5. After the minimum the stability increases again for test series DII_2 at a crest freeboard (R_c/D_n) of 1.5 but is still smaller than at a crest freeboard (R_c/D_n) of -3.

Figure 7.29 shows the number of rocking elements for the crest section. The crest section is least stable for crest freeboards (R_c/D_n) of -1, whereas for the most submerged and emerged breakwaters the stability increases. For emerged breakwaters the increase in the stability is largest, this is as expected because for conventional breakwaters no rocking elements are observed anymore at the crest. The two trend lines show a comparable trend for the different crest freeboards.

Figure 7.27 Rocking armour units, total wide crested breakwater, $s=2\%$

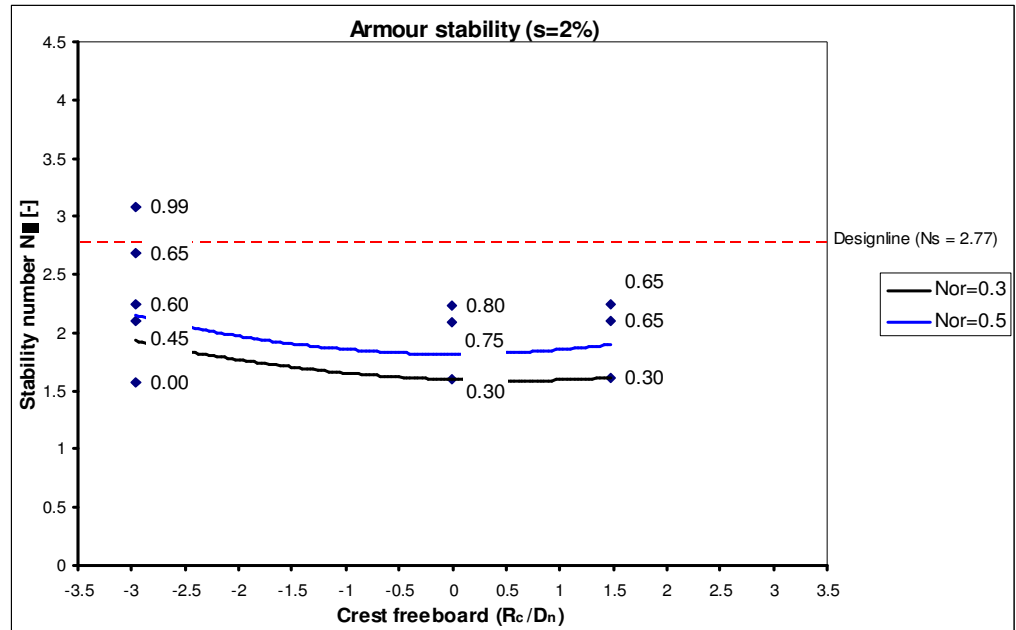


Figure 7.28 Rocking armour units, seaside slope wide crested breakwaters, $s=2\%$

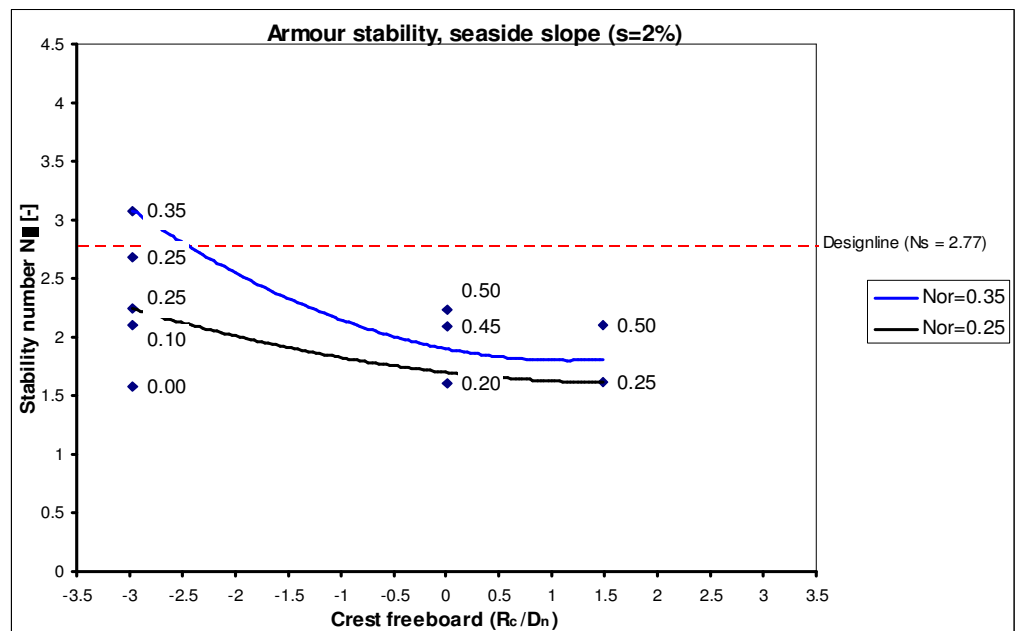


Figure 7.29 Rocking armour units, crest wide crested breakwater, $s=2\%$

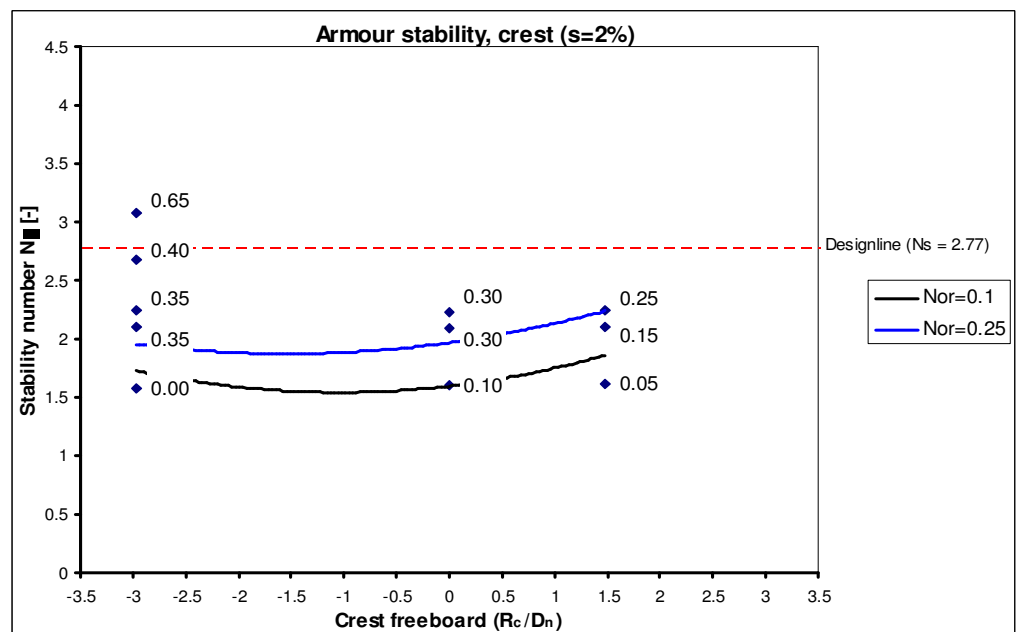


Figure 7.30 Damage ratios for the different breakwater sections, $s=2\%$

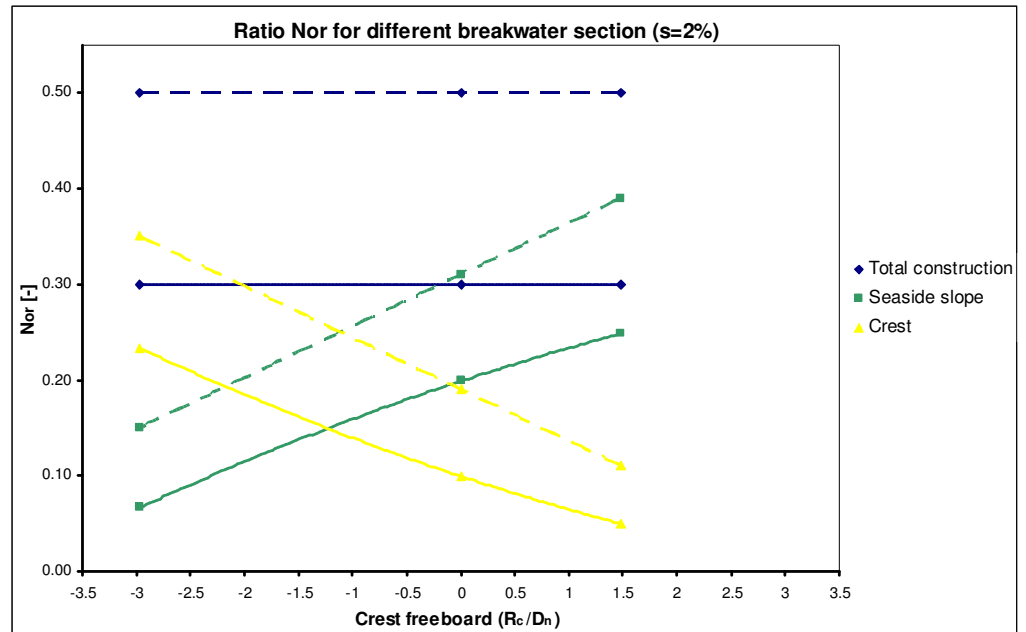


Figure 7.30 shows the ratios of damage for the different breakwaters sections. The dashed trend lines represent a number of rocking elements of 0.5 for the total breakwater, whereas the solid line represents a number of rocking elements of 0.3 for the total breakwater.

For submerged conditions most of the rocking elements are located at the crest whereas for increasing crest freeboards the number of rocking elements at the seaside slope becomes dominant from a crest freeboard (R_c/D_n) of -1.25. The intersection point of the trend lines for the seaside slope and crest for both damage levels is positioned at the same crest freeboard. This indicates that larger wave heights do not lead to a different ratio of the number of rocking elements over the different breakwater sections. An increase in the number of rocking elements ($N_{or}=0.5$) for the total breakwater causes an increased number of rocking elements at the seaside slope and crest. For submerged conditions the increase at the crest is largest whereas for emerged breakwaters this is seaside slope.

Small crested breakwater, $s=4\%$

Figure 7.31 shows the number of rocking armour units for the total breakwater armour layer and Figure 7.32, Figure 7.33 respectively the seaside slope and crest.

Figure 7.32 shows the number of rocking elements for the total breakwater. The stability decreases from submerged to emerged crest freeboards. At a crest freeboard (R_c/D_n) of 3 a slightly increasing trend line is visible which is as expected because it becomes a conventional breakwater. The stability is minimal for a crest freeboard (R_c/D_n) of 1.5. The two damage levels show a somewhat different line, but it is expected that this is caused by the uncertainties in the number of rocking elements.

Figure 7.32 shows the stability for the seaside slope. The stability of the seaside slope is minimal for a crest freeboard of 1.5 in case of $N_{or}=0.1$ and $N_{or}=0.15$ for a crest freeboard of 1. Subsequently the stability increases for increasing crest freeboards. For a small number of rocking elements the trend lines approaches the design stability number for conventional breakwaters ($R_c/D_n \geq 3.75$) which indicates a good reliability of the analysis.

Figure 7.33 shows the stability of the crest section. The crest is relatively unstable for submerged condition whereas the stability increases and becomes maximal between crest freeboards of 0 and 1.5. For positive crest freeboards the stability decreases again which is not in line with the expectations because for increasing crest freeboards wave overtopping decreases and thereby the load and the number of rocking elements.

Figure 7.31 Rocking armour units, total breakwater, $s=4\%$

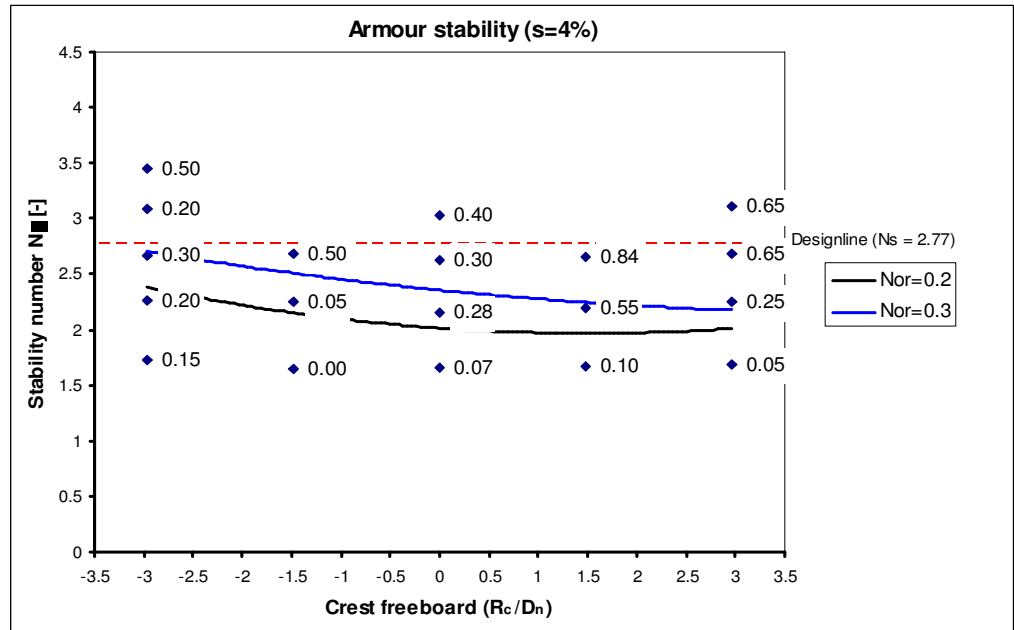


Figure 7.32 Rocking armour units, seaside slope, $s=4\%$

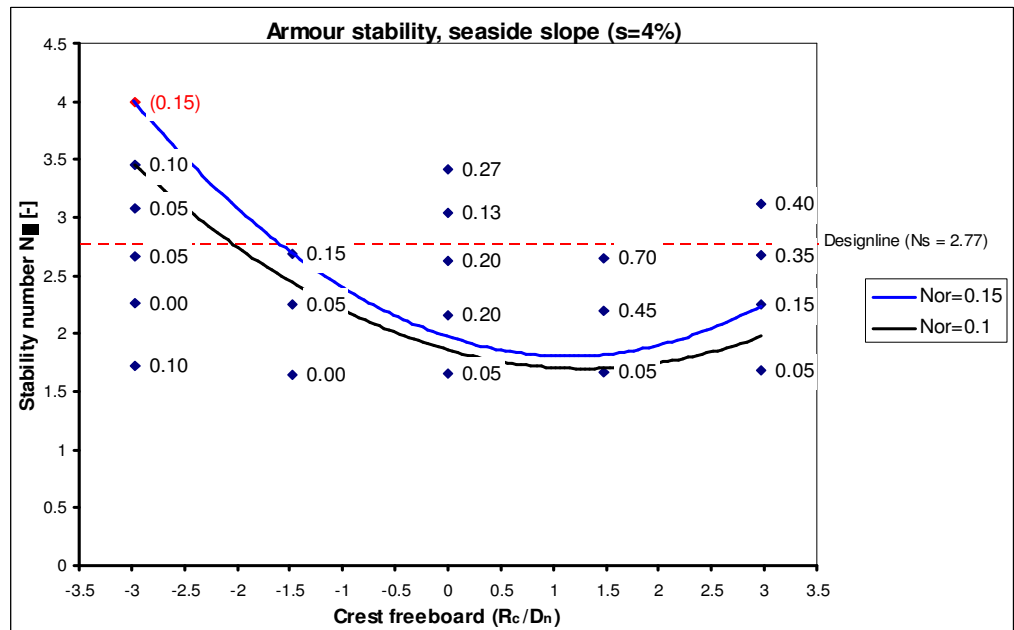


Figure 7.33 Rocking armour units, crest, $s=4\%$

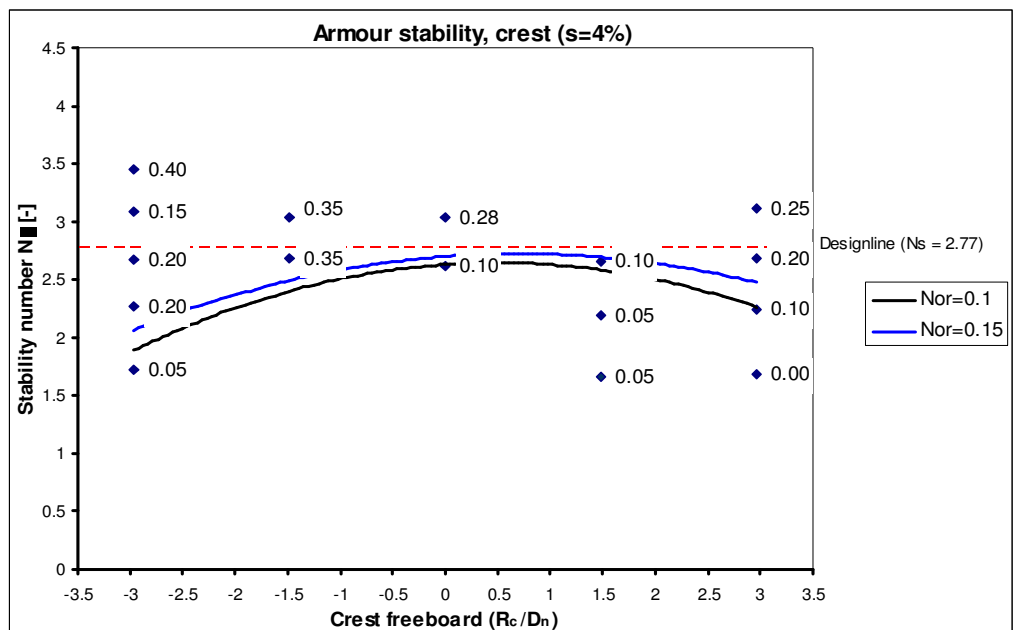


Figure 7.34 Damage ratios for the different breakwater sections, $s=4\%$

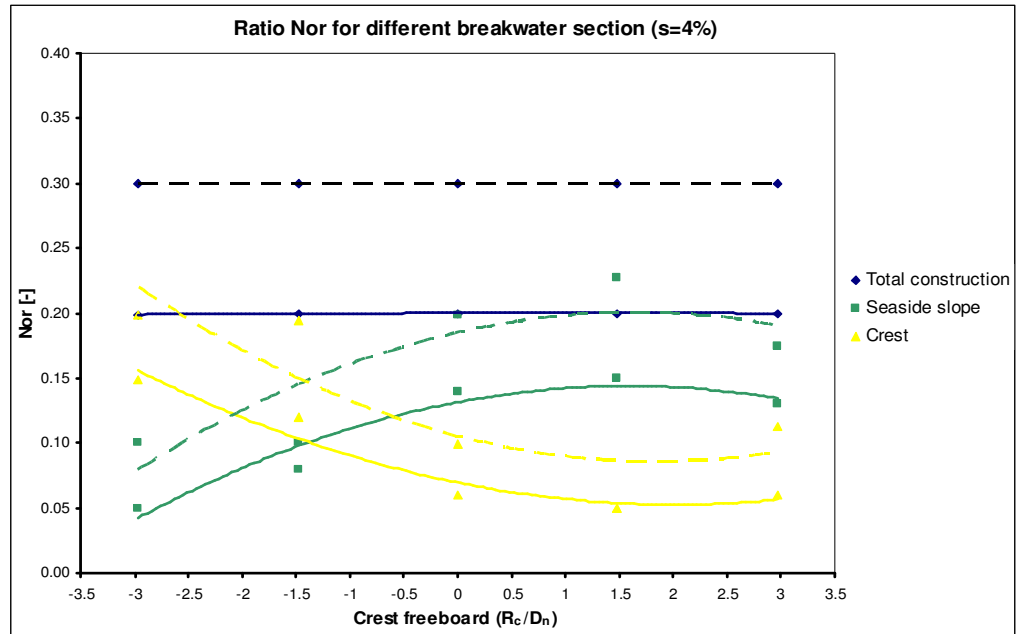


Figure 7.34 shows the ratios of damage for the different breakwaters sections. The dashed trend lines represent a number of rocking elements of 0.3 for the total breakwater, whereas the solid line represents a number of rocking elements of 0.2 for the total breakwater.

The contribution of the number of rocking elements at the seaside slope, to the total number of rocking elements for the total breakwater, increases from a negative crest freeboard to a crest freeboards (R_c/D_n) of 1.5 for both damage levels. Subsequently the contribution becomes less for larger crest freeboards. For the crest section exactly the opposite trend is perceptible. Until a crest freeboard (R_c/D_n) of -1.5 the crest shows the largest number of rocking elements whereas for larger crest freeboards this alters to the seaside slope, this holds for both damage levels. The total number of rocking armour units is correlated with the wave height, larger wave heights results in larger damage numbers, increasing wave heights could also change the location of maximal loading of the armour layer but this is not the case in Figure 7.34 because of the same intersection points of the seaside slope and crest for both damage levels. When the number of rocking elements increases for the total breakwater, the increase of the number of rocking element at the crest is slightly larger than for the seaside slope in case of negative crest freeboard. For positive crest freeboards it is the other way around, the seaside slope shows a relatively larger increase in the number of rocking elements than is the case for the crest.

Wide crested breakwater, $s=4\%$

Figure 7.35 shows the number of rocking armour units for the total wide crested breakwater armour layer and Figure 7.36, Figure 7.37 respectively the seaside slope and crest.

Figure 7.35 shows that the trend lines of fixed damage numbers show a different trend from each other for different crest freeboards. The stability in case of a number of rocking elements for $N_{or}=0.3$ is maximal for submerged conditions and becomes increasingly less stable for emerged breakwaters. Whereas for $N_{or}=0.5$ for crest freeboards (R_c/D_n) of 1.5 and -3 the stability is maximum and minimum at a crest freeboard (R_c/D_n) of -0.75. The minimum stability shifts from positive towards negative crest freeboard for increasing number of rocking elements.

Figure 7.36 shows the number of rocking element at the seaside slope. No trend line can be drawn for a fixed number of rocking elements. Therefore a conservative assumption has been made regarding the point at a crest freeboard (R_c/D_n) of -3 for plotting the trend lines. The stability decreases from submerged to emerged conditions and becomes minimum for a crest freeboard (R_c/D_n) of 1.5.

Figure 7.37 shows the number of rocking elements at the crest. The stability is maximal for emerged breakwaters and becomes minimal at a crest freeboard (R_c/D_n) of -0.75. For more negative crest freeboards the stability increases. The same trend is observed for both damage levels.

Figure 7.35 Rocking armour units, total wide crested breakwater, $s=4\%$

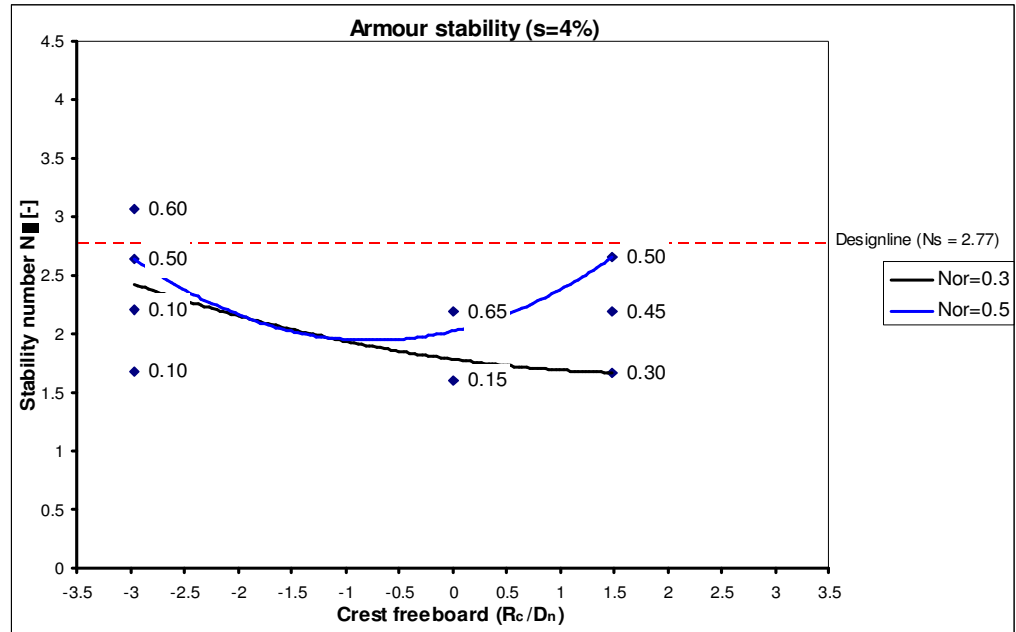


Figure 7.36 Rocking armour units, seaside slope wide crested breakwater, $s=4\%$

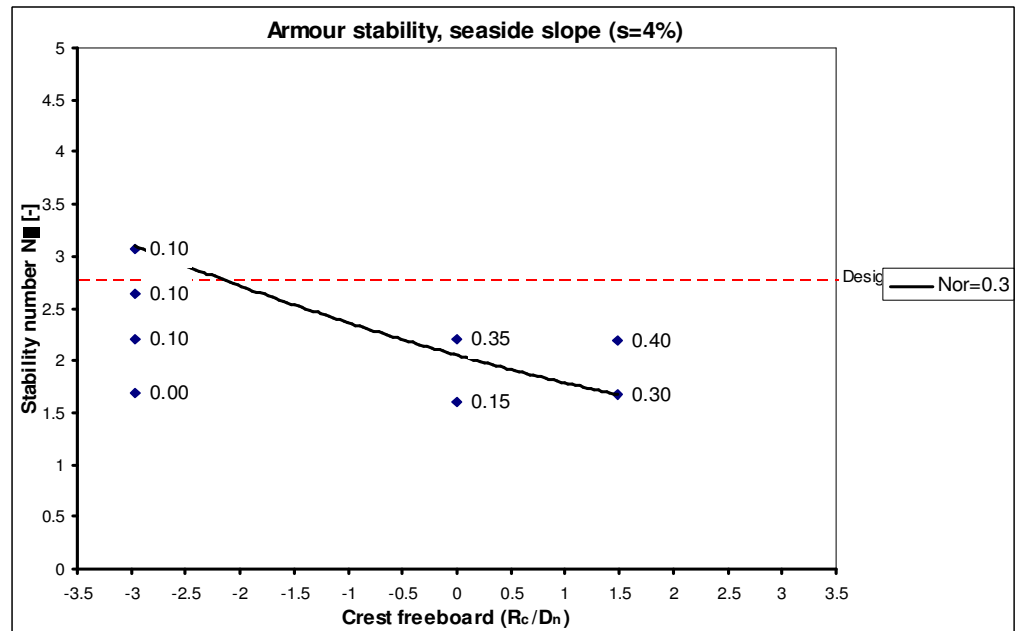


Figure 7.37 Rocking armour units, crest wide crested breakwater, $s=4\%$

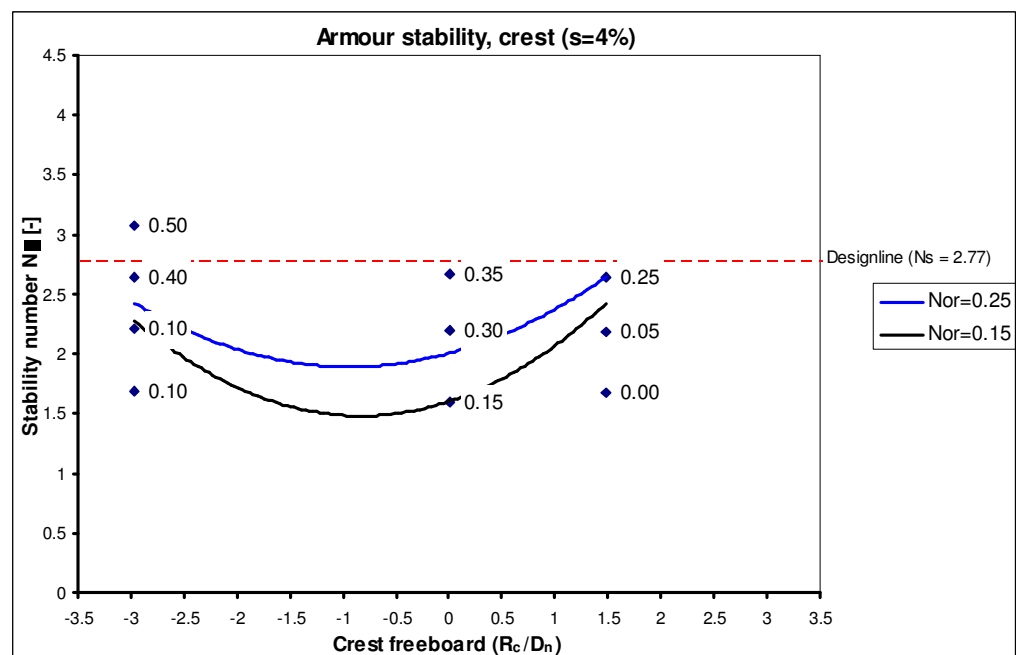


Figure 7.38 Damage ratios for the different breakwater sections, $s=4\%$

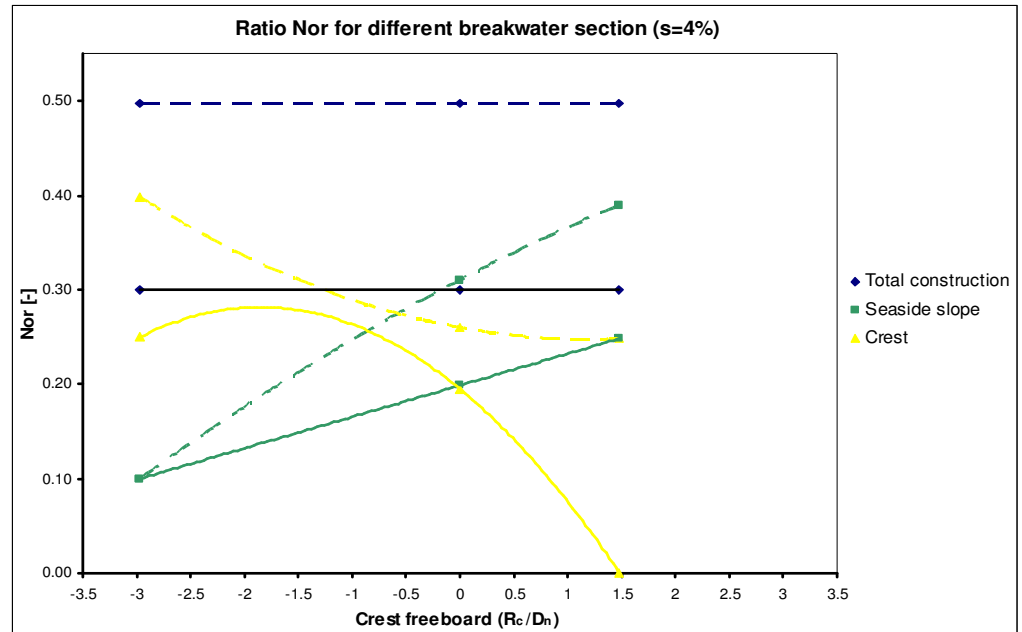


Figure 7.38 shows the ratios of damage for the different breakwaters sections. The dashed trend lines represent a number of rocking elements of 0.5 for the total breakwater, whereas the solid line represents a number of rocking elements of 0.3 for the total breakwater. For submerged conditions most of the rocking elements are located at the crest whereas for increasing crest freeboards the number of rocking elements at the seaside slope becomes dominant from a crest freeboard (R_c/D_n) of -0.5 and 0.1 for damage levels of $N_{or}=0.5$ and $N_{or}=0.3$ respectively. For a number of rocking elements of $N_{or}=0.3$ for the total breakwater no rocking armour units at the crest are observed in case of crest freeboard (R_c/D_n) of 1.5. The damage level of $N_{or}=0.3$ occurs at small wave heights at which almost no wave overtopping takes place, therefore no rocking elements are observed. An increase in the number of rocking elements for the total breakwater causes more rocking elements at the crest and not at the seaside slope for submerged conditions. For emerged condition both the seaside slope and crest show an increased number of rocking elements.

Conclusions

The crest freeboard has the following influence on the stability of the total breakwater, seaside slope and crest for all breakwater sections.

- Rocking occurs already for stability number smaller than the design stability number.
- 2% wave steepness
 - For the total breakwater the stability increases for increasing stability numbers until a crest freeboard of 1.5 after which it decreases slightly;
 - The seaside slope is most stable for submerged conditions and the stability decreases for positive crest freeboard;
 - The crest is least stable for submerged conditions and the stability increases for emerged conditions.
 - For increasing crest freeboards the number of rocking elements at the seaside slope increases whereas for the crest section it decreases.
 - For a total damage number of $N_{or}=0.2$ most of the rocking elements are observed at the seaside slope in case of submerged conditions. For increasing wave heights and thereby increasing total damage numbers $N_{or}=0.3$ the crest shows the most rocking elements, the number of rocking elements at the seaside slope remains the same as for the lower damage number.
 - For increasing crest freeboards the difference in the total number of rocking elements ($N_{or}=0.2$, $N_{or}=0.3$) is mainly caused by the higher damage numbers at the seaside slope.
- 4% wave steepness
 - The stability of the total breakwater decreases for increasing stability numbers, at a crest freeboard (R_c/D_n) of 3 a slight decrease of stability is present.
 - The seaside slope shows a large variation of the stability over crest freeboard. For submerged conditions the largest stability is reached whereas for a crest freeboard (R_c/D_n) between 0 and 1.5 the minimum stability is reached. For larger crest freeboards the stability increases, which is in accordance with the expectation of almost no rocking armour units at the design stability number for conventional breakwaters ($R_c/D_n \geq 1$);
 - The crest is most stable for crest freeboards (R_c/D_n) between 0 and 1.5 whereas for other crest freeboard the stability decreases. The absolute minimum is reached for the most submerged conditions.
 - Until a crest freeboard R_c/D_n of -1.5 the crest section shows the most rocking elements, for crest freeboards R_c/D_n larger than -1.5 seaside slope section shows most of the rocking elements.
 - The differences caused by the different total number of rocking armour units ($N_{or}=0.2$, $N_{or}=0.3$) is that for submerged breakwaters the increase of the number of rocking elements at the crest is largest whereas for a positive crest freeboard the seaside slope shows the largest number of rocking elements.

7.4.2. INFLUENCE CREST WIDTH AND RELATIVE PLACEMENT DENSITY

Two different crest widths are tested, three and nine armour units wide respectively. The wide crested breakwaters are performed with a relative placement density of 100% whereas the small crested breakwaters have a relative placement density of 103%. In this section the influence of a wide and small crest and the different relative placement densities are compared to each other for all breakwater sections. The difference in stability for the seaside slope between the wide and small crested breakwater is expected to be largely caused by the lower relative placement density, whereas the difference in the stability of the crest is expected to be caused by the crest width.

A trend line for a fixed number of rocking elements for both crest widths is plotted over the crest-freeboards. The plotted fixed number of rocking elements is not always the same for both the wide and small crested breakwaters, given the observed number of rocking elements. Therefore in some cases two different fixed numbers of rocking elements are plotted. The maximum tested crest freeboard (R_c/D_n) for wide crested breakwaters is 1.5, therefore the trend lines are extrapolated to a crest freeboard (R_c/D_n) of 3 to enable the comparison of the wide and small crested breakwater for all crest freeboards. The comparison is made for either wave steepness's.

Wave steepness 2%

Figure 7.39 shows the number of rocking elements at the total breakwater, whereas Figure 7.40 and Figure 7.41 shows the number of rocking elements at the seaside slope and crest respectively.

The total breakwater shows two different trends for the two breakwaters crest widths. At a crest freeboard (R_c/D_n) of -3 the stability is the same for both crest widths in case of a number of rocking elements (N_{or}) of 0.3. The stability of the wide crested breakwater decreases for increasing crest freeboards and attains a minimum for a crest freeboard (R_c/D_n) of 0.5. Whereas the stability of the small crested breakwater increases for increasing crest freeboards and attains a maximum at a crest freeboard of 1.5.

At the seaside slope the stability of wide crested breakwaters is smaller than in the case of small crested breakwaters. The plotted trend lines do not show a comparable number of rocking elements because this is not feasible due to the test results. As a consequence the results of the influence of crest width are larger than suggested by Figure 7.42 for the seaside slope. For both crest widths the same trend lines are observed, the difference between the trend lines is smallest for the most submerged conditions. As stated earlier the difference at the seaside slope is expected to be caused by relative placement density instead of the crest width itself.

The crest section shows that in general the wide crest is less stable than the small crest. Furthermore two different trends for the stability of the wide and small crested breakwaters are observed. At a crest freeboard (R_c/D_n) of -3 the stability is almost the same for both crest widths. For increasing crest freeboards the stability increases until a maximum stability is reached for a crest freeboard (R_c/D_n) of 0, after that the stability decreases again. The

stability for wide crested breakwaters shows that initially the stability decreases for increasing crest freeboards and increases again for crest freeboards (R_c/D_n) larger than -1.

Figure 7.39 Total number of rocking armour units, small and wide crested breakwater, $s=2\%$

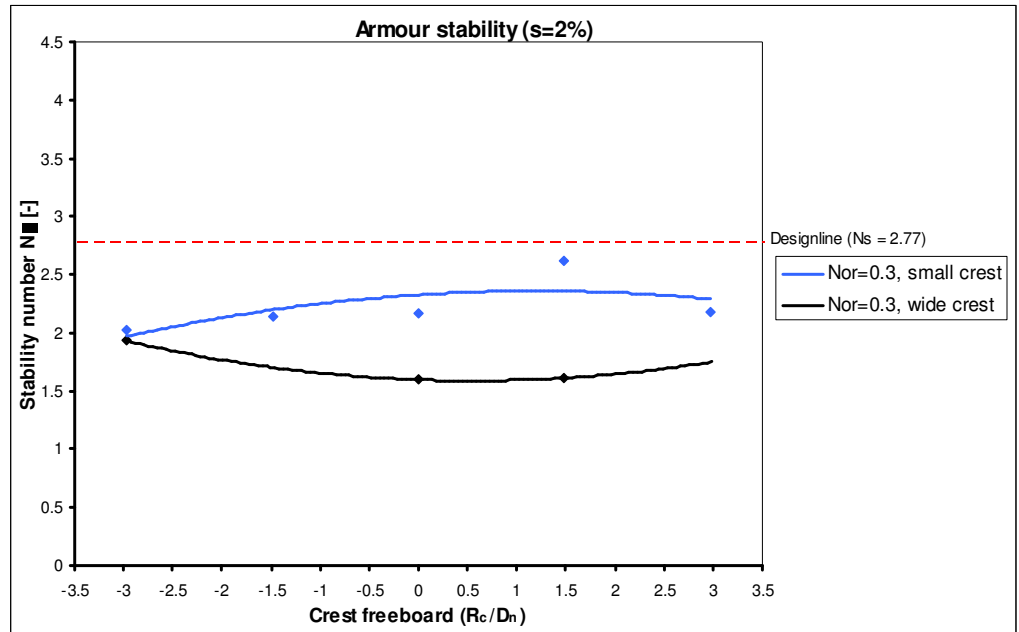


Figure 7.40 Rocking armour units at seaside slope, small and wide crested breakwater, $s=2\%$

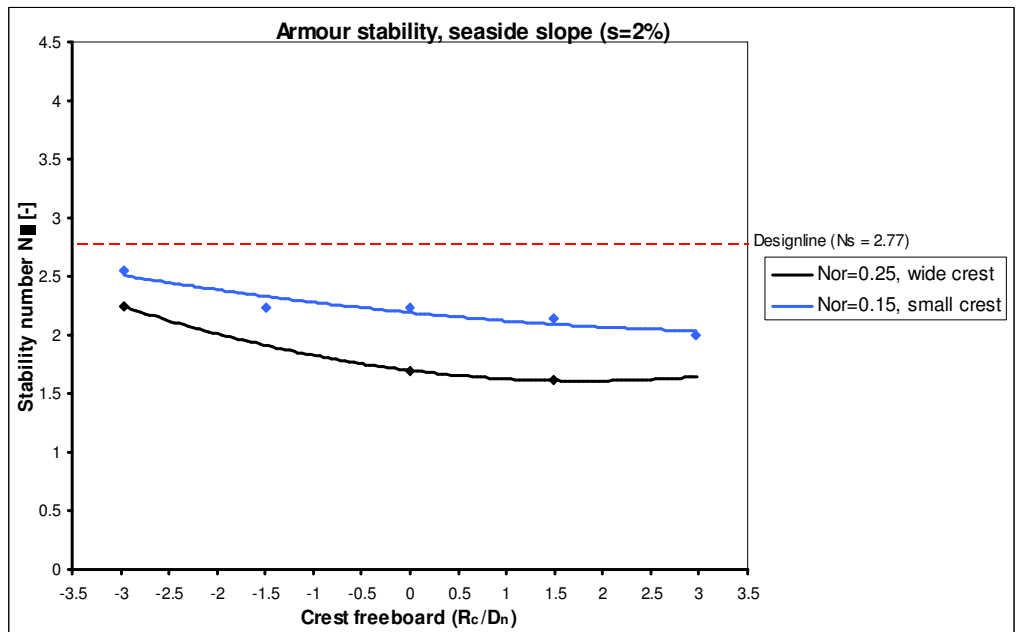
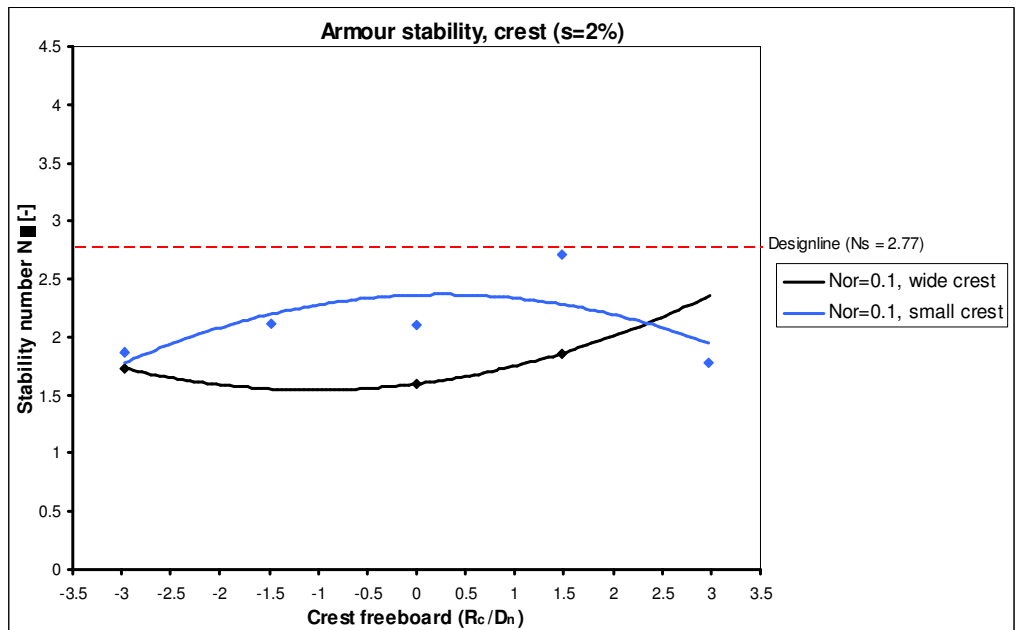


Figure 7.41 Rocking armour units at seaside slope, small and wide crested breakwater, $s=2\%$



Wave steepness 2%

Figure 7.42 shows the number of rocking elements at the total breakwater, whereas Figure 7.43 and Figure 7.44 shows the number of rocking elements at the seaside slope and crest respectively.

The stability of the total breakwater armour layer shows the same trend for both wide and small crested breakwaters, although some deviations of point from the trend line are present. The wide crested breakwater is the least stable and the difference in stability is smallest for a crest freeboard (R_c/D_n) of -3 and 1.5 although the trend line does not show it.

The seaside slope shows comparable trends for both crest widths, where the wide crested breakwater is the least stable. It was not possible to plot comparable damage levels for both crest widths, a damage level of $N_{or}=0.3$ for the small crested breakwater is more stable therefore the difference in stability between the two crest widths increases. At a crest freeboard (R_c/D_n) of 0 the difference between the stability for both crest widths is smallest and increases for more deviating crest freeboards. As stated earlier the difference at the seaside slope is expected to be caused by relative placement density instead of the crest width itself.

The stability for the crest section is almost the same for both wide and small crest breakwater in the case of the most submerged tested conditions. Both crest widths show an opposite trend, for the wide crested breakwater a decreasing trend towards a minimal stability at a crest freeboard (R_c/D_n) of -1 is present and for the small crested breakwater and increasing stability towards a maximum.

Figure 7.42 Total number of rocking armour units, small and wide crested breakwater, $s=2\%$

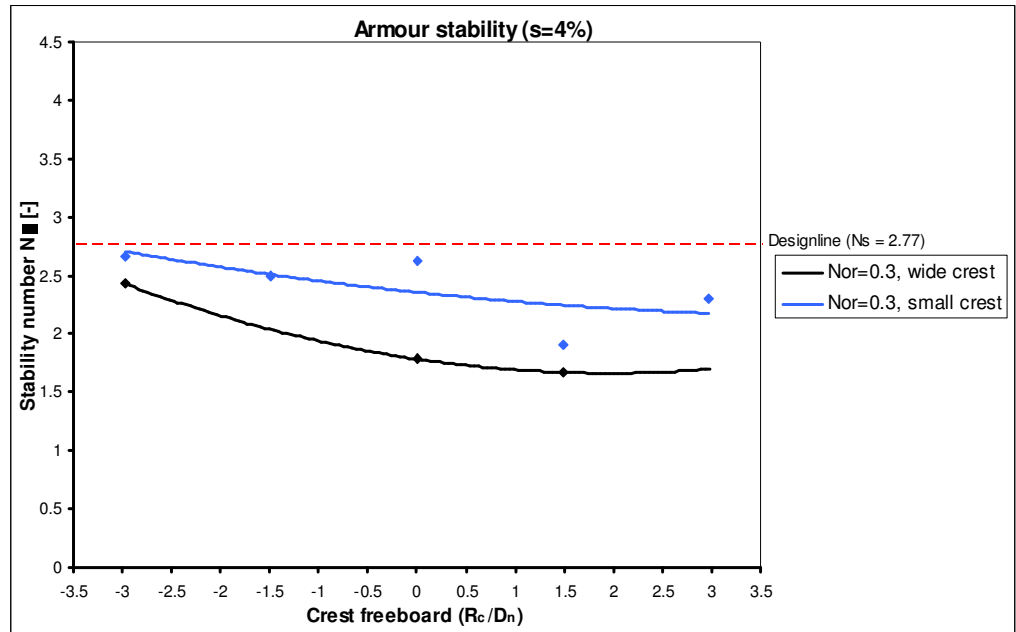


Figure 7.43 Rocking armour units at seaside slope, small and wide crested breakwater, $s=4\%$

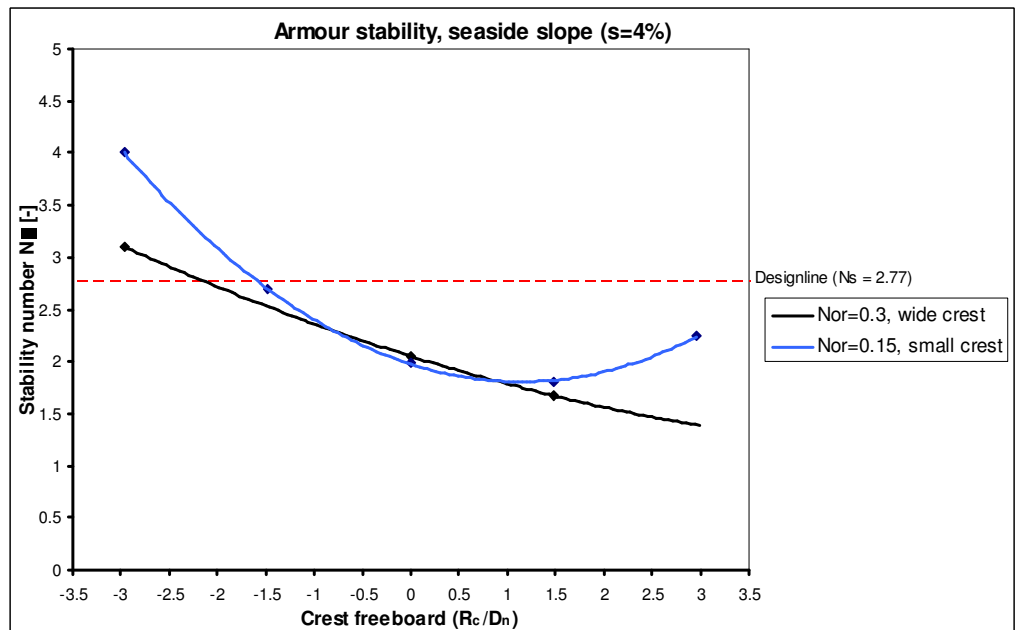
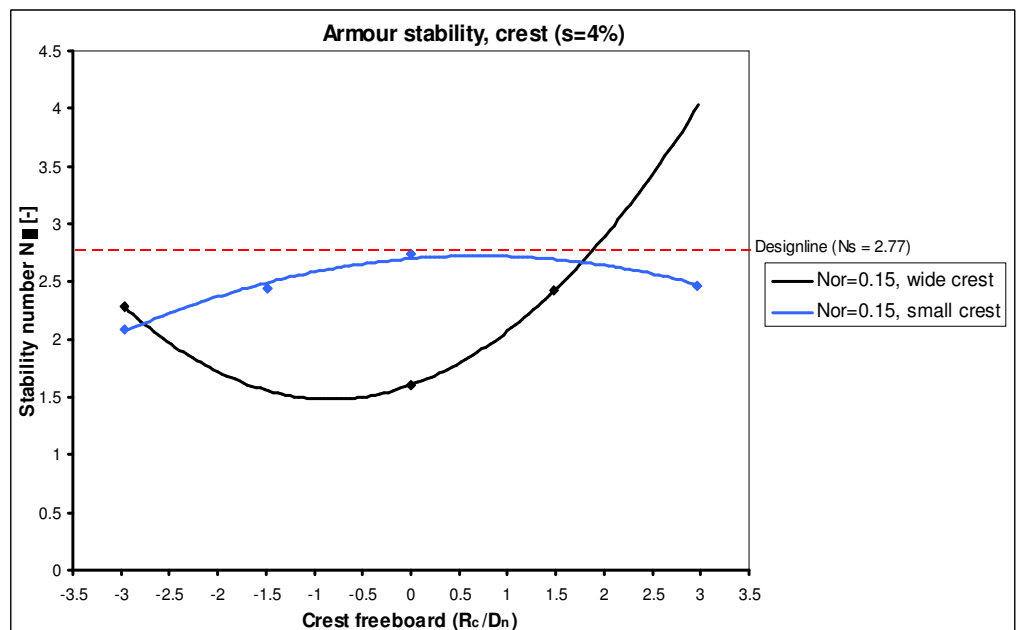


Figure 7.44 Rocking armour units at crest, small and wide crested breakwater, $s=4\%$



Conclusions

The following conclusions can be drawn regarding the crest width and the relative placement density:

- For all wide crested breakwaters the stability is lower than is the case for small crest breakwaters, this is caused due to the lower relative placement density and the increased potential number of rocking armour units at the total breakwater.
- The seaside slope shows for both wide and small crested breakwaters decreasing stability numbers for increasing crest freeboard, except for a wave steepness of 4% and crest freeboard (R_c/D_n) of 3 an increasing trend is observed.
- The crest shows for both wave steepness's the same trend for the wide and small crested breakwaters. The small crested breakwaters show an increasing stability from submerged conditions until a crest freeboard (R_c/D_n) of 0 and 1 for respectively wave steepness 2 and 4% where after the stability decreases again for increasing crest freeboards. The stability of the crest of the wide crested breakwater shows a relatively large stability for submerged and emerged breakwaters and is minimal in between.
- Almost the same the stability is reached for the total breakwater for both crest widths for the most submerged tested conditions. This indicates that the influence of both the crest width and the relative placement density does not have a large influence in the case of the most

7.4.3. INFLUENCE WAVE STEEPNESS

The previous discussed subjects are threaded separated for each wave steepness. In this section the influence of the wave steepness at the number of rocking elements is discussed. To this end, trend lines for a fixed number of rocking elements are draw for the different breakwater sections. The plots are made for both the small and wide crested breakwaters.

Small crested breakwater

Figure 7.45 shows the trend lines for the total breakwater, the trend line for the 4% wave steepness shows the opposite course of the 2% wave steepness. At negative crest freeboards waves with a steepness of 2% show more rocking elements than is the case for the 4% wave steepness. This alters at zero crest freeboard; the 4% waves show a larger number of rocking elements. For the most emerged tested breakwater almost the same number of rocking armour units are present. Only for zero and 1.5 crest freeboard (R_c/D_n) some deviations form the trend lines are present. Test series DI show the most rocking elements in case of 4% wave steepness whereas for the 2% wave steepness this test series show the least number of rocking elements. For wave steepness 2% most rocking armour units are observed for a crest freeboard (R_c/D_n) of -3.

Figure 7.46 shows the number of rocking elements at the seaside slope. The seaside slope is most stable for both a wave steepness of 2 and 4% in the case of submerged conditions. The stability in case of 2% wave steepness decreases almost linearly to the most emerged breakwater. Whereas the stability in case of 4% wave steepness decreases relatively fast and attains a minimum for a crest freeboard (R_c/D_n) of 1.5. After that, the stability increases again which is logical because the crest freeboard becomes larger and approach that of a conventional breakwater, where the design stability number is valid.

Figure 7.47 shows the number of rocking armour units for the crest. The armour units are less stable for the 2- than for the 4 percent wave steepness. The difference in stability for both wave steepness's decreases for increasing positive crest freeboards. For both the 2- as the 4% wave steepness the stability increases for increasing stability numbers.

Figure 7.45 Influence wave steepness on rocking armour units, small crested breakwaters, total breakwater,

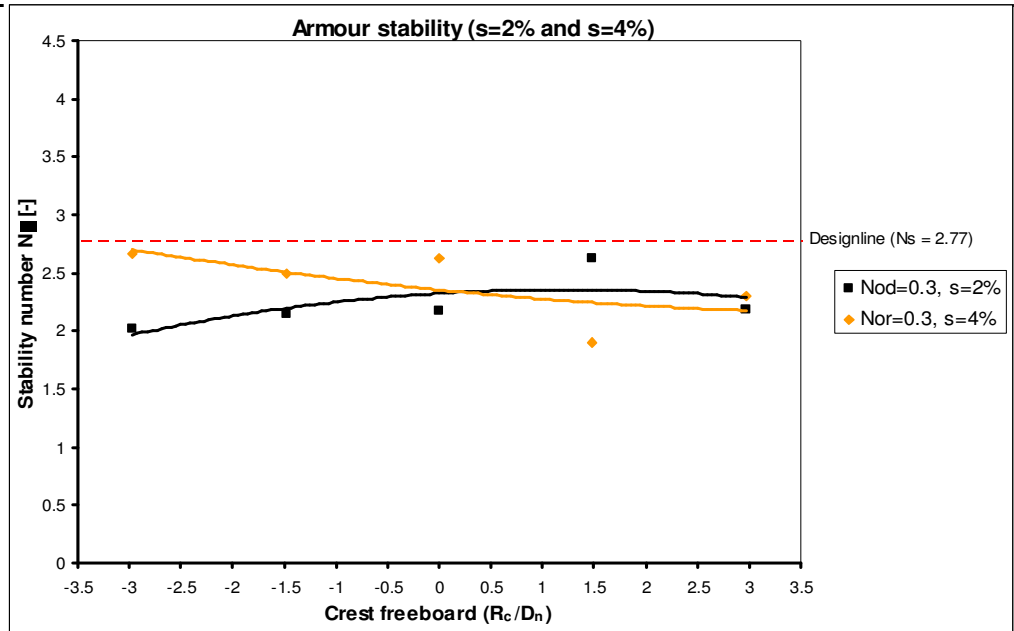


Figure 7.46 Influence wave steepness on rocking armour units, small crested breakwater, seaside slope section

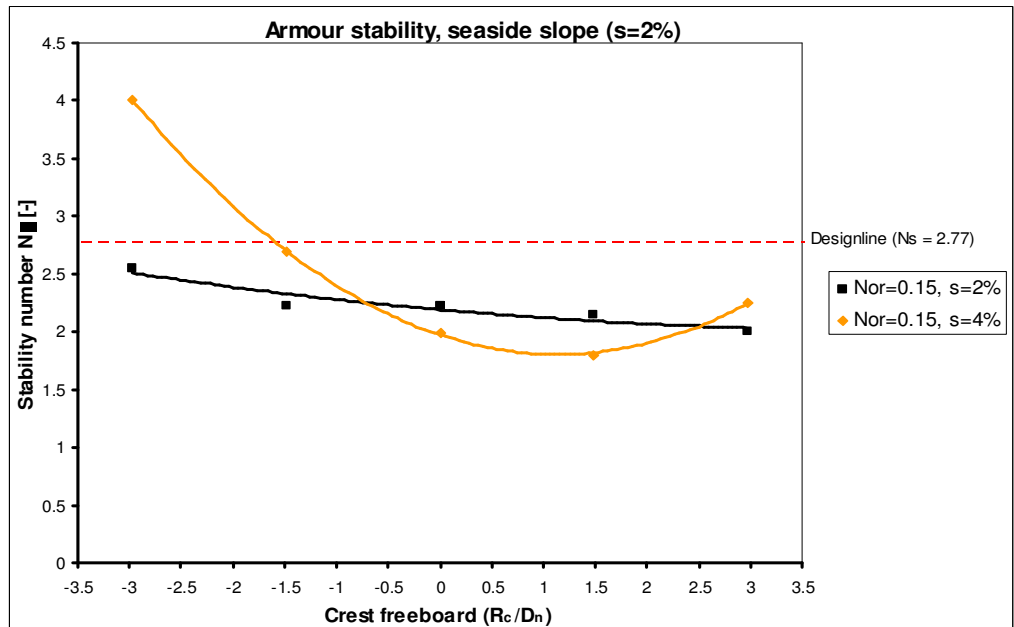
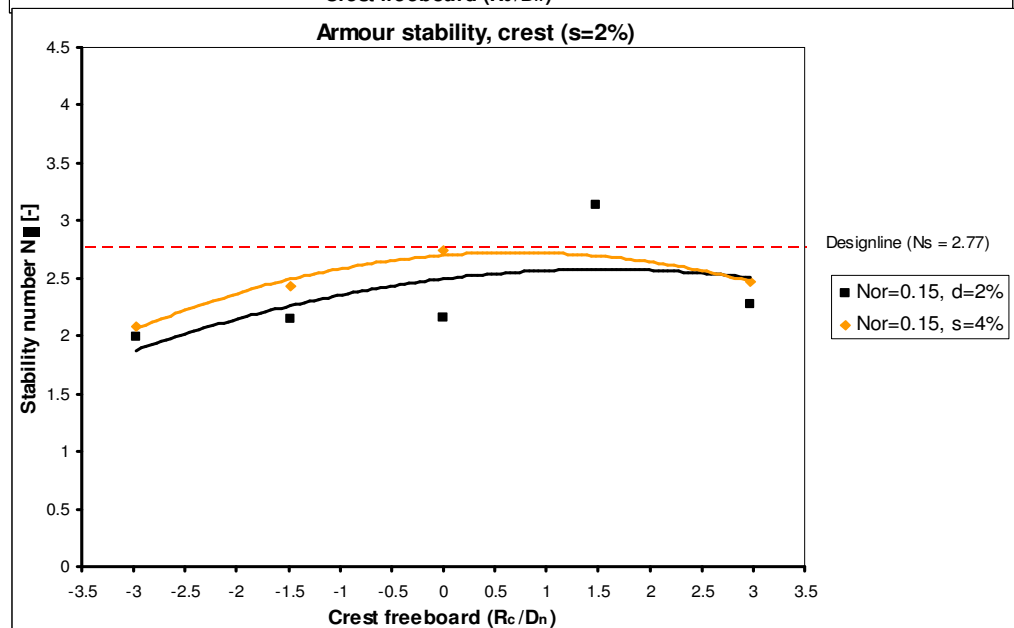


Figure 7.47 Influence wave steepness on rocking armour units, small crested breakwaters, crest section



Wide crested breakwater

Figure 7.48 shows the number of rocking elements for the total breakwater. The stability is maximal for submerged conditions and decreases for increasing crest freeboards to a minimum for zero crest freeboards in case of wave steepness 2% and a crest freeboard (R_c/D_n) of 1.5 for wave steepness 4%. For a wave steepness of 2 and 4% the stability is the same at a crest freeboard (R_c/D_n) of 1.5. Extrapolation of the trend lines shows that the stability increases again after the minimum stability. The 2% wave steepness shows a larger number of rocking elements compared to the 4% wave steepness for a specific stability number.

Figure 7.49 shows the stability for the seaside slope of the wide crested breakwaters. The stability number for a number of rocking armour units of 0.3 for a crest freeboard of -3 and a wave steepness of 4% is assumed because no measurement that damage are available. The armour units are less stable for two percent wave steepness than four percent wave steepness, except for a crest freeboard (R_c/D_n) of 1.5 where both wave steepness's are equally stable.

The crest is least stable for a wave steepness of 2% except for a crest freeboard (R_c/D_n) of -0.6 where they are equally stable. Both wave steepness's show a comparable trend, where the trend for 4% wave steepness is more pronounced.

Figure 7.48 Influence wave steepness on rocking armour units, wide crested breakwaters, total breakwater

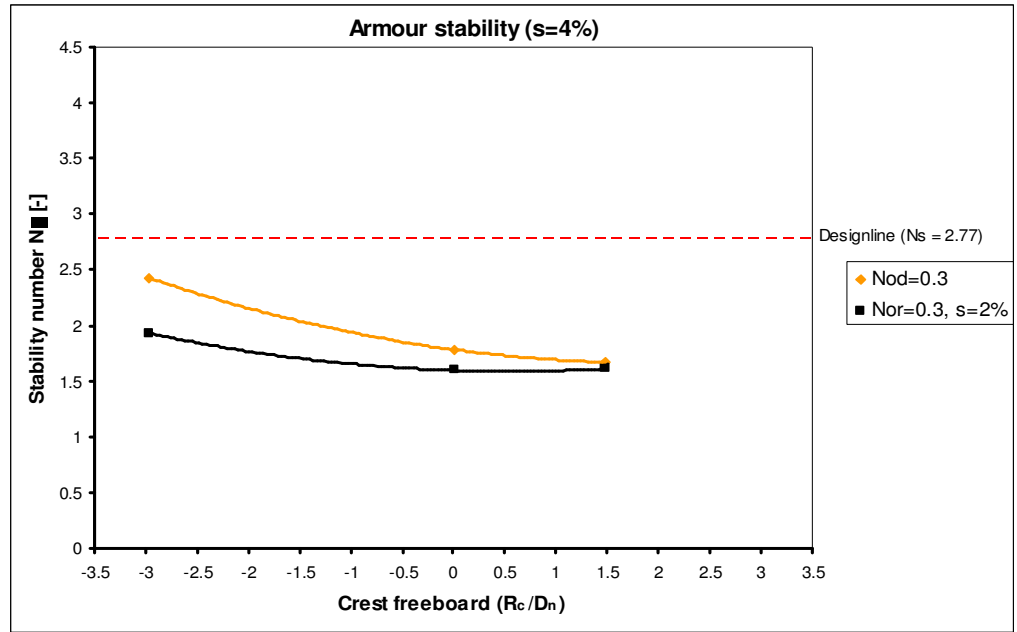


Figure 7.49 Influence wave steepness on rocking armour units, small crested breakwaters, seaside slope section

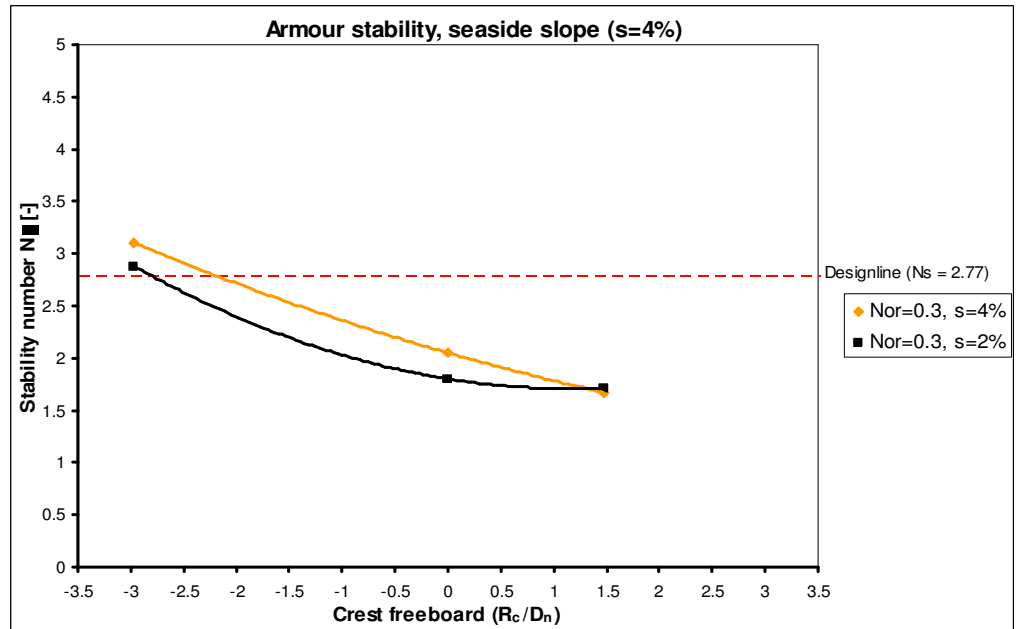
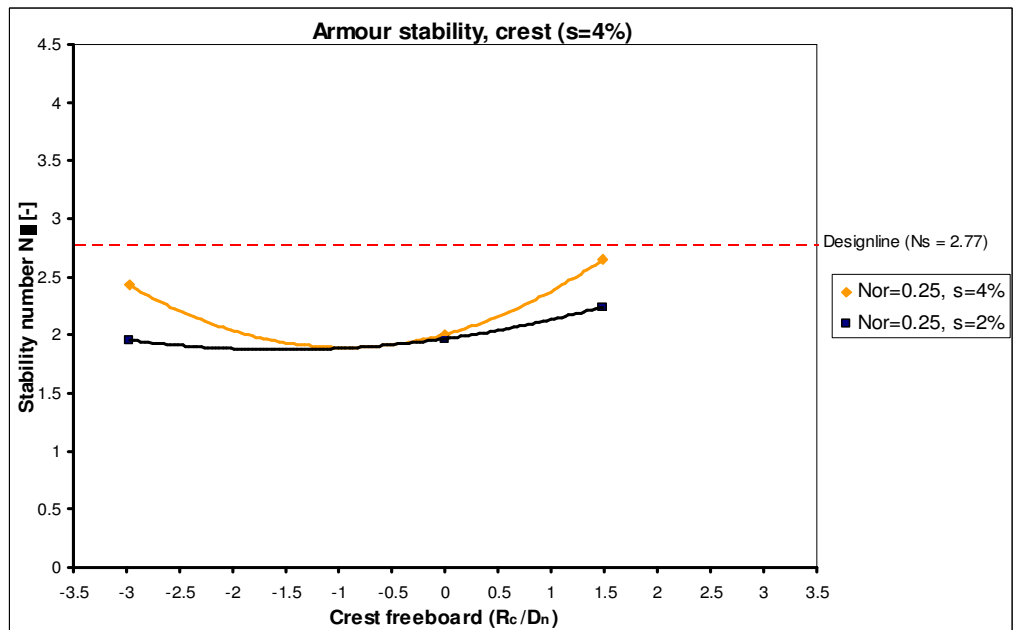


Figure 7.50 Influence wave steepness on rocking armour units, wide crested breakwaters, crest section



7.5. LOCATION OF ROCKING ARMOUR UNITS

The location of rocking armour units can be retrieved from the test results because the number of rocking armour units is given per breakwater section. The location of rocking Xbloc elements within the breakwater sections can however not be retrieved from the test results (§7.1), therefore the location of rocking Xbloc elements is plotted into figures like Figure 7.51 and Figure 7.52. These figures show with diamond shaped dots the location of the rocking elements for the reference cross section an wave steepness's 2 and 4%. For each test series these graphs are made, see Appendix K.

Figure 7.51 Location of rocking elements for reference test series (CI), wave steepness 2%

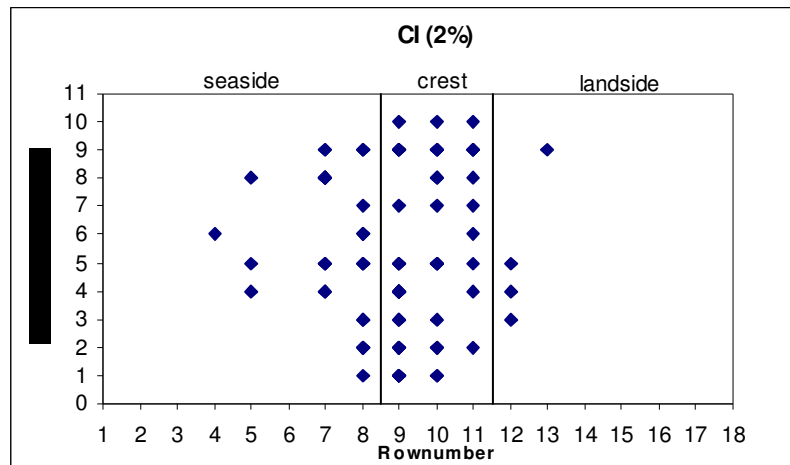
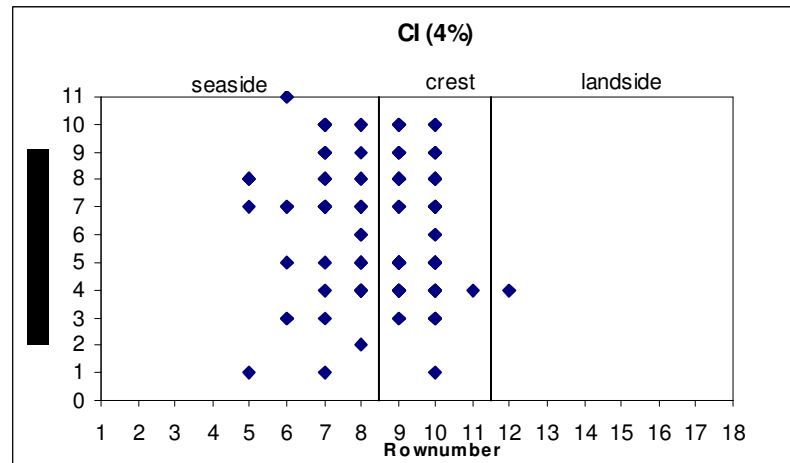


Figure 7.52 Location of rocking elements for reference test series (CI), wave steepness 4%.



8. DISPLACED ARMOUR UNITS

8.1. TEST RESULTS DISPLACED ARMOUR UNITS

In this section the test results concerning the stability of the armour layer are presented, on these results the analysis is based. Two damage levels are distinguished:

- start of damage, the displacement of one Xbloc armour units out of the armour layer, $N_{od} = 0.05$ (§0);
- failure, the displacement of ten Xbloc armour units out of the armour layer $N_{od} = 0.5$ (§0).

The results for start of damage and failure are plotted into graphs, the following applies for these graphs.

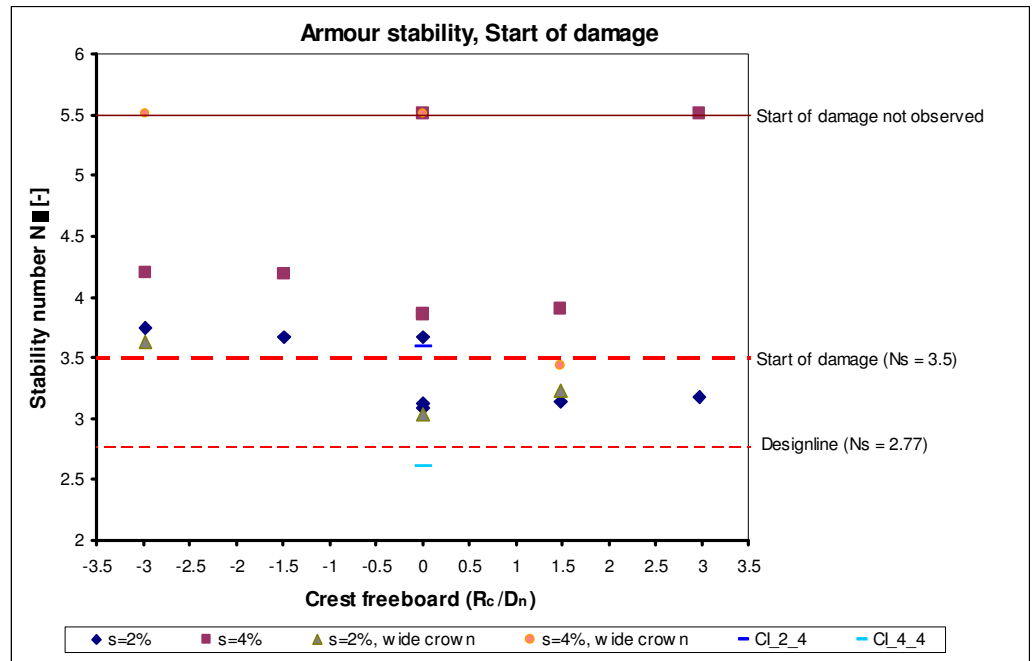
The results of clamped placed crest elements are not presented in the above figures (see §5.6.3). Tests with a wide crest and tests CI_2_4, CI_4_4 are executed with a relative placement density of 100%, whereas the relative placement density of the other tested cross section is 103%.

The test series are continued until 10 armour units are displaced, in the time required to stop the wave generator more elements may be displaced (Appendix d) but these are not taken into account in the analysis.

Start of damage

The stability numbers at which start of damage occurred for the entire armour layer are plotted in Figure 8.1 for various crest freeboards (R_c/D_n). In the foregoing text (§5 Model setup) R_c/H_s was used because the nominal diameter was not yet known, but from now on R_c/D_n is used. A distinction is made between the different wave steepness's and crest widths. Furthermore three lines are plotted in the figure, the bottom and the middle line represent the design stability number and start of damage ($N_{od} = 0.05$) for standard situations, respectively. The top line is a fictitious line which represents test series at which no start of damage occurred.

Figure 8.1 Results performed tests, Start of damage



Start of damage for wave steepness two percent is observed at approximately the same stability number for both wide and small crested breakwaters. For tests with four percent wave steepness this is not the case. Start of damage is not observed for wide crested breakwaters except for a test series with a crest freeboard of 1.5. In that case it actually occurs at a lower stability number than for the small crested breakwaters, in contrast to the other tests. Start of damage for test CI_2_4 occurs at the same stability number as is the case for the other tested breakwaters with a small crest, the opposite is true for test CI_4_4.

The reference situation $R_c/D_n = 0$ shows for both the two and four percent wave steepness one test which does not coincide with the other tests. The deviation is large for the four percent wave steepness.

It should be noted that start of damage in Figure 8.2 could be caused by losing one badly placed Xbloc armour unit. The placement of the Xbloccs can be seen as a stochastic process, due to the relatively small number of tests the results should be handled with care.

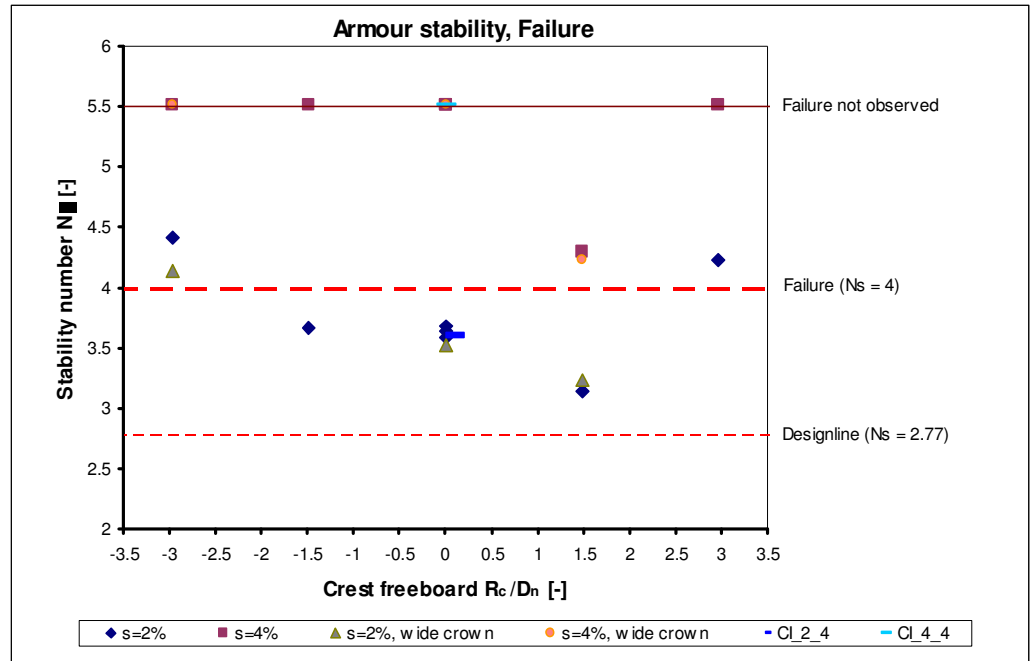
Some preliminary conclusions can be drawn from Figure 8.1:

- for breakwaters with crest freeboard of 0 or 1.5 the lowest stability numbers for start of damage occur;
- start of damage occurs at lower stability numbers for the two percent wave steepness than for four percent wave steepness;
- the difference in the stability numbers at which start of damage occurs is approximately constant for a wave steepness of four and two percent, only for crest freeboard 3 a considerable difference occurs.

Failure

The same graph as for start of damage is plotted for failure ($N_{od} = 0.5$) of the total armour layer in Figure 8.2. The middle line now represents the stability number at which failure normally occurs for a standard breakwater.

Figure 8.2 Results performed tests, failure



Failure for tests with four percent wave steepness is only observed for a crest freeboard (R_c/D_n) of 1.5, whereas in the case of two percent wave steepness failure occurs for all tests. No difference between the wide and small crested breakwater occurs, only for the test with wave steepness two percent the wide crested breakwater fails for a lower stability number as the small crested breakwater in the case of crest freeboard minus three.

Tests CI_2_4 and CI_4_4 coincide with the other tested reference breakwaters.

Both tests with four percent wave steepness and two percent wave steepness the stability is minimal for a crest freeboard of 1.5. Tests with two percent wave steepness show a trend of decreasing stability of the armour layer for increasing crest freeboard until a crest freeboard of 1.5, from there on the armour units become more stable. This is logical because the breakwater then becomes again a normal breakwater instead of a low-crested one. For submerged conditions less wave energy is dissipated which is favourable for the stability of the armour layer.

Some preliminary conclusions can be drawn from Figure 8.2:

- a clear trend for the stability of the armour layer in the case of wave steepness two percent occurs, the minimum occurs in case of a crest freeboard of 1.5;
- tests with four percent wave steepness show also a minimum stability at a crest freeboard of 1.5 in case of both a wide and small crest.

8.2. REFERENCE TEST SERIES

Tests at the reference cross section, zero crest freeboard and small crest width, are performed several times to acquire insight into the reliability of the test results. But it enables also the valuation of the reliability of test results for the other cross sections in further analysis.

In the case of wave steepness 2% tests CI_2_1, CI_2_2 and CI_2_3 are referred to as the reference tests whereas in case of the 4% wave steepness these tests are CI_4_1, CI_4_2, CI_4_3.

The results of the reference tests are visualised by plotting the number of displaced armour units (N_{od}) against the stability number (N_s). In this way the damage progression for increasing wave heights is obtained (see for example Figure 7.3). The mean number of displaced elements (CI_2 mean, CI_4 mean) of the reference tests per stability number is calculated and plotted together with its 90% confidence band interval. The lines which represent the upper and lower limit of the confidence band interval are plotted black dashed, whereas the mean number of displaced armour units is plotted in a solid line. No trend lines are added as in the case of rocking elements because at the moment of the displacement of the first element the breakwater fails at the same stability number. No real trends are present for the displacement of the crest elements.

Furthermore tests CI_4_4 and CI_2_4 are plotted in the same figures; these test series were performed with a relative placement density of 100%, whereas the reference tests had a relative placement density of 103%.

The above described figure is made for the total breakwater armour layer, seaside slope and crest (see §5.6.3 for a clear definition of the different breakwater sections). Also a distinction is made between the 2 and 4% wave steepness. First the figures of the 2% wave steepness are discussed (§7.2.1) and subsequently the 4% wave steepness (§7.2.2).

8.2.1. TWO PERCENT WAVE STEEPNESS

Figure 8.3, Figure 8.4 and Figure 8.5 shows the number of displaced armour units for the total breakwater, seaside slope and crest respectively. Most of the displaced armour units are displaced within one wave height, only for the crest section some elements are displaced for lower wave heights. The displacement of almost all elements until failure at the same wave height in combination with the small interval of tested wave heights indicates that damage and ultimately failure occurs within a small interval of stability numbers and that failure occurs without any warning in the form of earlier displaced elements. In general, from the total number of displaced elements relatively the largest part is displaced from the crest.

The 90% confidence band interval in case of the total breakwater increases for increasing wave heights from a stability number of 2.7 and subsequently becomes maximal after which the interval decreases to zero. This is caused due to the fact that failure of all reference test series occurred at the same wave

height for all tests. For the seaside slope the interval is everywhere zero except for the stability number at which failure occurred. The crest section shows an increasing confidence band interval from stability numbers of 2.7. The confidence band interval is just as large for the seaside slope as the crest.

Test series CI_2_4 are performed with a relative placement density of 100% whereas the reference test series have relative placement density of 103%. For test series CI_2_4 relatively a large number of element are displaced from the leeside slope section at the expense of the displacement of crest elements. Therefore the number of displaced elements at the crest falls outside the 90% confidence band interval. It is not certain of this is caused by to the lower relative placement density, it could well be a onetime phenomenon.

Figure 8.3 Number of displaced armour units, reference test series (s=2%), total breakwater

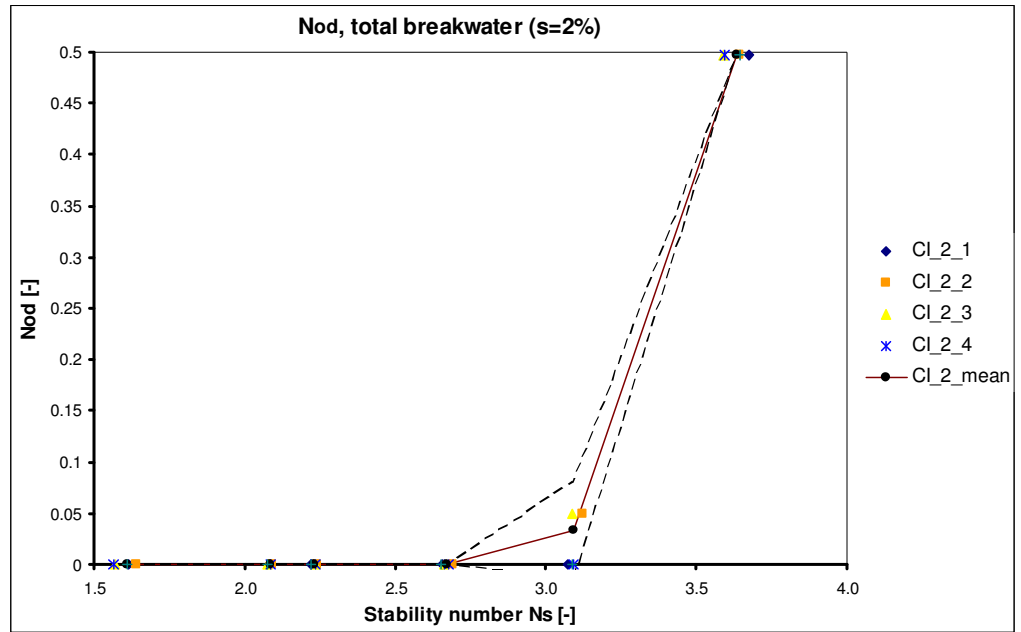


Figure 8.4 Number of displaced armour units, reference test series (s=2%), seaside slope

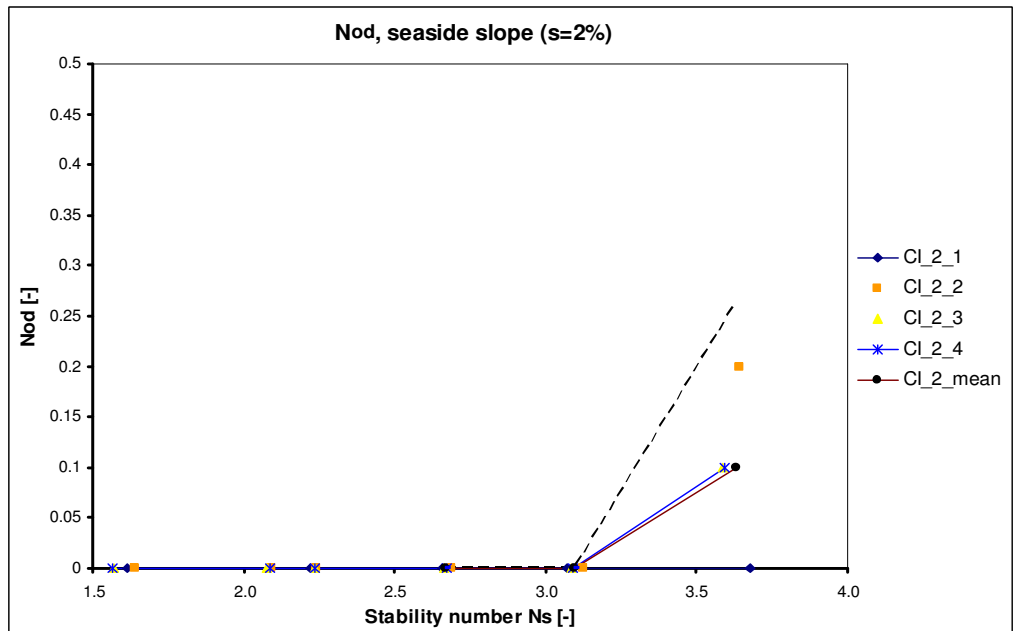
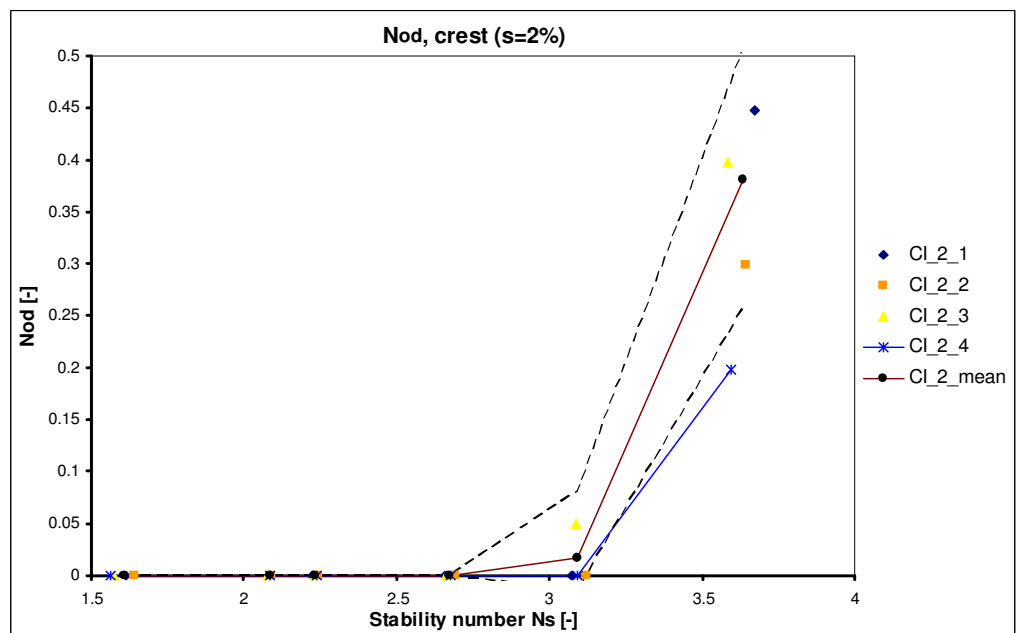


Figure 8.5 Number of displaced armour units, reference test series (s=2%), crest



8.2.2. FOUR PERCENT WAVE STEEPNESS

Figure 8.6, Figure 8.7 and Figure 8.8 shows the number of displaced armour units for the total breakwater, seaside slope and crest in case of 4% wave steepness. For the reference test series and a wave steepness of 4% no failure occurred, the maximum number of displaced armour units was $N_{od}=0.15$. Due to the small number of displaced elements the possibilities of the analysis of trends are limited.

The total breakwater, seaside slope and crest shows no displaced armour units for stability numbers smaller than 3.86. For the seaside slope and crest the number of displaced elements increases further for increasing stability numbers whereas the number of displaced elements at the seaside slope remains constant.

For the total breakwater and the crest section the confidence band interval increases for increasing stability numbers, whereas the seaside slope shows a constant confidence band interval. The lower limit of the confidence band interval is in all cases the x-axis ($N_{od}=0$). The largest confidence band interval is present for the crest section.

Test series CI_4_4 shows a larger number of displaced armour units for the total breakwater and the seaside slope than the average of the reference test series. But due to the results which are in the 90% confidence band interval no conclusions can be drawn.

Figure 8.6 Number of displaced armour units, reference test series (s=4%), total breakwater

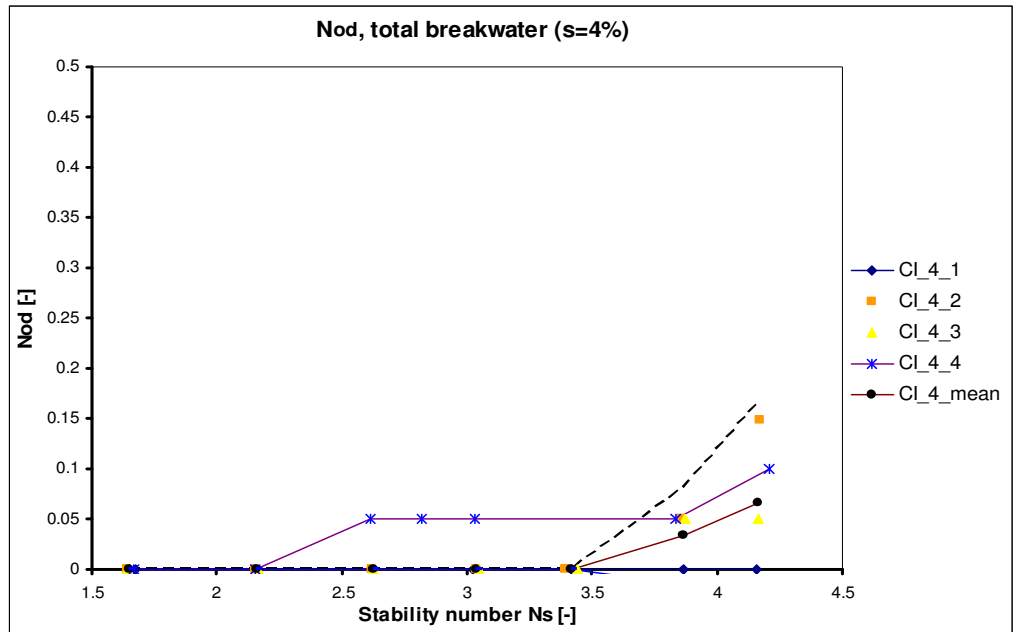


Figure 8.7 Number of displaced armour units, reference test series (s=4%), seaside slope

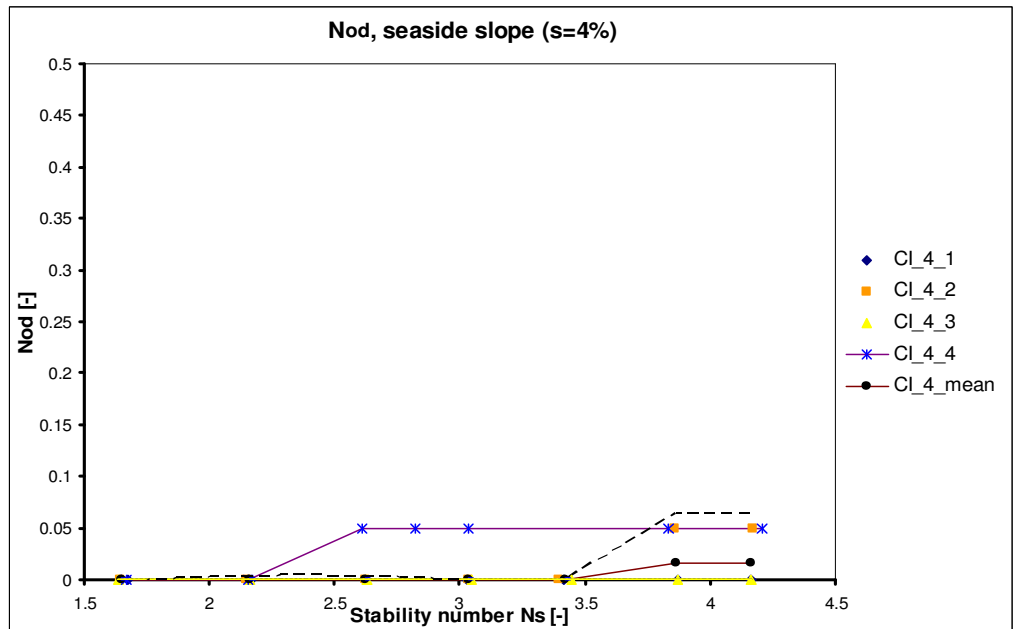
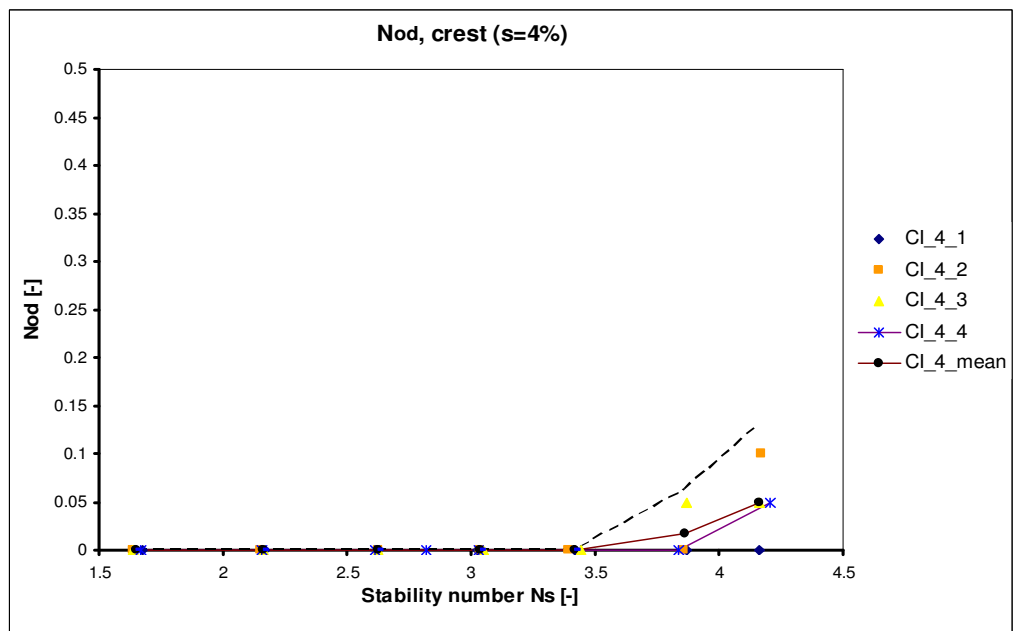


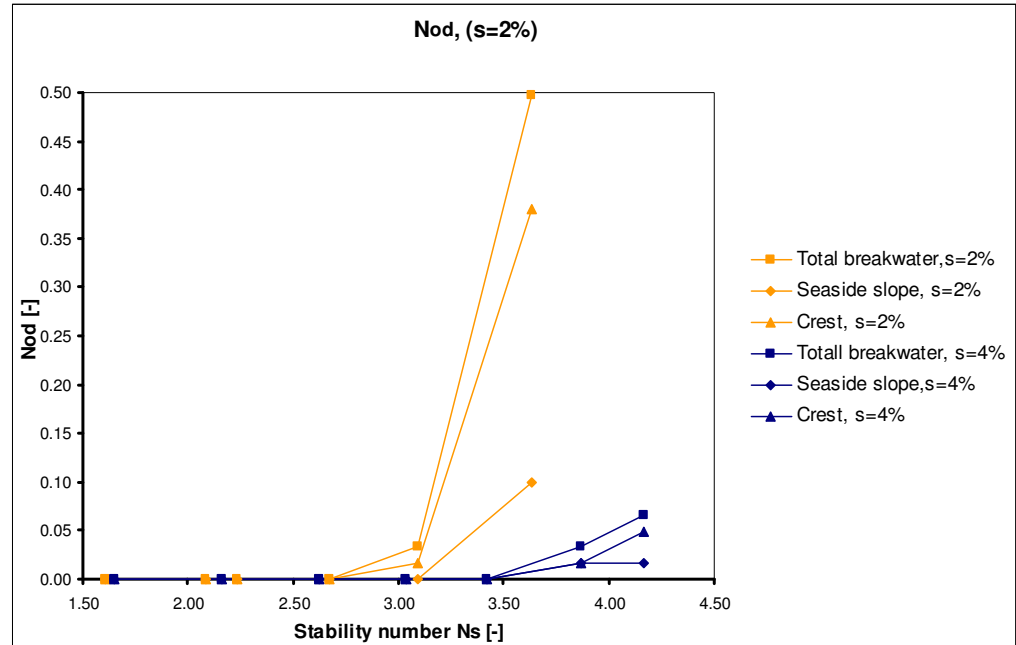
Figure 8.8 Number of displaced armour units, reference test series (s=4%), crest



8.2.3. CONCLUSIONS

A number of conclusions can be drawn from the analysis of the reference test for both the 2 and 4% wave steepness. All test results are plotted into Figure 8.9 to give an overview and enable the comparison of the test results for wave steepness of 2 and 4%.

Figure 8.9 Number of displaced armour units, reference test series, all breakwater cross section



The following conclusions can be drawn regarding the number of displaced armour units for the reference test series:

- Failure and start of damage occurs for higher stability numbers than the design stability number;
- Failure ($N_{or}=0.5$) in case of a wave steepness of 2% occurs at a significant lower stability number than is the case for 4% wave steepness;
- For both a wave steepness of 2 and 4% the crest section shows relatively to the crest section the most displaced armour units;
- Failure occurs within a relatively small interval of stability numbers for the 2% wave steepness, the damage development of the 4% wave steepness indicates a more gradual course;
- The distribution of the number of displaced elements over the seaside slope and crest show some scattered values but the number of displaced elements for the total breakwater is for each test series constant. This translated itself into the 90% confidence band interval;
- The 90% confidence band interval in case of the 4% wave steepness is larger for the crest than the seaside slope, the total breakwater shows the largest interval. Due to the low number of displaced elements the confidence band interval varies between $N_{or}=0$ and the upper limit of the interval.

8.3. ANALYSIS DISPLACED XBLOC ARMOUR UNITS

In this section all test series are discussed, a distinction in the analysis is made between:

- small crested breakwater, $s=2\%$ (§8.3.1);
- wide crested breakwater, $s=2\%$ (§8.3.2);
- small crested breakwater, $s=4\%$ (§0);
- wide crested breakwater, $s=4\%$ (§0).

It should be noted that the wide crested breakwaters have a relative placement density of 100% whereas the small crested breakwater 103%.

For all of the above stated tests, graphs with the number of displaced armour units are plotted against the stability number for the total breakwater (including the leeside slope), seaside slope and crest. Furthermore in every graph the mean number of rocking armour units for the reference test series is plotted together with the 90% confidence band interval (dashed lines), also for the wide crested breakwaters.

This analysis gives information on the rate of damage progression and shows which test series are least stable. The results of the 2% wave steepness analysis give more information than the 4% due to the larger number of displaced crest elements.

8.3.1. SMALL CRESTED BREAKWATERS, $S=2\%$

In this section all test series with a small crest and wave steepness 2% are considered.

Figure 8.10 Number of displaced armour units small crested breakwaters, all 2% wave steepness test series, all breakwater sections

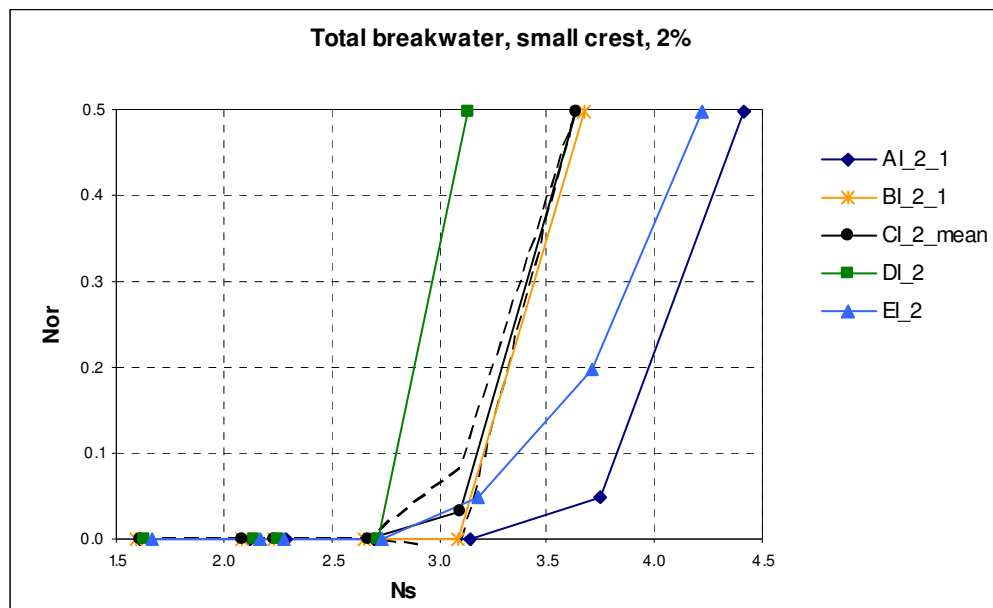


Figure 8.10 shows the number of displaced elements for the total breakwater. Failure for test series AI_2_1, CI_2_mean and EI_2 is reached within one or two wave heights after start of damage has occurred. For the other test series failure occurs within the same wave height of start of damage. Test series DI_2

is least stable of all tests whereas test series EI_2 is the second most stable. The larger part of all test series is outside the 90% confidence band interval of the reference test series which indicates that the test series really shows different trends.

Figure 8.11 Number of displaced armour units small cersted breakwaters, all 2% wave steepness test series, seaside slope

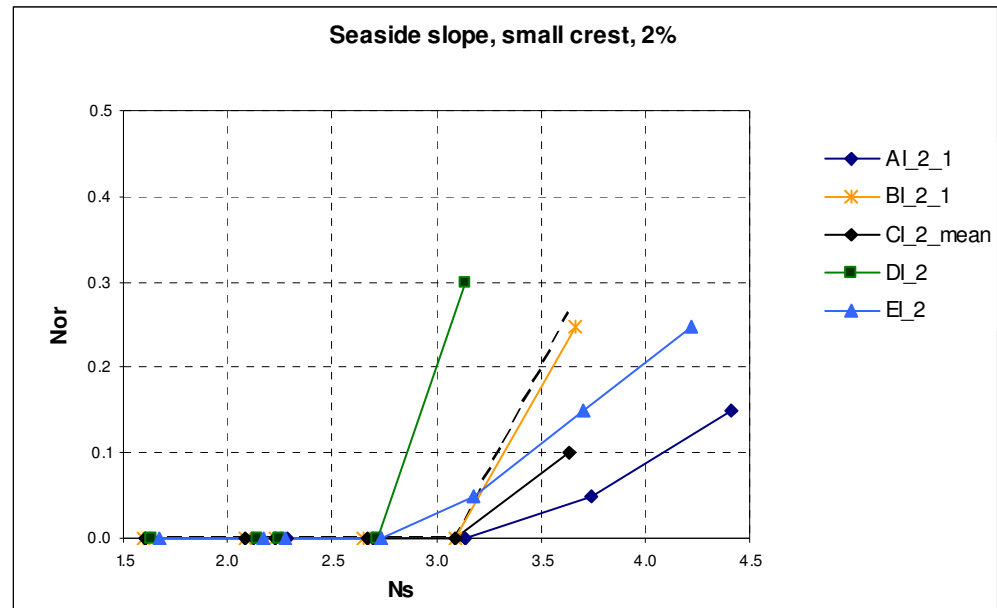


Figure 8.11 shows the number of displaced elements at the seaside slope. It clearly shows that test series DI_2 is the least stable and AI_2_1 the most stable. Start of damage for emerged breakwaters is observed at the same wave height, for test series DI_2 start of damage and failure take place at the same wave heights whereas for test series EI_2 the damage develops more gradual for increasing stability numbers. Start of damage for breakwaters with negative and zero crest freeboard all occur at the same stability number, for test series BI_2_1 and CI_2_mean for the same wave heights failure occurred. The total number of displaced seaside slope elements is maximal for test series DI_2 and minimal for test series CI_mean. Test series BI_2_1 and EI_2 show the same total number of displaced armour units. A direct comparison between the total numbers of displaced elements at the seaside slope is possible because failure occurred for all test series.

Figure 8.12 Number of displaced armour units small cersted breakwaters, all 2% wave steepness test series, crest

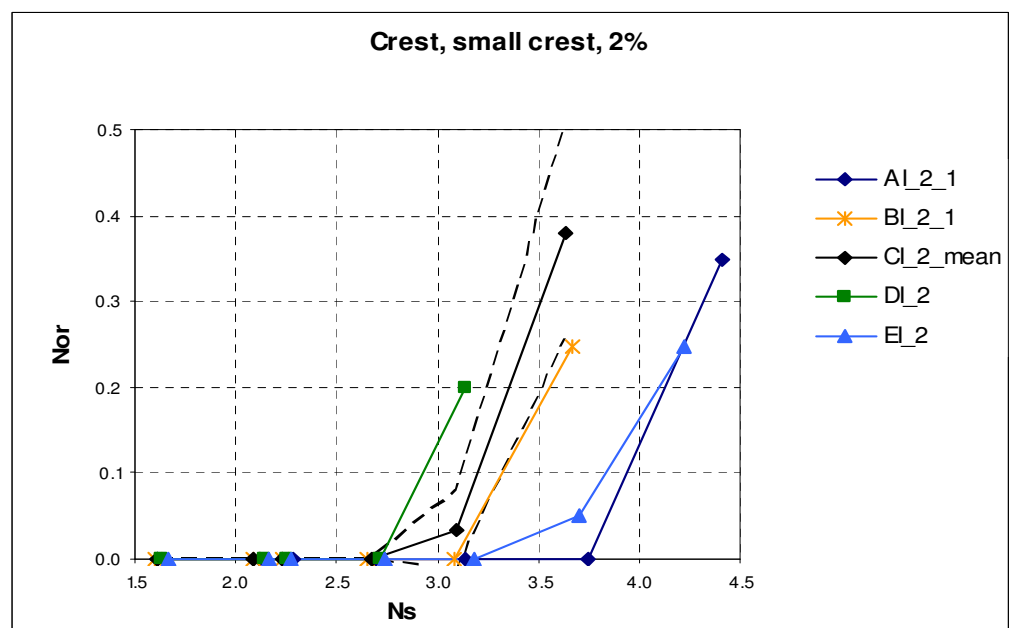


Figure 8.12 shows the number of displaced armour units at the crest. The stability increases from emerged to submerged conditions except for test series EI_2 which is slightly less stable than test series AI_2_1. Start of damage for test series DI_2 and CI_2_mean is observed at the same stability number, failure for test series DI_2 occurs at the same wave height. Start of damage and failure of the other test series occurs at the same wave height except for test series EI_2.

By comparing Figure 8.11(seaside slope) and Figure 8.12 (crest) for some test series the location of the first displaced element can be retrieved which shows the order of displacement of elements at the seaside slope and crest. For test series EI_2 and AI_2_1 the first elements are displaced from seaside slope whereas for test series CI_2_mean from the crest section the first elements are displaced.

8.3.2. WIDE CRESTED BREAKWATER, $S=2\%$

In this section all test series with a wide crest and wave steepness 2% are discussed.

Figure 8.13 shows the number of displaced armour units for the total breakwater. Failure occurred for all test series except for AII_2_1. Test series DII_2 is the least stable, the stability of the other test series increases for increasing crest freeboard. The 90% confidence band interval of the reference test series is largest for stability numbers between 2.7 and 3.1, the displacement of the first element ($N_{od}=0.05$) is observed within the confidence band interval in case of the two least stable test series. But failure occurs at a different stability number outside the confidence band interval. The stability of the reference test series is somewhat smaller than test series CII_2.

Figure 8.13 Number of displaced armour units wide crested breakwaters, all 2% wave steepness test series, crest

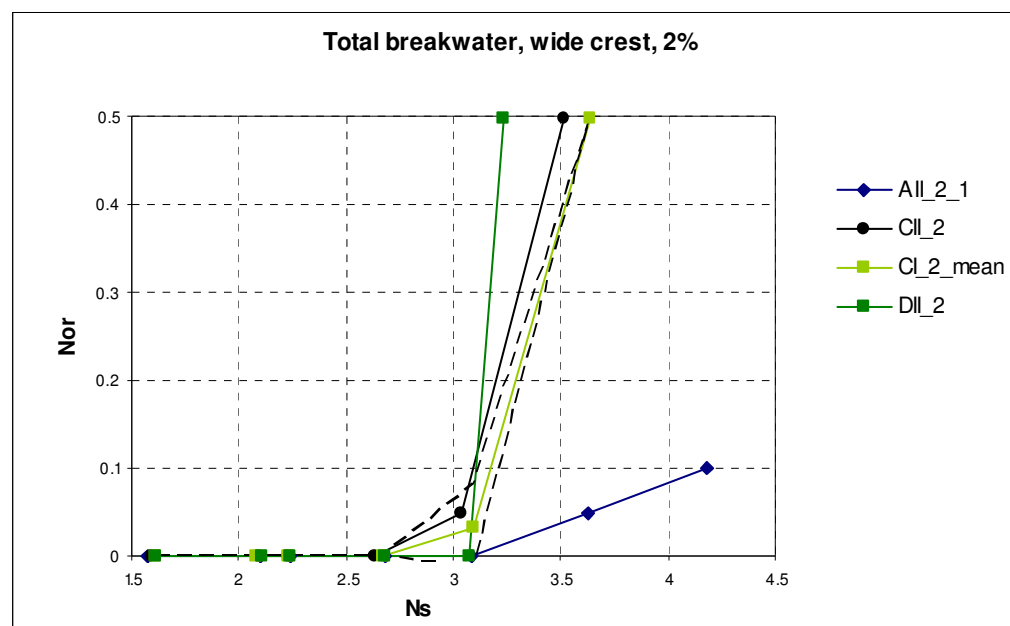


Figure 8.14 Number of displaced armour units wide crested breakwaters, all 2% wave steepness test series, crest

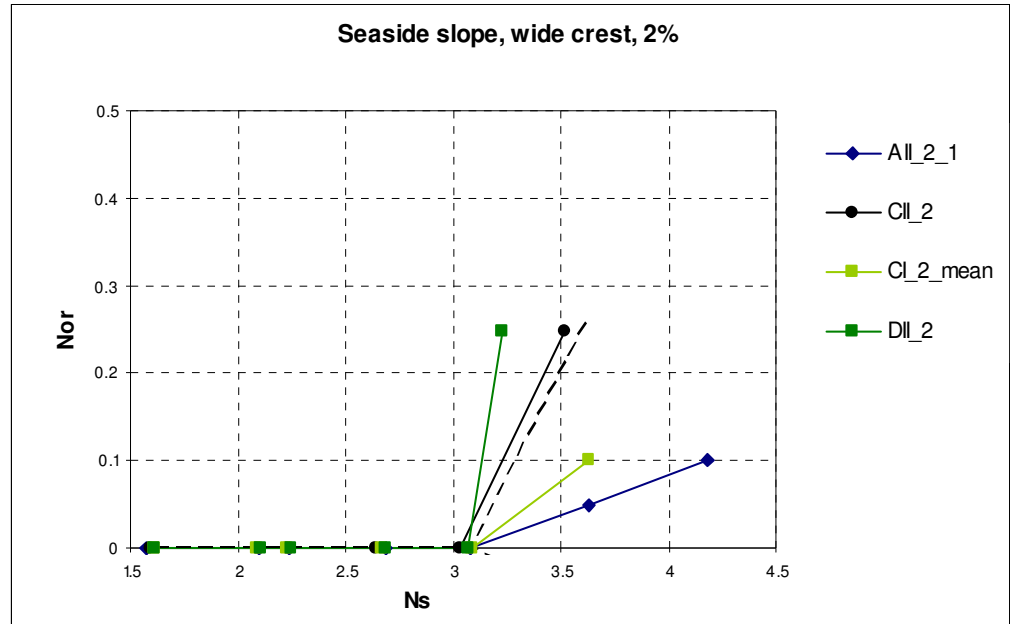


Figure 8.15 shows the number of displaced elements at the crest. The stability of the seaside slope increases from emerged to submerged breakwaters, test series DII_2 to AII_2_1. Start of damage occurs at the same stability number independently of the test series. Tests series CII_2 shows significant more displaced elements than the reference test series, CI_2_mean.

Figure 8.15 Number of displaced armour units wide crested breakwaters, all 2% wave steepness test series, crest

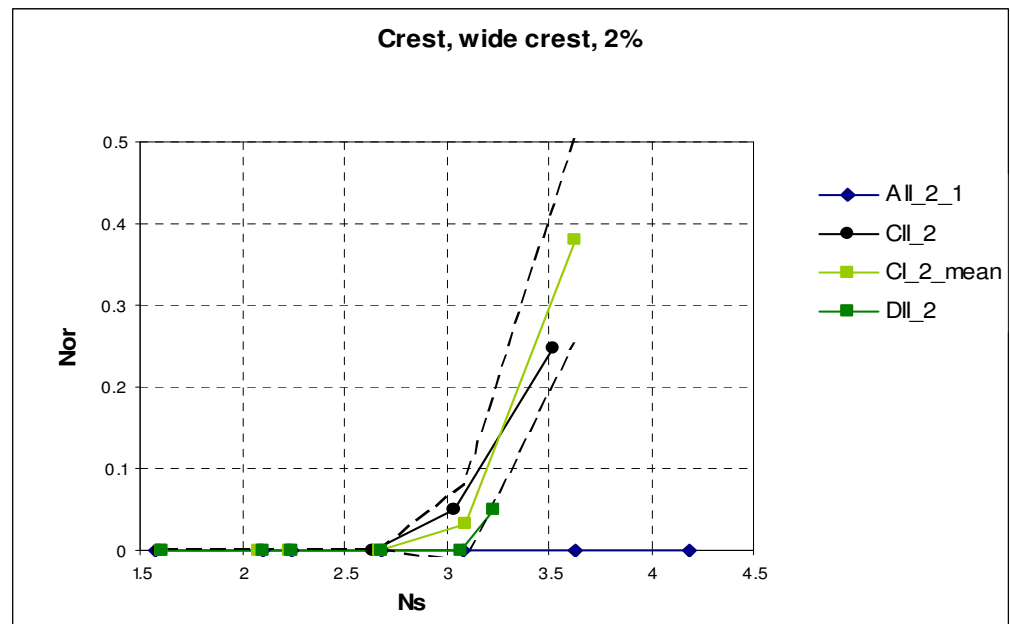


Figure 10.1 shows the number of displaced elements from the crest. The number of displaced elements from the crest is largest for zero crest freeboard and decreases for both positive and negative crest freeboard. The numbers of displaced crest elements are all in the 90% confidence band interval of the reference test series except test AII_2_1.

By comparison of Figure 10.1 and Figure 10.2 the first displaced element is retrieved in case of test series CII_2. This element is positioned at the crest, subsequently further damage at the crest and seaside slope results.

8.3.3. SMALL CRESTED BREAKWATERS, S=4%

In this section all test series with a small crest and wave steepness 4% are discussed. Due to the low number of displaced elements in case of the 4% wave steepness the results of the analysis are limited.

Figure 8.14 shows the number of displaced elements for the total breakwater. Only for test series DI_4 failure occurred whereas for the other test series none or only one element is displaced.

Figure 8.17 shows the number of displaced elements at the crest. Only for test series DI_4 and CI_4_mean some elements are displaced. For test series DI_4 failure occurred, Figure 8.17 shows that all elements are displaced from the seaside slope.

Figure 8.16 Number of displaced armour units wide crested breakwaters, all 2% wave steepness test series, total breakwater

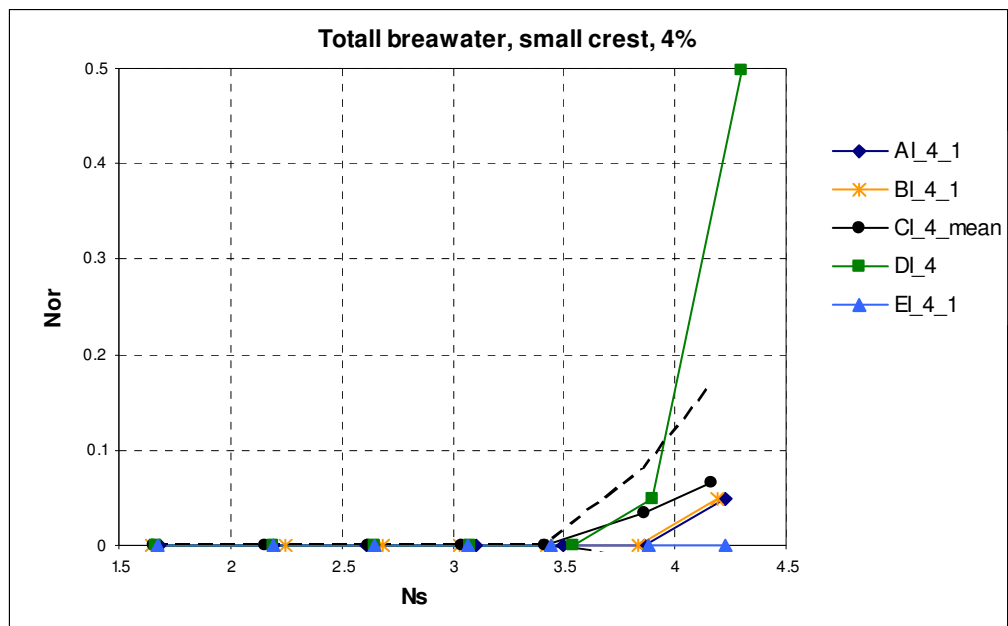


Figure 8.17 Number of displaced armour units wide crested breakwaters, all 2% wave steepness test series, crest

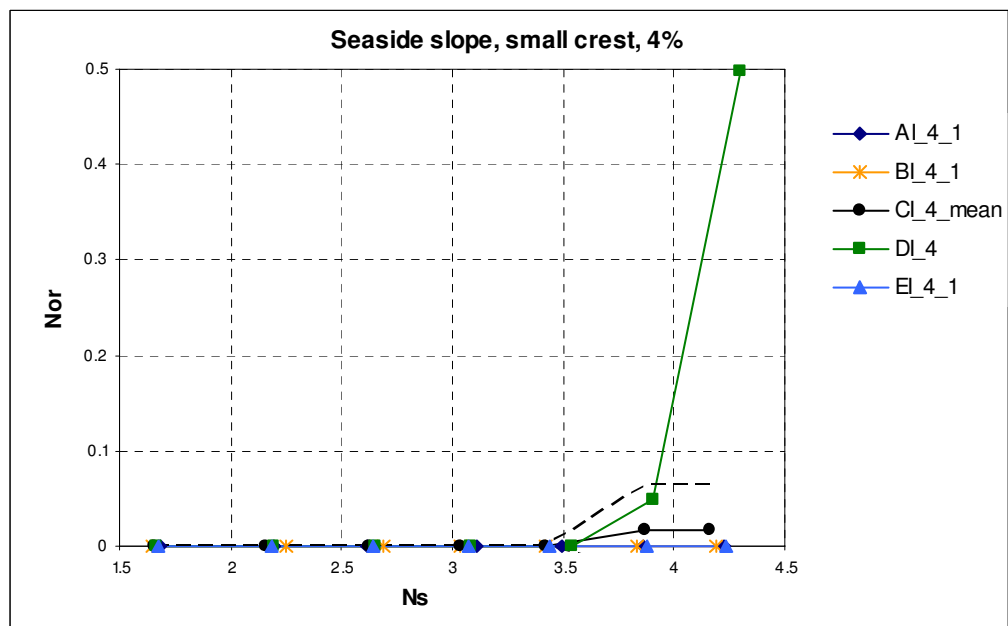


Figure 8.18 Number of displaced armour units wide crested breakwaters, all 2% wave steepness test series, crest

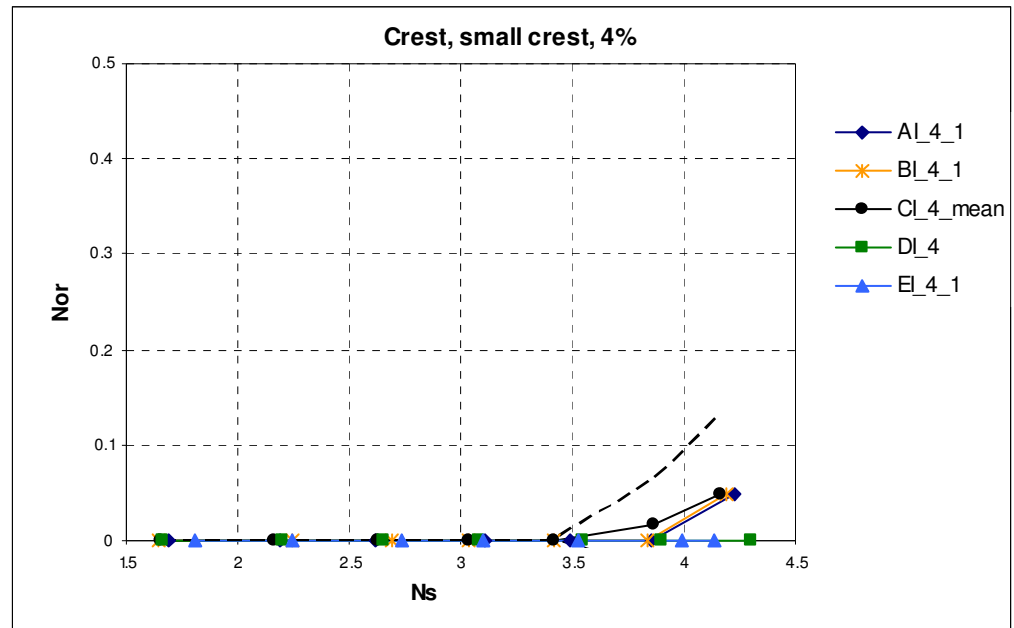


Figure 8.18 shows the number of displaced elements at the crest. For all negative and zero crest freeboard breakwaters some elements are displaced from the crest whereas for positive crest freeboard no elements are displaced.

8.3.4. WIDE CRESTED BREAKWATER, $S=4\%$

In this section tests with a wide crested breakwater and a wave steepness of 4% are discussed. Figure 8.19 shows the number of displaced armour units at the total breakwater. Test series DI_2 is clearly the least stable, further no armour units are displaced for the wide crested breakwaters. Test series CI_4_mean shows a number of displaced element whereas test series CII_4 not, this indicated that CII_4 is more stable. But due to the low number of displaced elements and the 90% confidence band interval of the reference test series this can not stated

Figure 8.20 shows the number of displaced armour units at the crest only for test series DII_4 some elements are displaced. The same holds for the crest section, Figure 8.21. The first displaced element originates from the crest, subsequently some elements are displaced alternately from the crest and the seaside slope.

Figure 8.19 Number of displaced armour units wide crested breakwaters, all 2% wave steepness test series, total breakwater

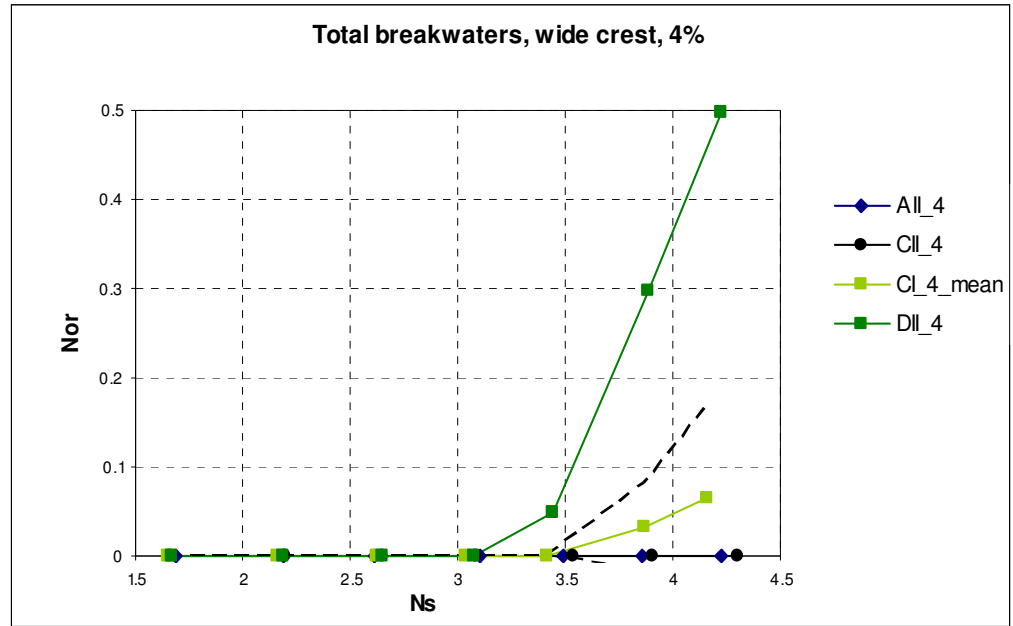


Figure 8.20 Number of displaced armour units wide crested breakwaters, all 2% wave steepness test series, seaside slope

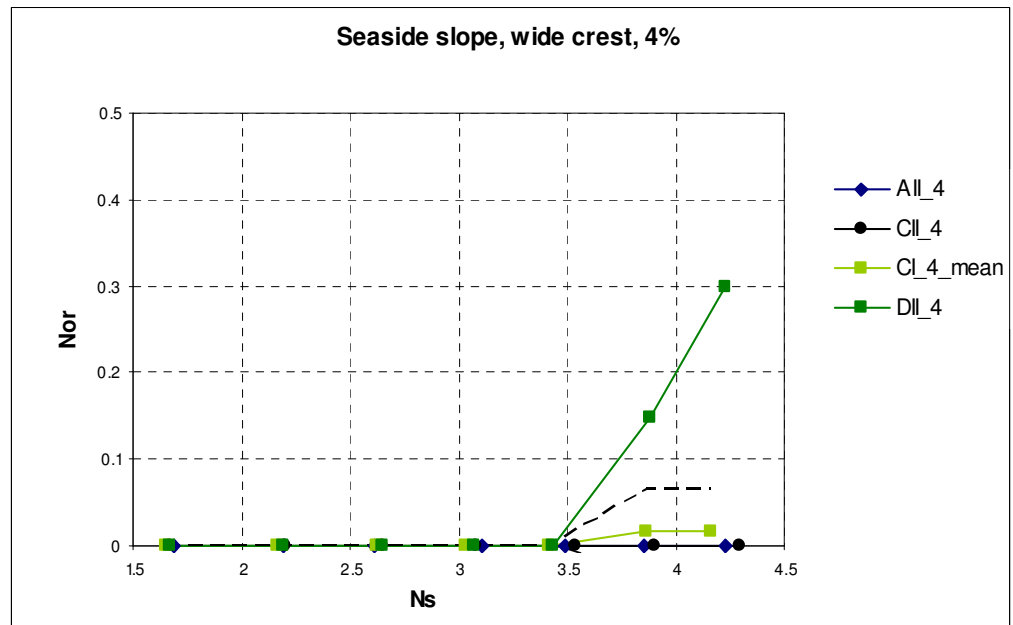
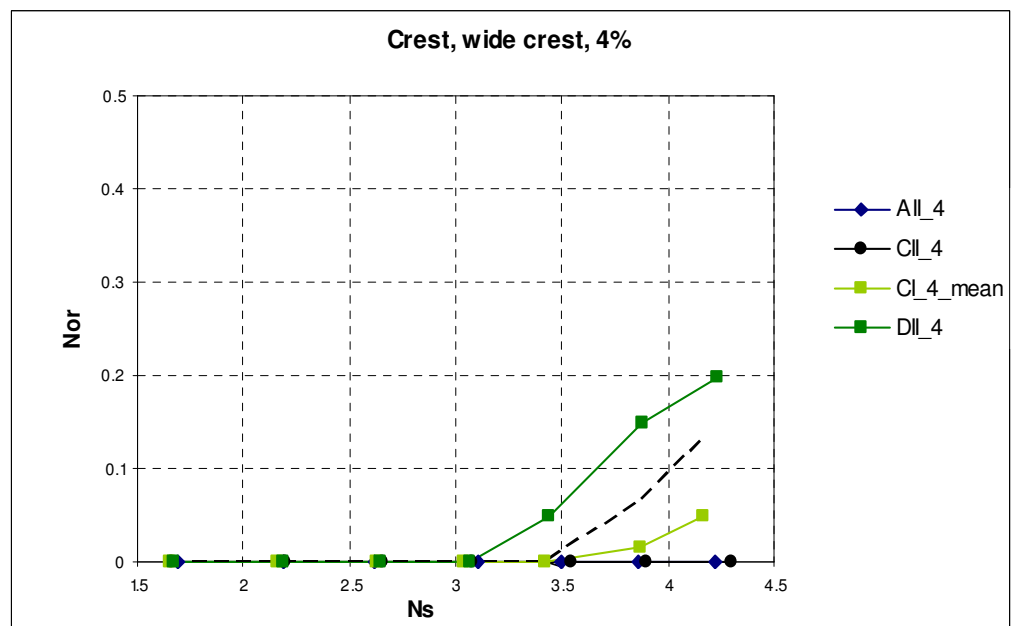


Figure 8.21 Number of displaced armour units wide crested breakwaters, all 2% wave steepness test series, crest



8.4. DISCUSSION TEST RESULTS

In this section the test results of the displaced armour units are discussed, the following subjects are treated:

- influence crest freeboard;
- influence crest width;
- influence wave steepness.

The study is aimed at the stability of the Xbloc single layer armour unit at low-crested breakwaters, therefore the influence of crest width and wave steepness is discussed in relation to the stability number and crest freeboard.

For each of the above given subjects the number of displaced armour units is plotted against the stability number (at the y-axis) and crest freeboard (at the x-axis). Through a fixed number of displaced armour units a trend line is drawn. For the reference test series the mean number of displaced armour units is used. Also the design and start of damage stability numbers are plotted to place the number of displaced elements in more perspective. The trend lines are not correlated with the other breakwater sections, $N_{or}=0.1$ at the seaside slope and crest does not imply that the number of rocking elements (N_{or}) at the total breakwater is 0.2. The ratios of the number of displaced elements at the different breakwater sections can thus not be retrieved from these results. In case the required number of displaced armour units for drawing the trend line falls between two points which present the number of displaced armour units the stability number is calculated by interpolation for the required number of displaced armour units.

The above described figures show for fixed damage levels the stability number over the crest freeboard. The figures don't give any easily readable information over the damage ratios for the different breakwater sections in case of a fixed damage number for the total breakwater. Therefore plots are made which show the number of displaced armour units at the crest and seaside slope for a fixed number of displaced elements at the total breakwater. To this end the number of displaced elements (N_{od}) is plotted at the y-axis and the crest freeboard on the x-axis. The summated number of displaced armour units for the seaside slope and crest are not always equal to the number of displaced armour units of the total breakwater, because in some cases elements are displaced from the leeside slope. These figures are of interest because for increasing wave heights (larger damage numbers) the wave structure interaction and the most severe loaded part of the breakwater can change.

Further the 90% confidence band intervals are plotted for 'Failure' and 'Start of damage'. The line which represents failure is not in the middle of the confidence band 'Failure', this is caused due to a safety factor.

8.4.1. INFLUENCE CREST FREEBOARD

The influence of the crest freeboard on the stability of the breakwater is discussed for:

- small crested breakwater, $s=2\%$;
- wide crested breakwater, $s=2\%$;
- small crested breakwater, $s=4\%$.

The influence of the crest freeboard for ‘wide crested breakwater, $s=4\%$ ’ is not discussed because of insufficient data points.

Small crested breakwater, $s=2\%$

Figure 8.22, Figure 8.23 and Figure 8.24 show the armour layer stability for different damage level at the total breakwater, seaside slope and crest respectively.

The stability of the total breakwater is maximal for the most submerged conditions in the tested range. It should be noted that the minimum stability according to the trend lines occurs at approximately zero crest freeboard whereas the actual minimum stability of the breakwater lies at a crest freeboard (R_c/D_n) of 1.5. This is caused by the large difference in stability for the reference test series and the tests series with a crest freeboard (R_c/D_n) of 1.5. The trend lines show in general an increasing curvature for higher damage levels, this indicates that the breakwater becomes more stable for higher damage levels.

The stability of the seaside slope is maximal for submerged conditions in the tested range and decreases for increasing crest freeboards towards a minimum at a crest freeboard of 1.5. For increasing crest freeboards the line which represents start of damage comes close to that of conventional breakwaters ($R_c/D_n > 3.75$) in case of extrapolation. The deviation of the trend line from test series with a crest freeboard of 1.5 is quite large.

The difference in stability over the crest freeboard is largest for the crest section compared to the total breakwater and the seaside slope. For both the most submerged and emerged tested breakwaters the stability is maximal. At a crest freeboard of 1.5 the stability is minimal although the trend line does not show that. For conventional breakwaters the stability of the crest section is not of importance anymore according to Figure 8.24 which is as expected.

Figure 8.22 Stability at different crest freeboards, total breakwater, small crest width (s=2%).

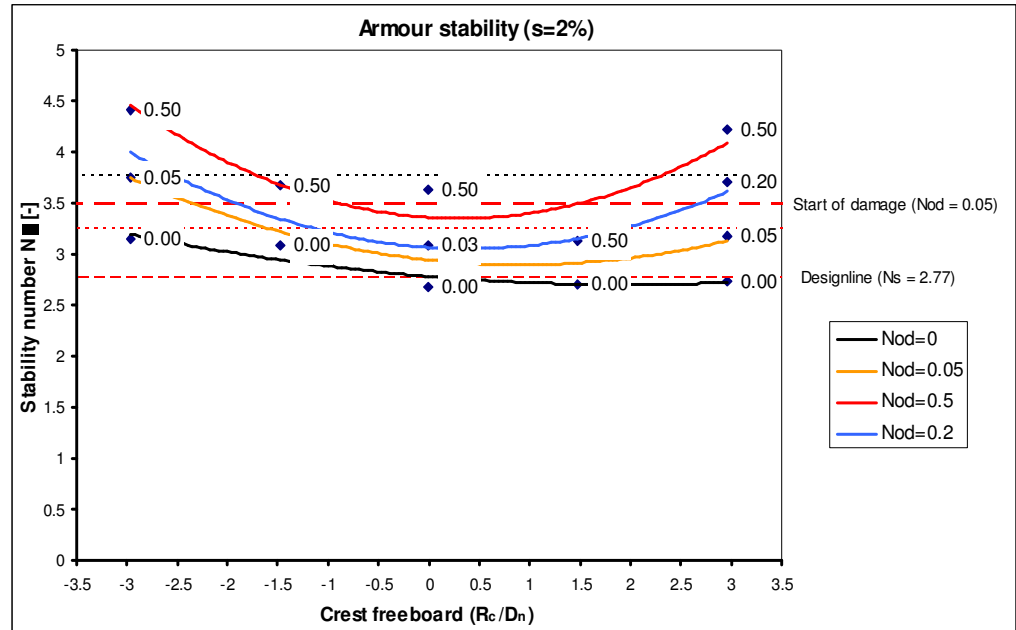


Figure 8.23 Stability at different crest freeboards, seaside slope, small crest width (s=2%).

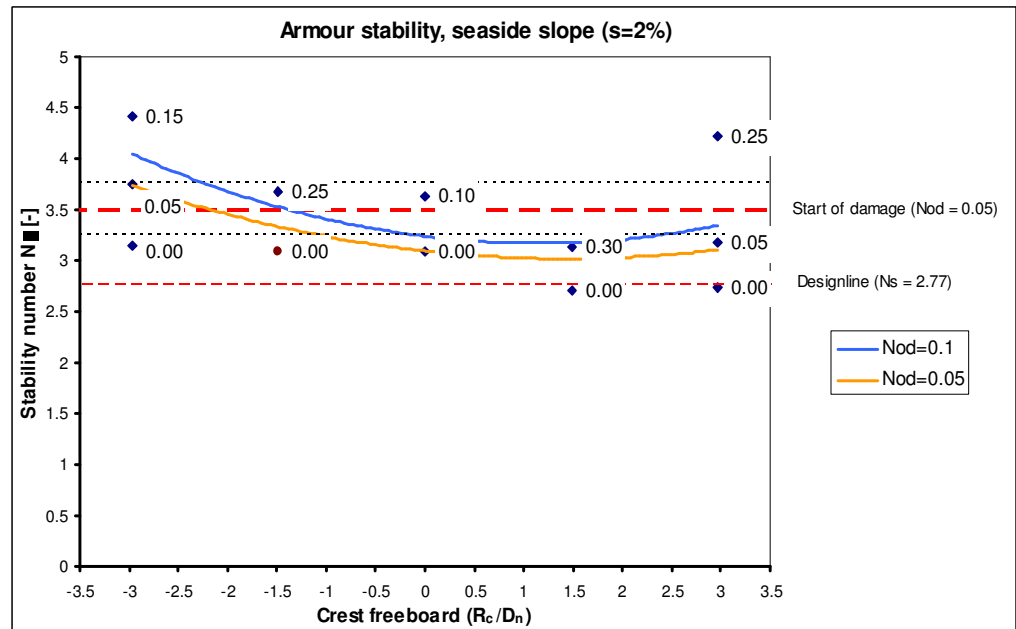
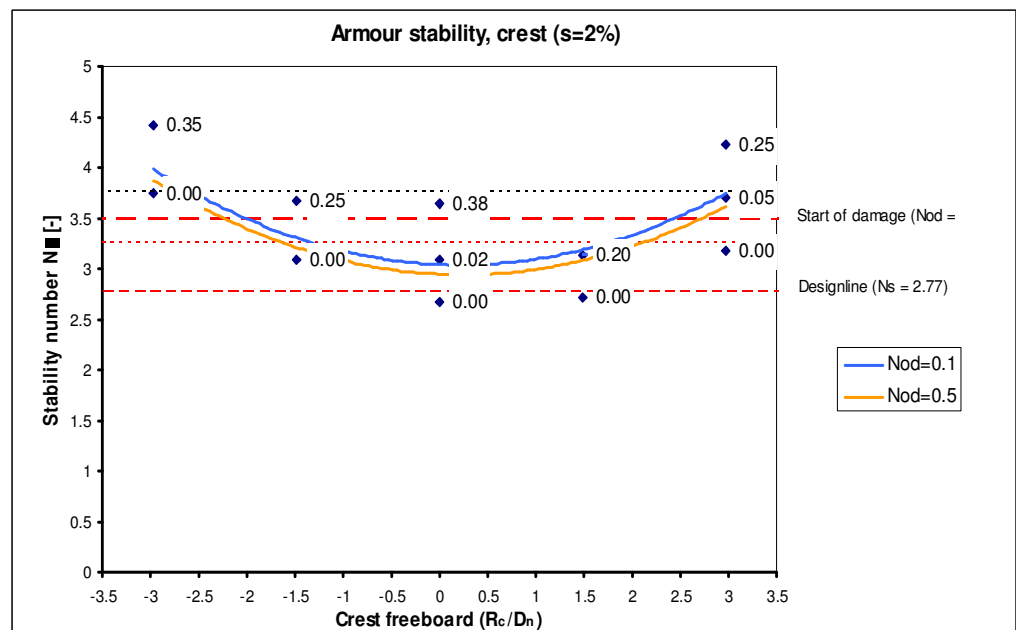


Figure 8.24 Stability at different crest freeboards, crest, small crest width (s=2%).



Wide crested breakwaters, $s=2\%$

Figure 8.25 show the number of displaced armour units from the total breakwater and Figure 8.26, Figure 8.27 respectively the seaside slope and crest. The wide crested breakwaters are performed with a relative placement density of 100% whereas the small crested breakwaters with 103%.

The stability of the total breakwater is maximal for emerged conditions and becomes less for increasing crest freeboards and attains a minimum for a crest freeboard of 1.5. No displaced armour units and failure for this test occurs within a small increase of the wave height. The stability increases for increasing

The seaside slope shows a comparable trend as for the total breakwater.

The trend lines for the fixed damage levels are based on stability numbers which are assumed for crest freeboards of -3. The dashed trend lines show possible other courses of the fixed damage number trend lines. Despite the absence of displaced armour units for submerged conditions Figure 8.27 shows the trend for the stability of the armour units.

Figure 8.25 Stability at different crest freeboards, total breakwater, small crest width ($s=2\%$).

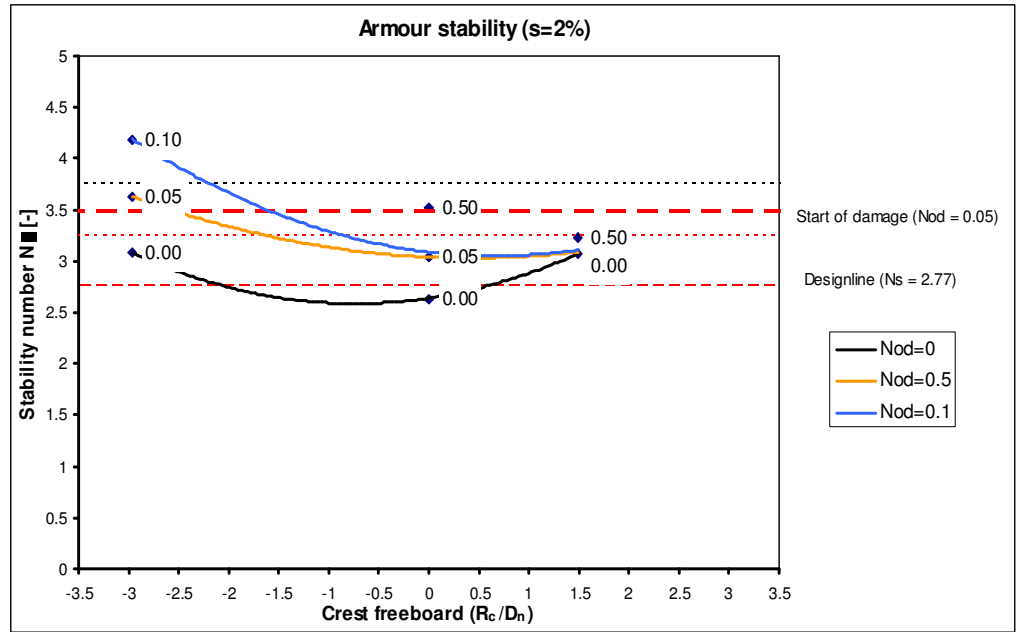


Figure 8.26 Stability at different crest freeboards, seaside slope, small crest width ($s=2\%$).

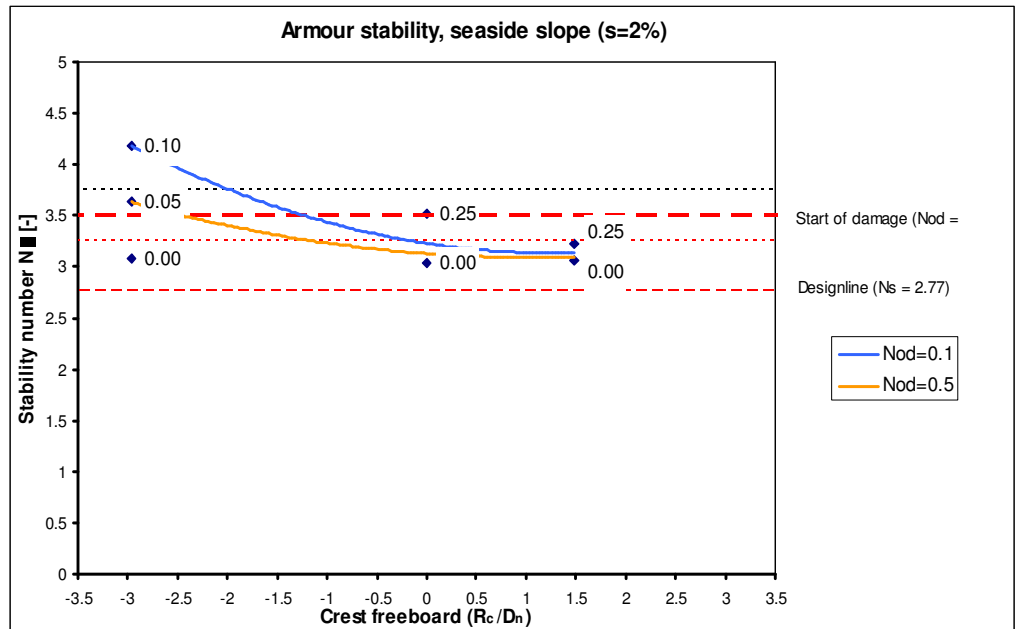
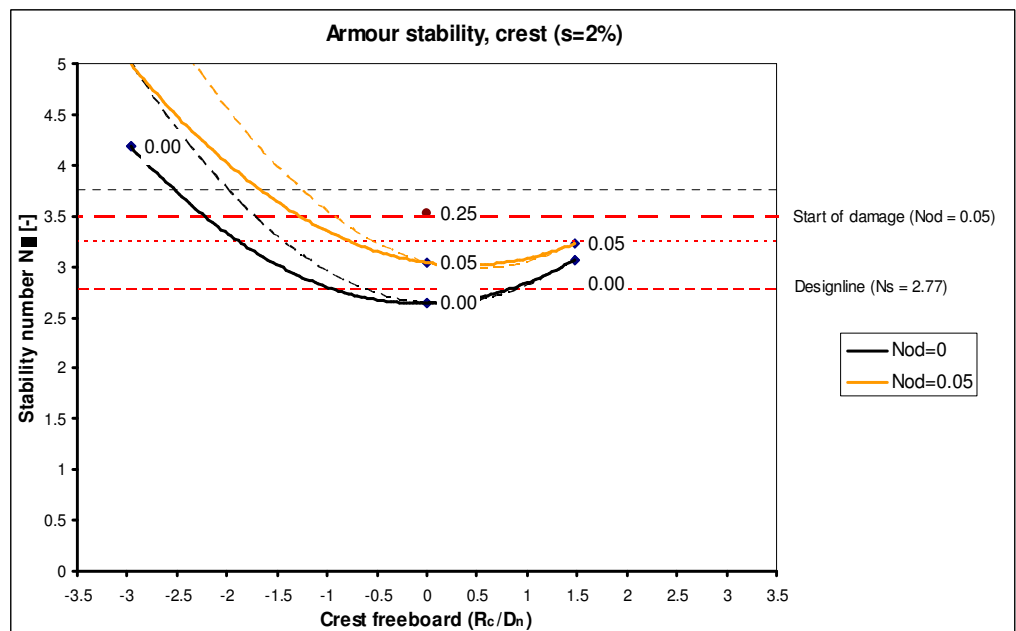


Figure 8.27 Stability at different crest freeboards, crest, small crest width ($s=2\%$).



Small crested breakwater, $s=4\%$

Figure 8.28 shows the number of displaced elements for the total breakwater and Figure 8.29, Figure 8.30 for the seaside slope and crest respectively.

Due to the low number of displaced elements (except for a crest freeboard of 1.5) only the trend line which represents no damage are plotted. For various test series no damage at all occurred therefore it is unknown if for higher stability numbers damage will occur. As a result the trend lines can be seen as lower limit at which no damage occurs.

The stability for the total breakwater and seaside slope is maximal for submerged and emerged conditions and minimal for crest freeboards of 1.5. The stability of the crest section is constant for submerged conditions and decreases slightly for zero crest freeboard. For positive crest freeboard no displaced element are observed while failure occurred for crest freeboard 1.5. All elements are thus displaced from the seaside slope. The trend lines show larger or equal stability numbers as for start of damage for conventional breakwaters.

Figure 8.28 Stability at different crest freeboards, total breakwater, small crest width ($s=4\%$).

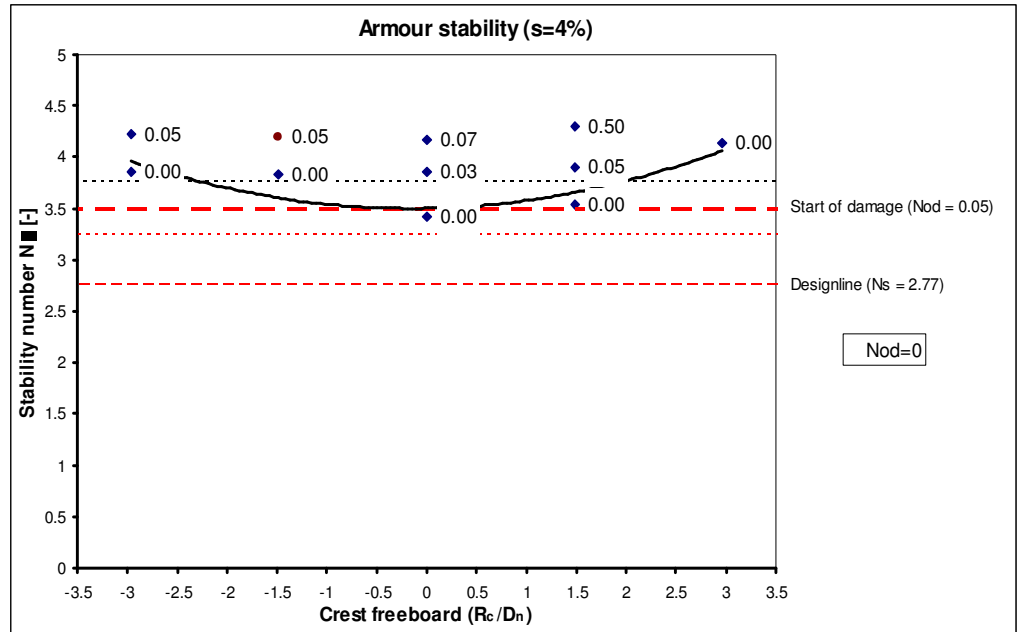


Figure 8.29 Stability at different crest freeboards, seaside slope, small crest width ($s=4\%$).

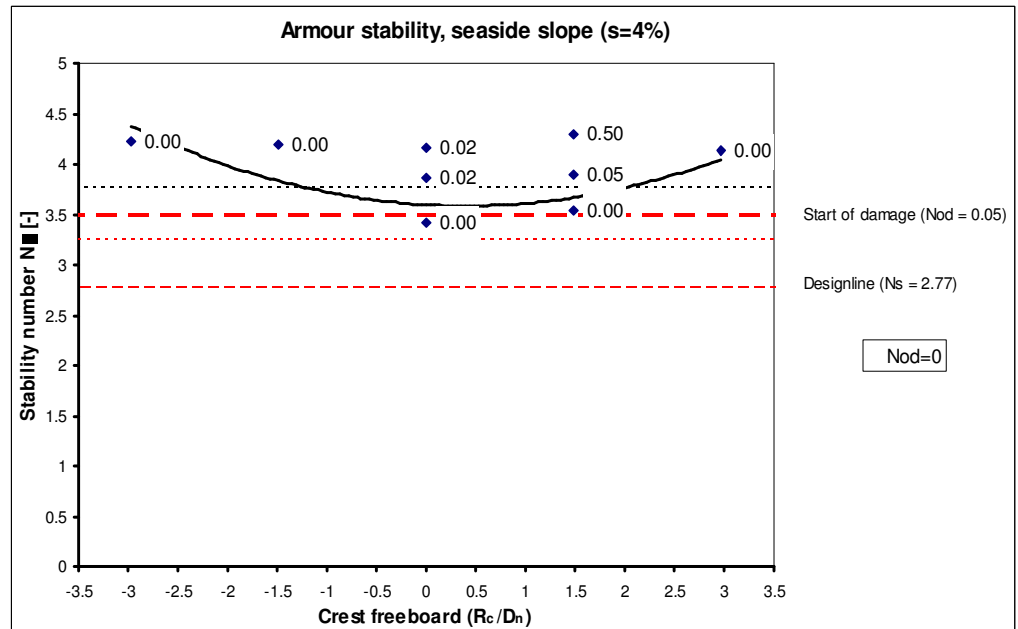
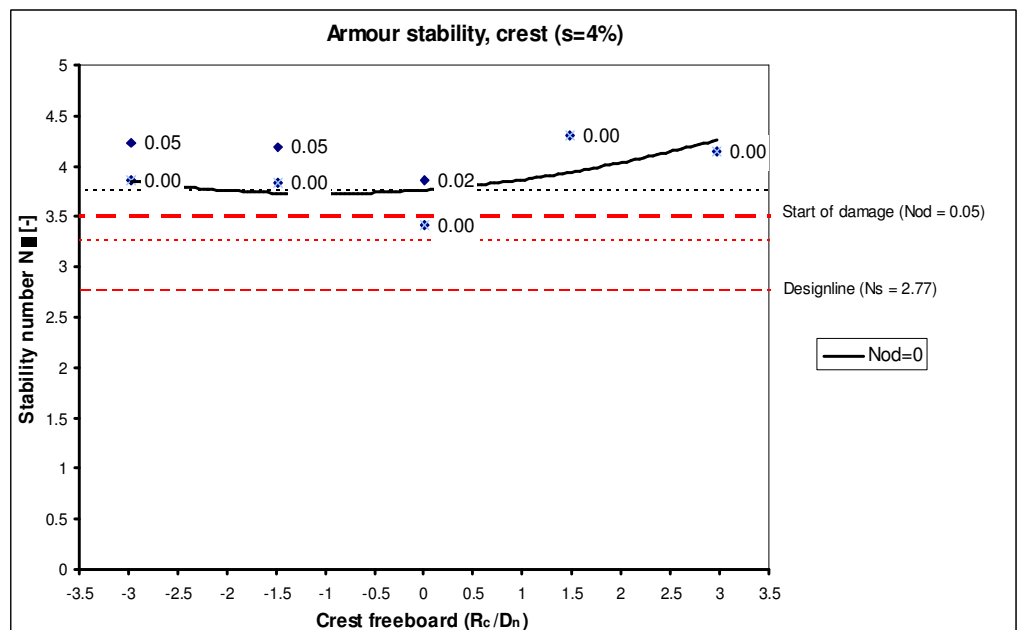


Figure 8.30 Stability at different crest freeboards, crest, small crest width ($s=4\%$).



Conclusions

The wide crested breakwaters and a wave steepness of 4% show only some displaced elements at a crest freeboard of 1.5. Therefore these results are not discussed. The following conclusions can be drawn for the wide and small crested breakwaters for 2 and 4% wave steepness:

- The total breakwater shows for all crest widths and wave steepness's the same trend. The stability is minimal for a crest freeboard of 1.5 although the trend lines do not always show it exactly right. For negative and positive crest freeboards the stability increases.
For low damage levels in the case of 2% wave steepness the stability for negative crest freeboards is larger than for emerged breakwaters, this is not the case for wave steepness of 4%
- The stability of the seaside slope is maximal for negative and positive crest freeboards, the minimum stability is obtained for a crest freeboard of 1.5. The increase in stability for positive crest freeboards is larger for the 4 than the 2% wave steepness.
- The crest sections shows a similar trend as the total breakwater, except for a wave steepness of 4% the stability is approximately constant for negative crest freeboards and increases for positive crest freeboards.

8.4.2. INFLUENCE CREST WIDTH AND RELATIVE PLACEMENT DENSITY

The influence of crest width on the number of displaced armour units is only described for the 2% wave steepness test series. For the wide crested breakwater and wave steepness 4% only at a crest freeboard of 1.5 elements are displaced, therefore it is not possible to compare both crest widths for a wave steepness of 4%.

Furthermore it should be noted that the relative placement density of wide crested breakwaters is 103% whereas for the small crested breakwaters it is 100%. Potential differences between the stability of the wide and small crested breakwater at the seaside slope are expected to be caused dominantly by the relative placement density whereas for the crest section the differences are expected to be caused by the crest width.

Trend lines are plotted for fixed damage levels over the crest freeboard for both crest widths. The trend line of the wide crested breakwater is extrapolated to a crest freeboard of 3 to enable the comparison of both crest widths for all crest freeboards.

Wave steepness 2%

Figure 8.31, Figure 8.32 and Figure 8.33 show the number of displaced elements for wide and small crested breakwaters for the total breakwater, seaside slope and crest respectively. For the total breakwater and the seaside slope the compared damage number for both the wide and small crested breakwater amounts $N_{od}=0.1$. For the crest section the stability numbers are compared at which no damage occurred.

The stability curves for the total breakwater show that the wide crested breakwater is slightly more stable than the small crested breakwater for all

crest freeboards. Almost all points of the wide crested breakwater are positioned above that of the small crested breakwater this shows that it is not any arbitrariness.

The stability of the armour units at the seaside slope is approximately the same for both crest widths. Only for the small crested breakwater the deviation from the observed number of displaced armour units to the trend line is quite large.

For the crest section trend lines are plotted which represent zero displaced armour units. Du to the fact that for a crest freeboard of -3 no elements are displaced it could be that still no damage is present for larger stability numbers, the dashed line represents the trend line which would result from that. The solid trend line can thus be seen as a lower limit for submerged conditions. For zero crest freeboard the stability for both crest widths is approximately the same, whereas for emerged and submerged crest freeboards the wide crested breakwater becomes more stable than the small crested.

Figure 8.31 Stability small versus wide crested breakwater, total stability, ($s=2\%$).

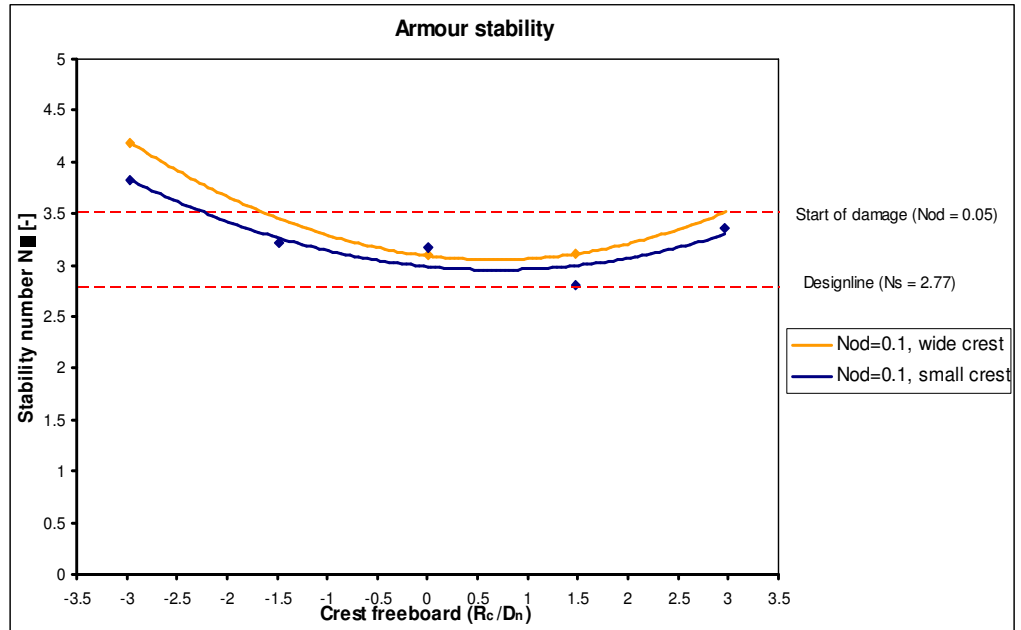


Figure 8.32 Stability small versus wide crested breakwater, seaside slope, ($s=2\%$).

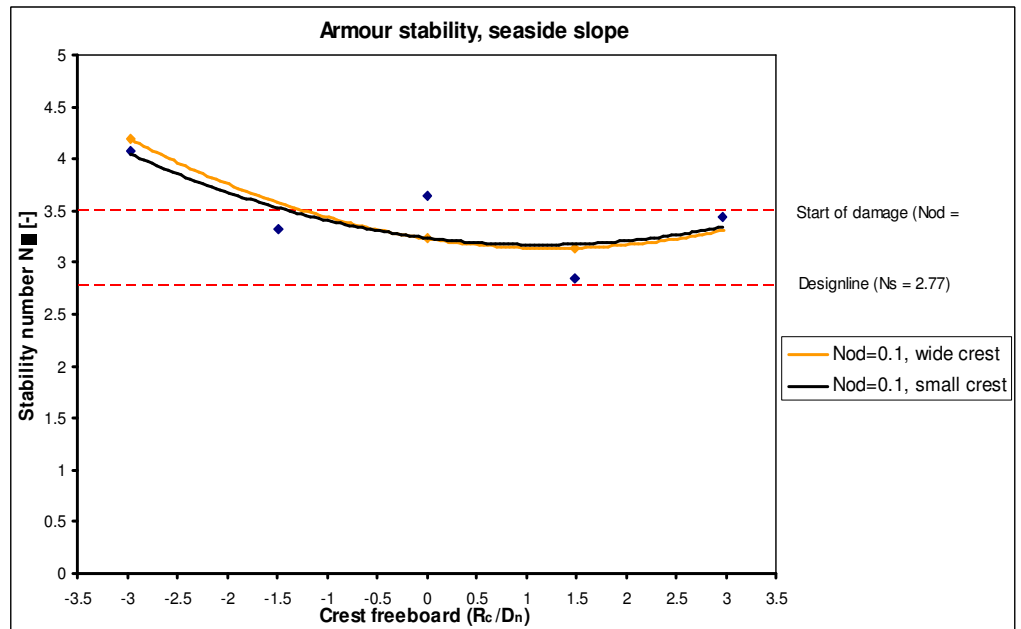
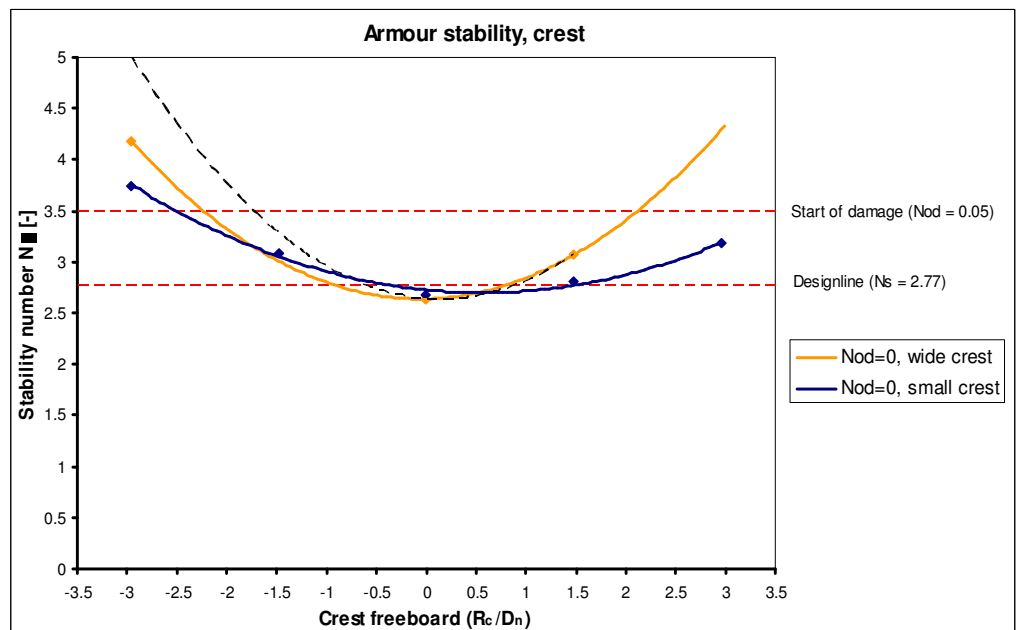


Figure 8.33 Stability small versus wide crested breakwater, crest, ($s=2\%$).



Conclusions

The crest width can only be compared for wave steepness 2% due to the absence of data points for the wide crested breakwater and wave steepness 4%.

For all breakwater sections similar trends are observed for both crest widths. The total breakwater is slightly more stable for the wide crested breakwater at all crest freeboards. The stability of the seaside slope is the same for both crest widths, this indicates that crest width does not have an influence on the stability of the seaside slope. The crest section is slightly less stable for the wide crested breakwater in the proximity of zero crest freeboard whereas for increasing positive and negative crest freeboard the small crested breakwater becomes less stable.

8.4.3. INFLUENCE WAVE STEEPNESS

The above described subjects are treated separately for all wave steepness's. In this section the influence of the wave steepness at the number of displaced armour units is discussed. To this end, trend lines for fixed damage levels are plotted over the different crest freeboards for both a wave steepness of 2 and 4% for the different breakwater sections. The plots are only made for the small crested breakwaters because for the wide crested breakwaters not enough elements are displaced in case of a wave steepness of 4%.

Trend lines for zero damage levels are plotted for the small crested breakwater, the comparison of other damage levels is not possible because of the low number of displaced armour units for the 4% wave steepness.

Small crested breakwater

The stability of the armour layer for the total breakwater is significant smaller for a wave steepness of 2% than for 4%. The stability is maximal for the most emerged tested breakwater in case of 4% wave steepness, whereas for 2% wave steepness the stability is minimal. The stability in case of 2% wave steepness shows a different trend than the 4% wave steepness for the most emerged breakwaters whereas for submerged conditions a similar trend is observed.

The stability of the armour layer at the seaside slope is significant smaller for the 2% than the 4% wave steepness. The stability in case of 4% wave steepness is maximal for the most positive and negative crest freeboards, while the stability in case of 2% wave steepness is constant for submerged conditions and subsequently decreases for increasing crest freeboards.

The stability at the crest is approximately the same for both wave steepness's in case of a crest freeboard of -3 and subsequently decreases for decreasing negative crest freeboard. The decrease in stability is larger for a wave steepness of 2% than for 4% and results in a minimum stability at a crest freeboard of 0 for both wave steepness's, although the 4% trend line does not show it. For crest freeboards larger than 0, both wave steepness's show a comparable trend.

Figure 8.34 Influence wave steepness on the displacement of armour units, small crested breakwater, total breakwater.

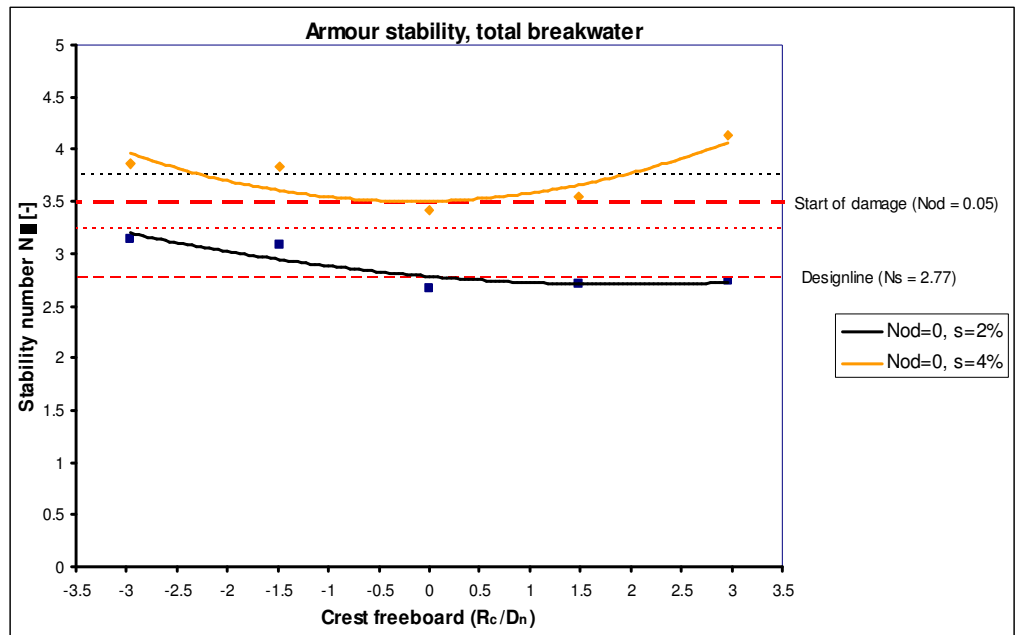


Figure 8.35 Influence wave steepness on the displacement of armour units, small crested breakwater, seaside slope.

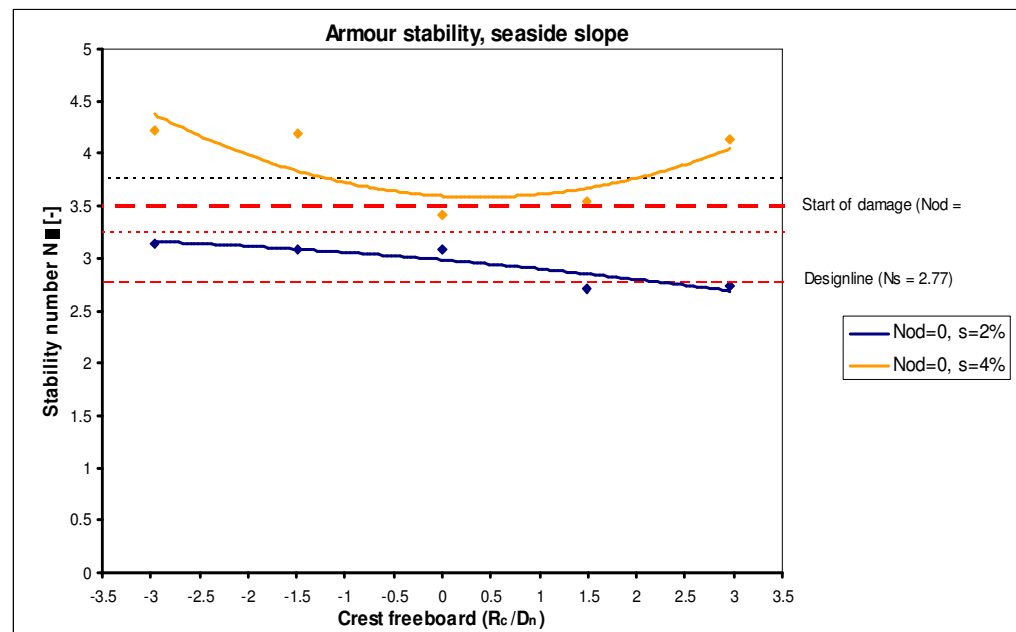
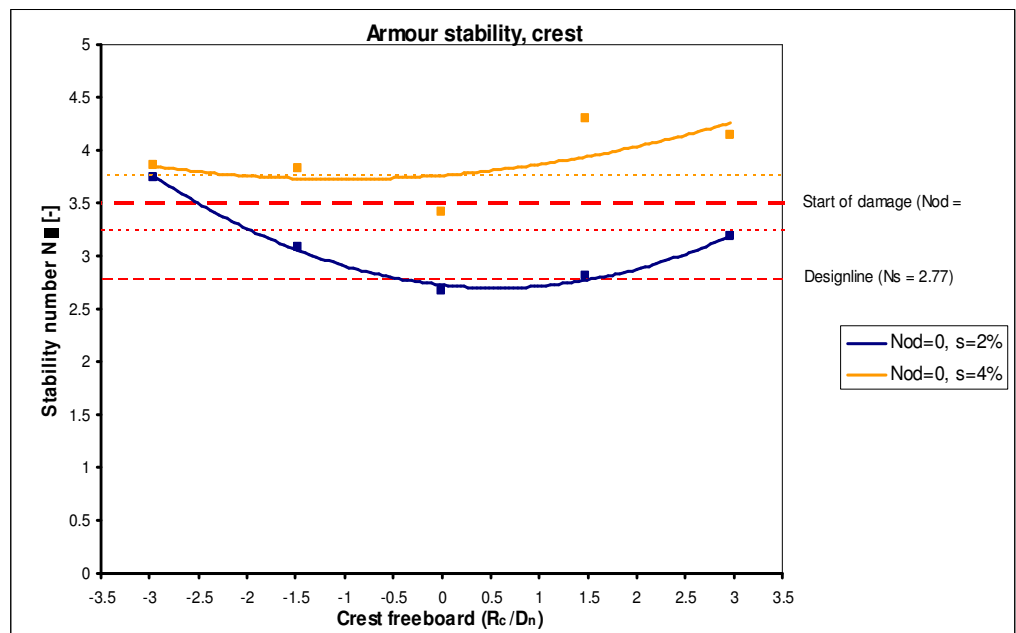


Figure 8.36 Influence wave steepness on the displacement of armour units, small crested breakwater, crest.



Conclusions

The comparison of wave steepness can only be made for the small crested breakwaters due to the absence of data points for the wide crested breakwater in case of 4% wave steepness. The stability in case of 2% wave steepness is always smaller than for the 4% wave steepness.

The stability of the total breakwater shows a different trend for positive crest freeboard for the 4% wave steepness than in case of 2% wave steepness. The stability of the armour layer for the seaside slope in case of wave steepness 4% shows a stability curve which is relatively large for submerged and emerged conditions and attains a minimum for a crest freeboard of zero. The stability of the 2% wave steepness decreases almost linearly from submerged conditions to emerged conditions.

For the most negative crest freeboard the stability is approximately the same for both the small and wide crested breakwaters. The difference in stability increases towards zero crest freeboard and stabilizes for positive crest freeboards.

8.5. LOCATION OF DISPLACED ARMOUR UNITS

The location of damage indicates the areas where the armour layer is loaded most heavily, insight is obtained in the most vulnerable sections. The initial location of the armour units, which are displaced by more than one armour unit dimension from the armour layer, up to a maximum of 10 (failure) are plotted in graphs. On the x-axis the Xbloc row numbers are plotted. No elements are dislocated lower than the third Xbloc row, therefore the numbering starts from the third row of the lee- and seaside slope (counted from upside down). On the y-axis the elements number is presented. The rows contain alternately 10 and 11 armour units, the numbering ranges from 1 to 10 and 1 to 11.

The location of damage is plotted for varying crest freeboard, wave steepness and crest width. The reference test series are plotted in Figure 8.37 and Figure 8.38, in Appendix L for all tests the location of displaced element is plotted.

Figure 8.37 Location of displaced armour units for reference test series (CI), wave steepness 2%.

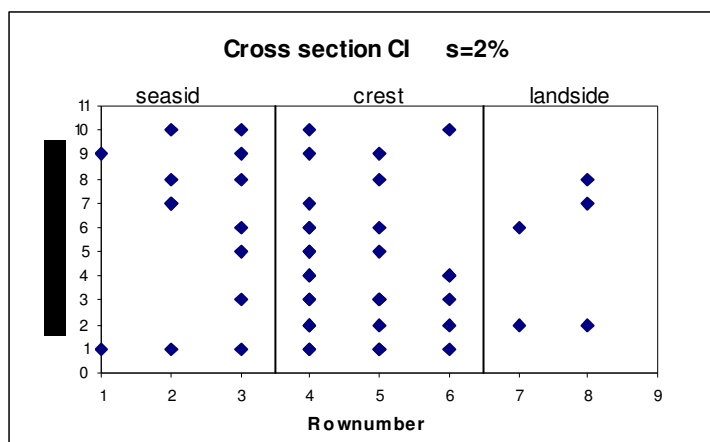
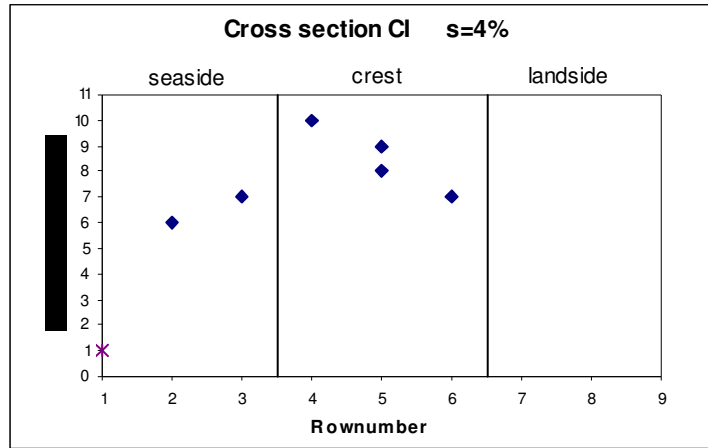


Figure 8.38 Location of displaced armour units for reference test series (CI), wave steepness 4%.



Most of the displaced elements are positioned at the upper part of the seaside slope and the seaside part of the crest. If the first element is displaced the exposed surface area to the wave induced motion of the surrounding elements increases, this in combination with the decreased stability of the armour units in the upper part of the seaside slope and crest (see §4.2.2) leads to further displacement of the surrounding elements. Most of the damage is therefore observed clustered.

9. COMPARISSION TEST RESULTS

In this section the discussed test results for rocking and displaced armour units are compared to each other (§9.1).

9.1. COMPARISSON ROCKING AND DISPLACED ELEMENTS

The comparison of the rocking and the displaced elements shows whether rocking and the displacement of armour units are correlated with each other. If this is the case rocking armour units can be seen as a first sign of further damage in the form of displaced elements. The comparison is made for:

- Small crested breakwater, $s=2\%$;
- Wide crested breakwaters, $s=2\%$;
- Small crested breakwater, $s=4\%$;
- Wide crested breakwaters, $s=4\%$.

To enable the comparison of the rocking and displaced elements different fixed damage levels for the number of rocking and displaced elements are plotted over the crest freeboard.

Small crested breakwater, $s=2\%$

Figure 9.1 shows the comparison of rocking and displaced armour units for the total breakwater and Figure 9.2, Figure 9.3 for the seaside slope and crest respectively. For all breakwater sections and crest freeboards rocking is present at lower stability numbers than the displacement of elements.

The total breakwater shows a different trend for both rocking and displaced elements. Rocking is least stable for the most submerged tested conditions whereas for the displacement of armour units it shows the largest stability. Furthermore failure occurred at the lowest stability number for a crest freeboard of 1.5, the fixed damage level for rocking however shows for that crest freeboard the highest stability.

The seaside slope shows for submerged conditions a comparable trend as for the displacement of the armour units. For emerged breakwaters the stability increases again for the displacement of armour units whereas the seaside slope shows an almost linear decreasing line for the number of rocking elements from negative to positive crest freeboard. The minimum stability for rocking and the displacement of elements does not coincide with each other. For larger damage levels in case of displaced element the deviations in stability between rocking and displacement becomes increasingly larger.

The seaside slope shows that the stability of the number of rocking armour units is smallest for negative crest freeboards and becomes maximal for a crest freeboard of 1.5 where after it decreases gradually. The stability of the number of displaced element shows the opposite trend, the minimum stability is obtained for a crest freeboard of 1.5. The maximum stability for rocking

elements coincide thus with the minimum stability of displaced armour units. For crest freeboards larger or smaller than 1.5 the difference in stability between rocking and displacement increases.

Figure 9.1
 Comparisson rocking and displacd armour units, total breakwater, s=2%.

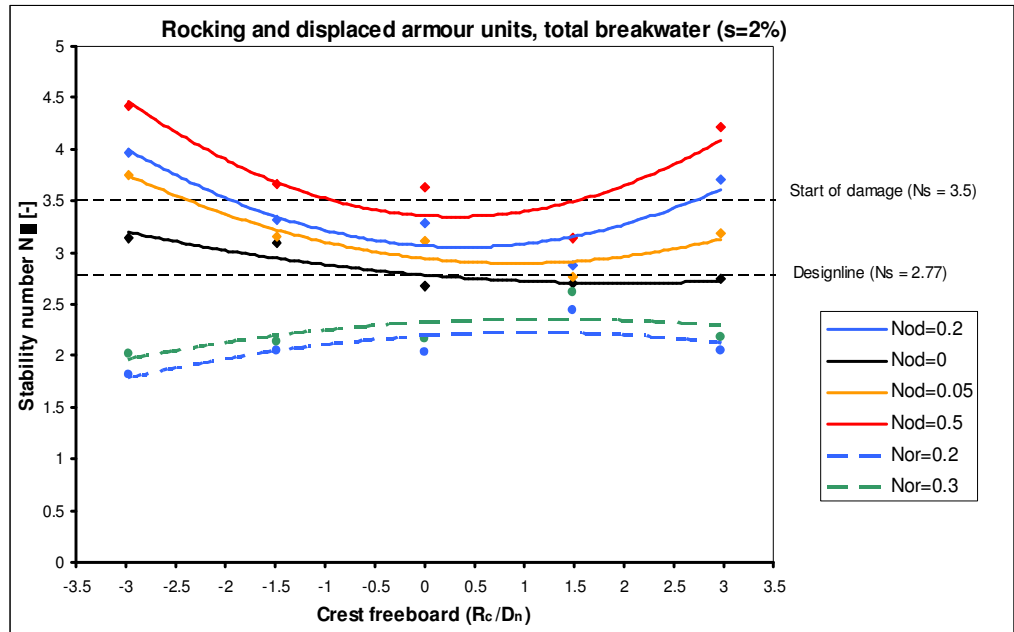


Figure 9.2
 Comparisson rocking and displacd armour units, seaside slope, s=2%.

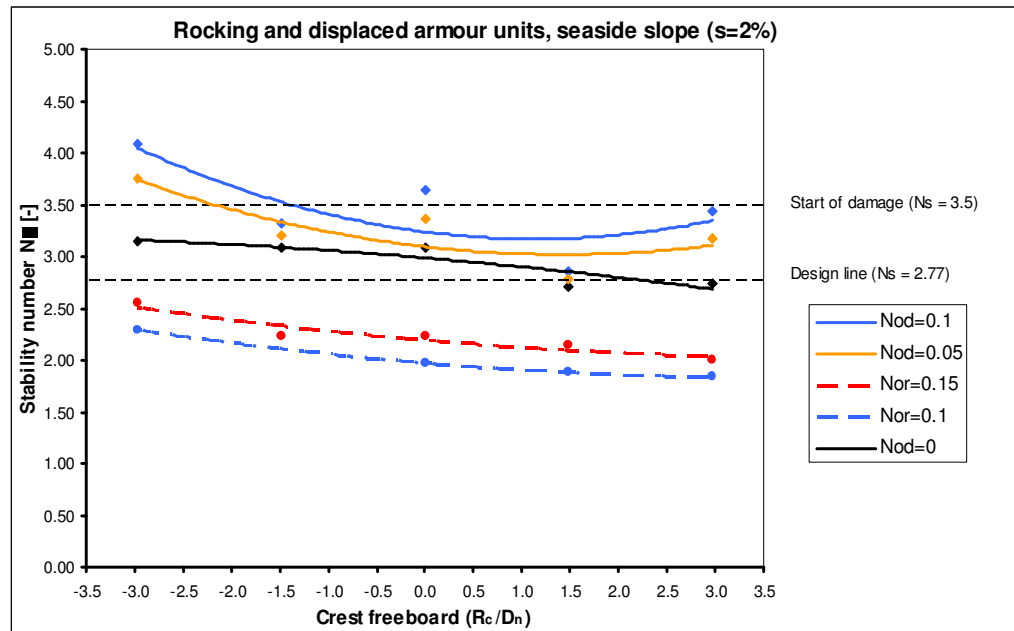
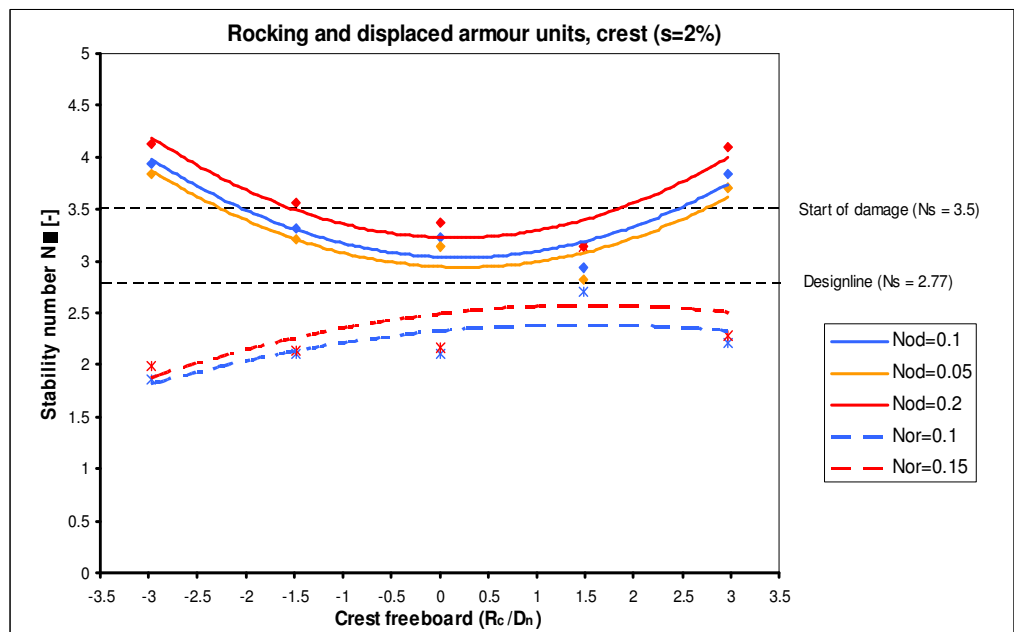


Figure 9.3
 Comparisson rocking and displacd armour units, crest, s=2%.



Wide crested breakwater, $s=2\%$

Figure 9.4 shows the comparison of rocking and displaced armour units for the total breakwater and Figure 9.5, Figure 9.6 for the seaside slope and crest respectively. Not only the crest width is changed compared to the small crested breakwater but also the relative placement density, which is 100% for the wide crested breakwater and 103% for the small crested breakwater. It is expected that possible differences compared to the small crested breakwater are caused due to the relative placement density in case of the seaside slope and the crest width for possible differences at the crest.

The stability of the total breakwater shows similar trends for both rocking and the displacement of elements, except for the trend line which represents zero displaced armour units. The increase in stability for submerged conditions is larger in case of the displaced armour units than for rocking.

The stability of the seaside slope shows a comparable trend for both rocking and the displacement of armour units. The stability decreases from submerged to emerged conditions. For a low number of rocking armour units the decrease in stability is almost linear as is the case for small crested breakwaters. The difference in stability between rocking and the displacement of armour units is not constant.

In Figure 9.6, crest section, the stability is plotted for the rocking and the displacement of elements. The two dashed trend lines represent possible other courses of the trend lines for the displacement of the armour units, for a crest freeboard of -3 no displaced elements are observed. The black trend line represents the most conservative assumption whereas the black dashed trend line a more progressive one.

Rocking and the displacement of elements show both a different trend for different crest freeboards. Also the difference in stability for rocking and the displacement of elements is not constant.

Figure 9.4 Influence wave steepness on the displacement of armour units, small crested breakwater, crest

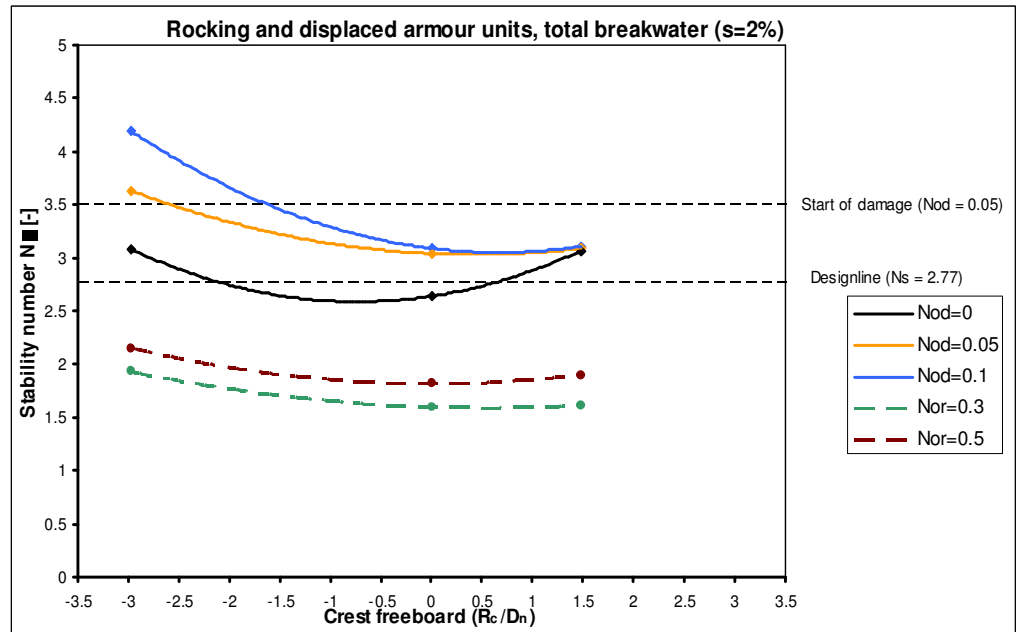


Figure 9.5 Influence wave steepness on the displacement of armour units, small crested breakwater, crest

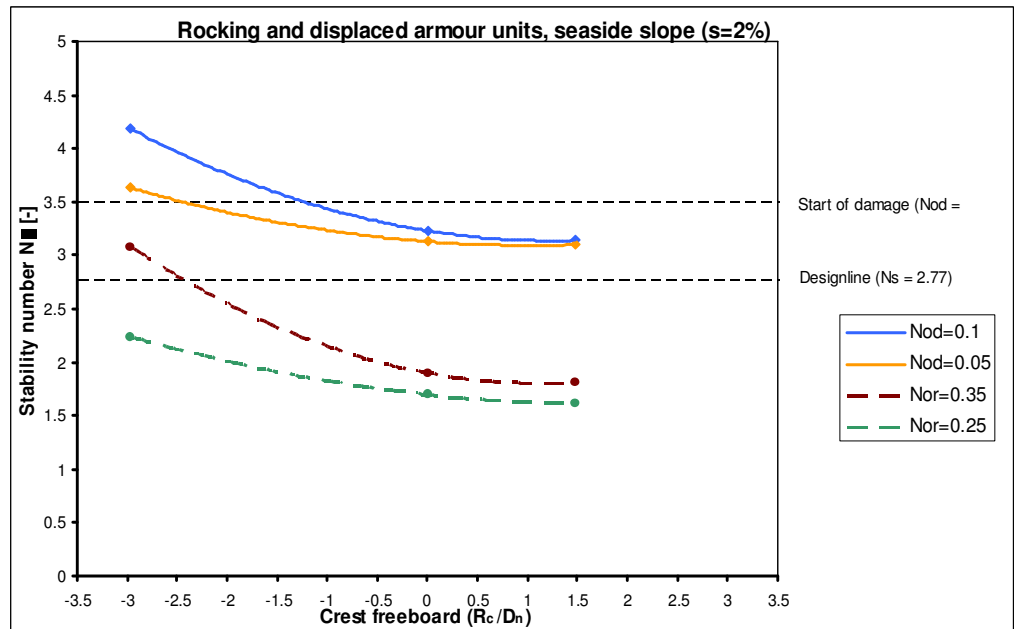
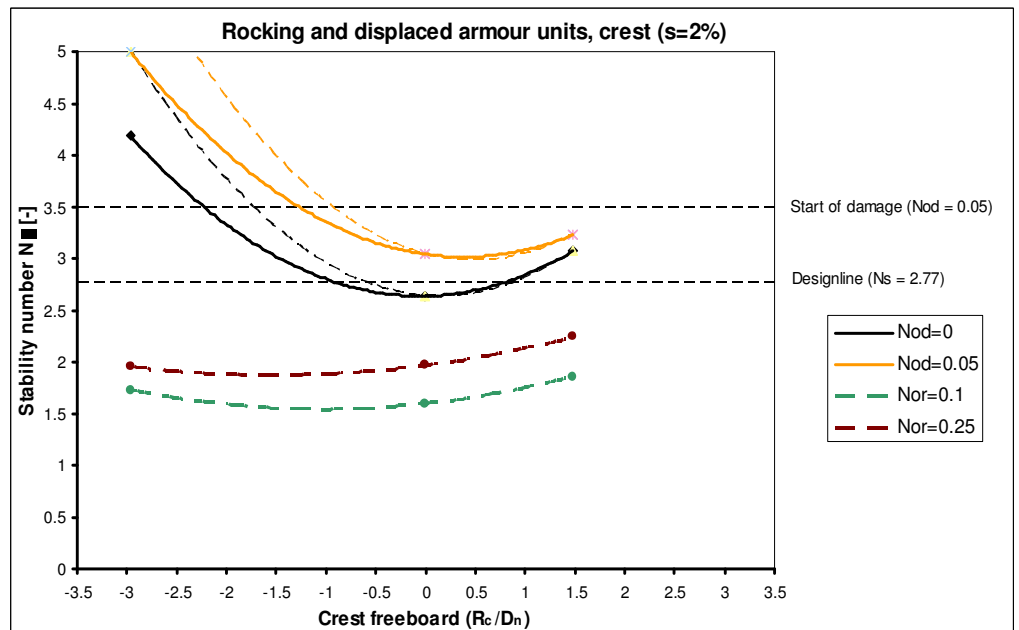


Figure 9.6 Influence wave steepness on the displacement of armour units, small crested breakwater, crest



Small crested breakwater, $s=4\%$

Figure 7.9 shows the stability for both rocking and the displacement of armour units for the total breakwaters, whereas Figure 9.8 and Figure 9.9 for the seaside slope and crest respectively.

Figure 7.9 shows the stability for the rocking and displaced elements. The least stable crest freeboard is 1.5, this can not be derived from the trend lines for both rocking and the displacement of elements.

Figure 9.7 Influence wave steepness on the displacement of armour units, small crested breakwater, crest

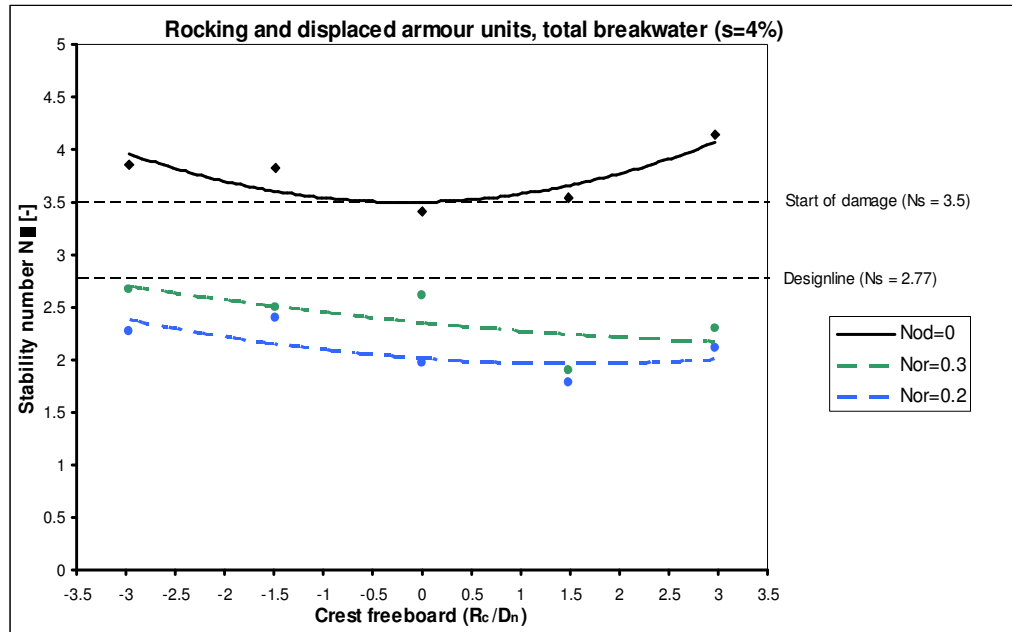


Figure 9.8 Influence wave steepness on the displacement of armour units, small crested breakwater, crest

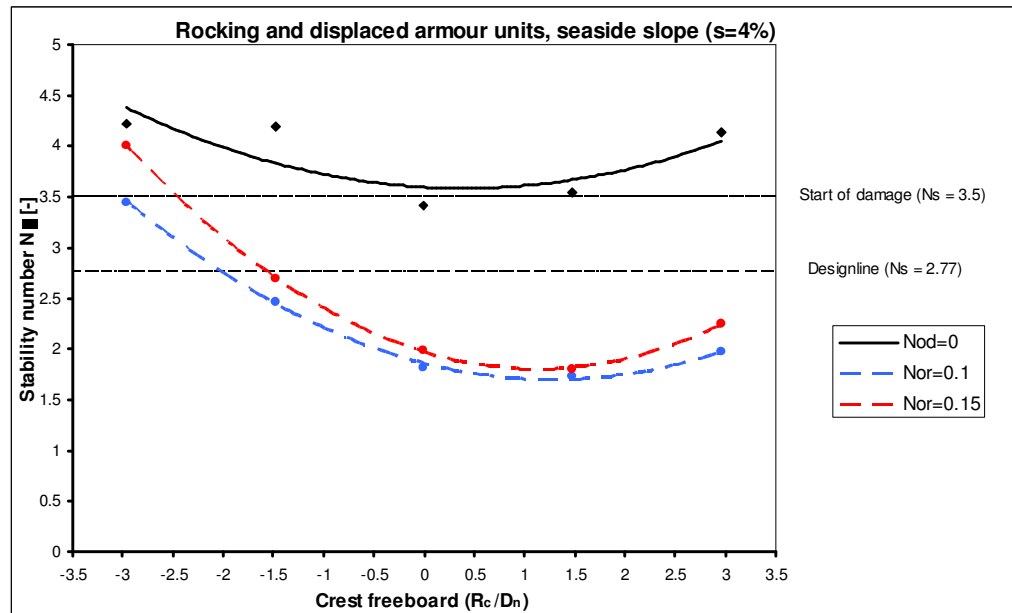
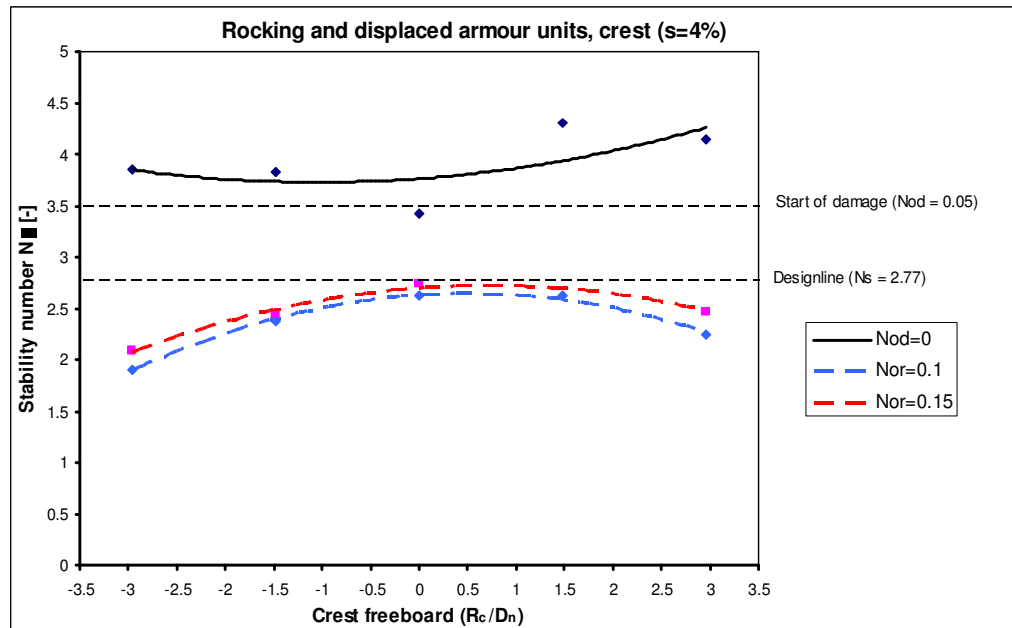


Figure 9.9 Influence wave steepness on the displacement of armour units, small crested breakwater, crest



10. WAVE TRANSMISSION

Low-crested breakwaters force the incoming waves to break and dissipate the wave energy. Many breakwaters of this type have been built at various locations to stabilize an eroded beach and to reduce damage to coastal and harbour structures due to severe wave action. To meet the requirements of the design successfully the transmitted wave height should be predicted in advance correctly. Therefore the measured transmitted wave height and period (which can be derived from the transmitted spectra, see Appendix F) are treated shortly, it is an elementary part in the design of low-crested breakwaters.

Wave transmission is a result of overtopping wave energy over the breakwater crest and a permeable core of the breakwater in combination with relatively long wave periods. The wave transmission coefficient is defined as:

$$K_t = \frac{H_t}{H_i} \quad (9.2)$$

In which:

H_t transmitted significant wave height [m];

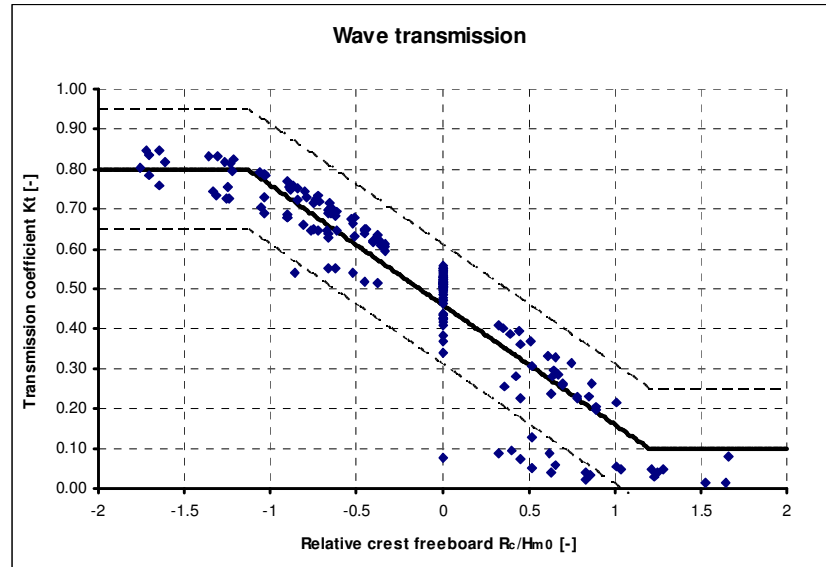
H_i incident significant wave height [m].

VAN DER MEER *et al.* 1994 gives the following formula for a rough estimate of the wave transmission:

$$\begin{aligned} K_t &= 0.80 & -2.00 < \frac{R_c}{H_{m0}} < -1.13 \\ K_t &= 0.46 - 0.3 \cdot \left(\frac{R_c}{H_{m0}} \right) & -1.13 < \frac{R_c}{H_{m0}} < 1.20 \\ K_t &= 0.10 & 1.20 < \frac{R_c}{H_{m0}} < 2.0 \end{aligned} \quad (9.3)$$

Formula (9.3) is plotted with the ninety percent confidence interval in Figure 10.1 together with the measured wave transmission for all test series.

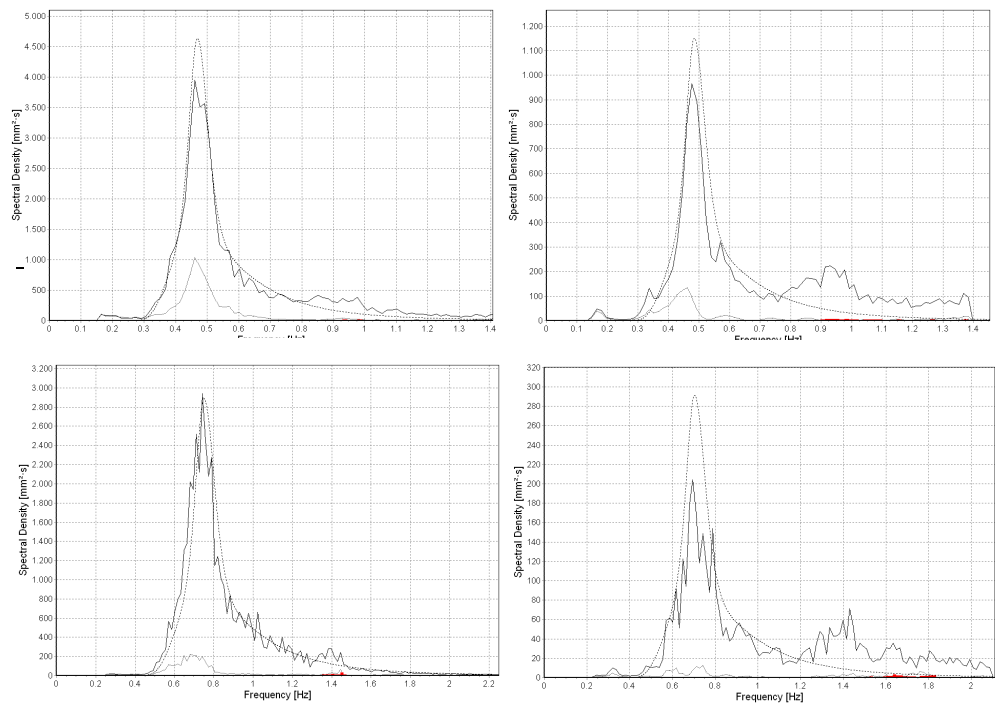
Figure 10.1 Measured wave transmission in relation to VAN DER MEER *et al.* (1994)



The data fit formula (9.3) quite well, only around $R_c/H_{m0} = 0.5$ there are a number of measured wave transmission points outside the confidence interval. These points correspond to test DII_2 and DII_4, the point outside the confidence interval at $R_c/H_{m0} = 0$ correspond to test CII_4 with 60% H_d . The formula predicts the wave transmission for structures with a wide crests and a crest freeboard of $R_c/H_{m0} = 0.5$ not good because the method is based on model test with relatively small breakwater crests.

Transmitted spectra are often different from incident spectra. Waves breaking over a low-crested structure may generate two or more transmitted waves on the lee side. The effect is that more energy is present at higher frequencies than for the incident spectrum. In Figure 10.2 the incident and transmitted spectra are shown for two tests where the design wave height was generated.

Figure 10.2 Wave spectra (for tests CI_2_1 and DI_4), incident at foreshore (left graph) and transmitted spectra behind the breakwater (right graph).



The spectra show that indeed more wave energy is present at higher frequencies and that at the peak frequency the wave energy reduced. Waves with two different periods are generated behind the structure, one of which approximately is the peak period of the generated spectrum. This is also the case for the emerged breakwater, cross section DI_4. More emerged tested cross sections show totally different transmitted spectra than described above, see Appendix F.

11. FINAL CONCLUSION

In this chapter the conclusions and recommendations of the performed study are presented. The Newbiggin case demonstrates the lack of knowledge for the stability of single layer armour units at low-crested breakwaters. One percent of the elements were broken one year after completion of the breakwater. The stability number used for calculation of the armour unit's size was the same as for conventional breakwaters which is not sufficient given the number of broken armour units.

To enlarge the understanding of the stability of Xbloc single layer armour units at low-crested breakwaters physical model tests are performed.

The influence of different parameters on the stability is discussed:

Wave height

- Increasing wave heights show an increasing number of rocking elements at the crest for breakwaters with negative crest freeboard whereas the increase in the number of rocking elements at the seaside slope is relatively small. For emerged breakwaters an opposite trend is observed.

Rocking armour units:

- Rocking and the displacement of armour units are not correlated with each other. Rocking shows a different trend at the total breakwater, crest and seaside slope for both wave steepness's than the trends for the displacement of armour units.
- For submerged conditions the stability of the armour units at the crest is smallest, this is caused by the oscillating flow of water over the breakwater crest. This flow of water is initiated by the overtopping waves and a gradient over the breakwater crest caused by a wave trough in front of the breakwater.
- Rocking armour units are observed well before failure and in most cases before the design stability number. At the moment of displacement of armour units a large amount of rocking elements is observed.
- Most of the rocking armour units are observed at the upper part of the seaside slope and the outer seaside row of the crest.
- The confidence band interval of the reference test series increases for increasing stability numbers.

Displaced armour units:

- Failure always occurs for stability number larger than the design stability number.
- Failure occurs in a small interval of stability numbers, most of the time start of damage and failure occurs at the same stability number.
- The confidence band interval of the reference test series for the total number of displaced armour units is small which indicates a good reliability of the model tests. The distribution of the displaced elements over the breakwater sections shows however a larger spreading.

Crest freeboard

- For both crest widths and wave steepness's the stability (of the displaced elements) of the total breakwater is smallest for a crest freeboard of 1.5. For more negative and positive crest freeboard the stability increases.
- The increase in stability for the total breakwater is largest for negative crest freeboard and wave steepness 2% whereas for wave steepness 2% the increase in stability is largest for positive crest freeboard.
- The stability for rocking elements at the total breakwater is largest for a crest freeboard of 1.5 in case of a wave steepness of 2% and smallest in case of wave steepness 4%.

Crest width

- In general the stability of wide crested breakwaters for rocking elements is observed for lower stability numbers than for small crested breakwaters. This could also be caused by the lower packing density of the armour units.
- The small crested breakwater is slightly more stable in case of the displacement of elements than the wide crested breakwater.

Wave steepness

- The armour units are less stable at all breakwater sections for wave steepness 2% than in the case of a wave steepness of 4% for the displacement of armour units.
- In case of rocking the stability of the total breakwater is smallest for submerged conditions and wave steepness 2%. Whereas for emerged breakwaters the stability is almost comparable for both wave steepness's.

Although start of damage and failure occurred for stability numbers larger than the design stability number rocking is observed for significant lower stability numbers than the design stability number. This could explain the damage in Newbiggin, the design of low-crested breakwaters should be based on rocking instead of the displacement of elements. Ultimately this leads to a non constant design stability number for low-crested breakwaters, the stability number varies for different crest freeboards and wave steepness's.

12. REFERENCES

- BAKKER, P., KLABBERS, M., MUTTRAY, M., VAN DER BERGE, A. (2005) Hydraulic performance of Xbloc armour units, published on <http://www.xbloc.com/htm/downloads.php>
- BREBNER A. (1978) Performance of Dolos blocks in an open channel situation, *Proceedings Coastal Engineering '78*, Hamburg, 2305 – 2307
- BRUUN P. AND GÜNBAK, A.R. (1977) Stability of sloping structures in relation to $\xi = \tan \alpha / \sqrt{H/L_0}$ risk criteria in design, *J. Coastal Engineering*, 1, 287-322
- BURCHARTH H.F. (1993) Structural integrity and hydraulic stability of Coastal engineering manual
- D'ANGREMOND K., AND VAN ROODE, F.C. (2001). Breakwaters and closure dams, Engineering the interface of soil and water 2, *VSSD, Delft Dolos armour layers*, Hydraulics & Coastal Engineering Laboratory, Department of Civil Engineering, Aalborg University, Denmark.
- De Rover, R. (2007) Breakwater stability with damaged single layer armour units, *MSC thesis, Delft University of Technology*.
- DORRINGTON METTAN, J. (1980) *Armour Formulae?*, *Proceedings Coastal Engineering '80*, Sydney, 2304 – 2325
- GARCIA, N., LARA, J.L. AND LOSADA, I.J. (2004) 2-D numerical analysis of near-field flow at low-crested permeable structures, *J. of Coastal Engineering*, 15, 991 - 1020
- GODA Y. (2000) *Random Seas and Design in Maritime Structures*. Advanced Series on Ocean Engineering, World scientific, 73-95
- HALD, T. AND BURCHARTH, H.F. (2000) An alternative stability equation for rock armoured rubble mound breakwaters, *Proceedings Coastal Engineering '00*, Sydney, 1921 – 1934
- HATTORI, M., YAUCHI, E. AND KASAHARA, Y. (1999) Hydraulic stability of armor units in single cover layer, *Coastal Structures '99*, Santander, Spain, pp 241-248.
- KRAMER M. AND BURCHARTH, H. (2003) Stability of low-crested breakwaters in shallow water short crested waves, *Proceedings Coastal Structures '03*, Portland, 137 -149
- KRAMER, M., ZANUTTIGH, B., VAN DER MEER, J.W., VIDAL, C. AND GIRONELLA, F.X. (2005) Laboratory experiments on low-crested breakwaters, *J. of Coastal Engineering*, 10-11, 867 – 885

KRAMER, M., ZANUTTIGH, B., VAN DER MEER, J.W., VIDAL, C., AND GIRONELLA, F.X. (2005) Laboratory experiments on low-crested breakwaters, *Proceedings Coastal Engineering '05, Delft*, 1375 – 1388

LOSADA, I.J., GARCIA, N. AND LARA, J.L. (2003) Report on turbulent flow velocities in the surface region of LCS. *Environmental design of low crested coastal defence structures (DELOS), D23 and D44*

MATSUDA S., MATSUMOTO, A., NISHIGORI, W., HANZAWA, M. AND MATSUOKA, M. (2003) Crown height effects on stability of flat type concrete armor blocks, *Proceedings Offshore and Polar engineering '03, Honolulu*, 631 - 638

MELBY, J.A. AND KOBAYASHI, N. (1996) Incipient motion of breakwater armor units, *Proceedings Coastal Engineering '96, Copenhagen*, 1803-1815

MIZUTANI N., IWATA, K., RUFIN JR., T.M. AND KURATA, K. (1992) Laboratory investigations on the stability of a spherical unit of a submerged breakwater, *Proceedings Coastal Engineering '92, Venice*, 1400 – 1413

MIZUTANI N., RUFIN JR., T.M. AND IWATA, K. (1994) Stability of armour stones of a submerged wide crown breakwater, *Proceedings Coastal Engineering '94, Kobe*, 1439 - 1453

MUTTRAY, M., REEDIJK, J., VOS-ROVERS, I., BAKKER, P. (2005) Placement and structural strength of Xbloc and other single layer armour units, published on <http://www.xbloc.com/htm/downloads.php>

PRICE, W.A. (1979) Static stability of rubble mound breakwaters, *J. Dock & Harbour Authority*, 60,

ROCK MANUAL, THE (2007) The use of rock in hydraulic engineering (2nd edition), CIRIA, London, England.

SCHIERECK, G.J. (2004) Introduction to bed, bank and shore protection, *VSSD, Delft*

VAN DER MEER J.W. (1988) Stability of cubes, tetrapods and accropode, *Proceedings Breakwaters Conference '88, Eastbourne*, 59 – 68

VAN DER MEER J.W. (1988) Rock slopes and gravel beaches under wave attack, PHd. Thesis, Delft University of Technology. Also in *Delft Hydraulics Communications* No. 396.

VAN DER MEER J.W. AND K.W. PILARCZYK (1990) Stability of low-crested and reef breakwaters, *Proc. Int. Conf. Coastal Engineering, Delft*, pp 1375 – 1388.

VAN DER MEER J.W., DAEMEN, I.F.R. (1994) Stability and wave transmission at low-crested rubble-mound structures, *ASCE Journal of Waterway, Port, Coast and Ocean Engineering*, New York, pp 1 - 19.

VAN GENT, M.R.A., SMALE, A.J., KUIPER, C. (2003) Stability of rock slopes with shallow foreshores, *Proceedings Coastal structures '03*, 100 – 112

VERHAGEN H.J., B. REEDIJK, M. MUTTRAY (2006) The effect of foreshore slope on breakwaters stability

VIDAL, C., LOPEZ, F. AND LOSADA, I. (2007) Stability of low crested and submerged rubble mound breakwaters: Relationship between flow characteristics and measured damage and stability formulas for low crested and submerged breakwaters, *Proceedings Coastal Structures'07, Venice*, 1697 – 1692

VIDAL, C., LOSADA, M.A., MEDINA, R., MANSARD, E.P.D. AND GOMEZ-PINA, G. (1992) A universal analyses for the stability of both low-crested and submerged breakwaters, *Proceedings Coastal Engineering '92, Venice*, 1679 - 1692

WAREING A. (2009) Armour unit placement, Coasts, Marine structures and Breakwaters 2009, Edingburgh Abstract

LIST OF FIGURES

Figure 1.1 Breakwater cross section breakwater Newbiggin	2
Figure 1.2 Breakwater Newbiggin with monument	2
Figure 1.3 Original crest height breakwater relative to steel tube pile foundation of the monument	3
Figure 1.4 Breakwater Newbiggin with noticeable bump	3
Figure 1.5 Plan view breakwater Newbiggin	3
Figure 1.6 Illustration of interlocking effect, one element is pulled out initiating contact forces (F_c)	4
Figure 1.7 Contribution of gravity, interlocking and surface to the total stability with varying slope angles [Price (1979)]	4
Figure 2.1 Conventional multi layer rubble mound breakwater, [CEM 2006] ..	8
Figure 2.2 Conventional breakwater	10
Figure 2.3 Berm breakwater	10
Figure 2.4 Low crested breakwater	11
Figure 2.5 Submerged breakwater	11
Figure 2.6 Overview of breakwater failure modes, [CEM 2006]	12
Figure 2.7 Breaker types as a function of the surf similarity parameter [CEM 2006]	13
Figure 2.8 Energy dissipation for two breaker types [SCHIERECK 2004]	14
Figure 2.9 Up and downrush on impermeable slope [CEM 2006]	14
Figure 2.10 Up and down rush on permeable slope [CEM 2006]	15
Figure 2.11 Typical armour failure modes [BURCHARTH 1993]	16
Figure 3.1 Forces on a stone in flow [SCHIERECK 2004]	17
Figure 3.2 Schematisation of incipient motion	19
Figure 3.3 Van der Meer formula	23
Figure 3.4 Model of tested submerged breakwater MIZUTANI et al. 1992	25
Figure 3.5 Methods of wave force and velocity measurements MIZUTANI et al. 1992	25
Figure 3.6 Variation of dimensionless maximum force MIZUTANI et al. 1994 ..	26
Figure 3.7 Design graph with reduction factor for rock diameter of low-crested structure, VAN DER MEER et al. 1994	28
Figure 3.8 Design curves with 90% confidence bands for $S = 2$	29
Figure 3.9 Plan view and cross section of model by VIDAL et al. 1992	29
Figure 3.10 Armour (rock) stability corresponding to initiation of damage, non depth limited waves perpendicular to the trunk, BURCHARTH et al. 2006	30
Figure 3.11 Trunk armour stability corresponding to initiation of damage BURGER 1995	31
Figure 3.12 Trunk cross section KRAMER et al. 2003	31
Figure 3.13 Sections prone to damage, filled black areas indicate exposed stones, KRAMER et al. 2003	32
Figure 3.14 Initiation of damage, KRAMER AND BURCHARTH 2003	33
Figure 3.15 Design graph for stability of low-crested breakwaters corresponding to initiation of damage KRAMER AND BURCHARTH 2003	33
Figure 3.16 Stability condition in depth limited waves, KRAMER et al. 2003 ..	34
Figure 3.17 Design graph corresponding to damage initiation, equation (3.37) ($\gamma = 0.6$, $\rho_s = 2.65 \text{ t/m}^3$), KRAMER et al. 2003	35

Figure 3.18 Damage with regular waves	36
Figure 3.19 Comparison stability armour layer units on different breakwater sections according to the formulas in Table 3-1	38
Figure 3.20 Snapshots of velocity field for different (positive, zero, negative) crest freeboards and t/T values.....	39
Figure 3.21 Mean (ensemble averaged) flow, zero crest freeboard (a), and positive crest freeboard (b)	39
Figure 3.22 Computed mean (ensemble averaged) velocity profiles, structure freeboard (a) zero crest freeboard, (b) positive crest freeboard	40
Figure 3.23 Computed phase-averaged maximum velocity field and computed time averaged velocity field for different crest widths	41
Figure 4.1 Contribution of gravity and surface friction to the total stability with varying slope angle [PRICE 1979].....	47
Figure 4.2 Results pullout tests [MUTTRAY et al. 2005]	47
Figure 4.3 Results pullout tests Xbloc armour unit, slope 3:4, rough under-layer.	48
Figure 4.4 Results pullout tests Xbloc armour unit, various slope angles.....	48
Figure 4.5 Sections with initial damage.....	49
Figure 4.6 Relation between $hc/H_{1/3}$ and N_s for an 1:2 and 1:5 slope.....	50
Figure 4.7 Comparison of stability of front plus crest with rear slope [De Jong (1996)]	51
Figure 5.1 Schematisation wave flume Delta Marine Consultants	53
Figure 5.2 Overall cross section	60
Figure 5.3 Gabions	61
Figure 5.4 Geometry Xbloc armour unit	62
Figure 5.5 Location wave gauges.....	66
Figure 5.6 Damaged armour layer, lower positioned element, seaside slope. .	69
Figure 5.7 Lateral displaced Xbases, test AII_2, fixed Xbase toe elements, test AII_2_1.	69
Figure 5.8 Calculation centre axis armour layer	70
Figure 5.9 Placement crown elements for 100% and 103% relative placement density respectively.	71
Figure 5.10 Spectra CI_2_1	74
Figure 5.11 Rayleigh waveheight distribution and measured wave height CI_2_1	75
Figure 6.1 Overtopping wave for cross section EI.....	77
Figure 6.2 Current in seaward direction over breakwater crest for test series BI_2	77
Figure 6.3 Waterflow in seaside direction for a wide crested breakwater.....	78
Figure 6.4 Water cushion between spilling breaker (from the foreshore) and breakwater crest, seaside slope.....	79
Figure 6.5 Collapsing breaker (test DI_4_100).....	80
Figure 6.6 Overtopping wave (the white lines show the path of the overtopping wave and the seaside slope).....	80
Figure 6.7 Overtopping wave, the forming of two in opposite propagating waves	81
Figure 6.8 Hydraulic conditions at which initial settlements occur	83
Figure 6.9 Top view reference breakwater with representation of settlements	84
Figure 6.10 Fractured armour layer for emerged breakwater at transition of the crest to the seaside slope (test DI_4_160)	86
Figure 6.11 Enlarged white boxed area in Figure 6.10.....	86

Figure 6.12 Displacement crest section, initial situation and situation after test with 153% Hd, the white lines are reference lines	88
Figure 6.13 Displacement Xbloc crest elements for different moments in time	90
Figure 6.14 Number of displaced armour units in seaside direction for breakwaters at which failure occurred (10 displaced armour units)	91
Figure 6.15 Displacement Xbloc element at the seaside slope for different moment in time.....	93
Figure 7.1 Test results rocking armour units, Total breakwater	97
Figure 7.2 Test results rocking armour units, Seaside slope.....	98
Figure 7.3 Test results rocking armour units, Crest	98
Figure 7.4 Number of rocking armour units, reference test series (s=2%), total breakwater	101
Figure 7.5 Number of rocking armour units, reference test series (s=2%), seaside slope	101
Figure 7.6 Number of rocking armour units, reference reference test series (s=2%), crest	101
Figure 7.7 Number of rocking armour units, reference reference test series (s=4%), total breakwater	103
Figure 7.8 Number of rocking armour units, reference test series (s=4%), seaside slope	103
Figure 7.9 Number of rocking armour units, reference test series (s=4%), crest	103
Figure 7.10 Number of rocking armour units, reference test series, all breakwater sections.....	104
Figure 7.11 Number of rocking armour units small crested breakwaters, all 2% test series, all breakwater sections.....	105
Figure 7.12 Number of rocking armour units small crested breakwaters, all 2% test series, seaside slope	106
Figure 7.13 Number of rocking armour units small crested breakwaters, all 2% test series, crest.....	106
Figure 7.14 Number of rocking armour units wide crested breakwaters, all 2% test series, all breakwater sections.....	107
Figure 7.15 Number of rocking armour units wide crested breakwaters, all 2% test series, all breakwater sections.....	107
Figure 7.16 Number of rocking armour units wide crested breakwaters, all 2% test series, all breakwater sections.....	108
Figure 7.17 Number of rocking armour units, all 2% test series, all breakwater sections.....	108
Figure 7.18 Number of rocking armour units, all 2% test series, all breakwater sections.....	109
Figure 7.19 Number of rocking armour units, all 2% test series, all breakwater sections.....	110
Figure 7.20 Number of rocking armour units, all 2% test series, all breakwater sections.....	110
Figure 7.21 Number of rocking armour units, all 2% test series, all breakwater sections.....	111
Figure 7.22 Number of rocking armour units, all 2% test series, all breakwater sections.....	111
Figure 7.23 Rocking armour units, total breakwater, s=2%	114
Figure 7.24 Rocking armour units, seaside slope, s=2%	114
Figure 7.25 Rocking armour units, crest, s=2%	114
Figure 7.26 Damage ratios for the different breakwater sections, s=2%.....	115

Figure 7.27 Rocking armour units, total wide crested breakwater, $s=2\%$	117
Figure 7.28 Rocking armour units, seaside slope wide crested breakwaters, $s=2\%$	117
Figure 7.29 Rocking armour units, crest wide crested breakwater, $s=2\%$	117
Figure 7.30 Damage ratios for the different breakwater sections, $s=2\%$	118
Figure 7.31 Rocking armour units, total breakwater, $s=4\%$	120
Figure 7.32 Rocking armour units, seaside slope, $s=4\%$	120
Figure 7.33 Rocking armour units, crest, $s=4\%$	120
Figure 7.34 Damage ratios for the different breakwater sections, $s=4\%$	121
Figure 7.35 Rocking armour units, total wide crested breakwater, $s=4\%$	123
Figure 7.36 Rocking armour units, seaside slope wide crested breakwater, $s=4\%$	123
Figure 7.37 Rocking armour units, crest wide crested breakwater, $s=4\%$	123
Figure 7.38 Damage ratios for the different breakwater sections, $s=4\%$	124
Figure 7.39 Total number of rocking armour units, small and wide crested breakwater, $s=2\%$	128
Figure 7.40 Rocking armour units at seaside slope, small and wide crested breakwater, $s=2\%$	128
Figure 7.41 Rocking armour units at seaside slope, small and wide crested breakwater, $s=2\%$	128
Figure 7.42 Total number of rocking armour units, small and wide crested breakwater, $s=2\%$	130
Figure 7.43 Rocking armour units at seaside slope, small and wide crested breakwater, $s=4\%$	130
Figure 7.44 Rocking armour units at crest, small and wide crested breakwater, $s=4\%$	130
Figure 7.45 Influence wave steepness on rocking armour units, small crested breakwaters, total breakwater,.....	133
Figure 7.46 Influence wave steepness on rocking armour units, small crested breakwater, seaside slope section	133
Figure 7.47 Influence wave steepness on rocking armour units, small crested breakwaters, crest section	133
Figure 7.48 Influence wave steepness on rocking armour units, wide crested breakwaters, total breakwater.....	135
Figure 7.49 Influence wave steepness on rocking armour units, small crested breakwaters, seaside slope section	135
Figure 7.50 Influence wave steepness on rocking armour units, wide crested breakwaters, crest section	135
Figure 7.51 Location of rocking elements for reference test series (CI), wave steepness 2%	136
Figure 7.52 Location of rocking elements for reference test series (CI), wave steepness 4%	136
Figure 8.1 Results performed tests, Start of damage.....	138
Figure 8.2 Results performed tests, failure	139
Figure 8.3 Number of displaced armour units, reference test series ($s=2\%$), total breakwater	142
Figure 8.4 Number of displaced armour units, reference test series ($s=2\%$), seaside slope.....	142
Figure 8.5 Number of displaced armour units, reference test series ($s=2\%$), crest.....	142
Figure 8.6 Number of displaced armour units, reference test series ($s=4\%$), total breakwater	144

Figure 8.7 Number of displaced armour units, reference test series ($s=4\%$), seaside slope	144
Figure 8.8 Number of displaced armour units, reference test series ($s=4\%$), crest	144
Figure 8.9 Number of displaced armour units, reference test series, all breakwater cross section	145
Figure 8.10 Number of displaced armour units small crested breakwaters, all 2% wave steepness test series, all breakwater sections	146
Figure 8.11 Number of displaced armour units small crested breakwaters, all 2% wave steepness test series, seaside slope	147
Figure 8.12 Number of displaced armour units small crested breakwaters, all 2% wave steepness test series, crest	147
Figure 8.13 Number of displaced armour units wide crested breakwaters, all 2% wave steepness test series, crest	148
Figure 8.14 Number of displaced armour units wide crested breakwaters, all 2% wave steepness test series, crest	149
Figure 8.15 Number of displaced armour units wide crested breakwaters, all 2% wave steepness test series, crest	149
Figure 8.16 Number of displaced armour units wide crested breakwaters, all 2% wave steepness test series, total breakwater	150
Figure 8.17 Number of displaced armour units wide crested breakwaters, all 2% wave steepness test series, crest	150
Figure 8.18 Number of displaced armour units wide crested breakwaters, all 2% wave steepness test series, crest	151
Figure 8.19 Number of displaced armour units wide crested breakwaters, all 2% wave steepness test series, total breakwater	152
Figure 8.20 Number of displaced armour units wide crested breakwaters, all 2% wave steepness test series, seaside slope	152
Figure 8.21 Number of displaced armour units wide crested breakwaters, all 2% wave steepness test series, crest	152
Figure 8.22 Stability at different crest freeboards, total breakwater, small crest width ($s=2\%$)	155
Figure 8.23 Stability at different crest freeboards, seaside slope, small crest width ($s=2\%$)	155
Figure 8.24 Stability at different crest freeboards, crest, small crest width ($s=2\%$)	155
Figure 8.25 Stability at different crest freeboards, total breakwater, small crest width ($s=2\%$)	157
Figure 8.26 Stability at different crest freeboards, seaside slope, small crest width ($s=2\%$)	157
Figure 8.27 Stability at different crest freeboards, crest, small crest width ($s=2\%$)	157
Figure 8.28 Stability at different crest freeboards, total breakwater, small crest width ($s=4\%$)	159
Figure 8.29 Stability at different crest freeboards, seaside slope, small crest width ($s=4\%$)	159
Figure 8.30 Stability at different crest freeboards, crest, small crest width ($s=4\%$)	159
Figure 8.31 Stability small versus wide crested breakwater, total stability, ($s=2\%$)	162
Figure 8.32 Stability small versus wide crested breakwater, seaside slope, ($s=2\%$)	162

Figure 8.33 Stability small versus wide crested breakwater, crest, ($s=2\%$). .. 162

Figure 8.34 Influence wave steepness on the displacement of armour units, small crested breakwater, total breakwater. 164

Figure 8.35 Influence wave steepness on the displacement of armour units, small crested breakwater, seaside slope. 164

Figure 8.36 Influence wave steepness on the displacement of armour units, small crested breakwater, crest. 164

Figure 8.37 Location of displaced armour units for reference test series (CI), wave steepness 2%. 165

Figure 8.38 Location of displaced armour units for reference test series (CI), wave steepness 4%. 166

Figure 9.1 Comparison rocking and displaced armour units, total breakwater, $s=2\%$ 169

Figure 9.2 Comparison rocking and displaced armour units, seaside slope, $s=2\%$ 169

Figure 9.3 Comparison rocking and displaced armour units, crest, $s=2\%$ 169

Figure 9.4 Influence wave steepness on the displacement of armour units, small crested breakwater, crest. 171

Figure 9.5 Influence wave steepness on the displacement of armour units, small crested breakwater, crest. 171

Figure 9.6 Influence wave steepness on the displacement of armour units, small crested breakwater, crest. 171

Figure 9.7 Influence wave steepness on the displacement of armour units, small crested breakwater, crest. 173

Figure 9.8 Influence wave steepness on the displacement of armour units, small crested breakwater, crest. 173

Figure 9.9 Influence wave steepness on the displacement of armour units, small crested breakwater, crest. 173

Figure 10.1 Measured wave transmission in relation to VAN DER MEER et al. (1994). 175

Figure 10.2 Wave spectra (for tests CI_2_1 and DI_4), incident at foreshore (left graph) and transmitted spectra behind the breakwater (right graph). 175

Figure 0.1 Locations for calculation pressure gradient and characteristic velocity in the core 194

LIST OF TABLES

Table 1-1 Design paramters breakwater Newbiggin	2
Table 3-1 Design stability formulas of the different rubble mount breakwater sections.....	37
Table 4-1 Development concrete armour units.....	44
Table 5-1 Varying paramters (cross section)	58
Table 5-2 Nummerical paramters, overall cross section.....	59
Table 5-3 Parameters model and prototype Xbloc	62
Table 5-4 Programme test series	66
Table 5-5 Programme test series	68
Table 5-6 Performed tests	68
Table 5-7 Mean theoretical relative placement density	70
Table 5-8 Clipped wave energy [%].....	71
Table 5-9 Measured mean (of all test series) incident waveheight and the target wave height	72
Table 5-10 Measured mean wave period and target wave period.....	73

APPENDIX A

Interlocking

Results Price [1979]

Unit	Average value	Standard deviation
	F/W	of F/W
Stabits (brick wall ¹)	6.28	0.46
Stabits (double layer ¹)	1.75	0.6
Tetrapods	1.53	0.51
Dolos	3.62	1.64
Stone	2.14	0.9

¹ The brick wall and double layer are different placement modes of Stabits.

APPENDIX B

Stability parameters

Mobility Parameter

$$MP = \frac{U^2}{(\Delta \cdot g \cdot D_{n50})}$$

In which U is the horizontal velocity.

Shields Parameter

$$SP = \frac{\tau_{cw}}{(\rho_w \cdot g \cdot \Delta \cdot D_{n50})}$$

In which τ_{cw} is the shear stress over the structures surface that can be expressed in terms of velocity near the structures surface:

$$\tau_{cw} = 0.25 \cdot \rho_w \cdot f_w \cdot U^2$$

Where f_w is the wave friction coefficient and can be expressed by:

$$f_w = \exp \left[-6 + 5.2 \cdot \left(\frac{A_c}{k_s} \right)^{-0.19} \right] \quad \text{for } (A_c/k_s) > 1.57$$

$$f_w = 0.3 \quad \text{for } (A_c/k_s) \leq 1.57$$

In which k_s is the bed roughness, that may be expressed in term of the diameter of the stones, $k_s = 2 \cdot D_{90}$ and A_c is the horizontal orbital amplitude at the crest level.

Morison's Drag Force Parameter

$$FDN = 0.5 \cdot C_d \cdot \rho_w \cdot D_{n50}^2 \cdot U \cdot |U| + \rho_w \cdot C_m \cdot D_{n50}^3 \cdot \frac{dU}{dt}$$

In which C_d and C_m are, respectively the drag and inertia coefficients.

Morison's Lift Force Parameter

$$FLN = 0.5 \cdot C_L \cdot \rho_w \cdot D_{n50}^2 \cdot U \cdot |U|$$

In which C_L is the lift coefficient.

Stability formula for rubble-mound submerged breakwaters

The Mobility parameter describes the damage best over the cross section of a submerged breakwater. A breakwater will be considered submerged when:

$$\frac{H_s}{-R_c} < 0.8$$

The observed damage is correlated with the maximum values of the Mobility parameter along the submerged cross-section. The Mobility Parameter is formulated with the maximum velocity value that occurs on the landward edge of the crest, U_{\max} .

$$MP = \frac{U_{\max}^2}{(\Delta \cdot g \cdot D_{n50})} \quad (9.4)$$

Where U_{\max} is the maximum orbital velocity over the landward crest edge. An improvement of the relationship between the MP_{\max} and the damage parameter could be obtained if MP is substituted by MP_{crit} , defined in formula (9.5) as a function between the maximum velocity in the landward edge of the crest and the velocity for the threshold of rubble movement $U_{\max} - U_{\text{crit}}$.

$$MP_{\text{crit}} = \frac{(U_{\max} - U_{\text{crit}})^2}{(\Delta \cdot g \cdot D_{50})} \quad \text{if } U_{\max} - U_{\text{crit}} > 0 \quad (9.5)$$

$$MP_{\text{crit}} = 0 \quad \text{otherwise}$$

Where the velocity for movement of threshold, U_{crit} of the armour units is given as:

$$U_{\text{crit}} = \left(\frac{2 \cdot (\rho_s - \rho_w) \cdot g \cdot D_{50} \cdot \Psi_{\text{crit}}}{\rho_w \cdot f_w} \right)^{0.5} \quad (9.6)$$

In wich:

$$\Psi_{\text{crit}} = \frac{0.24}{D^*} + 0.055 \cdot (1 - e^{-0.02 \cdot D^*}) \quad (9.7)$$

$$D^* = 25 \cdot D_{50} \quad [\text{mm}] \quad (9.8)$$

$$f_w = \exp \left(-6 + 5.2 \cdot \left(\frac{A_c}{k_s} \right)^{-0.19} \right) \quad \text{for } \left(\frac{A_c}{k_s} \right) > 1.57 \quad (9.9)$$

$$f_w = 0.3 \quad \text{for } \left(\frac{A_c}{k_s} \right) \leq 1.57$$

The fit between the MP_{crit} and the damage parameter ($R^2 = 0.7$) is given by:

$$S = 3.2 \cdot MP_{\text{crit}}^{1.45} - 0.30 \quad (9.10)$$

Expression (9.10) requires the knowledge of the maximum velocity during the wave cycle on the structures landward edge, U_{\max} , that depends on the wave height, wave period, structures freeboard and crest width, being the most relevant the wave height and the freeboard, so it will be possible to express the U_{\max} in terms of relative freeboard H_{50}/R_c . For that reason, expression (9.10) is converted in terms of the parameter, c , given by:

$$c = \frac{U_{\max}}{U_{\text{crit}}} \quad (9.11)$$

Using the parameter c , expression (9.10) transform to:

$$MP_{\text{crit}} = \frac{((c-1) \cdot U_{\text{crit}})^2}{(\Delta \cdot g \cdot D_{50})} \quad (9.12)$$

Using the numerical model, the value of c in terms of H_{50}/R_c can be determined. The value of c increase monotonically with H_{50}/R_c . The best fit expression for c is given by:

$$c = \frac{U_{max}}{U_{crit}} = 0.73 \cdot \ln\left(\frac{-H_{50}}{R_c}\right) + 2.3 \quad (9.13)$$

The formulas (3.38), (3.39) and (3.40) are applicable in the limits of the experimental range, given approximately by:

$$0.3 \leq \frac{-H_{50}}{R_c} \leq 0.9$$

The formula has been applied to the existing data base which exists in total out of 115 regular and irregular laboratory tests and 15 prototype cases. The following conclusions can be drawn:

- for low damage levels ($S < 1$) formula (9.10) slightly overestimates the damage while for high damage levels ($S > 7$), formula (9.10) underestimates S ;
- nearly 90% of the cases are inside the band $S_{calculated} = S_{measured} \pm 2.5$;
- The maximum measured damage that after the calculation gives no damage at all lower than $S=2$.

Vidal et al. (2007)

APPENDIX C

First the pore velocity is calculated for the prototype scale. A fictitious scale length factor (N_L) has to be chosen to transfer the model dimensions to prototype scale.

The pressure gradient in prototype is calculated at 6 locations in the breakwater core (see Figure 0.1 **Fout! Verwijzingsbron niet gevonden.**) for 6 different moments in time (from $t=0$ the time is increased to $t=0.5 \cdot T_p$ in steps of $0.1 \cdot T_p$). The pressure gradients can be calculated according to BURCHARTH et al. 1999 as:

$$I_x = -\frac{\pi \cdot H_s}{L'} e^{-\delta \cdot 2 \cdot \pi \cdot x / L'} \cdot \left[\delta \cdot \cos\left(\frac{2 \cdot \pi}{L'} \cdot x + \frac{2 \cdot \pi}{T_p} \cdot t\right) + \sin\left(\frac{2 \cdot \pi}{L'} \cdot x + \frac{2 \cdot \pi}{T_p} \cdot t\right) \right] \quad (3.1)$$

With the pressure gradient known the pore velocity (at 6 locations in the breakwater for 6 different moments in time) in the core can be calculated using the Forchheimer equation given in BURCHARTH AND ANDERSEN 1995:

$$I_x = \alpha \cdot \left(\frac{1-n}{n}\right)^2 \frac{v}{g \cdot d_{50}^2} \cdot \frac{U}{n} + \beta \cdot \frac{1-n}{n} \cdot \frac{1}{g \cdot d_{50}} \cdot \left(\frac{U}{n}\right)^2 \quad (3.2)$$

In which:

δ damping coefficient, $\delta = 0.0141 \cdot \frac{n^{0.5} \cdot L_p^2}{H_s \cdot b}$;

H_s significant wave height [m];

n porosity of the core [-];

b core width [m];

T_p wave period [s];

d_{50} the median sieve size [m];

L' wave length in the core $L' = L/D^{1/2}$ valid for $h/L < 0.5$ [m];

L incident wave length [m];

U pore velocity [m/s];

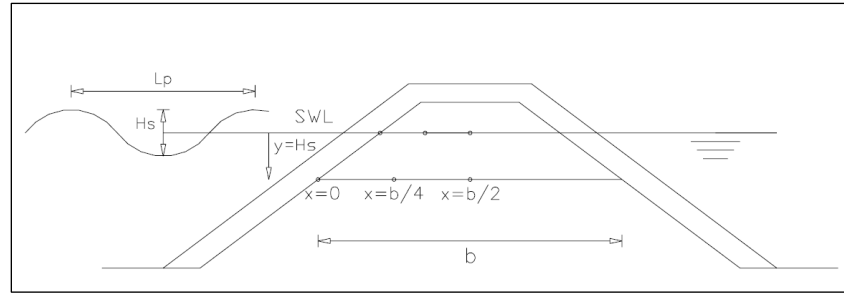
h water depth in front of the breakwater [m].

α, β coefficients depending on the Reynolds number, grain shape and grading, see text below and for values of α and β BURCHARTH *et al.* 1995 [-].

When in the Forchheimer equation (3.2) the coefficients α and β are set to $\alpha \neq 0$ and $\beta = 0$ the Darcy equation is obtained (the viscous term is dominant). The velocities are very small and the second convective inertia term can be neglected. If the velocities are larger, but the flow is still stationary and laminar, the complete Forchheimer equation describes the flow. For larger velocities, turbulence will occur. The inertia terms will for fully turbulent flow completely dominate over the viscous term, $\alpha = 0$, $\beta \neq 0$. If for fully turbulent

flow the Forchheimer equation is used, the linear term is only a fitting term which has no physical meaning.

Figure 0.1 Locations for calculation pressure gradient and characteristic velocity in the core



The time averaged velocity at the 6 locations in the breakwater can be calculated, hereafter the location averaged velocities are calculated with the time averaged velocities. In this manner the characteristic pore velocity in prototype is obtained. This prototype characteristic pore velocity is scaled using Froude scaling to acquire the desirable characteristic pore velocity in model:

$$\bar{U}_m = \bar{U}_p / \sqrt{N_L} \quad (3.3)$$

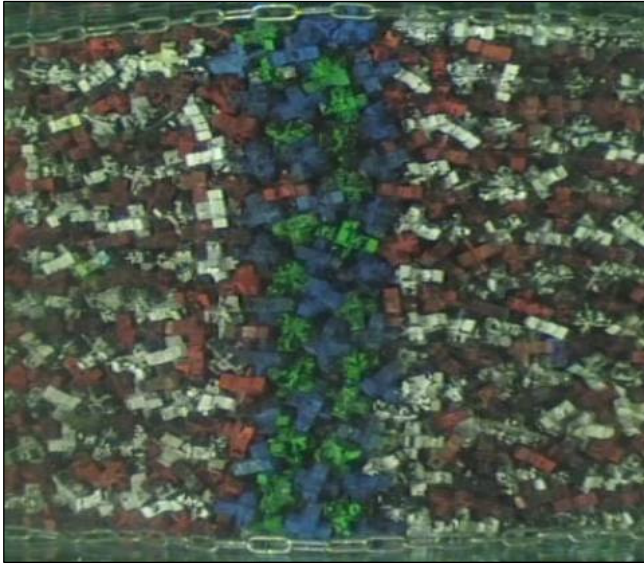
By choosing a value for d_{50} (for the model scale) and following the same procedure as described for the prototype scale the time and place averaged characteristic pore velocity can be determined. This calculated velocity has to be same as the one calculated with equation (3.3). If this is not the case the same procedure has to be repeated until the two calculated characteristic pore velocities are equal, than the median sieve size (d_{50}) is found for the core material in model tests.

After calculating the d_{50} with BURCHARTH et al. 1999 it has to be checked whether geometric scaling leads to a bigger median sieve size. The largest median sieve size has to be used.

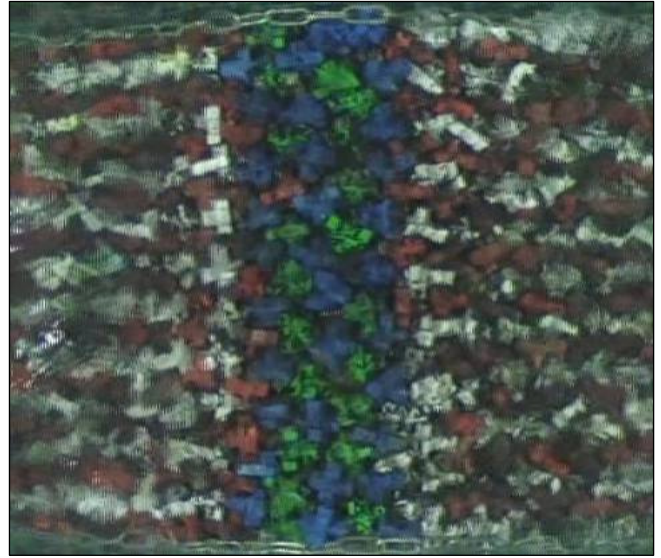
APPENDIX D

AI_2

Start



End

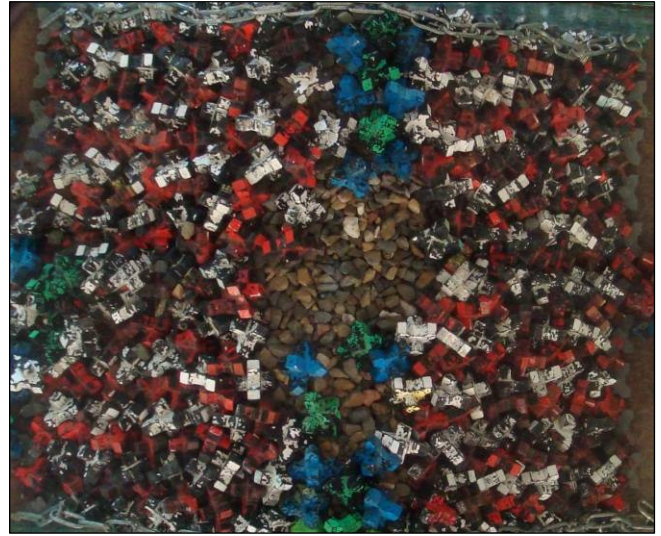


AI_2_1

Start



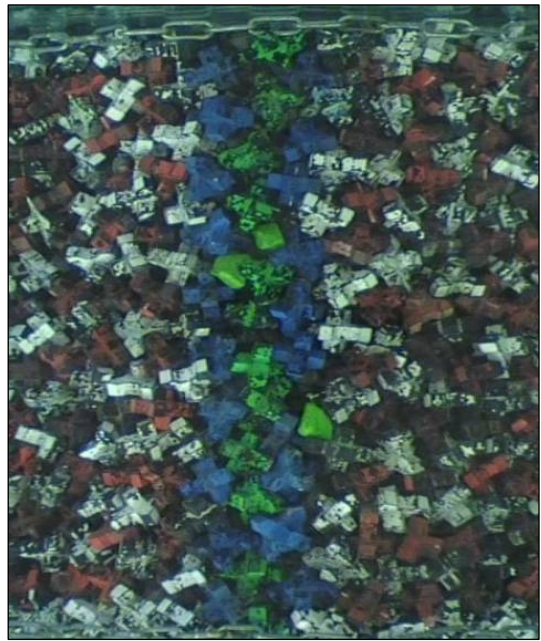
End



AI_4
Start



End

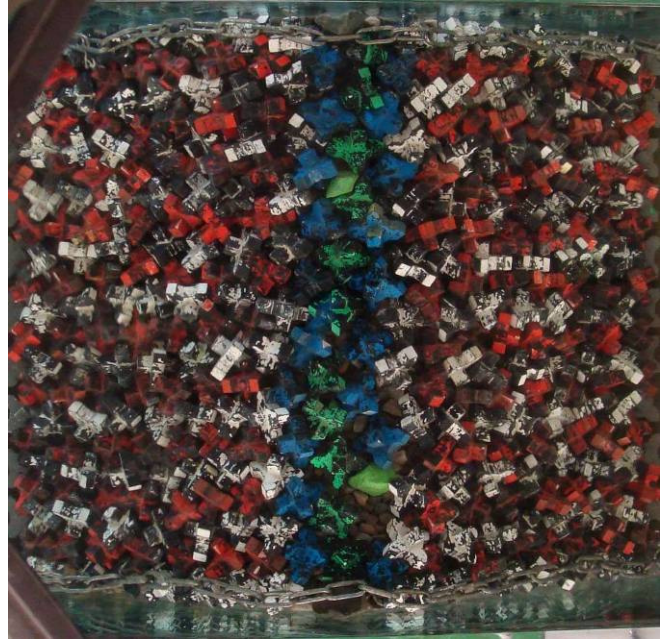


AI_4_1

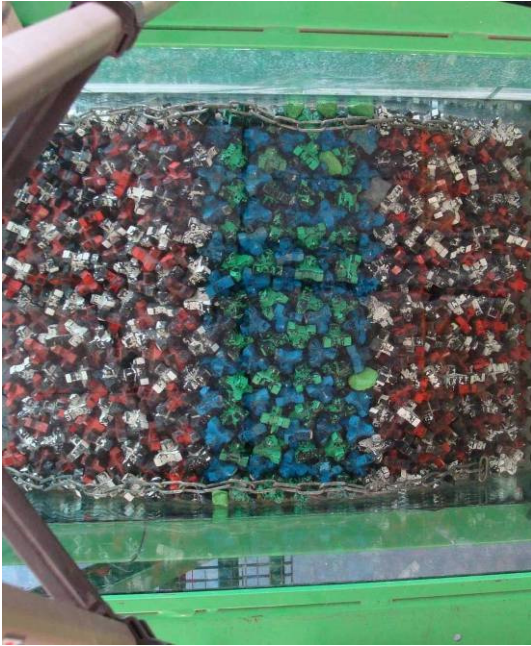
Start



End



AII_2
Start

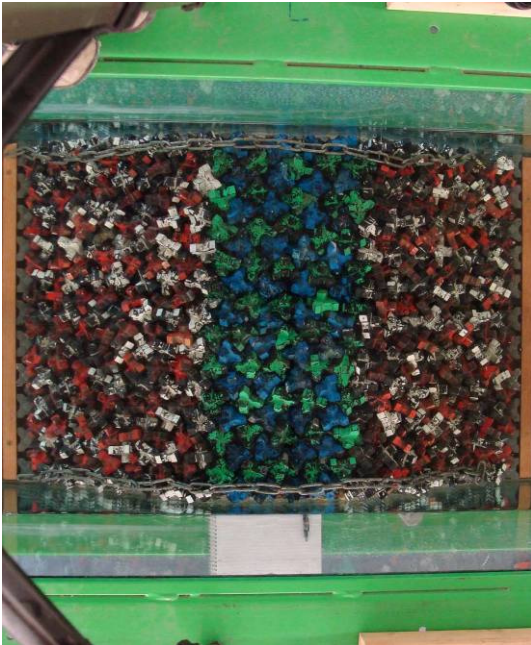


End



AII_2_1

Start

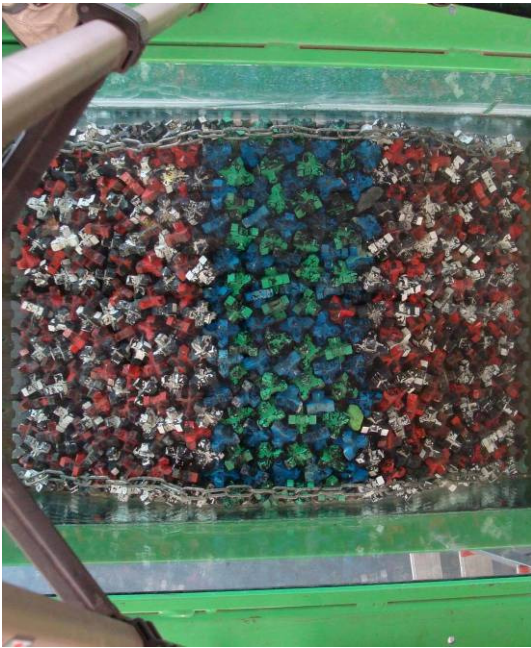


End

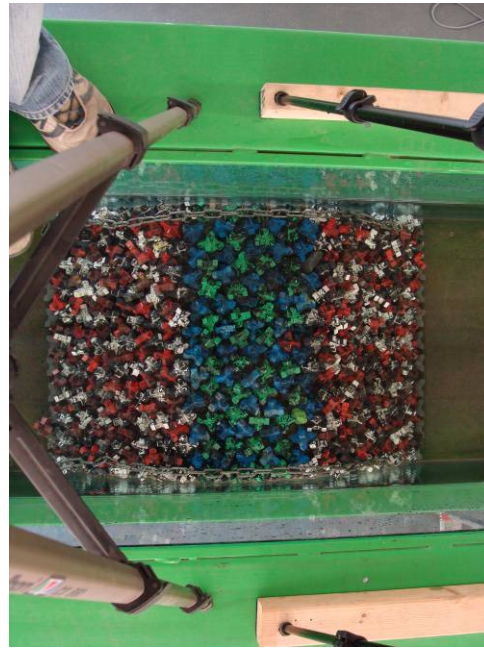


AII_4

Start

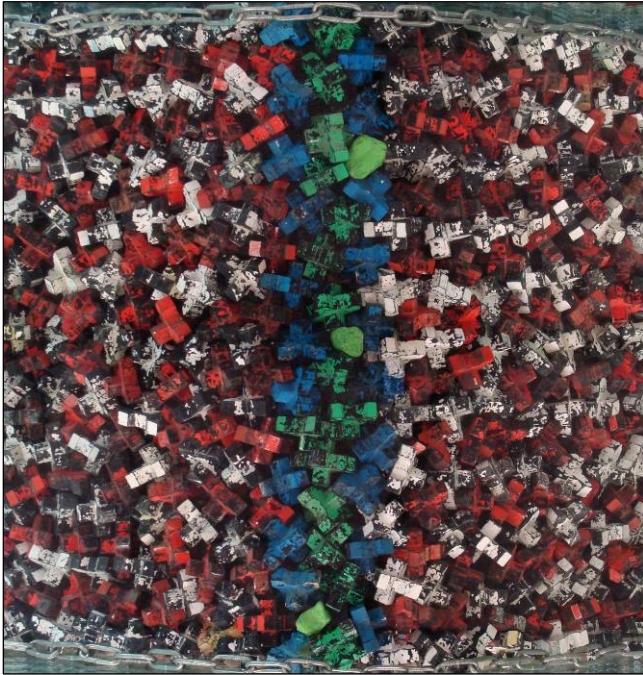


End

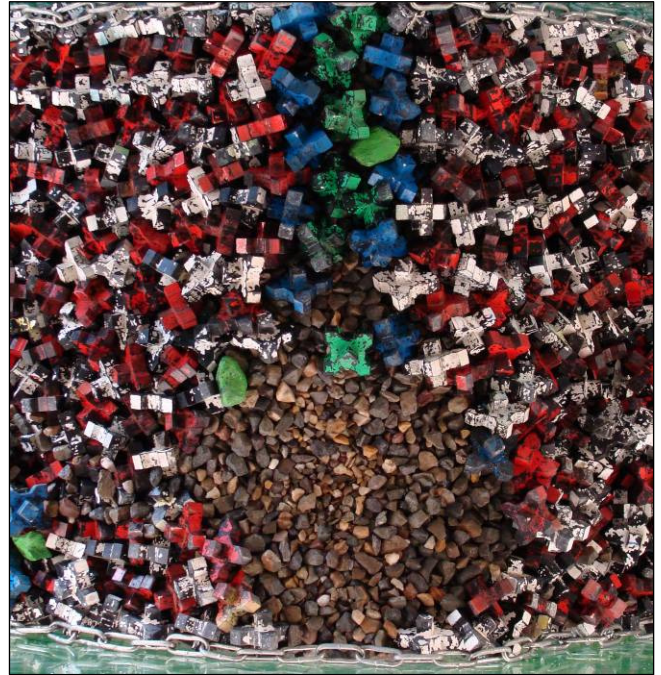


B1_2

Start

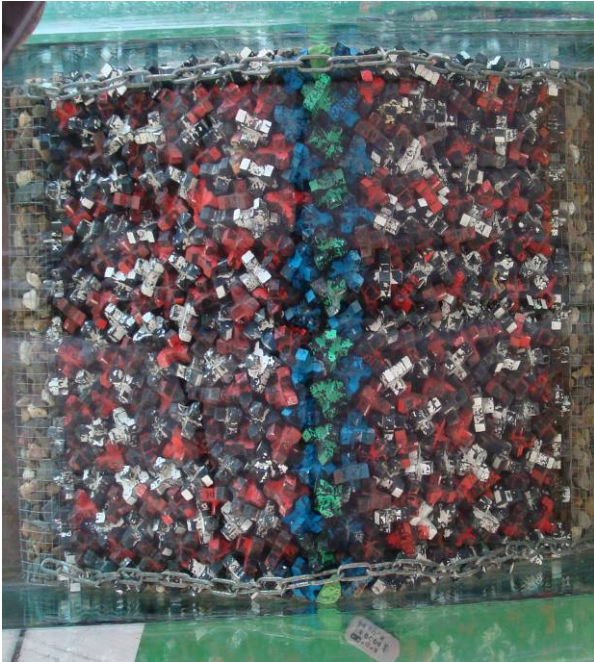


End



B1_2_1

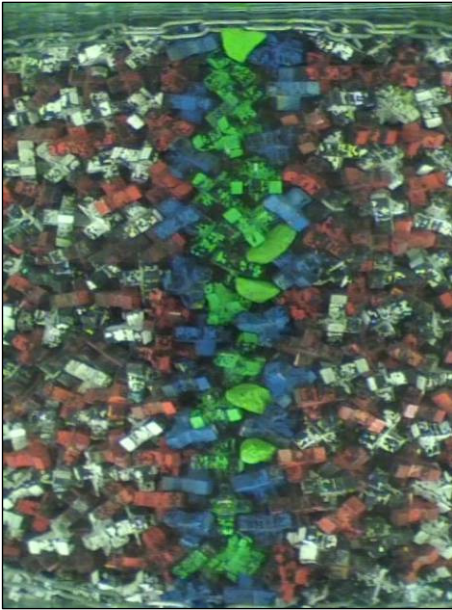
Start



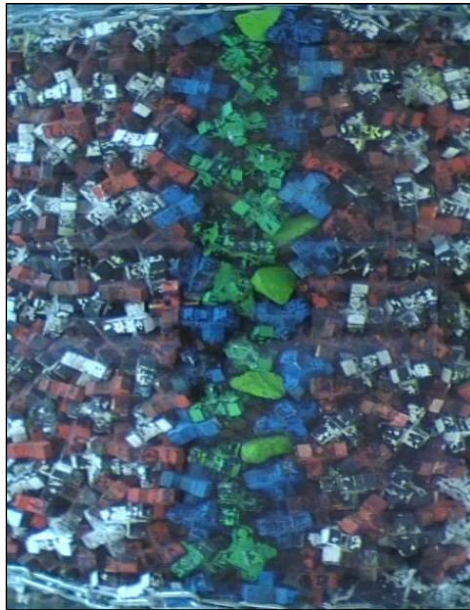
End



BI_4
Start



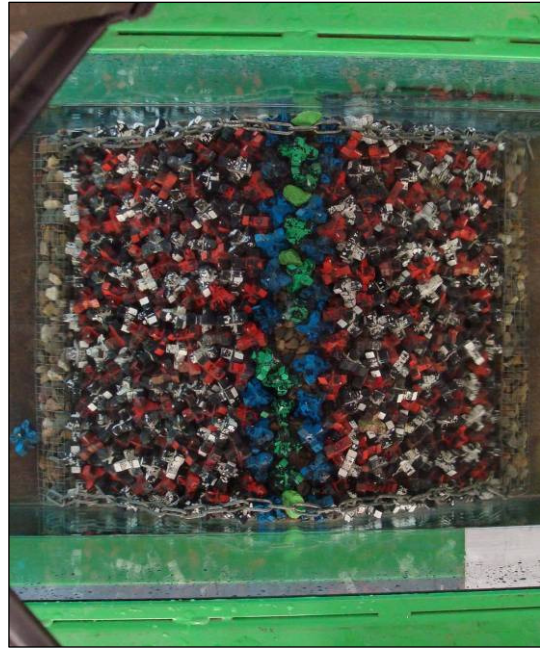
End



BI_4_1
Start



End



CI_2
Start

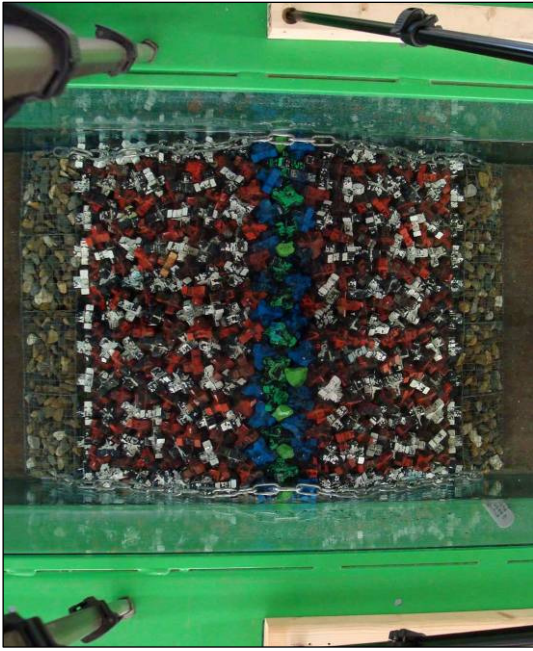


End

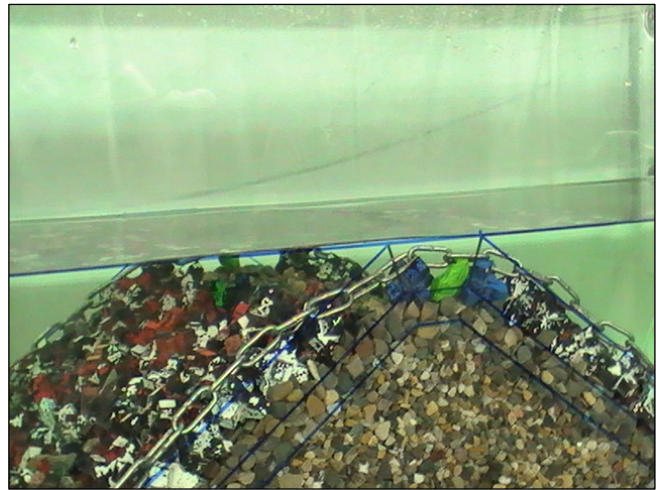
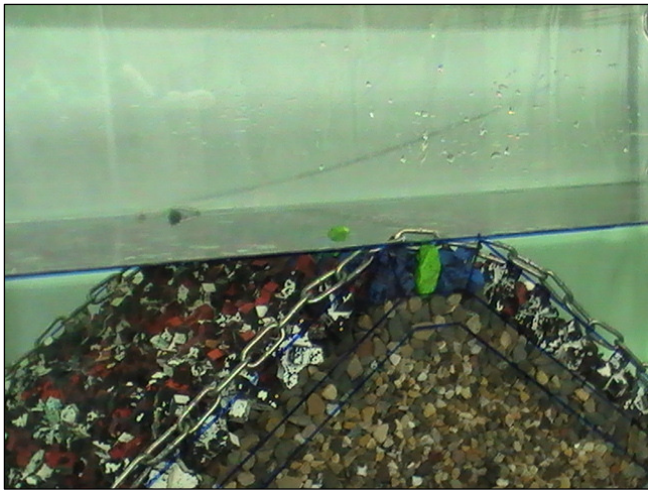
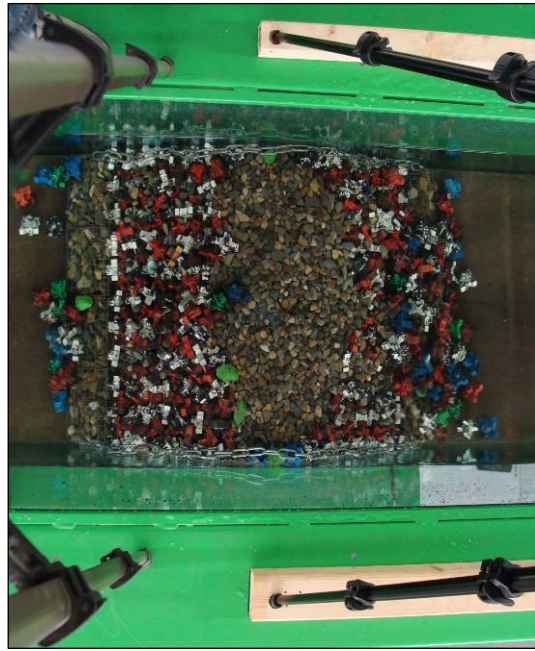


CI_2_1

Start



End



CI_2_2

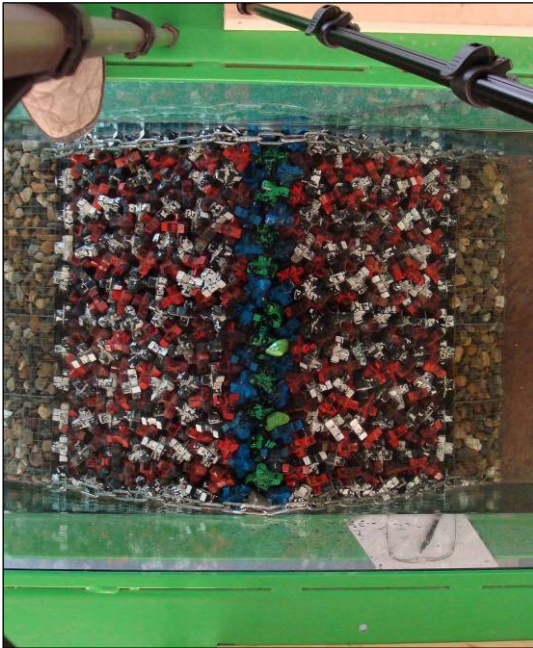
Start



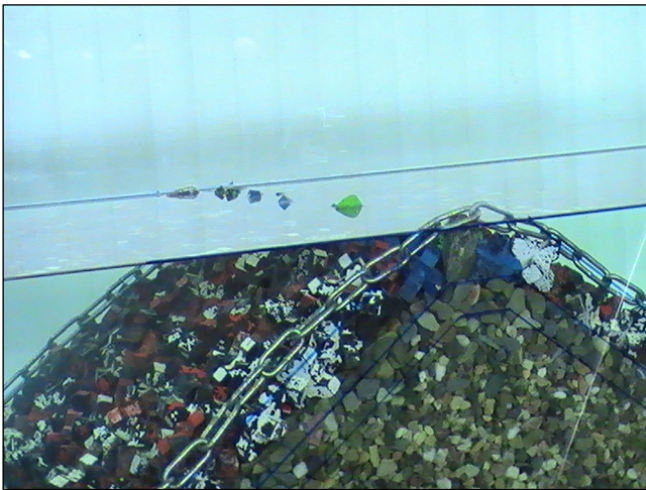
End



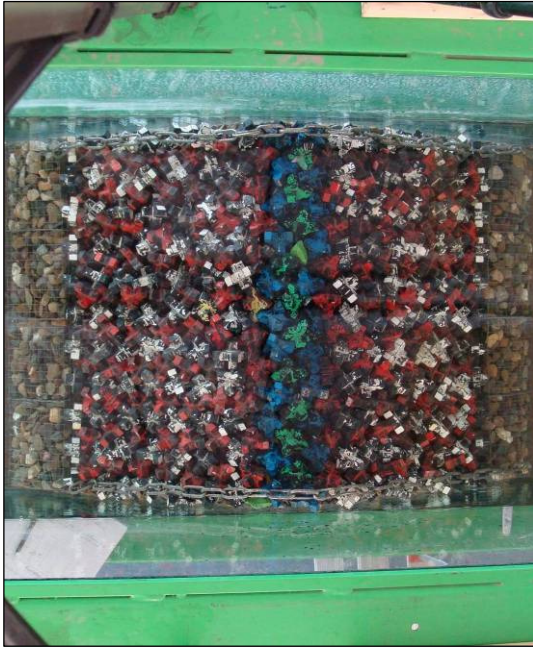
CI_2_3
Start



End



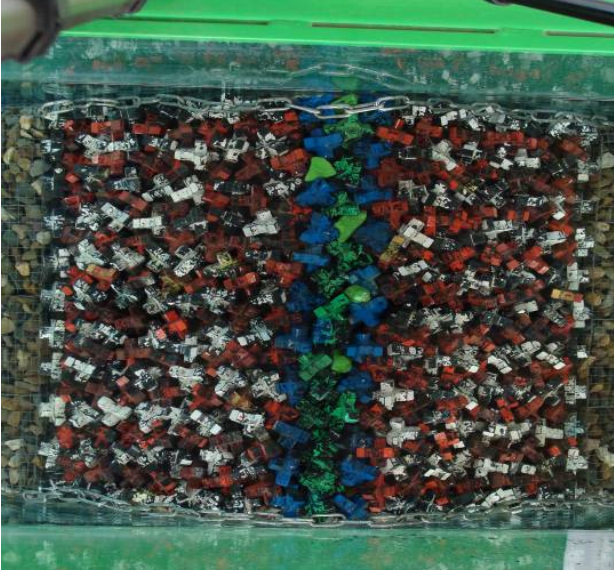
C1_2_4
Start



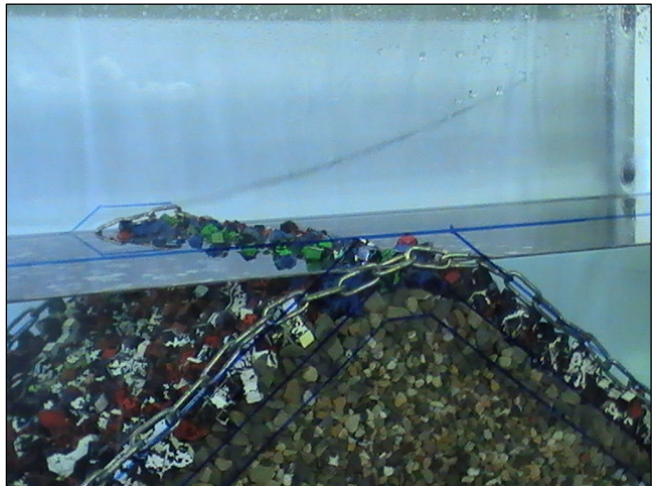
End



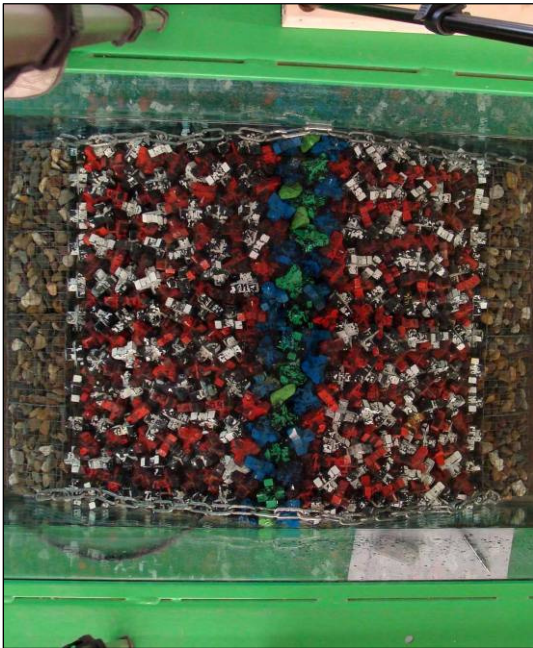
CI_4
Start



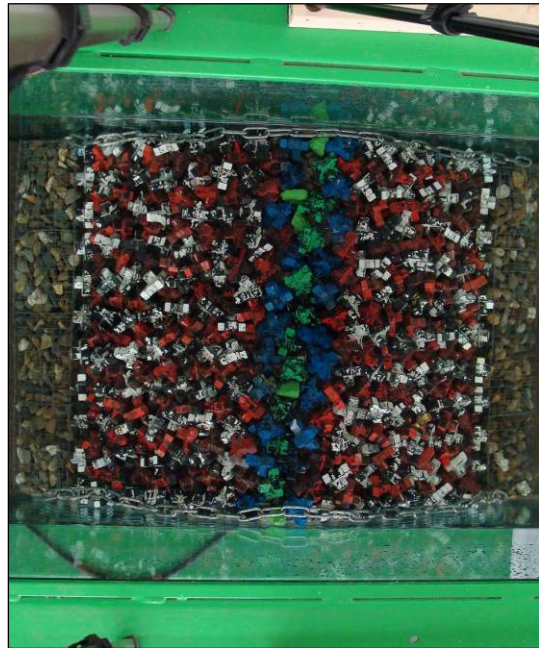
End



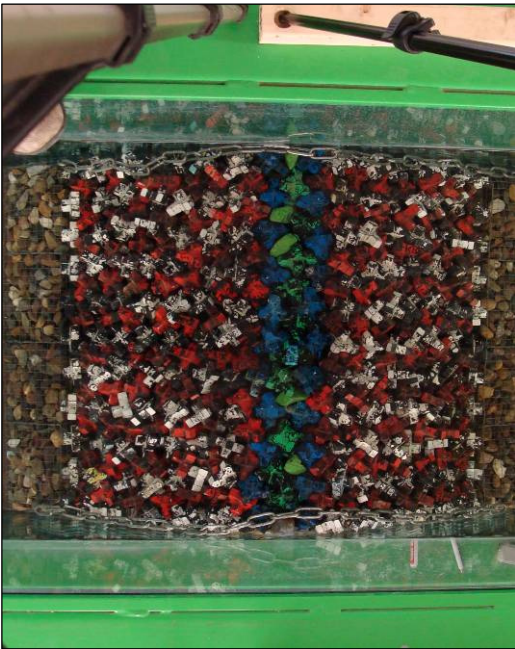
CI_4_1
Start



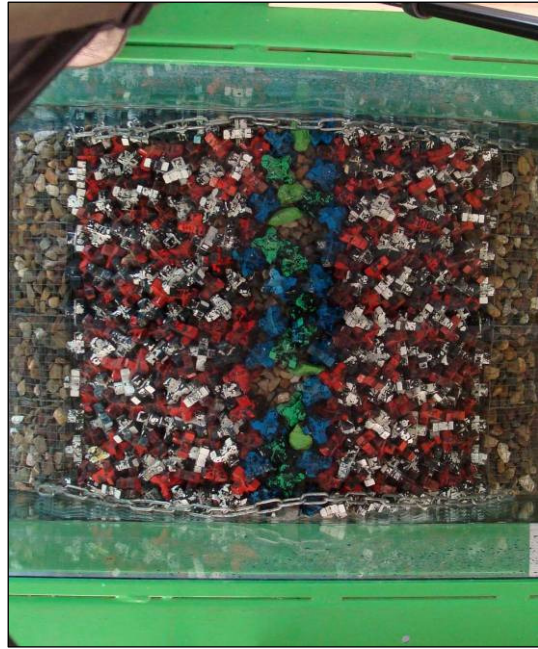
End



CI_4_2
Start

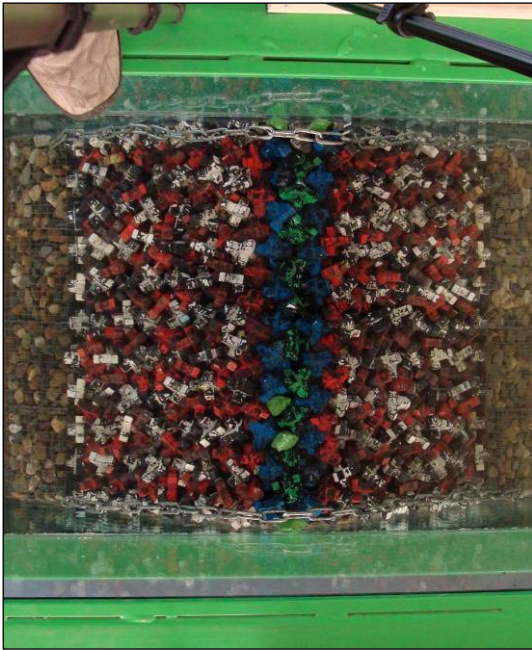


End

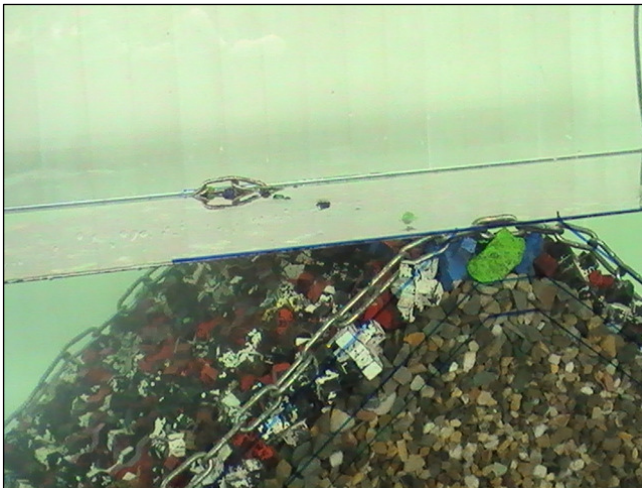


CI_4_3

Start



End

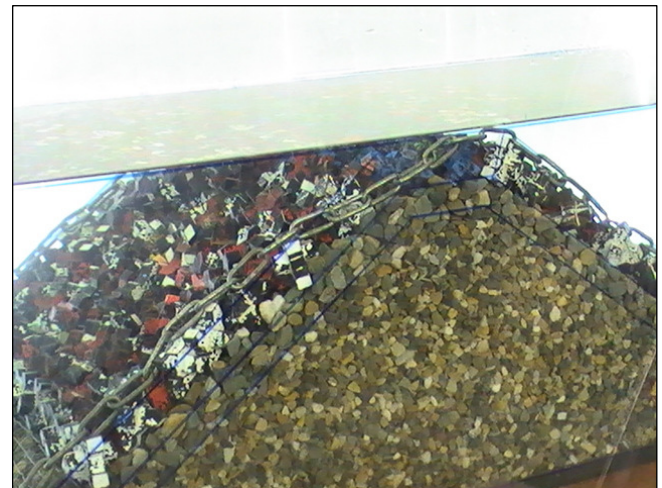
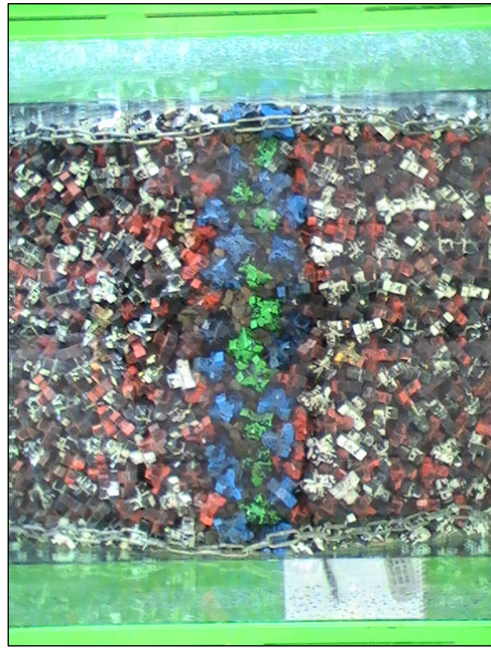


CI_4_4

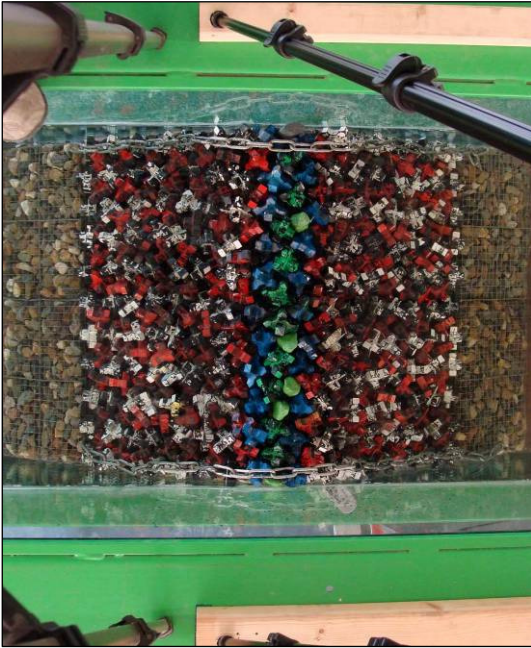
Start



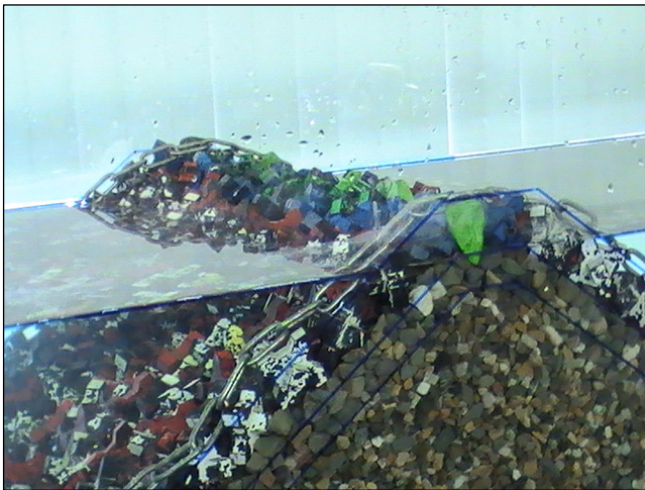
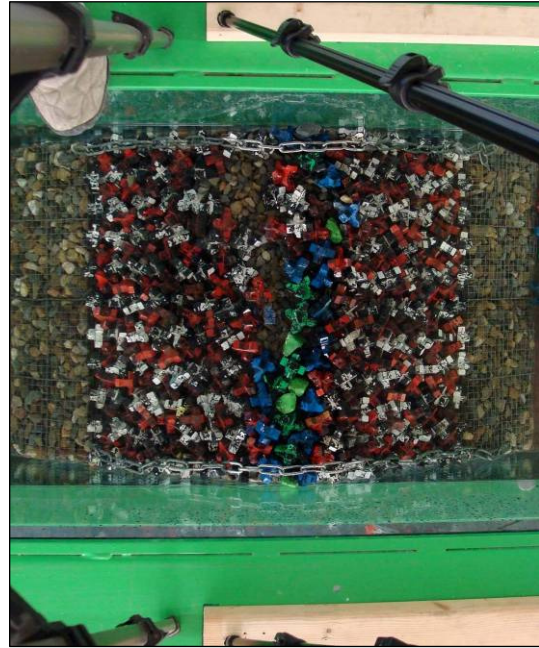
End



DI_2
Start



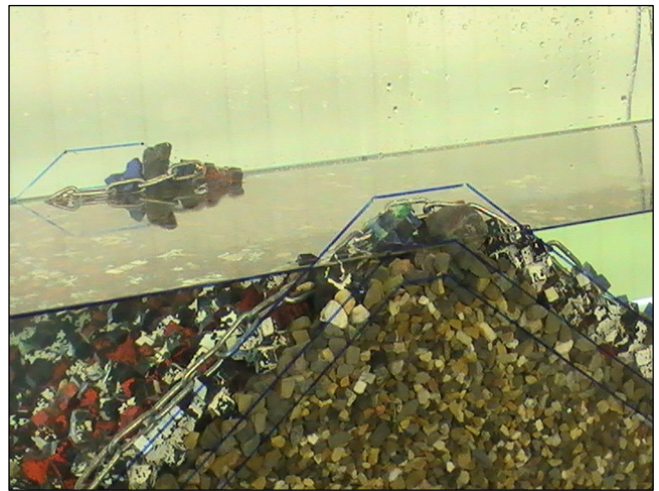
End



DI_4
Start



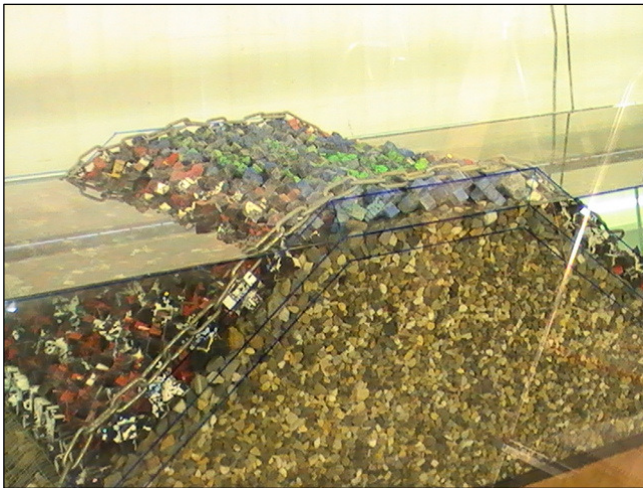
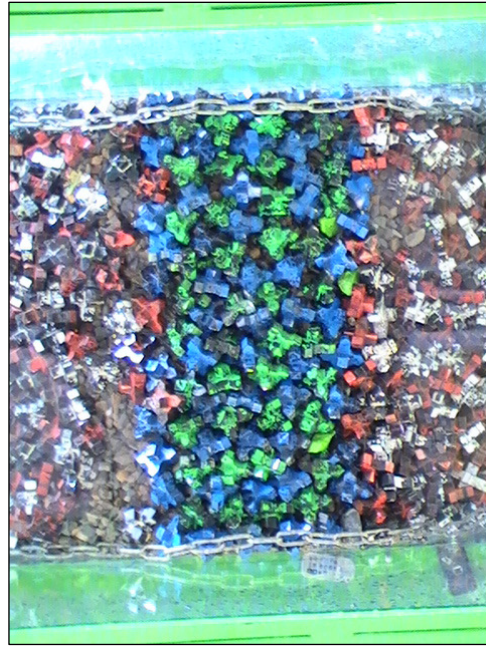
End



DII_2
Start

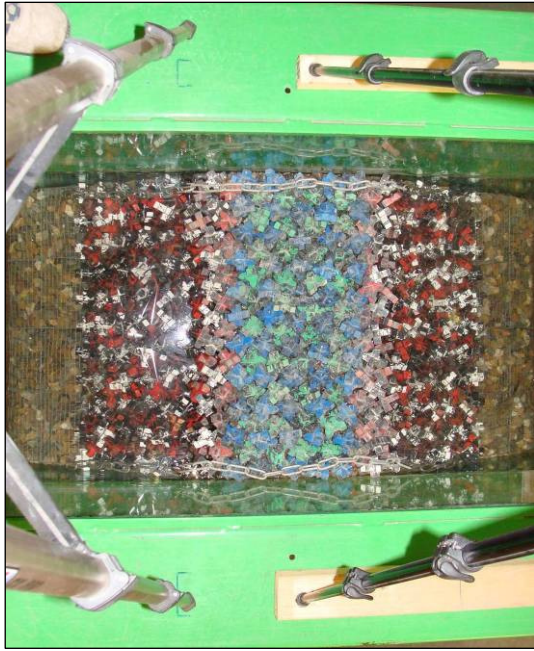


End

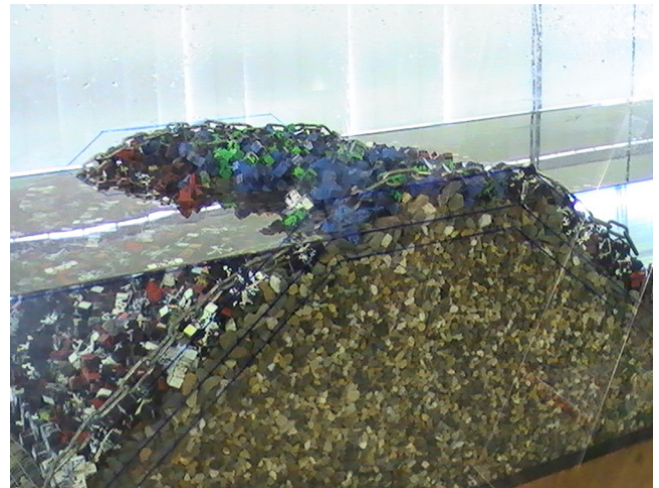
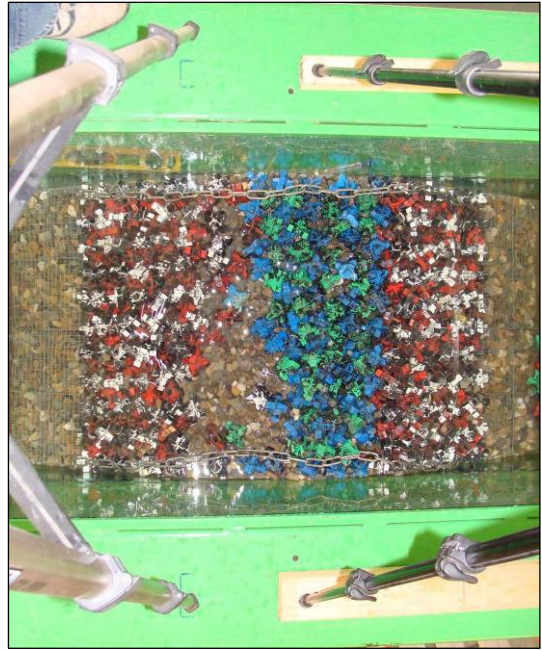


Not present

DII_4
Start



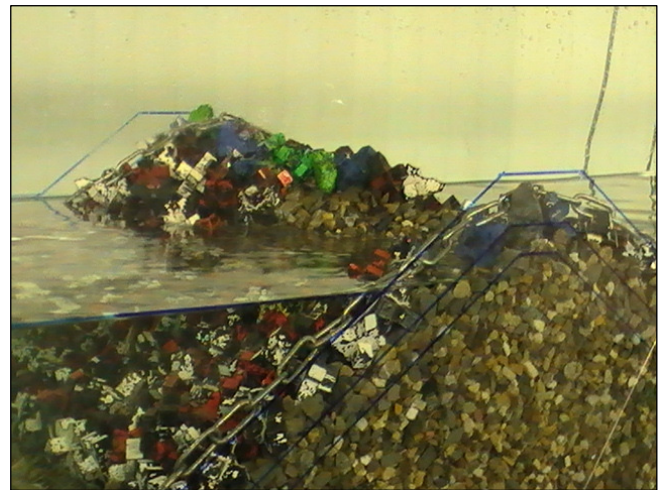
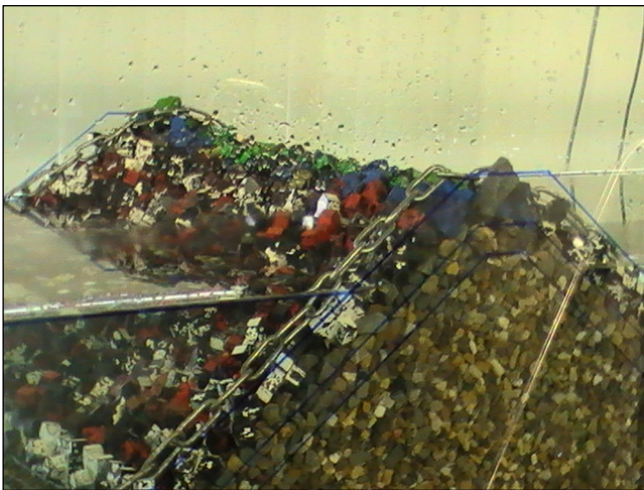
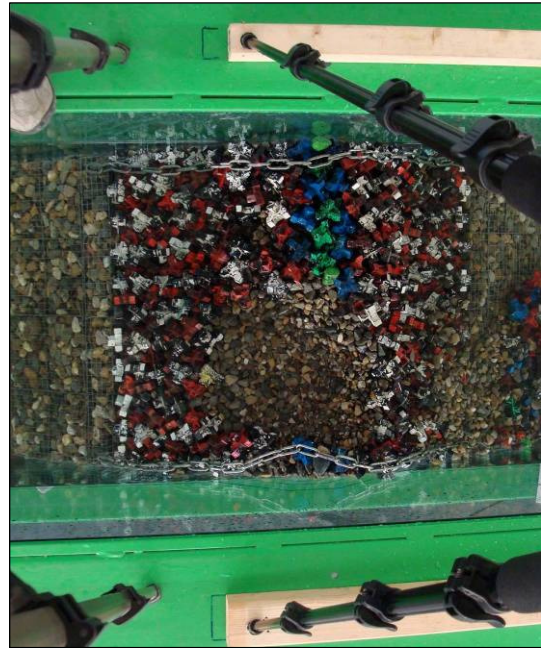
End



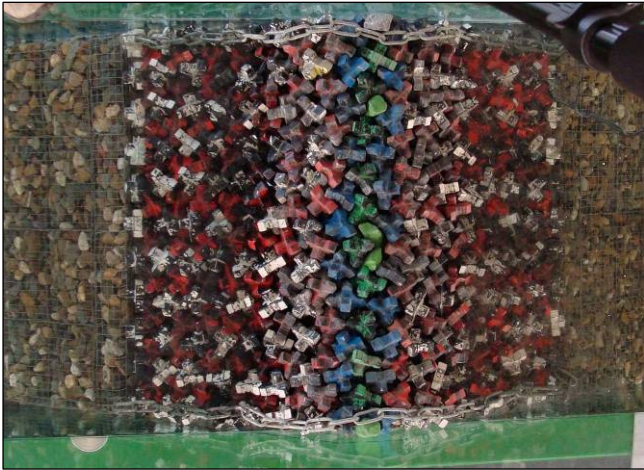
E1_2
Start



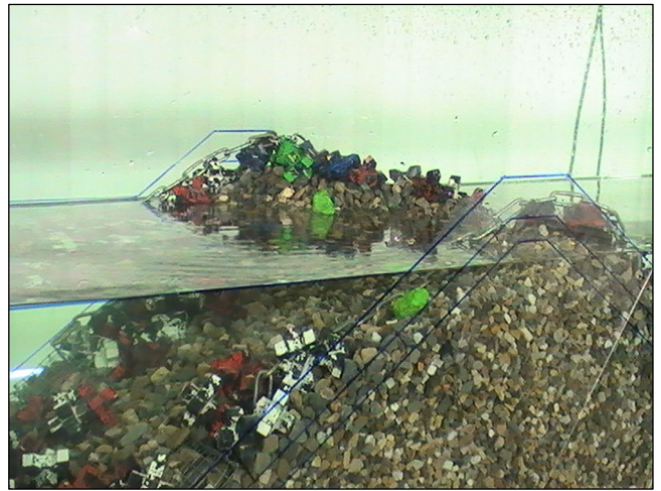
End



EI_4
Start



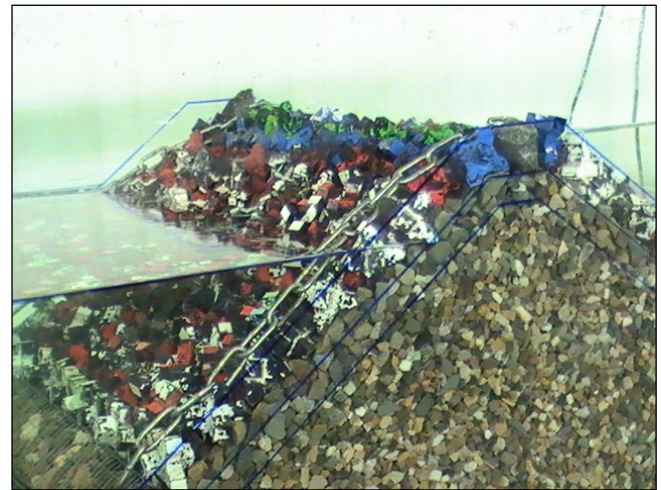
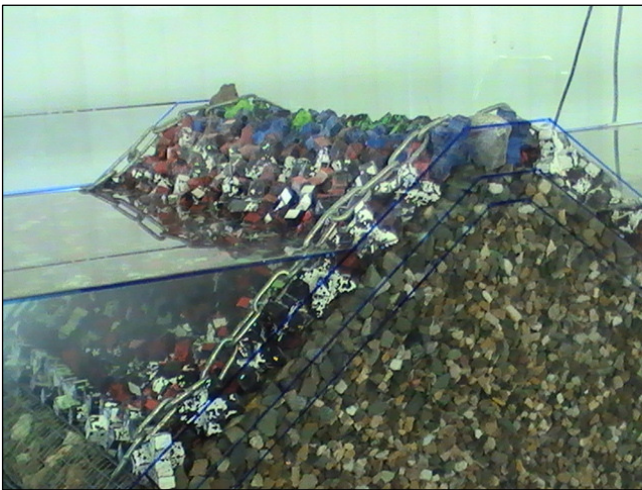
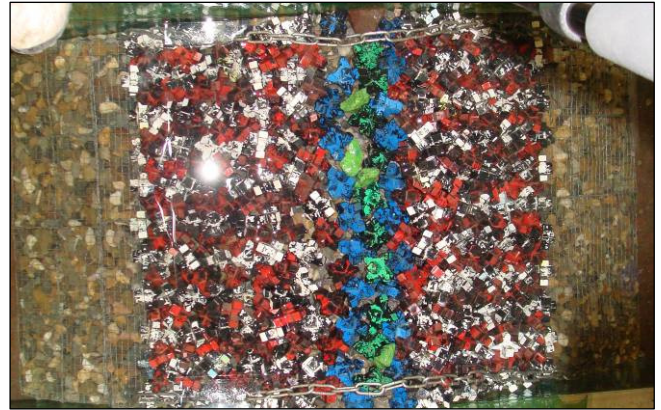
End



EI_4_1
Start



End



Title

Stability of single layer armour units on low-crested structures

APPENDIX E

Run	Incident wave height in front of foreshore			Incident wave height on foreshore			Incident wave height behind structure			Wave transmission	Rocking armour units				Displaced armour units			
	Model		Reflection	Model		Reflection	Model		Reflection	Ct=Ht/Hi	Total	Seaside slope	Crest	Leeside slope	Total	Seaside slope	Crest	Leeside slope
	Hm0,i	Tp		Hm0,i	Tp		Hm0,i	Tp										
[cm]	[s]	[-]	[cm]	[s]	[-]	[cm]	[s]	[-]	[-]	Nor [-]	Nor [-]	Nor [-]	Nor [-]	Nod [-]	Nod [-]	Nod [-]	Nod [-]	
AI_2_60	7.06	1.46	0.25	6.47	1.46	0.30	5.41	1.46	0.24	0.84	-	-	-	-	0.00	0.00	0.00	0.00
AI_2_80	8.75	1.73	0.30	8.14	1.73	0.34	6.78	1.73	0.29	0.83	-	-	-	-	0.00	0.00	0.00	0.00
AI_2_100	9.94	1.94	0.31	8.99	1.94	0.35	7.31	1.94	0.30	0.81	-	-	-	-	0.00	0.00	0.00	0.00
AI_2_120	11.59	2.13	0.32	10.65	2.13	0.36	8.41	2.07	0.31	0.79	-	-	-	-	0.00	0.00	0.00	0.00
AI_2_140	13.59	2.21	0.32	12.47	2.29	0.35	9.33	2.29	0.34	0.75	-	-	-	-	0.00	0.00	0.00	0.00
AI_2_160	16.60	2.37	0.29	14.80	2.37	0.32	10.59	2.37	0.37	0.72	-	-	-	-	0.00	0.00	0.00	0.00
AI_2_180	19.31	2.46	0.29	17.07	2.56	0.30	11.79	2.78	0.37	0.69	-	-	-	-	0.00	0.00	0.00	0.00
AI_2_1_60	6.73	1.46	0.24	6.42	1.46	0.28	5.44	1.46	0.20	0.85	0.10	0.10	0.00	0.00	0.00	0.00	0.00	0.00
AI_2_1_80	8.70	1.73	0.28	8.46	1.73	0.33	7.04	1.73	0.25	0.83	0.35	0.10	0.20	0.00	0.00	0.00	0.00	0.00
AI_2_1_100	9.29	1.94	0.30	9.14	1.94	0.35	7.53	1.94	0.26	0.82	0.50	0.10	0.40	0.00	0.00	0.00	0.00	0.00
AI_2_1_120	10.96	2.13	0.31	10.76	2.13	0.36	8.46	2.07	0.31	0.79	-	-	-	-	0.00	0.00	0.00	0.00
AI_2_1_140	12.76	2.21	0.32	12.55	2.21	0.36	9.47	2.21	0.36	0.75	-	-	-	-	0.00	0.00	0.00	0.00
AI_2_1_160	15.61	2.37	0.30	14.96	2.46	0.33	10.83	2.46	0.40	0.72	-	-	-	-	0.05	0.05	0.00	0.00
AI_2_1_180	18.83	2.46	0.28	17.63	2.67	0.31	12.20	2.78	0.41	0.69	-	-	-	-	0.50	0.15	0.35	0.00
AI_4_60	7.64	1.07	0.21	6.73	1.02	0.17	5.71	1.02	0.16	0.85	-	-	-	-	0.00	0.00	0.00	0.00
AI_4_80	9.65	1.16	0.24	8.75	1.21	0.22	7.16	1.26	0.18	0.82	-	-	-	-	0.00	0.00	0.00	0.00
AI_4_100	11.52	1.33	0.26	10.44	1.33	0.26	8.27	1.33	0.19	0.79	-	-	-	-	0.00	0.00	0.00	0.00
AI_4_120	13.09	1.46	0.25	12.41	1.46	0.28	9.36	1.46	0.19	0.75	-	-	-	-	0.00	0.00	0.00	0.00
AI_4_140	15.02	1.56	0.27	13.95	1.73	0.29	10.16	1.73	0.20	0.73	-	-	-	-	0.00	0.00	0.00	0.00
AI_4_160	16.76	1.73	0.27	15.40	1.73	0.30	11.10	1.73	0.22	0.72	-	-	-	-	0.00	0.00	0.00	0.00
AI_4_180	18.65	1.73	0.25	16.87	1.88	0.29	11.82	1.88	0.24	0.70	-	-	-	-	0.00	0.00	0.00	0.00
AI_4_1_60	7.79	1.07	0.20	6.87	1.02	0.17	5.61	1.02	0.15	0.82	0.15	0.10	0.05	0.00	0.00	0.00	0.00	0.00
AI_4_1_80	9.96	1.16	0.24	9.05	1.21	0.23	7.21	1.16	0.18	0.80	0.20	0.00	0.20	0.00	0.00	0.00	0.00	0.00
AI_4_1_100	11.37	1.31	0.25	10.64	1.33	0.27	8.37	1.33	0.18	0.79	0.30	0.05	0.20	0.00	0.00	0.00	0.00	0.00
AI_4_1_120	13.13	1.46	0.25	12.30	1.46	0.28	9.49	1.46	0.19	0.77	0.20	0.05	0.15	0.00	0.00	0.00	0.00	0.00
AI_4_1_140	15.13	1.56	0.26	13.79	1.60	0.30	10.29	1.73	0.20	0.75	0.50	0.10	0.40	0.00	0.00	0.00	0.00	0.00
AI_4_1_160	17.24	1.73	0.27	15.33	1.73	0.30	11.24	1.73	0.21	0.73	-	-	-	-	0.00	0.00	0.00	0.00
AI_4_1_180	19.30	1.73	0.25	16.79	1.73	0.30	11.99	1.88	0.22	0.71	-	-	-	-	0.05	0.00	0.05	0.00

Run	Incident wave height in front of foreshore			Incident wave height on foreshore			Incident wave height behind structure			Wave transmission	Rocking armour units				Displaced armour units			
	Model		Reflection	Model		Reflection	Model		Reflection	Ct=Ht/Hi	Total	Seaside slope	Crest	Leeside slope	Total	Seaside slope	Crest	Leeside slope
	Hm0,i	Tp		Hm0,i	Tp		Hm0,i	Tp										
[cm]	[s]	[-]	[cm]	[s]	[-]	[cm]	[s]	[-]	[-]	Nor [-]	Nor [-]	Nor [-]	Nor [-]	Nod [-]	Nod [-]	Nod [-]	Nod [-]	
All_2_60	6.94	1.46	0.17	6.48	1.46	0.21	5.08	1.46	0.14	0.78	0.25	0.10	0.15	0.00	0.00	0.00	0.00	0.00
All_2_80	8.90	1.73	0.24	8.32	1.73	0.29	6.19	1.73	0.15	0.74	0.40	0.15	0.25	0.00	0.00	0.00	0.00	0.00
All_2_100	9.37	1.94	0.29	8.87	1.94	0.34	6.70	1.94	0.18	0.76	0.40	0.15	0.25	0.00	0.00	0.00	0.00	0.00
All_2_120	11.05	2.13	0.30	10.67	2.13	0.36	7.77	2.07	0.30	0.73	0.84	0.10	0.75	0.00	0.00	0.00	0.00	0.00
All_2_140	12.81	2.21	0.32	12.24	2.21	0.37	8.42	2.21	0.37	0.69	-	-	-	-	0.00	0.00	0.00	0.00
All_2_160	15.62	2.37	0.30	14.73	2.46	0.35	9.59	2.29	0.44	0.65	-	-	-	-	0.05	0.00	0.00	0.00
All_2_180	18.47	2.37	0.29	16.51	2.67	0.35	10.69	2.78	0.50	0.65	-	-	-	-	0.10	0.00	0.00	0.00
All_2_1_60	6.88	1.46	0.1984	6.29	1.46	0.239	5.05	1.46	0.2376	0.80	0.00	0.00	0.00	0.00	0.00	0.00	0.00	0.00
All_2_1_80	8.80	1.73	0.26	8.39	1.73	0.3133	6.16	1.73	0.277	0.73	0.45	0.10	0.35	0.00	0.00	0.00	0.00	0.00
All_2_1_100	9.42	1.94	0.2975	8.94	1.94	0.3488	6.49	1.94	0.275	0.73	0.60	0.25	0.35	0.00	0.00	0.00	0.00	0.00
All_2_1_120	11.11	2.13	0.3068	10.71	2.13	0.3599	7.39	2.07	0.3175	0.69	0.65	0.25	0.40	0.00	0.00	0.00	0.00	0.00
All_2_1_140	12.65	2.21	0.3191	12.30	2.21	0.3654	8.35	2.21	0.3753	0.68	0.99	0.35	0.65	0.00	0.00	0.00	0.00	0.00
All_2_1_160	15.33	2.37	0.3007	14.50	2.46	0.3441	9.36	2.46	0.4333	0.65	-	-	-	-	0.00	0.05	0.00	0.00
All_2_1_180	18.38	2.46	0.2796	16.71	2.56	0.3345	10.46	2.78	0.4958	0.63	-	-	-	-	0.00	0.10	0.00	0.00
All_4_60	7.53	1.07	0.17	6.72	1.02	0.12	5.11	1.02	0.15	0.76	0.10	0.00	0.10	0.00	0.00	0.00	0.00	0.00
All_4_80	9.73	1.16	0.18	8.82	1.21	0.15	6.42	1.26	0.16	0.73	0.10	0.10	0.10	0.00	0.00	0.00	0.00	0.00
All_4_100	11.37	1.36	0.21	10.53	1.33	0.20	7.42	1.33	0.18	0.71	0.50	0.10	0.40	0.00	0.00	0.00	0.00	0.00
All_4_120	13.16	1.46	0.22	12.25	1.46	0.25	8.31	1.46	0.19	0.68	0.60	0.10	0.50	0.00	0.00	0.00	0.00	0.00
All_4_140	15.08	1.56	0.25	13.69	1.60	0.29	9.07	1.73	0.20	0.66	-	-	-	-	0.00	0.00	0.00	0.00
All_4_160	17.32	1.73	0.26	15.36	1.73	0.31	9.95	1.73	0.21	0.65	-	-	-	-	0.00	0.00	0.00	0.00
All_4_180	18.97	1.73	0.26	16.59	1.73	0.32	10.58	1.88	0.23	0.64	-	-	-	-	0.00	0.00	0.00	0.00
BI_2_60	6.71	1.46	0.26	6.58	1.46	0.30	4.76	1.46	0.19	0.72	0.00	0.00	0.00	0.00	0.00	0.00	0.00	0.00
BI_2_80	8.42	1.73	0.32	8.34	1.73	0.37	5.81	1.73	0.22	0.70	0.05	0.05	0.00	0.00	0.00	0.00	0.00	0.00
BI_2_100	8.98	1.94	0.34	9.06	1.94	0.39	6.28	1.94	0.23	0.69	0.50	0.15	0.35	0.00	0.00	0.00	0.00	0.00
BI_2_120	10.66	2.13	0.35	10.83	2.13	0.39	7.36	2.07	0.28	0.68	0.45	0.10	0.35	0.00	0.00	0.00	0.00	0.00
BI_2_140	12.24	2.21	0.34	12.36	2.21	0.37	8.05	2.21	0.34	0.65	-	-	-	-	0.00	0.00	0.00	0.00
BI_2_160	14.83	2.37	0.31	14.57	2.46	0.34	9.23	2.46	0.37	0.63	-	-	-	-	0.10	0.10	0.00	0.00
BI_2_180	17.52	2.37	0.30	16.64	2.56	0.34	10.22	2.78	0.40	0.61	-	-	-	-	0.50	0.20	0.30	0.00

Run	Incident wave height in front of foreshore			Incident wave height on foreshore			Incident wave height behind structure			Wave transmission	Rocking armour units				Displaced armour units			
	Model		Reflection	Model		Reflection	Model		Reflection	Ct=Ht/Hi	Total	Seaside slope	Crest	Leeside slope	Total	Seaside slope	Crest	Leeside slope
	Hm0,i	Tp		Hm0,i	Tp		Hm0,i	Tp										
[cm]	[s]	[-]	[cm]	[s]	[-]	[cm]	[s]	[-]	[-]	Nor [-]	Nor [-]	Nor [-]	Nor [-]	Nod [-]	Nod [-]	Nod [-]	Nod [-]	
BI 2 1 60	6.67	1.46	0.25	6.37	1.46	0.30	4.84	1.46	0.22	0.76	0.15	0.15	0.00	0.00	0.00	0.00	0.00	0.00
BI 2 1 80	8.65	1.73	0.33	8.32	1.73	0.38	5.74	1.73	0.29	0.69	0.20	0.15	0.05	0.00	0.00	0.00	0.00	0.00
BI 2 1 100	9.27	1.94	0.35	8.91	1.94	0.40	6.09	1.94	0.29	0.68	0.45	0.15	0.30	0.00	0.00	0.00	0.00	0.00
BI 2 1 120	10.79	2.13	0.34	10.57	2.13	0.40	7.02	2.07	0.34	0.66	0.70	0.20	0.50	0.00	0.00	0.00	0.00	0.00
BI 2 1 140	12.59	2.21	0.35	12.33	2.21	0.39	7.97	2.21	0.40	0.65	-	-	-	-	0.00	0.00	0.00	0.00
BI 2 1 160	15.44	2.37	0.32	14.65	2.46	0.36	9.12	2.37	0.44	0.62	-	-	-	-	0.50	0.25	0.25	0.00
BI 4 60	7.37	1.07	0.20	6.55	1.02	0.16	4.92	1.02	0.18	0.75	-	-	-	-	0.00	0.00	0.00	0.00
BI 4 80	9.41	1.16	0.24	8.56	1.26	0.22	6.04	1.26	0.19	0.71	-	-	-	-	0.00	0.00	0.00	0.00
BI 4 100	11.03	1.33	0.28	10.51	1.33	0.29	7.08	1.33	0.20	0.67	-	-	-	-	0.00	0.00	0.00	0.00
BI 4 120	12.64	1.46	0.30	12.18	1.46	0.32	7.90	1.46	0.21	0.65	-	-	-	-	0.00	0.00	0.00	0.00
BI 4 140	14.44	1.60	0.33	13.75	1.60	0.36	8.56	1.60	0.23	0.62	-	-	-	-	0.00	0.00	0.00	0.00
BI 4 160	16.51	1.73	0.33	15.42	1.73	0.38	9.49	1.73	0.24	0.62	-	-	-	-	0.00	0.00	0.00	0.00
BI 4 180	18.13	1.73	0.31	16.63	1.73	0.37	10.10	1.88	0.26	0.61	-	-	-	-	0.00	0.00	0.00	0.00
BI 4 1 60	5.88	1.00	0.31								0.00	0.00	0.00	0.00	0.00	0.00	0.00	0.00
BI 4 1 80	9.11	1.16	0.24	8.98	1.21	0.22	5.80	1.26	0.20	0.65	0.05	0.05	0.00	0.00	0.00	0.00	0.00	0.00
BI 4 1 100	10.97	1.33	0.28	10.73	1.33	0.29	6.76	1.31	0.24	0.63	0.50	0.15	0.35	0.00	0.00	0.00	0.00	0.00
BI 4 1 120	12.79	1.46	0.30	12.11	1.46	0.33	7.73	1.46	0.26	0.64	0.45	0.10	0.35	0.00	0.00	0.00	0.00	0.00
BI 4 1 140	14.64	1.56	0.33	13.66	1.60	0.37	8.42	1.73	0.29	0.62	-	-	-	-	0.00	0.00	0.00	0.00
BI 4 1 160	16.75	1.73	0.34	15.30	1.73	0.39	9.32	1.73	0.32	0.61	-	-	-	-	0.00	0.00	0.00	0.00
BI 4 1 180	18.78	1.73	0.33	16.74	1.73	0.39	9.93	1.73	0.35	0.59	-	-	-	-	0.05	0.00	0.05	0.00
CI 2 60	6.63	1.46	0.26	6.44	1.46	0.30	3.48	1.46	0.23	0.54	-	-	-	-	0.00	0.00	0.00	0.00
CI 2 80	8.50	1.73	0.33	8.29	1.73	0.38	4.57	1.73	0.26	0.55	-	-	-	-	0.00	0.00	0.00	0.00
CI 2 100	9.07	1.94	0.36	8.88	1.94	0.42	4.91	1.94	0.27	0.55	-	-	-	-	0.00	0.00	0.00	0.00
CI 2 120	10.68	2.13	0.38	10.59	2.13	0.44	5.72	2.07	0.32	0.54	-	-	-	-	0.00	0.00	0.00	0.00
CI 2 140	12.38	2.21	0.37	12.32	2.21	0.42	6.40	2.21	0.37	0.52	-	-	-	-	0.00	0.00	0.00	0.00
CI 2 160	15.16	2.37	0.34	14.55	2.37	0.40	7.48	2.37	0.41	0.51	-	-	-	-	0.50	0.25	0.20	0.05

Run	Incident wave height in front of foreshore			Incident wave height on foreshore			Incident wave height behind structure			Wave transmission	Rocking armour units				Displaced armour units			
	Model		Reflection	Model		Reflection	Model		Reflection	Ct=Ht/Hi	Total	Seaside slope	Crest	Leeside slope	Total	Seaside slope	Crest	Leeside slope
	Hm0,i	Tp		Hm0,i	Tp		Hm0,i	Tp										
[cm]	[s]	[-]	[cm]	[s]	[-]	[cm]	[s]	[-]	[-]	Nor [-]	Nor [-]	Nor [-]	Nor [-]	Nod [-]	Nod [-]	Nod [-]	Nod [-]	
CI 2_1_60	6.76	1.46	0.25	6.44	1.46	0.28	3.27	1.46	0.23	0.51	0.05	0.00	0.00	0.00	0.00	0.00	0.00	0.00
CI 2_1_80	8.56	1.73	0.33	8.33	1.73	0.37	4.48	1.73	0.27	0.54	0.20	0.00	0.15	0.05	0.00	0.00	0.00	0.00
CI 2_1_100	9.08	1.94	0.36	8.87	1.94	0.42	4.86	1.94	0.27	0.55	0.25	0.15	0.10	0.00	0.00	0.00	0.00	0.00
CI 2_1_120	10.72	2.13	0.38	10.61	2.13	0.44	5.64	2.07	0.32	0.53	0.20	0.05	0.15	0.00	0.00	0.00	0.00	0.00
CI 2_1_140	12.44	2.21	0.37	12.26	2.21	0.43	6.31	2.13	0.38	0.52	0.50	0.00	0.35	0.15	0.00	0.00	0.00	0.00
CI 2_1_160	15.36	2.37	0.35	14.67	2.37	0.41	7.49	2.37	0.42	0.51	-	-	-	-	0.50	0.00	0.45	0.05
CI 2_2_60	6.60	1.46	0.25	6.55	1.46	0.29	3.50	1.46	0.25	0.53	0.15	0.10	0.05	0.00	0.00	0.00	0.00	0.00
AI 2_2_80	8.39	1.73	0.33	8.34	1.73	0.37	4.61	1.73	0.30	0.55	0.30	0.25	0.05	0.00	0.00	0.00	0.00	0.00
CI 2_2_100	8.97	1.94	0.36	8.95	1.94	0.41	5.00	1.94	0.31	0.56	0.35	0.10	0.25	0.00	0.00	0.00	0.00	0.00
CI 2_2_120	10.59	2.13	0.38	10.74	2.13	0.43	5.83	2.07	0.38	0.54	0.55	0.20	0.35	0.00	0.00	0.00	0.00	0.00
CI 2_2_140	12.37	2.21	0.38	12.47	2.21	0.43	6.58	2.13	0.44	0.53	-	-	-	-	0.05	0.00	0.00	0.00
CI 2_2_160	15.01	2.37	0.35	14.54	2.37	0.42	7.47	2.37	0.48	0.51	-	-	-	-	0.50	0.20	0.30	0.00
CI 2_3_60	6.56	1.46	0.26	6.28	1.46	0.29	3.45	1.46	0.24	0.55	0.05	0.05	0.00	0.00	0.00	0.00	0.00	0.00
AI 2_3_80	8.57	1.73	0.34	8.30	1.73	0.38	4.54	1.73	0.28	0.55	0.15	0.10	0.05	0.00	0.00	0.00	0.00	0.00
CI 2_3_100	9.19	1.94	0.37	8.92	1.94	0.42	4.91	1.94	0.30	0.55	0.50	0.20	0.30	0.00	0.00	0.00	0.00	0.00
CI 2_3_120	10.83	2.13	0.38	10.63	2.13	0.44	5.73	2.07	0.36	0.54	0.89	0.30	0.60	0.00	0.00	0.00	0.00	0.00
CI 2_3_140	12.30	2.21	0.38	12.32	2.21	0.43	6.44	2.13	0.42	0.52	0.50	0.05	0.45	0.00	0.05	0.00	0.05	0.00
CI 2_3_160	14.23	2.37	0.36	14.32	2.37	0.42	7.30	2.37	0.46	0.51	-	-	-	-	0.50	0.10	0.40	0.00
CI 2_4_60	6.66	1.46	0.2361	6.25	1.46	0.2718	3.25	1.46	0.2521	0.52	0.30	0.20	0.10	0.00	0.00	0.00	0.00	0.00
AI 2_4_80	8.57	1.73	0.318	8.33	1.73	0.3678	4.40	1.73	0.295	0.53	0.70	0.40	0.30	0.00	0.00	0.00	0.00	0.00
CI 2_4_100	9.16	1.94	0.3561	8.93	1.94	0.4169	4.74	1.94	0.2927	0.53	0.40	0.15	0.25	0.00	0.00	0.00	0.00	0.00
CI 2_4_120	10.83	2.13	0.3734	10.68	2.13	0.4409	5.57	2.07	0.3367	0.52	-	-	-	-	0.00	0.00	0.00	0.00
CI 2_4_140	12.66	2.21	0.3758	12.34	2.21	0.4406	6.28	2.21	0.3954	0.51	-	-	-	-	0.00	0.00	0.00	0.00
CI 2_4_160	15.23	2.37	0.357	14.35	2.37	0.4282	7.06	2.37	0.4455	0.49	-	-	-	-	0.50	0.10	0.20	0.20

Run	Incident wave height in front of foreshore			Incident wave height on foreshore			Incident wave height behind structure			Wave transmission	Rocking armour units				Displaced armour units			
	Model		Reflection	Model		Reflection	Model		Reflection	Ct=Ht/Hi	Total	Seaside slope	Crest	Leeside slope	Total	Seaside slope	Crest	Leeside slope
	Hm0,i	Tp		Hm0,i	Tp		Hm0,i	Tp										
[cm]	[s]	[-]	[cm]	[s]	[-]	[cm]	[s]	[-]	[-]	Nor [-]	Nor [-]	Nor [-]	Nor [-]	Nod [-]	Nod [-]	Nod [-]	Nod [-]	
CI_4_60	7.16	1.07	0.18	6.64	1.02	0.15	3.22	1.02	0.23	0.49	0.00	0.00	0.00	0.00	0.00	0.00	0.00	0.00
CI_4_80	9.44	1.16	0.21	8.68	1.26	0.19	4.31	1.26	0.22	0.50	0.05	0.00	0.05	0.00	0.00	0.00	0.00	0.00
CI_4_100	11.04	1.33	0.25	10.51	1.33	0.25	5.29	1.33	0.25	0.50	0.05	0.05	0.20	0.00	0.00	0.00	0.00	0.00
CI_4_120	12.74	1.46	0.28	12.01	1.46	0.30	6.20	1.46	0.25	0.52	0.40	0.15	0.25	0.00	0.00	0.00	0.00	0.00
CI_4_140	14.54	1.60	0.31	13.66	1.60	0.35	6.90	1.60	0.27	0.51	-	-	-	-	0.00	0.00	0.00	0.00
CI_4_160	16.58	1.73	0.33	15.42	1.73	0.39	7.82	1.73	0.27	0.51	-	-	-	-	0.00	0.00	0.00	0.00
CI_4_180	18.14	1.73	0.33	16.63	1.83	0.40	8.41	1.88	0.28	0.51	-	-	-	-	0.05	0.00	0.05	0.00
CI_4_1_60	7.24	1.07	0.18	6.68	1.02	0.14	3.15	1.02	0.22	0.47	0.10	0.10	0.00	0.00	0.00	0.00	0.00	0.00
CI_4_1_80	9.09	1.16	0.22	8.65	1.21	0.20	4.14	1.26	0.22	0.48	0.25	0.20	0.05	0.00	0.00	0.00	0.00	0.00
CI_4_1_100	10.96	1.33	0.25	10.48	1.33	0.26	5.38	1.33	0.24	0.51	0.25	0.25	0.00	0.00	0.00	0.00	0.00	0.00
CI_4_1_120	12.56	1.46	0.29	12.08	1.46	0.31	6.27	1.46	0.25	0.52	0.25	0.10	0.15	0.00	0.00	0.00	0.00	0.00
CI_4_1_140	14.41	1.60	0.32	13.64	1.60	0.35	6.95	1.60	0.27	0.51	-	-	-	-	0.00	0.00	0.00	0.00
CI_4_1_160	16.29	1.73	0.33	15.44	1.73	0.38	7.76	1.73	0.28	0.50	-	-	-	-	0.00	0.00	0.00	0.00
CI_4_1_180	18.19	1.73	0.34	16.61	1.83	0.41	8.41	1.88	0.29	0.51	-	-	-	-	0.00	0.00	0.00	0.00
CI_4_2_60	7.30	1.07	0.17	6.55	1.02	0.14	3.47	1.02	0.23	0.53	0.10	0.05	0.05	0.00	0.00	0.00	0.00	0.00
CI_4_2_80	9.45	1.16	0.21	8.59	1.21	0.19	4.43	1.26	0.23	0.52	0.20	0.15	0.05	0.00	0.00	0.00	0.00	0.00
CI_4_2_100	11.24	1.33	0.25	10.47	1.33	0.25	5.47	1.33	0.25	0.52	0.15	0.15	0.00	0.00	0.00	0.00	0.00	0.00
CI_4_2_120	12.76	1.46	0.29	12.12	1.46	0.31	6.38	1.46	0.26	0.53	0.20	0.05	0.20	0.00	0.00	0.00	0.00	0.00
CI_4_2_140	14.62	1.60	0.31	13.55	1.60	0.35	7.08	1.60	0.27	0.52	0.50	0.15	0.30	0.00	0.00	0.00	0.00	0.00
CI_4_2_160	16.58	1.73	0.33	15.40	1.73	0.39	7.95	1.73	0.28	0.52	-	-	-	-	0.05	0.05	0.00	0.00
CI_4_2_180	18.20	1.73	0.33	16.64	1.83	0.40	8.47	1.88	0.29	0.51	-	-	-	-	0.15	0.05	0.10	0.00
CI_4_3_60	7.30	1.00	0.19	6.55	1.02	0.14	3.18	1.02	0.23	0.49	0.00	0.00	0.00	0.00	0.00	0.00	0.00	0.00
CI_4_3_80	9.35	1.16	0.22	8.64	1.21	0.20	4.34	1.26	0.23	0.50	0.40	0.25	0.15	0.00	0.00	0.00	0.00	0.00
CI_4_3_100	11.10	1.33	0.27	10.49	1.33	0.26	5.39	1.33	0.26	0.51	0.50	0.20	0.30	0.00	0.00	0.00	0.00	0.00
CI_4_3_120	12.61	1.46	0.30	12.17	1.46	0.32	6.33	1.46	0.28	0.52	0.75	0.25	0.50	0.00	0.00	0.00	0.00	0.00
CI_4_3_140	14.48	1.60	0.32	13.75	1.60	0.37	7.03	1.60	0.30	0.51	0.94	0.40	0.55	0.00	0.00	0.00	0.00	0.00
CI_4_3_160	16.44	1.73	0.34	15.45	1.73	0.40	7.90	1.73	0.32	0.51	-	-	-	-	0.05	0.00	0.05	0.00
CI_4_3_180	18.15	1.73	0.35	16.63	1.73	0.41	8.48	1.88	0.34	0.51	-	-	-	-	0.05	0.00	0.05	0.00

Run	Incident wave height in front of foreshore			Incident wave height on foreshore			Incident wave height behind structure			Wave transmission	Rocking armour units				Displaced armour units			
	Model		Reflection	Model		Reflection	Model		Reflection	Ct=Ht/Hi	Total	Seaside slope	Crest	Leeside slope	Total	Seaside slope	Crest	Leeside slope
	Hm0,i	Tp		Hm0,i	Tp		Hm0,i	Tp										
[cm]	[s]	[-]	[cm]	[s]	[-]	[cm]	[s]	[-]	[-]	Nor [-]	Nor [-]	Nor [-]	Nor [-]	Nod [-]	Nod [-]	Nod [-]	Nod [-]	
CI_4_4_60	7.29	1.07	0.1813	6.67	1.02	0.1449	3.08	1.07	0.2499	0.46	0.35	0.30	0.05	0.00	0.00	0.00	0.00	0.00
CI_4_4_80	9.24	1.16	0.208	8.61	1.21	0.1842	4.07	1.26	0.2755	0.47	0.70	0.50	0.20	0.00	0.00	0.00	0.00	0.00
CI_4_4_100	11.03	1.33	0.2427	10.43	1.33	0.2434	5.19	1.33	0.3048	0.50	1.09	0.80	0.30	0.00	0.05	0.05	0.00	0.00
CI_4_4_120	11.84	1.46	0.2763	11.26	1.46	0.2985	5.79	1.46	0.3231	0.51	-	-	-	-	0.05	0.05	0.00	0.00
CI_4_4_140	12.75	1.46	0.2734	12.11	1.46	0.2959	6.26	1.46	0.323	0.52	-	-	-	-	0.05	0.05	0.00	0.00
CI_4_4_160	16.67	1.73	0.3228	15.31	1.73	0.3881	7.77	1.73	0.3639	0.51	-	-	-	-	0.05	0.05	0.00	0.00
CI_4_4_180	18.62	1.73	0.329	16.79	1.83	0.4032	8.40	1.73	0.3691	0.50	-	-	-	-	0.10	0.05	0.05	0.00
CII_2_60	6.71	1.46	0.22	6.38	1.46	0.25	2.44	1.46	0.19	0.38	0.30	0.20	0.10	0.00	0.00	0.00	0.00	0.00
CII_2_80	8.57	1.73	0.28	8.33	1.73	0.33	3.41	1.73	0.26	0.41	0.75	0.45	0.30	0.00	0.00	0.00	0.00	0.00
CII_2_100	9.14	1.94	0.33	8.90	1.94	0.38	3.77	1.94	0.28	0.42	0.80	0.50	0.30	0.00	0.00	0.00	0.00	0.00
CII_2_120	10.58	2.13	0.35	10.53	2.13	0.42	4.50	2.07	0.35	0.43	-	-	-	-	0.00	0.00	0.00	0.00
CII_2_140	12.36	2.21	0.36	12.12	2.21	0.44	5.28	2.21	0.44	0.44	-	-	-	-	0.05	0.00	0.05	0.00
CII_2_160	14.80	2.37	0.36	14.05	2.37	0.44	6.11	2.37	0.49	0.44	-	-	-	-	0.50	0.25	0.25	0.00
CII_4_60	7.25	1.07	0.18	6.40	1.02	0.13	0.50	5.33	0.79	0.08	0.15	0.15	0.15	0.00	0.00	0.00	0.00	0.00
CII_4_80	9.38	1.16	0.20	8.77	1.21	0.17	2.97	1.26	0.28	0.34	0.65	0.35	0.30	0.00	0.00	0.00	0.00	0.00
CII_4_100	11.13	1.33	0.24	10.68	1.33	0.23	3.94	1.33	0.30	0.37	0.55	0.20	0.35	0.00	0.00	0.00	0.00	0.00
CII_4_120	12.68	1.46	0.27	12.03	1.46	0.28	5.02	1.46	0.32	0.42	-	-	-	-	0.00	0.00	0.00	0.00
CII_4_140	14.48	1.60	0.29	13.52	1.60	0.33	5.75	1.60	0.35	0.43	-	-	-	-	0.00	0.00	0.00	0.00
CII_4_160	16.53	1.73	0.30	15.17	1.73	0.37	6.63	1.73	0.33	0.44	-	-	-	-	0.00	0.00	0.00	0.00
CII_4_180	18.22	1.73	0.31	16.46	1.83	0.40	7.02	1.88	0.33	0.43	-	-	-	-	0.00	0.00	0.00	0.00
DI_2_60	6.76	1.46	67.61	6.52	1.46	0.35	1.50	1.46	0.29	0.23	0.05	0.05	0.00	0.00	0.00	0.00	0.00	0.00
DI_2_80	8.82	1.73	88.24	8.54	1.73	0.43	2.53	1.68	0.29	0.30	0.15	0.15	0.00	0.00	0.00	0.00	0.00	0.00
DI_2_100	9.16	1.94	91.62	8.99	1.94	0.48	2.98	2.00	0.29	0.33	0.10	0.10	0.00	0.00	0.00	0.00	0.00	0.00
DI_2_120	10.81	2.13	108.10	10.83	2.13	0.50	4.00	2.07	0.33	0.37	0.35	0.25	0.10	0.00	0.00	0.00	0.00	0.00
DI_2_140	12.55	2.21	125.50	12.52	2.21	0.49	4.93	2.91	0.40	0.39	0.30	0.15	0.15	0.00	0.50	0.30	0.20	0.00

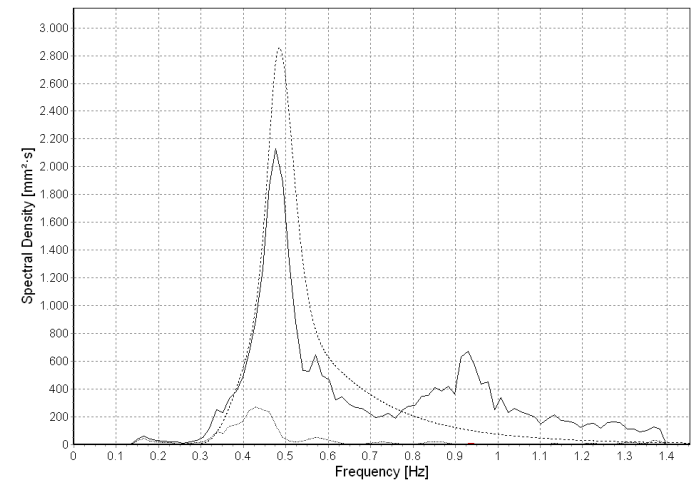
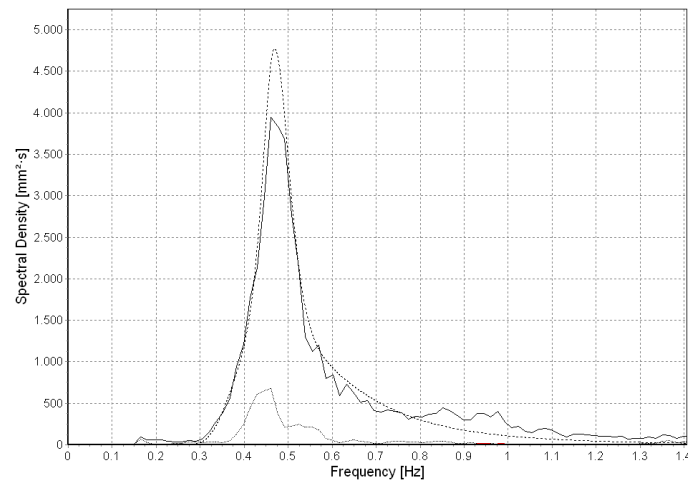
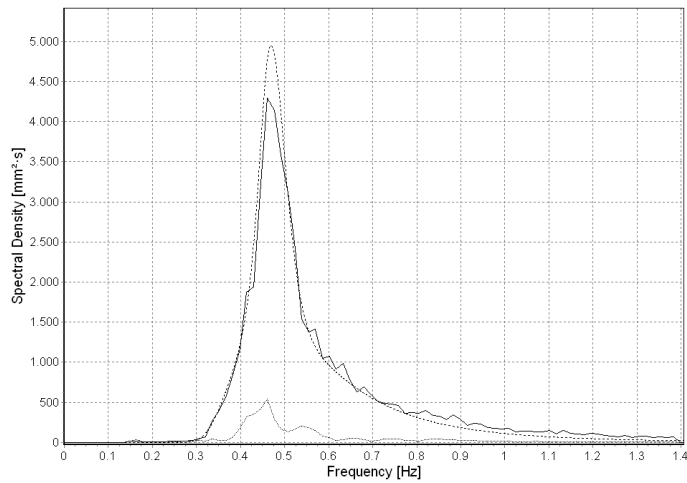
Run	Incident wave height in front of foreshore			Incident wave height on foreshore			Incident wave height behind structure			Wave transmission	Rocking armour units				Displaced armour units			
	Model		Reflection	Model		Reflection	Model		Reflection	Ct=Ht/Hi	Total	Seaside slope	Crest	Leeside slope	Total	Seaside slope	Crest	Leeside slope
	Hm0,i	Tp		Hm0,i	Tp		Hm0,i	Tp										
[cm]	[s]	[-]	[cm]	[s]	[-]	[cm]	[s]	[-]	[-]	Nor [-]	Nor [-]	Nor [-]	Nor [-]	Nod [-]	Nod [-]	Nod [-]	Nod [-]	
DI_4_60	7.62	1.07	0.24	6.65	1.02	0.22	0.28	5.33	0.87	0.04	0.10	0.05	0.05	0.00	0.00	0.00	0.00	0.00
DI_4_80	9.68	1.16	0.25	8.77	1.21	0.24	2.08	1.26	0.26	0.24	0.55	0.45	0.05	0.05	0.00	0.00	0.00	0.00
DI_4_100	11.65	1.33	0.28	10.59	1.33	0.28	3.27	1.42	0.24	0.31	0.84	0.70	0.10	0.05	0.00	0.00	0.00	0.00
DI_4_120	12.95	1.46	0.31	12.30	1.46	0.33	4.46	1.46	0.26	0.36	-	-	-	-	0.00	0.00	0.00	0.00
DI_4_140	14.97	1.56	0.33	14.14	1.60	0.37	5.50	1.60	0.30	0.39	-	-	-	-	0.00	0.00	0.00	0.00
DI_4_160	16.72	1.73	0.34	15.58	1.73	0.40	6.23	1.68	0.31	0.40	-	-	-	-	0.05	0.05	0.00	0.00
DI_4_180	18.14	1.73	0.34	17.16	1.83	0.43	7.05	2.00	0.32	0.41	-	-	-	-	0.50	0.50	0.00	0.00
DII_2_60	6.75	1.46	0.32	6.44	1.46	0.37	0.20	5.33	0.82	0.03	0.30	0.25	0.05	0.00		0.00	0.00	0.00
DII_2_80	8.71	1.73	0.38	8.41	1.73	0.45	0.49	5.33	0.67	0.06	0.65	0.50	0.15	0.00	0.00	0.00	0.00	0.00
DII_2_100	9.24	1.94	0.42	8.96	1.94	0.51	0.77	2.07	0.57	0.09	0.65	0.40	0.25	0.00	0.00	0.00	0.00	0.00
DII_2_120	10.88	2.13	0.44	10.71	2.13	0.53	1.35	2.07	0.55	0.13	-	-	-	-	0.00	0.00	0.00	0.00
DII_2_140	12.60	2.21	0.44	12.26	2.21	0.53	2.77	2.91	0.48	0.23	-	-	-	-	0.00	0.00	0.00	0.00
DII_2_160	13.60	2.46	0.42	12.90	2.46	0.52	3.64	2.91	0.53	0.28	-	-	-	-	0.50	0.25	0.05	0.20
DII_4_60	7.40	1.07	0.24	6.67	1.02	0.23	0.15	5.33	0.93	0.02	0.30	0.30	0.00	0.00	0.00	0.00	0.00	0.00
DII_4_80	9.56	1.16	0.25	8.74	1.21	0.24	0.34	5.33	0.89	0.04	0.45	0.40	0.05	0.00	0.00	0.00	0.00	0.00
DII_4_100	11.23	1.33	0.29	10.57	1.33	0.29	0.55	5.33	0.83	0.05	0.50	0.25	0.25	0.00	0.00	0.00	0.00	0.00
DII_4_120	12.92	1.46	0.32	12.26	1.46	0.35	0.87	5.33	0.76	0.07	-	-	-	-	0.00	0.00	0.00	0.00
DII_4_140	14.96	1.60	0.35	13.73	1.60	0.40	1.30	5.33	0.66	0.09	-	-	-	-	0.05	0.00	0.05	0.00
DII_4_160	17.09	1.73	0.35	15.50	1.73	0.42	3.94	1.68	0.33	0.25	-	-	-	-	0.30	0.15	0.15	0.00
DII_4_180	18.88	1.73	0.35	16.89	1.83	0.44	1.50	-	0.72	0.09	-	-	-	-	0.50	0.30	0.20	0.00
EI_2_60	6.85	1.46	0.36	6.66	1.46	0.40	0.53	1.60	0.43	0.08	0.15	0.15	0.00		0.00	0.00	0.00	0.00
EI_2_80	8.85	1.73	0.42	8.66	1.73	0.49	0.42	-	0.41	0.05	0.89	0.35	0.45	0.10	0.00	0.00	0.00	0.00
EI_2_100	9.38	1.94	0.46	9.09	1.94	0.55	0.43	-	0.34	0.05	0.80	0.60	0.20	0.00	0.00	0.00	0.00	0.00
EI_2_120	11.18	2.13	0.47	10.93	2.13	0.56	2.34	2.00	0.36	0.21	0.50	0.30	0.20		0.00	0.00	0.00	0.00
EI_2_140	13.02	2.21	0.47	12.70	2.21	0.56	3.32	2.91	0.41	0.26	-	-	-	-	0.05	0.05	0.00	0.00
EI_2_160	15.41	2.46	0.45	14.80	2.46	0.54	4.63	2.91	0.46	0.31	-	-	-	-	0.20	0.15	0.05	0.00
EI_2_180	18.07	2.46	0.43	16.86	2.46	0.54	5.56	2.78	0.50	0.33	-	-	-	-	0.50	0.25	0.25	0.00

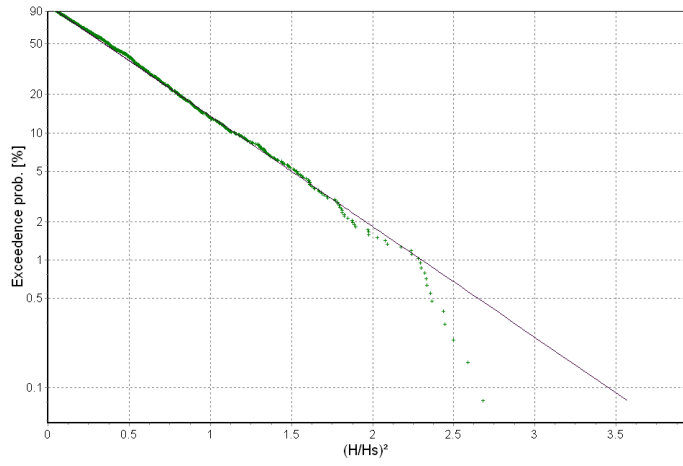
Run	Incident wave height in front of foreshore			Incident wave height on foreshore			Incident wave height behind structure			Wave transmission	Rocking armour units				Displaced armour units			
	Model		Reflection	Model		Reflection	Model		Reflection	Ct=Ht/Hi	Total	Seaside slope	Crest	Leeside slope	Total	Seaside slope	Crest	Leeside slope
	Hm0,i	Tp		Hm0,i	Tp		Hm0,i	Tp										
[cm]	[s]	[-]	[cm]	[s]	[-]	[cm]	[s]	[-]	[-]	Nor [-]	Nor [-]	Nor [-]	Nor [-]	Nod [-]	Nod [-]	Nod [-]	Nod [-]	
EI_4_60	7.86	1.07	0.25	7.23	1.02	0.25	0.11	5.33	0.90	0.02	0.00	0.00	0.00	0.00	0.00	0.00	0.00	0.00
EI_4_80	9.59	1.16	0.28	8.97	1.21	0.29	0.26	-	0.49	0.03	0.35	0.25	0.10	0.00	0.00	0.00	0.00	0.00
EI_4_100	12.58	1.33	0.32	10.91	1.33	0.32	0.61	-	0.00	0.06	0.60	0.60	0.00	0.00	0.10	0.05	0.00	0.00
EI_4_120	13.33	1.46	0.35	12.38	1.46	0.38	2.53	1.60	0.27	0.20	0.40	0.40	0.00	0.00	0.15	0.15	0.00	0.00
EI_4_140	15.21	1.60	0.38	14.09	1.60	0.43	3.27	1.60	0.28	0.23	-	-	-	-	0.20	0.15	0.00	0.00
EI_4_160	17.40	1.73	0.39	15.94	1.73	0.47	4.18	1.68	0.30	0.26	-	-	-	-	0.45	0.25	0.00	0.00
EI_4_180	18.24	1.73	0.39	16.52	1.83	0.49	4.69	1.73	0.31	0.28	-	-	-	-	0.50	0.50	0.00	0.00
EI_4_1_60	7.44	1.07	0.27	6.71	1.07	0.26	0.11	-	0.29	0.02	0.05	0.05	0.00	0.00	0.00	0.00	0.00	0.00
EI_4_1_80	9.61	1.16	0.29	8.85	1.26	0.29	0.34	-	0.16	0.04	0.25	0.15	0.10	0.00	0.00	0.00	0.00	0.00
EI_4_1_100	11.52	1.33	0.33	10.70	1.33	0.34	0.50	-	0.31	0.05	0.65	0.35	0.20	0.00	0.00	0.00	0.00	0.00
EI_4_1_120	13.41	1.46	0.37	12.43	1.46	0.39	2.43	1.60	0.29	0.20	0.65	0.40	0.25	0.00	0.00	0.00	0.00	0.00
EI_4_1_140	15.32	1.60	0.40	14.08	1.60	0.45	3.17	1.60	0.30	0.22	-	-	-	-	0.00	0.00	0.00	0.00
EI_4_1_160	17.50	1.73	0.40	15.93	1.73	0.48	4.12	1.68	0.31	0.26	-	-	-	-	0.00	0.00	0.00	0.00
EI_4_1_180	19.36	1.73	0.41	17.41	1.78	0.51	4.88	2.00	0.32	0.28	-	-	-	-	0.00	0.00	0.00	0.00

APPENDIX F

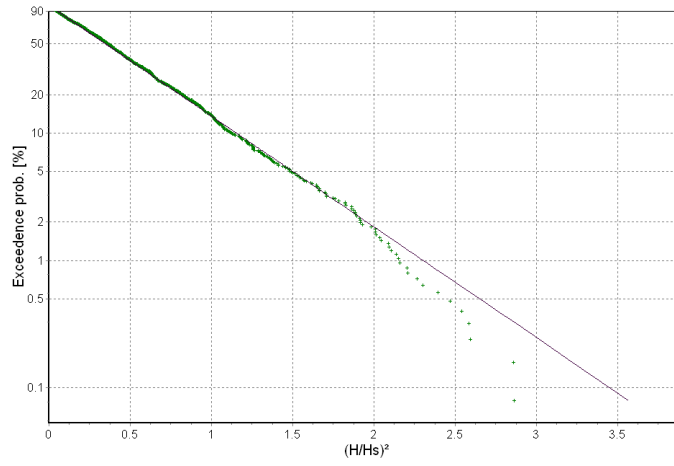
In this appendix the spectra for the three locations of the wave gauges are plotted for the design wave height.

AI_2_1

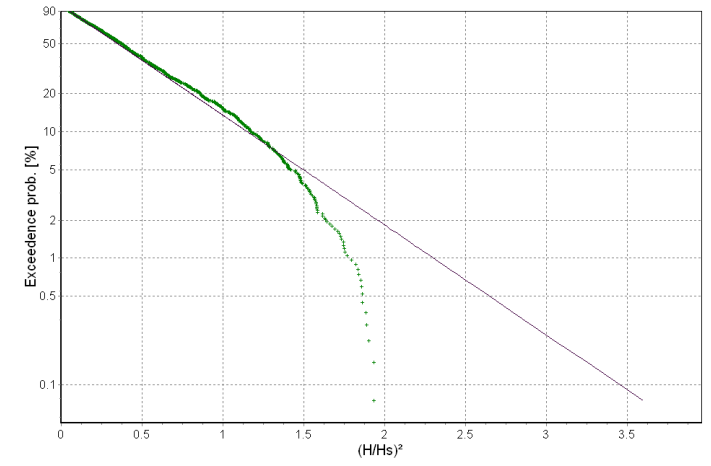




• Measured Incident — Rayleigh Incident

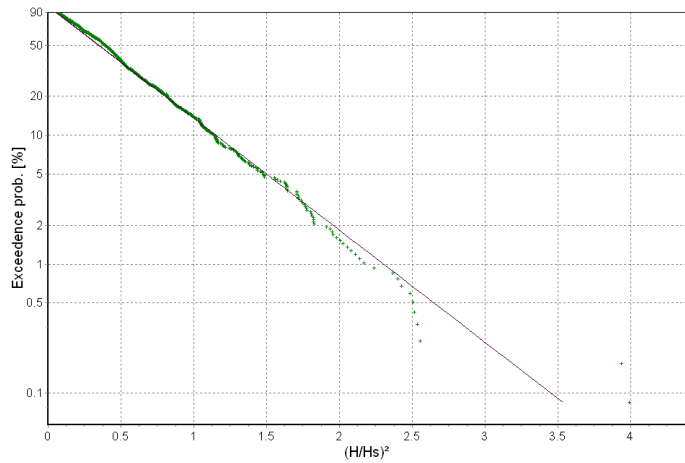
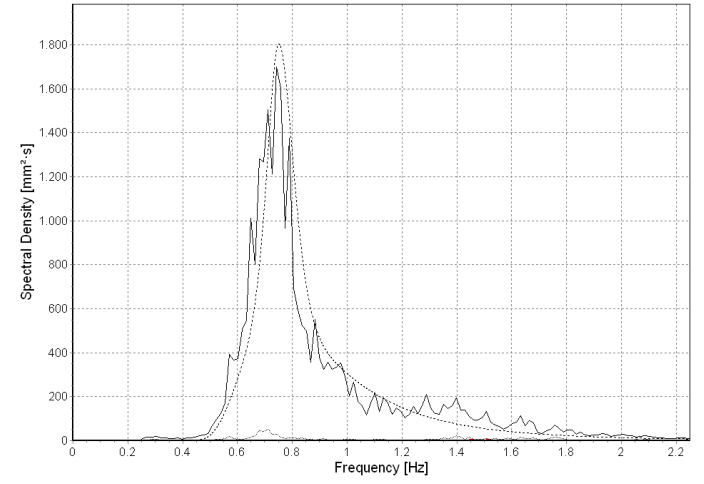
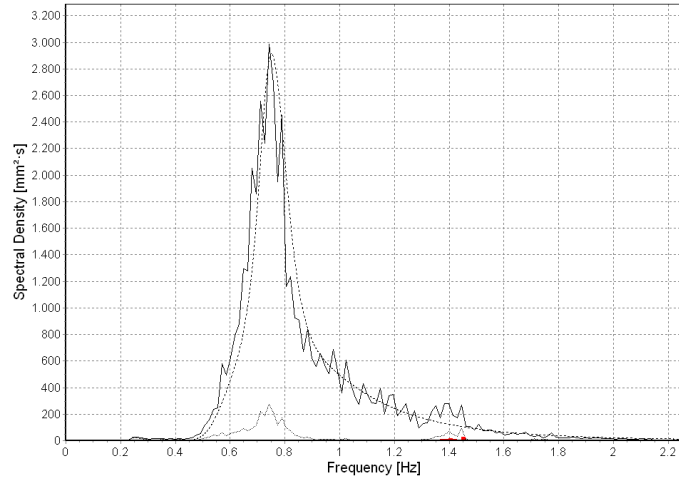
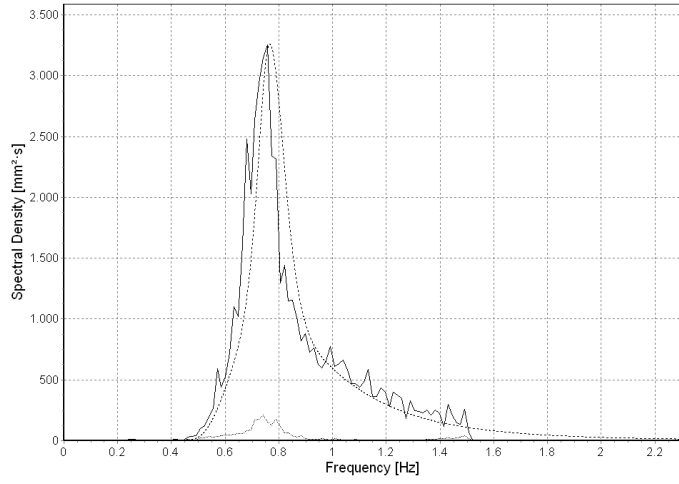


• Measured Incident — Rayleigh Incident

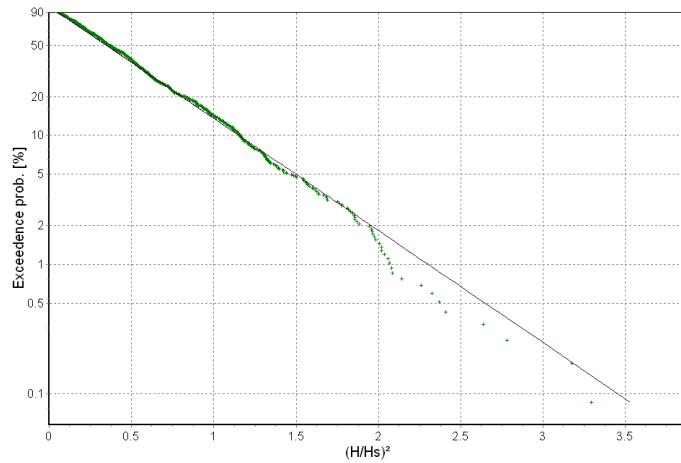


• Measured Incident — Rayleigh Incident

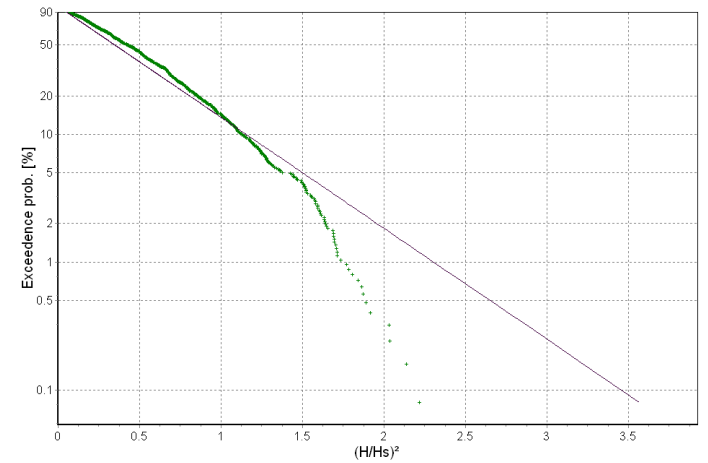
AI_4_1



• Measured Incident — Rayleigh Incident

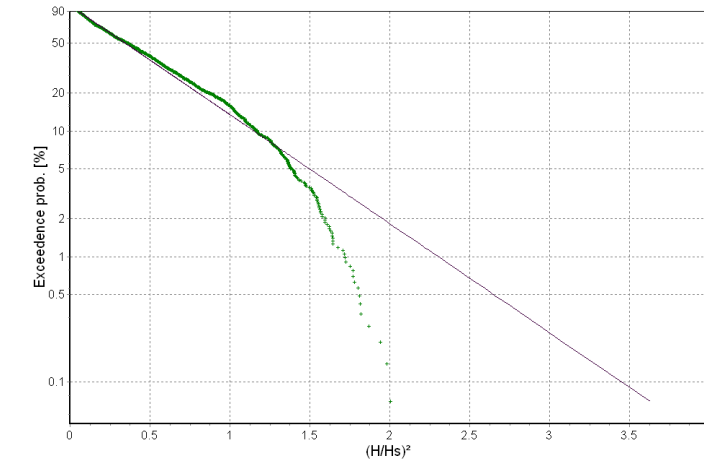
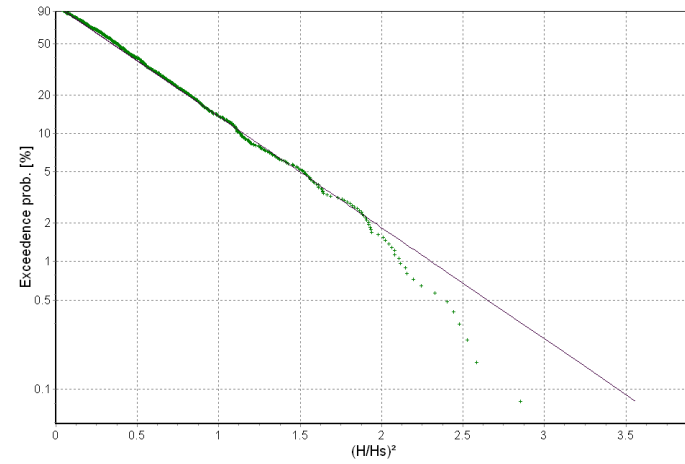
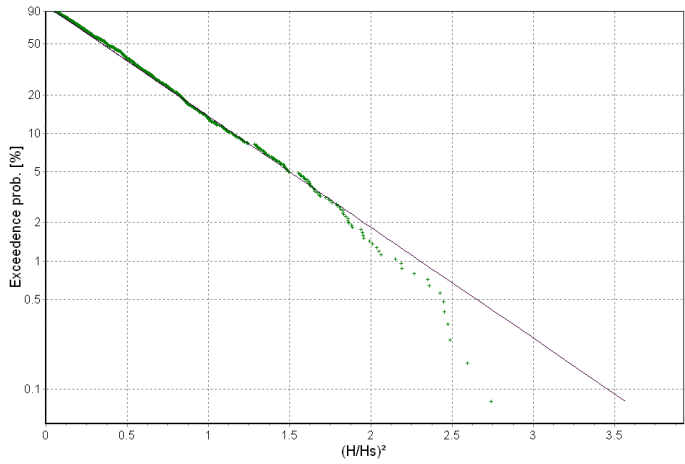
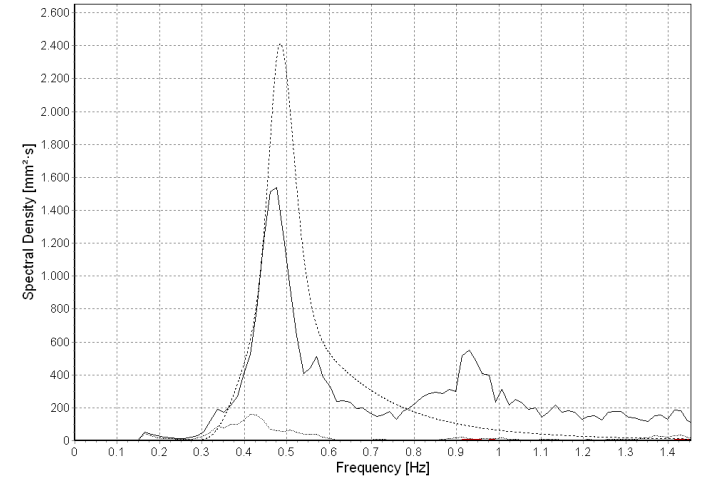
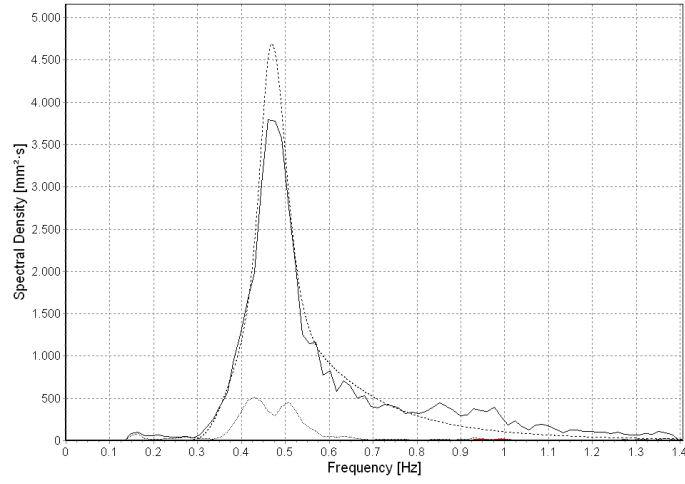
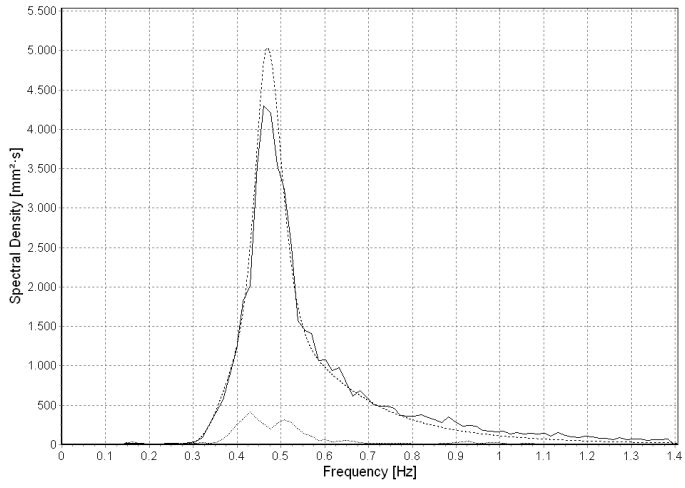


• Measured Incident — Rayleigh Incident



• Measured Incident — Rayleigh Incident

AII_2

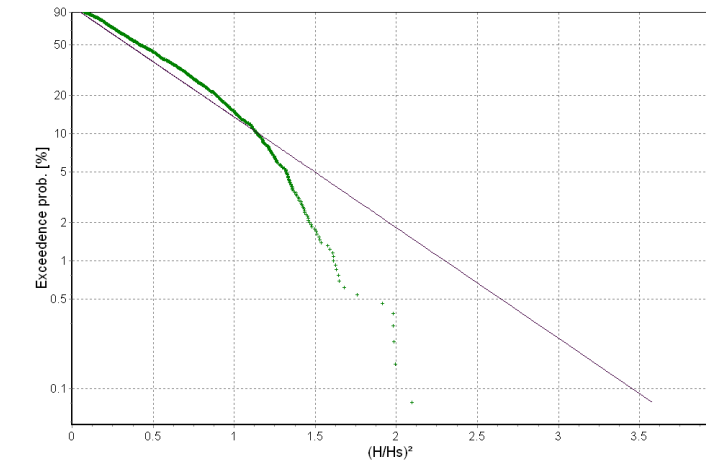
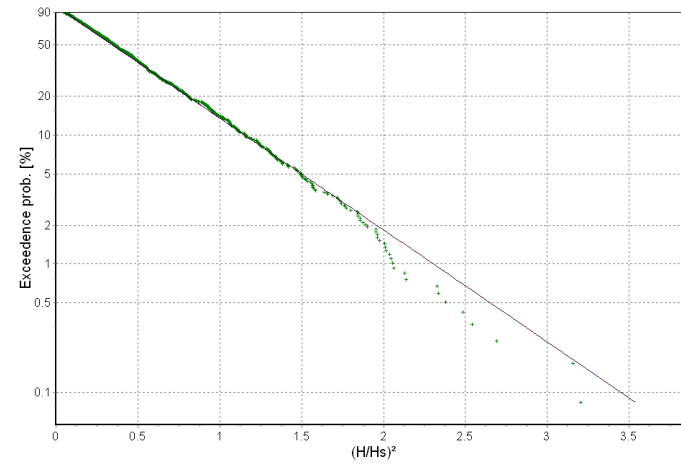
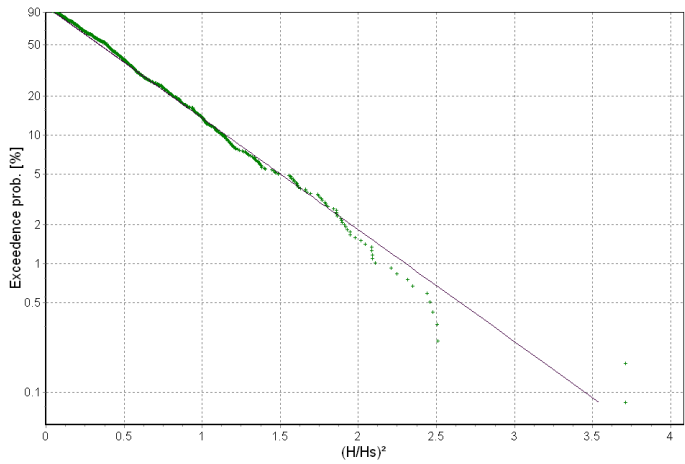
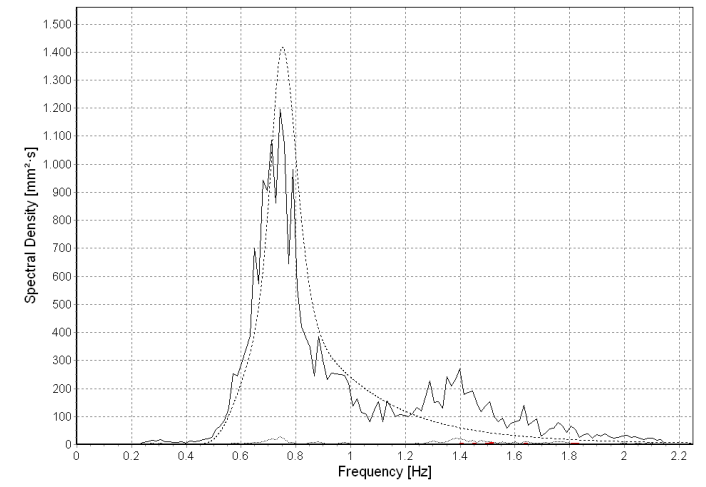
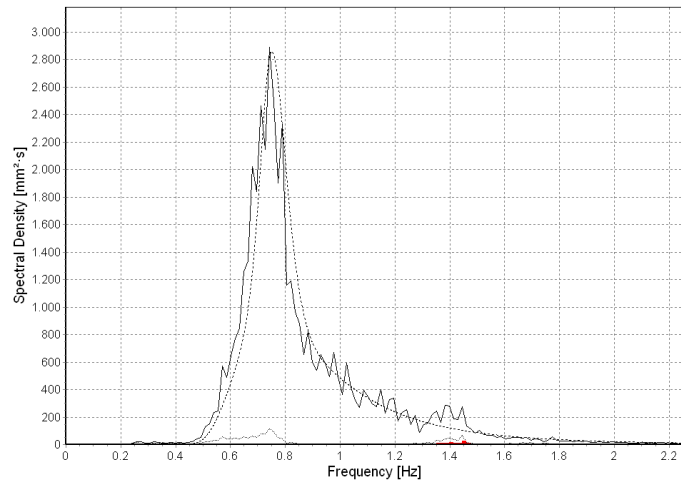
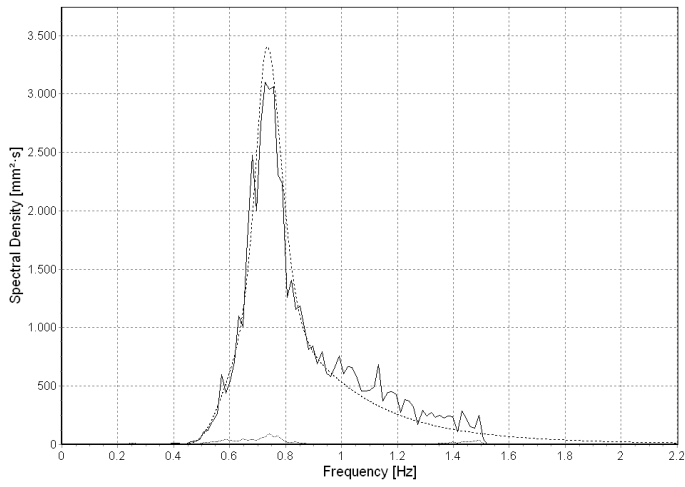


• Measured Incident — Rayleigh Incident

• Measured Incident — Rayleigh Incident

• Measured Incident — Rayleigh Incident

AII_4

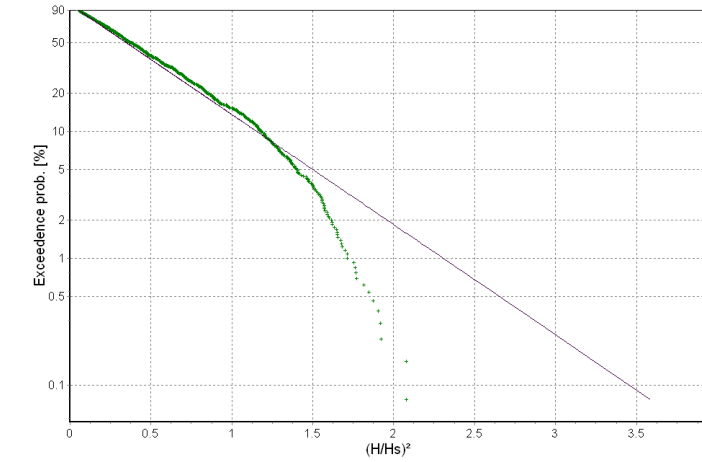
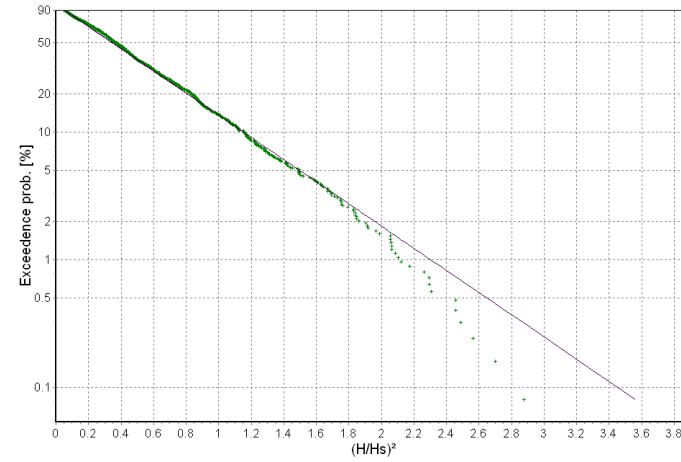
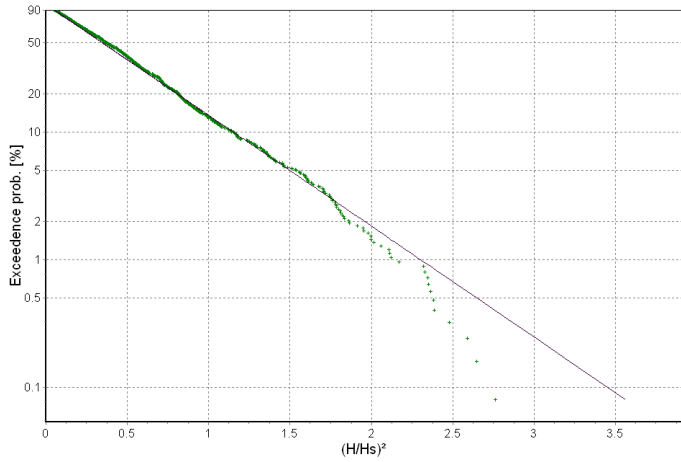
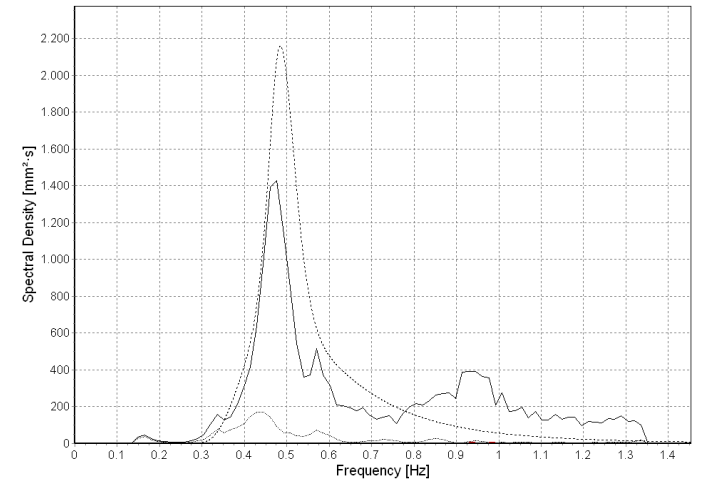
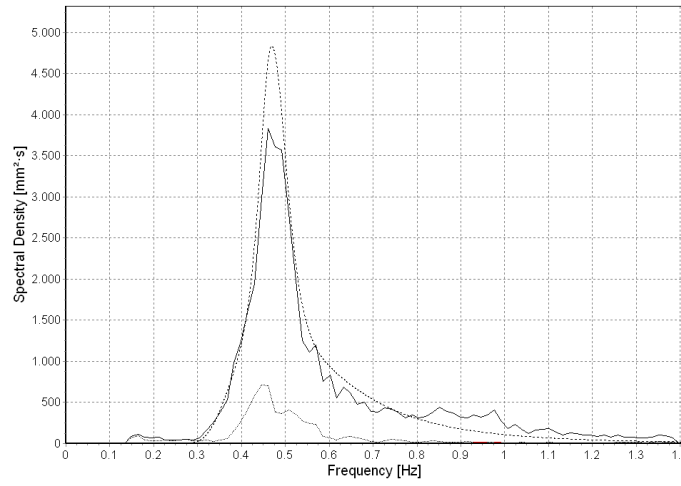
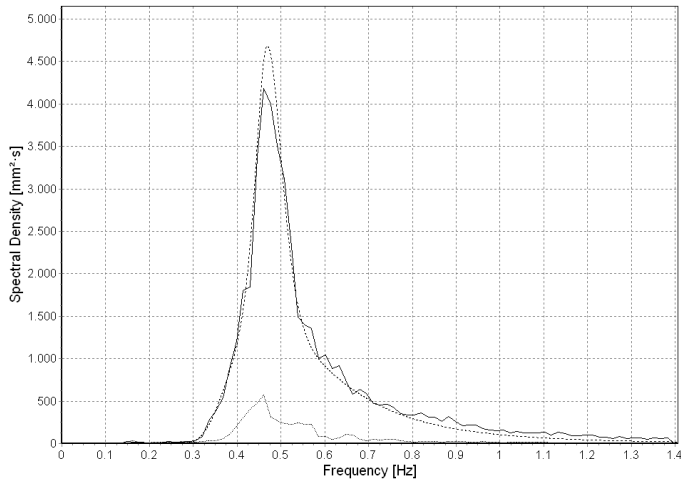


• Measured Incident — Rayleigh Incident

• Measured Incident — Rayleigh Incident

• Measured Incident — Rayleigh Incident

BI_2_1

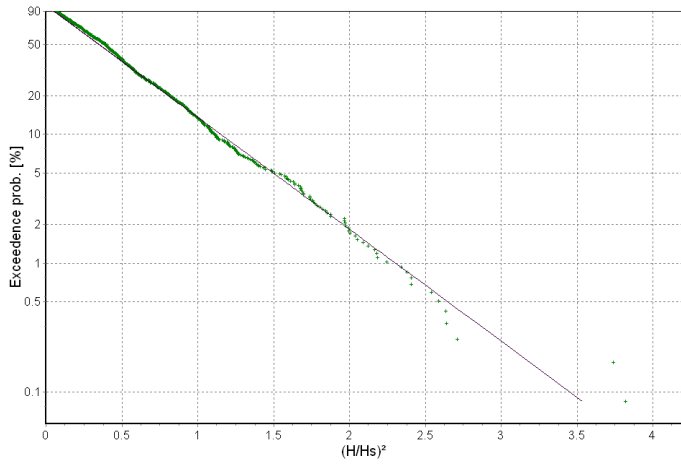
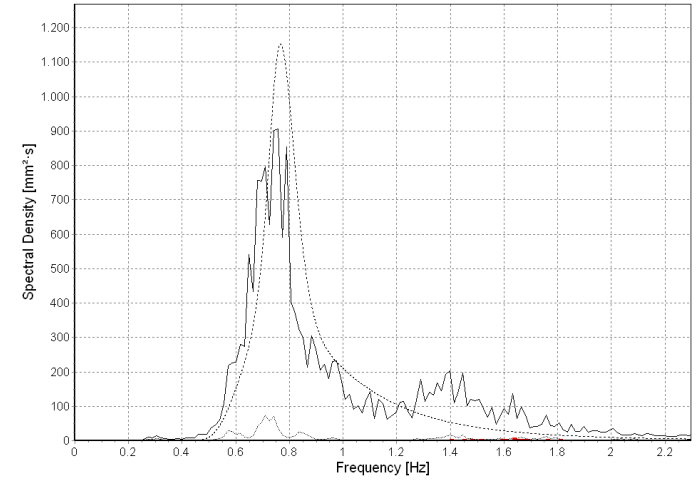
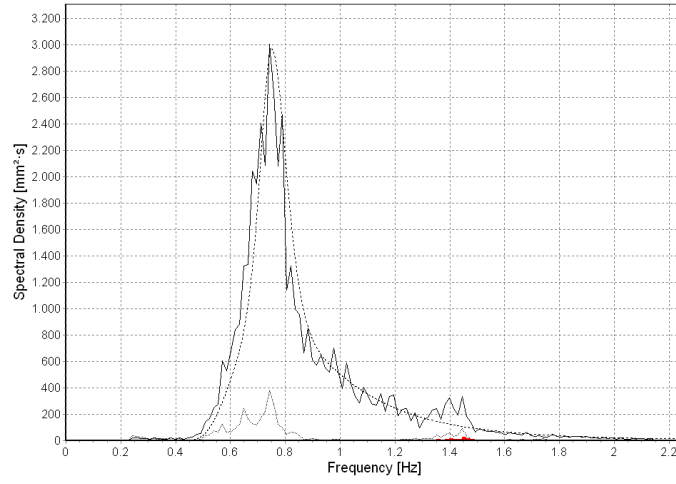
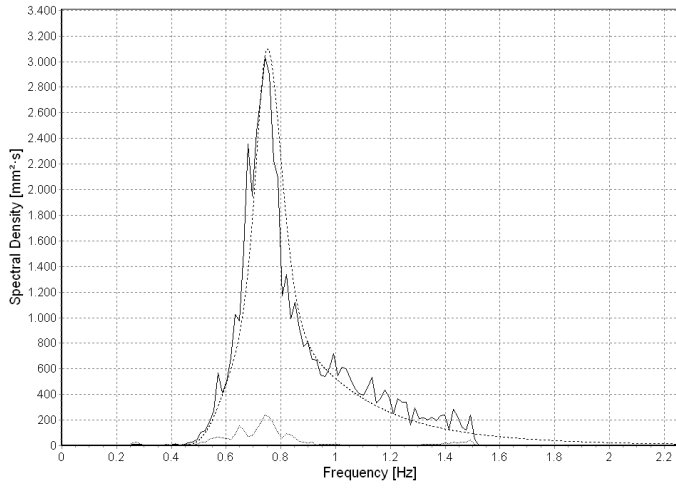


• Measured Incident — Rayleigh Incident

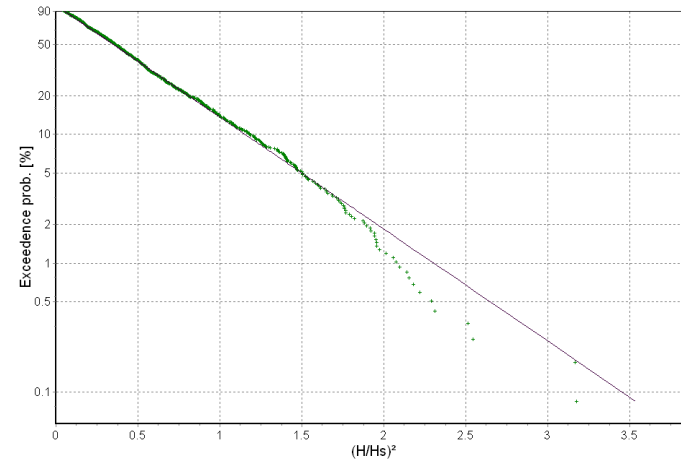
• Measured Incident — Rayleigh Incident

• Measured Incident — Rayleigh Incident

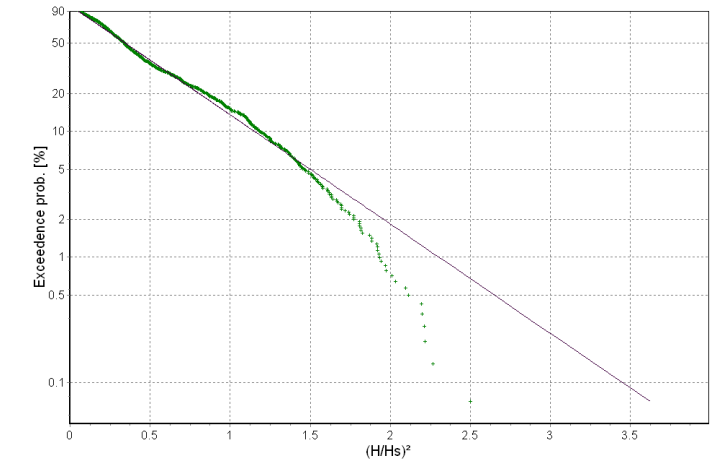
BI_4_1



• Measured Incident — Rayleigh Incident

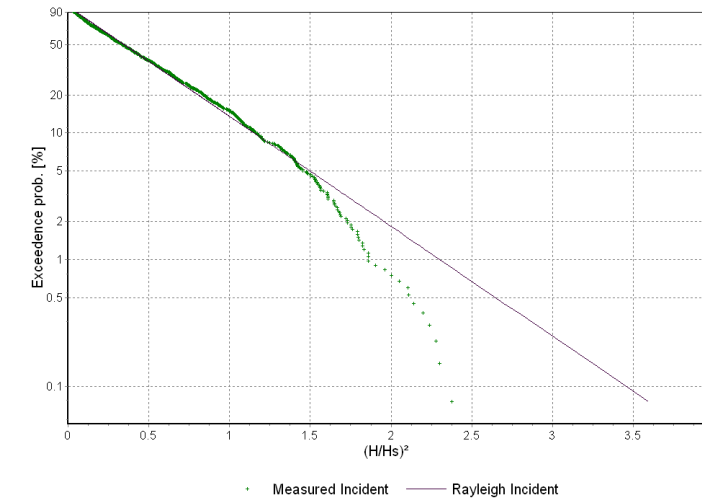
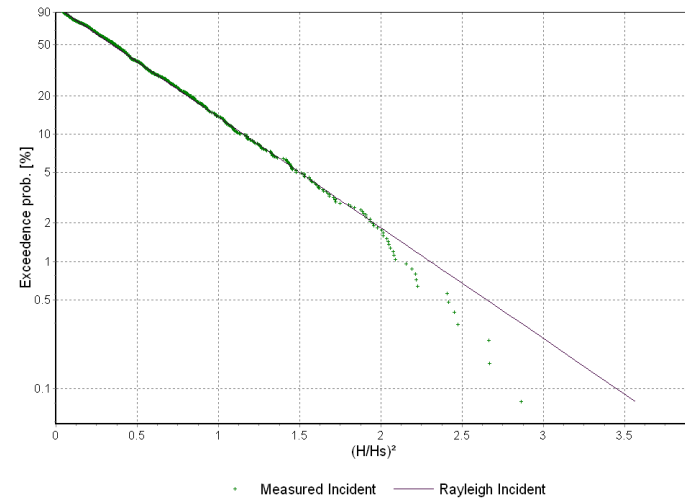
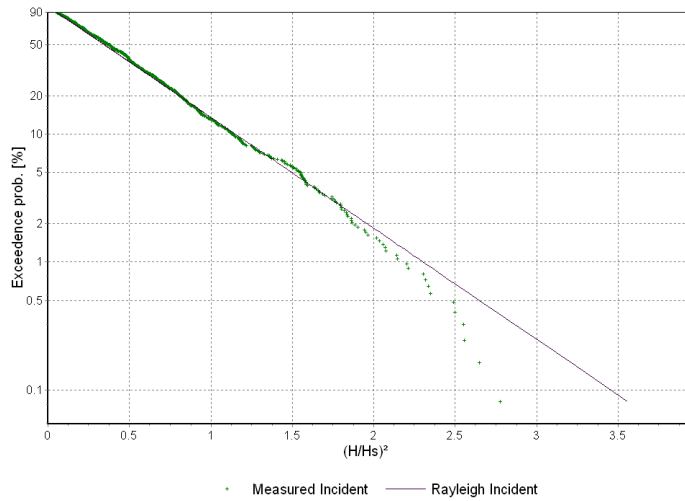
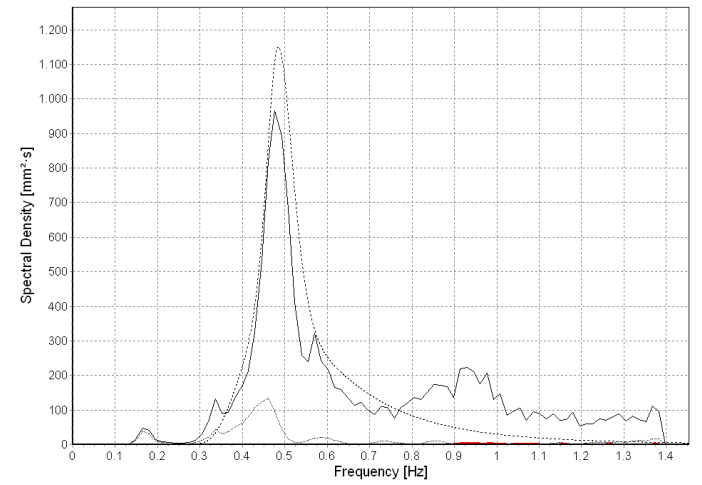
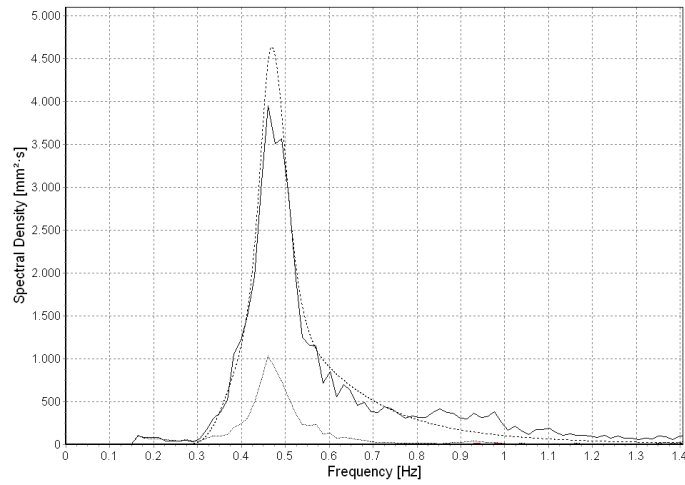
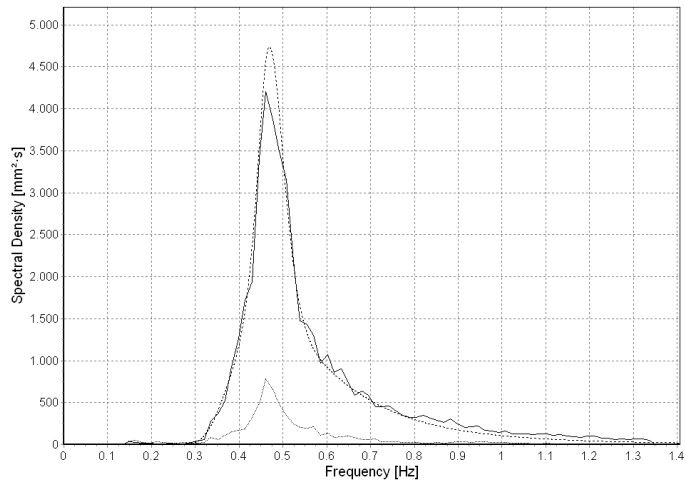


• Measured Incident — Rayleigh Incident

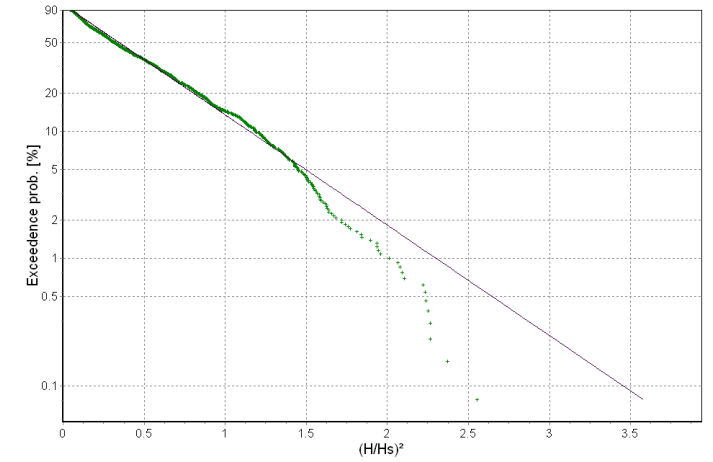
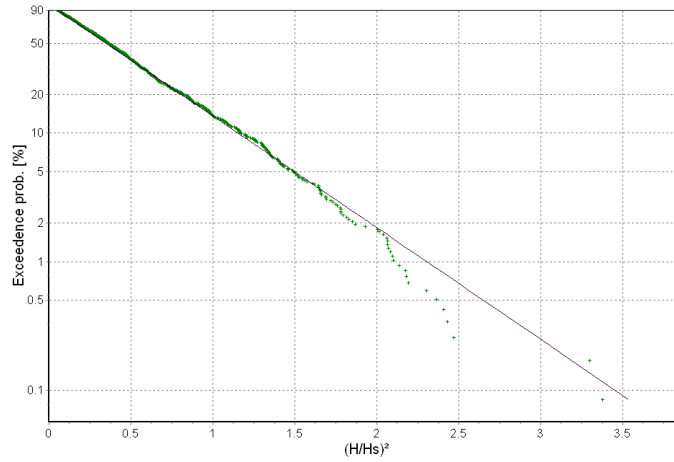
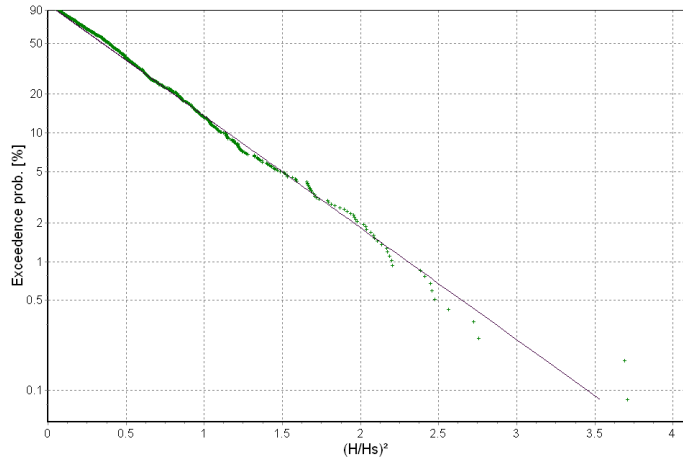
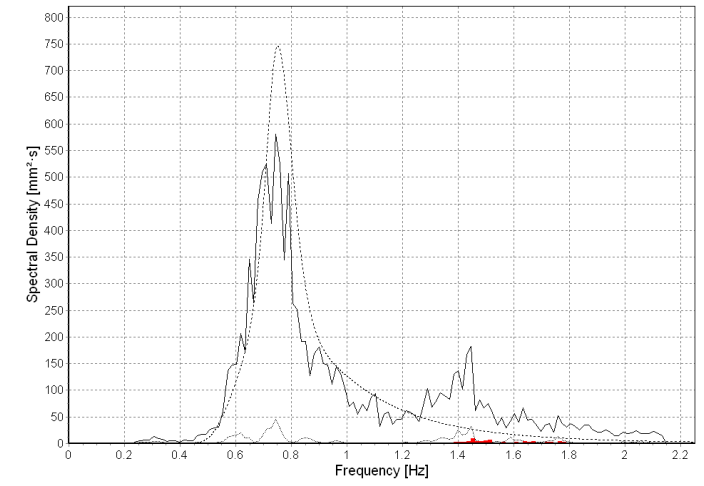
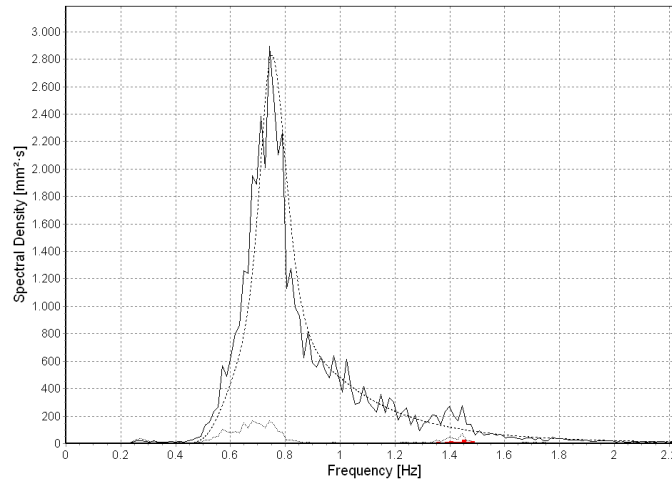
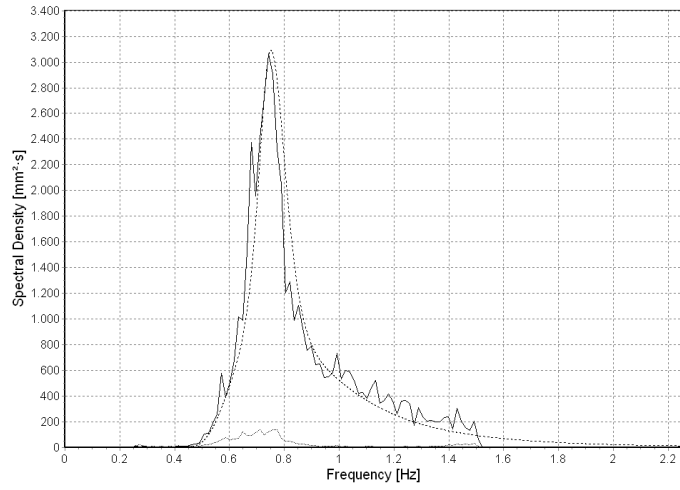


• Measured Incident — Rayleigh Incident

CI_2_1



CI_4_1

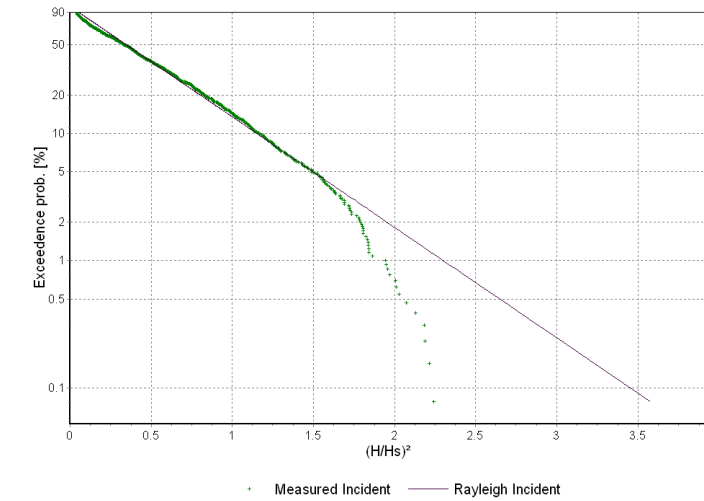
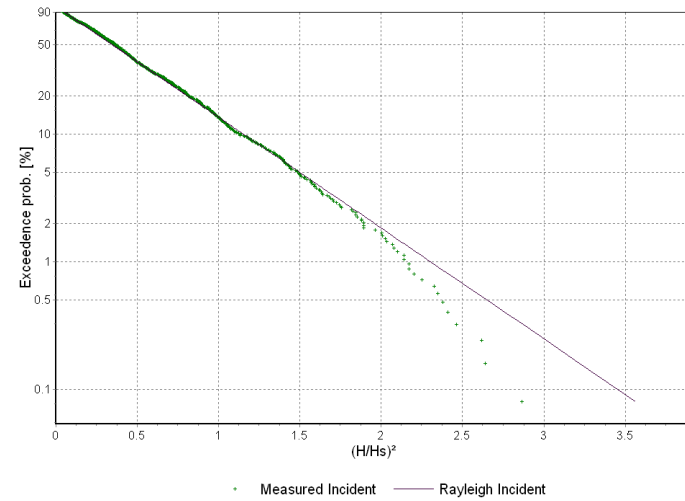
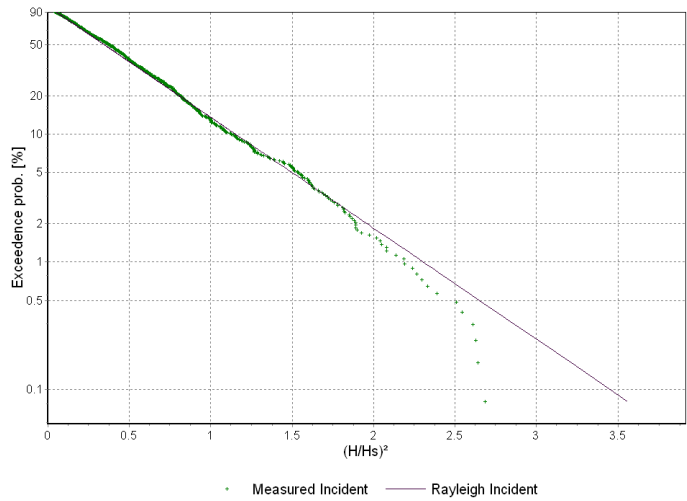
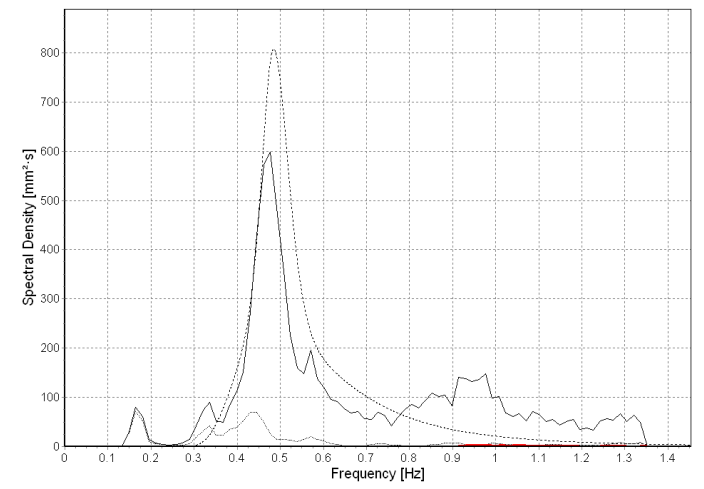
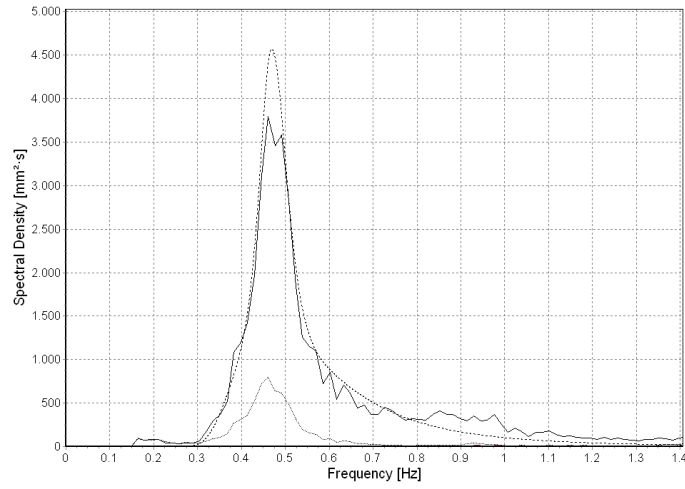
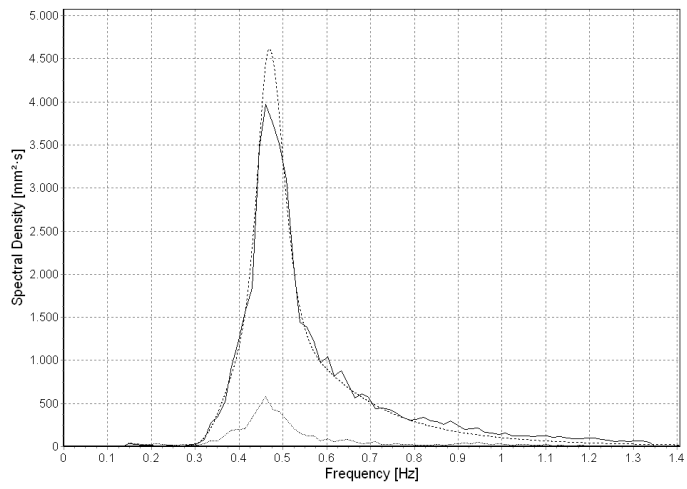


• Measured Incident — Rayleigh Incident

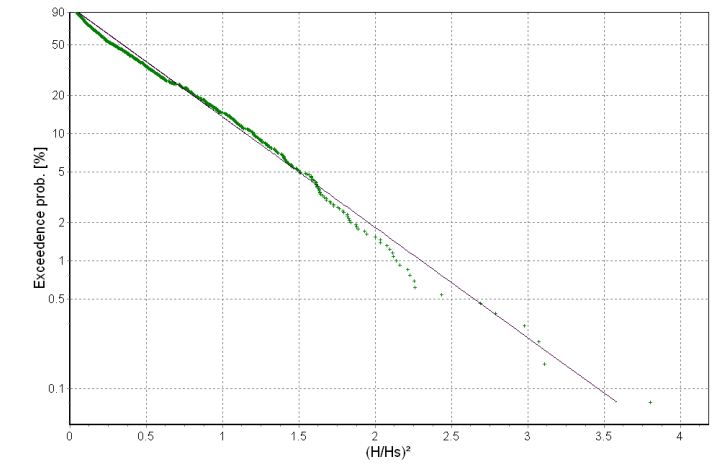
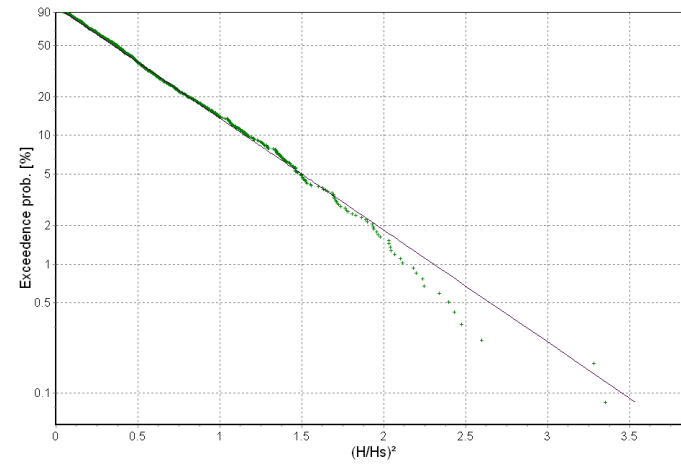
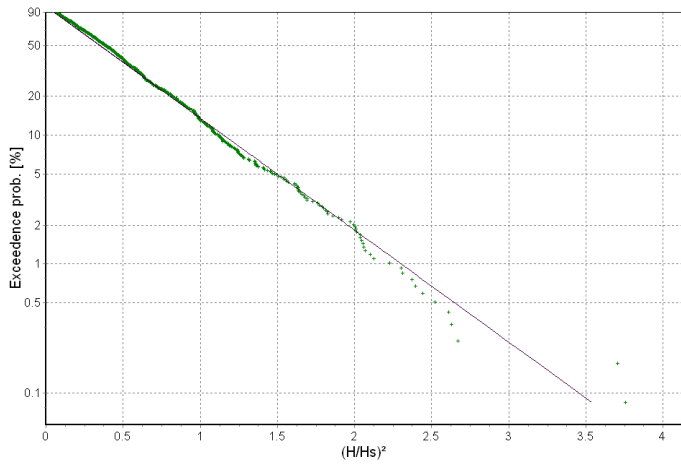
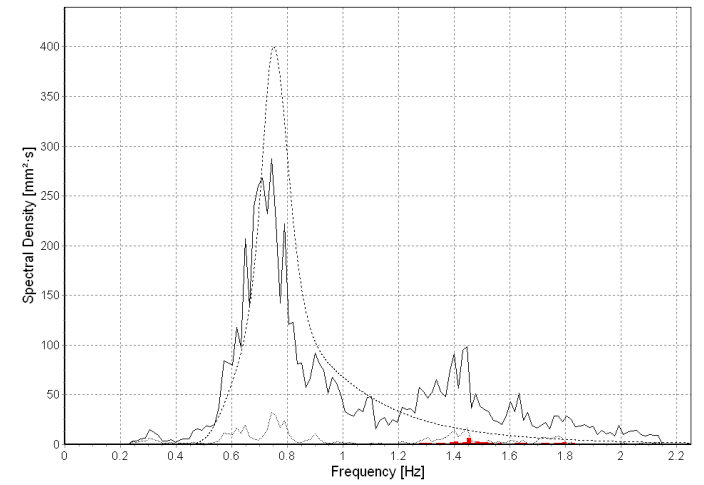
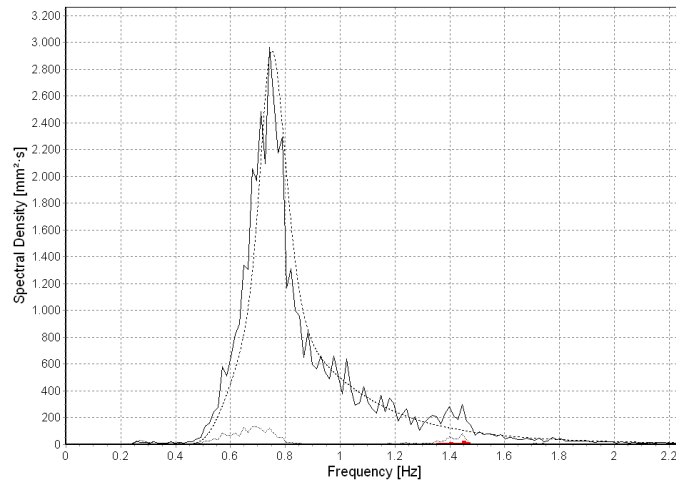
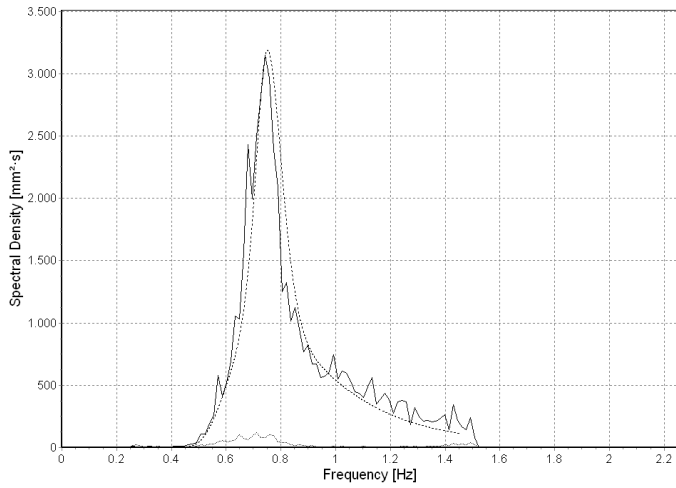
• Measured Incident — Rayleigh Incident

• Measured Incident — Rayleigh Incident

CII_2



CII_4

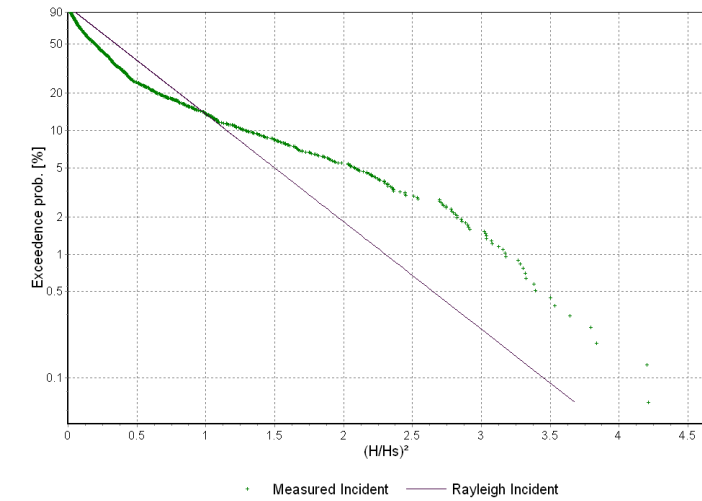
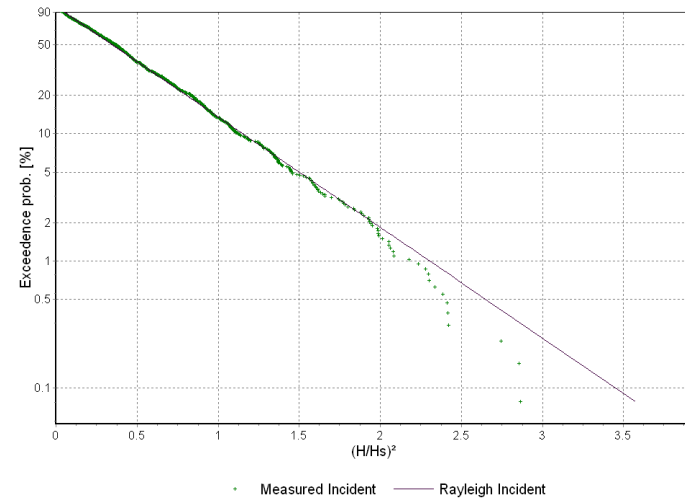
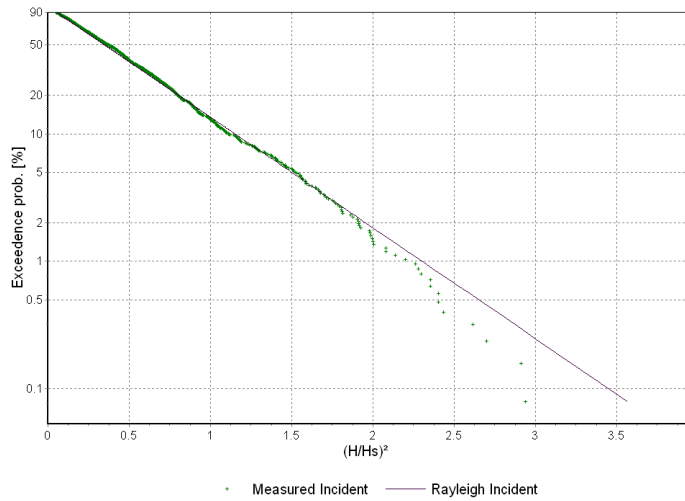
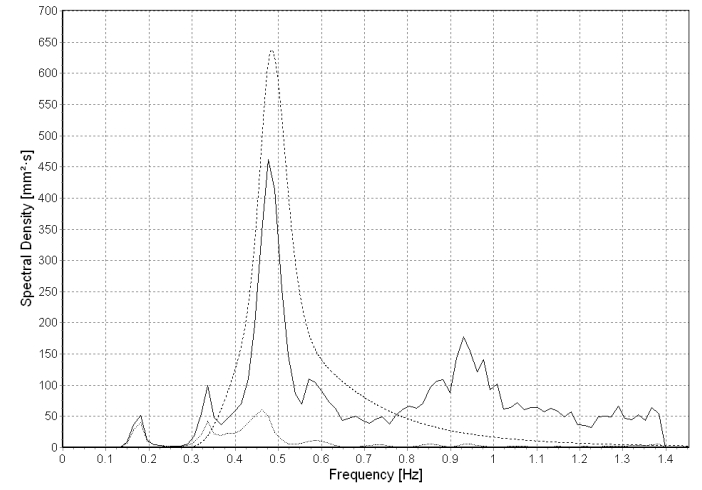
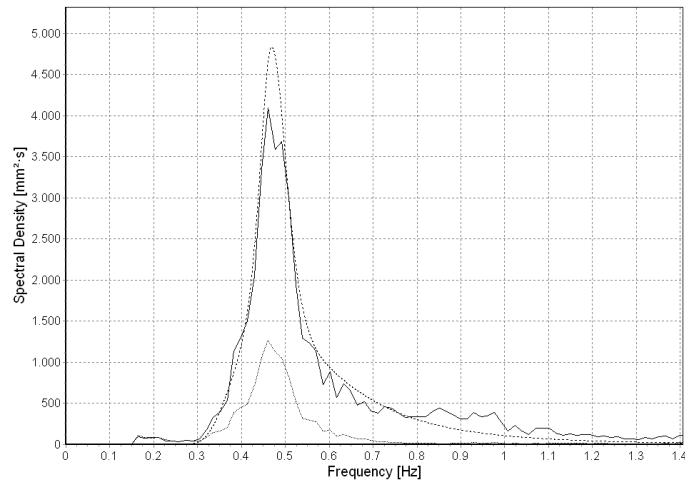
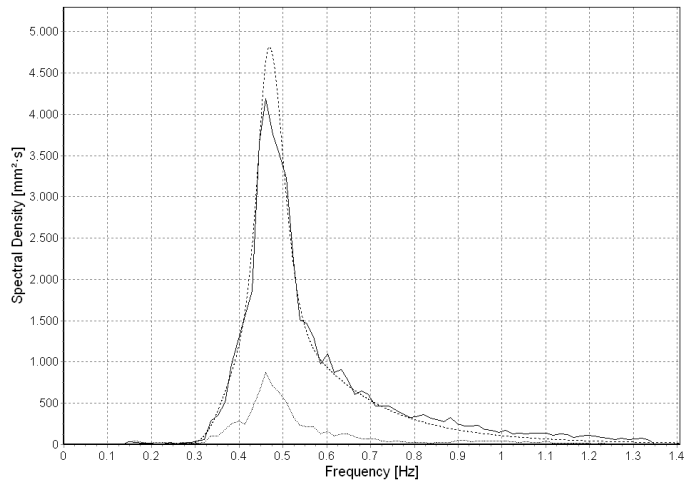


• Measured Incident — Rayleigh Incident

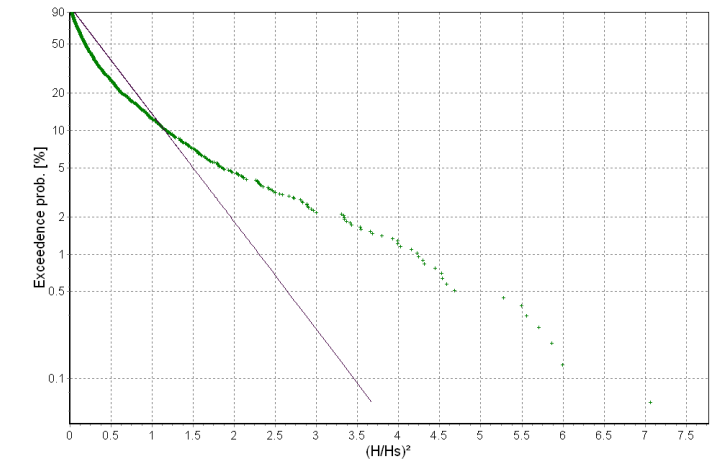
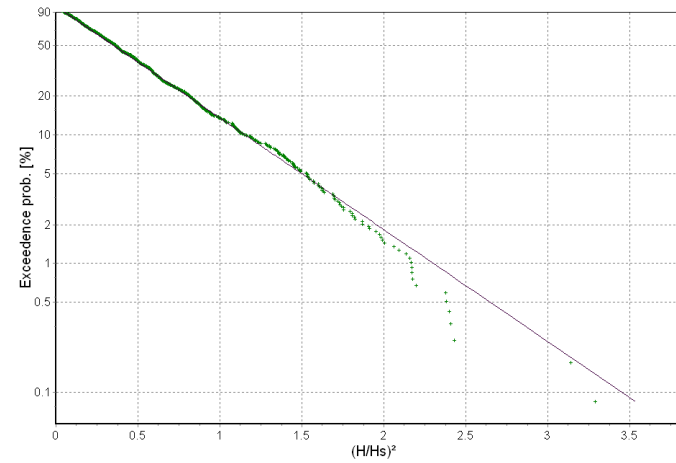
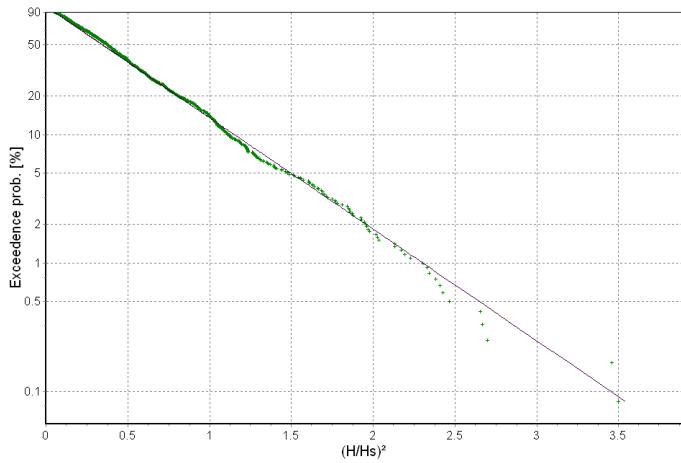
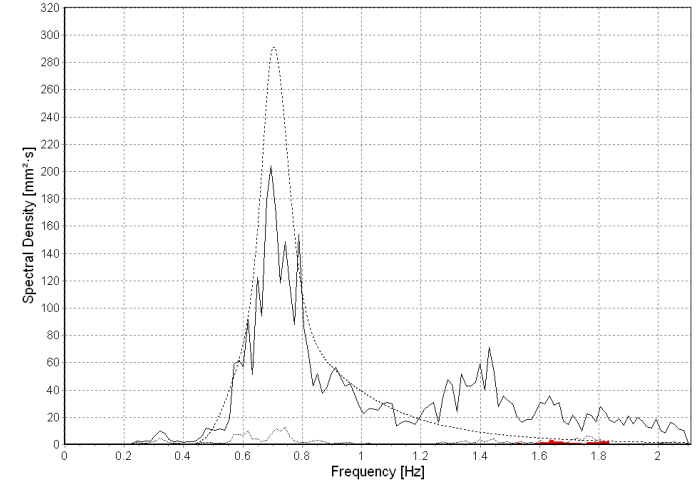
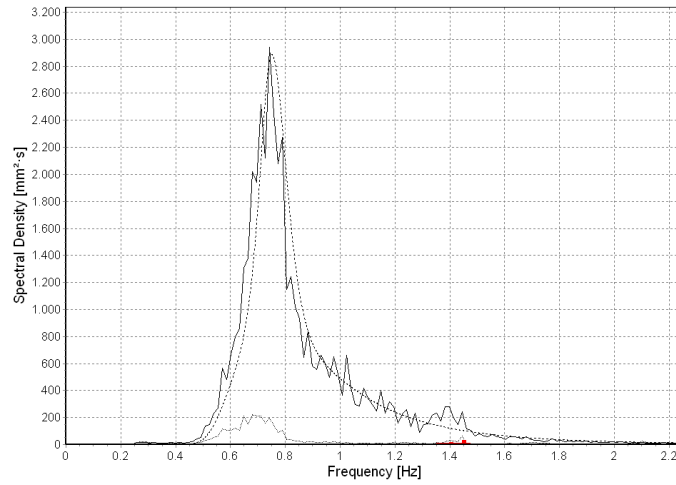
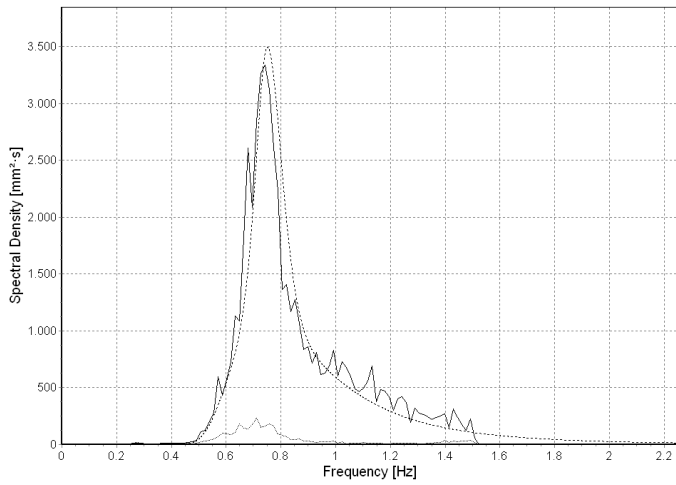
• Measured Incident — Rayleigh Incident

• Measured Incident — Rayleigh Incident

DI_2



DI_4

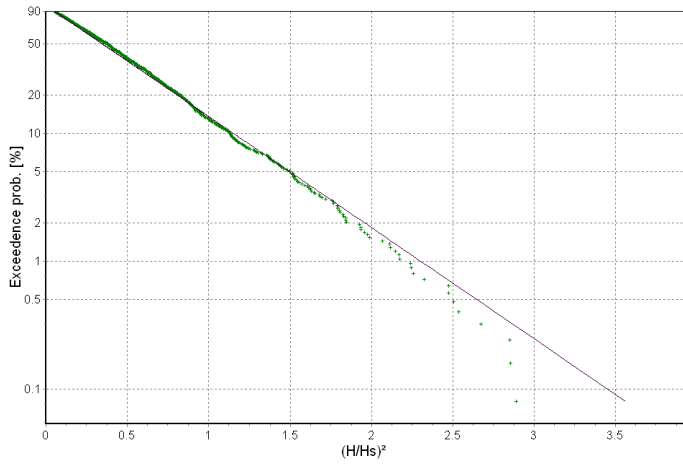
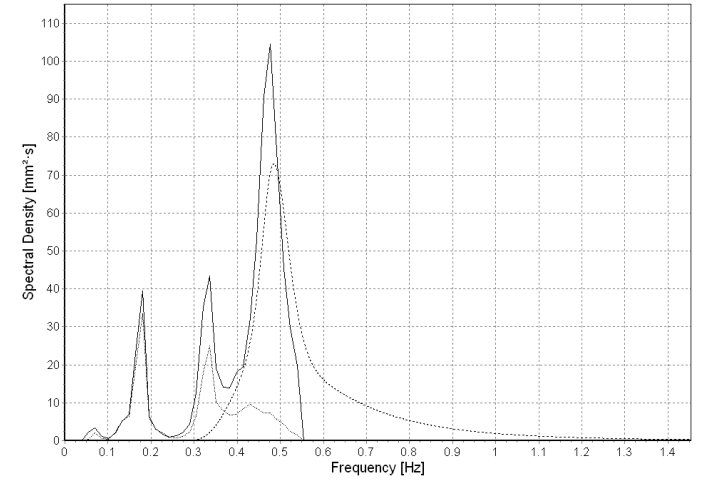
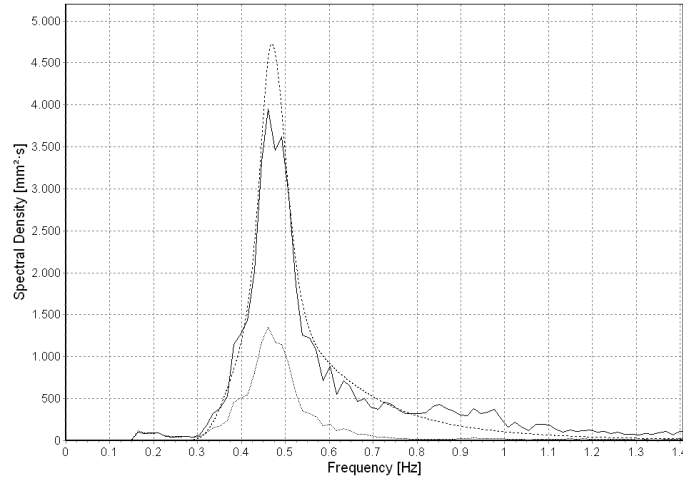
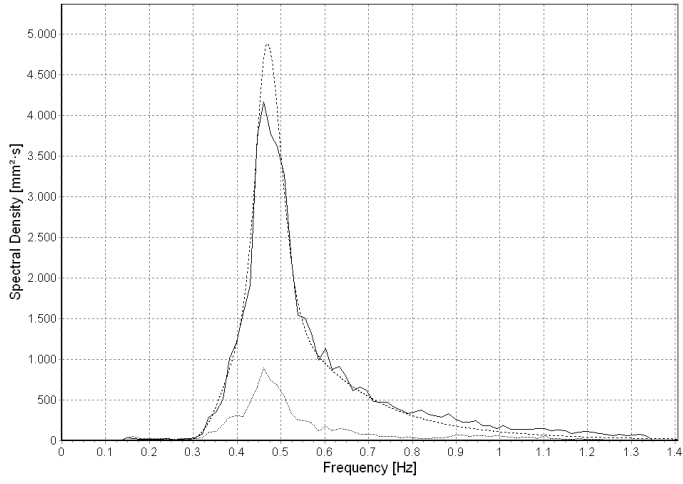


• Measured Incident — Rayleigh Incident

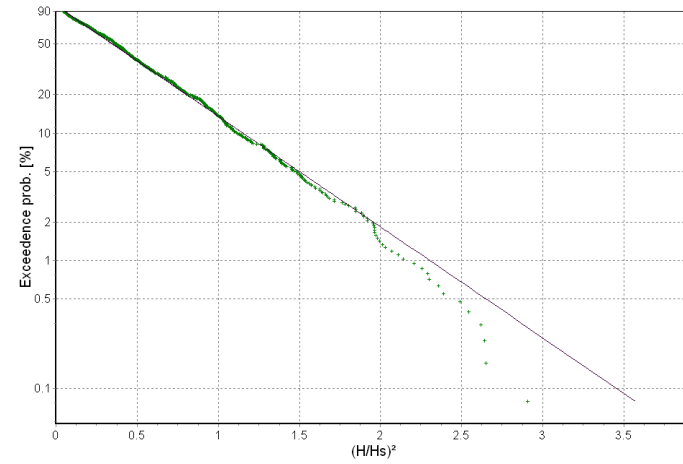
• Measured Incident — Rayleigh Incident

• Measured Incident — Rayleigh Incident

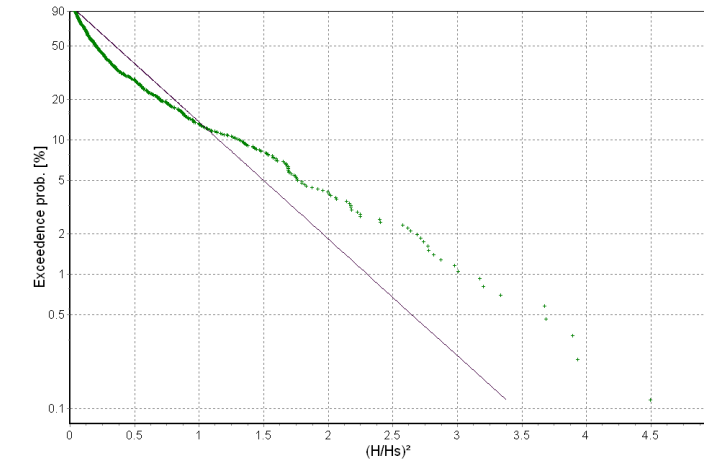
DII_2



• Measured Incident — Rayleigh Incident

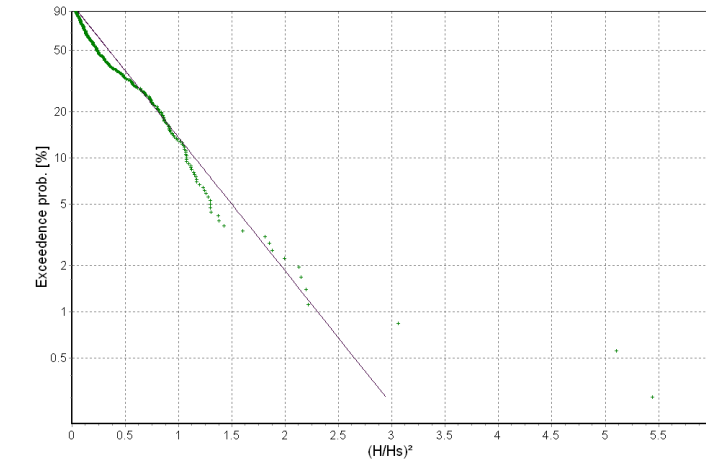
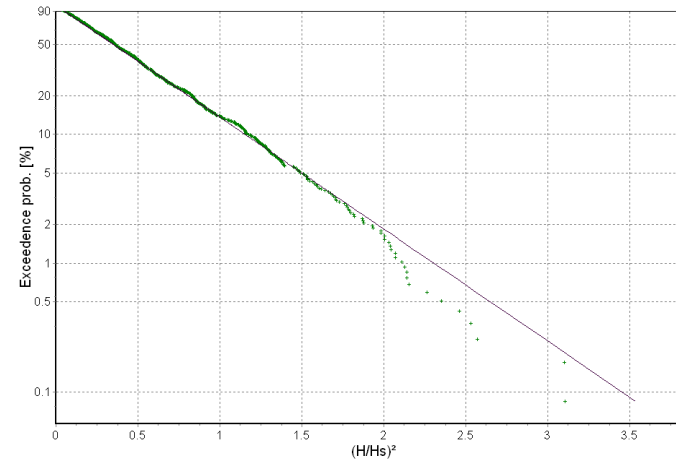
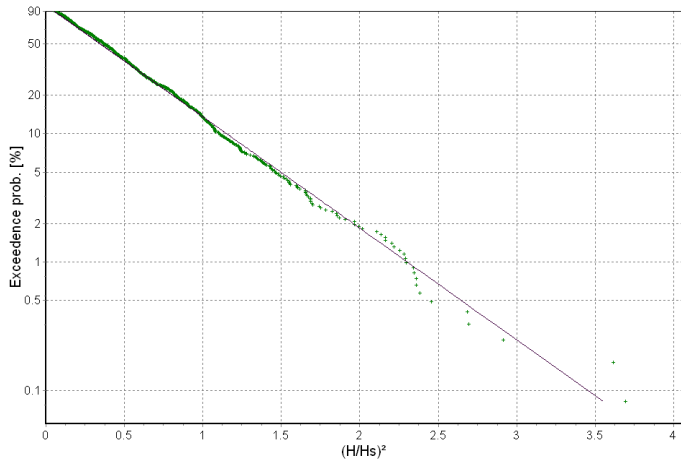
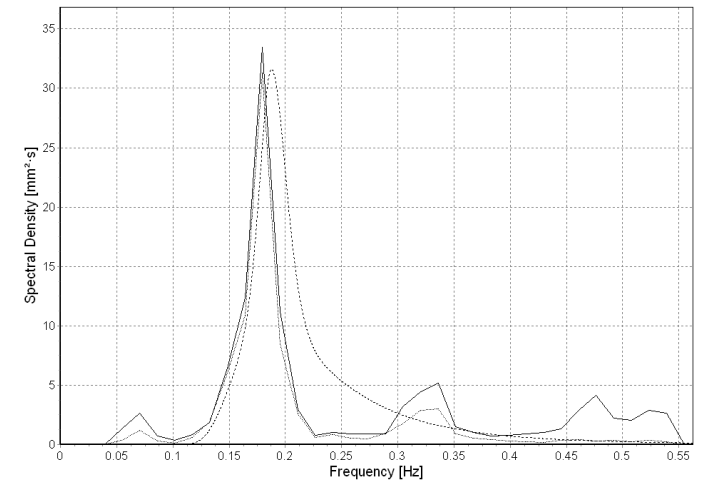
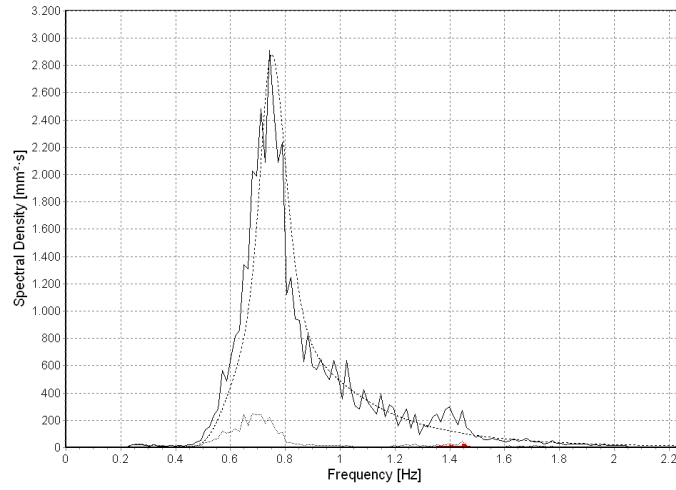
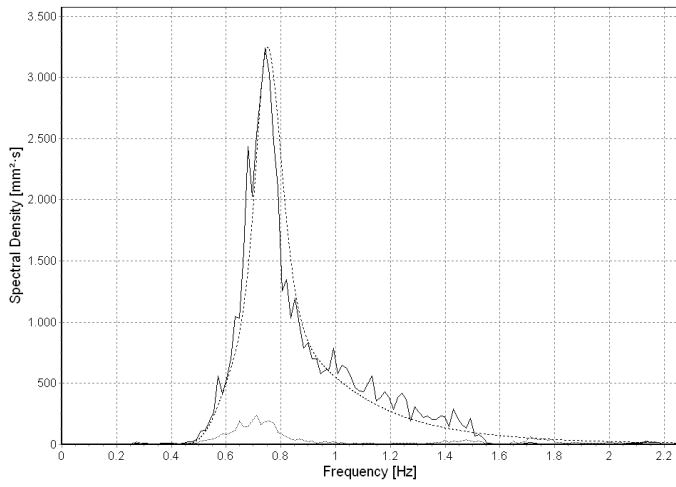


• Measured Incident — Rayleigh Incident



• Measured Incident — Rayleigh Incident

DII_4

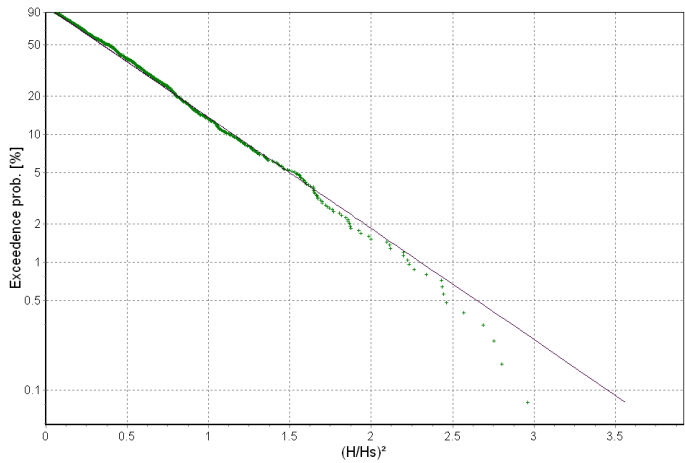
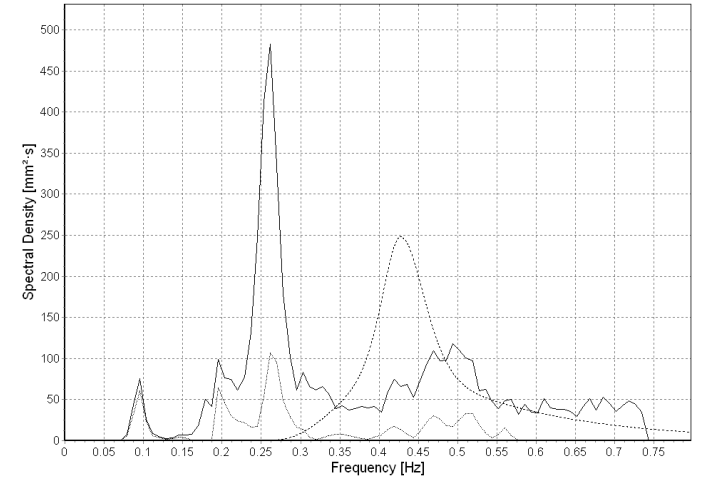
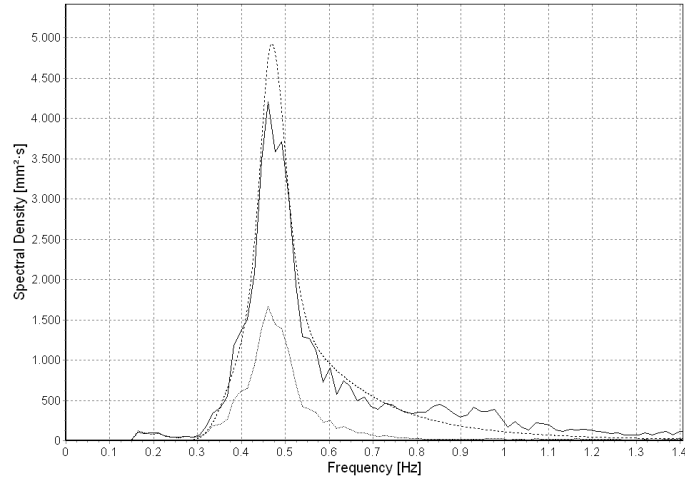
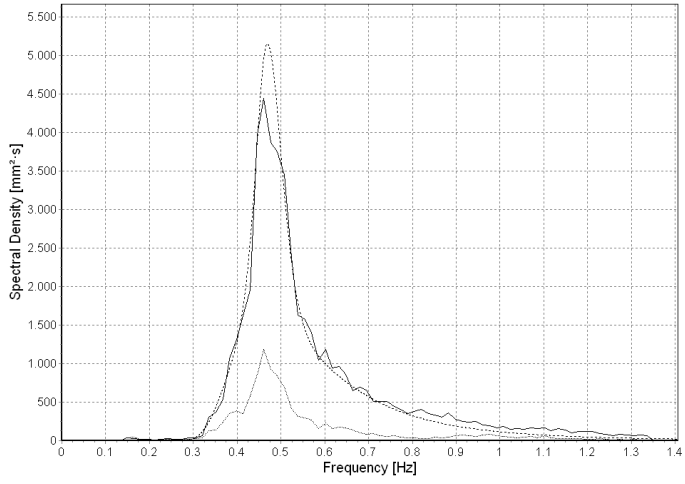


• Measured Incident — Rayleigh Incident

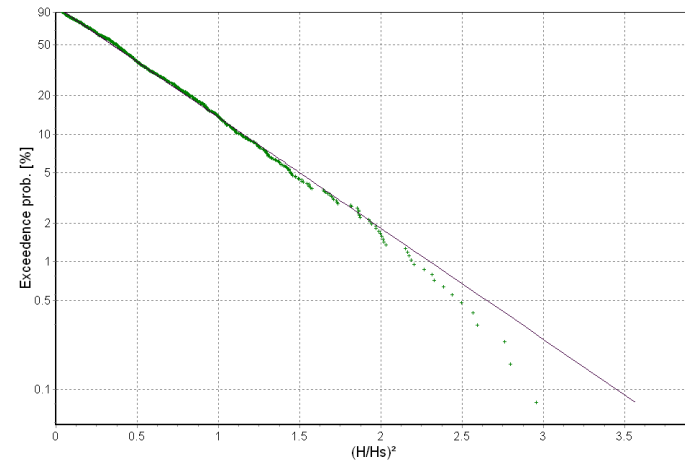
• Measured Incident — Rayleigh Incident

• Measured Incident — Rayleigh Incident

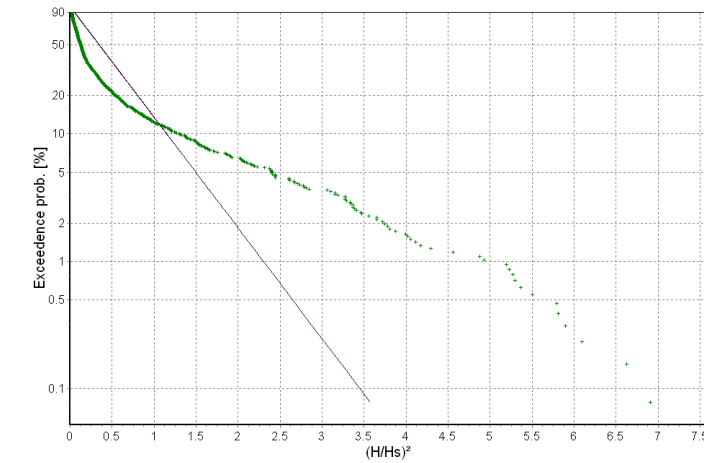
EI_2



• Measured Incident — Rayleigh Incident

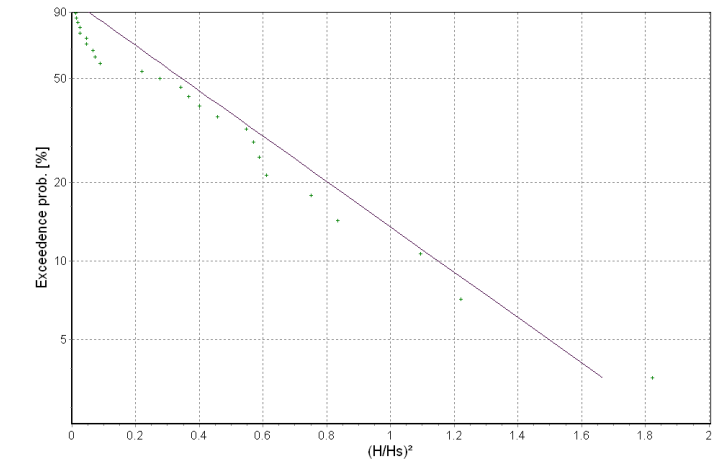
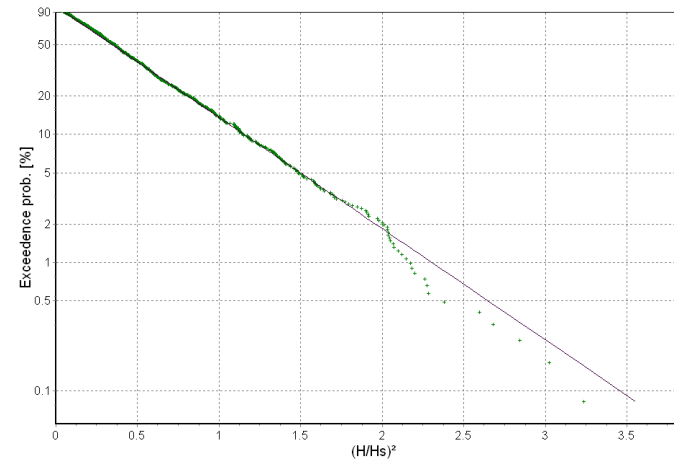
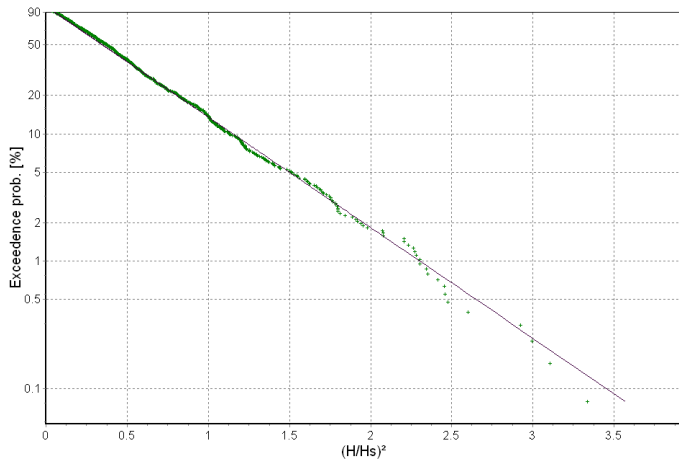
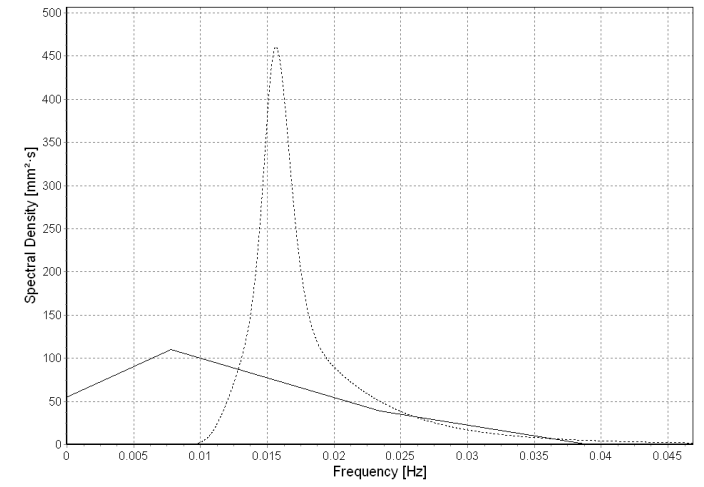
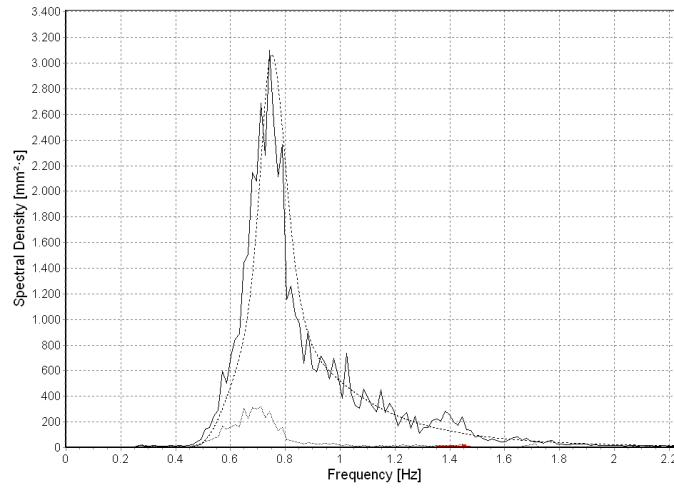
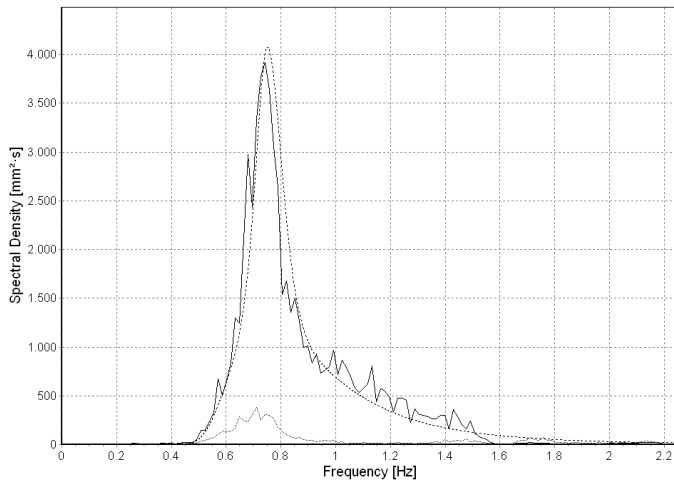


• Measured Incident — Rayleigh Incident



• Measured Incident — Rayleigh Incident

EI_4



• Measured Incident — Rayleigh Incident

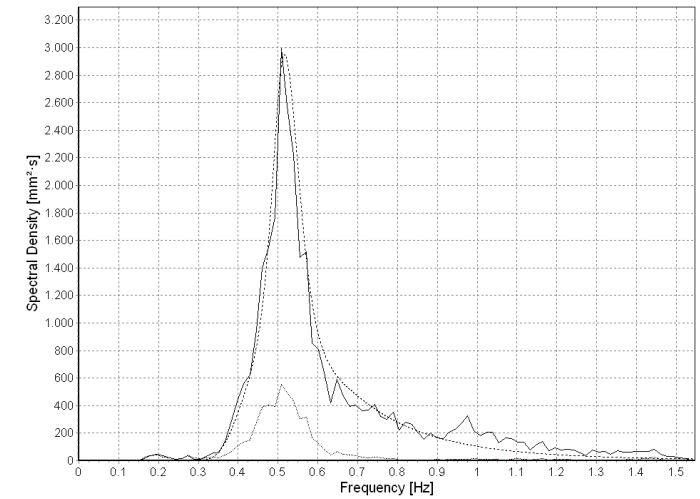
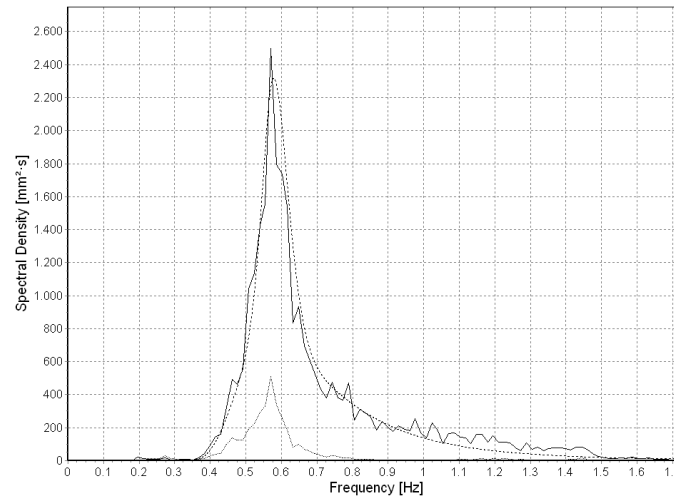
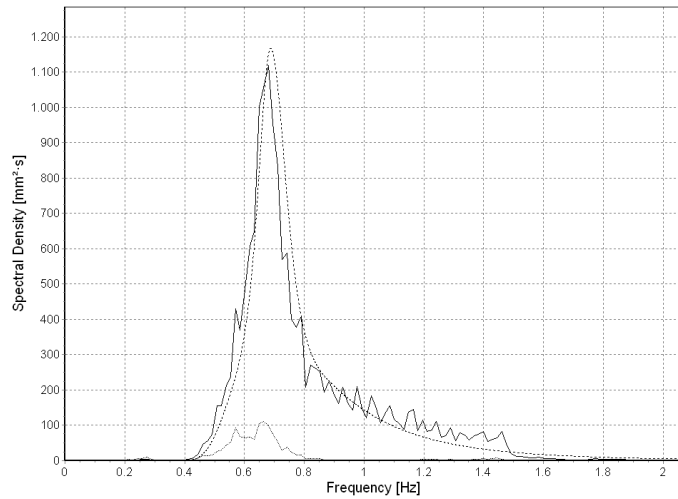
• Measured Incident — Rayleigh Incident

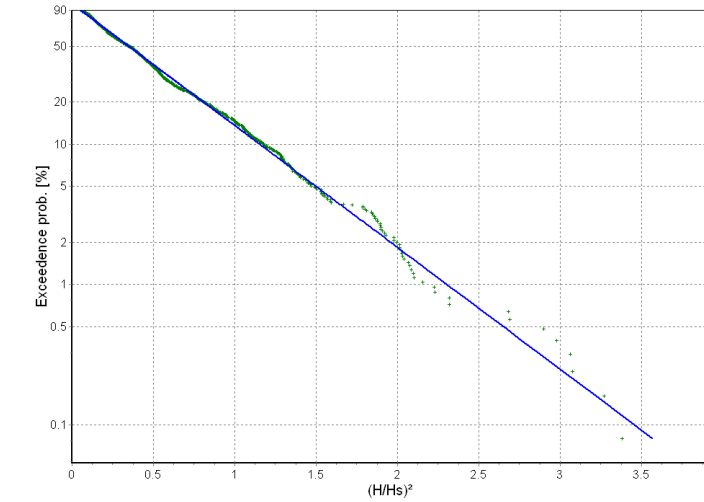
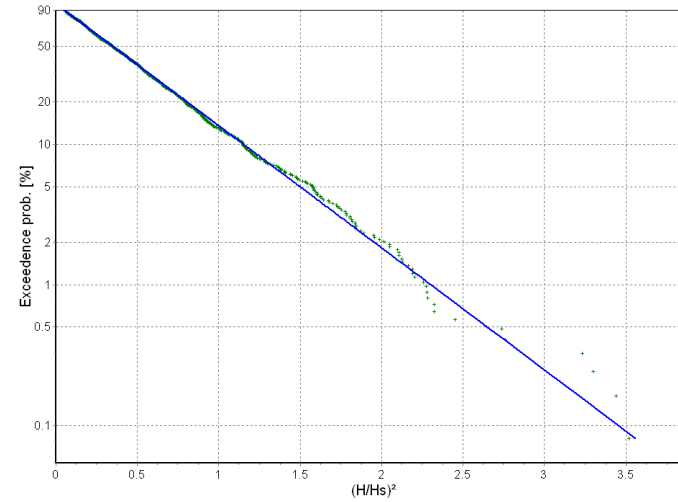
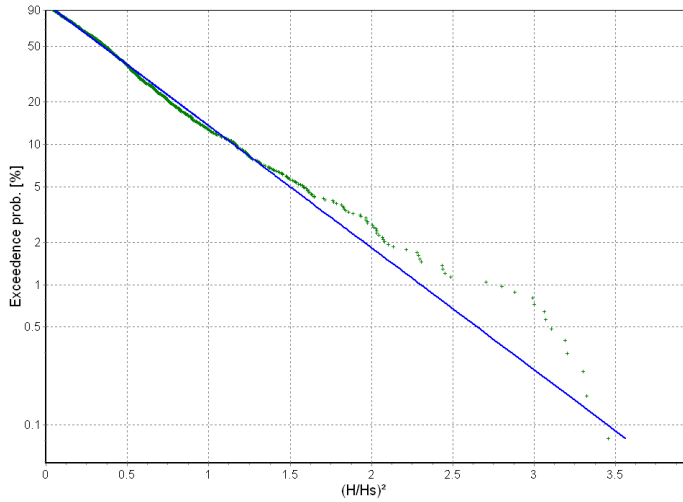
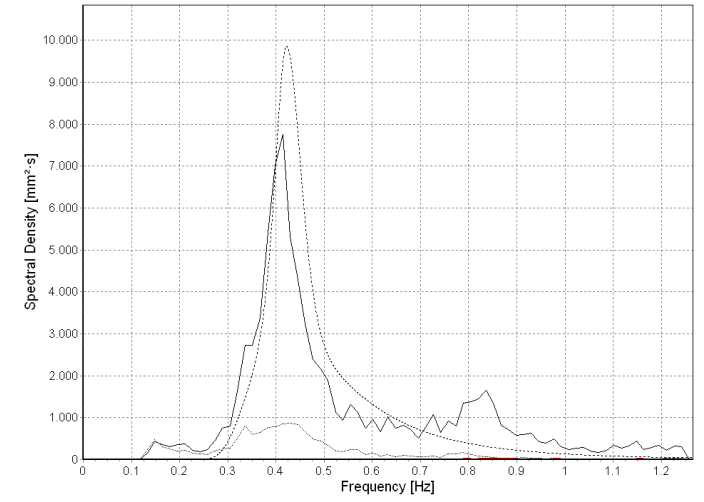
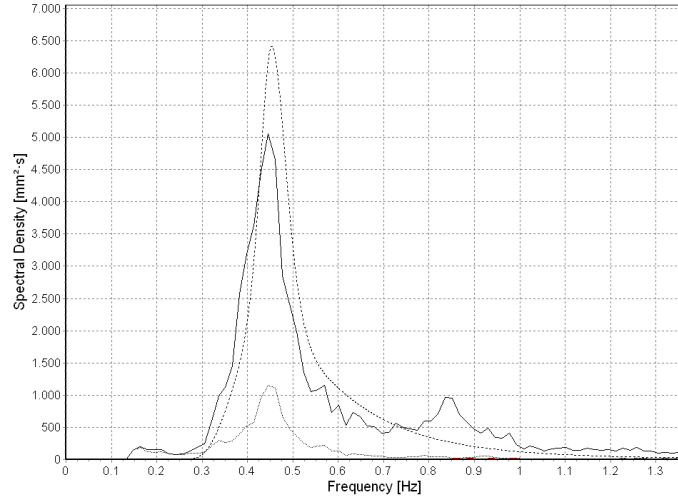
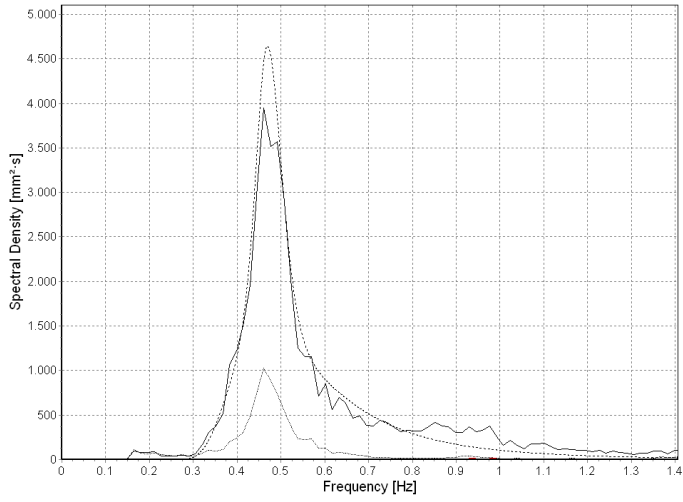
• Measured Incident — Rayleigh Incident

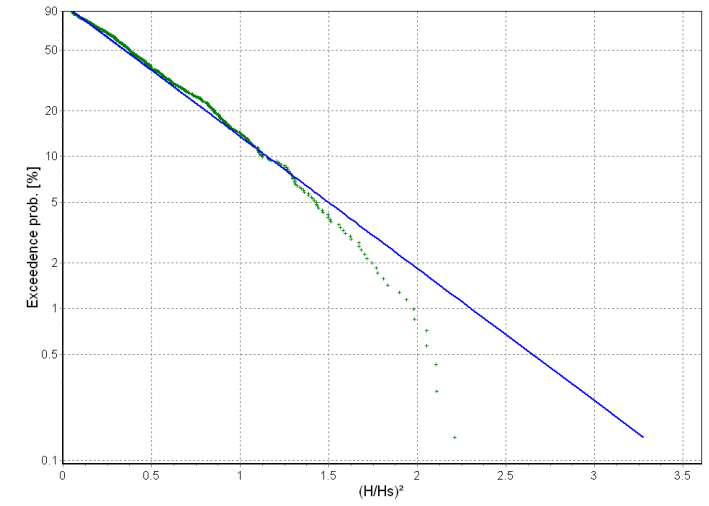
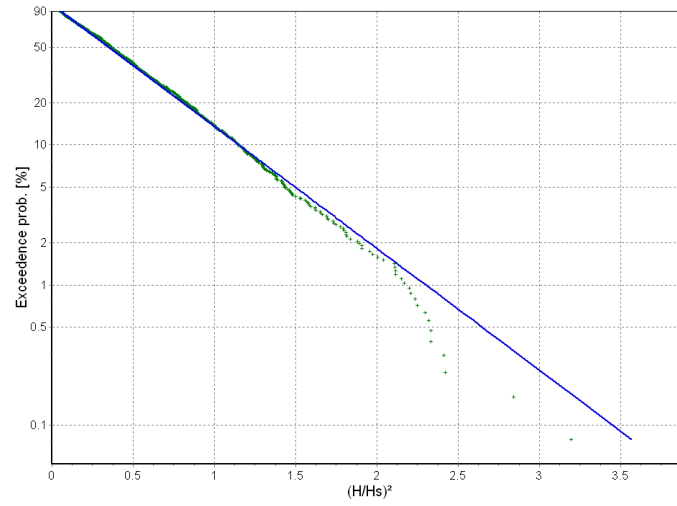
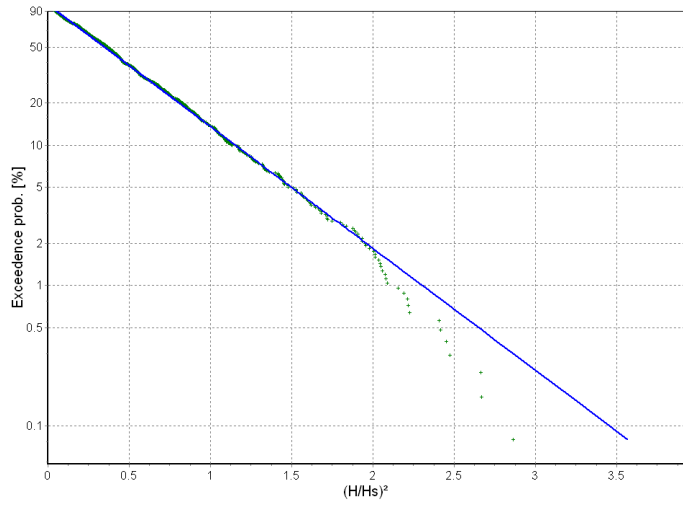
APPENDIX G

In this appendix the spectra and wave height distributions are plotted for one reference test series at the toe of the breakwater for increasing wave heights. For test series CI_2_1 plots are made for wave heights of 60% H_d up to 131% H_d and for CI_4_1 from 58% H_d up to 152% H_d .

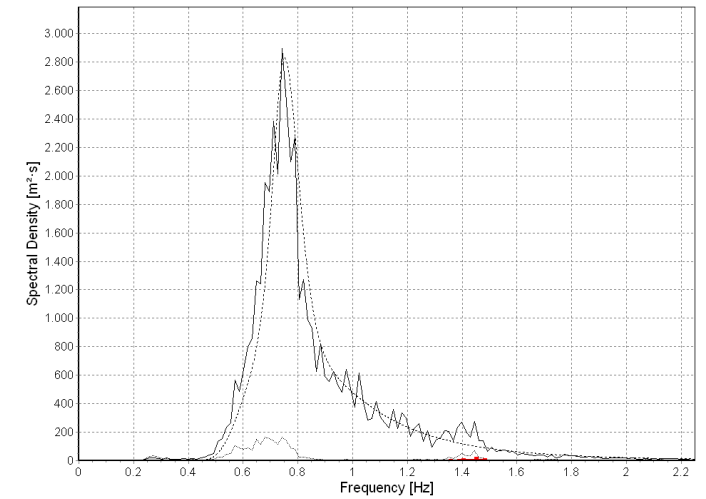
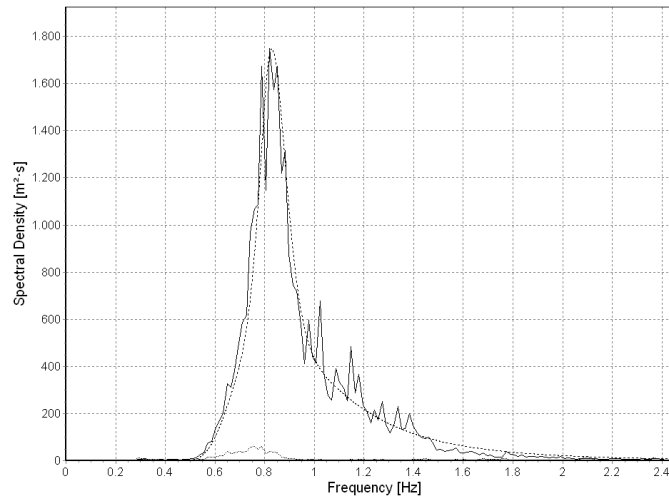
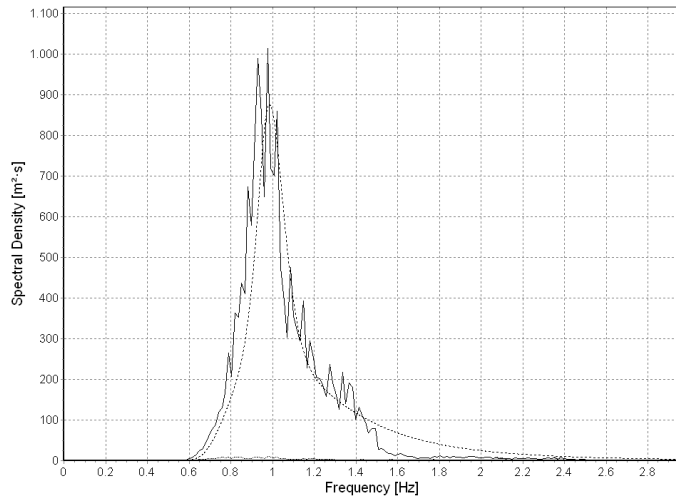
CI_2_1

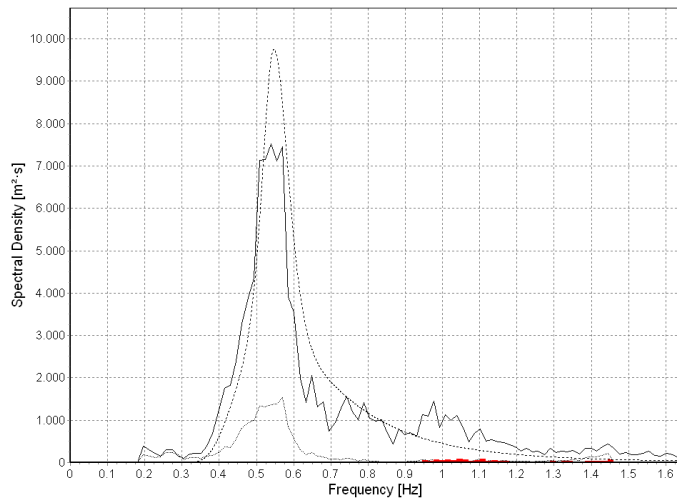
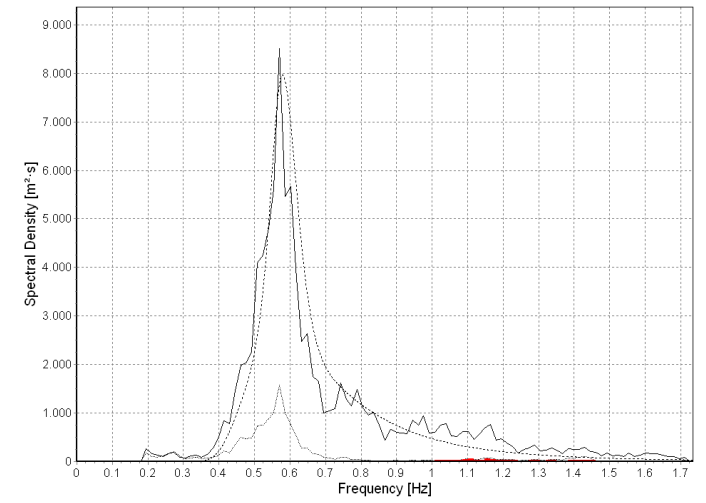
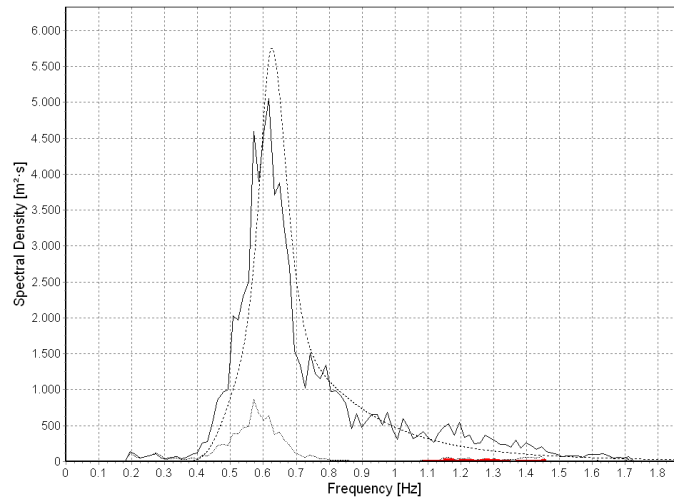
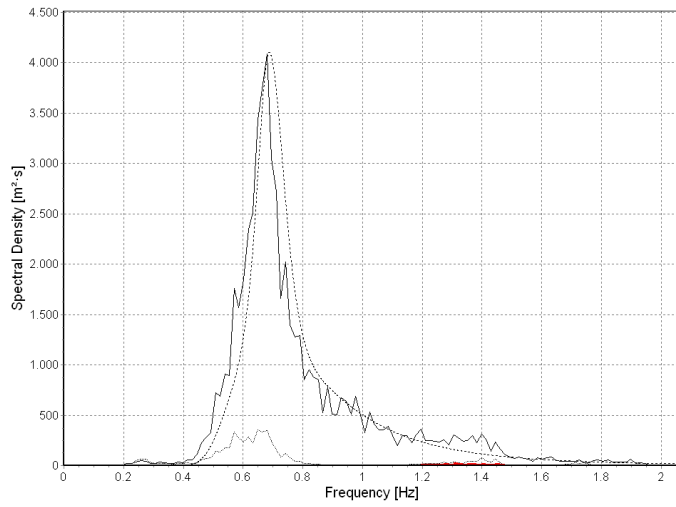


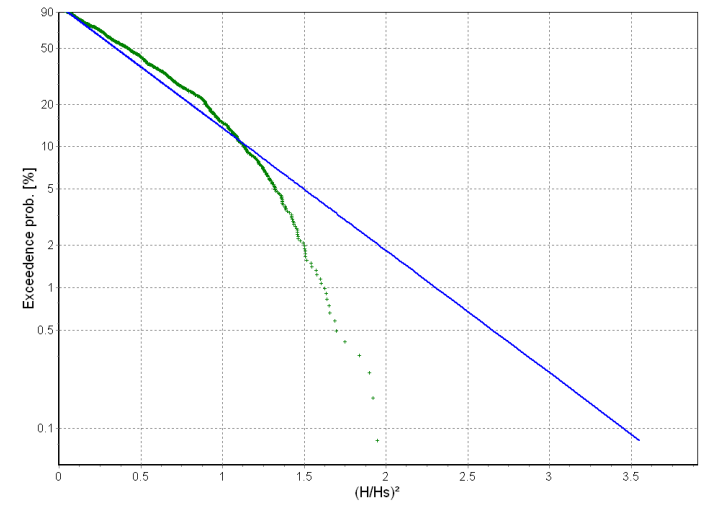
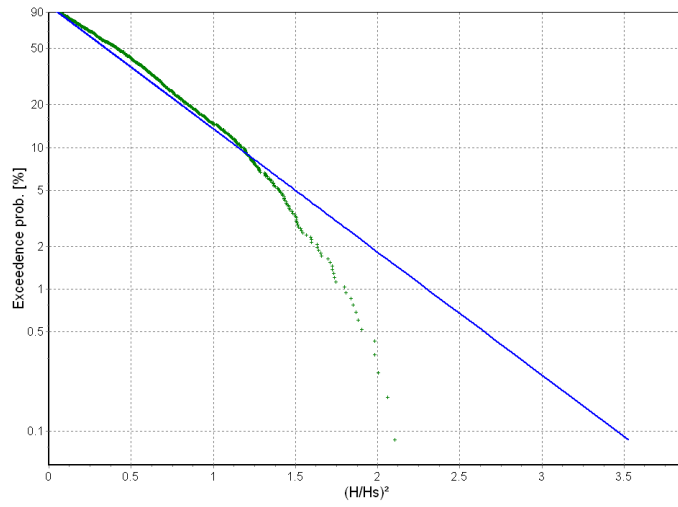
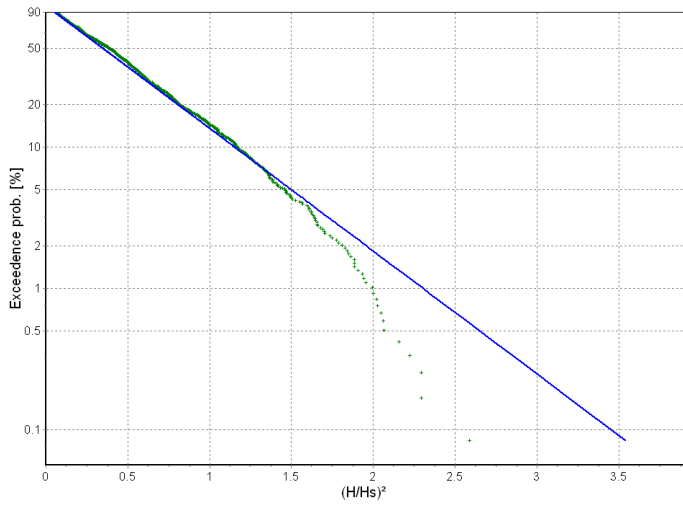
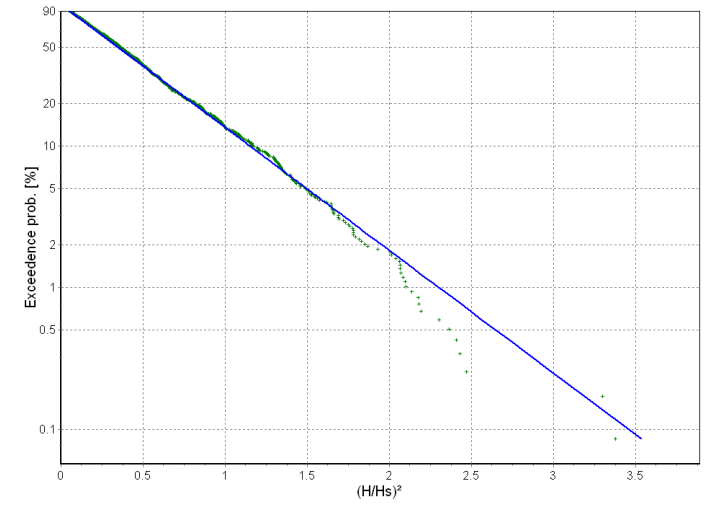
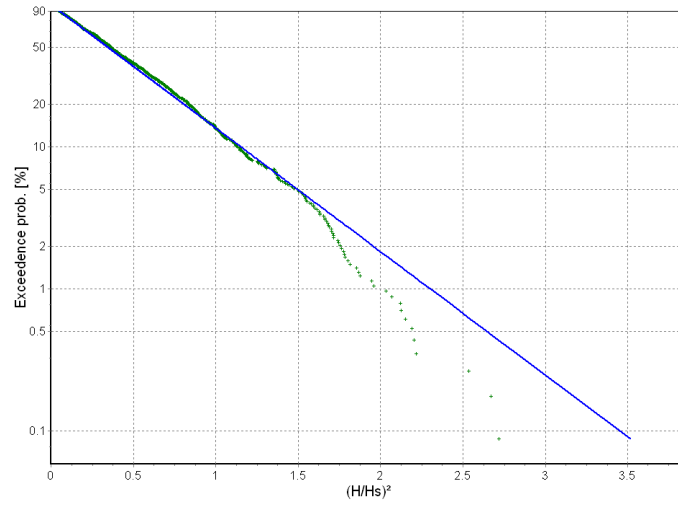
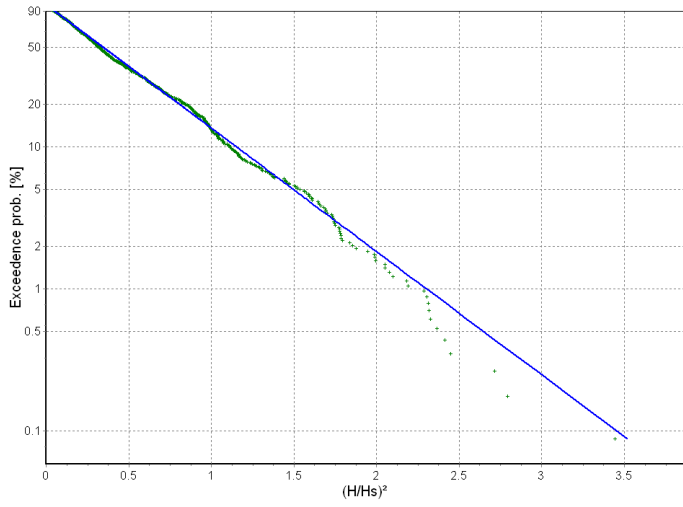




CI_4_1







Title

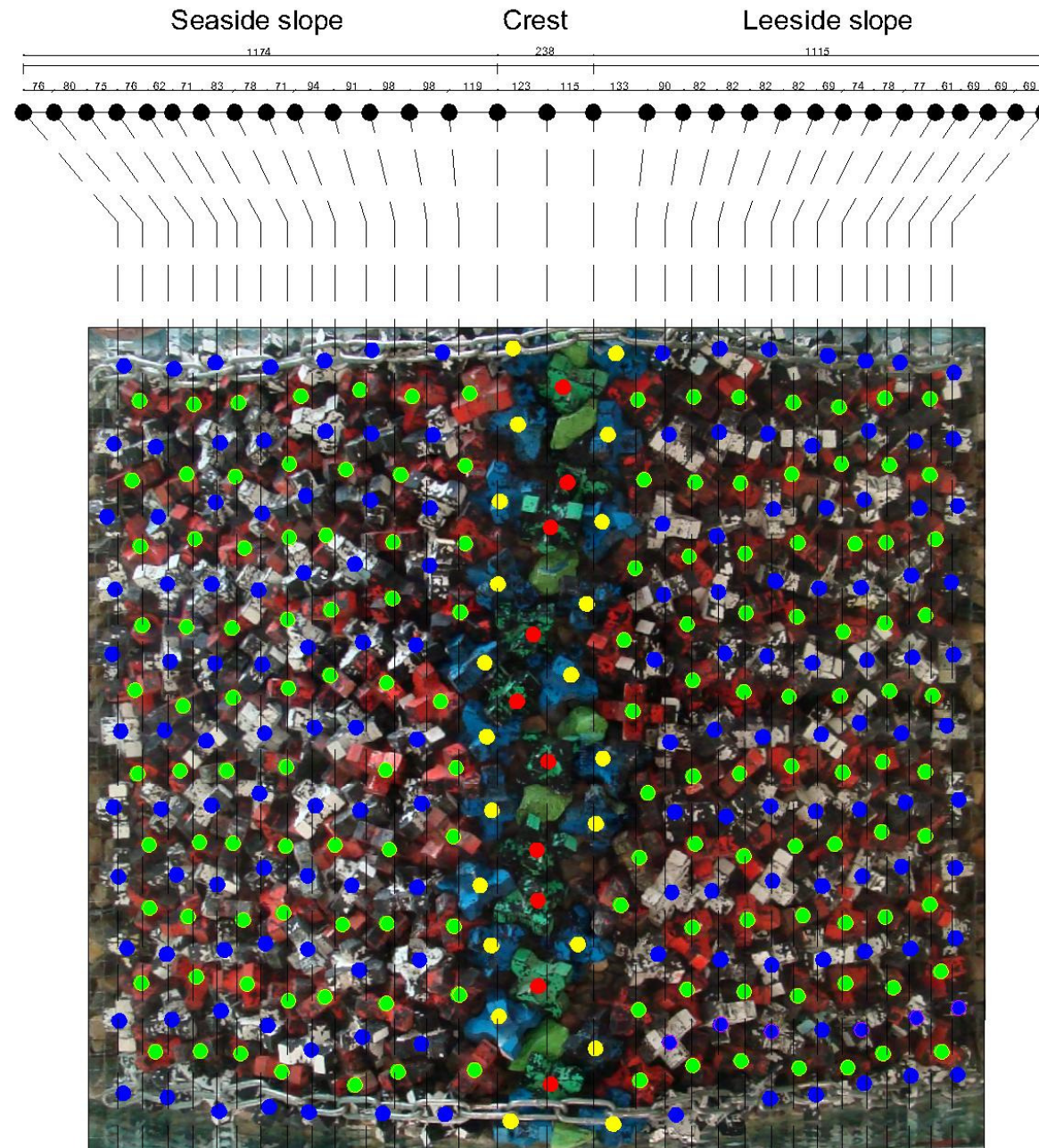
Stability of single layer armour units on low-crested structures

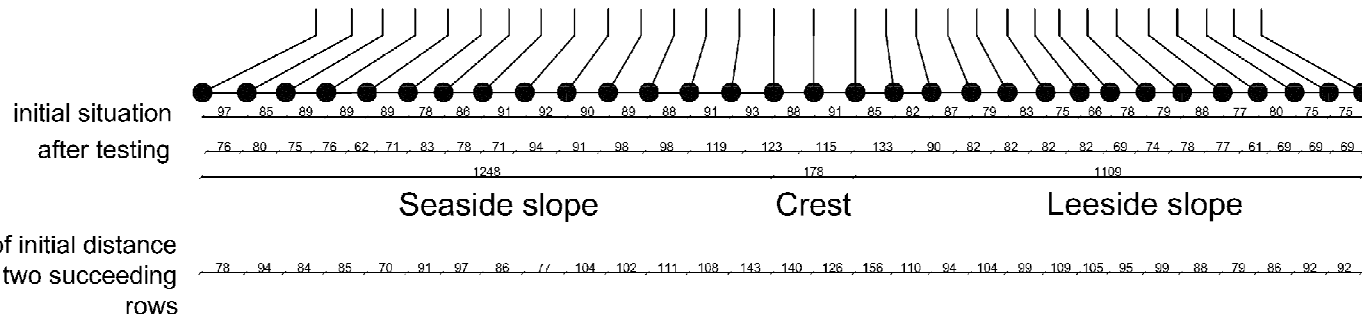
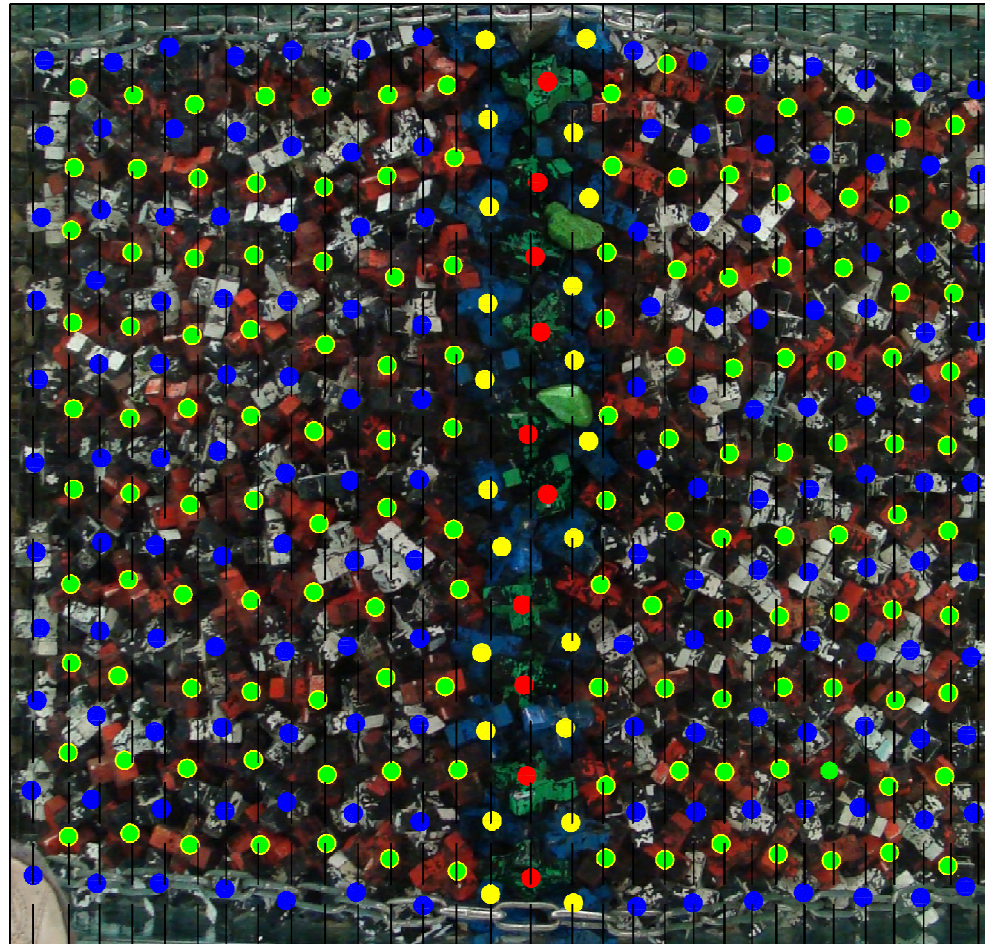
Waveheight distribution toevoegen 180%

Title

Stability of single layer armour units on low-crested structures

APPENDIX H





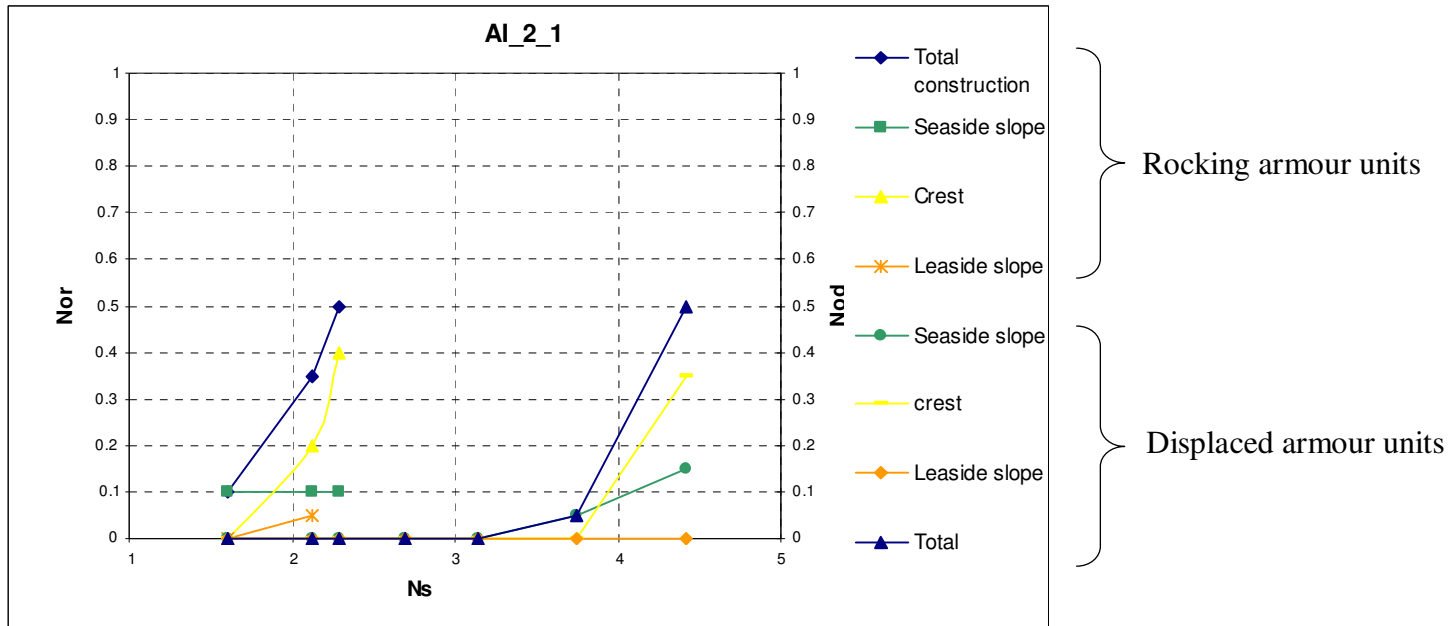
APPENDIX I

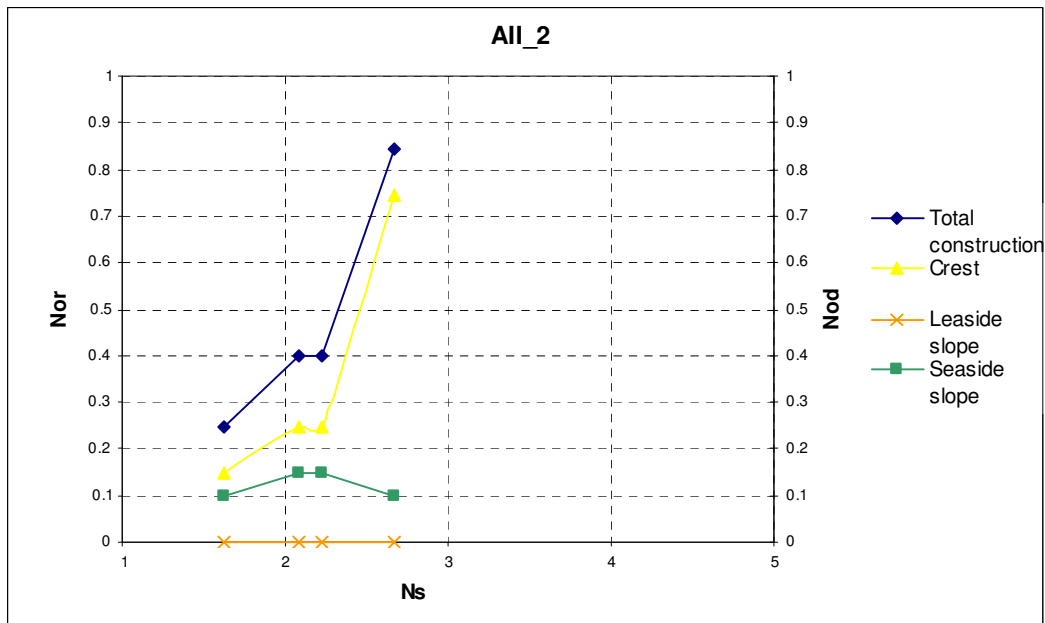
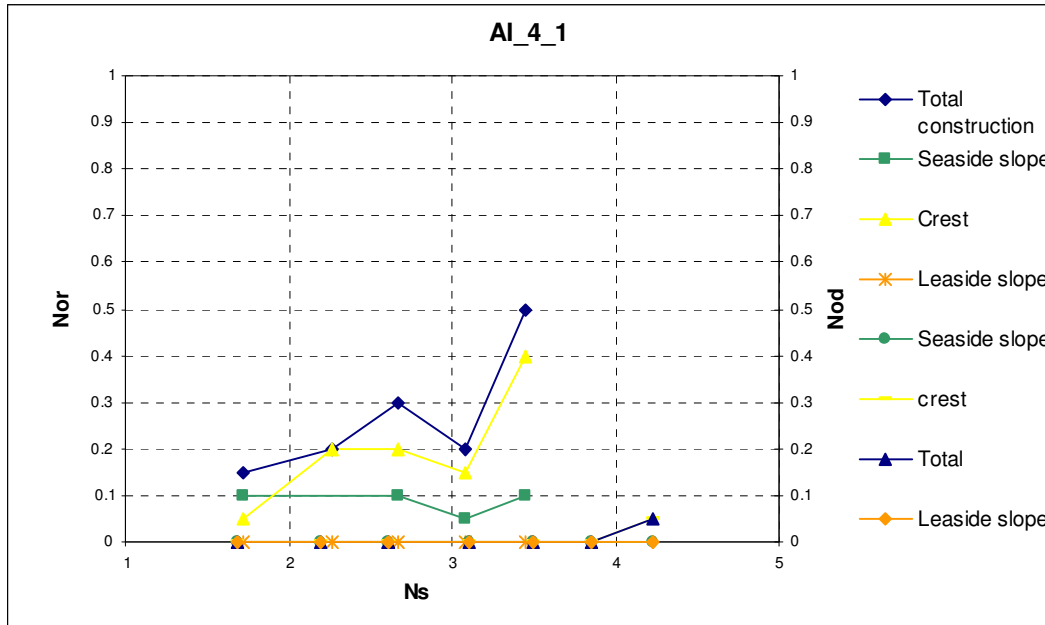
Direction (seaside (S.s) or landward (L.w.)) of displaced elements for the tested breakwater cross sections and the different breakwater sections.

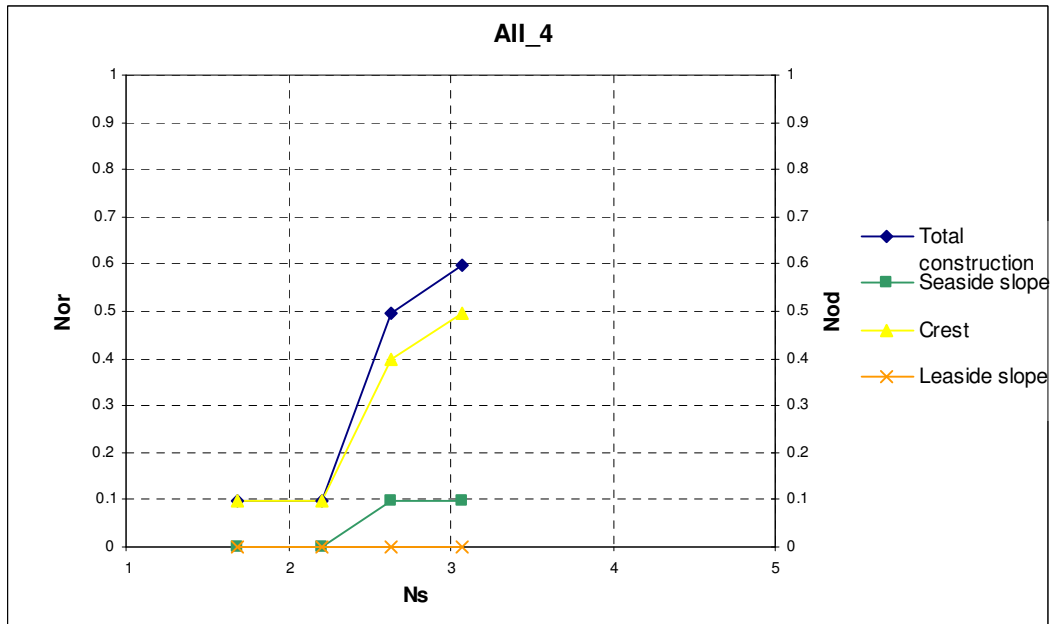
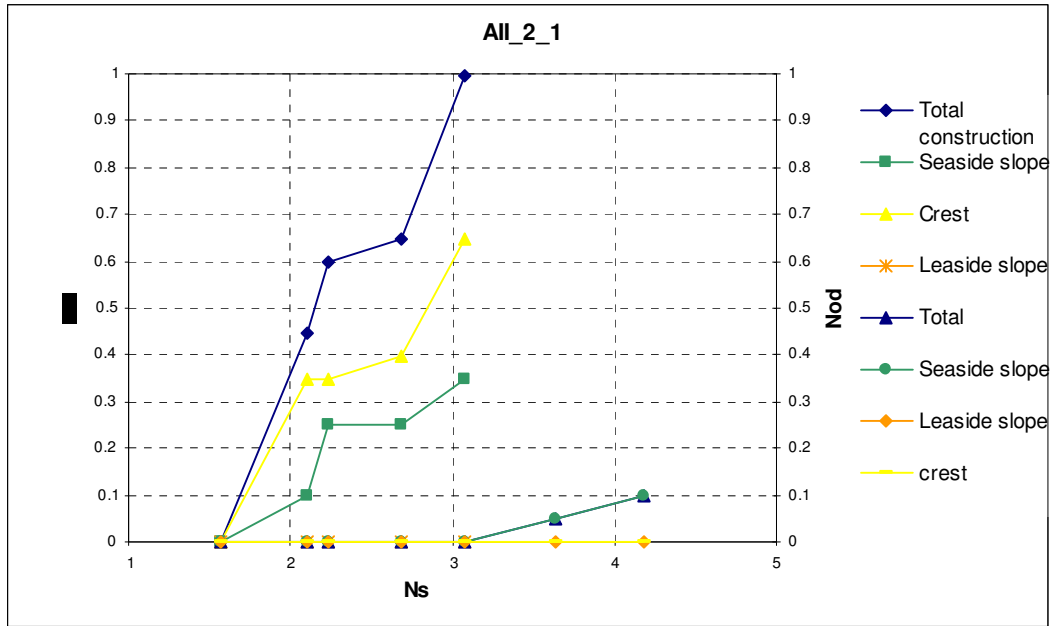
Test serie	Total		Seaside slope elements			Crest elements			Leaside slope elements			
	number of elements	S.s. direction	L.w. direction	number of elements	S.s. direction	L.w. direction	number of elements	S.s. direction	L.w. direction	number of elements	S.s. direction	L.w. direction
AI_2_1	10	10	0	3	3	0	7	7	0	0	0	0
AI_4_1	1	1	0	1	1	0	0	0	0	0	0	0
AII_2_1	10	10	0	3	3	0	7	7	0	0	0	0
BI_2	10	6	4	6	3	3	4	3	1	0	0	0
BI_2_1	10	7	3	5	4	1	5	4	1	0	0	0
BI_4_1	1	1	0	1	1	0	0	0	0	0	0	0
CI_2	10	3	7	4	0	4	5	3	2	1	0	1
CI_2_1	10	3	7	9	3	6	0	0	0	1	0	1
CI_2_2	10	6	4	6	3	3	4	1	3	0	0	0
CI_2_3	10	3	7	8	3	5	2	0	2	0	0	0
CI_2_4	10	3	7	2	0	2	4	3	1	4	0	4
CI_4	1	1	0	1	1	0	0	0	0	0	0	0
CI_4_2	3	0	3	2	0	2	1	0	1	0	0	0
CI_4_3	1	0	1	1	0	1	0	0	0	0	0	0
CI_4_4	2	0	2	1	0	1	1	0	1	0	0	0
CII_2	10	2	8	5	0	5	5	2	3	0	0	0
DI_2	10	0	10	6	0	6	4	0	4	0	0	0
DI_4	10	0	10	10	0	10	0	0	0	0	0	0
DII_2	10	0	10	4	0	4	6	0	6	0	0	0
DII_4	10	0	10	5	0	5	5	0	5	0	0	0
EI_2	10	0	10	4	0	4	6	0	6	0	0	0

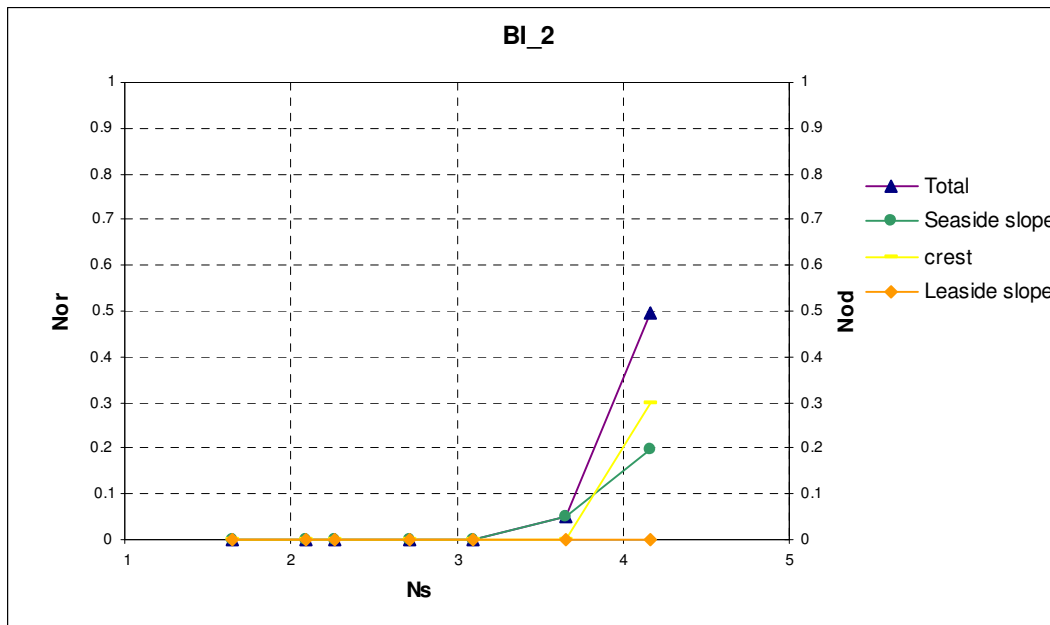
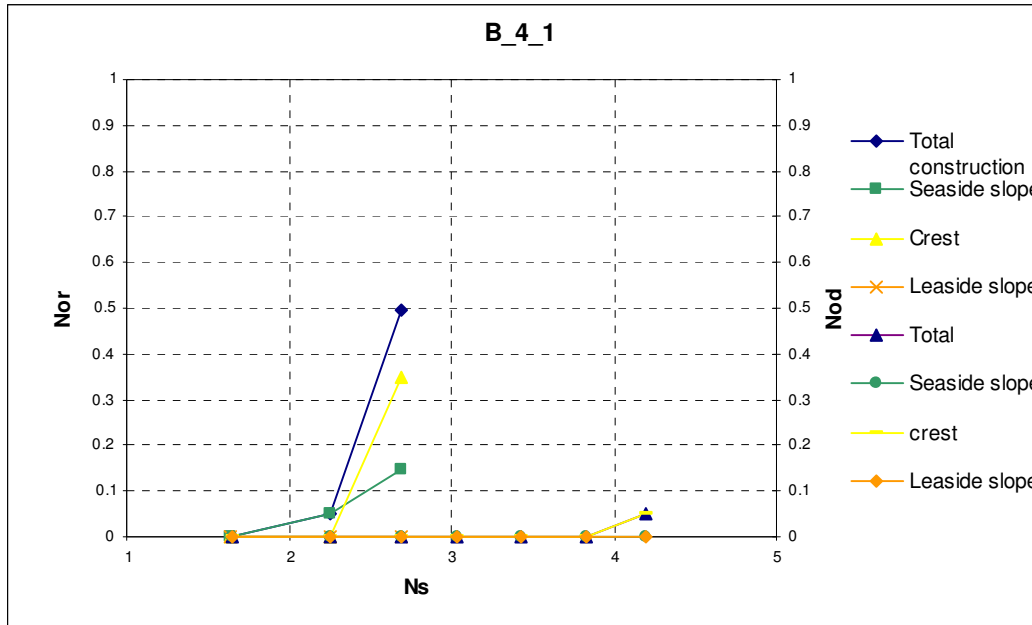
APPENDIX J

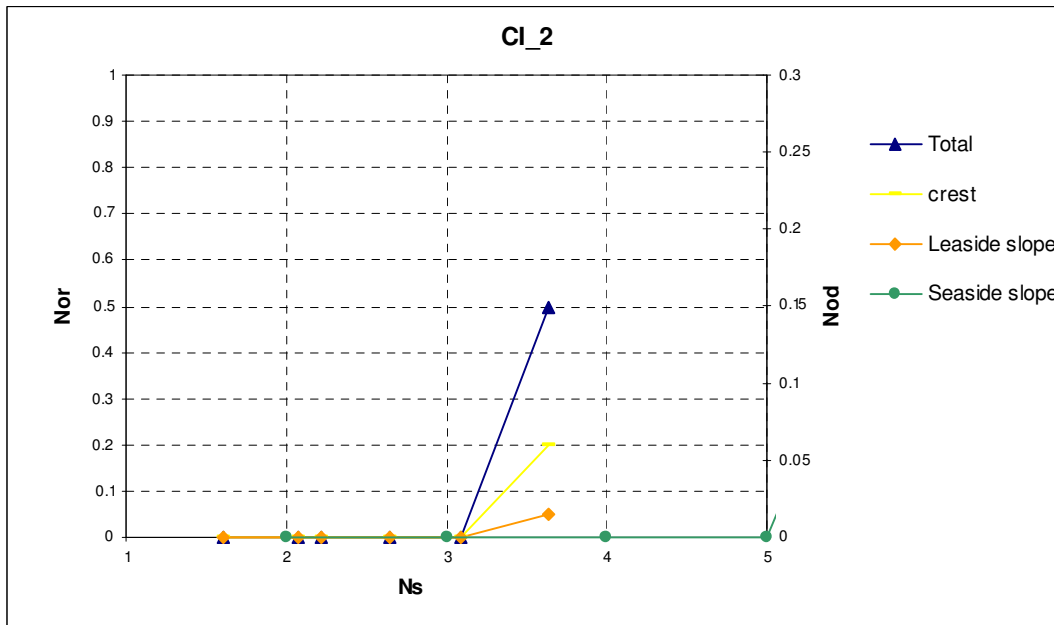
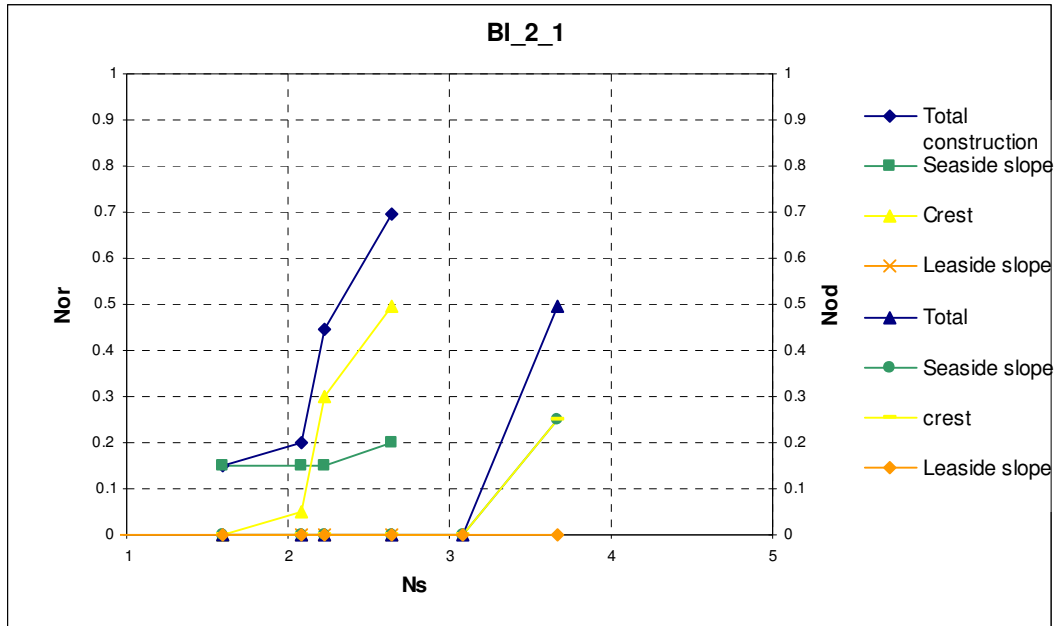
Damage progression lines for rocking Xbloc elements and displaced Xbloc elements.

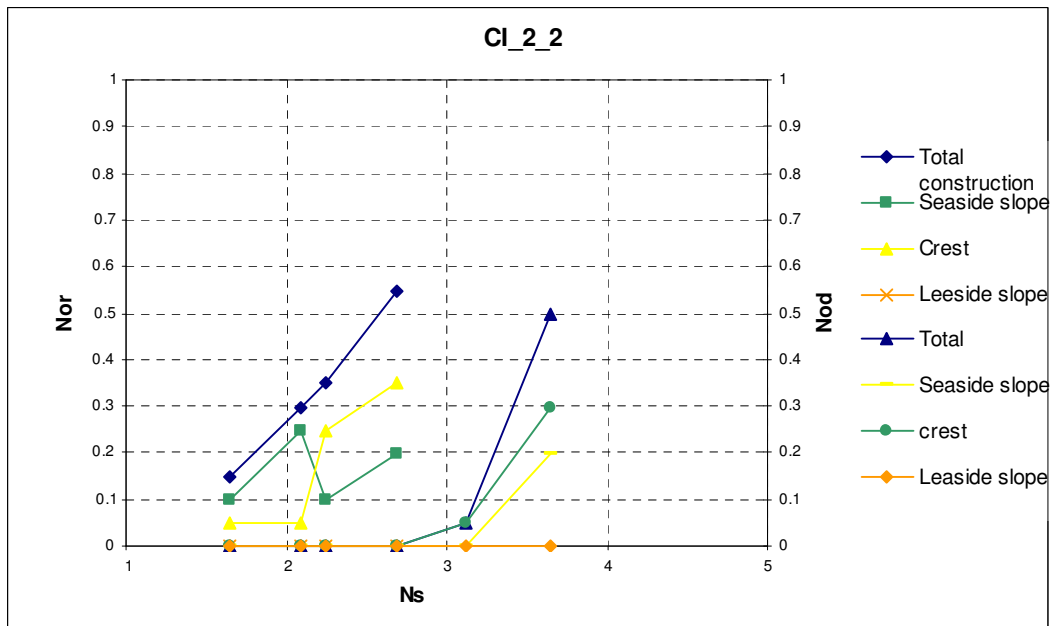
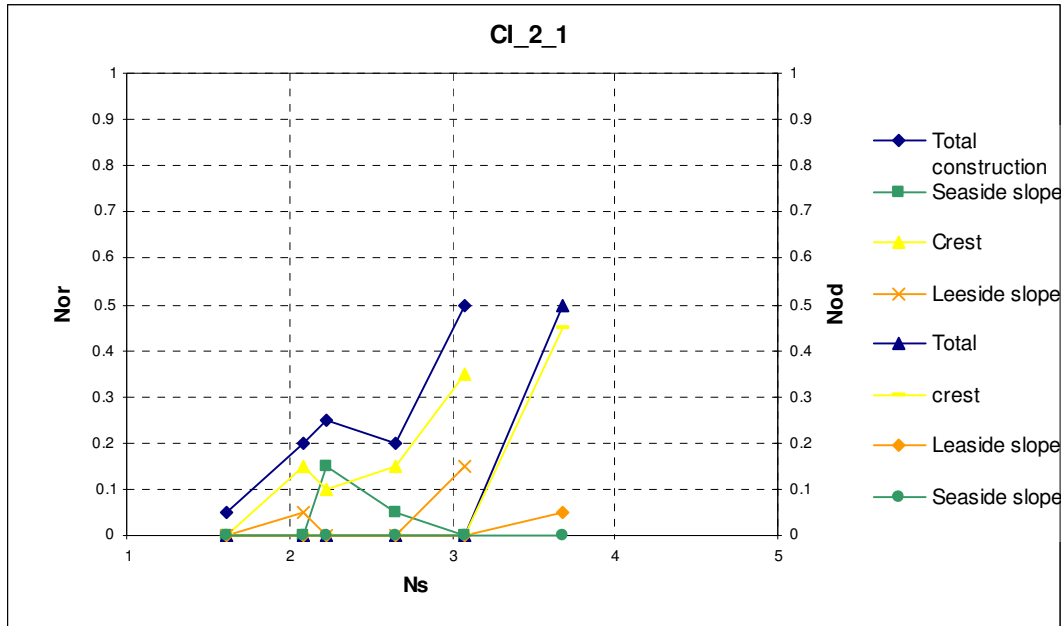


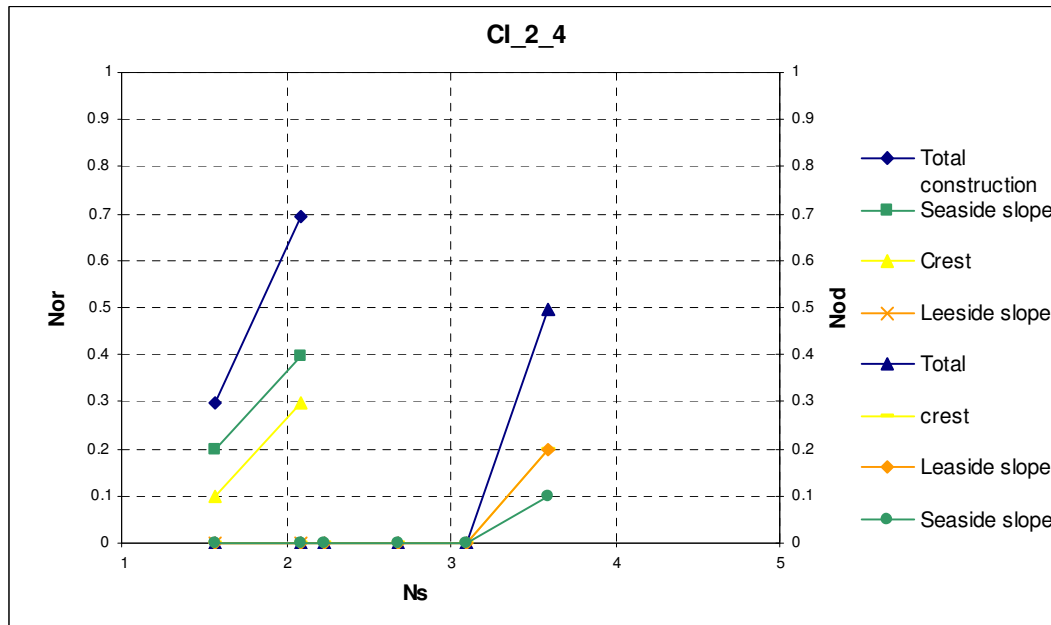
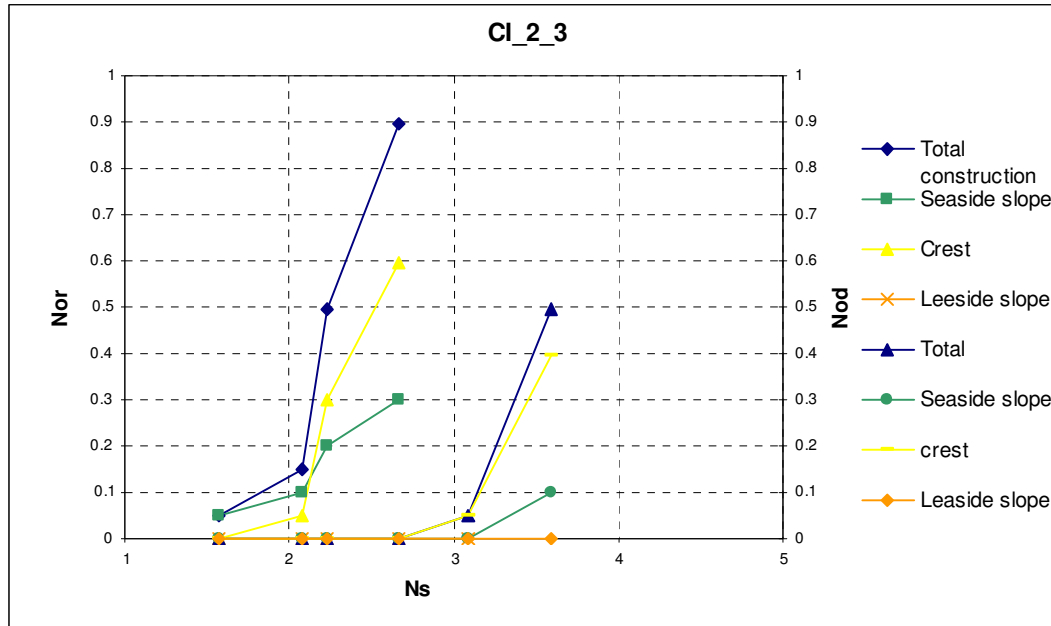


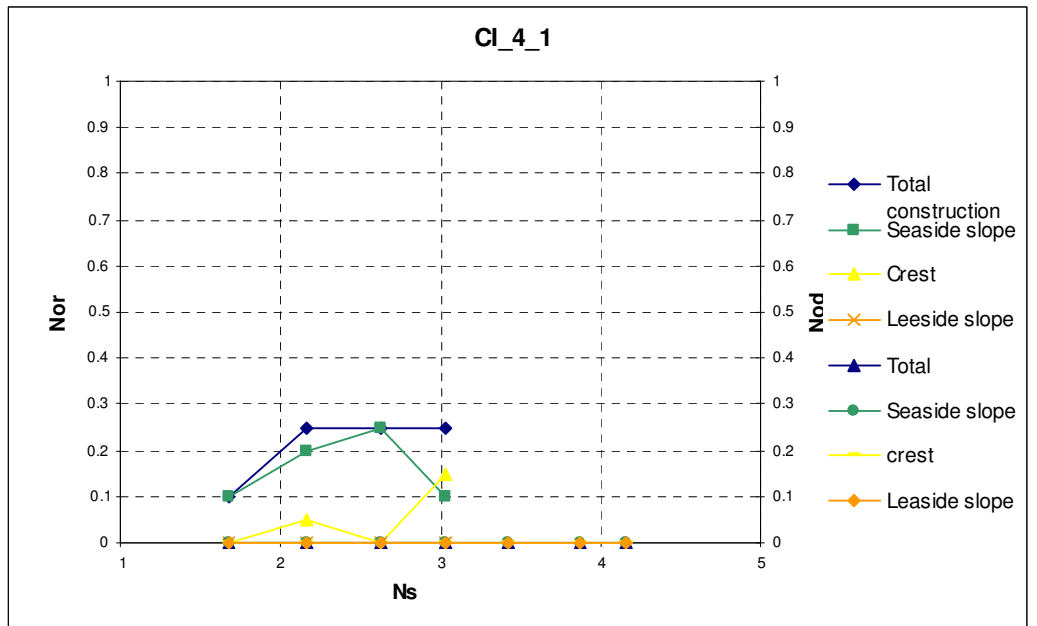
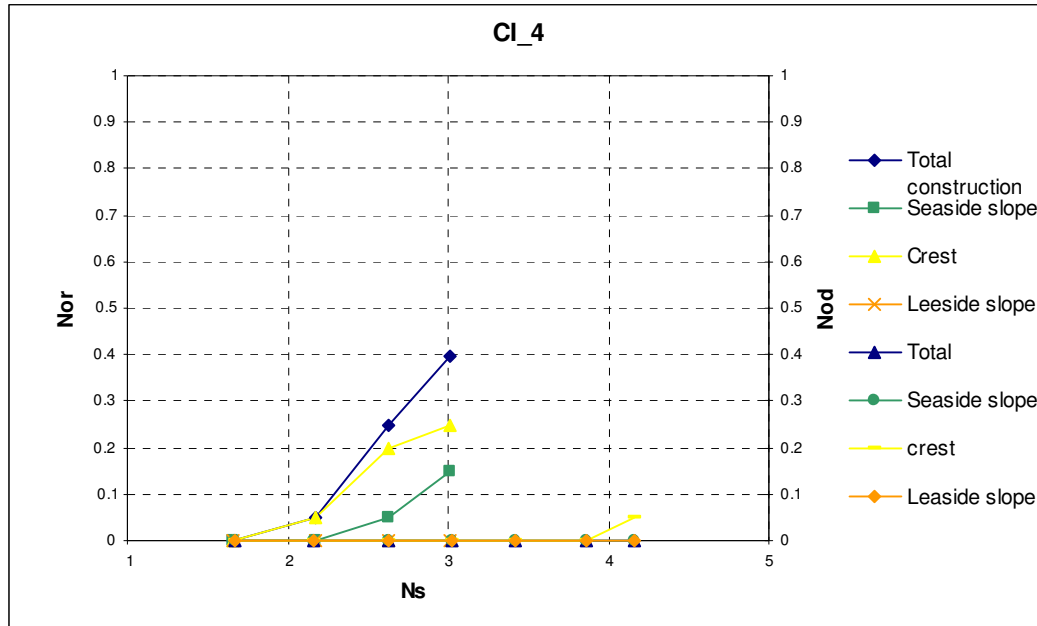


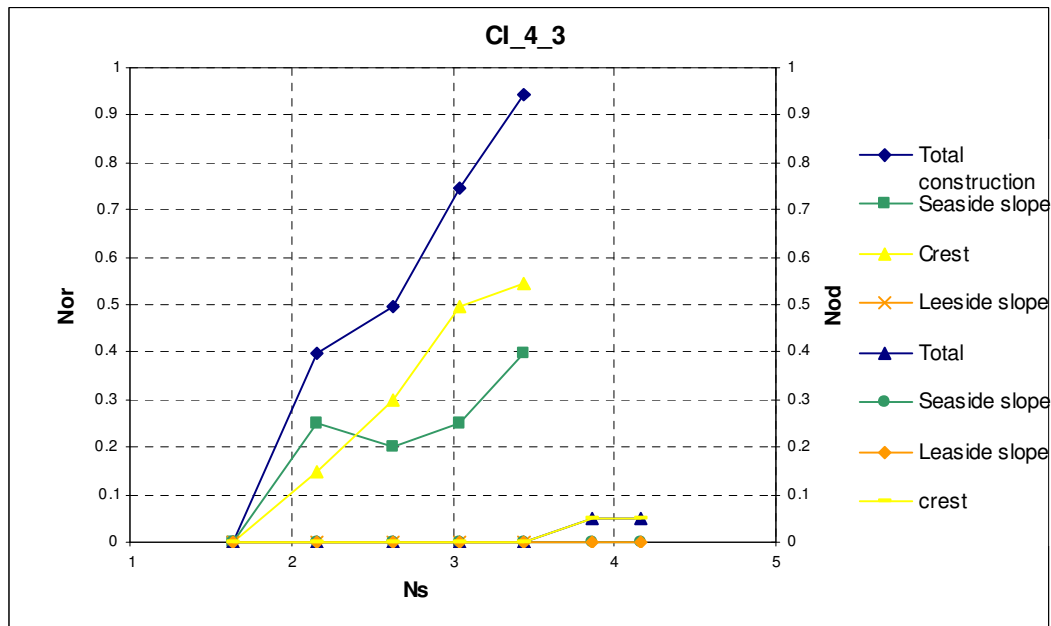
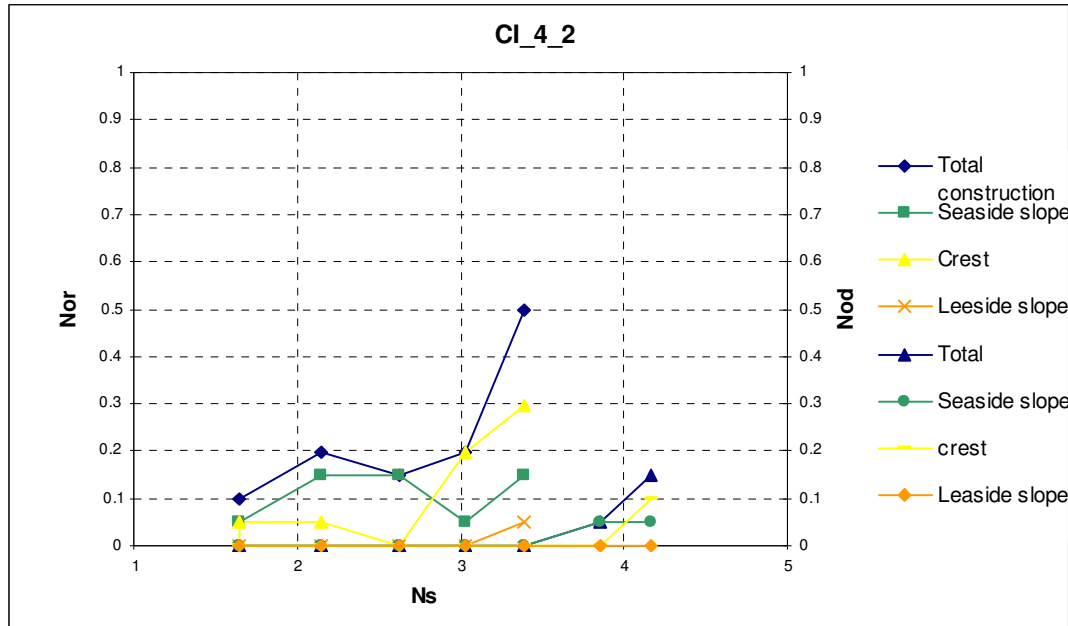


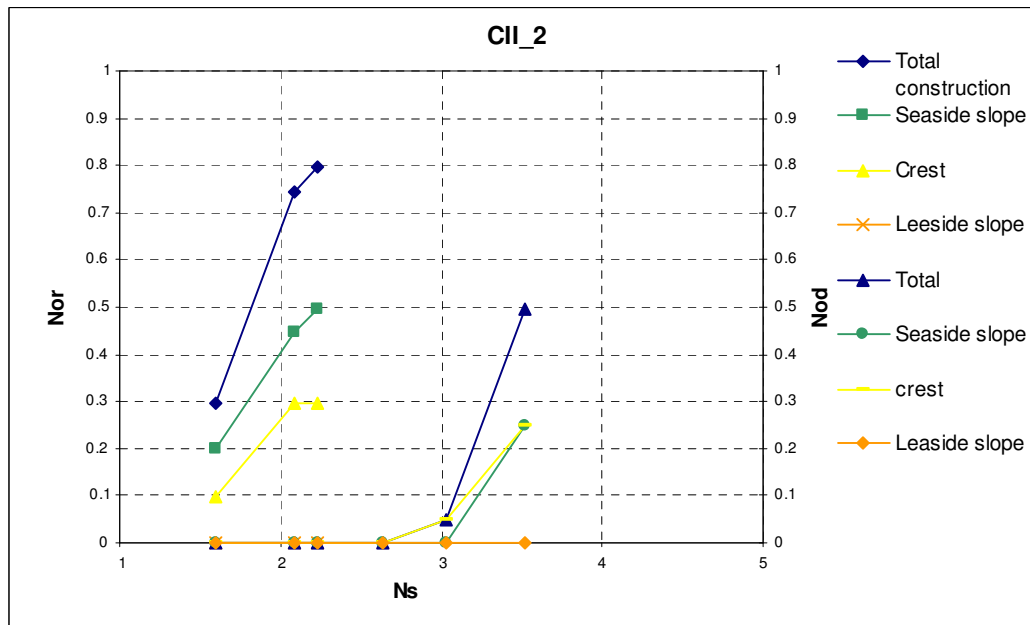
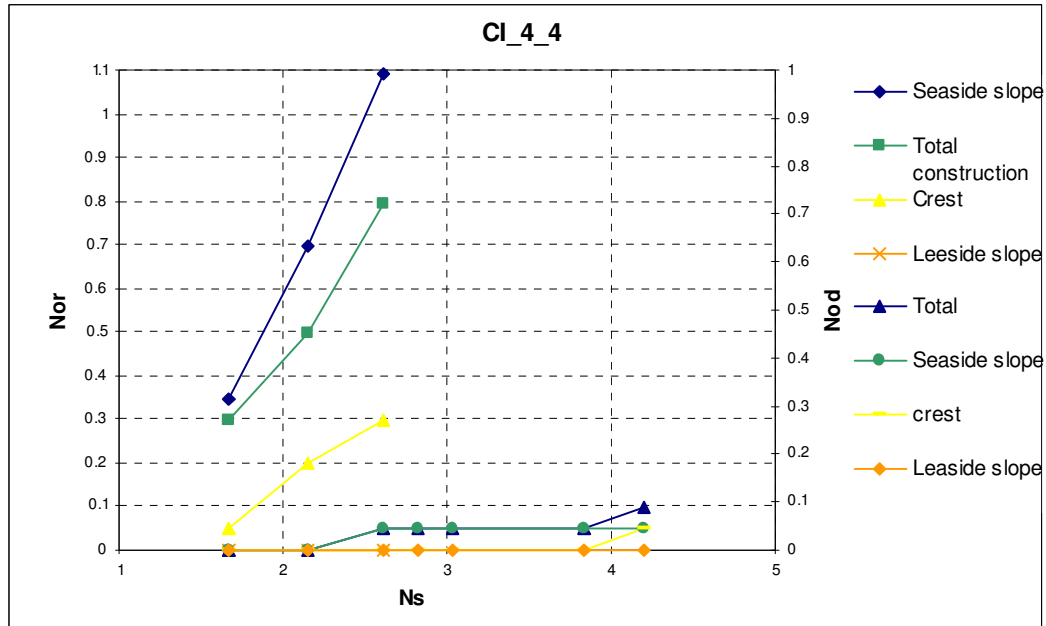


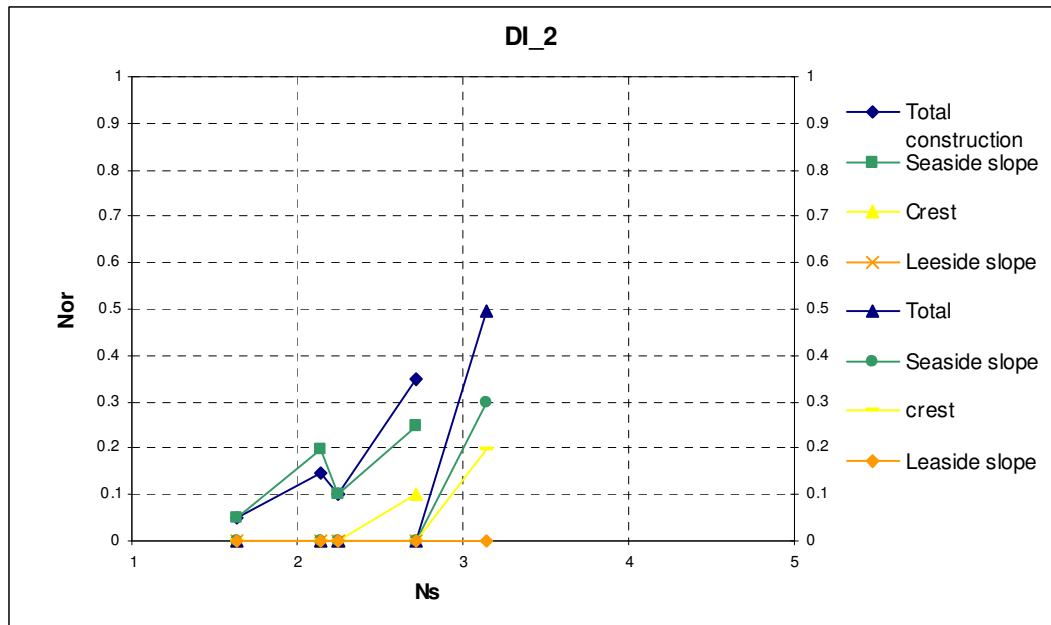
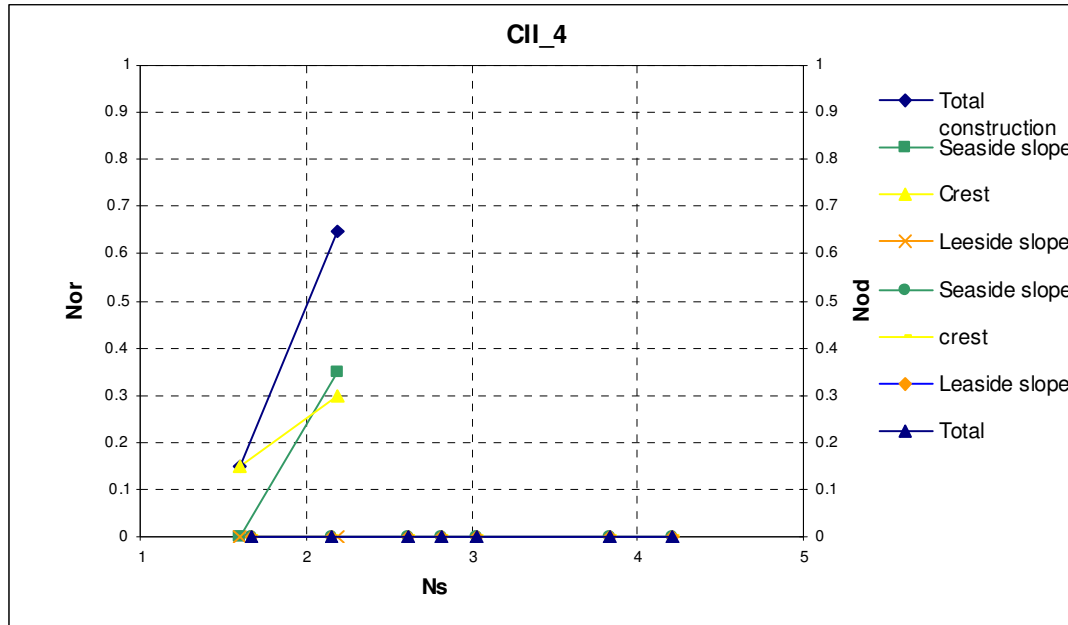


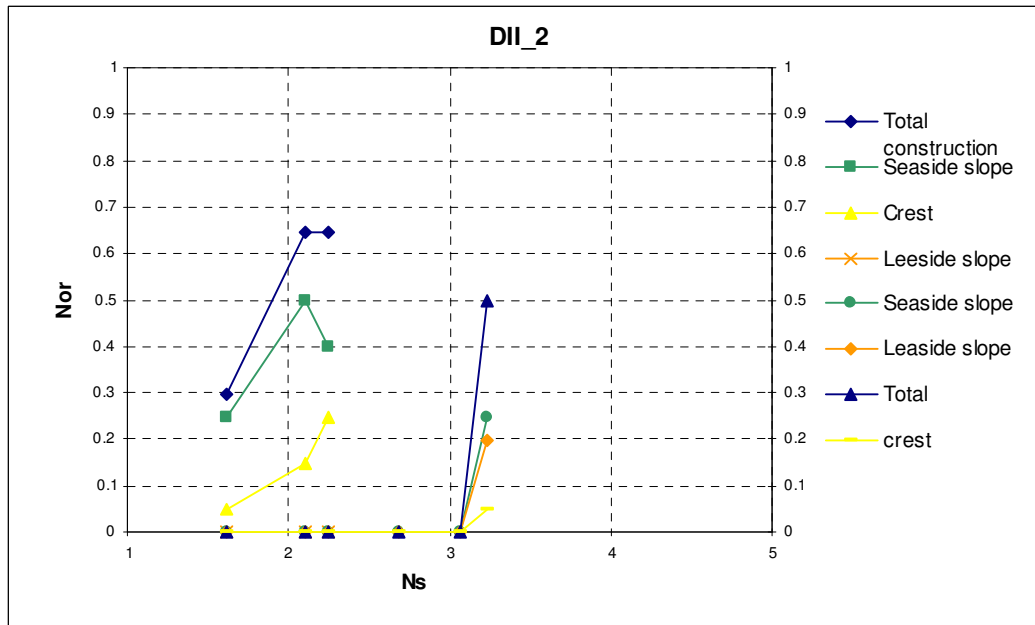
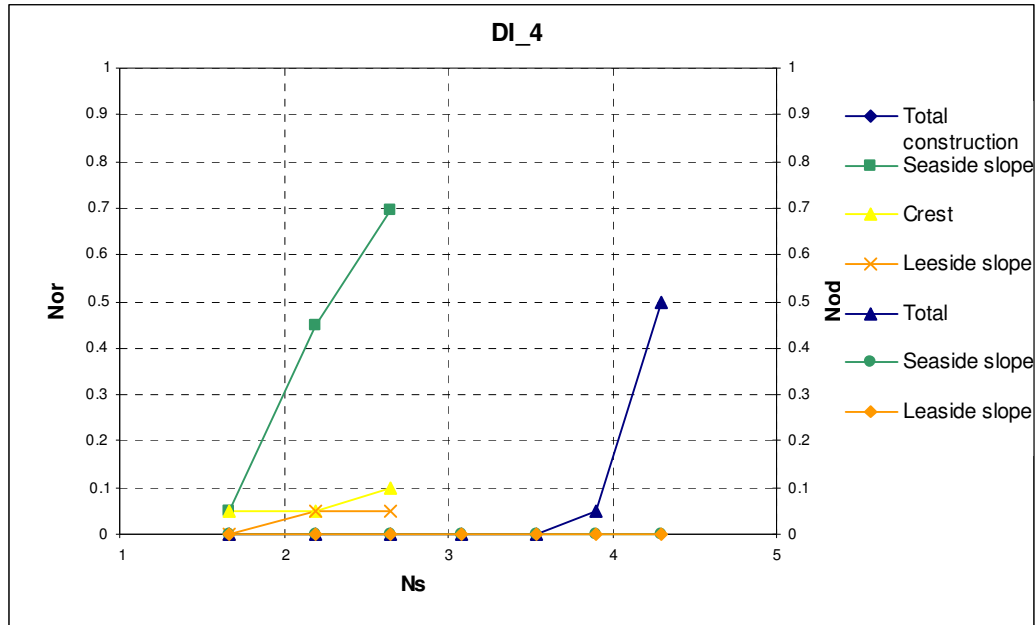


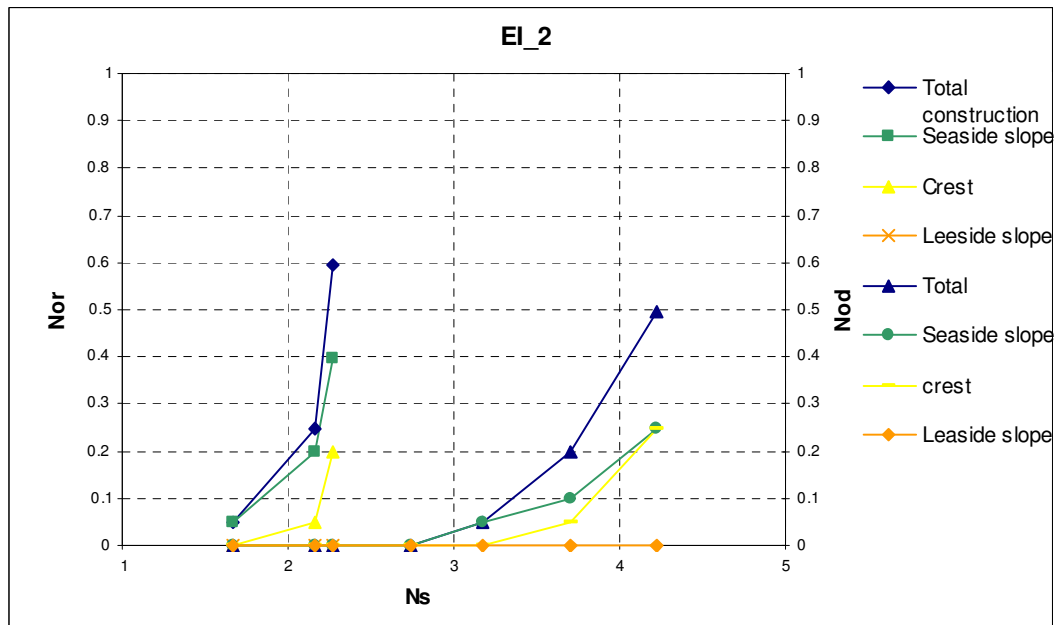
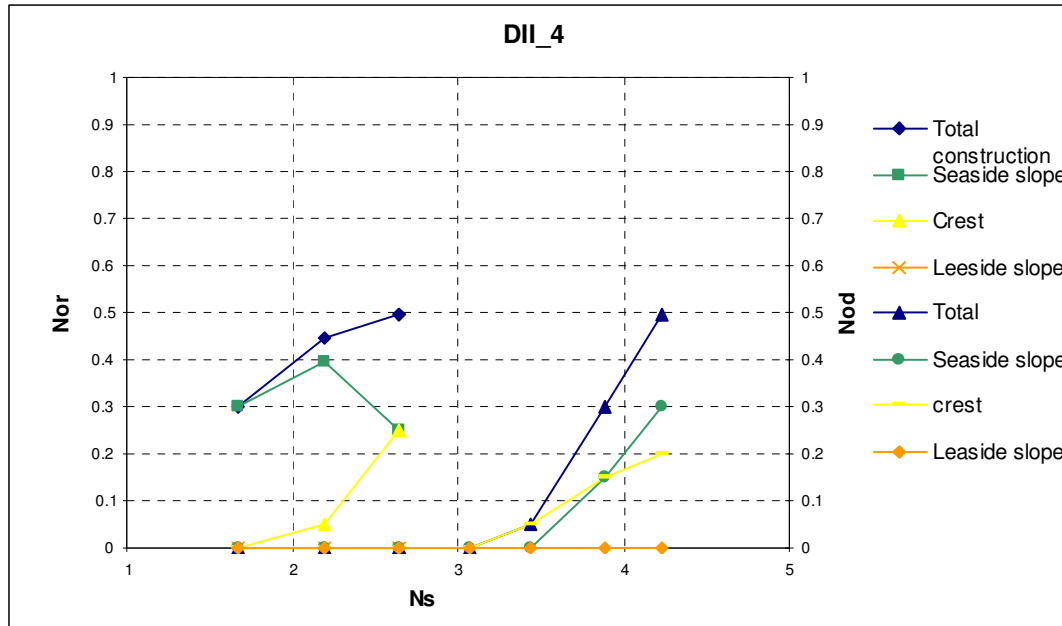


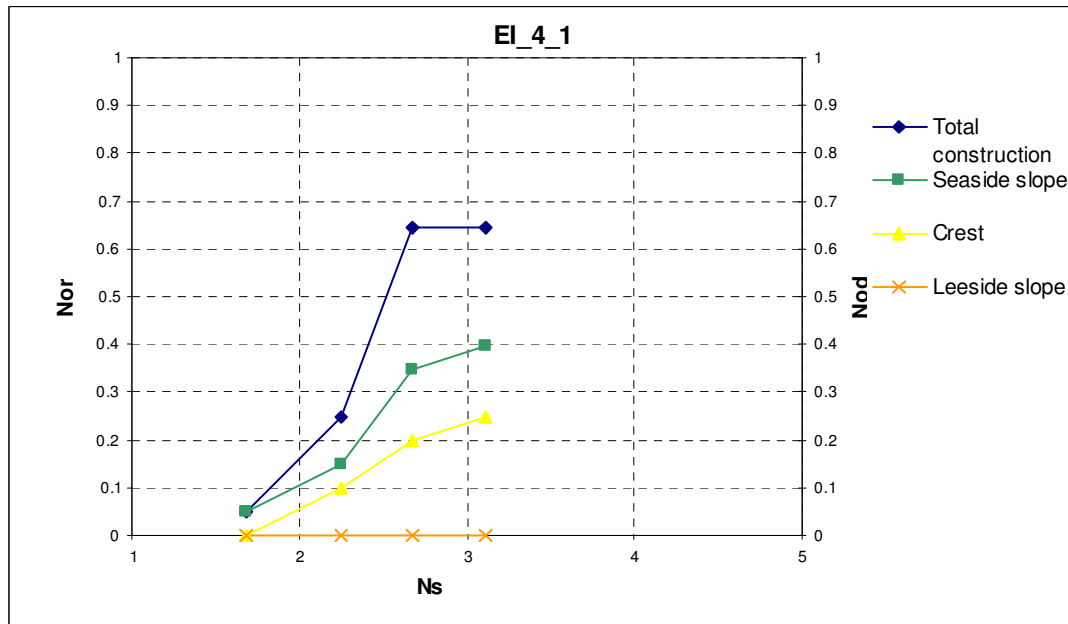
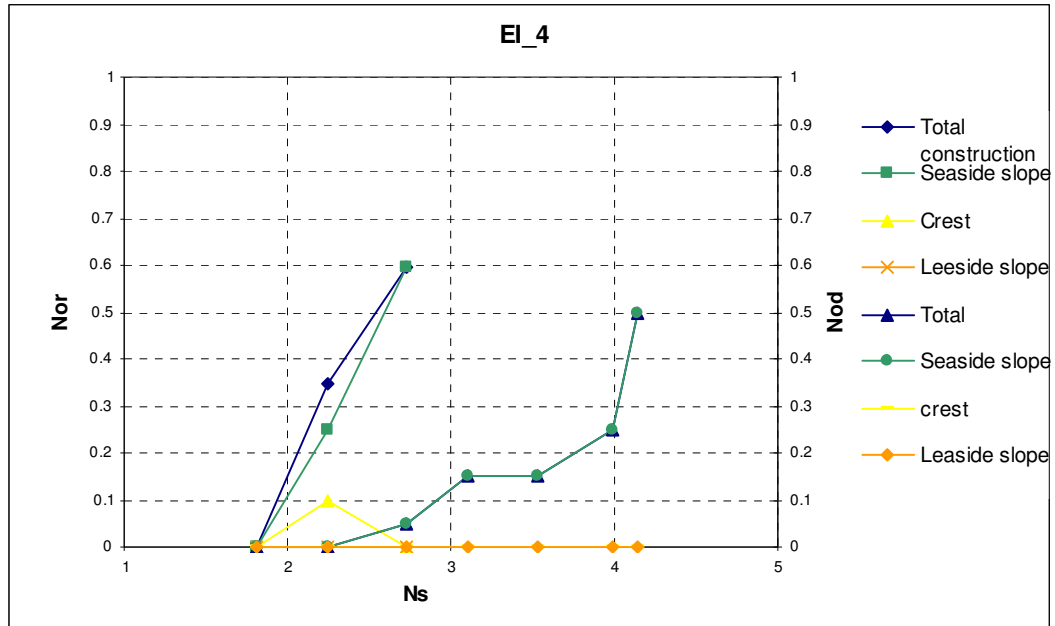






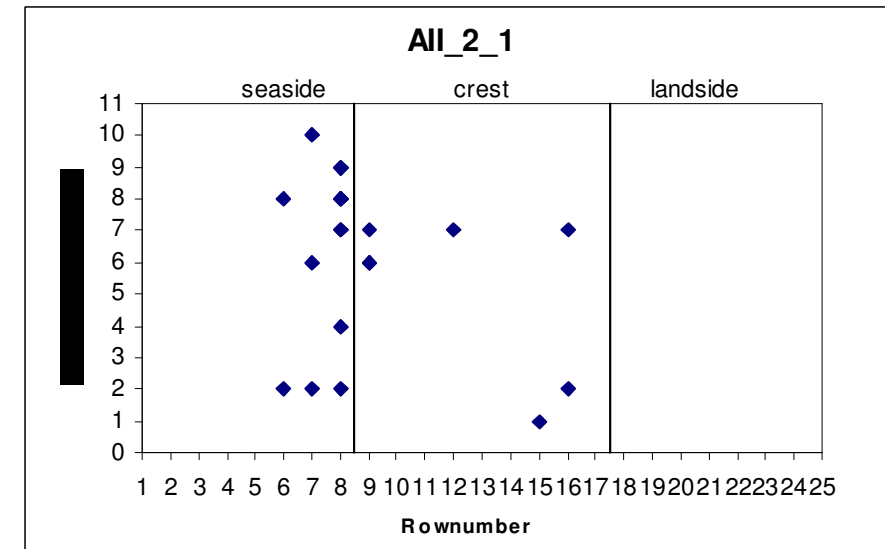
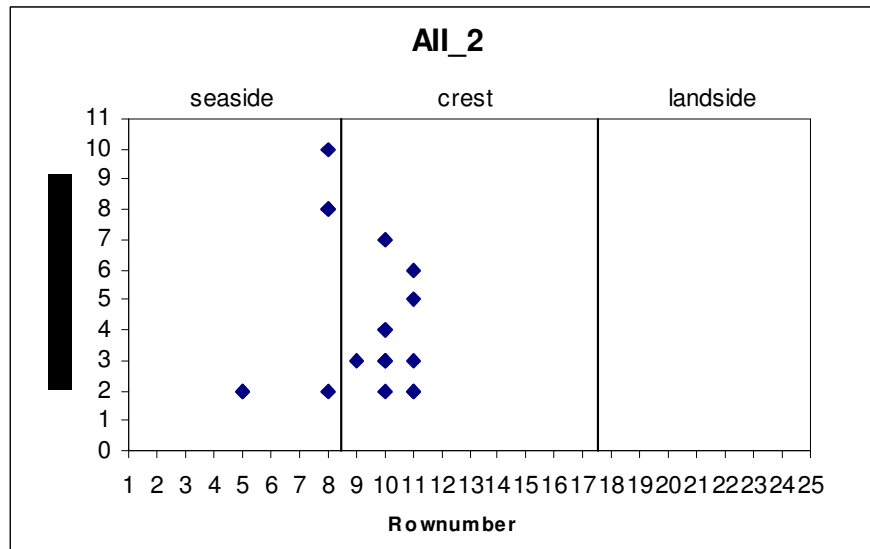
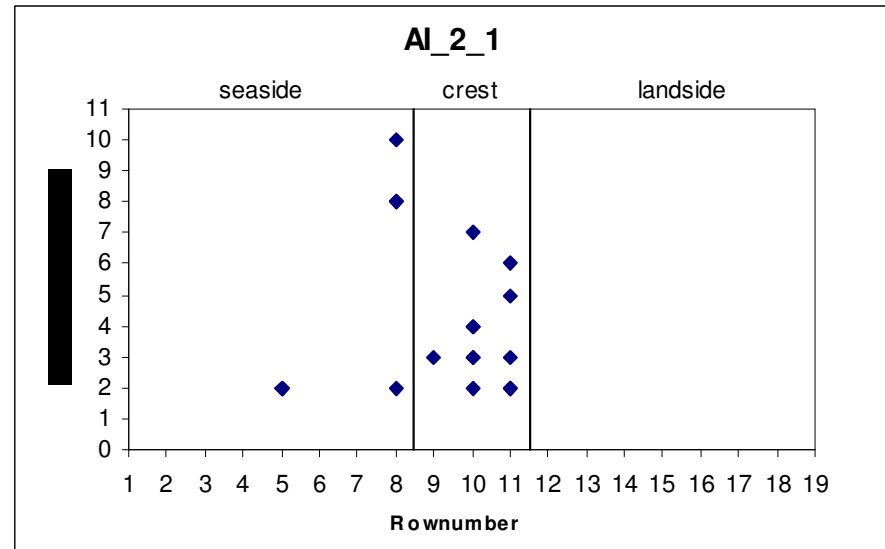
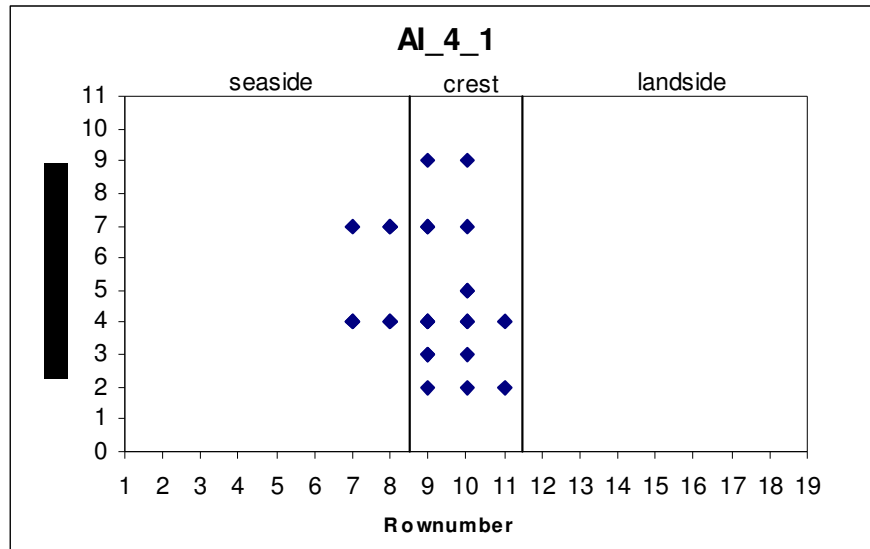


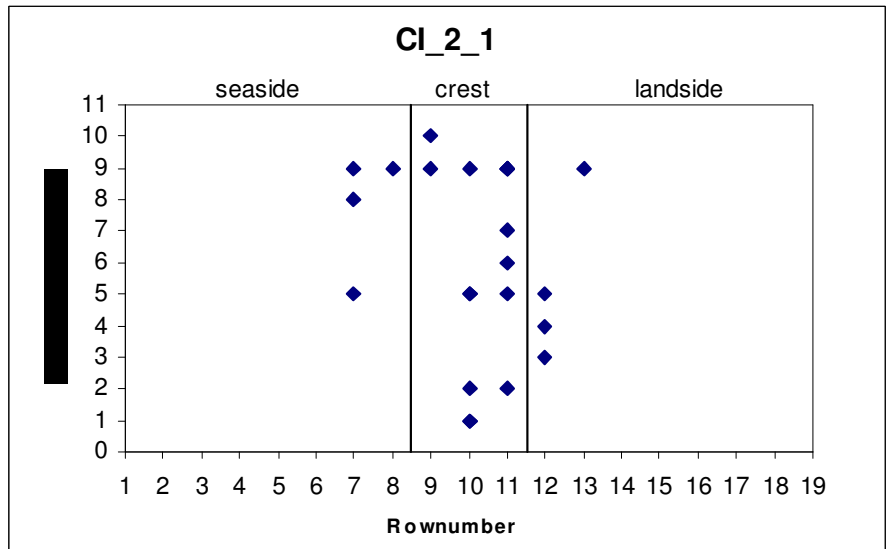
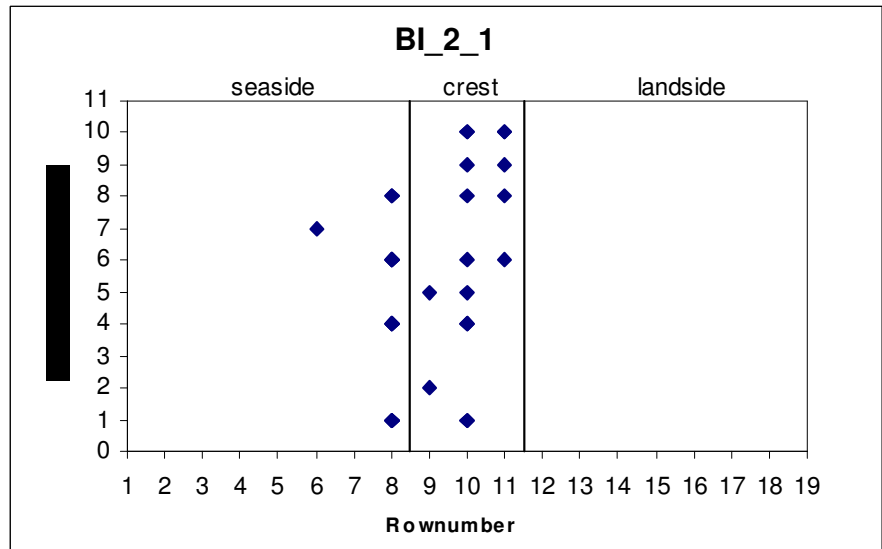
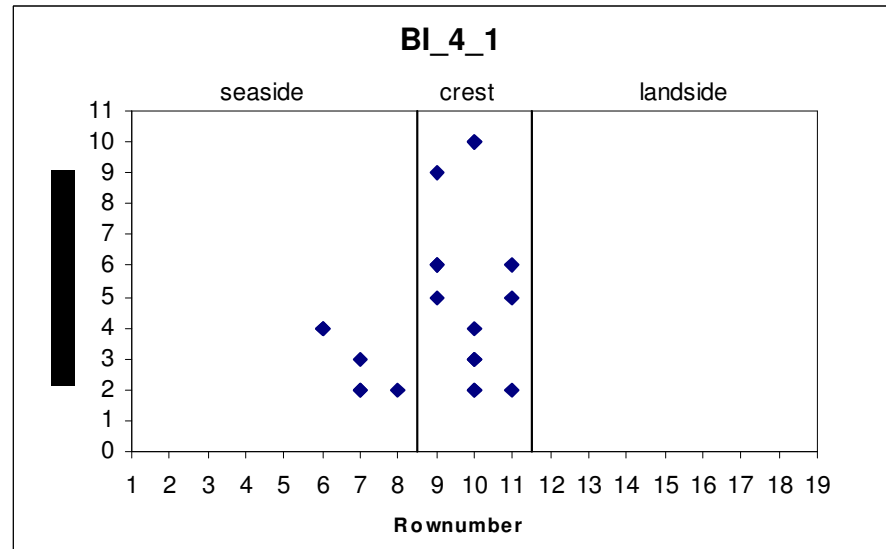
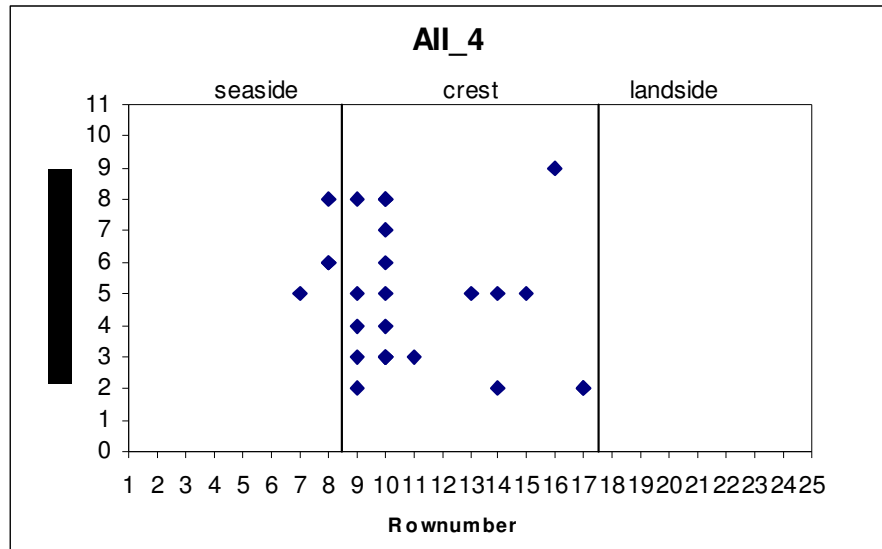


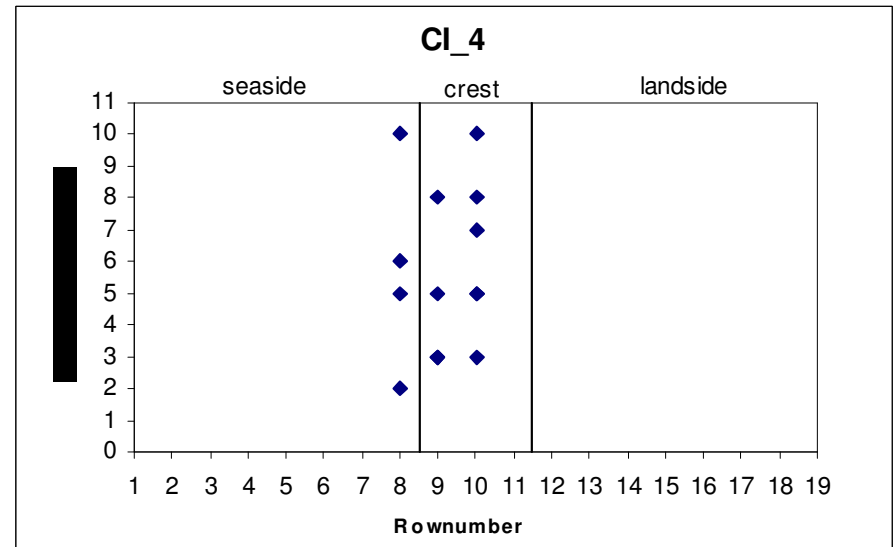
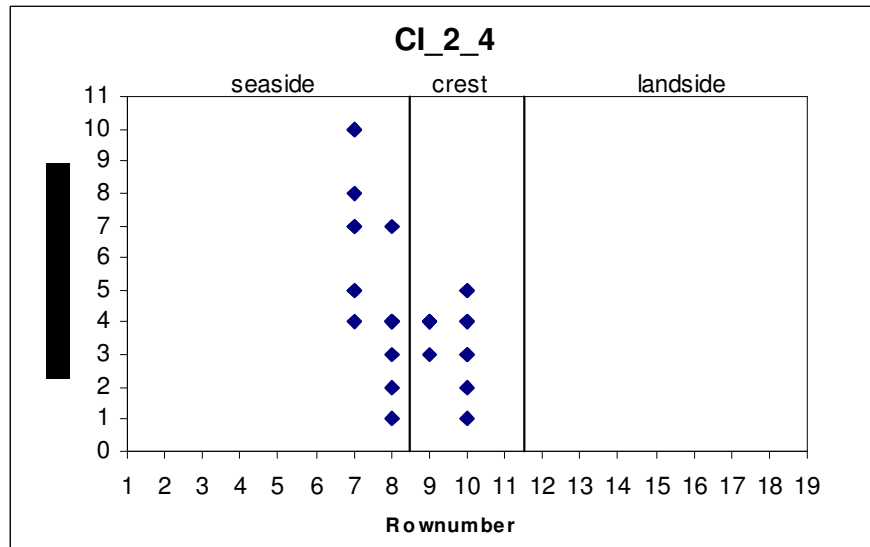
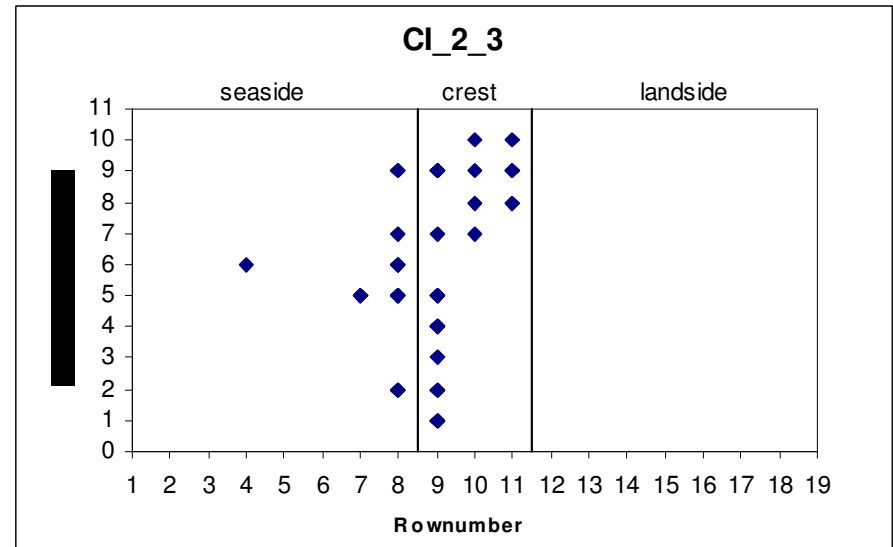
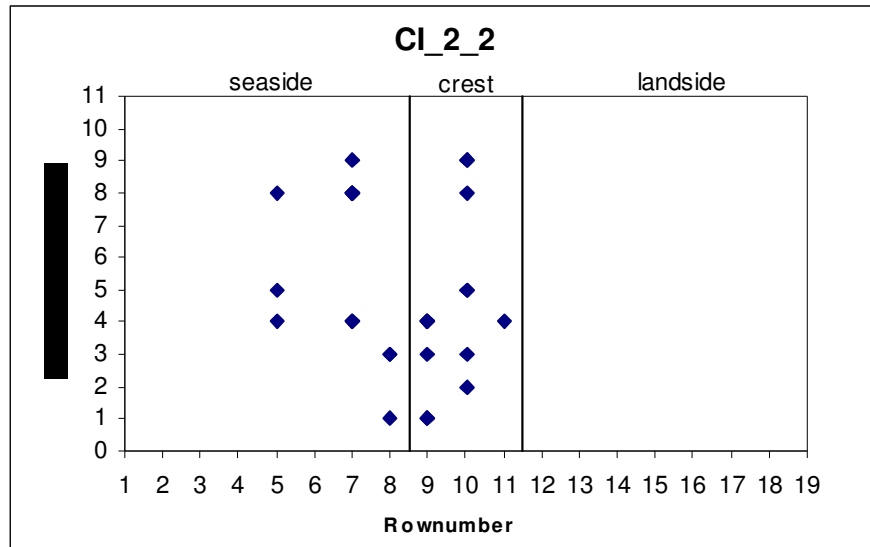


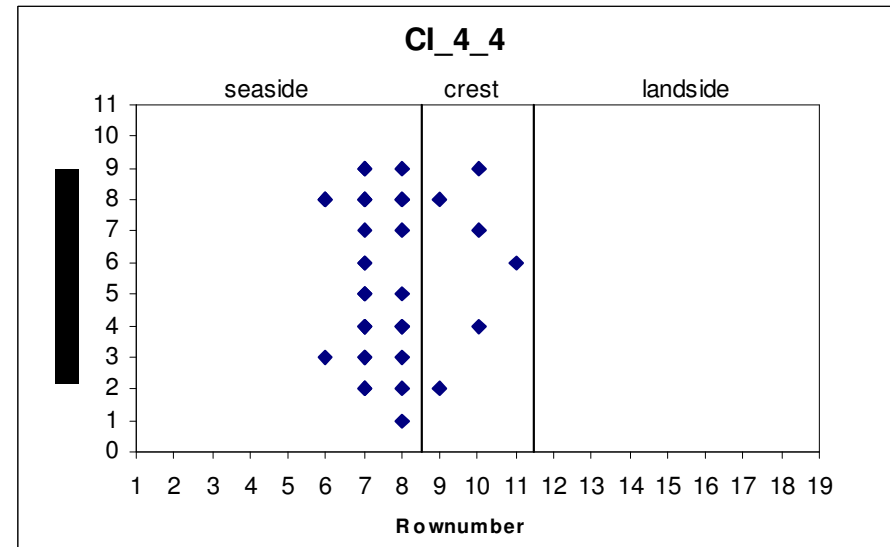
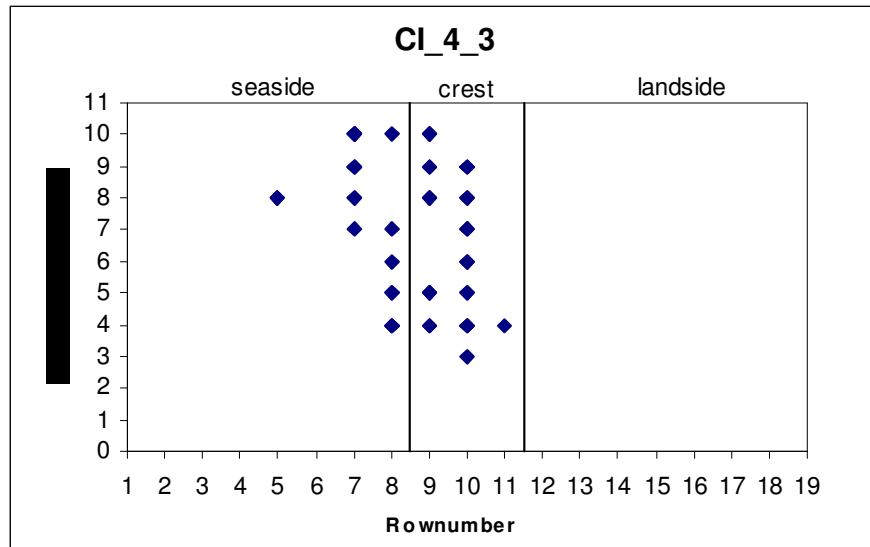
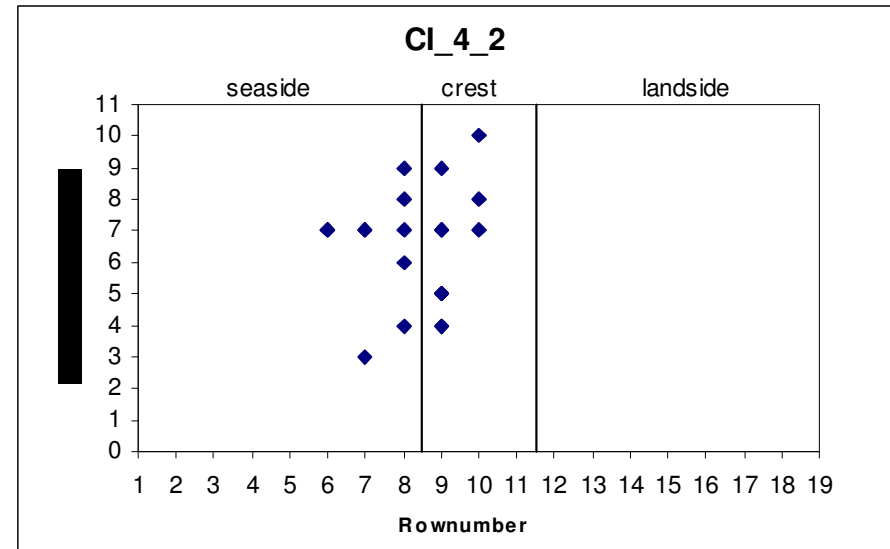
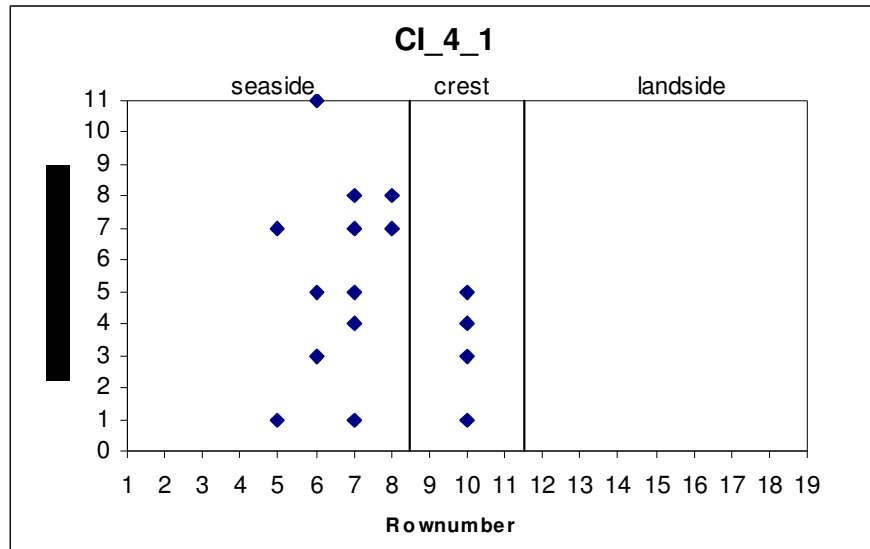
APPENDIX K

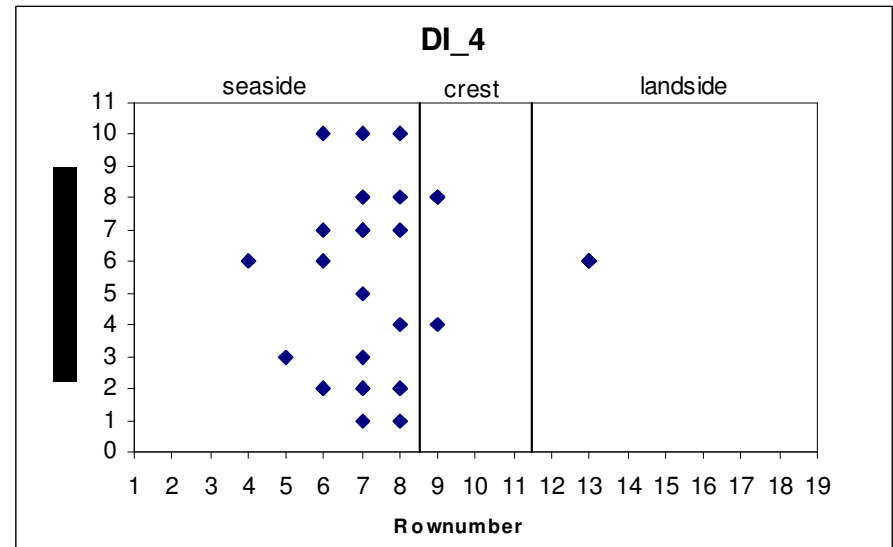
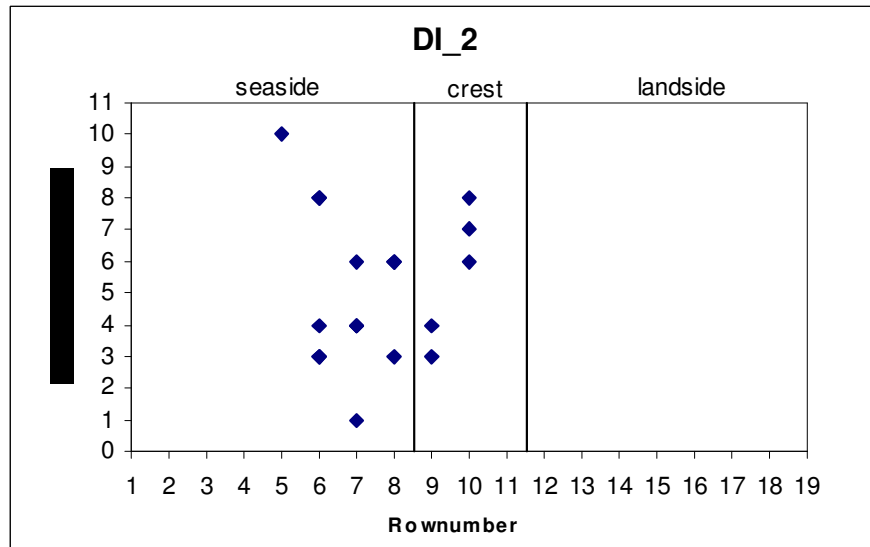
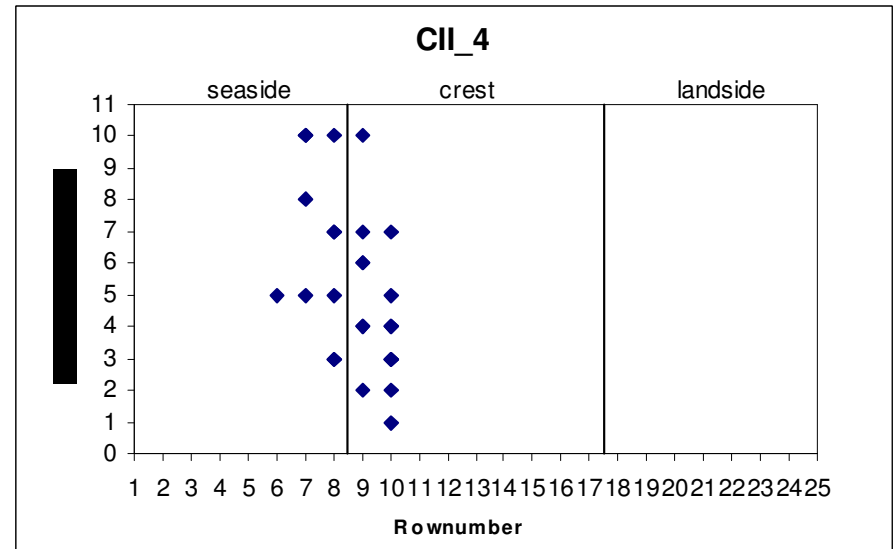
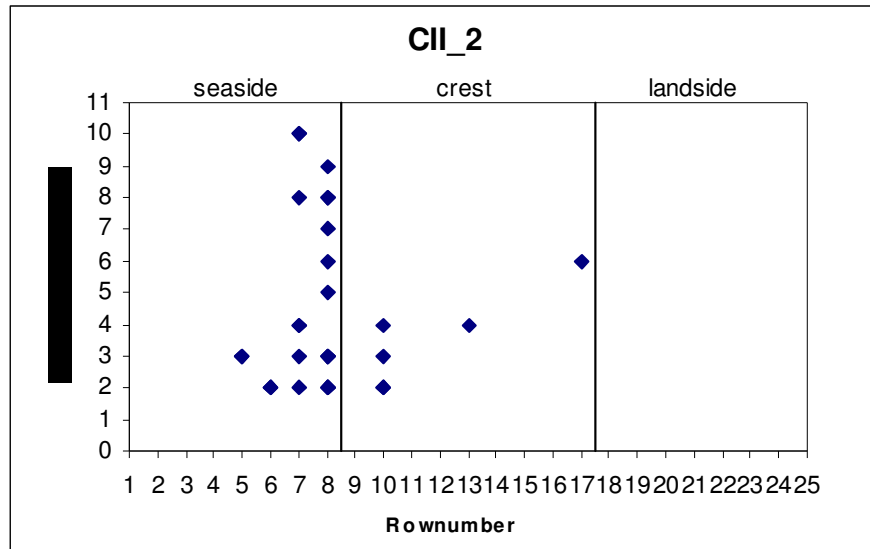
Appendix J shows the location of the rocking armour units.

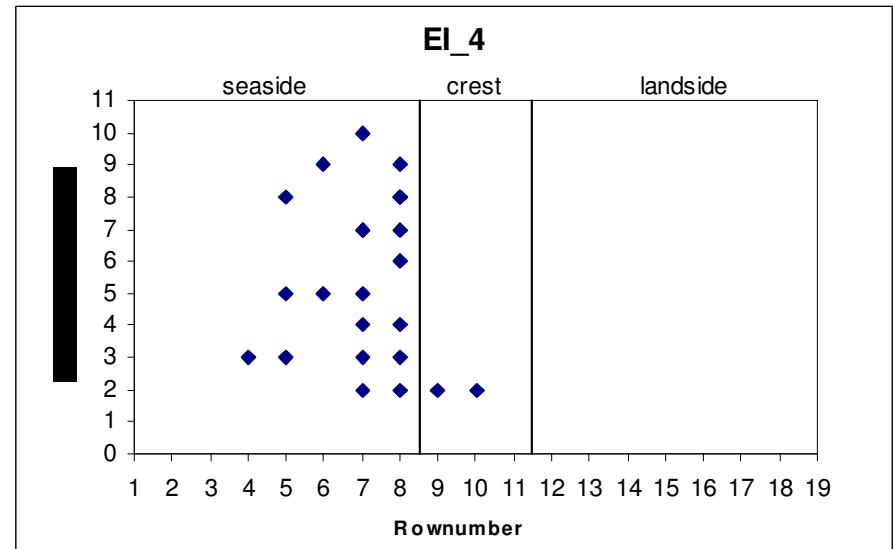
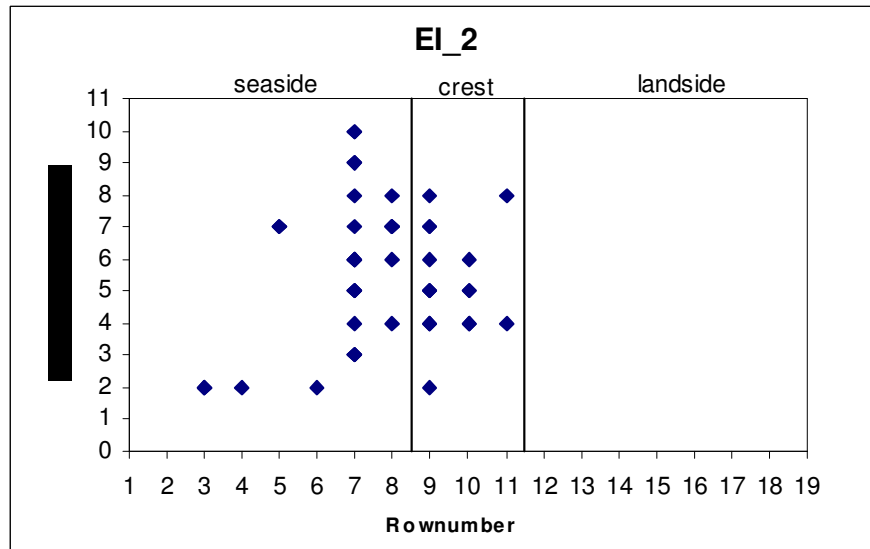
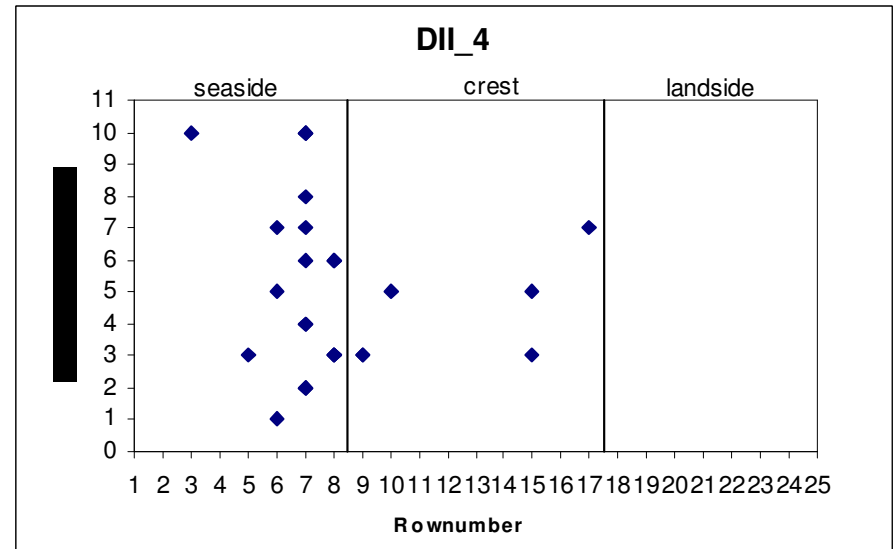
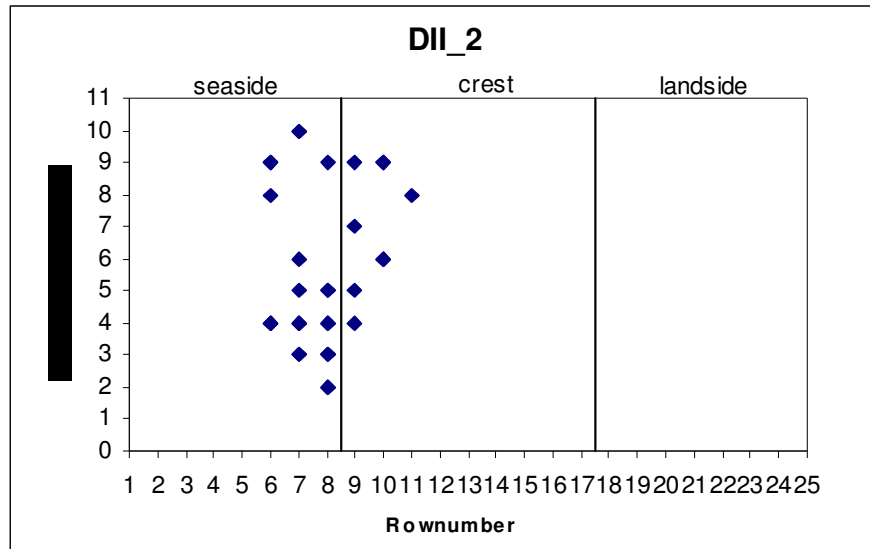


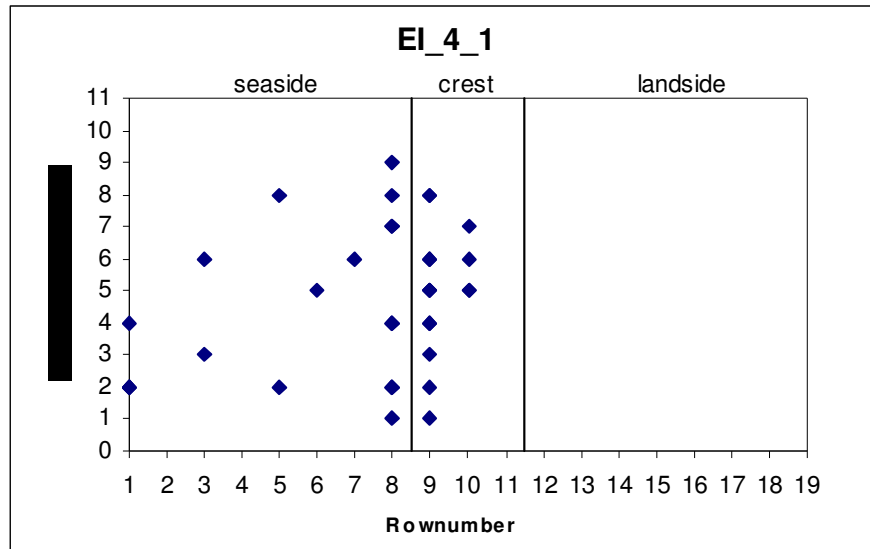










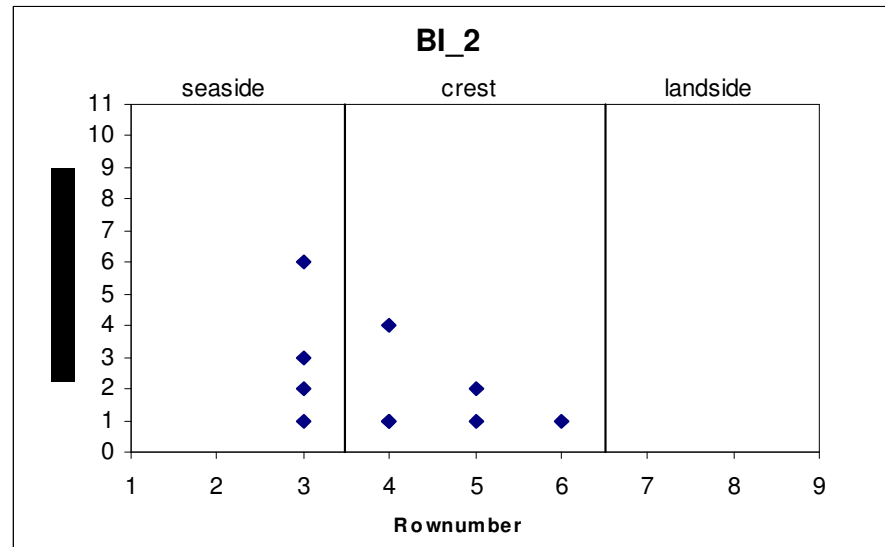
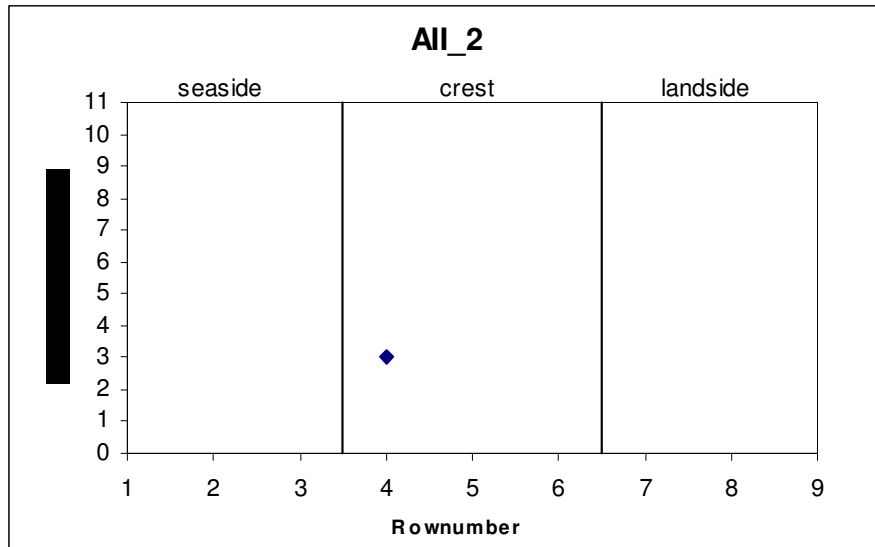
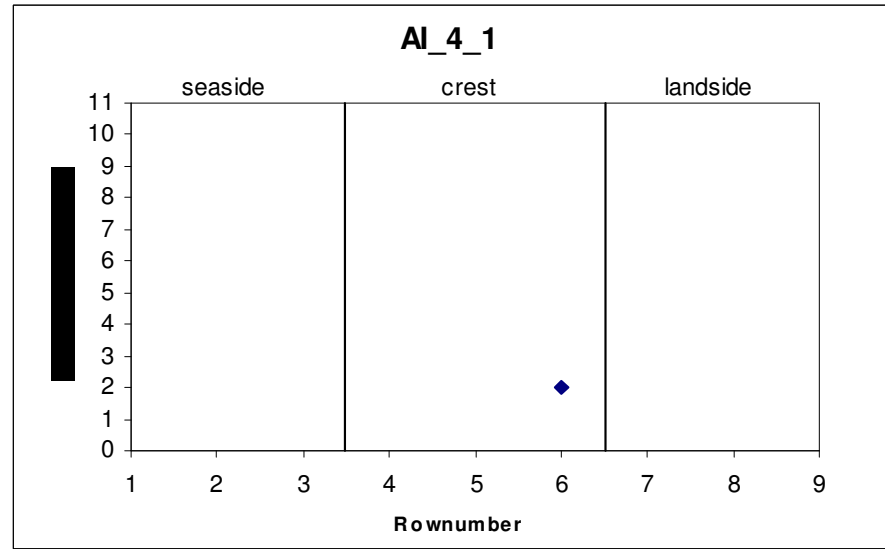
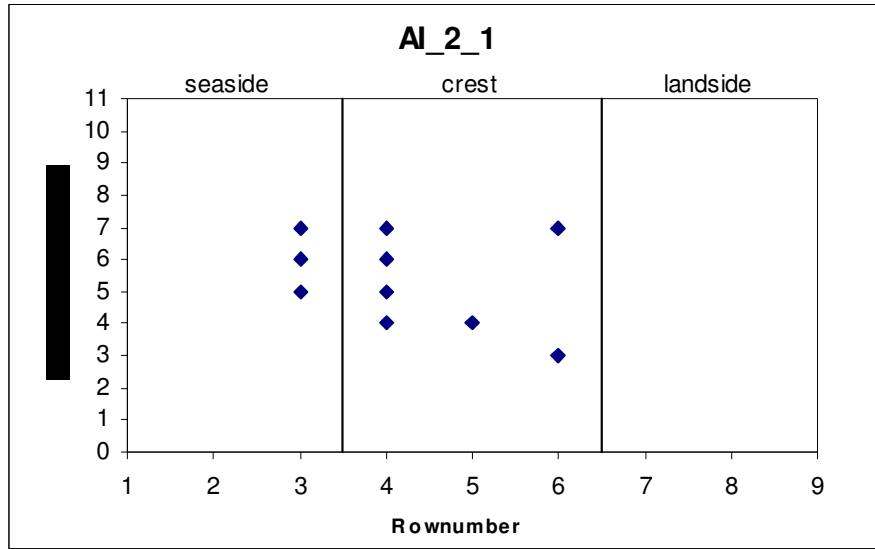


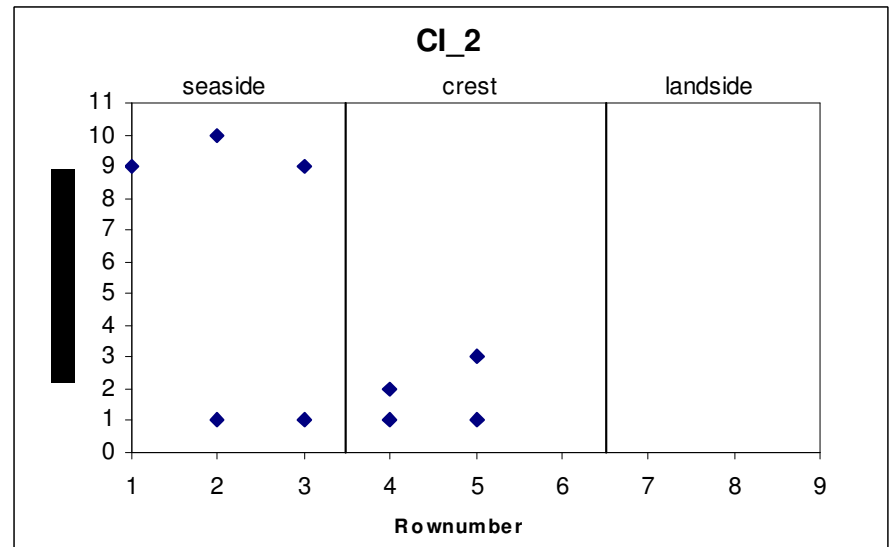
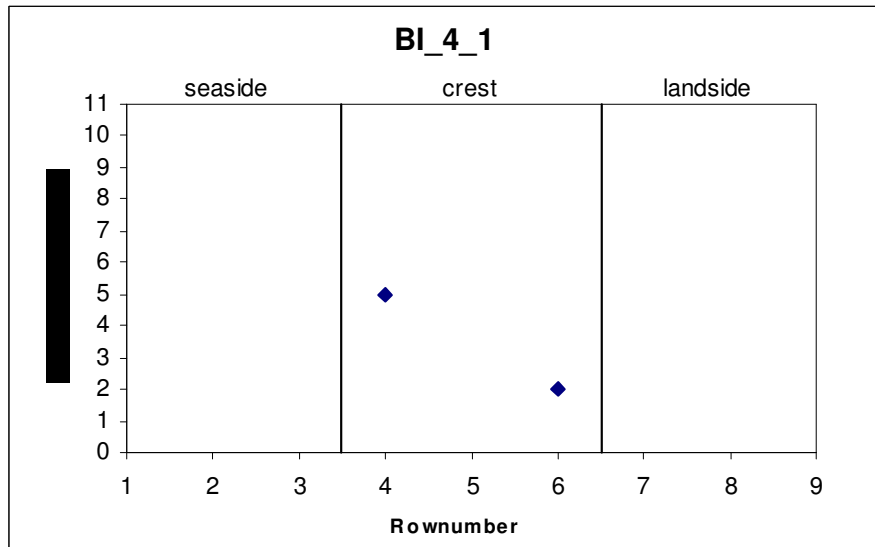
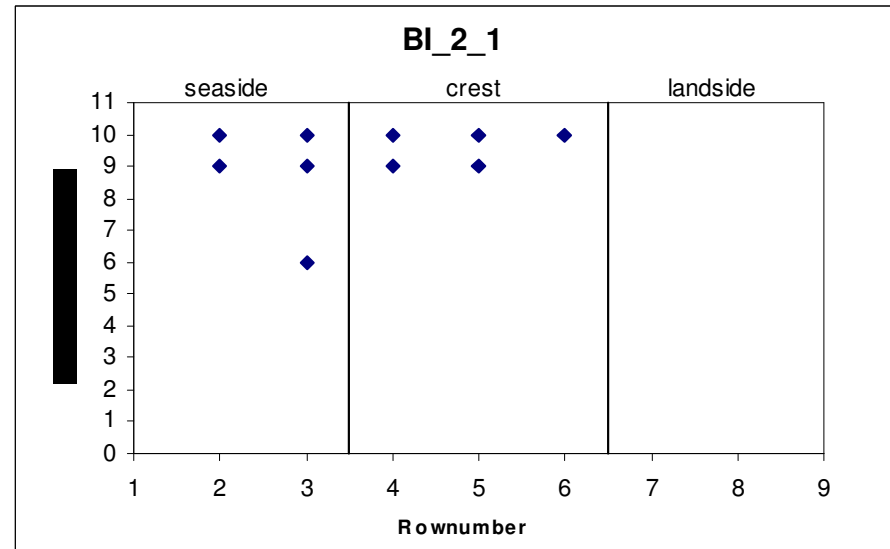
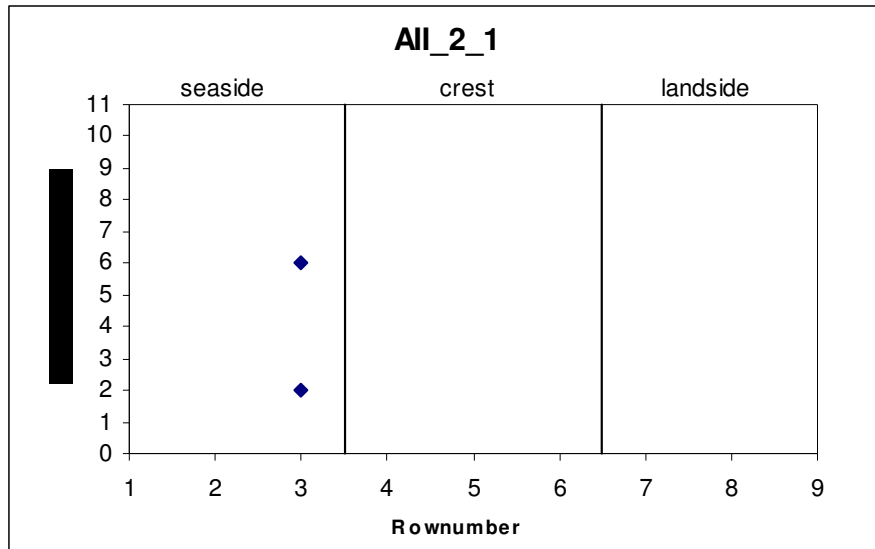
Title

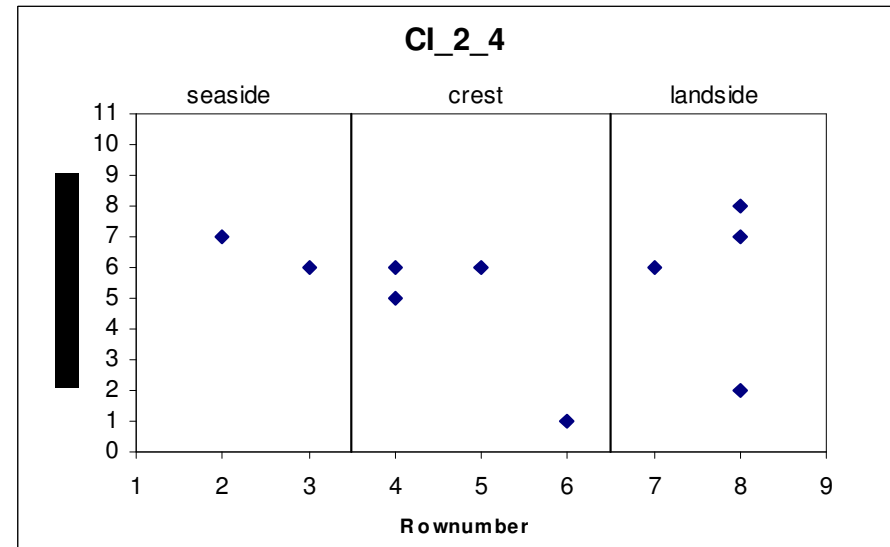
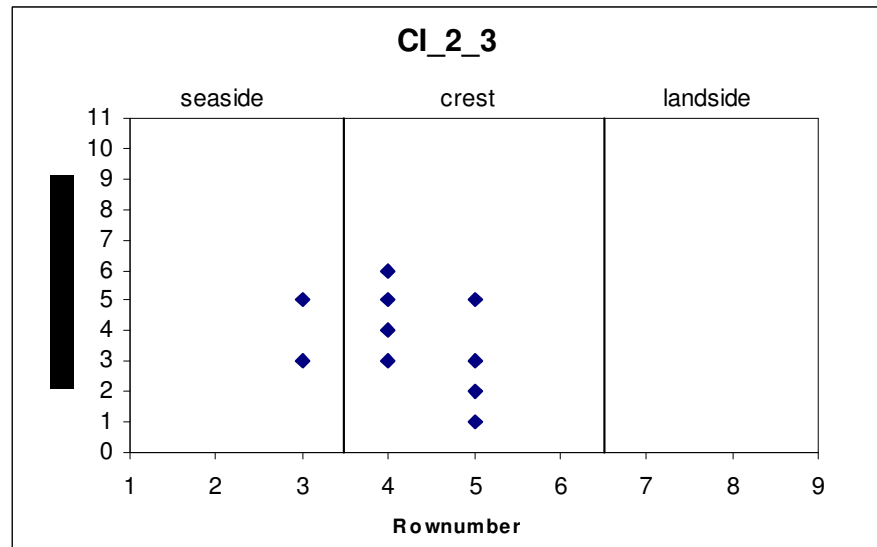
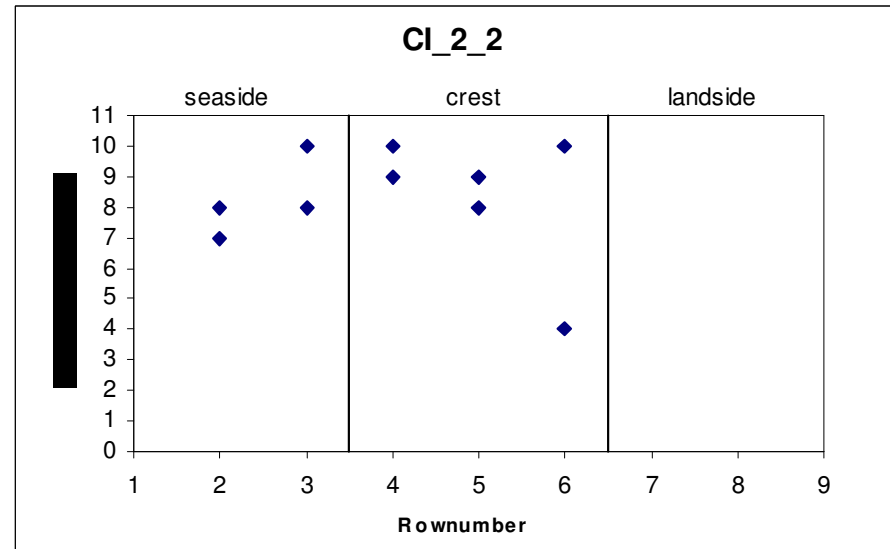
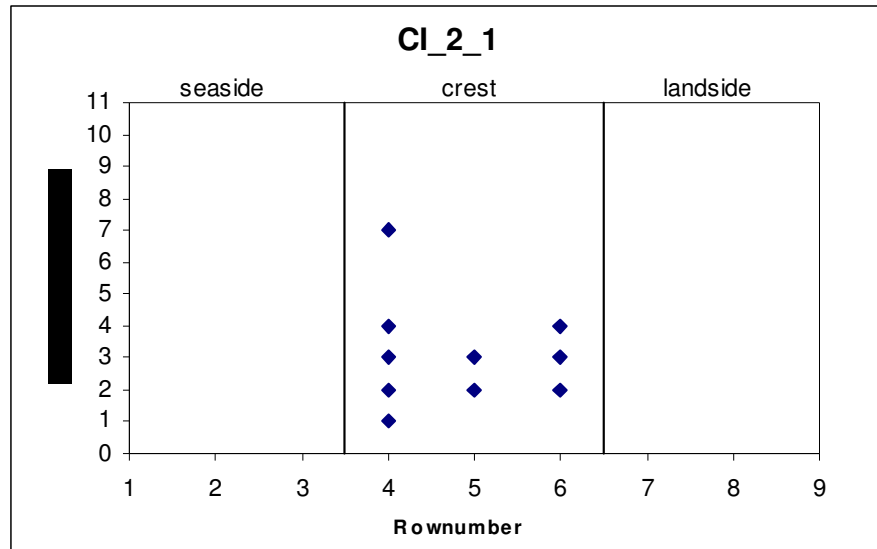
Stability of single layer armour units on low-crested structures

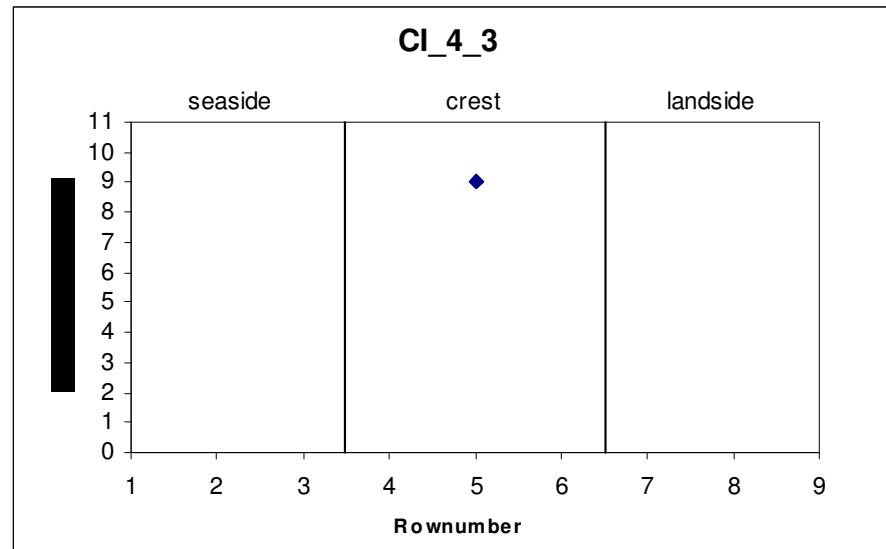
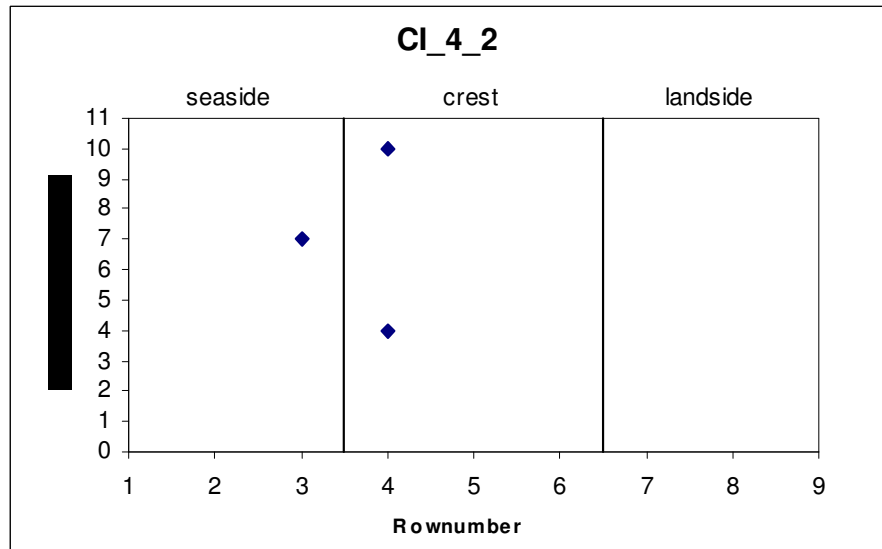
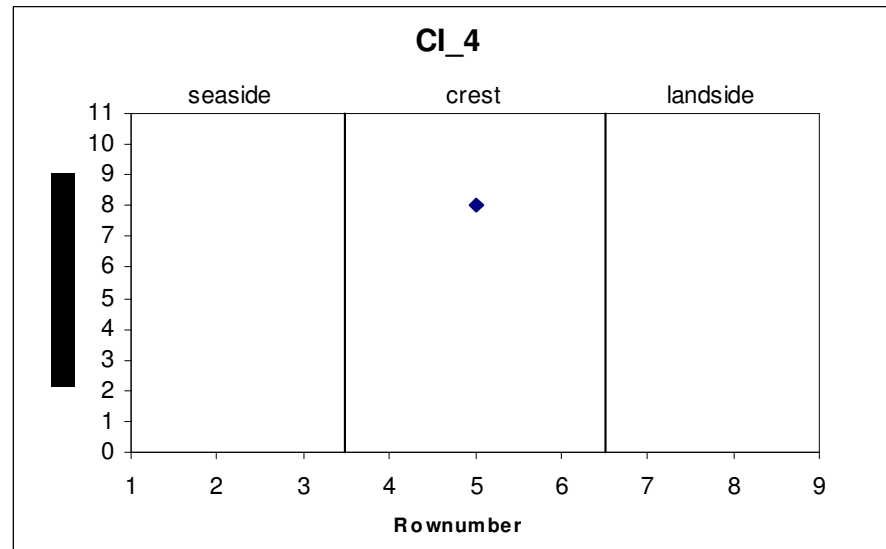
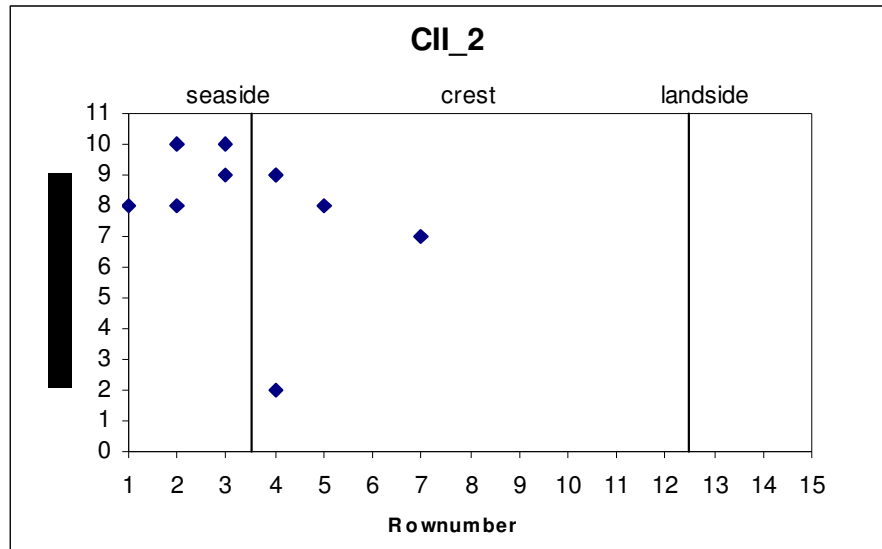
APPENDIX L

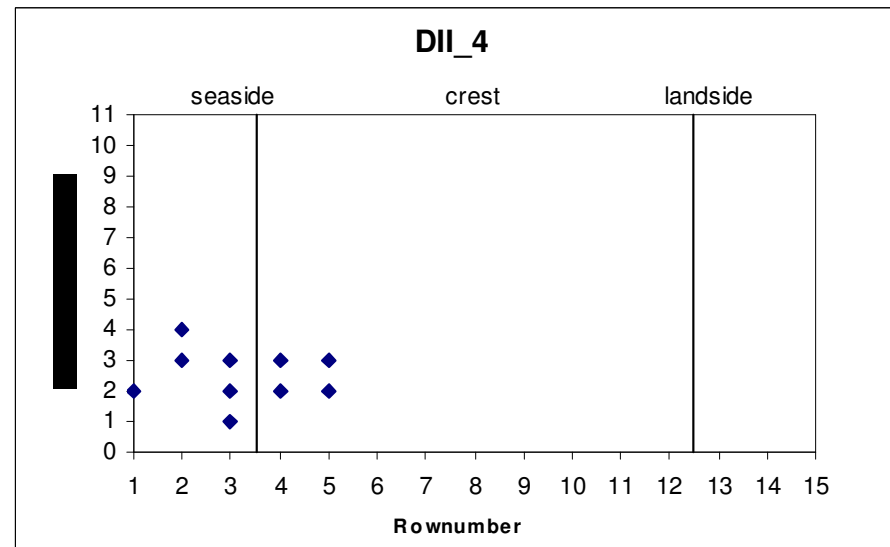
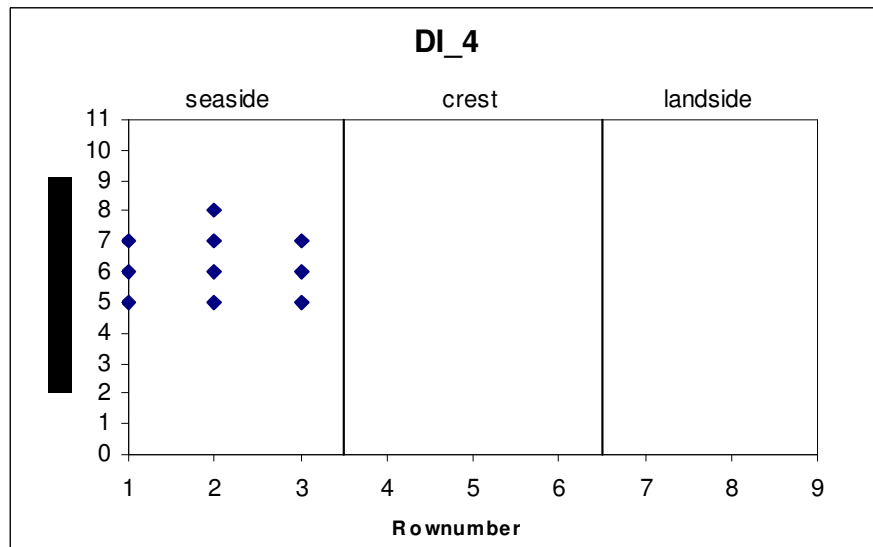
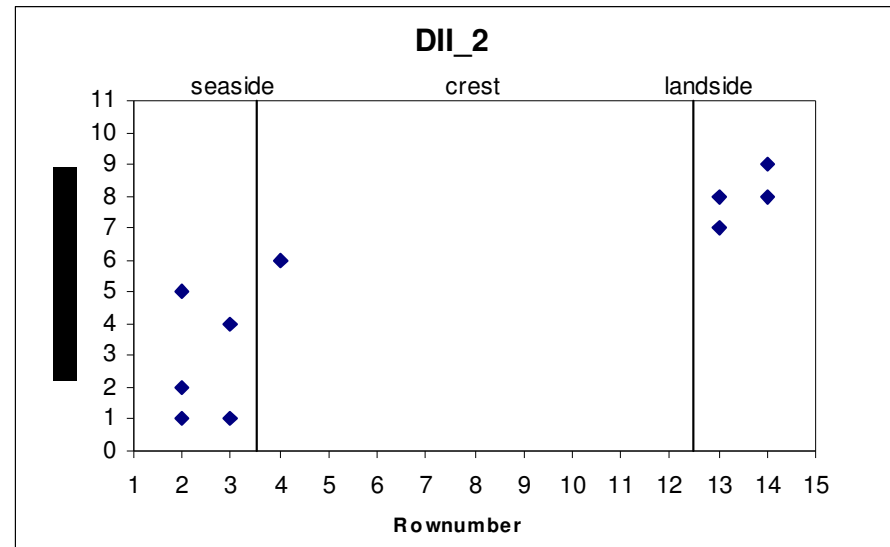
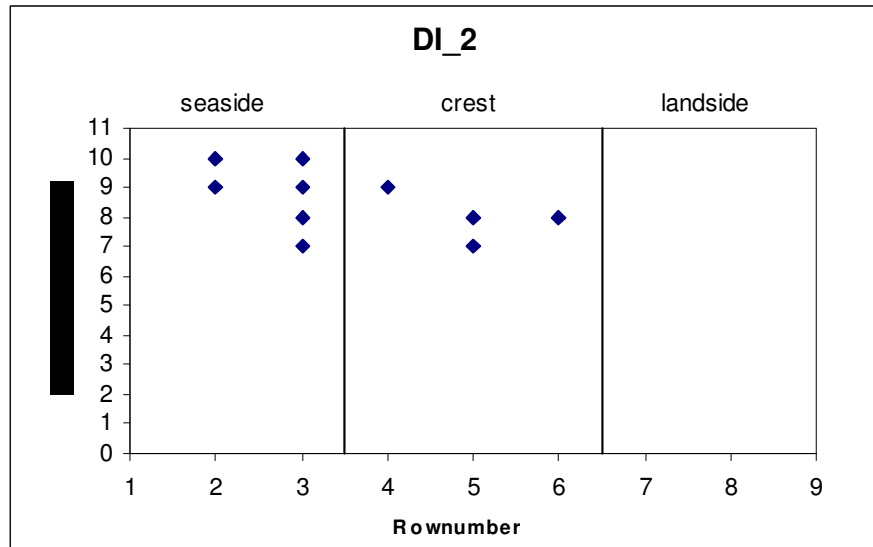
Appendix K shows the location of displaced armour units

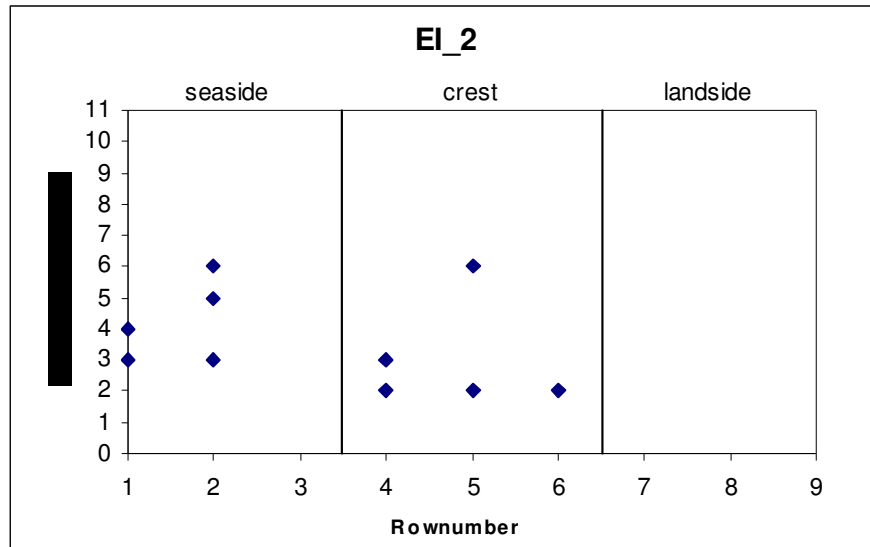












Title

Stability of single layer armour units on low-crested structures
